R-04-15

Preliminary site description

Forsmark area – version 1.1

Svensk Kärnbränslehantering AB

March 2004

SKB

Preliminary site description

Forsmark area – version 1.1

Svensk Kärnbränslehantering AB

March 2004

Preface

SKB started site investigations for a deep repository for spent nuclear fuel in 2002 at two different sites in Sweden, Forsmark and Oskarshamn. The investigations should provide necessary information for a license application aimed at starting underground exploration. For this reason, the site investigation data need to be interpreted and assessed into site descriptive models, which in turn are used for exploring design options, for safety assessment studies and for environmental impact assessment. Site descriptions are also needed for further planning of the site investigations.

A site description is an integrated description of the site and its regional setting, covering the current state of the geosphere and the biosphere as well as those ongoing natural processes which affect their long-term evolution. Development of site descriptions is an important activity during both the initial site investigation phase and the complete site investigation phase. Before the start of the initial phase in Forsmark, version 0 of the site descriptive model was developed /SKB, 2002a/. The results of the initial site investigation phase will be compiled into a preliminary site description (version 1.2). Late in 2002, SKB launched a project with the purpose of developing a preliminary site description for the Forsmark area. A parallel project was set up for the Oskarshamn area. The present report documents the first step in this work for the Forsmark area – the development of an interim version (1.1) of the preliminary site description.

The basis for the site description is quality-assured, geoscientific and ecological field data from Forsmark that are available in the SKB databases at pre-defined dates. The date for "data freeze" is 30 April 2003 for the interim version (model version 1.1).

The specific objectives of model version 1.1 were:
- demonstrate the application of the site descriptive methodology,
- find and establish a structure for the modelling work, and
- give recommendations on continued investigations.

The work has been conducted by a project group and other discipline-specific working groups or persons engaged by members of the project group. The members of the project group represent the disciplines geology, rock mechanics, thermal properties, hydrogeology, hydrogeochemistry, transport properties and surface ecosystems. In addition, some group members have specific qualifications of importance in this type of project e.g. expertise in RVS modelling, GIS modelling and in statistical data analysis. During the work, experts on Quaternary geology and near-surface hydrology were included in the project group.

The overall strategy to achieve a site description is to develop discipline-specific models by interpretation and analyses of the primary data. The different discipline-specific models are then integrated into a site description. Methodologies for developing the discipline-specific models are documented in methodology reports or strategy reports. A forum for technical coordination between the sites/projects is active and also sees to that the methodology is applied as intended and developed if necessary. The group consists of specialists in each field as well as the project leaders of both modelling projects.

The following individuals contributed to the project and/or to the report:
- Kristina Skagius – project leader and editor
- Lennart Ekman – investigation data
- Michael Stephens, Jan Hermanson – geology
- Anna Hedenström – Quaternary deposits
- Rolf Christiansson, Flavio Lanaro, Jan Sundberg – rock mechanics, thermal properties
- Sven Follin – hydrogeology
- Per-Olof Johansson - hydrology
- Marcus Laaksoharju – hydrogeochemistry
- Jan-Olof Selroos – transport properties
- Björn Söderbäck – ecosystems
- Johan Andersson – confidence assessment, and finally
- Martin Stigsson and Anders Lindblom

Anders Ström
Site Investigations – Analysis

Summary

This report presents the interim version (model version 1.1) of the preliminary Site Descriptive Model for Forsmark. The basis for this interim version is quality-assured, geoscientific and ecological field data from Forsmark that were available in the SKB databases SICADA and GIS at April 30, 2003 as well as version 0 of the Site Descriptive Model.

The new data acquired during the initial site investigation phase to the date of data freeze 1.1 constitute the basis for the updating of version 0 to version 1.1. These data originate from surface investigations on the candidate area with its regional environment and from drilling and investigations in boreholes. The surface-based data sets were rather extensive whereas the data sets from boreholes were limited to information from one c 1,000 m deep cored borehole (KFM01A) and eight c 150 to 200 m deep percussion-drilled boreholes in the Forsmark candidate area.

Discipline specific models are developed for a selected regional and local model volume and these are then integrated into a site description. The current methodologies for developing the discipline-specific models and the integration of these are documented in methodology reports or strategy reports. In the present work, the guidelines given in those reports were followed to the extent possible with the data and information available at the time for data freeze for model version 1.1.

Compared with version 0 there are considerable additional features in the version 1.1, especially in the geological description and in the description of the near surface. The geological models of lithology and deformation zones are based on borehole information and much higher resolution surface data. The existence of highly fractured sub-horizontal zones has been verified and these are now part of the model of the deformation zones. A discrete fracture network (DFN) model has also been developed. The rock mechanics model is based on strength information from SFR and an empirical, mechanical classification by depth at KFM01A and at outcrops. A first model of thermal properties of the rock has been developed, although still rather immature due to few site-specific data in support of the model. The hydrogeological description is based on the new geological (structure) model and the fracture transmissivity distribution of the DFN model is based on the data from depth (cored borehole KFM01A). The fracture intensity and permeability are very low below 400 m depth. Hydrogeological simulations of the groundwater evolution since the last glaciation have been performed and compared with the hydrogeochemical conceptual model. The conceptual model of the development of post-glacial hydrogeochemistry has been updated. Also, the salinity distribution, mixing processes and the major reactions altering the groundwaters have been described down to a depth of 200 m. A first model of the transport properties of the rock has been presented, although still rather immature due to lack of site-specific data in support of the model. For the near-surface, there is additional information regarding the stratigraphic distribution of glacial till and water-laid sediment, with related updates in the description.

There is much uncertainty in version 1.1 of the site descriptive model, but the main uncertainties have been identified, some are also quantified and others are left as input to alternative hypotheses. However, since a main reason for uncertainty in version 1.1 is lack of data and poor data density and as much more data are expected in coming data freezes, it has not been judged meaningful to carry the uncertainty quantification or the alternative model generation too far.

Advances have been made on some of the important site specific questions that were formulated in planning the execution programme for the Forsmark area. Concerning the *shape of the tectonic lens*, the understanding of the three dimensional shape of the rock domains in the local model area is now fair, even if there still remain uncertainty on the extension of rock domain boundaries at depth, especially outside the candidate area. A special study has evaluated the *ore potential* of the site. It concludes that the Forsmark candidate area is virtually sterile with respect to ore, although some additional assessments and measurements might be advisable to completely rule out the possibility. Concerning the *occurrence of gently dipping fracture zones*, model version 1.1 contains some near-horizontal, permeable fracture zones, but it is also noted that the extension in both the strike and dip directions as well as the hydraulic properties of these zones are still uncertain. Furthermore, other sub-horizontal zones may possibly exist in addition to the ones in the version 1.1 model. This

issue of sub-horizontal deformation zones remains after model version 1.1 and so does the issue of potential *high rock stresses.* Due to lack of on-site rock stress measurement in data freeze 1.1 the understanding of the rock stress distribution has not advanced very much in model version 1.1. The very low fracture intensity and very tight rock below 400 m in borehole KFM01A was more extreme than expected. This may also have rock mechanical implications.

Recommendations on continued field investigations during the initial site investigation are given based on results and experience gained during the work with the development of the site descriptive model version 1.1. During the course of the modelling work, information exchange with the site investigation has continuously taken place, e.g. concerning the siting of new boreholes. Recommendations on field investigations in order to reduce uncertainties in the model version 1.1 are also given, although it is recognised that a main reason for these uncertainties is lack of data and poor data density and that much more data are expected in coming data freezes from already planned investigations.

Contents

1 Introduction

1.1 Background

SKB started site investigations in the Forsmark and Oskarshamn areas in 2002. The aim of these investigations at both sites is to produce a *site description* that will serve the needs of both Design and Safety Assessment with respect to repository layout and construction and its long-term performance. It also provides a basis for the environmental impact assessment. A site description is an integrated description of the site and its regional setting, covering the current state of the geosphere and the biosphere as well as those ongoing natural processes that affect their long-term evolution. The site description includes two main components:

- a *written synthesis* of the site summarising the current state of knowledge as well as describing ongoing natural processes which affect their long-term evolution, and

- one or several *site descriptive models*, in which the collected information is interpreted and presented in a form which can be used in numerical models for rock engineering, environmental impact and long-term safety assessments.

More about the general principles for site descriptive modelling and its role in the site investigation programme can be found in the general execution programme for the site investigations /SKB, 2001a/.

The site investigation is divided into an initial site investigation and a complete site investigation. Development of site descriptions is an important activity during both these phases. Before the start of the initial site investigation in Forsmark, version 0 of the site descriptive model was developed /SKB, 2002a/. This model version 0 serves as a platform for the development of new versions during the site investigation phase. The results of the initial site investigation phase will be compiled into a "preliminary site description" (version 1.2).

Late in 2002, SKB launched a project with the purpose of developing a preliminary site description for the Forsmark area. A parallel project was set up for the Oskarshamn (i.e. Simpevarp) area. The present report documents the first step in this work for the Forsmark area – the development of an interim version (1.1) of the preliminary site description.

1.2 Scope and objectives

The development of an interim version of the preliminary site description (this report) was set up to be a learning exercise with the same main objectives as the overall project (see below), i.e. to produce a site description and to provide recommendations on continued field investigations. The specific objectives of the interim version are:

- To demonstrate application of the site descriptive methodology.

- To define and establish a structure for the modelling work within the project and in relation to other main activities (field investigation, design and safety assessment)

The main objectives of the overall project are:

- To develop and present a preliminary site description of the Forsmark area based on field data collected during the initial site investigation phase using version 0 of the site description for Forsmark as a starting point. The result is presented in the form of a site descriptive model on a local and a regional scale with an accompanying synthesis of the current understanding of the site.

- To give recommendations on continued field investigations during the initial site investigation and in preparation for the complete site investigation, based on results and experiences gained during the work with the development of site descriptive model versions.

The preliminary site description should be sufficiently detailed to provide a basis for a decision to continue with complete site investigation. The site description shall also allow for provision of responses to site-specific questions raised in FUD-K /SKB, 2001b/.

The basis for both the interim version (model version 1.1) and the preliminary site description (model version 1.2) is quality-assured, geoscientific and ecological field data from Forsmark that are available in the SKB databases SICADA and GIS at pre-defined dates. These dates for "data freeze" are 30 April 2003 for the interim version (model version 1.1) and 1 July 2004 for the preliminary site description (model version 1.2). All new information that becomes available up to these dates will be used to re-evaluate the pre-existing knowledge built into the version 0 and version 1.1 of the site description, respectively, in order to re-asses the validity of the previous model version.

It needs to be emphasised that this report is a first draft version of the preliminary site description. There are large uncertainties in the model description and in many aspects the confidence is low. The reason for this is two-fold; lack of primary data and too little time to carry out supporting exploratory analyses and modelling exercises.

1.3   Setting

The Forsmark site is located in northern Uppland within the municipality of Östhammar, about 170 km north of Stockholm. The candidate area is located along the shoreline of Öregrundsgrepen and it extends from the Forsmark nuclear power plant and access road to the SFR-facility in the northwest towards Kallrigafjärden in the southeast (Figure 1-1). The candidate area is approximately 6 km long and 2 km wide.

The water composition and water movement in Öregrundsgrepen are affected by the freshwater discharge from rivers which flow into the Gävle bay north of Öregrundsgrepen and by the wind. The freshwater discharge from Gävle bay moves south along the coast and passes Öregrundsgrepen, causing a lower salinity in this area compared with the part of the Baltic sea located east of the island Gräsö.

Östhammar municipality is situated on the border between two different landscape types – "Woodlands south of Limes Norrlandicus" and "Coast and archipelagos of the Baltic sea" /NMR, 1984/. The vegetation in the coastal area, where the candidate area is located, is dominated by forest with pine as the dominating forest type. Wetlands are frequent in the coastal area. The coastal and archipelago area is also valuable from a nature conservancy viewpoint and the south-easterly extension of the candidate area is bounded by a protected area, the Kallriga nature reserve.

The region is part of the sub-Cambrian peneplain belonging to the Fennoscandian shield and is relatively flat with a gentle slope to the NE. The candidate area lies at low altitude. The area immediately to the SW, between Fiskarfjärden and the river Forsmarksån, is slightly elevated. Quaternary deposits are more dominant than exposed bedrock or bedrock with only a thin Quaternary cover in the version 0 model area.

The predominating rock type in the region is grey to red, equigranular, metagranitoids. The major part of the bedrock was formed about 1,900 million years ago and it has been affected by both ductile and brittle deformation. The ductile deformation has resulted in large-scale ductile high-strain zones and the brittle deformation has given rise to large-scale faults and fracture zones. "Tectonic lenses", in which the bedrock is much less affected by ductile deformation, are enclosed between the ductile high-strain zones. The candidate area is located in one of these tectonic lenses.
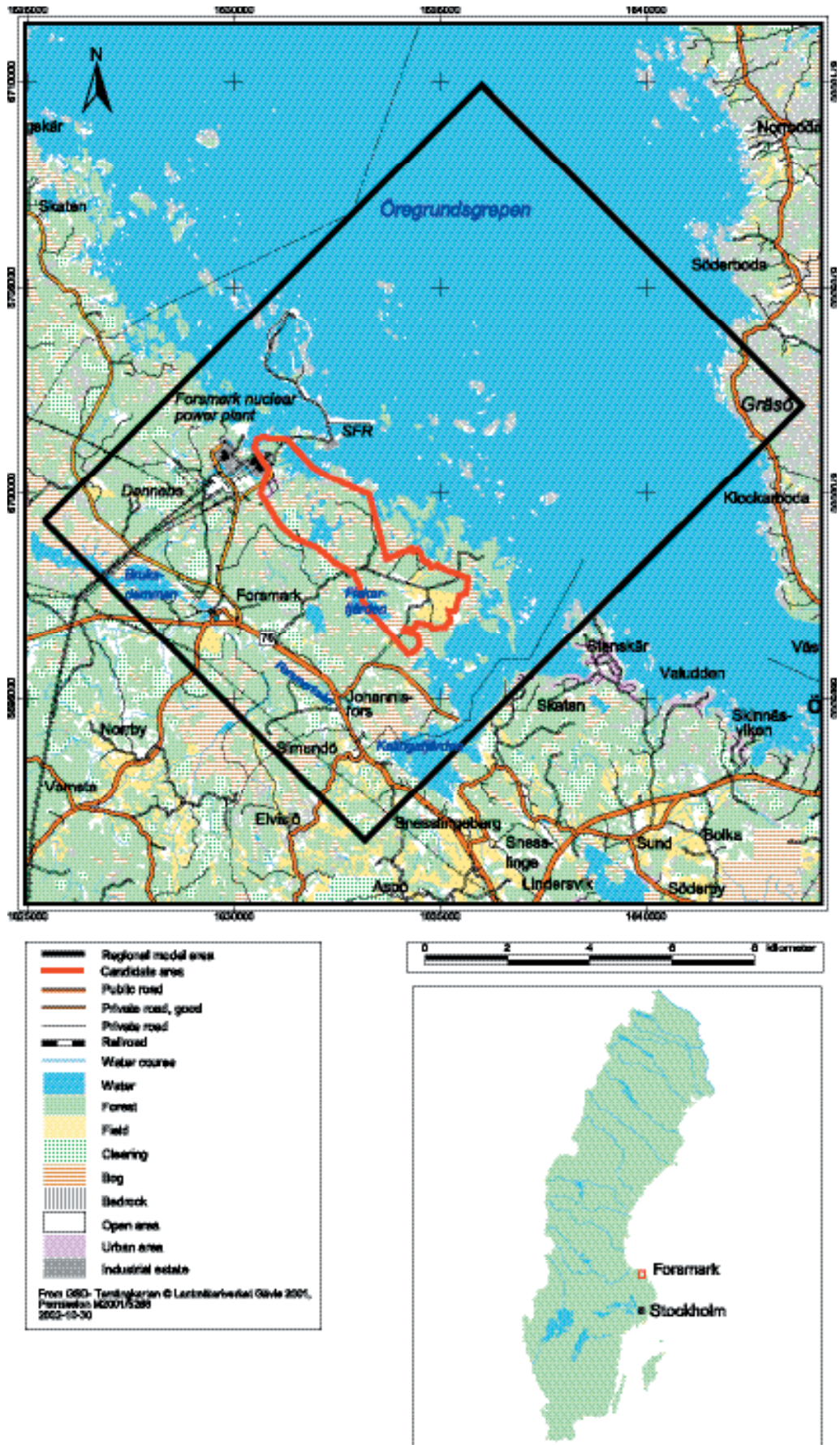
Figure 1-1. *The Forsmark candidate area (red) and the regional model area (black) in the preliminary site descriptive model.*

1.4 Methodology and organisation of work

1.4.1 Methodology

The project is multi-disciplinary in that it should cover all potential properties of the site that are of importance for the overall understanding of the site, for the design of the deep repository, for safety assessment and for the environmental impact assessment. The overall strategy to achieve this (illustrated in Figure 1-2) is to develop discipline-specific models by interpretation and analyses of the quality-assured primary data that are stored in the two SKB databases, SICADA and GIS. The different discipline-specific models are then integrated into a site description.

The site descriptive modelling comprises the iterative steps of primary data evaluation, of descriptive and quantitative modelling in 3D and of overall confidence evaluation. A strategy for achieving sufficient integration between disciplines in producing site descriptive models is documented in a separate strategy document for *integrated evaluation* /Andersson, 2003/, but has been developed further during the work with model version 1.1.
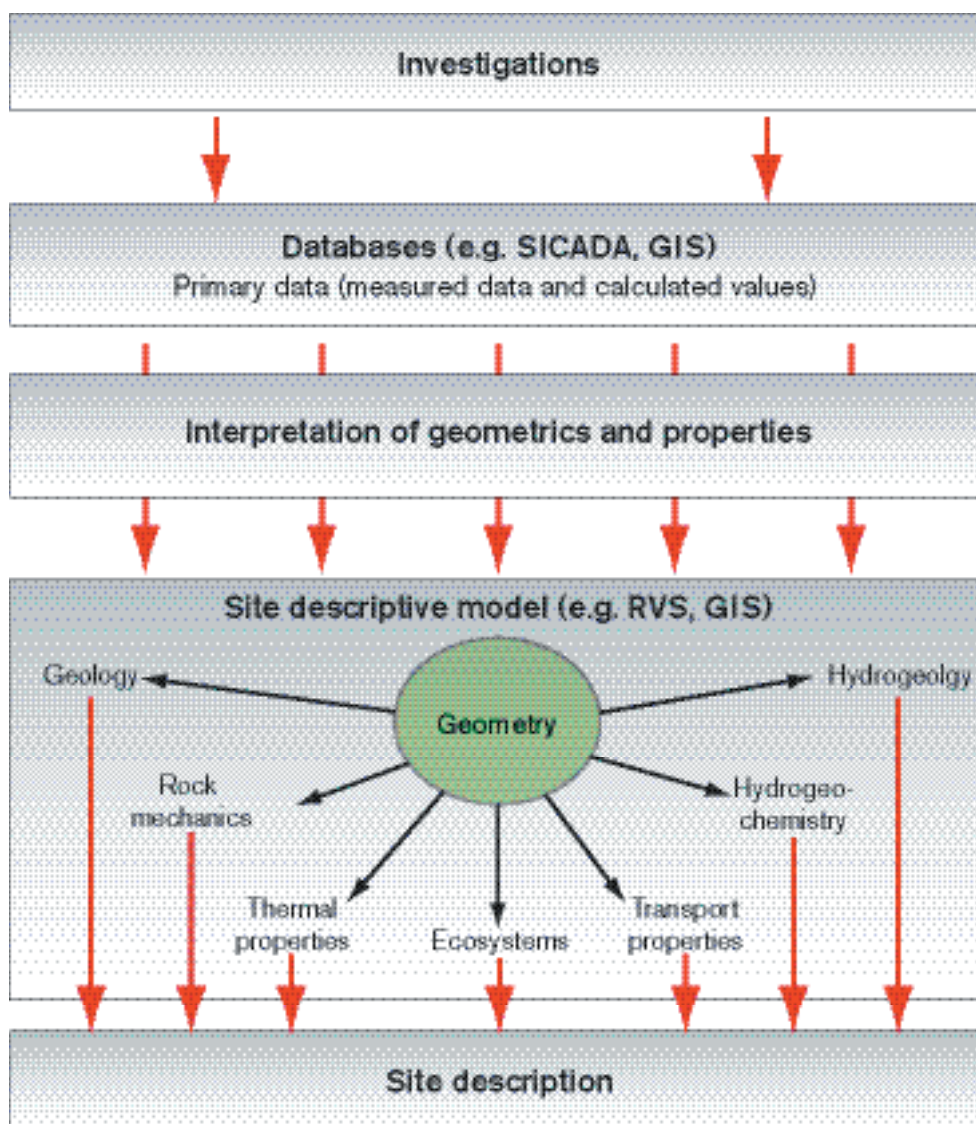
Figure 1-2. From site investigations to site description. Primary data from site investigations are collected in databases. Data are interpreted and presented in a site descriptive model, which consists of a description of the geometry of different units in the model and the corresponding properties of the site /from SKB, 2002a/.

Data are first evaluated within each discipline and then the evaluations are checked between the disciplines. Three-dimensional modelling, with the purpose of estimating the distribution of parameter values in space as well as their uncertainties, follows. The geometrical framework is taken from the geological model and is in turn used by the rock mechanics, thermal and hydrogeological modelling etc (see Figure 1-3). The three-dimensional description should present the parameters with their spatial variability over a relevant and specified scale, with the uncertainty included in this description. If required, different alternative descriptions should be provided.

Methodologies for developing site descriptive models are based on experiences from earlier SKB projects, e.g. the Äspö and the Laxemar modelling projects. Before the underground laboratory in Äspö was built, forecasts of the geosphere properties and conditions were made based on pre-investigations carried out around Äspö. Comparisons of these forecasts with observations and measurements in tunnels and boreholes under ground and evaluation of the results showed that it is possible to reliably describe geological properties and conditions with the aid of analyses and modelling /Rhén et al, 1997a,b,c; Stanfors et al, 1997/. The Laxemar modelling project /Andersson et al, 2002a/ was set up with the intention to explore the adequacy of available methodology for site descriptive modelling based on surface and borehole data and to identify potential needs for the development and improvements in methodology. The project was a methodology test using available data from the Laxemar area.

The current methodologies for developing the discipline-specific models are documented in methodology reports or strategy reports. In the present work, the guidelines given in those reports have been followed to the extent possible with the data and information available at the time for data freeze for model version 1.1. How the work was carried out is described further in Chapters 4 and 5 and for more detailed information on the methodologies the reader is referred to the methodology reports. These are:

- Geological Site Descriptive Modelling /Munier et al, 2003/.
- Rock Mechanical Site Descriptive Modelling /Andersson et al, 2002b/.
- Thermal Site Descriptive Modelling /Sundberg, 2003a/.
- Hydrogeological Site Descriptive Modelling /Rhén et al, 2003/.
- Hydrogeochemical Site Descriptive Modelling /Smellie et al, 2002/.
- Transport Properties Site Descriptive Modelling /Berglund and Selroos, 2004/.
- Ecosystem Descriptive Modelling /Löfgren and Lindborg, 2003/.

According to /Andersson, 2003/, the overall confidence evaluation should be based on the results of the individual discipline modelling and involve the different modelling teams. The confidence is assessed by carrying out checks concerning e.g. the status and use of primary data, uncertainties in derived models, and various consistency checks such as between models and with previous model versions. This strategy has been followed when assessing the overall confidence of model version 1.1. The core members of the project and the activity leaders from the Forsmark site investigation group together accomplished protocols addressing uncertainties and biases in primary data, uncertainty in models and potential for alternative interpretations, consistency and interfaces between disciplines, consistency with understanding of past evolution and consistency with previous model versions. The results are described in Chapter 6.
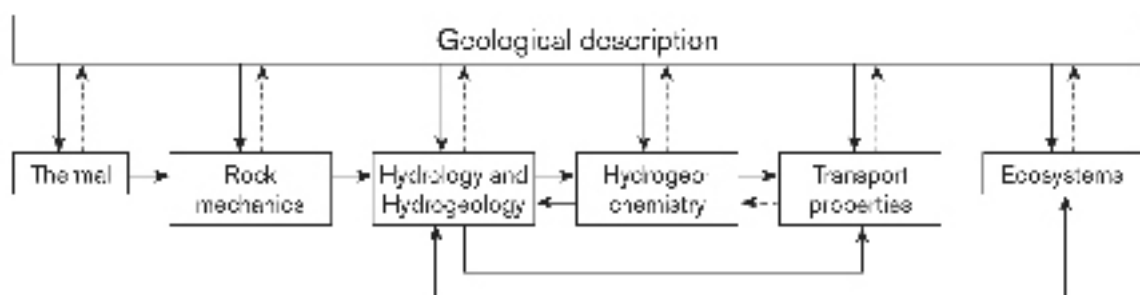
Figure 1-3. *Interrelations and feedback loops between the different disciplines in site descriptive modelling where geology provides the geometrical framework /from Andersson, 2003/.*

1.4.2 Organisation of work

The work has been conducted by a project group and other discipline-specific working groups or persons engaged by members of the project group. The members of the project group represent the disciplines of geology, rock mechanics, thermal properties, hydrogeology, hydrogeochemistry, transport properties and surface ecosystems. In addition, some group members have specific qualifications of importance in this type of project e.g. expertise in RVS (Rock Visualisation System) modelling, GIS-modelling and in statistical data analysis. During the work, experts on Quaternary geology and near-surface hydrology were included in the project group, as it became more and more evident that the project would benefit from such an extension of the coverage of the near-surface system.

Each discipline representative in the project group has taken the responsibility for the assessment and evaluation of primary data and for the modelling work. This has been done either by the representatives themselves or together with other experts or groups of experts outside the project group. Supporting reports have been produced for some of the discipline-specific work carried out within the framework of model version 1.1. References to these supporting reports are given at the appropriate places in the following chapters of this report.

The project group has met at regular intervals to discuss the progress of the work and specific questions that have emerged during the modelling work. In addition, the project group has had a workshop together with activity leaders from the Forsmark site investigation team addressing uncertainties and overall confidence in the data gathered and in the models produced (see Section 1.4.1). The information exchange between the modelling project and the site investigation team is an important component of the project, which is facilitated by the fact that some of the project members are also engaged as experts in the site investigation team. Other activities that have been undertaken to ensure a good information exchange is that several of the members of the modelling project have regularly participated in the activity leader meetings arranged by the site investigation team. Furthermore, the investigation leader at Forsmark has participated in several of the modelling project meetings.

1.5 This report

The structure of the report essentially follows the methodology applied in the modelling work, but with two introductory chapters that provide the prerequisites of the work and a third chapter that provides a description of the present understanding of the long-term history of the site.

Chapter 2 gives a summary of the model version 0 and the field investigations that have provided new data that were available at the time of data freeze for model version 1.1. Sources to these data and short descriptions of how these data have been used in the modelling, with references to sections in the report where these data are evaluated and utilised, are tabulated. In Chapter 3, the current understanding of the long-term historical development of the site is described in terms of the geological evolution of the crystalline bedrock and the evolution during the Quaternary period. Historical aspects of importance for the modelling and understanding of the past evolution of surface and groundwater are described, e.g. shoreline displacement, as well as the historical development of the surface ecosystem.

In Chapter 4, the disciplinary evaluation of primary data and inter-disciplinary comparisons are described. Chapter 5 describes how the results of the data evaluations are entered into the modelling and how the modelling has been carried out, discipline by discipline. Here also uncertainties and comparisons with previous model versions are addressed. Chapter 6 summarises the assessment of the overall confidence in model version 1.1, as derived by the use of auditing protocols. The Site Descriptive Model version 1.1 is presented in Chapter 7 in terms of surface- and ecosystem properties and properties of the bedrock. Chapter 8 summarises experience from the work with model version 1.1 and lists the implications of the work for the ongoing site investigations and for the forthcoming version 1.2 modelling activities.

2   Investigations, available data and other prerequisites for the modelling

The site description is developed and updated successively as the site investigations proceed and as new information concerning the geosphere and biosphere of the investigated areas becomes available. The first model developed was the site descriptive model, version 0 /SKB, 2002a/, which serves as a platform for subsequent model versions for all scientific disciplines involved in the site investigations, especially on a regional scale. Model version 0 is briefly described and commented on in Section 2.2.

In this chapter, the data behind model version 0 are presented together with the new data acquired during the initial site investigation extending over the period February 2002–April 2003. The new data constitute the basis for the updating of version 0 to version 1.1, the result of which is the ultimate objective of this report. An overview of the data available for model version 1.1 is given in Section 2.1 and more detailed descriptions are given in Sections 2.3 to 2.6. In Section 2.7, all data that are included in the development of model version 1.1 are tabulated, and references are given to the appropriate sections of this report where the usage of the data is described.

This chapter also presents the regional and local model volumes selected for the preliminary site descriptive model and the arguments behind the selection (Section 2.8).

2.1   Overview of investigations

This section presents an overview of the investigations made during the period February 14th 2002 (the date of permission from the County Administrative Board for SKB to commence site investigations at Forsmark) until late April 2003. The data associated with this period is denoted *data freeze 1.1*. These data comprise:

1. Primary data used in model version 0.

2. Data not previously considered in model version 0 (i.e. predominantly new data).

2.1.1   Primary data acquired before commencing the site investigation

As described in /SKB, 2002a/, the major sources of data for the Forsmark site descriptive model, version 0, developed prior to the start of the site investigations at Forsmark, were:

*   Information from the feasibility studies /SKB, 2000a/.

*   Some other "old" data sources.

*   Additional data collected and compiled during the preparatory work for the site investigations, especially regarding the discipline "Ecosystems".

The work, which later resulted in model version 0, started with an inventory of relevant data from the Forsmark regional area, as described in /SKB, 2002a/. The results of the inventory included a general description of available geographical data, most of which were stored in the SKB GIS database. As concerns the development of model version 0 for the geosphere, information from the feasibility studies /SKB, 2000a/ turned out to provide the most important data set, see also Section 2.2 below.

A survey was made of data already stored in the SKB Site Characterisation database, SICADA, and an inventory carried out of other data sources, whose information had not yet been evaluated and/or inserted in SICADA or GIS (i.e. not yet converted to digital form). Data sources relevant to the Forsmark regional model area, which, at least to some degree, need to be evaluated/converted/ inserted in the SKB databases, include a large amount of information describing the siting and construction of the three nuclear reactors (Forsmark 1–3), the feasibility study for an underground spent fuel interim storage facility at Forsmark, the pre-investigations and construction of the SFR,

and the SAFE project /SKB, 2002a/. These data are of potential interest when modelling the geosphere in the northwestern part of the Forsmark area. However, the time needed for the process of data transformation described above is such that the work with insertion in the SKB databases could not be completed in time for data freeze 1.1.

The level of knowledge of the surface ecosystems in the Forsmark regional model area is described in a condensed form in /SKB, 2002a/. The description refers to, and draws examples from, a series of SKB background reports which have been produced since the completion of the Östhammar feasibility study, and a number of other sources of information, which were gathered for the first time in /SKB, 2002a/. The version 0 compilation of data sources and contents was intended to provide guidelines for the investigations to come, in order to achieve the aims identified above.

2.1.2   Data freeze 1.1 – investigations performed and data acquired

The site investigations that were initiated early in 2002 comprised of surface investigations, drilling, investigations during drilling and borehole investigations performed after completion of drilling of the respective boreholes. The major part of the investigations made between mid February 2002 and late April 2003 were included in *data freeze 1.1*.

Surface investigations

The surface investigations embraced the following items:

- Mapping of rock types.

- Mapping of ductile and brittle structures.

- Mapping of Quaternary deposits.

- Airborne and ground geophysical investigations.

- Hydrogeochemical sampling/analysis of surface waters.

- A variety of surface ecological inventories and investigations.

Drilling activities

The drilling activities included drilling of:

- One c 1,000 m deep cored borehole of which the upper 100 m was percussion drilled (KFM01A).

- Percussion drilling of the upper 100 m of a second cored borehole (KFM02A).

- Eight percussion-drilled boreholes in solid rock with lengths between 26 m and 222 m.

- 53 boreholes (here called soil boreholes) through the Quaternary deposits.

Borehole investigations during drilling are described in Section 2.5.

Borehole investigations after drilling

The borehole investigations performed after the completion of individual boreholes may be divided into those using the following methods:

- Logging of core-drilled and percussion-drilled boreholes in solid rock with the BIPS colour TV-camera, borehole radar and conventional geophysical logging methods (electric, magnetic and radiometric methods).

- Detailed mapping of the core-drilled boreholes using the drill core supported by BIPS-images and geophysical logging data from the borehole, so called Boremap-mapping.

- Rock mechanical testing of the drill core.

- Boremap-mapping of percussion-drilled boreholes in solid rock. Since no drill cores exist, the mapping is based on samples of drill cuttings supported by BIPS-images and geophysical logging data.

- Hydraulic measurements in core-drilled boreholes as well as in percussion-drilled boreholes in solid rock and in soil boreholes.

- Groundwater sampling in core-drilled boreholes, percussion-drilled boreholes in solid rock and in soil boreholes.

Besides the single-hole methods, hydraulic interference tests between percussion-drilled boreholes were also carried out.

The investigations performed during 2002 and early 2003 have resulted in a large quantity of new data, especially from the candidate area, where intense surface investigations as well as borehole investigations were carried out during the period in question. Investigations were also conducted in the areas enclosing the candidate area, but these surveys have so far been restricted to surface investigations (including airborne geophysics).

The new data sets represent several geoscientific and biological disciplines. Furthermore, the character of data is highly diversified. All data are stored in the SKB databases SICADA or GIS. The results are also presented in a series of reports, printed in the SKB series P or R, see tables in Section 2.7.

2.2 Previous model versions

The version 1.1 site descriptive model of the Forsmark site is the first model including data from the initial site investigation phase. The point of departure for this version of the model is the *Forsmark site descriptive model, version 0* /SKB, 2002a/.

The site descriptive model version 0 contains different levels of complexity as regards the description of the biosphere compared with the geosphere description. The biosphere description focuses on a systematic overview of data needs and availability for developing a site descriptive model, whereas the geosphere description is the result of a more detailed treatment of the existing database and its transformation into the format of a site descriptive model. The present section mainly focuses on a presentation of version 0 for the geosphere.

Version 0 was developed out of the information available at the start of the site investigations. This information, except data from tunnels and drillholes at the sites of the Forsmark nuclear reactors and the SFR repository, is mainly 2D in nature (areal data), and is general and regional, rather than site-specific, in content. For this reason, the Forsmark site descriptive model, version 0, was developed on a regional scale, covering a rectangular area, 15 km in a southwest-northeast and 11 km in a northwest-southeast direction, see Figure 2-3. This area, which encloses the area identified in the feasibility study as favourable for further investigations, has been designated the *Forsmark regional model area* (see also Section 2.8).

The available information on the geosphere prior to the site investigations was rather extensive (e.g. information from SFR).

The lithological model was essentially 2D in character. The structural data suggested an anastomosing system of subvertical zones of high ductile strain, which have undergone reactivation by brittle faulting, providing a basis for preliminary RVS modelling, i.e. 3D modelling, procedures. The first attempt to develop such a 3D geological and geometrical framework for rock engineering and hydrogeological purposes was in model version 0 accompanied by a discussion of how best to assess uncertainty in relation to geological data, depending on the scale of compilation, the current level of knowledge and the interpretation of surface geometry /SKB, 2002a/. Furthermore, the version 0-report contains a geological evolution model for the Forsmark area, from c 1,900 million years to the Quaternary period, as well as a description of the Quaternary deposits in the Forsmark area based on the data available for the version 0 model.

The modelling activities within the disciplines rock mechanics, hydrogeology and hydrogeochemistry were confined to parameterisation exercises using the data that were available from the Forsmark regional model area. Mean values and uncertainty ranges of in situ stress magnitudes and orientations as well as ranges of values for rock mechanical properties were predicted with the lithological and structural model as a framework, using data from the area including the power station and SFR, and also stress data from the Finnsjön area.

Results of previous hydrogeological modelling studies in the Forsmark region and the data used in these modelling activities were used to place limits on hydrogeological properties of the fracture zones and the bedrock between fracture zones and for defining initial and boundary conditions. In this work, structural model version 0 was considered, but no actual testing of the hydrological aspects of the model was carried out.

The hydrogeochemical interpretation/modelling involved the formulation of a conceptual model and the use of a calculational model to describe the origin and evolution of the deep groundwater. No data for deep groundwater in the Forsmark area were available, but results obtained for the Olkiluoto and Hästholmen sites in Finland were given as estimates for the Forsmark regional area because of the similarity in latitude as well as in distance to the Baltic Sea.

An important result of the work with the version 0 model was the data inventory, in which the locations and scope of all potential sources of data were documented and the data were evaluated with respect to their usefulness for site descriptive modelling. This inventory contains data that, at that time, already were stored in the SKB databases SICADA and GIS, but also data that were not evaluated and/or inserted in the databases, but nevertheless relevant for site descriptive modelling.

2.3   Geographic data

/SKB, 2002a/ presents the geographical data available for the *site descriptive model, version 0*. The presentation includes:

- The co-ordinate system.

- Available maps (general map, topographic map, cadastral index map).

- Digital orthophotos.

- Elevation data.

This information is, with exception for the co-ordinate system, still relevant for data freeze 1.1. With reference to the co-ordinate system, all data described are presented in the Swedish national grid. The co-ordinate system is in /SKB, 2002a/ said to be for:

- X/Y (N/E): the national 2.5 gon V, RT 90 system ("RAK").

- Z (elevation): the national RH 70 levelling system.

***The above description should be replaced by the following complete description*:**

- X/Y (N/E): the national 2.5 gon V 0:-15, RT 90 system ("RAK").

- Z (elevation): the national RHB 70 levelling system.

One of the activities initiated in the site investigation in 2002 was to establish *a local net of fixed points* covering the local model area as well as part of the regional model area. In total, 19 reference points were established by rock dowels or steel pipes. All points were positioned by detailed GPS-measurements and levelled with a precision levelling instrument /Geocon, 2002/.

Elevation data covering the land area are available for the whole of Sweden from the GSD-Elevation database. These data are produced on a 50 m grid. Elevation data have an average error less than ± 2.5 m per 50x50 m grid cell, and are delivered with a resolution of 1 m. The latest revision of the database was completed in 1993.

A digital elevation model (DEM) of the Forsmark area has also been developed /Brydsten, 1999a/ for prediction of future shoreline displacement. The current site investigations have demonstrated certain level differences between the GSD-elevation data and the DEM-model data. An activity was there-fore initiated in May 2003 and the field work was undertaken during the following summer months with the objective of identifying and quantifying possible defects in the data sources used. The result of this work was not available in time for data freeze 1.1. Until the question-marks associated with the elevation data have been straightened out, these data should be treated with some caution.

2.4 Surface investigations

Surface investigations were performed within the entire regional model area, see Figure 2-6, and covered the disciplines:

1. Bedrock geology.

2. Quaternary geology.

3. Geophysics.

4. Hydrochemistry.

5. Surface ecology.

6. Hydrology.

The investigations that have generated data to data freeze 1.1 are outlined below for each discipline. Bedrock geological and geophysical data are treated together, due to their close interrelation. References to the documentation of data are given in tables in Section 2.7.

2.4.1 Bedrock geology and geophysics

Bedrock mapping started early in 2002 and has continued during 2003. Available data at data freeze 1.1 were:

- Rock type and ductile structural data from 1,054 outcrops. Also data of frequency and orientation of fractures at 44 outcrops were included.

- Data from detailed bedrock mapping with special emphasis on fractures from two uncovered outcrops at drillsites 2 and 3.

- Data from petrographic and geochemical analyses made on surface samples collected on outcrops during the bedrock mapping.

- Data from petrophysical measurements of samples from surface outcrops and in situ gamma-ray spectrometric data collected in connection with the rock sampling.

- Airborne geophysical data (Magnetic, EM, VLF and gamma-ray spectrometric data).

- Interpretation of the airborne geophysical data, including the identification of lineaments.

- Interpretation of topographic data on land.

- High-resolution seismic reflection data along five separate profiles with a total length of c 16 km.

- Ground geophysical data (magnetic and EM-data) close to drillsites 1, 2 and 3.

- Data from regional gravity measurements.

- Data from electric soundings.

2.4.2 Quaternary geology

The mapping of Quaternary deposits was initiated in 2002 and the field work has continued during 2003. Data freeze 1.1 includes data, which has been divided into stratigraphic data and surface-based data. The former were derived from excavations and soil sampling during drilling through the Quaternary deposits, including lake sediments. Surface-based data were acquired mainly from the regular mapping of Quaternary deposits.

Stratigraphical data

- Stratigraphic data on the Quaternary deposits obtained until data freeze 1.1 and analytical data on soil samples (grain size distribution).

- Field classifications of borehole sequences (till stratigraphy).

- The stratigraphical distribution and field characteristics of sediments in lakes.

Surface-based data

Surface-based data available at data freeze 1.1 were limited to:

- Field data from mapping of Quaternary deposits up to data freeze 1.1.

- Results from investigations of late- and post-glacial features performed up to data freeze 1.1.

2.4.3 Hydrochemistry

The hydrochemical surface investigations included in data freeze 1.1 were:

- Sampling and analysis of precipitation.

- Sampling and analysis of surface waters from a large number of sampling points.

2.4.4 Surface ecology

The discipline "Surface ecosystems" is to some extent dependent on making use of data from other disciplines (e.g. Quaternary geology, hydrogeology, hydrochemistry). Investigations made exclusively for Surface ecology within the site investigation, resulting in data used in data freeze 1.1, are listed below:

- A bird population survey.

- A mammal population survey.

- A vegetation inventory.

2.4.5 Hydrology

A limited number of data from hydrological activities performed during the site investigation were used in data freeze 1.1. These data comprise:

- Results from some simple, sporadic runoff measurements in the area.

- Surface-water levels.

2.5 Borehole investigations

Borehole investigations generating data for data freeze 1.1 were performed in the core- and percussion-drilled boreholes displayed in Figure 2-1 and in the soil boreholes illustrated in Figure 2-2. The borehole investigations performed within the site investigation may be subdivided into:

1. Investigations made during or immediately after completion of the drilling.

2. Investigations made after drilling.

Each of the three borehole categories, core-drilled boreholes, percussion-drilled boreholes in solid rock, and boreholes in soil (the latter category may be e.g. percussion-drilled or auger-drilled), was associated with a specific investigation programme during drilling and another programme after drilling. These programmes are presented in Sections 2.5.1 and 2.5.2, respectively, together with a comment on the outcome for the boreholes up to data freeze 1.1.
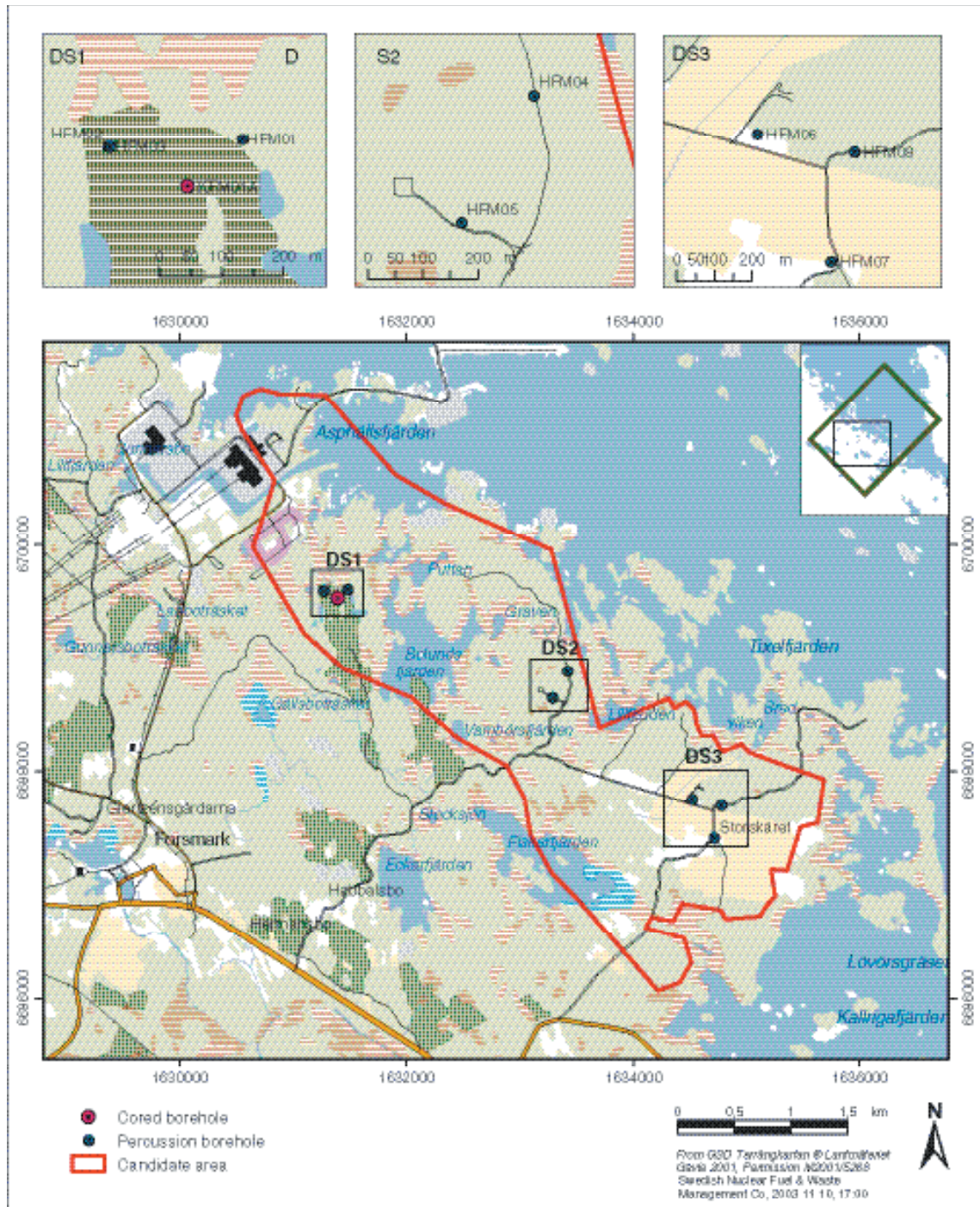
Figure 2-1. *Core-drilled (KFM01A) and percussion-drilled (HFM01–08) boreholes in solid rock from which data are included in data freeze 1.1.*
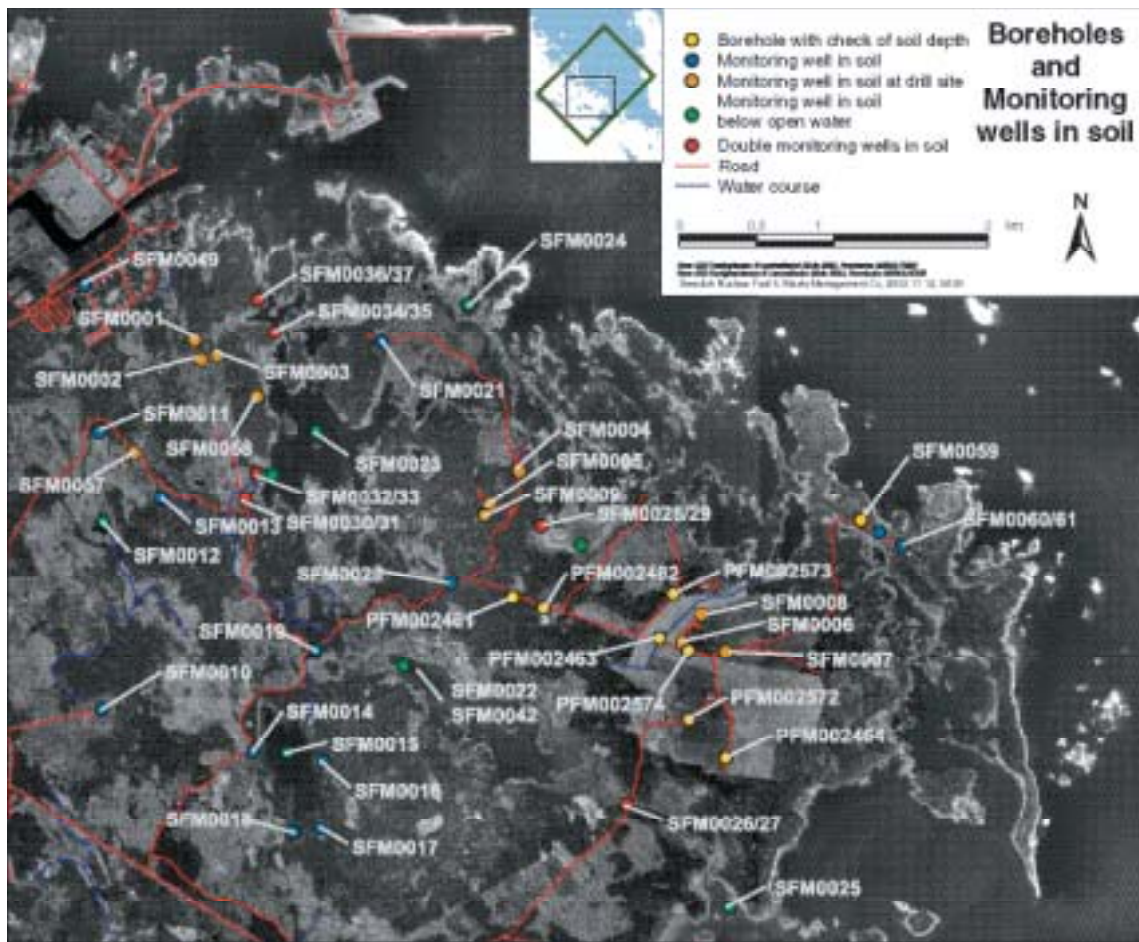
Figure 2-2. Boreholes in soil from which data are included in data freeze 1.1.

2.5.1 Borehole investigations during and immediately after drilling

Core-drilled boreholes

Borehole investigations during and immediately after core-drilling normally include
(see SKB MD 620.004):

- Overview mapping of the drill core.

- Hydraulic tests with a special test-tool (the wireline-probe).

- Absolute pressure measurements with the wireline-probe.

- Water sampling with the wireline-probe.

- Borehole deviation measurements.

- Weighing of drill cuttings.

- Registration of flushing and return water parameters (flow rate, flushing water pressure, electric conductivity, content of tracer dye, content of dissolved oxygen).

- Registration of drill-technical parameters of which some may be useful for geoscientific evaluation (e.g. penetration rates and feed pressure).

If the core-drilled borehole is prioritized for rock mechanical investigations, stress measurements by overcoring are also normally carried out during the drilling process.

Comments, telescopic borehole KFM01A

Only one deep borehole, KFM01A, is included in data freeze 1.1. This borehole, like most of the deep boreholes produced in the site investigation, is telescopic-drilled, implying that the upper 100 m are percussion-drilled with a large dimension (254 mm), and cased. The borehole section c 100–1,000 m, i.e. the major part of the borehole, is core-drilled. Therefore, in telescopic boreholes, the investigation programmes for both percussion-drilled and core-drilled boreholes are applied.

The investigation programme for percussion boreholes during drilling of borehole KFM01A, section 0–100 m, was carried out without divergence.

Regarding the investigation programme for core-drilled boreholes, the following deviations were made:

1. No tests or water sampling with the wireline-probe (except instrument tests) were performed, due to technical problems in combination with a very limited inflow of groundwater at depth in the borehole.

2. Registration of flushing water parameters was performed with individual data loggers from the beginning to c 600 m drilling length. During the subsequent drilling, the newly developed DMS-system (Drilling Measurement System) was implemented.

Borehole KFM01A was initially intended as a telescopic borehole of SKB chemistry type. Therefore, one of the most important investigations planned for the borehole was an extensive water sampling/analysis campaign, so called complete hydrogeochemical characterization down to, and, if possible, below repository depth. However, due to the very limited water inflow into the core-drilled part of the borehole, only two relatively shallow borehole sections, at 110–121 m and 177–184 m, could be sampled. Only the results from section 110–121 m were available in time for data freeze 1.1. Borehole KFM01A is now planned to be used for rock stress measurements by hydrofracturing and HTPF-measurements.

Percussion-drilled boreholes

Borehole investigations during (and immediately after) percussion drilling in solid rock comprise (see SKB MD 610.003):

- While drilling through the unconsolidated overburden (if any), sampling of soil with a frequency of one sample per metre; preliminary examination on site.

- Sampling of drill cuttings from the solid rock with a frequency of one sample per metre; preliminary examination on site.

- Manual measurement of the penetration rate at every 20 cm.

- Observation of the flow rate (if any) at every 20 cm; when a significant increase of the flow rate is noticed, it is measured.

- Observation of the water colour at every 20 cm.

- Measurement of the electric conductivity of the groundwater every third metre.

- Deviation measurements after completion of drilling.

Comments, percussion drilled boreholes HFM01–08

No deviations from the measurement programme were made during drilling of the eight percussion-drilled boreholes included in data freeze 1.1.

Boreholes in soil

Borehole investigations during percussion drilling in soil are divided into:

1. Investigations in soil boreholes in association with drillsites for deep telescopic-drilled boreholes. The boreholes of this category included in data freeze 1.1 are SFM0001–08.

2. All other soil boreholes.

Since the first category of boreholes was drilled with the same percussion drilling machine as was used for percussion drilling in solid rock, the same investigation programme was applied as for percussion drilled holes in rock, except deviation measurements, i.e.:

- Collecting of one soil sample per metre.

- Collecting of one sample of drill cuttings from the bedrock.

- Manual measurement of the penetration rate every 20 cm.

- Observation of groundwater flow rate (if any) and water colour every 20 cm and a measurement of the flow rate at each major flow change observed.

- Measurements of one value of the electrical conductivity of the sampled groundwater (if any) every third metre.

The investigation programme for the second category of boreholes could differ from borehole to borehole (see SKB MD 630.003). However, soil sampling and observation of groundwater inflow was always made.

Comments, boreholes in soil

The analyses of soil samples that were collected during drilling through the soil layer (soil boreholes and percussion boreholes) are reported as stratigraphic data within the activity characterised as mapping of Quaternary unconsolidated deposits (see Table 2-6). Regarding drill cuttings from the rock surface sampled during drilling of soil boreholes, analysis will be performed later and the results reported in the data freeze for model version 1.2.

2.5.2 Borehole investigations after drilling

A base-programme is carried out after drilling in all core-drilled as well as percussion-drilled boreholes. Depending on whether the borehole is prioritized for hydrogeochemical or rock stress measurements, the supplementary data after the base-programme will differ from borehole to borehole /SKB, 2000b/:

Core-drilled boreholes

Only data from the core-drilled borehole KFM01A are included in data freeze 1.1. The borehole investigations performed and reported in data freeze 1.1 are summarised below.

Borehole section 29–51 m (percussion-drilled)

The casing length is 29 m. An instability in the borehole wall at c 51 m prevented investigations below that level. The full diameter, 254 mm, of the percussion-drilled part of KFM01A was achieved by performing the drilling in two sequences. After the first sequence the diameter was 165 mm. At this stage, the following investigations were carried out.

- BIPS-logging.

- Borehole radar logging.

- Conventional geophysical logging.

- Boremap-mapping.

- HTHB-testing (pumping tests and flow logging).

- Groundwater sampling.

- Groundwater-level measurements.

After the above mentioned investigations, the borehole was reamed to 254 mm and cased, and the gap between the casing and borehole wall was cement-grouted. The remaining part of the borehole was core-drilled with a diameter of c 76 mm.

Borehole section 100–1000 m (core-drilled)

- BIPS-logging.

- Borehole radar logging.

- Boremap-mapping.

- Difference flow logging.

- Groundwater-level measurements.

- Hydrogeochemical characterization of the borehole section over 110–121 m.

- Analyses of uranine tracer in drilling water during core drilling.

- Sampling of the drill core for geological, rock mechanical, geochemical and transport analyses.

Percussion-drilled boreholes

The following borehole investigations were performed in the eight percussion-drilled boreholes in the bedrock, HFM01–HFM08:

- BIPS-logging.

- Borehole radar logging.

- Conventional geophysical logging.

- Boremap-mapping.

- HTHB-logging.

Besides the above single-hole measurements, hydraulic interference tests were performed between boreholes HFM01, HFM02 and HFM03.

Comments to radar logging in core-drilled and percussion-drilled boreholes:

Regarding borehole radar logging, only measurements with the dipole antenna resulted in QA-approved data. Due to technical difficulties, data achieved from the directional antenna probably must be rejected and new measurements must be performed later.

Part of the conventional geophysical data have been found to be of poor quality and were excluded from the analysis.

Boreholes in soil

Slug tests were performed in the following boreholes in soil: SFM0001–0006, SFM0008–0021, SFM0023–0037 and SFM0049.

2.6   Other data sources

As mentioned previously in this chapter, the storage of "old data" into the SKB databases SICADA and GIS was not completed in time for the data freeze for model version 1.1. These data were identified during the compilation of data for model version 0 and include information from the siting and construction of the three nuclear reactors (Forsmark 1–3), the feasibility study for an underground interim storage facility for spent fuel at Forsmark, the pre-investigations and construction of the SFR, and from the SAFE project. Some of these data were used in model version 0 and are also included in model version 1.1. The "old data" that have entered the model version 1.1 are included in the compilation tables in Section 2.7.

In the hydrogeochemical evaluation, data from SICADA that reflects the groundwater conditions at other Swedish sites are used as background information together with data from Finnish sites /Pitkänen et al, 1999/.

No measurements of site-specific retention parameters for the rock were at hand at the time of the data freeze for model version 1.1. The evaluation of sorption- and rock-matrix diffusion has therefore utilised results from various experimental investigations of these parameters carried out within the SKB-programme over the past years. For that purpose, a compilation of sorption and diffusion data evaluated from measurements in samples from Finnsjön was made together with any information available from the experiments on geology/mineralogy of the rock samples and hydrochemical conditions during the experiments.

2.7   Databases

The data that were available at the time of the data freeze for model version 1.1 are compiled in tables in this section. The purpose with these tables is to give a reference and account of which data were considered in the development of the site descriptive model (columns 1 and 2 in the table), as well as to give a reference to where in the following sections of the report the data are utilised (columns 3 and 4 in the table). How the data have entered into the modelling work is described in the different sections in Chapters 4 and 5. Data not included in the modelling/site description work are commented upon in the last column of the table.

For simplification and traceability reasons, the information is split into several tables, Table 2-1 to Table 2-7. Complete references to the site-data reports are given in Table 2-8.

The process of data collection and development of the data bases SICADA and GIS includes an auditing of the results before the data are stored in the data bases. The general concept of Quality Assurance of data is given in the general execution programme /SKB, 2001a/. The details of QA procedures for each discipline are given in the internal SKB Method Description documents. Any problem that occurs during a specific field activity is traceable through non-confirming reporting at the site. The remarks in the last column of Table 2-1 to Table 2-7 indicate problems that have been reported.

A number of studies involving data interpretation and modelling have been carried out within the framework of developing model version 1.1. In some cases, these studies are reported in separate reports, which are not included as references in the tables in this section. However, references to these supporting documents are given in Chapters 4 and 5.

Table 2-1. Available bedrock geological and geophysical data and handling in model version 1.1.

Available site data		Utilised in model version 1.1		Not utilised in version 1.1
Data specification	Ref	Analysis/Modelling	cf section	Motivation
Data from core-drilled boreholes				
Technical data in connection with drilling.	Data in SICADA, P-report not yet published	Siting and orientation of borehole KFM01A.	5.1 (rock domain and structural models)	
Radar and BIPS logging in KFM01A.	P-03-45	Identification of fracture zones in the interval 100–996 m.	4.4.1, 5.1 (structural models)	BIPS logging utilised in boremap mapping of KFM01A (100–1,001 m).
Boremap mapping of KFM01A (including the section 29–51 m in the percussion-drilled part).	P-03-23	Rock type, ductile deformation in the bedrock, fracture statistics and identification of fracture zones down to 1,001 m.	4.4.1, 5.1 (rock domain and structural models)	

| Available site data | | Utilised in model version 1.1 | | Not utilised in version 1.1 |
Data specification	Ref	Analysis/Modelling	cf section	Motivation
Data from percussion-drilled boreholes				
Technical data in connection with drilling.	P-03-30	Siting and orientation of boreholes HFM01, HFM02 and HFM03.	5.1 (rock domain and structural models)	
Technical data in connection with drilling.	P-03-51	Siting and orientation of boreholes HFM04 and HFM05.	5.1 (rock domain and structural models)	
Technical data in connection with drilling.	Data in SICADA, P-report not yet published	Siting and orientation of boreholes HFM06, HFM07 and HFM08.	5.1 (rock domain and structural models)	
Geophysical, radar and BIPS logging in HFM01, HFM02, HFM03 and the percussion-drilled part of KFM01A.	P-03-39	Identification of fracture zones down to 200.2 m in HFM01, 100 m in HFM02, 26 m in HFM03 and in the section 29–51 m in KFM01A.	4.4.1, 5.1 (structural models)	Geophysical data not utilised. Poor quality. BIPS logging utilized in Boremap mapping of HFM01, HFM02 and HFM03 and the 29–51 m section in KFM01A.
Geophysical, radar and BIPS logging in HFM04 and HFM05 and the percussion-drilled part of KFM02A.	P-03-53	Identification of fracture zones down to 221.7 m in HFM04, 200.1 m in HFM05 and 101 m in KFM02A.	4.4.1, 5.1 (structural models)	BIPS logging utilised in Boremap mapping of HFM04 and HFM05.
Geophysical, radar and BIPS logging in HFM06, HFM07 and HFM08.	P-03-54	Identification of fracture zones down to c 106 m in HFM06, c 120 m in HFM07 and c 140 m in HFM08.	4.4.1, 5.1 (structural models)	BIPS logging utilised in Boremap mapping of HFM06, HFM07 and HFM08.
Boremap mapping of HFM01, HFM02 and HFM03.	P-03-20	Indication of rock type and identification of fracture zones down to 200.2 m in HFM01, 100 m in HFM02 and 26 m in HFM03.	4.4.1, 5.1 (rock domain and structural models)	
Boremap mapping of HFM04 and HFM05.	P-03-21	Indication of rock type and identification of fracture zones down to 221.7 m in HFM04 and 200.1 m in HFM05.	4.4.1, 5.1 (rock domain and structural models)	
Boremap mapping of HFM06, HFM07 and HFM08.	P-03-22	Indication of rock type and identification of fracture zones down to 110.7 m in HFM06, 122.5 m in HFM07 and 143.5 m in HFM08.	4.4.1, 5.1 (rock domain and structural models)	
Other borehole and tunnel data				
Older geological and geophysical data from the Forsmark nuclear reactor sites.	Some data in SICADA but report planned after 30 April 2003			The assessment of these data has been moved forward to model version 1.2 due to the incomplete character of the data submitted on 2003-04-30, the absence of a complementary report and the limited time available for the completion of model version 1.1.
SFR structural models.	R-98-05, R-01-02	The sub-vertical zones 3, 8 and 9 have been extracted from /Axelsson and Hansen, 1997/. The sub-horizontal zone H2 has been extracted from the SAFE model by /Holmén and Stigsson, 2001/. On account of its length, the subvertical zone 6 /Axelsson and Hansen, 1997/ has not been included in the modelling carried out during the version 1.1.	5.1	

Available site data Data specification	Ref	Utilised in model version 1.1 Analysis/Modelling	cf section	Not utilised in version 1.1 Motivation
Surface-based data				
Bedrock mapping − outcrop data (rock type and ductile structures at 1054 outcrops; frequency and orientation of fractures at 44 outcrops).	P-03-09	Rock type, ductile deformation in the bedrock, fracture statistics and identification of fracture zones at the surface.	4.2.2, 4.2.4 5.1 (rock domain and structural models, DFN modelling in the local model area)	Data also utilised for the interpretation of airborne geophysical data.
Detailed bedrock mapping with special emphasis on fractures (two sites: KFM02A and KFM03A).	P-03-12	Rock type, ductile and brittle deformation in the bedrock, fracture statistics.	4.2.2, 4.2.4 5.1 (DFN modelling in the local model area)	
Petrographic (including QAPF) and geochemical analyses.	P-03-75	Mineralogical and geochemical properties of the bedrock. Structural analyses of ductile and brittle structures.	4.2.2, 4.2.4 5.1 (rock domain and structural models, DFN modelling in the local model area)	
Petrophysical rock parameters and in situ gamma-ray spectrometric data.	P-03-26	Physical properties of the bedrock.	4.2.2, 5.1 (rock domain models).	Data also utilised for the interpretation of airborne geophysical data.
High-resolution seismic reflection data along five separate profiles with a total length c 16 km.	R-02-43	Identification of inhomogeneities in the bedrock that may correspond to boundaries between different types of bedrock or deformation zones.	4.2.5, 5.1 (rock domain and structural models)	
Production of orthorectified aerial photographs and digital terrain model.	P-02-02		4.2.3	Data utilised for the interpretation of lineaments (topographic). Interpretation carried out during the site investigation programme.
Airborne geophysical data (magnetic, EM, VLF and gamma-ray spectrometric data).	P-03-41		4.2.3	Data utilised for the interpretation of lineaments (magnetic, EM and VLF). Interpretation carried out during the site investigation programme.
Ground geophysical data (magnetic and EM data) around DS1, DS2 and DS3.	P-02-01	Identification of lineaments/ fracture zones.	4.2.5, 5.1 (structural models)	
Regional gravity data.	P-03-42			The data have not yet been interpreted and are only of broad regional significance.
Electric soundings.	P-03-44			These data provide a support in the interpretation of the airborne EM data.
Interpretation of topographic data on land.	P-03-40	Identification of topographic lineaments.	4.2.3, 5.1 (structural models)	
Interpretation of airborne geophysical data.	P-03-102 P-04-29	Identification of lineaments based on magnetic, EM and VLF data.	4.2.3, 5.1 (structural models)	
Forsmark site descriptive model version 0.	R-02-32	Various aspects, particularly in the regional model area, where new data are not yet available from the site investigation programme.	4.2.2, 4.2.3 5.1 (rock domain and structural models)	

Table 2-2. Available rock mechanics site data and handling in model version 1.1.

Available site data Data specification	Ref	Utilised in model version 1.1 Analysis/Modelling	cf section	Not utilised in version 1.1 Motivation
Data from core-drilled boreholes				
Stress measurements in DBT1, DBT3.	/Carlsson and Olsson, 1982/ SICADA	Re-interpretation of old data, transient strain analysis, stress model.	4.6.1 5.2.3	
P-wave velocity in KFM01A.	P-03-38 SICADA	Evaluation of stress relaxation.	4.6.1 5.2.3	
Young's modulus, Poisson's ratio of intact rock, Shear tests on fractures, Point load tests on core samples from SFR boreholes KFR21, KFR22, KFR23, KFR24, KFR25, KFR27.	/Hagkonsult, 1982a,b/ SICADA	Characterisation of the rock mass by RMR, Q; empirical determination of the rock mass mechanical properties.	4.6.3 5.2.4	
Young's modulus, Poisson's ratio of intact rock, Point load tests on core samples from SFR boreholes KFR31, KFR32, KFR 35,KFR37.	SICADA	Characterisation of the rock mass by RMR, Q; empirical determination of the rock mass mechanical properties.	4.6.3 5.2.4	
Young's modulus, Poisson's ratio of intact rock, Point load tests on core samples from SFR boreholes KFR19, KFR20.	/Stille et al, 1985/ SICADA	Characterisation of the rock mass by RMR, Q; empirical determination of the rock mass mechanical properties.	4.6.3 5.2.4	
RQD, Rock types, Frequency, Fracture mapping properties from KFM01A.	P-03-38, SICADA	Characterisation of the rock mass by RMR, Q; empirical determination of the rock mass mechanical properties.	4.6.3 5.2.4	
Tilt tests on fractures from KFM01A.	P-03-128 SICADA	Characterisation of the rock mass by RMR, Q.	4.6.3	
Q-logging from KFM01A.	P-03-29	Comparison of Q-logging from different methods; empirical determination of the rock mass mechanical properties.	4.6.3 5.2.4	
Q-logging of surface exposures.	/Barton, 2004/	Comparison of Q-logging from different methods; empirical determination of the rock mass mechanical properties.	4.6.3 5.2.4	

Table 2-3. Available rock thermal data and handling in model version 1.1.

Available site data Data specification	Ref	Utilised in model version 1.1 Analysis/Modelling	cf section	Not utilised in version 1.1 Motivation
Data from core-drilled boreholes				
Temperature logging in KFM01A.	SICADA	Temperature and temperature gradient distribution.	4.7	
Density logging in KFM01A.	SICADA	Density distribution to indicate the distribution of thermal properties.	4.7	
Boremap mapping of KFM01A.	P-03-23	Rock type distribution.	5.3	
Surface-based data				
Modal analyses.	SICADA	Modelling of thermal conductivity from mineralogical properties of the bedrock. Statistical analysis.	4.7, 5.3	
Measurement of thermal properties.	P-03-08	Thermal transport properties for some samples. Comparison with modelled results.	4.7, 5.3	

Table 2-4. Available meteorological, hydrological and hydrogeological site data and handling in model version 1.1.

Available site data Data specification	Ref	Utilised in model version 1.1 Analysis/Modelling	cf section	Not utilised in version 1.1 Motivation
Meteorological data				
Regional data on precipitation, temperature, wind, humidity, global radiation.	R-99-70 TR-02-02 R-02-32	Characterisation, conceptual modelling of surface runoff and groundwater recharge.	4.3.1, 5.4.2, 5.4.4	
Snow depth, frost in ground and ice cover.	SICADA	Characterisation.	4.3.1	
Hydrological data				
Topographical information for delineation of catchment areas.	P-02-02 SKB GIS database	Characterisation of catchment areas.	3.3, 4.3.2, 5.4.2	
Regional runoff data.	R-99-70 TR-02-02 R-02-32	Characterization and conceptual modelling.	4.3.2, 5.4.2	
Simple, sporadic runoff measurements in the area.	SICADA	Characterization and conceptual modelling.	4.3.2, 5.4.2	
Data from core-drilled boreholes				
Pumping tests SFR.	R-02-14	Fracture zone transmissivity.	4.5	
Difference flow logging KFM01A.	P-03-28	No of conductive test sections. Transmissivity of conductive 5-m-sections and individual fractures.	4.5	
Data from percussion-drilled boreholes				
Pumping tests and flow logging DS1.	P-03-33	Fracture zone transmissivity.	4.5	
Pumping tests and flow logging DS2.	P-03-34	Fracture zone transmissivity.	4.5	
Pumping tests and flow logging DS3.	P-03-36	Fracture zone transmissivity.	4.5	
Interference tests DS1.	P-03-35	Fracture zone transmissivity and storativity.	4.5	
Data from boreholes in soil				
Drilling and sampling in soil.	P-03-64	Stratigraphy and thickness of the Quaternary deposits including bedrock elevation.	4.3.3, 5.4.2	
Slug tests in observation holes in soil.	P-03-65	Hydraulic conductivity data for the Quaternary deposits.	4.3.3, 5.4.2	
Surface-based data				
Ground elevation data and bathymetry of the Baltic Sea.	TR-99-16	Topography and bathymetry.		Used as it is, i.e. errors included.
Bathymetry of freshwater lakes.	SKB GIS database	Conceptual modelling of surface water.	4.3.2, 5.4.2	Not used in mathematical groundwater modelling because the resolution of the model's top layer is not sufficient.
Lake sediment characterisation.	P-03-24	Conceptual modelling of surface water – groundwater contact	5.4.2	Not used in mathematical groundwater modelling because the resolution of the model's top layer is not sufficient.

Table 2-5. Available hydrochemical and hydrogeochemical site data and handling in model version 1.1.

Available site data Data specification	Ref	Utilised in model version 1.1 Analysis/Modelling	cf section	Not utilised in version 1.1 Motivation
Data from core-drilled boreholes				
KFM01A – complete chemical characterisation.	AP-PF-400-02-38	All hydrochemical modelling and visualisation. Groundwater quality and representativeness.	4.8 and 5.5	
KFM02A – hydrochemical logging.	AP-PF-400-02-38	All hydrochemical modelling and visualisation. Groundwater quality and representativeness.	4.8 and 5.5	Not used for complete hydro-chemical modelling. Flushing water content is very high (80–90% in the lower half of the borehole).
KFM01A – Uranine analyses during core drilling.	AP-PF-400-02-03	DIS (Drilling impact study). Groundwater quality and representativeness.	4.8 and 5.5	Data in SICADA, but report not published (P-03-32).
KFM02A – Uranine analyses during core drilling.	AP-PF-400-02-42	DIS (Drilling impact study). Groundwater quality and representativeness.	4.8 and 5.5	Data in SICADA, but report not published (P-03-52).
Data from percussion-drilled boreholes				
GW analyses – DS1 KFM01A (0–100m), HFM01, HFM02, HFM03 + monitoring wells.	P-03-47	All hydrochemical modelling and visualisation. Groundwater quality and representativeness.	4.8 and 5.5	
GW analyses – DS2 KFM02A (0–100m), HFM04, HFM05 + monitoring wells.	P-03-48	All hydrochemical modelling and visualisation. Groundwater quality and representativeness.	4.8 and 5.5	
GW analyses – DS2 HFM06, HFM07, HFM08 + monitoring wells.	P-03-49	All hydrochemical modelling and visualisation. Groundwater quality and representativeness.	4.8 and 5.5	
Surface-based data				
Precipitation.	AP-PF-400-02-41	All hydrochemical modelling and visualisation. Groundwater quality and representativeness.	4.8 and 5.5	Draft version.
Surface sampling.	P-03-27	All hydrochemical modelling and visualisation. Groundwater quality and representativeness.	4.8 and 5.5	

Table 2-6. Available Quaternary geologic site data and handling in model version 1.1.

Available site data Data specification	Ref	Utilised in model version 1.1 Analysis/Modelling	cf section	Not utilised in version 1.1 Motivation
Surface-based data				
Mapping of Quaternary deposits, description.	P-03-11 SGU Ae	Distribution of Quaternary deposits.	3.2, 4.2.1, 5.1.1	
Outcrop map.	SKB-GIS	Distribution of bedrock outcrops.	4.2.1, 5.1.1,	
Neotectonic movements.	P-03-76	Late- or postglacial faulting.	4.2.1	
Stratigraphic data				
Mapping of Quaternary deposits, stratigraphic and analytical data. HFM01–HFM08 SFM001–SFM008.	P-03-14	Stratigraphic distribution and characterisation of Quaternary deposits from percussion-drilled holes.	4.2.1, 5.1.1, 7.1.4	
Marine and lacustrine sediment.	P-03-24 R-01-12 TR-03-17	Stratigraphic distribution and field characterization of sediment in lakes.	4.2.1, 5.1.1,	
Stratigraphic sections SFM009–SFM049 PFM002461–65 PFM002472–74.	P-03-64.		4.2.1, 5.1.1, 7.1.4	

Table 2-7. Available surface ecological site data and handling in model version 1.1.

Available site data Data specification	Ref	Utilised in model version 1.1 Analysis/Modelling	cf section	Not utilised in version 1.1 Motivation
Terrestrial – abiotic				
Digital Elevation Model – see Table 2-4.				
Mapping of regolith (Quaternary deposits) – see Table 2-6.				
Marine and lacustrine sediments – see Table 2-6.				
Meteorology data (regional) – see Table 2-4.				
Terrestrial – biotic				
Bird population survey.	P-03-10	Description.	4.10.1, 5.7.2	
Mammal population survey.	P-03-18	Description.	4.10.1, 5.7.2	
Vegetation mapping.	R-02-06	Description, biomass modelling.	4.10.1, 5.7.2	
Vegetation biomass.	P-03-90	Biomass modelling.	4.10.1, 5.7.2	
Humans and land use.	Not yet published	Description.	4.10.2, 5.7.3	Only part of the information utilised in v 1.1.
Compilation of existing information 2002.	R-02-08	Description.	4.10.1, 7.1.5	
Surface waters – abiotic				
Surface water chemistry data – see Table 2-5.				
Surface waters – biotic				
Compilation of existing information 2002.	R-02-08	Description.	4.10.1, 7.1.5	

Table 2-8. Reports in the SKB series P-, R- and TR- that are referred to in Table 2-1 to Table 2-7.

P-02-01	**Thunehed H, Pitkänen T**. Markgeofysiska mätningar inför placering av de tre första kärnborrhålen i Forsmarksområdet.
P-02-02	**Wiklund S.** Digitala ortofoton och höjdmodeller. Redovisning av metodik för platsundersöknings-områdena Oskarshamn och Forsmark samt förstudieområdet Tierp Norra.
P-03-08	**Adl-Zarrabi B.** Outcrop samples from Forsmark. Determination of thermal properties by the TPS-method.
P-03-09	**Stephens M B, Bergman T, Andersson J, Hermansson T, Wahlgren C-H, Albrecht L, Mikko H.** Forsmark bedrock mapping. Stage 1 (2002) – Outcrop data including fracture data.
P-03-10	**Gren M.** Fågelundersökningar inom SKB:s platsundersökningar 2002. Forsmark.
P-03-11	**Sohlenius G, Rudmark L, Hedenström A.** Forsmark. Mapping of unconsolidated Quaternary deposits. Field data 2002.
P-03-12	**Hermanson J, Hansen L, Olofsson J, Sävås J, Vestgård J.** Detailed fracture mapping at the KFM02 and KFM03 drill sites.
P-03-14	**Sohlenius G, Rudmark L.** Forsmark site investigation. Mapping of unconsolidated Quaternary deposits. Stratigraphical and analytical data.
P-03-18	**Cederlund G, Hammarström A, Wallin K.** Surveys of mammal populations in the areas adjacent to Forsmark and Tierp. A pilot study 2001–2002.
P-03-20	**Nordman C.** Forsmark site investigation. Boremap mapping of percussion boreholes HFM01–03.
P-03-21	**Nordman C.** Forsmark site investigation. Boremap mapping of percussion boreholes HFM04 and HFM05.
P-03-22	**Nordman C.** Forsmark site investigation. Boremap mapping of percussion boreholes HFM06–08.
P-03-23	**Petersson J, Wängnerud A.** Forsmark site investigation. Boremap mapping of telescopic drilled borehole KFM01A.
P-03-24	**Hedenström A.** Forsmark site investigation. Investigation of marine and lacustrine sediments in lakes. Field data 2003.
P-03-26	**Mattsson H, Isaksson H, Thunehed H.** Forsmark site investigation. Petrophysical rock sampling, measurements of petrophysical rock parameters and in situ gamma-ray spectrometry measure-ments on outcrops carried out 2002.
P-03-27	**Nilsson A-C, Karlsson S, Borgiel M.** Forsmark site investigation. Sampling and analysis of sur-face waters. Results from sampling in the Forsmark area, March 2002 to March 2003.
P-03-28	**Rouhiainen P, Pöllänen J.** Forsmark site investigation. Difference flow logging of borehole KFM01A.
P-03-29	**Barton N.** KFM01A. Q-logging.
P-03-30	**Claesson L-Å, Nilsson G.** Drilling of flushing water well, HFM01 and two groundwater monitoring wells, HFM02 and HFM03 at drillsite DS1.
P-03-33	**Ludvigson J-E, Jönsson S, Levén J.** Forsmark site investigation. Pumping tests and flow logging. Boreholes KFM01A (0–100 m), HFM01, HFM02 and HFM03.
P-03-34	**Ludvigson J-E, Jönsson S, Svensson T.** Forsmark site investigation. Pumping tests and flow logging. Boreholes KFM02A (0–100 m), HFM04 and HFM05.
P-03-35	**Ludvigson J-E, Jönsson S.** Forsmark site investigation. Hydraulic interference tests. Boreholes HFM01, HFM02 and HFM03.
P-03-36	**Källgården J, Ludvigson J-E, Jönsson S.** Forsmark site investigation. Pumping tests and flow logging. Boreholes KFM03A (0–100 m), HFM06, HFM07 and HFM08.
P-03-38	**Tunbridge L, Cryssantanthakis P.** Forsmark site investigation. Borehole: KFM01A. Determination of P-wave velocity, transverse borehole core.
P-03-39	**Gustafsson C, Nilsson P.** Forsmark site investigation. Geophysical, radar and BIPS logging in boreholes HFM01, HFM02, HFM03 and the percussion drilled part of KFM01A.
P-03-40	**Isaksson H.** Forsmark site investigation. Interpretation of topographic lineaments 2002.
P-03-41	**Rønning H J S, Kihle O, Mogaard J O, Walker P, Shomali H, Hagthorpe P, Byström S, Lindberg H, Thunehed H.** Forsmark site investigation. Helicopter borne geophysics at Forsmark, Östhammar, Sweden.
P-03-42	**Aaro S.** Forsmark site investigation. Regional gravity survey in the Forsmark area, 2002 and 2003.
P-03-44	**Thunehed H, Pitkänen T.** Forsmark site investigation. Electric soundings supporting inversion of helicopterborne EM-data.
P-03-45	**Aaltonen J, Gustafsson C.** Forsmark site investigation. RAMAC and BIPS logging in borehole KFM01A.

P-03-47	**Nilsson A-C.** Forsmark site investigation. Sampling and analyses of groundwater in percussion drilled boreholes and shallow monitoring wells at drillsite DS1. Results from the percussion boreholes HFM01, HFM02, HFM03, KFM01A (borehole section 0–100 m) and the monitoring wells SFM0001, SFM0002 and SFM 0003.
P-03-48	**Nilsson A-C.** Forsmark site investigation. Sampling and analyses of groundwater in percussion drilled boreholes and shallow monitoring wells at drillsite DS2. Results from the percussion boreholes HFM04, HFM05, KFM02A (borehole section 0–100 m) and the monitoring wells SFM0004 and SFM 0005.
P-03-49	**Nilsson A-C.** Forsmark site investigation. Sampling and analyses of groundwater in percussion drilled boreholes at drillsite DS3. Results from the percussion boreholes HFM06 and HFM08.
P-03-51	**Claesson L-Å, Nilsson G.** Drilling of flushing water well, HFM05 and a groundwater monitoring well, HFM04, at drillsite DS2.
P-03-53	**Nilsson P, Gustafsson C.** Forsmark site investigation. Geophysical, radar and BIPS logging in boreholes HFM04, HFM05 and the percussion drilled part of KFM02A.
P-03-54	**Nilsson P, Aaltonen J.** Forsmark site investigation. Geophysical, radar and BIPS logging in boreholes HFM06, HFM07 and HFM08.
P-03-64	**Johansson P-O.** Forsmark site investigation. Drilling and sampling in soil. Installation of groundwater monitoring wells and surface water level gauges.
P-03-65	**Werner K, Johansson P-O.** Forsmark site investigation. Slug tests in groundwater monitoring wells in soil.
P-03-75	**Stephens MB, Lundqvist S, Bergman T, Andersson J, Ekström M.** Forsmark site investigation. Bedrock mapping. Rock types, their petrographic and geochemical characteristics, and a structural analysis of the bedrock based on Stage 1 (2002) surface data.
P-03-76	**Lagerbäck R, Sundh M.** Forsmark site investigation. Searching for evidence of late- or post-glacial faulting in the Forsmark region. Results from 2002.
P-03-90	**Fridriksson G, Öhr J.** Assessment of plant biomass of the ground, field and shrub layers of the Forsmark area. Forsmark site investigations.
P-03-102	**Isaksson H, Mattsson H, Thunehed H, Keisu M.** Interpretation of petrophysical surface data. Stage 1 (2002).
P-03-128	**Chryssanthakis P.** Borehole KFM01A – Results of tilt testing.
P-04-29	**Isaksson H, Thunehed H, Mattsson H, Keisu M.** Interpretation of airborne geophysics and integration with topography. Stage 1 (2002).
R-98-05	**Axelsson C-L, Hansen L M.** Update of structural models at SFR nuclear waste repository, Forsmark, Sweden.
R-99-70	**Lindell S, Ambjörn C, Juhlin B, Larsson-McCann S, Lindquist K.** Available climatological and oceanographical data for site investigation program.
R-01-02	**Holmén J G, Stigsson M.** Modelling of future hydrogeological conditions at SFR.
R-01-12	**Bergström E.** Late Holocene distribution of lake sediment and peat in NE Uppland, Sweden.
R-02-06	**Boresjö Bronge L, Wester K.** Vegetation mapping with satellite data of the Forsmark and Tierp regions.
R-02-08	**Berggren J, Kyläkorpi L.** Ekosystemen i Forsmarksområdet. Sammanställning av befintlig information.
R-02-14	**Axelsson C-A, Ekstav A, Lindblad Påsse A.** SFR – Utvärdering av hydrogeologi.
R-02-32	**SKB.** Forsmark – site descriptive model version 0.
R-02-43	**Juhlin C, Bergman B, Palm H.** Reflection seismic studies in the Forsmark area – stage 1.
TR-99-16	**Brydsten L.** Shore line displacement in Öregrundsgrepen.
TR-02-02	**Larsson-McCann S, Karlsson A, Nord M, Sjögren J, Johansson L, Ivarsson M, Kindell S.** Meteorological, hydrological and oceanographical information and data for the site investigation program in the communities of Östhammar and Tierp in the northern part of Uppland.
TR-03-17	**Hedenström A, Risberg J.** Shore displacement in northern Uppland during the last 6500 calender years.

2.8   Model volumes

In agreement with the general execution program /SKB, 2001a/, the site descriptive modelling is performed on two different scale model volumes, the *regional* and the *local* model volumes. Generally, the local model should cover the volume within which the repository is expected to be placed, including accesses and the immediate environs. In addition to the description on the local

scale, a description is also devised for a much larger volume, the regional model, in order to place the local model in a larger context and to allow for a sensitivity analysis of, mainly, hydrogeological boundary conditions. This section presents and motivates the model volumes selected in this study.

2.8.1 General

The difference between the regional and local model volumes is primarily a matter of scale of presentation. The local volume description should be detailed enough for the needs of the design and safety assessment groups. It is primarily the users of the descriptions who can judge whether the local volume is sufficiently large. The site modelling group may then choose to enlarge this minimum volume in order to find more natural boundaries with the regional description. The regional volume scale should allow a justifiable interface with the local description. Thus, the existence of very detailed data outside the "needed" local volume is not by itself a reason to expand the local volume.

The need for pre-defined model volumes also stems from demands of the integrated representation in the SKB Rock Visualisation System, RVS. As discussed and explained by /Munier et al, 2003/, the property predictions should cover the entire volume of a model and be of the same resolution (scale). However, since the information density varies, the confidence in the description will generally vary within the model volume. Furthermore, the verbal descriptions of the site need not be restricted to the size of the RVS-representation. Furthermore, boundaries of numerical models used in subsequent analyses need not coincide with the RVS-representation boundary. Selection of boundaries and boundary conditions is left to the discretion of the numerical modeller and should be decided on the basis of the purpose of the modelling. Naturally, it is an advantage if the boundaries coincide. In addition, the following rules of thumb apply /Andersson, 2003/:

- The local site descriptive model should cover an area of about 5–10 km^2, i.e. large enough to include the potential repository and its immediate surroundings. This also means that the location of this model area needs to be agreed upon by both the design and site modelling groups.

- The regional descriptive model should be large enough to allow for a sensitivity analysis of boundary conditions and to provide site understanding to the local model.

- If possible, model domains selected in previous versions should be retained. Deviations should be well motivated and their basis fully documented.

- The models should include the main sources of new information (e.g. deep boreholes and areas of extensive surface geophysics).

- The local domain should be large enough to allow meaningful hydrogeological flow simulations within the domain, even if information for boundary conditions or an encompassing regional scale hydrogeological model may need to be taken from the regional domain – or beyond.

- Potentially important features, such as lineaments, rock type boundaries etc, should be considered when selecting the size of the model volumes.

However, practical considerations demand that the model domains should not be too large in relation to the selected resolution (scale) of the description.

2.8.2 Regional model volume

Generally, the geographic scope of the regional models depends on the local premises and is controlled by the need to achieve understanding of the conditions and processes that determine the conditions at the site /SKB, 2001a/. The regional model should encompass a sufficiently large area that the geoscientific conditions that can directly or indirectly influence the local conditions, or help in understanding the geoscientific processes in the repository area, are included. In practical terms, this may entail a surface area of "a few hundred square kilometres."

Figure 2-3 shows the Forsmark regional model area selected for version 1.1. It is the same as the regional model area in version 0 /SKB, 2002a/, but the rationale for its selection has been re-assessed, see below. In addition, the depth of the model volume is now set to 2.2 km (100 m above present sea-level and 2,100 m below).

Figure 2-3. *Regional model area in version 1.1 (same as in version 0). The depth of the volume is set to 2.2 km. The figure also shows the lineaments (dashed lines) and fracture zones (solid lines) identified in version 0. The selected regional model area captures relevant portions of the regional deformation zones.*

The regional model volume has been selected on the basis of the following considerations:

- It includes the candidate area and it is not prohibitively large as it has a surface area of 165 km² (see Figure 2-3),

- It captures relevant portions of the extensive regional deformation zones which strike in a north-westerly direction and surround the candidate area (see Figure 2-3). Any expansion of the regional model area to the northwest or southeast would not provide any significant changes in the regional geological picture.

- It adequately covers the variations in rock type in the candidate area and its immediate surroundings.

- It captures the main hydrogeological features of the region, as the boundaries perpendicular to the shoreline are judged to be sufficiently far away from each other so that they do not influence the groundwater flow in the candidate area. The boundary to the southwest lies on the south-western side of a local topographic divide and the boundary to the northeast lies northeast of a major bathymetric break in Öregrundsgrepen. The area includes potential discharge areas even after consideration has been taken for considerable shoreline displacements (see Figure 2-4 and Figure 2-5).

- A depth of 2.1 km below sea-level is considered to provide a reasonable vertical extent for the local description and is the maximum depth down to which any meaningful extrapolations of deformation zones could be made.
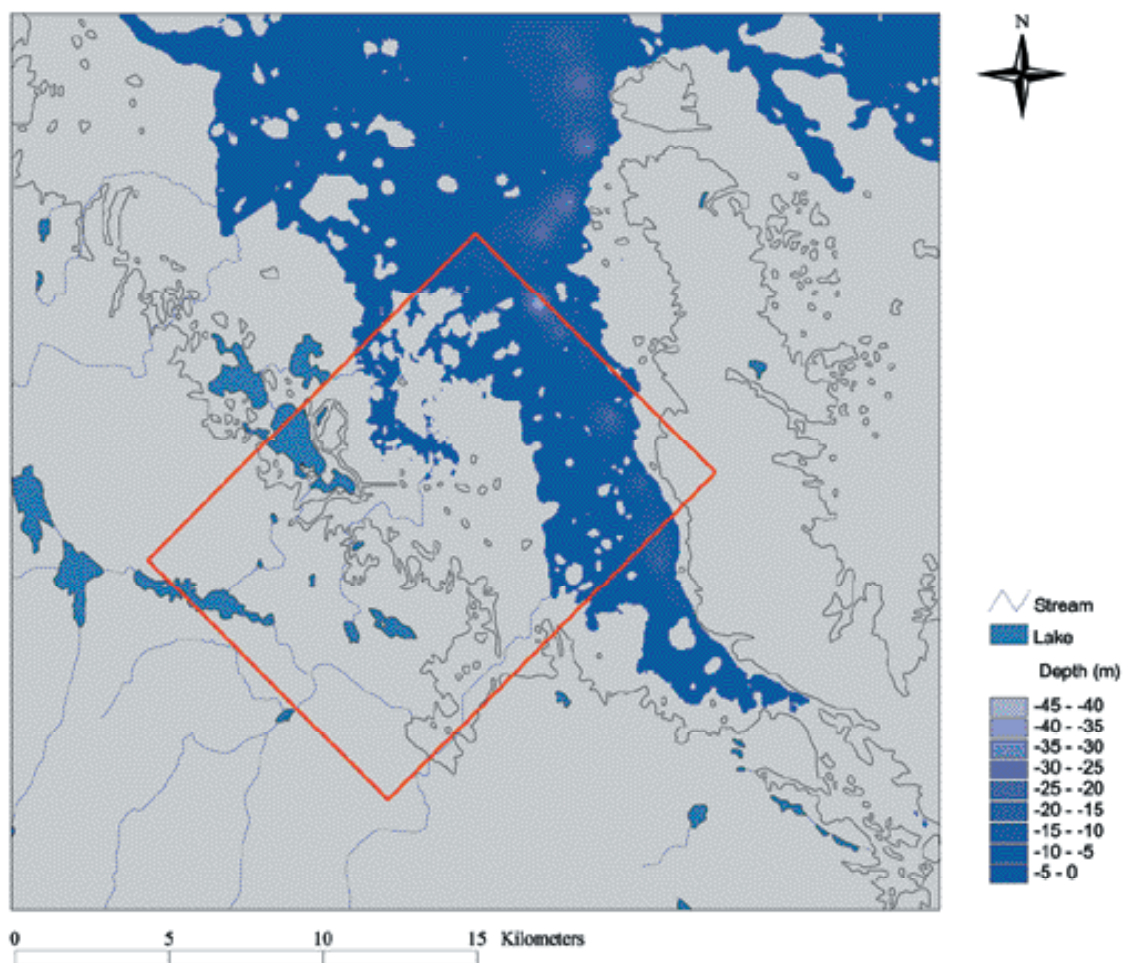
Figure 2-4. *The selected regional model area includes potential discharge areas also after considerable shoreline displacement. The figure shows the predicted shoreline at 4,500 AD /Brydsten, 1999a/.*
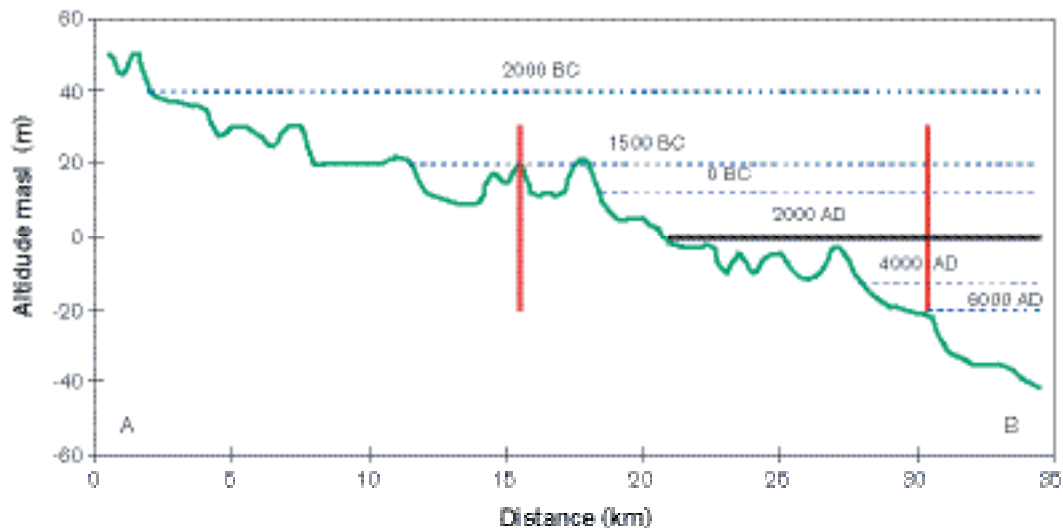
Figure 2-5. *Topographic relief along a line transverse the shore (A=1620000, 6683000 and B=1639000, 6713000). The horizontal blue lines show the sea level at c 2,000 BC, 1,500 BC, 0 BC, 2,000 AD, 4,000 AD and 6,000 AD /Påsse, 1996/. The vertical red lines indicate the location of the upstream and downstream vertical sides of the Forsmark regional model area. Modified after /Stigsson et al, 1998/.*

2.8.3 Local model volume

The horizontal area of the deep repository (at repository depth) is ideally about 2 km². This area includes a fully built repository with approximately 4,500 canisters. The surface facility and the access routes to the deep repository are not included in this area since their plan requirement depend on whether a straight ramp, a spiral ramp or a shaft will be used. The geometrically ideal case will not be achieved in reality, since the layout of the deep repository will be adapted to conditions in the bedrock (fracture zones, etc). The more deposition areas the deep repository is divided up into and the more irregular these geometries are, the larger total repository area will be required, since intervening unutilized "corridors" must also be included in the total "encompassing" area. The local investigation and model area should also be considerably larger than the repository area, above all because it is not otherwise possible to try alternative repository layouts and gradually arrive at the optimal placement and adaptation to rock conditions. The local model should therefore encompass a surface area of 5–10 km² /SKB, 2001a/.

Figure 2-6 shows the Forsmark local model area selected for version 1.1. The depth range is selected to be 1,100 m below sea-level and 100 m above sea-level. The rationale for volume selection is given below.

The local model volume has been selected on the basis of the following considerations:

- It provides the minimum volume which includes the candidate area, the parts of the 'tectonic lens' below the current reactor site as well as potential access ramps from the SFR peninsula. Thus, the volume encompasses any possible location of the deep repository at the Forsmark site, i.e. where a high resolution description may be needed.

- Both to the northeast and southwest, it includes the boundaries to more inhomogeneous and banded bedrock outside the candidate area.

- It includes key rock boundaries within and immediately adjacent to the candidate area which help to define the structural framework within the 'tectonic lens'.

- A depth of 1,100 m beneath sea-level will permit inclusion of all information from the deep boreholes that will be drilled at the site.

- It is larger than the recommended size, but not prohibitively large as it has a surface area of 31.5 km² (see Figure 2-6).
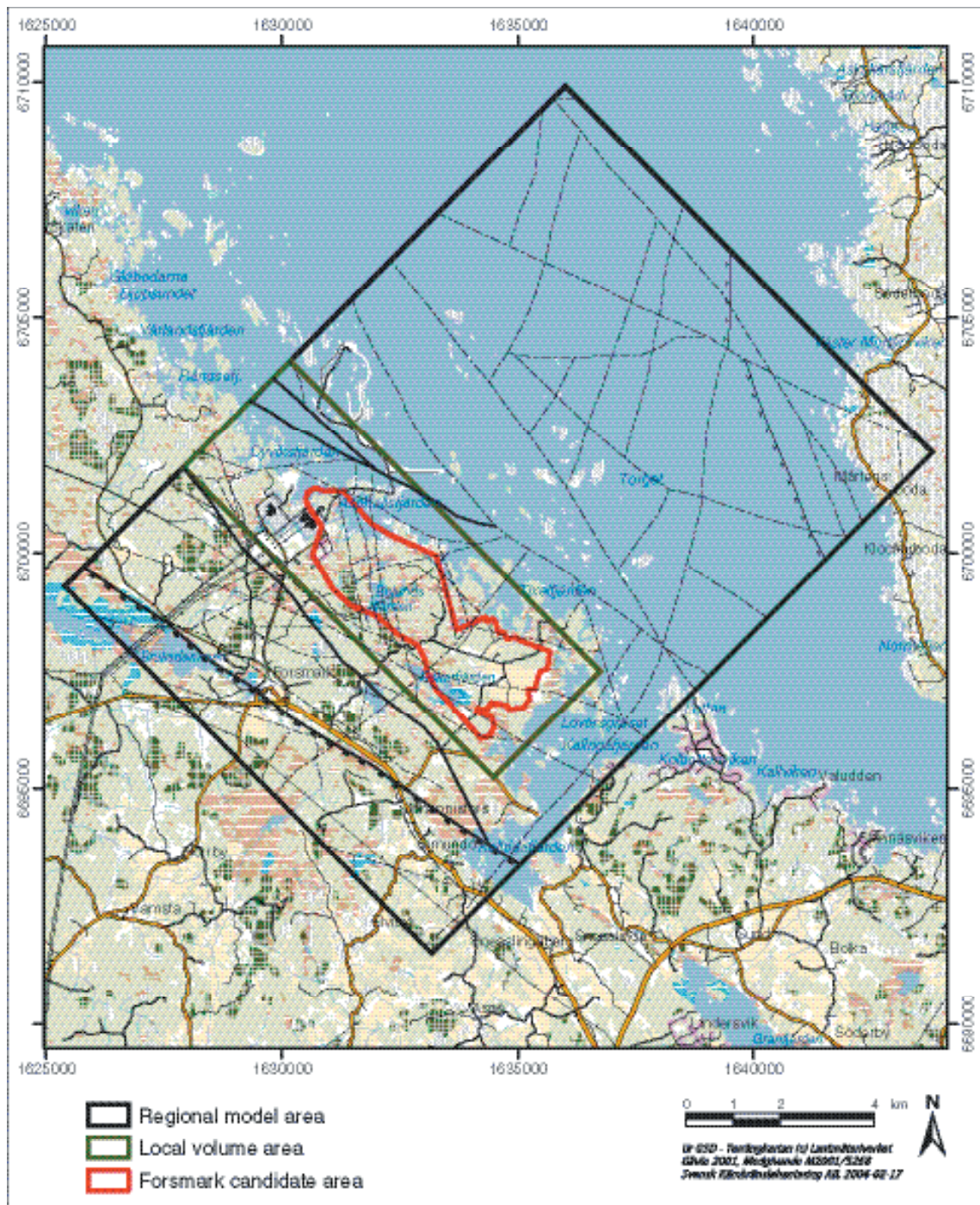
Figure 2-6. *The local volume area (green line) just surrounds the Forsmark candidate area (red line). Thereby it will cover the potential repository volume, including access ramps, and its immediate surroundings. The depth is selected to 1,100 m below sea-level and 100 m above sea-level. The figure also shows the lineaments (dashed lines) and fracture zones (solid lines) identified in version 0.*

In selecting the local model volume, it was initially considered whether to enlarge the model volume to also include the surrounding regional fracture zones with northwesterly strike and major topographic features. However, there are several arguments against such an enlargement:

- The level of confidence in a high-resolution-scale description outside the candidate area will always be quite small, except for patches like the SFR-volume. A too large local volume area may thus provide a misleading picture of the actual confidence or may draw unmotivated resources to improve confidence in details not really required.

- The resource requirements needed to handle a very large local model volume are not prohibitive, but are significant. A larger local model volume would still not be sufficiently large to capture all features required in the regional model (see Section 2.8.2).

Evidently, the limits of the model size selected mean that e.g. hydrogeological model simulations usually cannot treat boundaries of the local model as physical boundaries. If a larger model domain is needed, the regional fracture zones surrounding the candidate area as well as the major topographic features will be included. However, this is not a problem for the simulation models as they can handle nested volumes.

3 Evolutionary aspects of the Forsmark site

3.1 Crystalline bedrock from c 1,900 million years to the Quaternary

The Forsmark regional model area in central Sweden forms part of an old area of Precambrian crystalline rocks, referred to as the Fennoscandian Shield. Forsmark lies within a broader lithological province, which extends from the Loftahammar-Linköping area in the south to the Hudiksvall-Ånge area in the north. This province consists of metagranitoids with associated metavolcanic and metasedimentary rocks (Figure 3-1). The meta-igneous rocks within this province vary in age from 1,906 to 1,840 million years, rocks younger than 1870 million years being especially conspicuous north of Gävle. It includes one of Sweden's important ore provinces – Bergslagen and adjacent areas that is situated between Örebro and Gävle /Frietsch, 1975; Åkerman, 1994/.

Forsmark lies within the southernmost part of a complex, structural domain with predominantly high-grade metamorphic rocks. This domain extends from the coastal area in the northern part of Uppland to the Hudiksvall-Ånge area to the north and is referred to as structural domain 1 in Figure 3-1. It is characterized by a relatively high concentration of ductile high-strain zones with NW to NNW strike, which anastomose around lenses in which the bedrock is folded and generally displays lower strain. These so-called tectonic lenses are also conspicuous on a smaller scale within the Forsmark regional model area.

In accordance with other older Precambrian shield areas, a complex network of ductile-brittle and brittle fracture zones transects the Fennoscandian Shield. In eastern areas, these zones initiated their development after c 1,700 million years ago. Locally, for example at Forsmark /Larsson, 1973; Carlsson, 1979/, it has been shown that individual zones were active at different times during the last 1,700 million years.

In order to understand the geological evolutionary aspects of the Forsmark site, it is necessary to view the site in a broader geological context. For this purpose, attention is focused here on the area in the central-eastern part of Sweden that extends from Loftahammar and Linköping in the south to Hudiksvall and Ånge in the north (Figure 3-1). A model for the geological evolution of central-eastern Sweden, within which the Forsmark regional model area is situated (Figure 3-1), is presented for six key phases related to different time periods (Table 3-1). Much of the bedrock in this part of Sweden formed during phases 1 and 2. Where the effects of geological events are of more limited character and, in general, less well understood (phases 3–6), information from outside the Loftahammar-Ånge area has also been taken into account.

The evolutionary model for the crystalline bedrock has utilized the following information:

- Countrywide compilations of the bedrock geology both in cartographic /Stephens et al, 1994/ and text /Fredén, 1994; Stephens et al, 1997/ form.

- A review of tectonic régimes in the Fennoscandian Shield during the last 1,200 million years /Larson and Tullborg, 1993/.

- A reconstruction of the tectonic history of the Fennoscandian Shield during the last 100 million years, based on data available along its margins to the south and west /Muir Wood, 1995/.

- Summaries of the geology of central Sweden in several county reports /Antal et al, 1998a,b,c,d; Bergman et al, 1999a,b; Gierup et al, 1999/.

- Some key references of more local interest which are referred too directly in the text.

Figure 3-1. *Simplified map of the bedrock geology of Sweden. The position of the Forsmark regional model area is shown. Modified after /Stephens et al, 1994/.*

The internationally accepted geological time scale that has been used in this report is presented in Figure 3-2 and an overview of phases 1–6 is provided in Table 3-1. Some indication of the level of knowledge concerning the relevance of each phase for the geological evolution of the Forsmark site is also presented in this table. The continuous southward and westward growth of the shield, with variable crustal movement directions during the different time phases, is illustrated in a series of diagrams (Figure 3-3, Figure 3-4 and Figure 3-5). Younger geological events, principally around the margins of the shield, are also shown (Figure 3-6 and Figure 3-7). A short description of each phase completes this section.
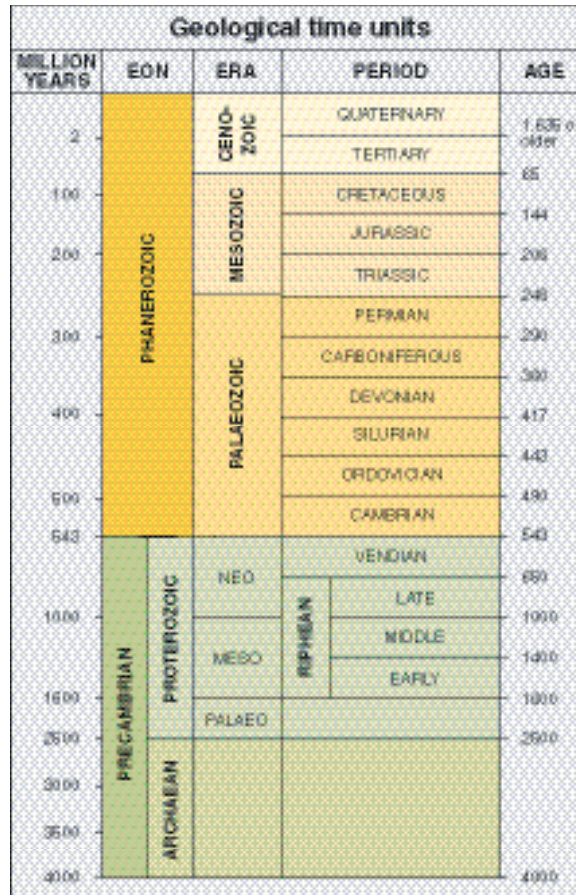
Figure 3-2. Geological time scale used in this report. Modified after /Koistinen et al, 2001/.

Table 3-1. Overview of geological activity in the crystalline bedrock from 1,910 million years to the Quaternary period.

Phase	Time period	Geological activity	Geological activity in the Forsmark area
1	1,910 to 1,870 (1,860) million years	Sedimentation, major igneous activity, and crustal deformation associated with growth and early-stage reworking of the crust (Svecokarelian orogeny, early stage).	Formation of major part of bedrock. Ductile deformation?
2	1,870 to 1,750 million years	Major igneous activity, sedimentation and crustal deformation associated primarily with reworking of the newly-formed crust (Svecokarelian orogeny, late stage). Slow exhumation of deeper crustal levels and erosion.	Formation of younger intrusive rocks. Ductile deformation.

Phase	Time period	Geological activity	Geological activity in the Forsmark area
3	1,750 to 900 million years	Far-field effects of : • Continued crustal growth and crustal reworking with deformation and metamorphism to the south and west (including Gothian and Hallandian orogenies). • Crustal reworking with deformation and metamorphism related to the assembly of the supercontinent Rodinia (Sveconorwegian orogeny). Geological activity in eastern Sweden includes: • Continued exhumation of deeper crustal levels and erosion. • Igneous activity at high crustal levels. • Local subsidence and formation of sedimentary basins during the Mesoproterozoic. • Subsidence and formation of a foreland sedimentary basin to the east of the Sveconorwegian orogenic belt, related to the exhumation of deeper crustal levels and erosion within this belt.	Uncertain. Indications of brittle deformation in Uppland.
4	900 to 400 million years	Far-field effects of: • The break-up of Rodinia with the formation of the ocean Iapetus and the continent Baltica. • The rotation and drift of Baltica northwards over the globe. • The destruction of Iapetus and the birth of the continent Laurussia (Caledonian orogeny). Geological activity in eastern Sweden includes: • Rifting, erosion and final establishment of the sub-Cambrian peneplain. • Marine transgression and deposition of sedimentary cover during the Early Palaeozoic. • Subsidence and formation of an Upper Silurian to Devonian, foreland sedimentary basin to the east of the Caledonian orogenic belt, related to the exhumation of deeper crustal levels and erosion within this belt.	Uncertain. Disturbance of sub-Cambrian peneplain in vicinity of the Forsmark site. Possible brittle deformation.
5	400 to 250 million years	Far-field effects of: • Hercynian-Variscan orogeny in central Europe and final assembly of the supercontinent Pangaea. • Rifting along the southern margin of the Fennoscandian Shield. Geological activity in eastern Sweden includes: • Some exhumation of deeper crustal levels and erosion. • Possible disturbance of the sub-Cambrian peneplain.	Uncertain. Disturbance of sub-Cambrian peneplain in vicinity of the Forsmark site. Possible brittle deformation.
6	250 million years to the start of the Quaternary period	Far-field effects of: • Rifting along the southern and western margins of the Fennoscandian Shield and marine transgression during the Cretaceous (especially the Late Cretaceous). • Alpine orogeny in southern Europe. • Opening and spreading of the North Atlantic Ocean. Geological activity in eastern Sweden includes: • Some exhumation of deeper crustal levels and erosion. • Possible disturbance of the sub-Cambrian peneplain. • Plate motion from 60–0 million years related to opening and spreading of the North Atlantic Ocean.	Uncertain. Disturbance of sub-Cambrian peneplain in vicinity of the Forsmark site. Possible brittle deformation.

3.1.1   Phase 1 – Period 1,910 to 1,870 (1,860) million years

Prior to 1,910 million years ago, there was considerable deposition of sediments in large parts of Sweden and Finland. During this time, the region was situated marginal to or outboard of a continental nucleus to the northeast (Figure 3-3) and the crustal development was at a very primitive stage.

From 1,910 to 1,760 million years, the shield area in eastern Sweden and in much of Finland was affected by major igneous activity (Figure 3-3). Three associations of igneous rock are present. These are referred to, in intrusive rock terms, as follows:

• Granitoid-Dioritoid-Gabbroid (GDG) rock association.

• Granite-Syenitoid-Dioritoid-Gabbroid (GSDG) rock association.

• Granite-Pegmatite (GP) rock association.

In any one region of the shield, the GSDG and GP rocks appear to have intruded after the GDG rocks and after the initiation of ductile deformation in the bedrock.

During the time frame from 1,910 to 1,870 million years, much of the continental crust in central-eastern Sweden, including the Forsmark site, was formed or initially reworked in connection with an early stage of the Svecokarelian orogeny. Evidence for crustal deformation and metamorphism prior to 1,860 million years ago is apparent.

The sedimentary rocks west of Stockholm (blue colour in Figure 3-1) form the oldest rocks in central-eastern Sweden. These volcanogenic, distal turbidites are older than 1,906 million years in age and pass stratigraphically upwards /Ambros, 1988; Stephens et al, 2000/ into volcanic and synvolcanic intrusive rocks that formed during the period 1,906 to 1,891 million years (Figure 3-3). Rhyolitic compositions dominate in western areas, dacitic and andesitic compositions to the east /Lundström, 1988; Allen et al, 1996/.

In the relatively well-preserved rocks northwest of Örebro (Figure 3-1), both main volcanic and waning volcanic stages have been documented /Allen et al, 1996/. Juvenile volcaniclastic rocks, lava domes and synvolcanic intrusions dominate the main volcanic stage. Reworked volcanic rocks, skarn deposits, carbonate rocks and mafic dykes or sills are prominent components during the waning stage of the volcanism. After 1,891 million years ago, deposition of post-volcanic, sedimentary rocks occurred. During the period 1,891 to 1,870 million years and possibly earlier, tonalites, granodiorites, granites and associated intermediate to mafic rocks (GDG rock association) intruded the supracrustal rocks (Figure 3-3).

The volcanic rocks in the area between Gävle and Örebro (Figure 3-1) host Fe-, Fe-Mn and Zn-Pb-Ag-(Cu-Au) mineral deposits. This region (Bergslagen and adjacent areas) is historically the most prosperous mining district in Sweden. During the 18th and 19th centuries, iron ore from over 3,000 workings in this area provided much of Sweden's wealth. The important base-metal deposits are associated with skarn deposits and carbonate rocks that were deposited during the waning stage of the volcanic activity. Mineralisations hosted by volcanic rocks are a significant bedrock component close to the Forsmark site /Lindroos et al, 2004/.

All rocks older than 1,870 million years in age are affected by ductile deformation and metamorphism with the development of a planar grain-shape fabric, including a gneissosity in higher-grade rocks. The intrusion-deformation relationships in the area south of Örebro indicate that deformation and metamorphism had initiated prior to 1,860 million years ago /Wikström, 1996; Wikström and Karis, 1998/.

The tectonic setting has been coupled to subduction of oceanic lithosphere and continental back-arc basin evolution similar to that observed in, for example, New Zealand at the present day /Allen et al, 1996/. A comparison with the Finnish segment of the Fennoscandian Shield suggests important, dextral transpressive deformation. The transpression was taken up in the Finnish segment by dextral displacement along ductile high-strain zones with NW strike, combined with shortening across an older continental margin which also trends NW (thrusting to the NE). Oblique collision against the older continental margin with a NS to NNW-SSE crustal movement direction is inferred (Figure 3-3).
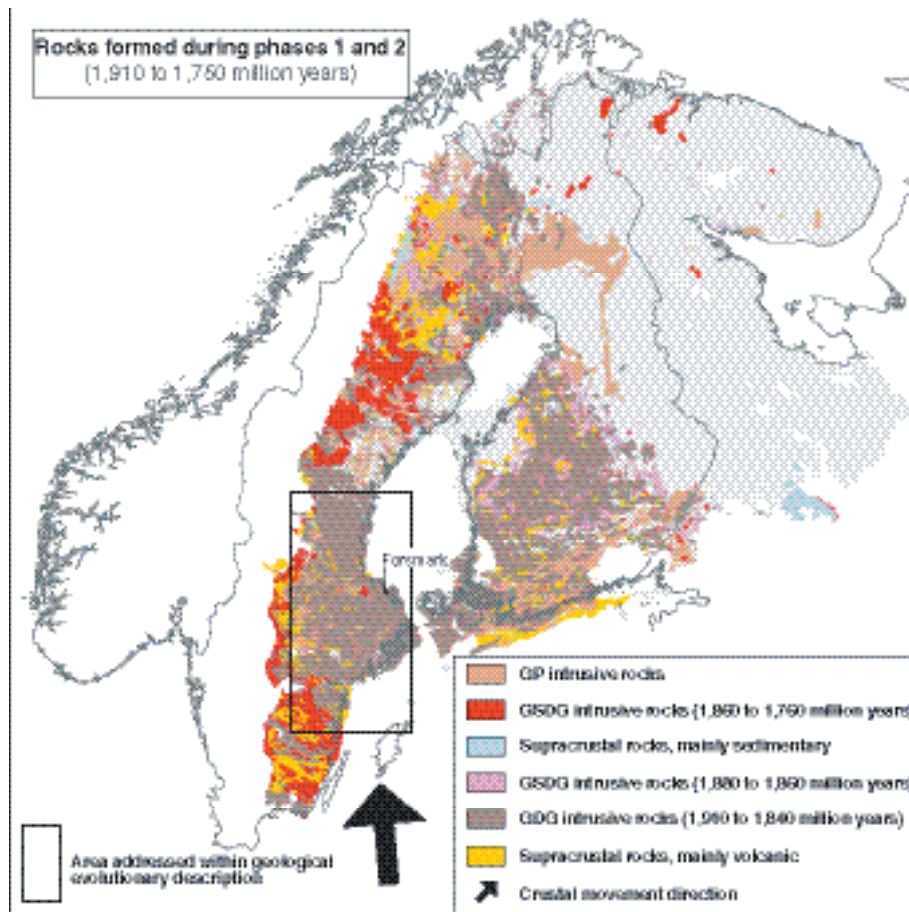
Figure 3-3. *Rocks formed during phases 1 and 2 (1,910 to 1,750 million years). All the bedrock shown in grey had formed prior to 1,910 million years ago. The figure is based on the database presented by /Koistinen et al, 2001/.*

3.1.2 Phase 2 – Period 1,870 to 1,750 million years

During the period 1,870 to 1,750 million years ago, there was considerable igneous activity, sedimentation and crustal deformation in central-eastern Sweden (Figure 3-3). Some of the intrusive rocks in the Forsmark area are inferred to have formed during this phase. These geological events were predominantly associated with reworking of older crust, in connection with the later stage of the Svecokarelian orogeny. Additions of newly formed crust also occurred.

North of Mora and Gävle (Figure 3-1), sedimentary rocks including quartzites, that are older than c 1,870 million years, pass stratigraphically upwards into a bimodal volcanic sequence of rhyolites and basalts, and younger sedimentary rocks /Lundqvist, 1968; Delin and Persson, 1999/. The volcanic rocks are 1,870 to 1,860 million years in age. During the period 1,870 to 1,840 million years, rocks of the GDG association intruded these supracrustal rocks (Figure 3-3).

By contrast, in especially the southern and western parts of central-eastern Sweden, there was extensive intrusion of granites, quartz monzonites, monzonites and associated intermediate to mafic rocks (GSDG rock association) during the periods 1,860 to 1,840 and 1,825 to 1,760 million years (Figure 3-3). Supracrustal rocks, that belong to the younger of these suites, are also present. Several granites that belong to the GP rock association, with ages around 1,800 million years, show high U and Th contents. They are also associated with W-Mo mineralisation.

All the rocks that were formed during 1,870 to 1,840 million years display ductile deformation and metamorphism with development of the following features:

• A tectonic foliation.

• Regional-scale folding which deforms earlier planar fabrics.

- An intense, linear grain-shape fabric.

- High-strain zones that assisted the exhumation of deeper crustal levels and erosion.

Gradual waning of the ductile deformation under lower-grade metamorphic conditions and at shallower crustal depths occurred after c 1,800 million years.

The geodynamic régime involved dextral transpressive deformation. This deformation was absorbed by major folding between ductile high-strain zones as well as dextral displacement along ductile high-strain zones with NW strike, combined with shortening in a NE direction across the zones (Figure 3-1) /Stephens and Wahlgren, 1996; Högdahl, 2000; Beunk and Page, 2001/. Continued oblique collision against the older continental margin to the northeast, with a NS to NNW-SSE crustal movement direction, as indicated for phase 1, is inferred.

3.1.3 Phase 3 – Period 1,750 to 900 million years

After 1,750 million years ago, the focus of igneous activity, sedimentation and crustal deformation shifted progressively westwards and southwards, away from the central-eastern part of Sweden (Figure 3-4 and Figure 3-5). The geological events in these areas are an expression of continued crustal growth and crustal reworking of the Fennoscandian Shield, in connection with and following the Gothian (1,700–1,560 million years), Hallandian (1,460–1,420 million years and possibly later) and Sveconorwegian (1,100–900 million years) orogenies. By c 900 million years ago, our planet had probably passed through a critical milestone, with the assembly of the major supercontinent Rodinia.
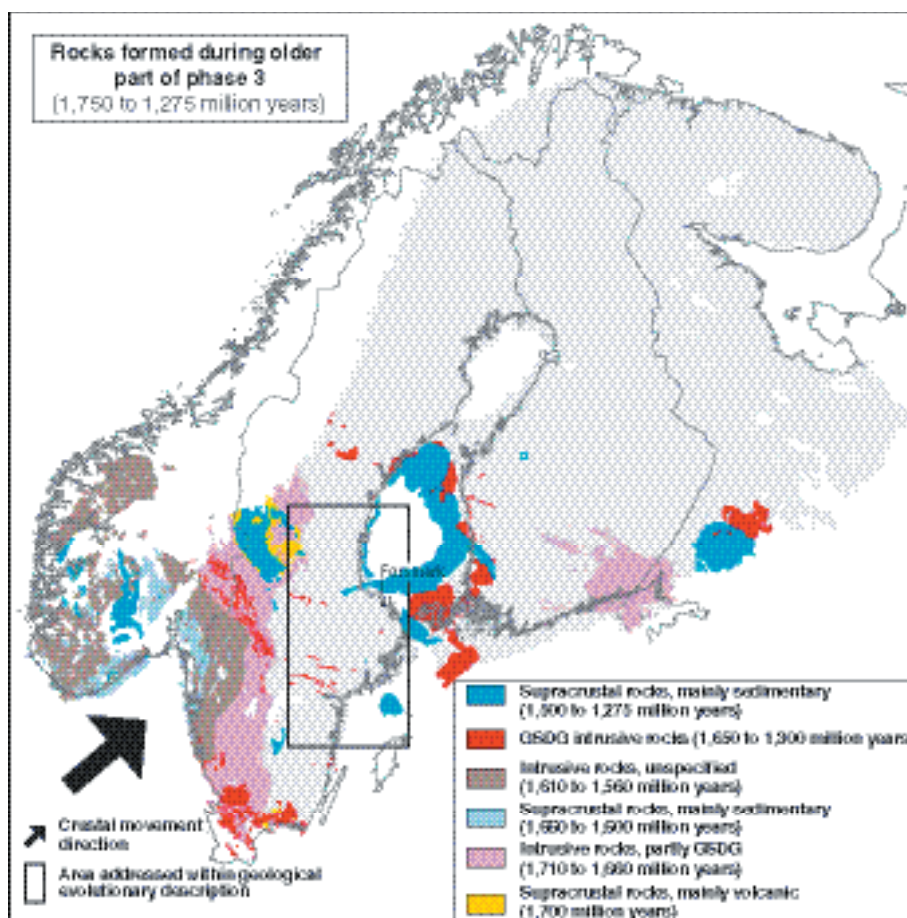
Figure 3-4. *Rocks formed during older part of phase 3 (1,750 to 1,275 million years). All the bedrock shown in grey had formed prior to 1,750 million years ago. The figure is based on the database presented by /Koistinen et al, 2001/.*
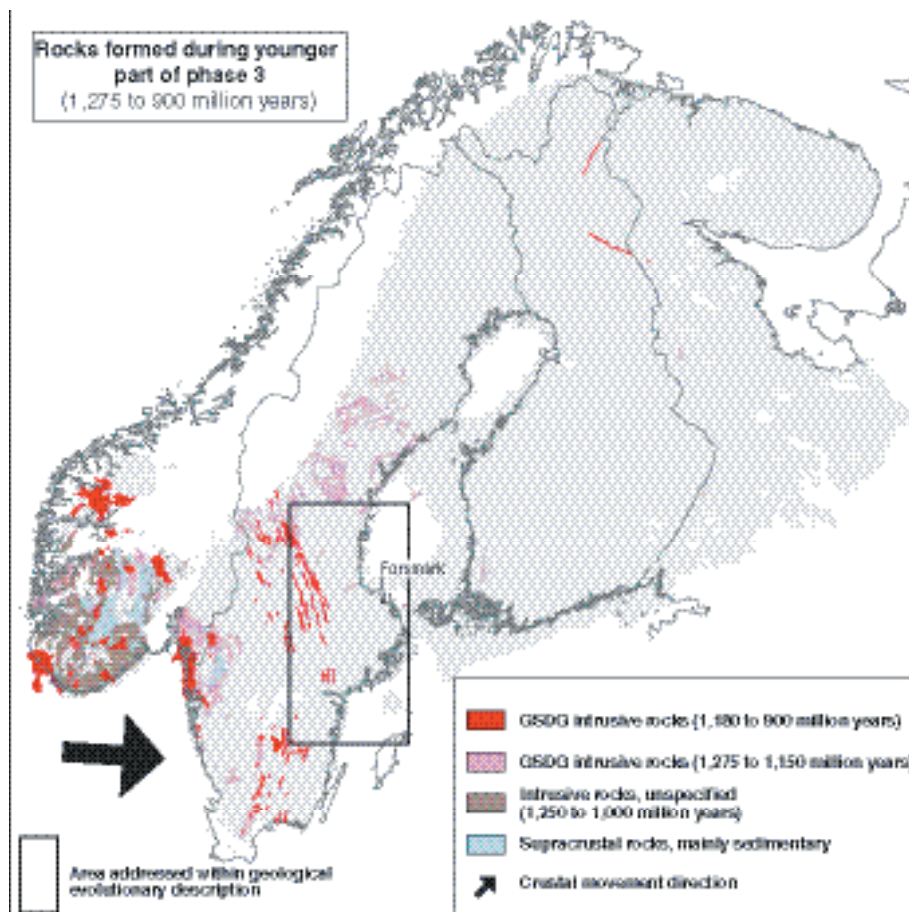
Figure 3-5. *Rocks formed during younger part of phase 3 (1,275 to 900 million years). All the bedrock shown in grey had formed prior to 1,275 million years ago. The figure is based on the database presented by /Koistinen et al, 2001/.*

The far-field effects of the important geological events in the western and southern parts of the Fennoscandian Shield are present in the areas to the east, including the central-eastern part of Sweden. Igneous activity, faulting and sedimentation witness the continued crustal and, in particular, thermal disturbance in the eastern areas (Figure 3-4 and Figure 3-5). However, the effects in the Forsmark area are not well understood.

Within the period 1,710 to 1,660 million years, GSDG igneous activity and sedimentation occurred in the westernmost parts of central-eastern Sweden (Figure 3-4). North of Mora (Figure 3-1), a ductile high-strain zone with NNW strike was also active. This deformation zone shows dextral displacement along the zone, together with shortening across the zone /Bergman and Sjöström, 1994/. The transpressive deformation can be explained in terms of an oblique collision with a NE-SW crustal movement direction (Figure 3-4).

During the period 1,560 to 1,460 million years, dykes and several isolated bodies of minor intrusive rocks that belong to the GSDG suite injected the bedrock in central-eastern Sweden. These include:

• Mafic dykes with a WNW strike (Figure 3-4) and an age of c 1,560 million years.

• Intrusions of rapakivi granite, quartz syenite and dykes with an ENE strike. These rocks have yielded ages in the time span 1,500 to 1,460 million years.

More widespread volumes of intrusive rocks, including rapakivi granites, with ages in the range 1,580 to 1,500 million years are present north of Sundsvall, on Åland and in southwestern Finland (Figure 3-4). Furthermore, an alkaline intrusive rock that is exposed at Norra Kärr, east of Vättern, has yielded an age of 1,545 million years. A similar alkaline intrusive body at Almunge, between

50

Stockholm and Forsmark, may also have intruded during the early part of the Mesoproterozoic. However, the age of this intrusion is not known.

Local subsidence and formation of sedimentary basins with extensive deposition of sandstones also occurred during the period 1,500 to 1,275 million years (Figure 3-4). Furthermore, U-Pb dating of pitchblende in quartz-, calcite- and chlorite-filled fractures and Rb-Sr dating of epidote-filled fractures have yielded ages between c 1,590 and 1,450 million years /Welin, 1964; Wickman et al, 1983/. The pitchblende occurs, together with hematite and various sulphides, along fractures that strike, for example, WNW or NW. This age-dating work has been carried out at several localities in Uppland. The dates indicate the development of brittle fracturing of the bedrock during the early part of the Mesoproterozoic, in areas close to Forsmark.

Much of the sedimentation and igneous activity in the Fennoscandian Shield during the period 1,275 to 900 million years took place in southwestern Sweden and southern Norway (Figure 3-5). Nevertheless, the occurrence of mafic sills and dykes, with ages of 1,275 million years and 1,000 to 900 million years, provide evidence for significant igneous activity and the development of thermal anomalies in central-eastern Sweden during this time period (Figure 3-5). Subsidence related to the development of a Sveconorwegian foreland basin in southeastern Sweden has also been proposed /Tullborg et al, 1996; Larson et al, 1999/.

Ductile deformation and metamorphism affected southwestern Sweden and southern Norway during the period 1,100 to 900 million years (Sveconorwegian orogeny). Deformation along a major, Sveconorwegian high-strain zone with NW to NS strike is sinistral transpressive in character /Stephens et al, 1996/. Extensional ductile deformation has also been identified along this zone /Berglund, 1997/. West of Örebro, in the frontal part of the Sveconorwegian orogen, ductile-brittle high-strain zones with NE strike show dextral transpressive strain /Wahlgren et al, 1994/. These kinematic studies suggest a WNW-ENE to EW crustal movement direction during this important collisional event (Figure 3-5).

Brittle deformation with the same kinematics is potentially of major significance in more easterly areas, including the Forsmark area. Rb-Sr dating of prehnite- and calcite-filled fractures in Uppland have yielded ages between 1,250 and 1,100 million years. These data confirm the development of brittle fracturing of the bedrock during the later part of the Mesoproterozoic, in areas close to Forsmark.

3.1.4   Phase 4 – Period 900 to 400 million years

Following the assembly of Rodinia, the Fennoscandian shield was situated at high southerly latitudes. The following geological events dominated during the period 900 to 400 million years:

- The break-up of Rodinia with the formation of the ocean Iapetus and the continent Baltica, c 600 million years ago.

- The rotation and drift of Baltica northwards over the globe.

- The destruction of Iapetus and the birth of the continent Laurussia during the Caledonian orogeny that took place 510–400 million years ago.

Much of the evidence for this geodynamic development occurs in the bedrock exposed in the Caledonian orogenic belt (Figure 3-6) and only the far-field effects of these tectonic events are present in the eastern part of Sweden. The effects at the Forsmark site are poorly understood.

In the Vättern area (Figure 3-1), sedimentation in connection with aborted continental rifting occurred during the period 800–700 million years before present. Ultimate continental break-up and formation of the ocean Iapetus and the new continent Baltica occurred to the northwest, c 600 million years ago. An isolated alkaline intrusive body, with an age around 610 to 530 million years, intruded the Fennoscandian Shield at Alnön in the Sundsvall area.

Following rifting, erosion and establishment of the sub-Cambrian peneplain, a major marine transgression occurred during the early part of the Cambrian, 543 to 520 million years ago. This transgression was accompanied by deposition of mature sandstone, siltstone and shale. Deposition

of shale and limestone followed during the later part of the Cambrian, during the Ordovician and during the Silurian, 520 to 420 million years ago. All these sediments were deposited over large areas on top of the deeply eroded shield in a stable, continental shelf environment. However, they are only preserved today in offshore areas and in isolated, fault-controlled outliers on land (Figure 3-6). The calcareous character of the moraine at Forsmark is related to the widespread occurrence of Ordovician limestone to the north of the Forsmark area (Figure 3-6).

Deposition of the sediments on the continental shelf occurred at the same time as sedimentation, igneous activity and crustal deformation dominated areas to the northwest, along the margin of the continent Baltica. This Caledonian orogenic activity was related to continent-arc and continent-continent collisions with shortening in a WNW-ENE direction (Figure 3-6) and major thrusting to the east. Extensional collapse and sinistral strike-slip deformation followed in the western parts of the orogeny. Subsidence related to the development of a foreland basin has been inferred to be present in the areas that lie east of the Caledonian orogenic belt /Tullborg et al, 1995, 1996; Larson et al, 1999/.

The faults that bound the various Lower Palaeozoic outliers on land strike approximately NS and EW. They disturb both the sub-Cambrian peneplain and the Lower Palaeozoic rocks, and were active during or after the Caledonian orogeny (or both). Disturbance of the sub-Cambrian peneplain has been noted in northern Uppland /Lidmar-Bergström, 1994; Bergman et al, 1999/ and faulting that took place during or after the Caledonian orogeny (or both) is potentially of major significance at the Forsmark site.
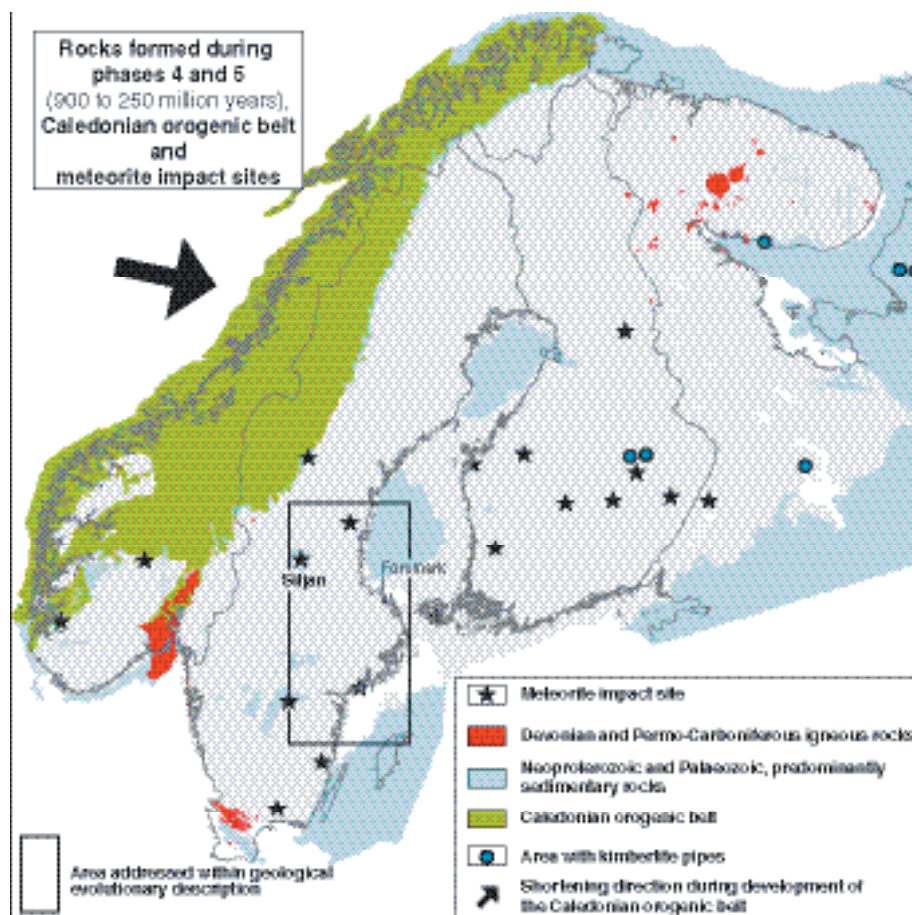
Figure 3-6. Rocks formed during phases 4 and 5 (900 to 250 million years). All the bedrock shown in grey had formed prior to 900 million years ago. The figure is based on the database presented by /Koistinen et al, 2001/.

3.1.5 Phase 5 – Period 400 to 250 million years

There is very poor control concerning the lithological and structural developments in central-eastern Sweden, including the Forsmark site, during this period. During the late Devonian and Carbonifereous (360 to 295 million years), the focus of sedimentation, igneous activity and crustal deformation had shifted southwards to the central part of Europe, in connection with the Hercynian-Variscan orogeny. This orogenic event resulted in the final assembly of the supercontinent Pangaea.

During the late Carboniferous and Permian (295 to 275 million years), extensional deformation and associated volcanic and intrusive activity prevailed in the Oslo graben, Norway (Figure 3-6). During the same time period, dextral transtensional deformation and intrusion of mafic dykes and sills occurred along the Sorgenfrei-Tornquist Zone, in the southernmost part of Sweden (Figure 3-6). Furthermore, an isolated alkaline body intruded the Fennoscandian Shield near Särna, northwest of Mora, at the same time as the igneous activity took place in the Oslo graben to the southwest.

Far-field effects of the Hercynian-Variscan orogeny and, more confidently, the late Carboniferous and Permian rifting can be estimated in central-eastern Sweden. The disturbances of the sub-Cambrian peneplain may be related to faulting during this phase. Permian faulting, at least in the area around the lake Vättern, has been proposed /Månsson, 1996/.

Recent work has suggested the presence of meteorite impact structures in the Fennoscandian Shield and its cover sedimentary rocks /Wickman, 1988; Henkel and Pesonen, 1992/. A rounded topographic, geological or geophysical feature has often triggered such speculations. By far the best-documented structure, with a diameter of c 50 km, occurs in the Siljan area, close to Mora in central-eastern Sweden (Figure 3-6). This structure formed c 360 million years ago, during the late Devonian or early Carboniferous periods.

3.1.6 Phase 6 – Period 250 million years to the Quaternary period

As for phase 5, there is very poor control concerning the geological developments in the central-eastern part of Sweden during the period 250 million years up to the Quaternary, i.e. during the Mesozoic era and the Tertiary part of the Cenozoic era. Sedimentary (and, locally, volcanic) rocks are only preserved in the southernmost part of Sweden and in offshore areas surrounding Norden and Russia (Figure 3-7). However, it is possible that some of the brittle structures at, for example, the Forsmark site are coupled to tectonic events that occurred around the margins of the shield during this period.

During the early part of the Mesozoic, differential subsidence controlled by transtensional defor-mation occurred along the Sorgenfrei-Tornquist Zone in southernmost Sweden /Erlström and Sivhed, 2001/. Volcanic activity was also prevalent in this area during the Jurassic and Cretaceous (Figure 3-7). The tectonic environment radically changed during the later part of the Cretaceous and the earliest part of the Tertiary (95 to 60 million years), when a marine transgression and inversion tectonics with dextral transpressional deformation along the Sorgenfrei-Tornquist Zone took place /Erlström and Sivhed, 2001/. The geological events during the later part of the Cretaceous and into the Tertiary correspond temporally with the initiation of the Alpine orogeny in southern Europe and the collision between Africa and Eurasia. A maximum principal stress (σ_1) in a NNE-SSW direction has been inferred during this period (Figure 3-7) /Muir Wood, 1995/.

From 60 million years and onwards, the North Atlantic Ocean started to open and to spread. During this time, plate movements associated with spreading of the North Atlantic Ocean appear to have dominated the geodynamics of northern Europe. After c 12 million years, a maximum principal stress (σ_1) in a NW-SE direction has prevailed in this region (Figure 3-7) /Muir Wood, 1995/.

It is probable that there were far-field effects of the rifting, opening and spreading of the North Atlantic Ocean as well as Alpine collisional tectonics in the Fennoscandian Shield. At least some of the documented disturbances of the sub-Cambrian peneplain may be related to faulting during this period. The broad geomorphological framework of Fennoscandia, with high mountains to the west, steep slopes down to the Norwegian Sea and gentle, southeasterly slopes to the east, is considered to have been established during Tertiary uplift /Holtedahl, 1953; Lidmar-Bergström, 1996/. It is possible that there is a relationship between this broad geomorphological framework and the tectonic developments in southern Europe and the North Atlantic region during this period.

Figure 3-7. Rocks formed during phase 6 (250 million years to the Quaternary period). All the bedrock shown in grey had formed prior to 250 million years ago. The figure is based on the database presented by /Koistinen et al, 2001/.

3.2 Geological evolution during the Quaternary period

A model for the regional geological evolution with focus on north-eastern Uppland during the Quaternary period is presented for the main climatic stages of the late Quaternary. The model has utilised the compilations made in connection with the Östhammar feasibility study /Bergman et al, 1996/ and information in the 3rd edition of the National Atlas of Sweden /Fredén, 2002/ together with the references given in the text in the remainder of this section.

The Quaternary Period is the youngest in the earth's history, characterised by alternating *glacial* and *interglacial* stages with further subdivision into cold phases, *stadials* and warm phases, *interstadials*. A combination of climatic oscillations with large amplitude, together with the intensity of the colder periods, is characteristic of the Quaternary Period. Oxygen isotope records in deep-sea sediment suggest as many as fifty glacial/interglacial cycles during the Quaternary /Shackelton et al, 1990/. The duration of the Quaternary has been a subject of debate within the geological community. The Tertiary/Quaternary transition was determined to 1.65 million years at the Geological Congress in London, 1948. More recent research, however, suggests an older date for the start of the Quaternary and a consensus is possibly developing for a longer chronology for the Quaternary, starting at the Matuyama/Gauss palaeomagnetic boundary c 2.4 million years before present /e.g. Ŝibrava, 1992; Shackelton, 1997/.

The Quaternary Period is subdivided into two epochs: the Pleistocene and the Holocene, Table 3-2. The major part of the Quaternary Period belongs to the Pleistocene, whereas the Holocene started during the latest deglaciation, c 11,000 years ago /Fredén, 2002/. The chronology used in Quaternary studies is often based on various dating methods and correlations between lithological units.

Table 3-2. The geological timescale showing the subdivision of the late Quaternary period with climatic stages from /Fredén, 2002/. The ages are approximate and given in calendar years before present From: Sveriges Nationalatlas, www.sna.se.
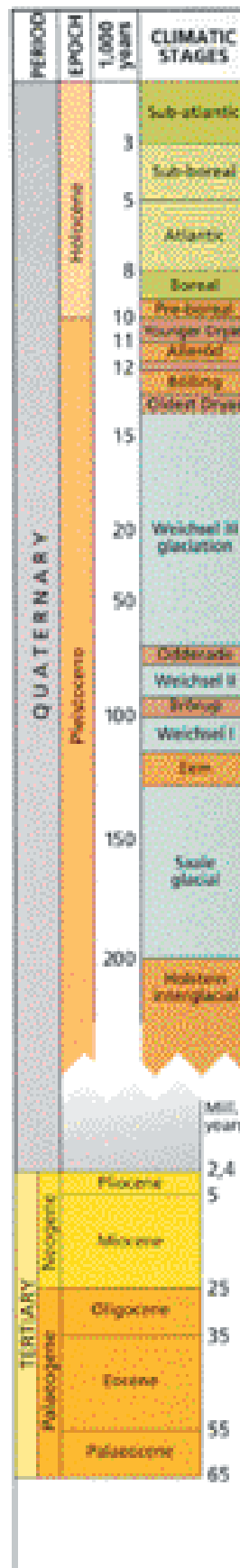
Terrestrial data from Sweden may be correlated with the Marine Oxygen Stages from deep-sea sediment or Greenland ice cores. However, the absolute ages are sometimes uncertain, because of doubts as to the appropriate stage which to correlate. This is especially valid for dating of events and lithological units originating from phases older than the latest glacial-interglacial cycle. The ages given in this section are mainly based on the chronology in /Fredén, 2002/ stated as calendar years before present.

The general concept of the impact of glacial erosion has earlier been that each glacial cycle erodes the existing unconsolidated deposits and gives rise to a new generation of glacial deposits. For areas where the inland ice has been cold based, this opinion has partly been revised during the last decades. In northern Sweden, for example, landforms and ventifacts from phases older than the latest glaciation have been preserved, although the area has been subject to subsequent glaciations /e.g. Hättestrand and Stroeven, 2002; Lagerbäck, 1988a,b; Lagerbäck and Robertsson, 1988/. Also the presence of deep-weathered bedrock surfaces within glaciated areas has been interpreted to reflect a non-erosive glacial regime /e.g. Lundqvist, 1985; Lidmar-Bergström et al, 1997/.

The alternating glacial/interglacial periods resulted in major palaeogeographical variations due to glacioisostatic movements and eustatic sea level variations. During the glacial stages, large water volumes were stored in the ice caps. Hence, the global sea level has been at considerably lower levels than the present. During the latest glaciation, the global sea level was in the order of 120 m lower than the present /Fairbanks, 1989/ and the glacio-isostatic effect pressed down Fennoscandia with as much as c 800 m /Fredén, 2002/.

3.2.1   The Pleistocene

The preserved geological information from the early Quaternary in Sweden is very fragmentary. The oldest organic deposits, dated to the *Holsteinian interglacial* (c 230,000 years ago) are described from the Alnarp depression in Skåne and at Öje in western Dalarna. Fossils show that the forests contained coniferous trees such as larch and Serbian spruce. The climate was oceanic, i.e. warm and moist with small annual variation. The glacial till underlying the Holsteinian deposits is the oldest known Quaternary deposit in Sweden, possibly originating from the Elsterian Glaciation (>250,000 years ago). The Elsterian ice cap at its maximum extension is estimated to have covered all of Fennoscandia, reaching approximately to southern Poland.

The glacial expansion that followed, the Saale, lasted for approximately 70,000 years and reached approximately as far south in Europe as the Elsterian. The next interglacial, the *Eemian* occured between c 130,000 and 115,000 years ago. Eemian deposits are known from several widely spread places in Sweden. The climate was periodically milder than it has been since the last deglaciation with e.g. forests including hardwood further north than during the subsequent interglacial. The history of the Baltic basin during the Eemian is described from sediment at Bollnäs and in the Dellen region, Nyköping and Skulla in central Uppland. The sediment at Bollnäs and in the Dellen region contains evidence for brackish water conditions at altitudes of 50–100 masl[1] /Robertsson et al, 1997/. Since the major part of north-eastern Uppland is situated at lower altitudes, the region was at least periodically situated beneath the surface of the Eemian Sea (Figure 3-8). The extent of and environment in the Eemian Sea has been described from Finland, where detailed studies have discovered that the marine Eemian Sea was preceded by a lacustrine stage, comparable with the Ancylus Lake stage of the Holocene Baltic Basin /Grönlund, 1991 a,b/.

At c 115,000 years ago, global cooling initiated the latest glaciation, the Weichselian. The Weichselian glaciation is subdivided into three colder phases, *stadials*, interrupted by milder phases, *interstadials*. The interstadials, however, either did not reach full interglacial climatic conditions or lasted for too short time for forest vegetation to develop. The interstadials are instead characterised by tundra climate and shrub vegetation. The information on the extension of the inland ice during the first Weichselian stadial is sparse. However, thick till beds are documented in Norrland and northernmost Finland, and are interpreted to originate from this stage. The extension of the inland ice is estimated to have reached approximately to Dalarna and Hälsingland with tundra climate in north-eastern Uppland (Figure 3-8).

---

[1] masl = metres above sea level.

The Eemian Interglacial
c. 130 000–115 000 years B.P.

The first Weichselian Stadial
c. 115 000–100 000 years B.P.

The Jämtland/Brörup Interstadial
c. 100 000–90 000 years B.P.

The second Weichselian Stadial
c. 90 000–80 000 years B.P.

The Tärendö/Odderade Interstadial
c. 80 000–70 000 years B.P.

The start of the Weichselian Glaciation's main phase, c. 50 000 years B.P.

Borders
Shore line
National border

Vegetation
Glacier
Lake
Ocean
Tundra
Birch forest
Coniferous forest
Temperate forest of broad-leaf trees

0 200 400 800 1200 km

Figure 3-8. *Palaeogeographical maps showing the distribution land/sea together with vegetation zones during the Eemian Interglacial and the main climatic stages of the Weichselian glaciation /Fredén, 2002/. Note that the Baltic Basin was marine during the Eemian and lacustrine during the early and middle Weichselian.*

At c 100,000–90,000 years ago, the *Jämtland interstadial*, correlated to the continental Brörup interstadial and Finnish Peräpohjola took place (Figure 3-8). The climate at that time was cooler than the present with tundra conditions in northernmost Sweden and coniferous forests dominating the vegetation in north-eastern Uppland. The presence of continental ice caps resulted in a global sea level lower than the present with a lacustrine Baltic basin.

The information regarding the conditions in Sweden during the second Weichselian stadial (c 90,000–80,000 years ago) is also restricted. A consistent feature of the till stratigraphy in central and northern Sweden, however, is the occurrence of a characteristic dark, bluish grey clayey till, often covered by a younger till /Björnbom, 1979/. The clayey till has been interpreted to represent the stadial between the Jämtland and the Tärendö interstadials, the second Weichselian stadial. Based on the spatial distribution of the till, traced to southern central Sweden, the ice cap is estimated to have reached approximately south of Lake Mälaren (Figure 3-8). In north-eastern Uppland, several occurrences of a hard clayey till have been described /e.g. Persson, 1992/. The exact age of the lithological unit is, however, still a subject to research.

At c 80 000–70 000, the *Tärendö* interstadial, correlated to the Odderade on the continent, took place (Figure 3-8). The climate during the Tärendö interstadial is known to have been very cold /Lagerbäck, 1988a/. In northern Sweden, outcrops and boulders were polished by snow crystals, suggesting temperatures of c –40°C. North-eastern Uppland was probably covered by sparse, tundra-like birch forest and a lacustrine Baltic basin with a lake level below the present, leaving north-eastern Uppland above shoreline.

The main phase of the Weichselian glaciation started c 70,000 years ago. Compared to the Saale and Elsterian glacial maximum, the Weichselian did not reach as far south. The maximum extension of the inland ice was around 20,000 years ago and reached approximately northern Germany and central Denmark, covering all of Sweden and the Baltic basin. In northern Europe, several slightly warmer interstadials within this stage have been recorded. The west-coast of Norway, for example, was probably ice free at two of these interstadials. There is, however, no clear evidence of interstadial conditions from central Sweden during the main Weichselian glaciation, although this is a topic for discussion.

The major part of the glacial till in north eastern Uppland is generally considered to originate from the latest glacial stage and the subsequent deglaciation. The oldest glacial striae recorded in north-eastern Uppland are orientated from the north-west, a younger system from the north-north west and the youngest striae are approximately from the north /Persson, 1992/. This suggests a clockwise shift in the ice flow direction during the deglaciation. Glacial till is the dominating unconsolidated Quaternary deposit in the region. The grain size distribution of the till reflects e.g. the variation in the composition of the bedrock material. Several till types are observed in north-eastern Uppland /Persson, 1992/. Sandy till, dominated by Precambrian bedrock material, has the largest areal extent. Along the Uppland coast, however, a clayey till is frequently exposed. The thickness of the till is generally in the order of 1–5 m. In areas with continuous till cover, the thickness may be considerably greater; 8–15 m is not unusual. Morphologic features, such as moraine ridges, are rare in the region. Instead, the till fills depressions in the bedrock, leaving a flat upper surface. Fabric analyses generally indicate that the major part of the till cover was deposited from an ice movement that predominated during the late phase of the ice recession. Sections with more than one till bed, i.e. a complex till stratigraphy, are documented at several localities in northern eastern Uppland /Persson, 1992/. The observations, however, give no evidence for a general pattern in the till stratigraphy. At some localities, a sandy till covers a clayey one, whereas at other localities, the reverse is recorded. An oscillating ice front during the retreat may cause thrust faults that may give rise to reversals in the till stratigraphy.

The latest deglaciation took place during the Preboreal climatic stage, c 11,000 years ago /Fredén, 2002; Persson, 1992; Strömberg, 1989/. According to extrapolations from clay varve investigations from central and northern Uppland and Åland, the ice recession had a rate of c 300–350 m per year in northern Uppland. The ice at the front was in the order of 300 m thick, melting into the open water of the Yoldia Sea stage of the Baltic. Plastic deformations in glacial silt and clay have been described from the Gävle area /Eriksson and Lidén, 1988; Grånäs, 1985; Sandegren et al, 1939; Sandegren and Asklund, 1948; Strömberg, 1989/. The deformational structures are interpreted to be caused by glaciotectonic processes, which possibly could indicate a re-advance of the ice sheet during the deglaciation.

3.2.2   The Holocene

A major crustal phenomenon that has affected and continues to affect northern Europe, following the latest melting of inland ice, is the interplay between isostatic recovery on the one hand and eustatic sea level variations on the other. In northern Sweden, isostatsy has been the dominating component, resulting in regressive shoreline movement since deglaciation /e.g. Lundqvist, 1963; Miller and Robertsson, 1979; Renberg and Segerström, 1981/. Along the southern part of the Swedish east coast, the isostatic component was less intense and declined earlier during the Holocene, resulting in a more complex shore displacement with alternating transgressive and regressive phases /e.g. Berglund, 1971; Fromm, 1976; Risberg, 1991/. In north-eastern Uppland, the highest Holocene coastline was developed during the Yoldia Sea stage of the Baltic. The highest shoreline was situated c 80 km to the west of the present shoreline location, presently uplifted to c 190 masl.

The Yoldia Sea stage of the Baltic is subdivided into an initial lacustrine phase, a short brackish phase followed by a final lacustrine phase (Table 3-3). The brackish water phase of the Yoldia Sea lasted c 120 years, as recorded e.g. by ostracods and foraminifers in varved clay from central Sweden /Wastegård et al, 1995; Schoning, 2001/. Marine water entered the Baltic basin through the topographic lowland in Närke, known as the Närke Strait. An anticlockwise circulation brought the saline water southward along the Swedish east coast /Heinsalu, 2001/. The short duration of the brackish phase together with freshwater supply from the melting ice probably resulted in only minor, if any, influence of saline water in north-eastern Uppland during this stage.

The next Baltic stage, the Ancylus Lake, was lacustrine with initial outlet through the Lake Vänern basin /Björck, 1995/. The isostatic uplift was faster in the north, resulting in the Ancylus transgression in regions situated south of the outlet /e.g. Svensson, 1989/. The northern limit of the Ancylus transgression along the Swedish east coast is recorded in eastern Södermanland /Hedenström and Risberg, 1999/. Thus, north-eastern Uppland was situated in a region with regressive shore displacement also during this stage.

Ongoing eustatic sea level rise, in combination with reduced isostatic rebound in the south enabled marine water to enter the Baltic basin through the Danish straits, marking the onset of the Litorina Sea *sensu lato*. In south-eastern Uppland, an initial stage when the salinity was stable and low lasted for approximately 1,000 years before the onset of the brackish water Litorina *sensu stricto* /Hedenström, 2001/. Within north-eastern Uppland, the first land areas emerged c 6,500 years ago /Robertsson and Persson, 1989; Bergström, 2001; Hedenström and Risberg, 2003/ i.e. during the most saline phase of the Litorina Sea correlated with the Holocene climatic optimum during the Atlantic climatic stage (Table 3-3) /Westman et al, 1999/. Along the southern shores of the Baltic, transgressive sea levels during the Litorina Sea stage have been documented with a 0-isobase recorded in south eastern Uppland /Hedenström, 2001/. In the northern part of Uppland, shoreline displacement studies /Robertsson and Persson, 1989; Bergström, 2001; Hedenström and Risberg, 2003/ have documented a continuous regression during the last c 6,500 years. At present, the land in north eastern Uppland is rising with respect to the sea level at the rate of c 60 cm per 100 years /Ekman, 1996/.

The major part of the Forsmark regional model area was still covered by water until c 2,500 years ago (Figure 3-9a). A few scattered islands, situated close to the church of Forsmark, are the first local land areas to emerge from the Baltic, c 2,500 years ago. The surface of the islands was covered by sandy till and exposed bedrock, similar to the present situation on the islands within the regional model area. Palaeo-ecological studies from the Florarna mire complex, situated c 30 km west of the regional model area, indicated a local humid and cold climate at approximately this time /Ingmar, 1963/.

At 1,500 years ago (Figure 3-9b), the Baltic still covered the Forsmark candidate area. In the more elevated areas in the south-western part of the map, land-areas presently covered by peat had emerged. At that time, these sedimentary basins were newly isolated from the Baltic and most probably a number of very small and shallow freshwater lakes/ponds existed. At the same time

Table 3-3. Summary of the stages of the Baltic Sea, years before present /Fredén, 2002; Westman et al, 1999/.

Baltic stage	Calender year BP	Salinity	Environment in Forsmark
Baltic Ice Lake *not applicable in Forsmark*	15,000–11,550 *not applicable in Forsmark*	Glacio-lacustrine *not applicable in Forsmark*	Covered by inland ice.
Yoldia Sea	11,500–10,800	Lacustrine/Brackish /Lacustrine	Deglaciation, regressive shoreline from c 190 – c 170 masl. Minor influence of brackish water.
Ancylus Lake	10,800–9,500	Lacustrine	Regressive shoreline from c 170–75 masl.
Litorina Sea *sensu lato*	9,500–present	Brackish	Regressive shoreline from 75–0 masl. Most saline period 6,500–5,000 calendar years BP. Present Baltic Sea during approximately the last 2000 years.

the isolation process of the larger Lake Bruksdammen started. A grave mound, the oldest known archaeological site in the area, is located on the crest of an island situated c 1 km east of the church of Forsmark. At 500 years ago (Figure 3-9c), the major part of the candidate area had emerged and several freshwater lakes were isolated from the Baltic, e.g. Eckarfjärden, Gällsboträsket and Djupträsket. The Börstil esker and Storskäret formed islands exposed to the sea. The present distribution of Quaternary deposits in the Forsmark area is displayed in the last picture (Figure 3-9d). Glacial till covers the major part of the area together with organic deposits, especially in the south-western part of the map. Lake Bolundsfjärden is still in contact with the Baltic whereas Lake Fiskarfjärden just recently has been isolated.
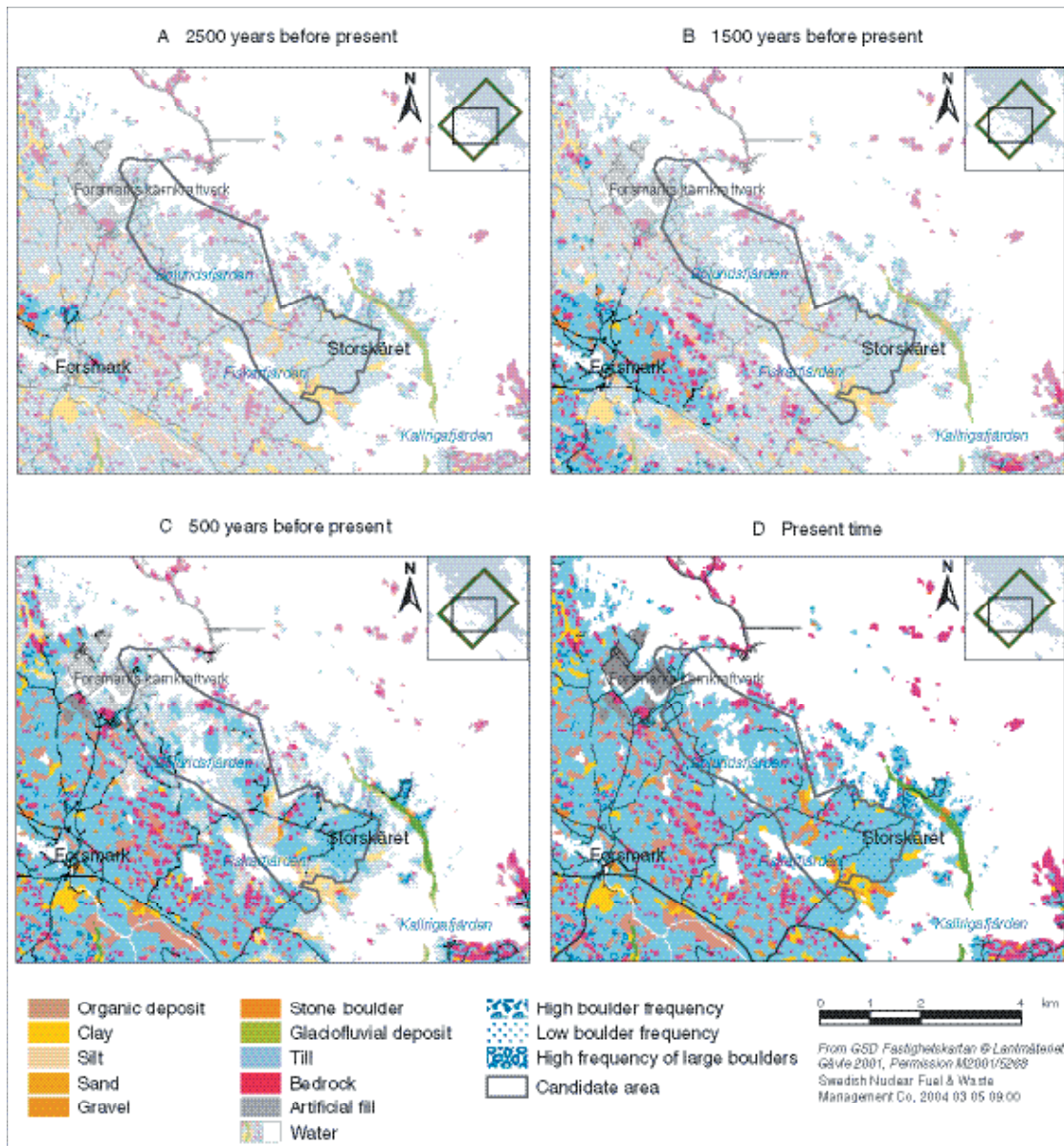
Figure 3-9a–d. *A series of palaeogeographical maps showing the distribution land/sea at 2,500, 1,500 and 500 and 0 calendar years before present. The land areas show the distribution of the unconsolidated Quaternary deposits from /Persson, 1985, 1986/. The shore displacement curve used derives from /Påsse, 1997, 2001/ and the ages are given in calendar years before present. The modelled shore displacement curve for Forsmark is based on an interpolation between Gävle and Stockholm.*

Pollen-analytical levels recorded in northern Uppland are the Elm decline, c 5,200 years BP, and the spread of spruce at c 3,400–2,700 years BP /Robertsson and Persson, 1989/. At the Hållnäs peninsula, c 35 km north of the regional model area, biostratigraphical investigations have been performed in connection with archaeological investigations /Ranheden, 1989/. Settlements from the Viking age and medieval period were identified in the fossil record, i.e. humans have been occupying the archipelago successively as new land emerges from the Baltic.

3.2.3 Late- or post-glacial crustal movement, and seismic activity in historical time

The Forsmark regional model area is situated east of a belt that extends from southwestern Sweden via the coastal areas of Norrland to inland Norrbotten, along which there is a relatively high concentration of registered earthquake epicentres with a magnitude of 5 or less on the Richter scale. Apart from frequent yet minor seismic activity registered during the 1980's in the Dannemora and Finnsjön areas, southwest of the regional model area, which is thought to have been caused by human activity /Bergman et al, 1996/, natural earthquake epicentres are sparse in the northern part of the county of Uppsala. The strongest earthquake registered in the county (year 1776) had an epicentre c 10 km northwest of Tierp and a magnitude of 3.6 on the Richter scale. Recent seismic activity has been related to ongoing plate-tectonic processes including spreading of the North Atlantic Ocean /Slunga and Nordgren, 1990/. However, this activity may also be related to post-glacial rebound, i.e. there is no consensus that it is due to plate-tectonic processes alone.

Evidence for the presence of late- or post-glacial faulting in the northern part of Uppland is lacking. Furthermore, the mapping of Quaternary deposits on map-sheets 12I Östhammar NO and 13I Österlövsta SO/13J Grundkallen SV by SGU during 1982 and 1983 /Persson, 1985, 1986/ did not yield any observations which could be interpreted as supporting the presence of late- or post-glacial faults in these areas. A discussion of a bolder-rich area, the Gillberga gryt, was summarised by /Bergman et al, 1996/. /Agrell, 1981/, /Sjöberg, 1994/ and /Mörner, 2003/ interpreted the boulder-cave to represent the result of a neotectonic event. /Persson, 1990/ favours a glaciotectonic origin of the boulder cave, an opinion also favoured by /Lagerbäck and Sundh, 2003/ after a field inspection of the site. A study of late- or post-glacial faulting in northern Uppland was initiated during 2002 and will continue within the site investigation programme during 2004 /Lagerbäck and Sundh, 2003/.

During the construction of the Forsmark Power plant, a characteristic feature in the uppermost rock mass was found to be the occurrence of horizontal and sub-horizontal fractures (see Section 4.6.5). The bedrock was covered by glacial till and the open fractures contained fine-grained sediment /Carlsson, 1979; Pusch et al, 1990/. Investigations of the pollen flora from sediment in the open fractures indicated that the sediment contained re-deposited interglacial or interstadial material, i.e that the sediment was pre-Holocene, possibly early or middle Weichselian in age /Stephansson and Eriksson, 1975/.

3.3 Premises for surface and groundwater evolution

3.3.1 Premises for surface water evolution

As shown in Figure 3-9, almost the whole regional model area was covered by sea water until 2,500 years ago. The evolution of the salinity of the sea water since the onset of the Litorina period, as used in model version 1.1, is shown in Figure 3-10. In Figure 3-11 the time since the land emerged from the Baltic Sea is presented as an iso-chronic map based on /Brydsten, 1999a/. From the map it can be seen that the whole candidate area was covered by the sea until less than 1,500 years ago. This means that the Quaternary deposits in the area have been exposed to groundwater recharge and soil forming processes for a very limited time.
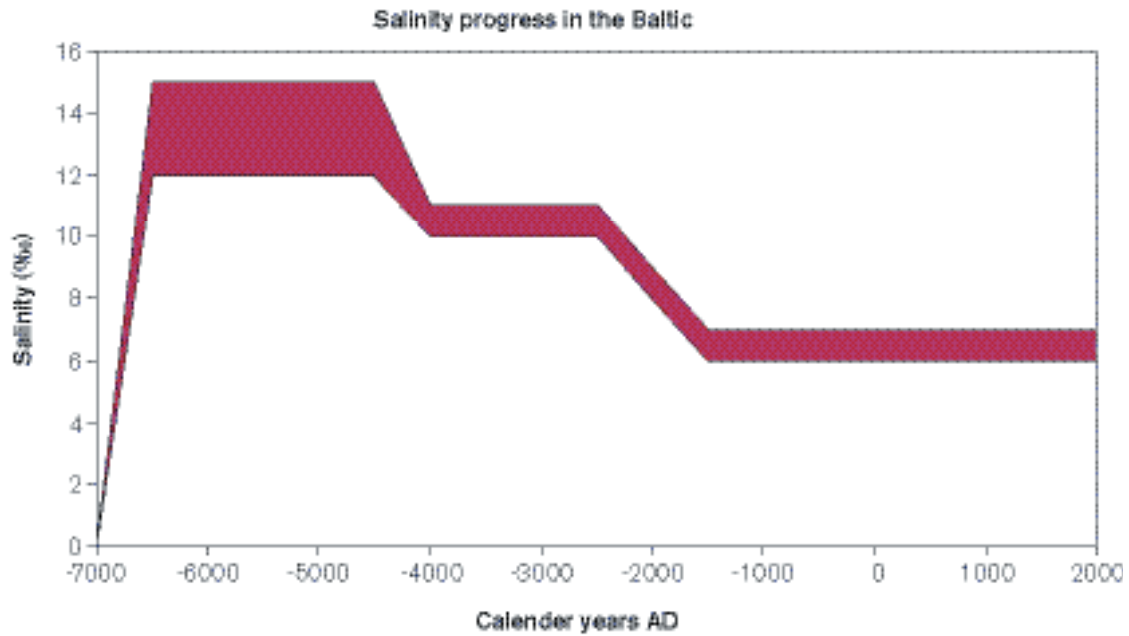
Figure 3-10. *Water salinity of the Baltic from the onset of the Litorina period until today. Modified after /Westman et al, 1999/.*
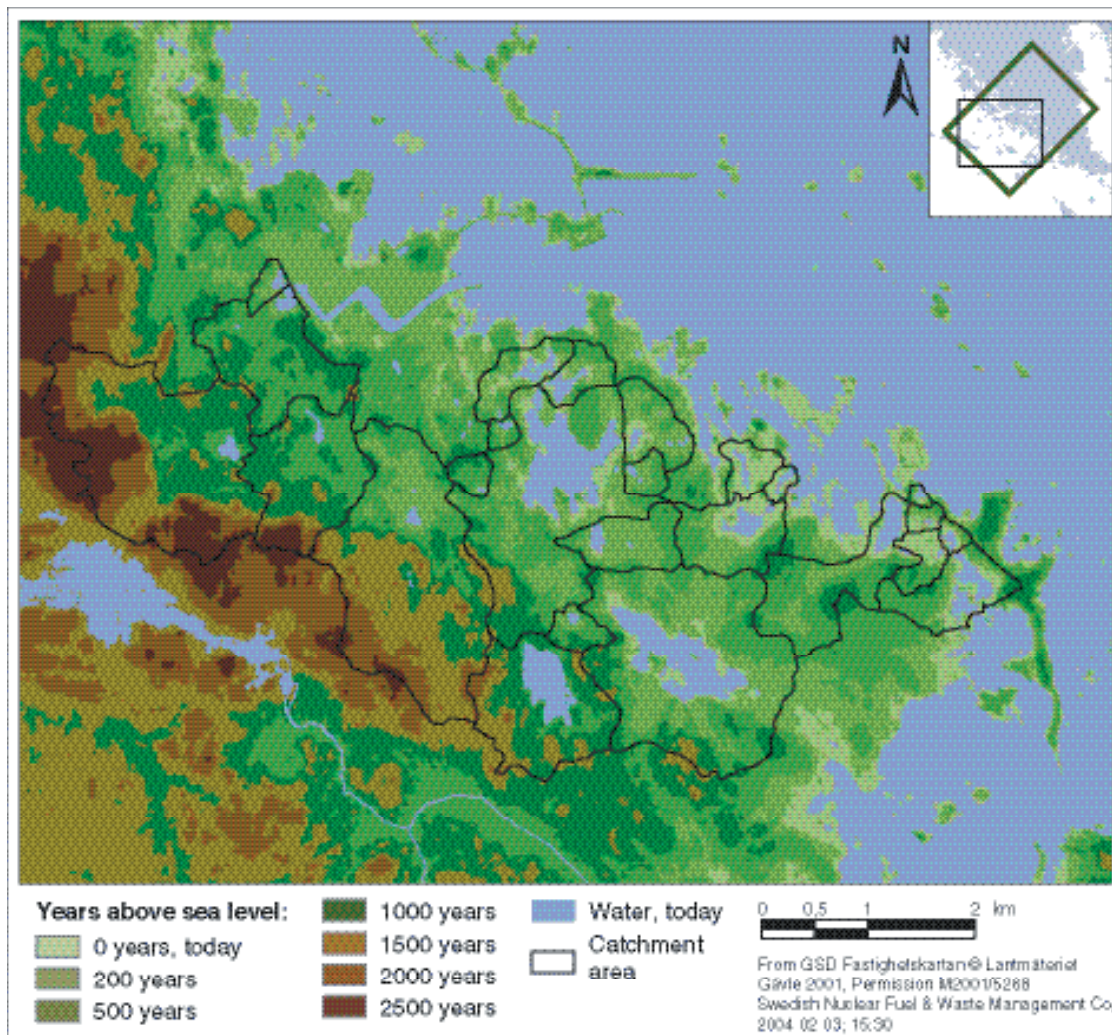
Figure 3-11. *Iso-chronic map showing the time since the land emerged from the Baltic Sea.*

3.3.2 Post-glacial conceptual model of groundwater evolution

The first step in the groundwater evaluation is to construct a conceptual postglacial scenario model (Figure 3-12) for the site. This is based on known palaeo-hydrogeological events indicated by Quaternary geological investigations. This model can be helpful when evaluating data, since it provides constraints on the possible groundwater types that may occur. The glacial/post-glacial events that might have affected the Forsmark site are based on information from various sources including /Fredén, 2002/, /Hedenström and Risberg, 2003/, /Westman et al, 1999/ and /SKB, 2002a/.

When the continental ice sheet was formed 100,000 BP permafrost formations ahead of the advancing ice sheet probably extended to depths of several hundred metres. According to /Bein and Arad, 1992/ the formation of permafrost in a brackish lake or sea environment (e.g. similar to the Baltic Sea) produced a layer of highly concentrated salinity ahead of the advancing freeze-out front. Since this saline water would be of high density, it would subsequently sink to lower depths and potentially penetrate into the bedrock where it would sink and eventually mix with formational groundwaters of similar density. Where the bedrock was not covered by brackish lake or sea water similar freeze-out processes would occur on a smaller scale within the hydraulically active fractures and fracture zones, again resulting in formation of a higher density saline component which would gradually sink and eventually mix with existing saline groundwaters. Laboratory experiments at the University of Waterloo, Canada, /Frape, pers comm, 2003/ indicate that the volume of highly saline water produced from brackish waters by this freeze-out process would be much less than initially considered by Bein and Arads (op. cit.) and would tend to form restricted pockets of high density saline water rather than a continuous horizon of high salinity in the case of a lake or sea environment.

With continued evolution and movement of the ice sheet, areas previously subject to permafrost would be eventually covered by ice, accompanied by a rise in temperature of the underlying rock and a slow decay of the permafrost layer. Hydrogeochemically, this decay may have resulted in distinctive signatures being imparted to the groundwater and fracture minerals.

During subsequent melting and retreat of the ice sheet, the following sequences of events are thought to have influenced the Forsmark area:

- When the continental ice melted and retreated c 11,000 years BP, glacial meltwater was hydraulically injected under considerable head pressure into the bedrock close to the ice margin. The exact penetration depth is still unknown, but depths exceeding several hundred metres are possible according to hydrodynamic modelling /e.g. Svensson, 1996/. Some of the permafrost decay groundwater signatures may have been disturbed or destroyed during this stage.

- Different non-saline and brackish lake/sea stages then transgressed the Forsmark site during the period c 11,000 BP to the present. Of these, two periods with brackish water can be recognised; a short period of the Yoldia Sea stage (11,500 to 10,800 BP) and the Litorina Sea *sensu lato* (9,500 BP to the present cf Table 3-3). The Yoldia period has probably resulted in only minor contributions to the subsurface groundwater since the water was very dilute and brackish from the large volumes of glacial meltwater it contained. Furthermore, the brackish-water phase of the Yoldia Sea lasted only for c 120 years. The Litorina period in contrast had a salinity maximum of about twice the present Baltic Sea and this maximum prevailed from 6,500 to 5,000 BP. During the last 2,000 years the salinity has remained almost equal to the present Baltic Sea values /Westman et al, 1999 and references therein/. Dense brackish seawater such as the Litorina Sea water was able to penetrate the bedrock resulting in a density turnover which affected the groundwater in the more conductive parts of the bedrock. The density of the intruding seawater in relation to the density of the groundwater determined the final penetration depth. As the Litorina Sea stage contained the most saline groundwater, it is assumed to have had the deepest penetration depth eventually mixing with the glacial/brine groundwater mixtures already present in the bedrock.

- When the Forsmark region was gradually raised above sea level, the major parts of the regional model area during the last 1,500 years, fresh meteoric recharge water formed a lens on top of the saline water because of its low density. As the present topography of the Forsmark area is flat and the time elapsed since the area rose above the sea is short, the out flushing of saline water has been limited and the freshwater lens remains at shallow depths (from the surface down to 25–100 m depending on hydraulic conditions).
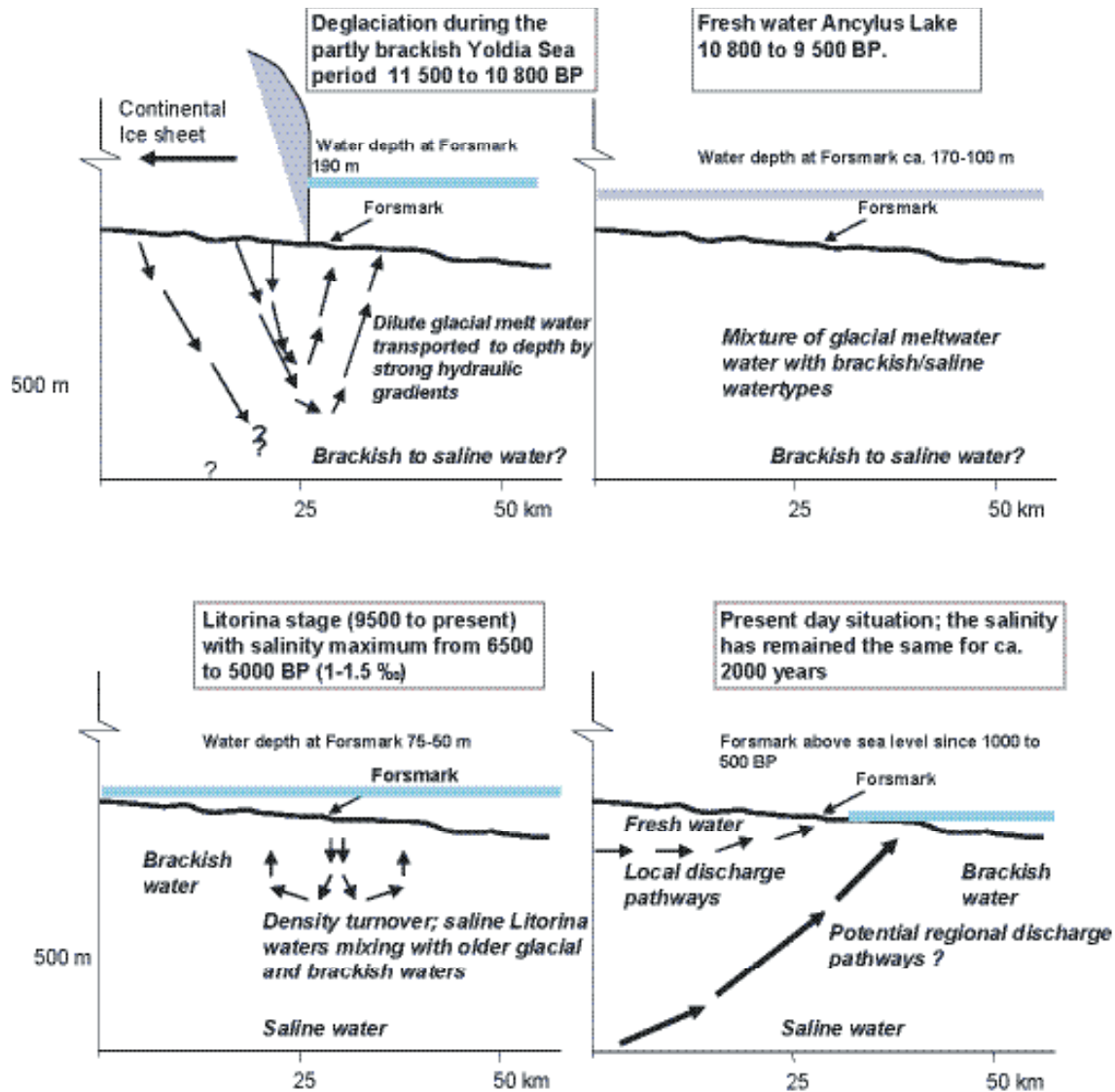
Figure 3-12. *An updated conceptual postglacial scenario model for the Forsmark site. The figures show possible flow lines, density driven turnover events and non-saline, brackish and saline water interfaces. Possible relation to different known post-glacial stages such as land uplift which may have affected the hydrochemical evolution of the site is shown: a) Yoldia Sea stage including deglaciation, b) Ancylus Lake stage, c) Litorina Sea stage, and d) present day Baltic Sea stage. From this conceptual model it is expected that glacial meltwater and deep and marine water of various salinities have affected the groundwater. Based on information from /Fredén, 2002/, /Hedenström and Risberg, 2003/, /Westman et al, 1999/ and /SKB, 2002a/.*

Many of the natural events described above may be repeated during the lifespan of a repository (thousands to hundreds of thousands of years). As a result of the described sequence of events, brine, glacial, marine and meteoric waters are expected to be mixed in a complex manner at various levels in the bedrock, depending on the hydraulic character of the fracture zones, groundwater density variations and borehole activities prior to groundwater sampling. For the modelling exercise which is based on the conceptual model of the site, groundwater end-members reflecting, for example, glacial meltwater and Litorina Sea water composition were added to the data set /cf Laaksoharju et al, 2004/.

The uncertainty of the updated conceptual model increases with modelled time. The largest uncertainties are therefore associated with the stage showing the flushing of glacial melt water. The driving mechanism behind the flow lines in Figure 3-12 is the shore level displacement, which in turn is driven by the land uplift.

3.4   Historical development of the surface ecosystems

Patterns in the present-day surface ecosystems are a result of physical and biological processes over time, e.g. land uplift, climate change, vegetation development and human impact. These processes are often combined, where one process sets the limits for others. For example, climate and land uplift often determine vegetation development, which in turn controls human settlements and land use. The strongest impact on the historical development of the surface ecosystems in the Forsmark area is caused by direct or indirect effects of the latest glaciation. A direct effect, still strongly affecting the systems, is shoreline displacement, but other factors like soils, altitude, and the prerequisites for creation of lakes and watersheds are also determined by the latest glaciation.

3.4.1   The Baltic Sea

When the glacial ice cover started to retreat about 11,000 years ago, the Forsmark regional model area was situated about 190–170 m below the surface level of the Yoldia Sea, at that time a freshwater stage of the Baltic Sea (cf Table 3-3). The conditions in the Forsmark area remained principally lacustrine for approximately 1,500 years, until the onset of the Litorina Sea stage. From Litorina until today, the Baltic Sea has been brackish with varying salinity and with an estimated maximum salinity level about twice as high as today, occurring during the period 6,500–5,000 BP /Westman et al, 1999/. The post-glacial climate in the Baltic Sea area has changed several times between cold and warm periods, and the varying salinity may at least partly be related to climate variations with decreased salinity during periods of climate deterioration /Westman et al, 1999/.

As described above, the first islands in the Forsmark regional model area appeared approximately 2,500 years ago (cf Figure 3-9 and Figure 3-11). Accordingly, the post-glacial ecosystems have been dominated by marine stages, and no terrestrial or lacustrine ecosystems have existed in the area until the last 2,500 years. Today, the Forsmark area is situated on the border between two different landscape types: "Woodlands south of Limes Norrlandicus" and "Coasts and archipelagos of the Baltic sea" /NMR, 1984/. Because of the shoreline displacement, all terrestrial and freshwater parts of the model area have relatively recently belonged to the latter type and the border between the two types is continuously moving to the east. This means that both the aquatic and the terrestrial ecosystems have gone through substantial changes during the post-glacial period, and they are still changing continuously, especially near the shoreline.

3.4.2   Lacustrine ecosystems

In Scandinavia, a majority of the present lakes were formed during the last glaciation, when geomorphological processes substantially altered the entire landscape. As the glacier retreated, erosion, transport, and deposition of material resulted in the formation of numerous lake basins in the landscape. Due to present land uplift in the Forsmark area, freshwater lake basins are continuously formed along the coast as bays become isolated from the brackish water of the Baltic Sea. Immediately after the formation of a lake, an ontogenetic process starts, where the basin ultimately is filled with sediments, and thereby develops towards extinction of the lake. Depending on local hydrological and climatic conditions the lake may be converted to a final stage of a bog or to forest /Wetzel, 2001/. A usual pattern for lake ontogeny is the subsequent development of more and more eutrophic conditions as lake depth and volume decreases. In later stages, aquatic macrophytes speed up the process by colonising large areas of the shallow sediments /Wetzel, 2001/.

All lakes in the Forsmark area, as well as all other lakes below the highest shoreline of the Baltic Sea (and its previous lake and sea stages), have their origin as depressions at the bottom of these large aquatic systems /Brunberg and Blomqvist, 2000/. The lakes of Uppsala County can be divided into three categories, based on their ecosystem functioning: shallow and oligotrophic hardwater lakes, shallow alkaline brownwater lakes, and deeper highly eutrophic lakes /Brunberg and Blomqvist, 2000/. All three lake categories occur within or in the vicinity of the Forsmark area, but the lakes in the area differ in several aspects from lakes in Uppsala County in general /Brunberg and Blomqvist, 2000/. Because of their location close to the Baltic Sea in a low-land area, they are generally younger than the inland, more elevated lakes. Other characteristics of the Forsmark lakes are that they are smaller, shallower and have smaller volume of water than the lakes of Uppsala County in general.
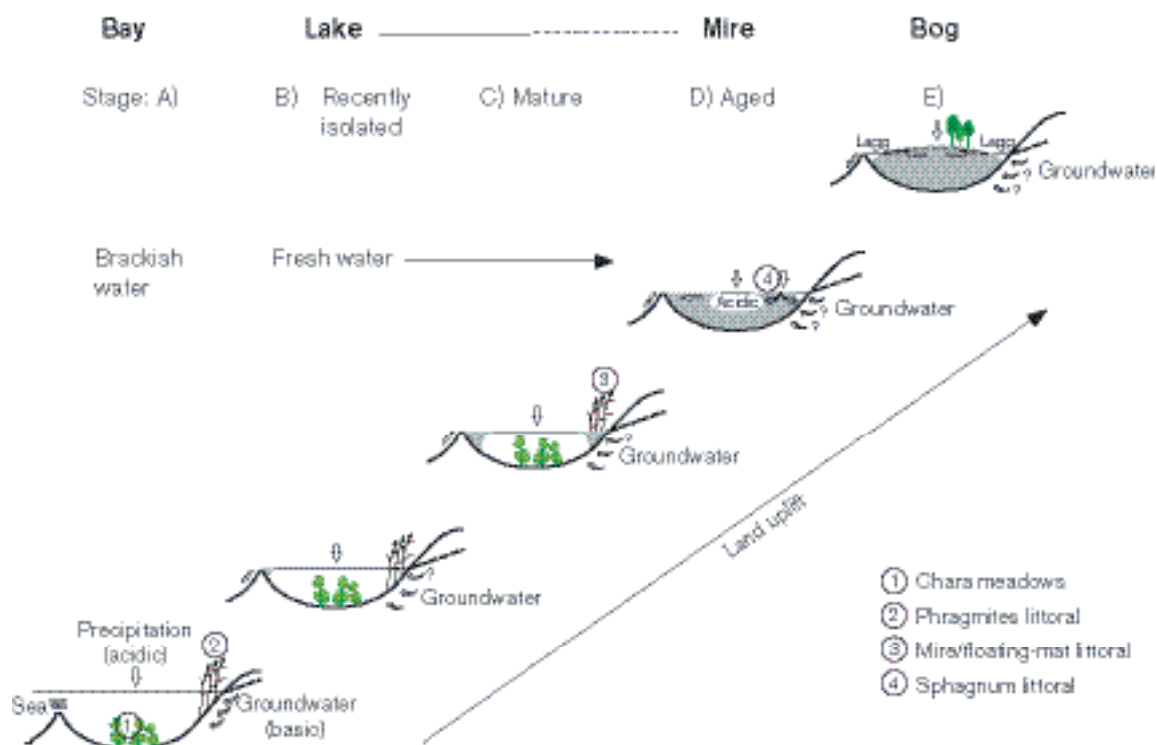
Figure 3-13. *Suggested ontogeny of the oligotrophic hardwater lakes in the Forsmark area. The numbers in the figure represent different major components of the ecosystem: 1 = Chara meadow, 2 = Phragmites littoral, 3 = mire/floating-mat littoral, 4 = Sphagnum littoral /from Brunberg and Blomqvist, 2000/.*

Shallow oligotrophic hardwater lakes, which are totally dominant among the present lakes in the Forsmark regional model area, can be regarded as ephemeral in that they shift to alkaline brownwater conditions approximately 1,000–1,500 years after isolation from the sea /Brunberg and Blomqvist, 2003/. Thereafter, they are successively filled with allocthonus (from the drainage area) and autocthonous material (produced in the lake basin itself), the final stage being a wetland forest or a bog (Figure 3-13). Due to the small catchment areas with minor topographic variation dominated by wave-washed till and wetlands, there are few sources of allocthonus material. Thus, the sediment of the lakes in the area shows a high degree of autochthonous origin compared with many other lakes. There seems to be very few, if any, lakes or previous lakes in the Forsmark area that have followed the general pattern of more and more eutrophic conditions during lake ontogeny /Brunberg and Blomqvist, 2000/. Several lakes connected to the river Forsmarksån have been strongly affected by anthropogenic activity (see Section 3.4.5).

3.4.3 Vegetation

Vegetation development after the latest glaciation has been primarily controlled by land uplift and climatic changes. The general vegetation development, after the retreat of the glacial ice cover, is very much the same all over Stockholm archipelago /Jerling et al, 2001/. However, the first islets appears in the Forsmark area around 2,500 years BP, which is some 4,000 years later than for the earliest parts of the archipelago. This affects the time period of vegetation development, unaffected by humans, which is quite short compared to other areas in the archipelago. On the other hand, the general processes controlling the successional development of vegetation are the same, regardless of when the succession begins.

The historical vegetation development is examined by using data from pollen analysis /Jerling et al, 2001/. Such analyses have shown that the first vegetation in the Stockholm archipelago was dominated by typical early colonising tree species like Pine (*Pinus sylvestris),* Birch (*Betula spp*) and Hazel (*Corylus avellana*). Some tree species are fast colonisers and occur early in succession (Figure 3-14). However, a major part of the early succession species is short-lived herbs
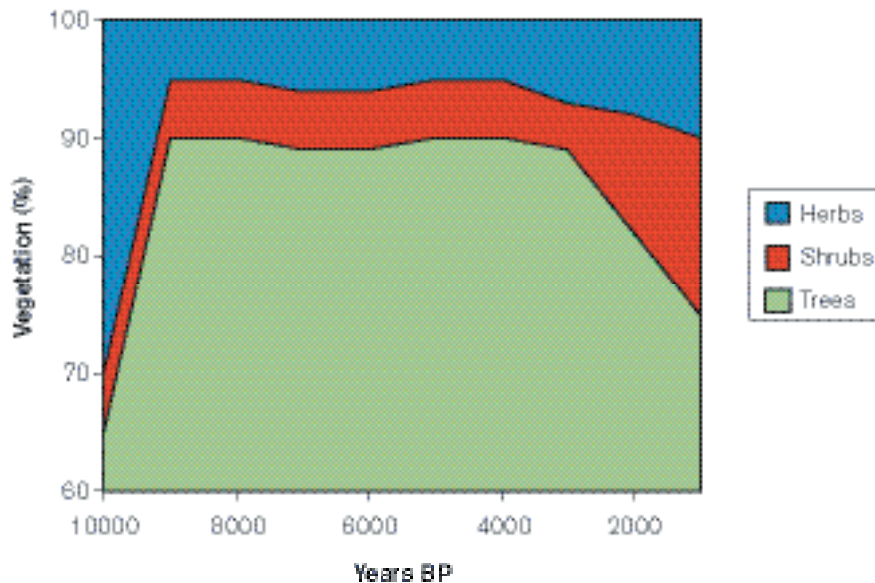
Figure 3-14. *Pollen diagram showing the relative amount of trees, shrubs and herbs in the Stockholm archipelago /after Jerling et al, 2001/.*

and grasses, but since they are light dependent they disappear later in the succession, when the vegetation canopy is closing. The Boreal period was totally dominated by Birch (*Betula spp*) and Pine (*Pinus sylvestris*), whereas the Atlantic period was characterised by the expansion of nemoral (thermophilous) forest trees, like Oak (*Quercus robur*), Elm (*Ulmus glabra*), Lime (*Tilia cordata),* Ash (*Fraxinius excelsior)*, because of warmer climate. Spruce (*Picea abies*) had its expansion much later, about 2,500 BP /Jerling et al, 2001/. In conclusion, a major part of the immigrating plants were already established in the coastal area of Uppsala County when the first islands in the Forsmark area emerged from sea. There is a consensus that Uppsala county never has been so forested as today /Lindborg and Schüldt, 1998/. Thus, in several areas today's forests are the first generation of woodlands since the first settlement, as a result of agriculture.

During the last 200 years, human activities have had a major impact on the development of the vegetation in the Forsmark area. Historical vegetation and land use development can be reconstructed by combining data from pollen analysis, old cadastral maps, soil and bedrock maps and archaeological data, with shoreline displacement models /Cousins, 2001/. Although land use alters the "natural" vegetation processes, all of the area has not been equally exploited through time, depending on differences in Quaternary deposits. For example, deposits on the flat sub-Cambrian peneplain are naturally rich in nutrients and thus frequently used in agriculture, but the areas closer to the coast have more exposed bedrock, resulting in less opportunity for agriculture /Jerling et al, 2001/. Moreover, as new land emerges, new immigrating species can establish and the primary succession, comparable to the one occurring after the glaciation, continues. Thus, land class distribution on the border of the coastal region changes little even though local spatial patterns are continuously changing.

Due to the strong influence by man on terrestrial ecosystems, it is difficult to evaluate the relative importance of natural factors affecting the conifer forests. As the iron industry became more organised in the 16th century, forests were cut down to feed furnaces and mines with wood and charcoal. Many regions, including Forsmark, were almost depleted of trees at the end of this period /Welinder et al, 1998/. Tar and lumber also became commercially important.

3.4.4 Wild fauna

Archaeological excavations make it possible to document the diet of early settlers by identifying bones from animals /cf Bratt, 1998/. However, abundances of specific species are not possible to estimate based on these findings. Food remains from the Stone Age imply that seal and different

fish species were common in the food of man in the Stockholm archipelago. Further inland there are frequent traces of moose, red deer, wild boar and bear in the remains /Bratt, 1998/. During the most intense hunting period, some two hundred years ago, many large mammals were locally extinct in Uppsala County, e.g. bear, beaver, and wolf /Lindborg and Schüldt, 1998/. Documenting earlier fauna in the Forsmark area specifically has not been done, and may be difficult due to few excavations in this area. However, information on the occurrence of large mammals during the last 50 years are available for Forsmark area, based on bag records registered by local hunters /Lång et al, 2004/.

3.4.5 Population and land use

The first documented settlement close to the Forsmark area is from c 4,000 BP, when people began to cultivate the large peneplain of Uppsala /Lindborg and Schüldt, 1998/. Due to low altitude, the Forsmark area emerged from the sea relatively late compared to other areas in the archipelago. The first settlers were not able to colonise until after 1,500 BP, when the first island emerged in the area /Brydsten, 1999a/. No specific historical land use data have been analysed for the Forsmark area. However, many of the general historical changes are applicable also to Forsmark.

The first islands in the Forsmark area emerged during the late Iron Age, which is about the same time as the population in other parts of the archipelago became more settled. The few islands that had existed long enough to develop a forest were cut in favour of agriculture. As methods for agriculture were improved, fields became more productive and traces of the same cereals as are common today are documented. During the Medieval period the agricultural land expanded and meadows and pastures became an important land use because of substantial cattle breeding /Gustafsson and Ahlén, 1996/. In the coastal area, islands in the outer archipelago were often exclusively used for livestock grazing and mowing.

The more recent land use may be studied by using cadastral maps from the late 17th century and written historical documents. However, only land close to villages was mapped and only when the villagers asked for land redistribution. Generally, the cultural landscape (i.e. field boundaries) described in such maps was to a large extent established in the late Iron Age /Widgren, 1983; Welinder et al, 1998/. During the period 1700–1850, the communally owned land was divided to the individual farms, and the fields were reorganised. Technology also altered the cultural landscape as lakes and wetlands were drained and cultivated, which is also documented in the Forsmark area. Better iron tools made it possible to till the earth deeper and dig ditches and thus drain sodden areas. During the late 19th century, much of the former forested and more unsuitable areas also became agricultural land. Due to population expansion people started to move into cities or emigrate. During the 1930's less than half of the population lived off the land. Today 80% of the population lives in cities and only 2–3% are farmers. From 1850 to 1950, farming practises became more and more mechanised. Small scale farming and the associated mosaic landscape disappeared during the 20th century and successively changed to large scale, rationalised agriculture. Hence, only small remnants of the ancient rural landscape are left today.

The forests in the landscape have not been mapped to the same extent over historical time. Forests and wood have only recently been regarded as an economic resource, which has implication for the historical documentation of forestry in the Forsmark area. Forestry was, however, a major industry in the northern part of the Uppland County between the 11th and the 19th century. Iron mining has played an important role in the region since the Iron Age (Mattson and Stridberg, 1980). From the 17th to the beginning of the 20th century, there were several furnaces and ironworks established in the Forsmark region, e.g. Lövsta Bruk, Österby Bruk and Forsmarks Bruk. The latter is situated within the Forsmark area and became, in 1570, a so called "kronobruk" /Anonymous, 1997/. The area surrounding Forsmark was heavily influenced by logging for charcoal and wood to supply the furnaces all around Bergslagen. The life close to the mines shaped the landscape into a mosaic of small-scale traditional agriculture landscape, ironworks and forest industry. The water from the river Forsmarksån was also regulated for mining. These places are today of national interest for their cultural history /Lindborg and Schüldt, 1998/. During the last few hundreds of years, a major part of the Forsmark region has been used in forestry, first owned by Forsmarks bruk and later by Assi-Domän and Sveaskog.

4 Evaluation of primary data

The site descriptive modelling comprises the iterative steps of primary data evaluation, descriptive and quantitative modelling in 3D, and overall confidence evaluation. The means and results of the first of these steps, evaluation of the site data available at data freeze, are described in this chapter. The primary data need to be checked for consistency and to be interpreted into a format more amenable for three-dimensional modelling. Furthermore, while cross-discipline interpretation is encouraged there is also a need for transparency. This means that the evaluations are made within each discipline. The results are used as input to the next step, the descriptive and quantitative modelling, which is described in Chapter 5.

4.1 Topography and bathymetry

The Digital Elevation Model, DEM, is built from several different sources with different resolution and accuracy. Four regions of accuracy and resolutions are identified; sparse land, dense land, sparse sea and dense sea, see Figure 4-1.

According to /Brydsten, 1999a/, the sparse data on land is collected from two sources – the existing DEM from the Swedish national land survey in a grid with 50 m squares and elevation lines from the digital map with a scale of 1:10,000. The dense data on land comes from a special survey with a grid with 10 m squares /Wiklund, 2002/. None of these data sets contains any bathymetric data. Hence, the elevation coincides with the water surfaces of the lakes.
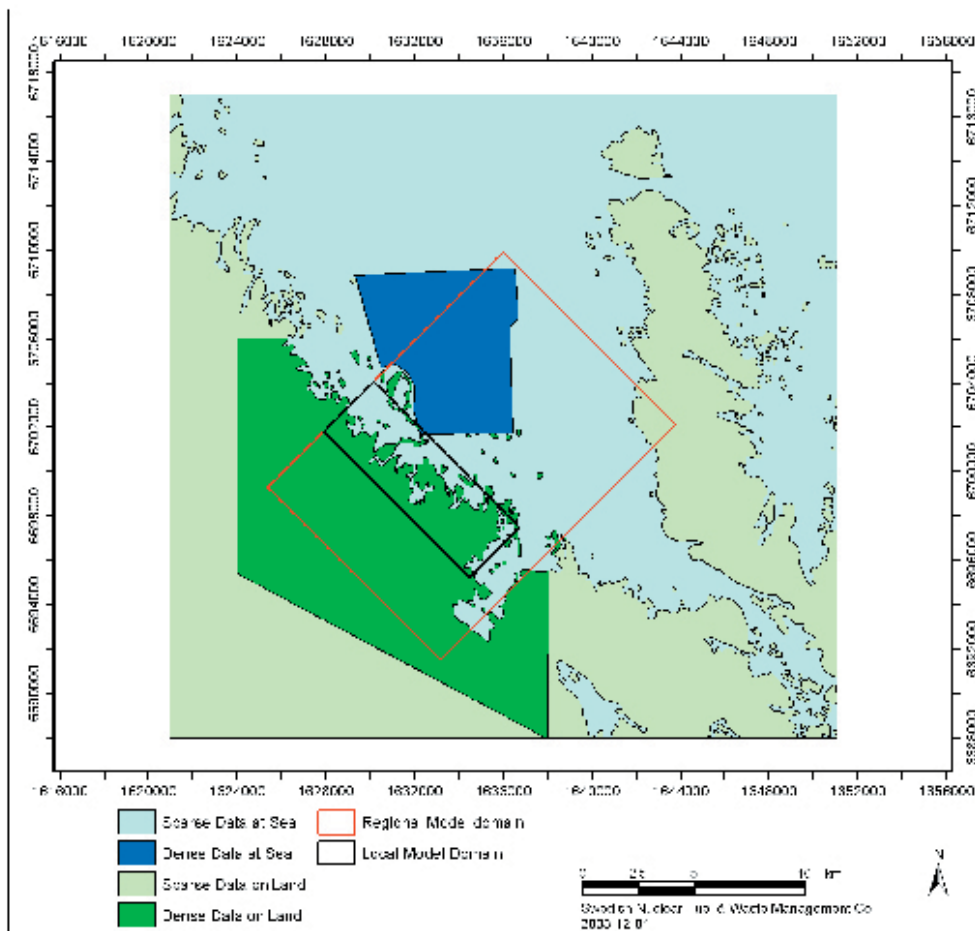
Figure 4-1. *Data density for the Digital Elevation Model, DEM.*

Elevation at sea for the sparse area is obtained partly from the digital chart produced by the Swedish National Administration of Shipping and Navigation, and partly from point depth measurements. The digital chart has depth lines for 3, 6, 10, 15, 25 and 50 m, but lack the point depths that are present on the paper chart. These values were manually digitized. For the dense area at sea, the base map for the charts was used to digitize the point depth data. This approach was in accord with /Brydsten, 1999a/.

Some of the source data are old and hence not in the Swedish national Cartesian system, RT90. Therefore, these data have been transformed to the national 2.5 gon V 0:-15, RT90 system. All the transformed data were interpolated in ArcGIS using kriging algorithms in accord with the methodology reported by /Brydsten, 1999a/.

The interpolated DEM is shown in Figure 4-2. The white line corresponds to the coast line from the cadastrial map. The discrepancies, especially in Kallrigafjärden, are due to lack of data at sea.
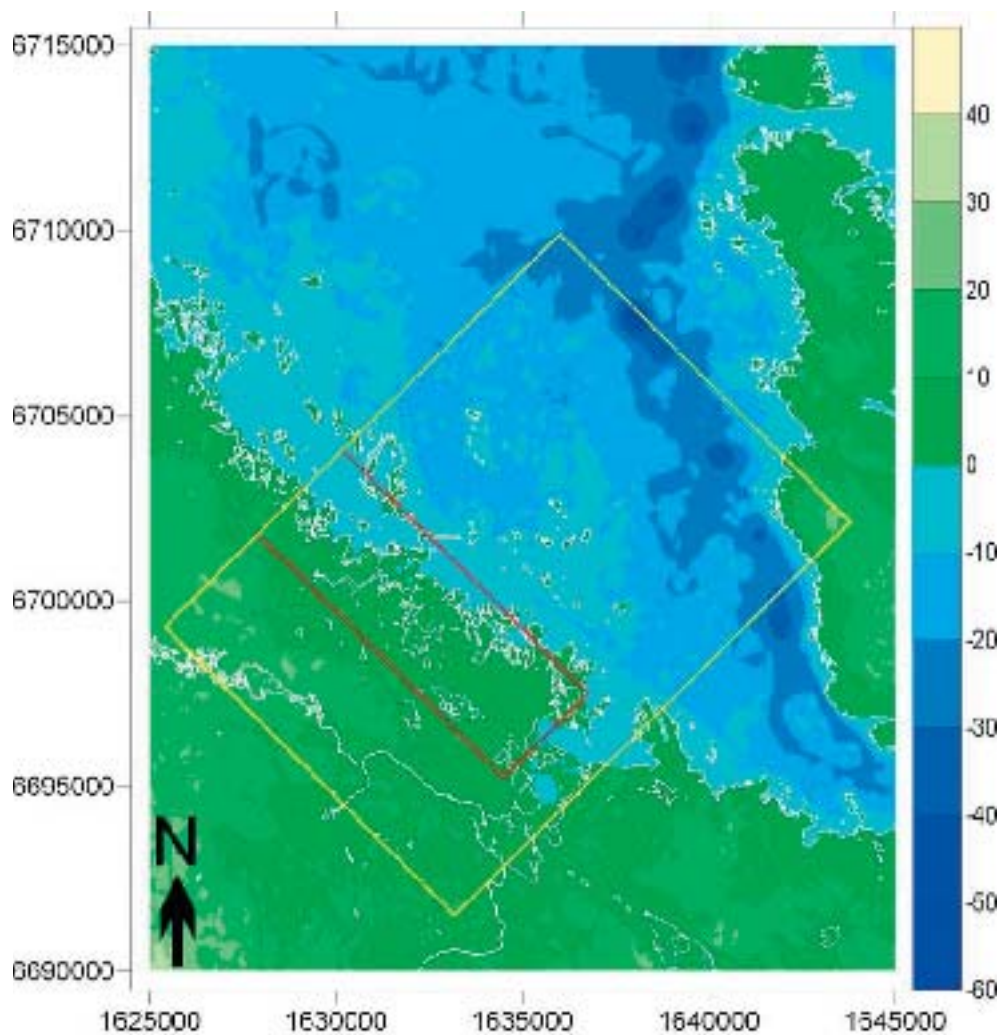
Figure 4-2. *The interpolated digital elevation model, DEM.*

4.2 Geologic evaluation of surface based data

4.2.1 Quaternary deposits and other regoliths

Regoliths will be called Quaternary deposits and includes glacial deposits such as till, glaciofluvial deposits and clay, as well as postglacial deposits such as marine and lacustrine sediment and peat. The description of the distribution and composition of Quaternary deposits in the Forsmark regional model area is based on the compilations made in connection with the Östhammar feasibility study /Bergman et al, 1996/ in combination with the observations from the initiated site investigations /Sohlenius and Rudmark, 2003/.

Surface based data

Quaternary deposits occupy c 82% of the land area in the regional model area and artificial fill, principally around the Forsmark nuclear power station and an area close to Johannisfors, c 3%. Exposed bedrock or bedrock with only a thin (< 0.5 m) Quaternary cover occupies c 15% of the land area. The Quaternary deposits consist of two components:

- Glacial deposits which were deposited either directly from the inland ice or from the water derived from the melting of this ice. These deposits include till, glaciofluvial sand and gravel, and varved glacial clay. Glacial striae on bedrock outcrops are common and indicate an older ice movement from the NW to NNW and younger movements from the north.

- Post-glacial deposits which were formed after the inland ice had melted and retreated from the area c 11,000 years ago /Fredén, 2002/. The post-glacial deposits include sand and clay and organic deposits such as peat and gyttja.

The information from the ongoing site investigations confirms the general knowledge from earlier geological maps. Based on a comparison with the initial geological map, the areas mapped in support of model version 1.1 represent a variety of Quaternary deposits. Thus, the information gained from the investigations this far can be regarded as representative for the area to be mapped, even though only approximately 25% of the total area has been investigated (Figure 4-3) and only descriptive data are available for comparison with the initial map. New information regarding the spatial distribution of Quaternary deposits derived within the site investigation can be divided into two groups:

1. A small-scale pattern of Quaternary deposits as well as the distribution of bedrock outcrops, including surfaces down to 10 m in cross section. This information is the result of the differences in scale between earlier information and the ongoing mapping.

2. The character and distribution of water-laid sediment and organic deposits.

The distribution of bedrock outcrops, i.e. areas with no Quaternary deposits, is based on field observations as well as interpretations from infrared aerial photographs. The frequency of outcrops varies within the mapped area. Areas with low frequency of outcrops are e.g. the eastern part at Storskäret and west of Lake Bolundsfjärden. Areas with high frequency of bedrock outcrops are e.g. the south-western part of the mapped area and the coast north of Lake Bolundsfjärden. Many of the outcrops are Roches mountonnées with a smooth abraded northern side and a rough, steep plucked side towards the south. Ice moving from $350 \pm 10°$ formed the majority (c 80%) of the glacial striae. Striae from the north-west are preserved on lee side positions and one striae from 5° east is observed.

Glacial till is the dominating Quaternary deposit. Based on the surface layer, three areas with different till types were distinguished:

I   The western and northern parts of the mapped area, east and northwest of Lake Eckarfjärden and north of Lake Bolundsfjärden are dominated by sandy till. Gravely till was also identified, mainly close to drillsite 1. Medium bolder frequency dominates.

II At Storskäret and east of Lake Fiskarfjärden, a clayey till dominates. The boulder frequency is low and the area is used for cultivation.

III The easternmost part of the mapped area, close to the Börstilåsen esker, is dominated by a high frequency of large boulders.
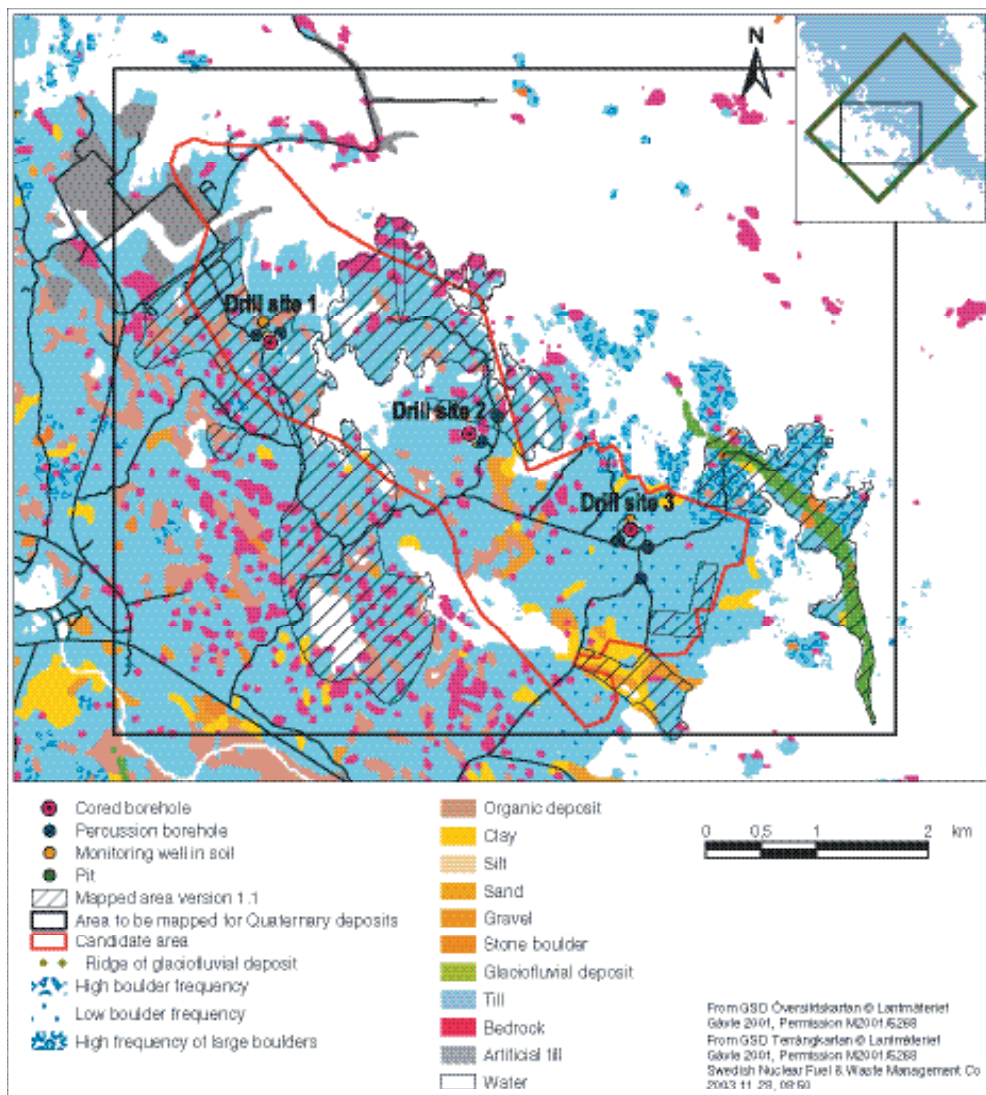
Figure 4-3. *Map showing the distribution of Quaternary deposits (version 0 data) and the area mapped 2002 (striped). The locations for analytical data are indicated. Green labels are surface-based data from pits. Blue and orange labels are stratigraphic data from corings.*

Grain size analyses were performed on 12 surface samples from pits within the mapped region (Figure 4-4). For three of the samples, the field classification deviated from the laboratory results. In all three samples the field classification (sandy till) underestimated the clay content (clayey till). Ordovician limestone is a conspicuous component in the till deposits. All samples analysed contained calcium carbonate, except one sample of wave-washed sandy gravel collected at 0.4 m depth. Clay from the same pit at 0.55 m depth consisted of 25% $CaCO_3$. The upper decimetres of the till have generally been washed clear from clay and silt. At exposed positions the uppermost layer consists of shingle.

Glaciofluvial sediments are deposited in a small esker, the Börstilåsen esker, with a flat crest reaching c 5 m above the present sea level. Wave washing has also affected the esker, where a raised shingle shoreline is developed.

Post-glacial sediment and peat form the youngest group of Quaternary deposits. In general, they overlie till and, locally, glacial clay or crystalline bedrock. The post-glacial Quaternary deposits are dominated by organic sediment and re-deposited, wave-washed sand and gravel. A large number of small (< 50 m) wetlands were discovered during the field investigations, but not presented in the

Figure 4-4. *Within the areal mapping of Quaternary deposits, pits were dug and surface samples collected for textural and chemical analyses.*

version 0 geological maps /Persson, 1985, 1986/. A genetic/principal discrepancy with version 0 data is that peat covers less extensive areas. Clay gyttja or gyttja clay are the dominating organic deposits in the surface of the wetlands whereas peat accumulations > 50 cm are rare. Actual peat accumulations were concentrated in the more elevated areas, e.g. south east of Lake Eckarfjärden. The organic sediment is often thinner than 1 m, underlain by sand or gravel and till or glacial clay.

Stratigraphic data

The glacial till is generally considered to be less than 5 m thick. The stratigraphical distribution and thickness of the Quaternary deposits were investigated using three methods: percussion corings, auger drillings and a Russian peat corer. Figure 4-5 shows the location of these investigations.

The percussion corings are clustered in areas close to drillsites 1–3. The drilling and sampling processes result in disturbed bulk-samples which often contains bedrock fragments or crushed boulders. Samples from each half metre coring depth were used for field classification, thus the stratigraphic distribution is not based on contiguous layers. Since the corings continued into bedrock, the thickness of the regolith is regarded as reliable. From the percussion corings close to drillsite 1–3, 33 samples were selected for analyses of grain-size distribution /Sohlenius and Rudmark, 2003/.

At drillsite 1, 5 of 18 samples analysed were wrongly classified in the field. The thickness of the Quaternary deposits varied between c 12 m and 4 m in the eight corings, located within c 200 m of the drillsite. However, the upper surface of the till is very flat and varies between c 4 and 2 masl. All samples analysed contained calcium carbonate, $m = 15 \pm 3\%$ (Table 4-1). From the ground surface downward, three stratigraphic till units were defined. These are gravely till, sandy till and silty till closest to bedrock (Table 4-1).
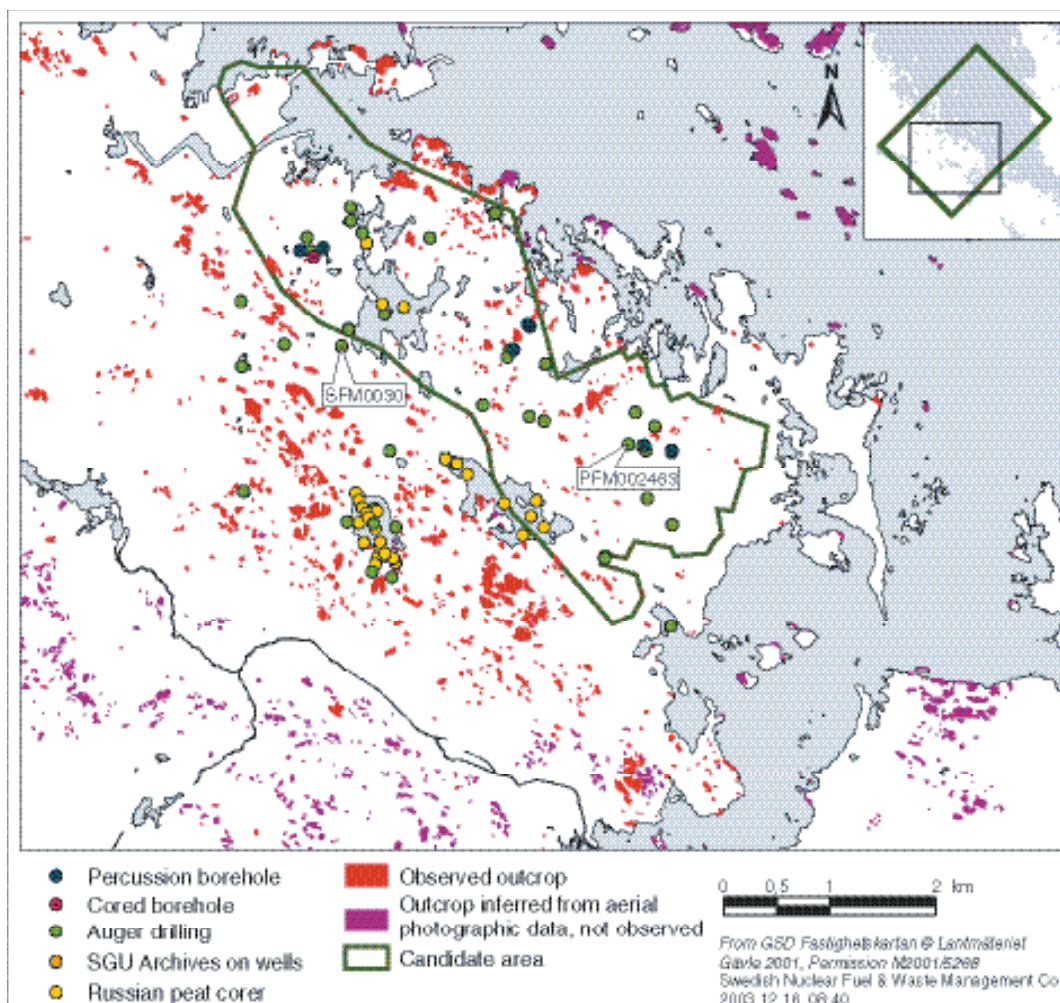
Figure 4-5. *Map showing the location of the stratigraphic information based on percussion corings, auger drillings and Russian peat corer as well as the information from SGU archives on wells.*

Table 4-1. Results from grain-size analyses together with calcium carbonate content of samples collected at corings close to drillsite 1.

ID code	Depth (m)	Quaternary deposit	CaCO$_3$ (%)
HFM01	1	Sandy till	15.5
HFM01	5.5	Sandy till	17
HFM01	8.5	Sandy-silty till	9
HFM02	1.5	Gravely till	14
HFM02	3.5	Gravely till	14
HFM02	10.5	Sandy-silty till	20.5
HFM03	1	Gravely till	8
HFM03	5.5	Sandy till	15
HFM03	8.5	Sandy-silty till	16
SFM0001	1.5	Gravely till	19
SFM0001	2.5	Gravely till	19.5
SFM0001	3.5	Clayey sandy-silty till	12.5
SFM0002	1	Sandy till	17
SFM0002	3	Sandy till	14
SFM0002	4.5	Sandy till	12.5
SFM0003	1	Sandy till	12.5
SFM0003	3.5	Sandy till	13.5
SFM0003	8.5	Sand	18

At drillsite 2, the field classification of one sample (sandy till) underestimated the clay content (clayey sandy till). All samples analysed contained calcium carbonate, m = 24 ± 4% (Table 4-2). The thickness of the glacial till varies between 0.5 and 4.5 m. There are too few corings to establish a general stratigraphy.

At drillsite 3, all 10 samples were described with the same field classification as the laboratory tests. The method for sampling has been improved since the first corings at drillsite 1, probably reflected in a more accurate field classification at drillsites 2 and 3. All samples contained calcium carbonate, m = 28 ± 4% (Table 4-3). The thickness of the glacial till varies from 1.5 to 5 m. A preliminary stratigraphy includes an upper unit with clayey till and a lower unit with a sandy till.

Table 4-2. Results from grain size analyses and calcium carbonate content of samples collected at corings close to drillsite 2.

ID code	Depth (m)	Quaternary deposit	CaCO$_3$ (%)
HFM04	0.5	Gravely till	18
HFM05	2	Clayey, sandy-silty till	23
HFM05	3	Clayey, sandy till	22
SFM0004	2.5	Clayey, sandy till	30
SFM0005	1	Sandy till	25

Table 4-3. Results from grain-size analyses together with calcium carbonate content of samples collected at corings close to drillsite 3.

ID code	Depth (m)	Quaternary deposit	CaCO$_3$ (%)
HFM06	1	Clayey, sandy till	27
HFM07	1.5	Boulder clay	27
HFM08	2	Clayey, sandy-silty till	27
HFM08	4.5	Clayey till	33
SFM0006	1.5	Clayey, sandy-silty till	31
SFM0007	2.0	Clayey, sandy-silty till	23
SFM0007	4.5	Clayey, sandy till	30
SFM0008	1.5	Boulder clay	19
SFM0008	4.5	Sandy till	30
SFM0008	5.0	Clayey, sandy till	31

The auger drillings were performed at the installation of groundwater monitoring wells. The drillsites are spread out within the area and cover mainly the different types of glacial till, except the region with high frequency of boulders. The auger drilling provides continuous sequences of till, better suited for a stratigraphic description. The thickness of the Quaternary deposits was between 1.4 and 17 m. However, the auger drillings on lakes and at locations where no wells were installed did not always for certain reach bedrock, which is why these values are minimum depths to bedrock. Detailed lithologic descriptions or analytical data are not yet available from the auger corings.

Information on the spatial distribution of marine and lacustrine sediment was gained by the investigations of sediment in lakes. Site investigation data comprise field classifications of sediment from 19 lakes and small ponds in the Forsmark area /Hedenström, 2003/. Information from corings and stratigraphical sections from Lake Eckarfjärden and Lake Fiskarfjärden has previously been published by /Bergström, 2001/. The sedimentary sequences were generally thin, often less than 3 m from the lake upper surface to the glacial till underlying the sediment. The data from /Bergström, 2001/ penetrated down to glacial clay whereas the corings from the site investigation program aimed at reaching the glacial till or bedrock below the sediment. Analyses of the borehole samples indicate that there are some differences in the evaluation technique between the data sets. The differences are mostly a question of detail, but are rather consistent and easy to spot.

- Data from /Bergström, 2001/ have a less detailed partition of layers than data from the site investigations. This is especially evident in the layers of algae gyttja and calcareous gyttja.

- The interpretation of the uppermost layer differs between the sample sets. In the first set the layer is identified as mud, but in the second set it is left as an unclassified layer of detritus.

A general stratigraphy was recorded with the following sediment types:

Lithology
Unclassified detritus
Calcareous gyttja
Algal gyttja
Gyttja clay/clay gyttja
Sand, gravel
Postglacial clay
Glacial clay

The data from the sediment investigation have been used to build three-dimensional models of the sediment in Lake Eckarfjärden and Lake Bolundsfjärden (see Section 5.1.1 and 7.1.4). Analytical data of e.g. grain size and calcite will be available for version 1.2 of the site descriptive model.

Offshore Quaternary deposits

A survey of the marine geology offshore Forsmark was conducted during 2002. However, these new site-specific data were not available for version 1.1 of the site descriptive model.

The Offshore Quaternary deposits in the area directly northeast of the Forsmark nuclear power station and above SFR have been studied previously. In these areas, the Quaternary deposits are dominated by till that rests on the bedrock. Locally, till is covered by fine sediment (clay). In the small area studied in detail above SFR /Sigurdsson, 1987/, the clay is glacial in character and is overlain by a thin layer of sand and gravel. The clay in this area occurs most conspicuously in a narrow belt, which trends in a NNW direction. /Carlsson et al, 1985/ have speculated that the occurrence of clay, in some cases, may be linked to fracture zones in the bedrock. The thickness of the offshore Quaternary deposits varies considerably from < 2.5 m to > 10 m /Carlsson et al, 1985/. In the area above SFR, till varies in thickness between 4 and 14 m and clay between 0 and 4 m.

Late- or post-glacial faulting

The search for evidence of late or post-glacial faulting in the Forsmark region includes literature review, air-photo interpretation, field reconnaissance and stratigraphic investigations in one machine-cut trench /Lagerbäck and Sundh, 2003/.

The air-photo interpretation identified 35 fairly pregnant escarpments and crevasses of which most were later checked in the field. The candidates for young fault movements turned out to be glacially eroded, i.e. not post-glacial in age.

About 40 gravel- and sandpits were visited. In 11 sections, sandy, silty deposits regarded as susceptible to seismically induced liquefaction were observed, but no major distortions were noted. Contorted and folded sequences of glacial clay were encountered at several locations, but these were interpreted as being a result of sliding.

A survey of glacially polished bedrock outcrops in the archipelago was performed, but no indications of post-glacial fault movements were found. One c 80 m long trench on the eastern flank of the Börstilåsen esker was excavated (Figure 4-6). No signs of earthquake vibrations were found. Deformation of the primary sedimentary structures caused by drop-stones and sliding occurred frequently. No distinct indications of late or post-glacial faulting have appeared so far, but the investigations are still in their early stages. Furthermore, the crucial test, the search for seismically generated distortions in strategically located trenches, remains to be done.

Figure 4-6. *One example of a machine-cut trench, studied for seismically induced liquefaction. The trench is c 80 m long, located on the eastern flank of the Börstilåsen Esker. No distinct indications of late or postglacial faulting have appeared so far. The investigations are planned to continue throughout 2004.*

4.2.2   Rock type – distribution, description and age

Data

The field and analytical data, which permit an assessment of the distribution, description and age of the various rock types at the surface, are of variable quality over the regional model area. Three areas, that contain data of different quality, are recognised (Figure 4-7):

- The area between road 76 and the coast, including the candidate area.
- The areas that are situated south of road 76 and on the islands northeast of the candidate area.
- The outboard area to the northeast under Öregrundsgrepen and on Gräsö.

Between road 76 and the coast, detailed bedrock mapping and analytical work have been carried out during 2002 and reported during 2003, in connection with the site investigation programme at Forsmark. The concentration of high-quality surface bedrock data in this area is judged to be high (Figure 4-7).

No such mapping was completed during 2002 south of road 76 and on the islands that are situated northeast of the candidate area. For this reason, the surface distribution of rock types in these areas has been adopted for modelling purposes (see Section 5.1.2) from the Site Descriptive Model version 0 bedrock map /SKB, 2002a/. It is difficult to judge the quality of the surface bedrock data in these two areas. Only map compilations at the scale 1:50,000 /Svenonius, 1887; Stålhös, 1991/ and c 1:30,000 /Hansen, 1989/ were used in the Site Descriptive Model version 0 work. An estimate of the concentration of high-quality base data in these two areas is medium (Figure 4-7).

In the outboard areas further to the northeast, the surface distribution of rock types has also been adopted for modelling purposes (see Section 5.1.2) from the Site Descriptive Model version 0 bedrock map /SKB, 2002a/. Surface bedrock data is entirely absent under Öregrundsgrepen. Furthermore, it is difficult to judge the quality of the surface bedrock data on Gräsö, since only a map compilation at the scale 1:50,000, based on old field data /Svenonius, 1887/, was used in the Site Descriptive Model version 0 work. An estimate of the concentration of high-quality base data in the outboard areas to the northeast is low to zero (Figure 4-7).
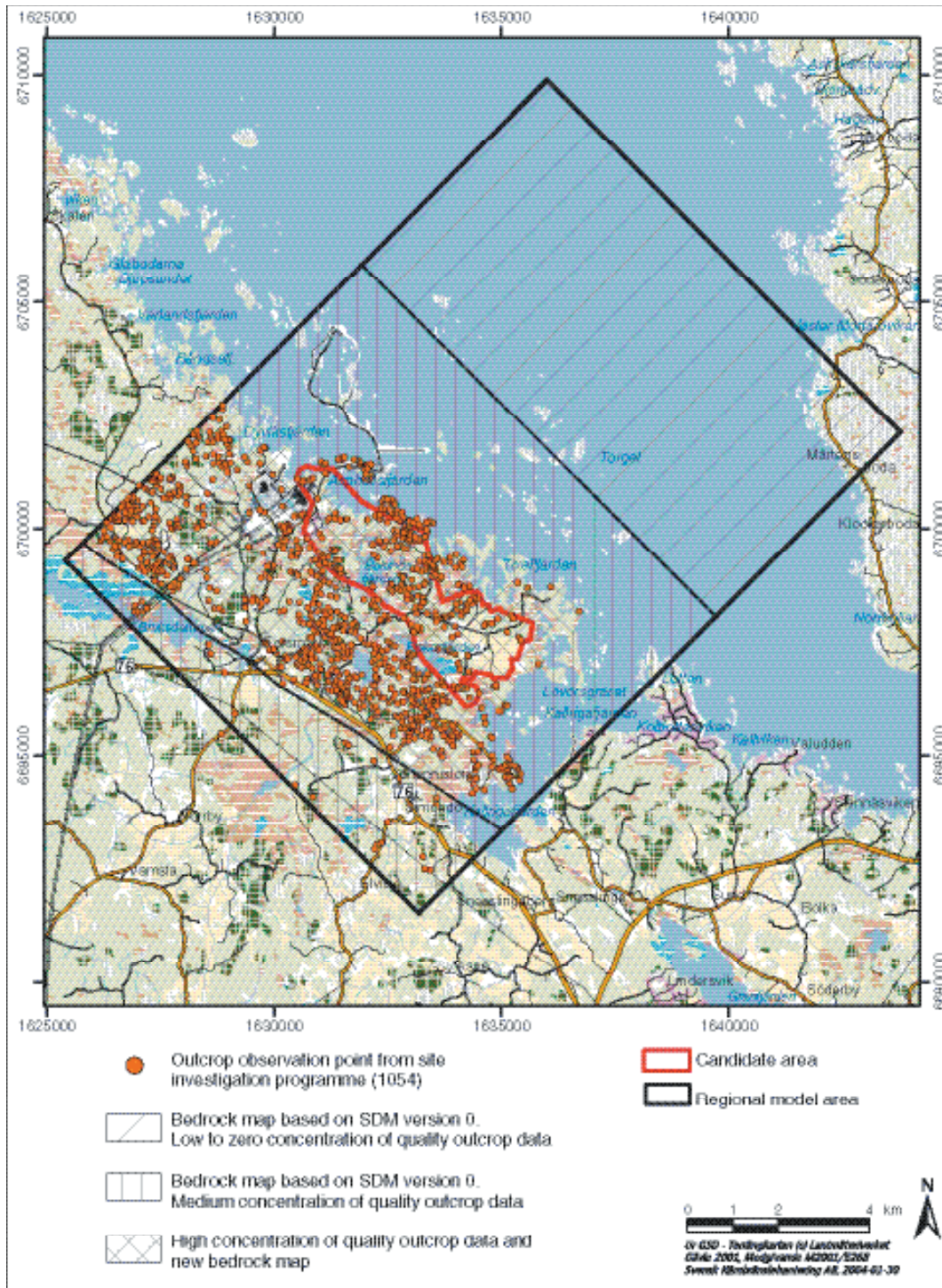
Figure 4-7. Summary of base data used to assess the distribution, description and age of rock types in the regional model area.

The distribution, description and age of the various rock types at the surface are documented with the help of the following information in the area between road 76 and the coast:

- The database with 1,054 outcrop observations (Figure 4-7) that was assembled in connection with the field activities during 2002 and subsequently synthesized /Stephens et al, 2003a/. These data include measurements of the magnetic susceptibility of different rock types at 853 of the 1,054 outcrops. The magnetic susceptibility data were subsequently evaluated and interpreted in /Isaksson et al, 2004a/.
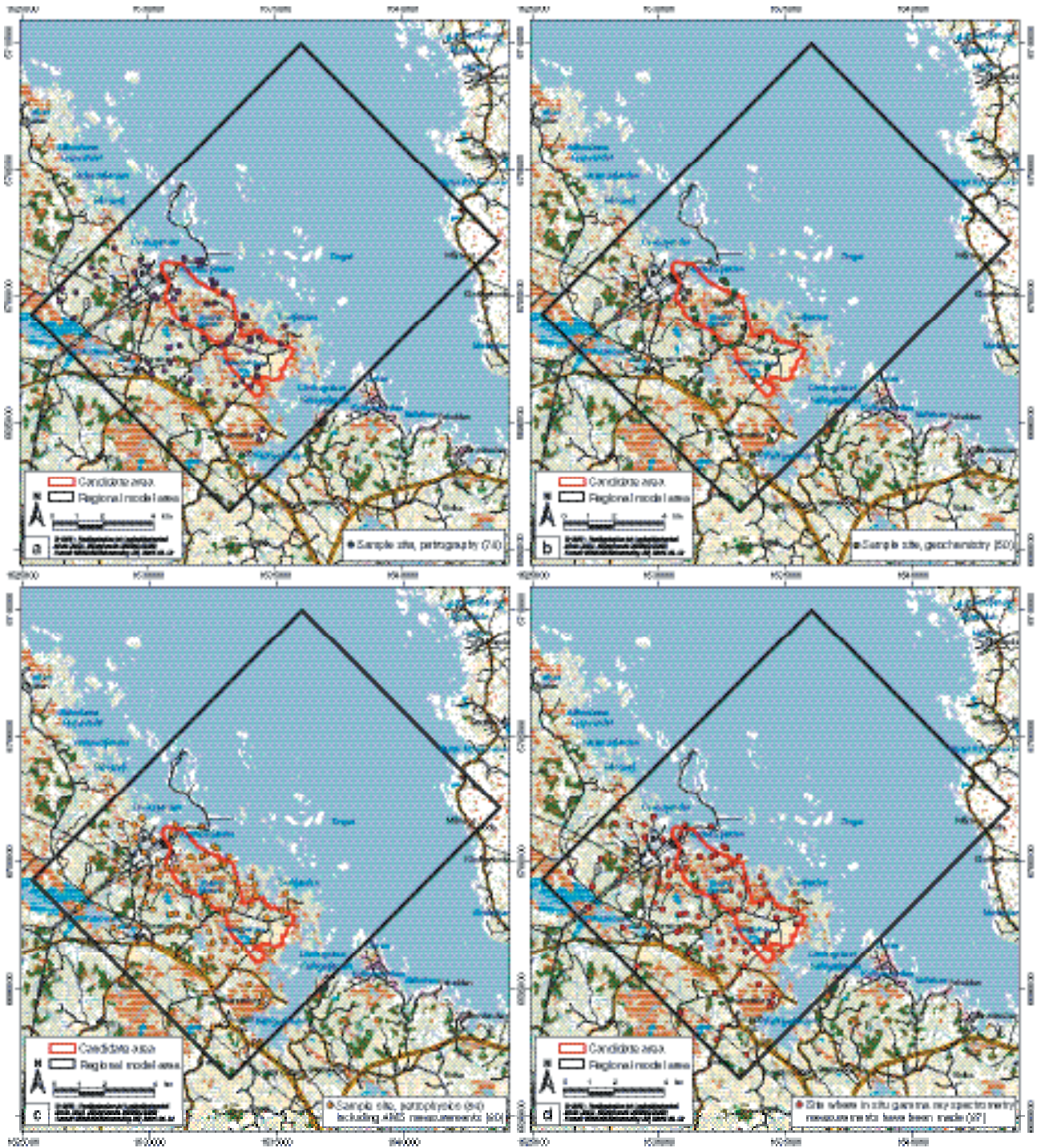
Figure 4-8. Sites where samples have been taken for the measurements of petrographic (a), geochemical (b) and petrophysical (c) data and where in situ, gamma-ray spectrometric measurements have been carried out (d).

- The petrographic data from 78 surface samples (Figure 4-8a) and the evaluation and interpretation of these data in /Stephens et al, 2003b/. This data set includes 71 modal analyses recalculated to QAPF values /Streckeisen, 1976, 1978/.

- The geochemical data from 50 surface samples (Figure 4-8b) and the evaluation and interpretation of these data in /Stephens et al, 2003b/.

- The laboratory measurements of petrophysical data on samples taken from 84 sites (Figure 4-8c) /Mattsson et al, 2003/, and the later evaluation and interpretation of these data in /Isaksson et al, 2004a/.

- The measurements of in situ, gamma-ray spectrometry data at 87 sites (Figure 4-8d) /Mattsson et al, 2003/, and the later evaluation and interpretation of these data in /Isaksson et al, 2004a/.

- The bedrock geological map (version 1.1) that was compiled with the help of available outcrop data and airborne magnetic data during the early part of 2003 (field note Forsmark 22 and Figure 4-9).
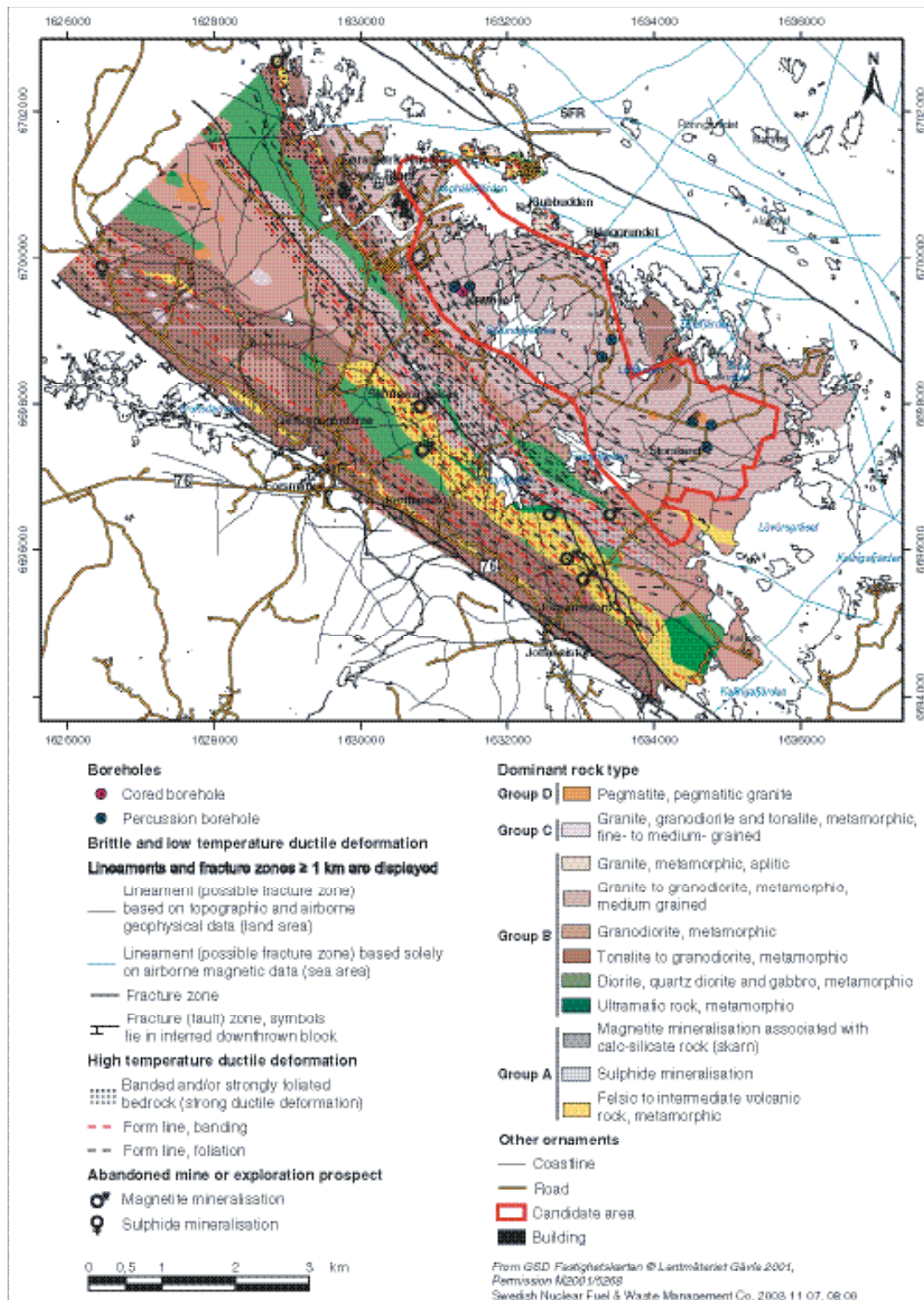
Figure 4-9. *Map of the bedrock geology in the area between road 76 and the coast, including the candidate area.*

Attention is focussed in this report on the composition, grain-size, density, magnetic susceptibility and uranium content in the various rock types that occur in the area between road 76 and the coast. Rock composition has been determined on the basis of the QAPF analyses. Both gamma-ray spectrometry and geochemical values are available for the determination of uranium contents. Knowledge of uranium content in the bedrock is important since anomalously high values of this element, and, in particular, the dominant isotope uranium-238, can give rise to high values of radon-222. Geochronological information has been derived from the Geological Survey of Sweden's geochronology database.

Evaluation

The Forsmark area is dominated by intrusive igneous rocks, whilst supracrustal rocks (metamorphosed volcanic rocks and magnetite mineralisation) form a subordinate component (Figure 4-9). Apart from some younger granites and pegmatitic rocks, which display only a weak foliation, all rocks are more or less affected by ductile deformation. This deformation is associated with recrystallization that occurred under amphibolite-facies (> 500–550°C) metamorphic conditions and at depths probably greater than 15 km. For this reason, most of the rock names are prefixed with the term "meta".

The bedrock-mapping programme indicates that four major groups of rock types (Table 4-4) and eleven mappable rock units (Figure 4-9) have been identified in the area between road 76 and the coast. Rock groups A, B and C represent a stratigraphic sequence with older, predominantly volcanic rocks represented in Group A, major plutonic rocks with variable compositions represented in Group B, and younger, minor intrusive rocks represented in Group C. The minor intrusive rocks in Group D are younger than the rocks in Groups A and B. However, there are variable time relationships between the rocks in Groups C and D.

Table 4-4. Major groups of rock types recognised during the bedrock-mapping programme 2002.

Rock types
All rocks affected by brittle deformation. The fractures generally cut the boundaries between the different rock types (sealed boundaries).
Rocks in Group D affected, in part, by ductile deformation and metamorphism.

Group D (1,850–1,750 million years)	Fine- to medium-grained granite, aplite, pegmatitic granite and pegmatite. Occur as dykes and minor bodies that are commonly discordant to earlier ductile deformation. Variable age relationships with respect to Group C.

Rocks in Group C affected by ductile deformation under amphibolite-facies metamorphic conditions.

Group C (1,870–1,840 million years)	Fine- to medium-grained granodiorite, tonalite and subordinate granite. Occur as lenses and dykes in Groups A and B. Intruded after some ductile deformation in the rocks belonging to Groups A and B.

Rocks in Groups A and B affected by ductile deformation under amphibolite-facies metamorphic conditions.

Group B (1,903–1,840 million years)	Biotite-bearing granite (to granodiorite) and aplitic granite, both with amphibolite as dykes and irregular inclusions.
	Granodiorite and tonalite to granodiorite with amphibolite enclaves.
	Quartz diorite to gabbro, ultramafic rock.
Group A (1,906–1,891 million years)	Volcanic rocks and iron oxide mineralisation. Sulphide mineralisation.

The candidate area at Forsmark (Figure 4-9) is situated within the northwestern part of a tectonic lens that extends from northwest of the Forsmark nuclear power plants to Kallrigafjärden and further to the southeast. This tectonic lens is characterised by an inferred, generally lower degree of ductile deformation relative to that observed in the marginal domains, both to the southwest and to the northeast (see also Section 4.2.4).
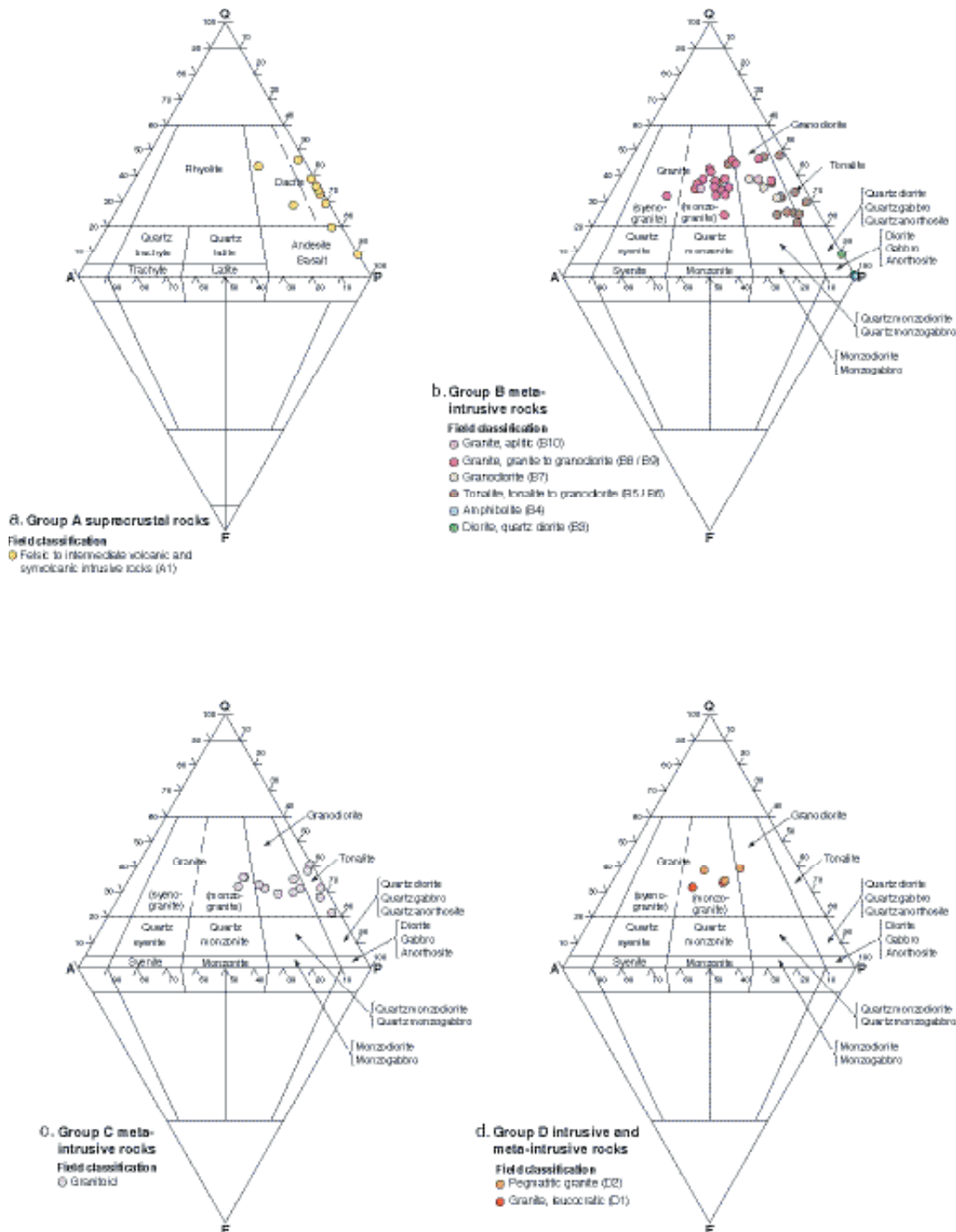
Figure 4-10. QAPF modal classification of the analysed samples in the different rock groups /after Stephens et al, 2003b/. The classification is based on /Streckeisen, 1976, 1978/.

The dominant rock type within the candidate area is a biotite-bearing metagranite that belongs to Group B (Table 4-4). Amphibolite as well as younger felsic meta-intrusive rocks, including pegmatitic rocks, that belong to Groups C and D, form subordinate rock components within the biotite-bearing metagranite. Metamorphosed tonalite to granodiorite and granodiorite form subordinate, mappable rock units within the parts of the candidate area that are situated northwest and south of Storskäret, respectively (Figure 4-9).

Metavolcanic rocks and mineralisation (Group A)

Metavolcanic rocks (yellow colour in Figure 4-9) are a volumetrically important component in the bedrock that occur both to the northeast and to the southwest of the candidate area (Figure 4-9). Due to the effects of ductile deformation and recrystallization under amphibolite-facies metamorphic conditions, considerable uncertainty remains concerning whether these rocks represent juvenile pyroclastic rocks, lavas, synvolcanic intrusions, resedimented volcaniclastic deposits, post-eruptive, volcanogenic sedimentary rocks, or a combination of these possibilities. For purposes of simplification, they are referred to here as metamorphosed volcanic (metavolcanic) rocks.

The metavolcanic rocks are fine-grained and show a medium-K, dacitic or andesitic composition with a dominance of dacites (Figure 4-10a). Most density values are greater than or equal to 2,700 kg/m^3 (Figure 4-11a). These values are consistent with the mineralogical classification based on the QAPF values. Two concentrations of magnetic susceptibility values, at high and low values, appear to be present in the metavolcanic rocks (Figure 4-11a). Uranium contents are not anomalous (Figure 4-12a). The metavolcanic rocks are enriched in large ion lithophile (LILE) relative to high field strength (HFSE) elements (Figure 4-13a), with negative anomalies for Nb and Ta relative to primordial mantle values. These features suggest the influence of a source region for these rocks that was affected, at some stage in its history, by subduction-related processes.

Most samples display evidence for secondary alteration processes. At least some of the volcanic rocks have been affected by an alteration that modified the relative contents of the alkali elements Na and K. Plagioclase feldspar is commonly affected by saussuritization and/or sericitization. Epidote and chlorite (after biotite) are also common secondary minerals. Other secondary minerals include goethite (after pyrite), prehnite and calcite.

Iron oxide mineralisation, that is associated with calc-silicate rock (skarn) and, locally, contains base metal sulphides, is the most important type of mineralisation in the Forsmark area *(darker grey colour and symbols in Figure 4-9)*. Density and magnetic susceptibility values for two samples are 4,225 and 4,130 kg/m^3 and 0.124 and 0.122 SI units, respectively. The metavolcanic rocks that are situated to the southwest and northwest of the candidate area host this type of mineralisation. Seven localities are present where some mining or exploration activity (or both) has taken place in historical time (Figure 4-9). A metagranodiorite (Group B) in the westernmost part of the mapped area hosts a second type of mineralisation that consists of *base metal and iron sulphides (paler grey colour and symbol in Figure 4-9)*. A more detailed documentation of metallic mineralisations and industrial minerals in the Forsmark area, and the potential of this area for exploration and exploitation activities, are addressed in a complementary report /Lindroos et al, 2004/.

The metavolcanic rocks and the iron oxide mineralisations belong to the Svecofennian, predominantly supracrustal rocks that are common in the Bergslagen area and its surroundings in central-eastern Sweden. These rocks show a range of U-Pb (zircon) ages of c 1,906–1,891 million years. The metavolcanic and iron oxide mineralisations are inferred to have formed during phase 1 of the geological evolution of this part of the Fennoscandian Shield (see Section 3.1).

Ultramafic, mafic, intermediate and felsic (quartz-rich) meta-intrusive rocks (Group B)

The plutonic rocks within this group are, volumetrically, the most important group of rock types in the Forsmark area. Medium-grained, equigranular intrusive rocks dominate and show a wide variety of compositions that range from ultramafic (olivine-hornblende pyroxenite) to mafic (gabbro), intermediate (diorite, quartz diorite) and felsic (tonalite, granodiorite and granite). This range in compositions is also reflected in the wide variation in density values (Figure 4-11b). Ductile deformation and recrystallization under amphibolite-facies metamorphic conditions have affected all the rocks in Group B.

The ultramafic-intermediate rocks form isolated plutons that are commonly strongly drawn out in the direction of the mineral stretching lineation (see Section 4.2.4). These bodies are prominent both to the southwest and to the north of the candidate area (Figure 4-9) /SKB, 2002a/. Plutons dominated by *ultramafic rocks (darker green colour in Figure 4-9)* have been separated on the geological map from plutons dominated by *gabbro, diorite and quartz diorite (paler green colour in Figure 4-9)*. The major ultramafic body in the southeastern part of the mapped area corresponds to a high magnetic anomaly.
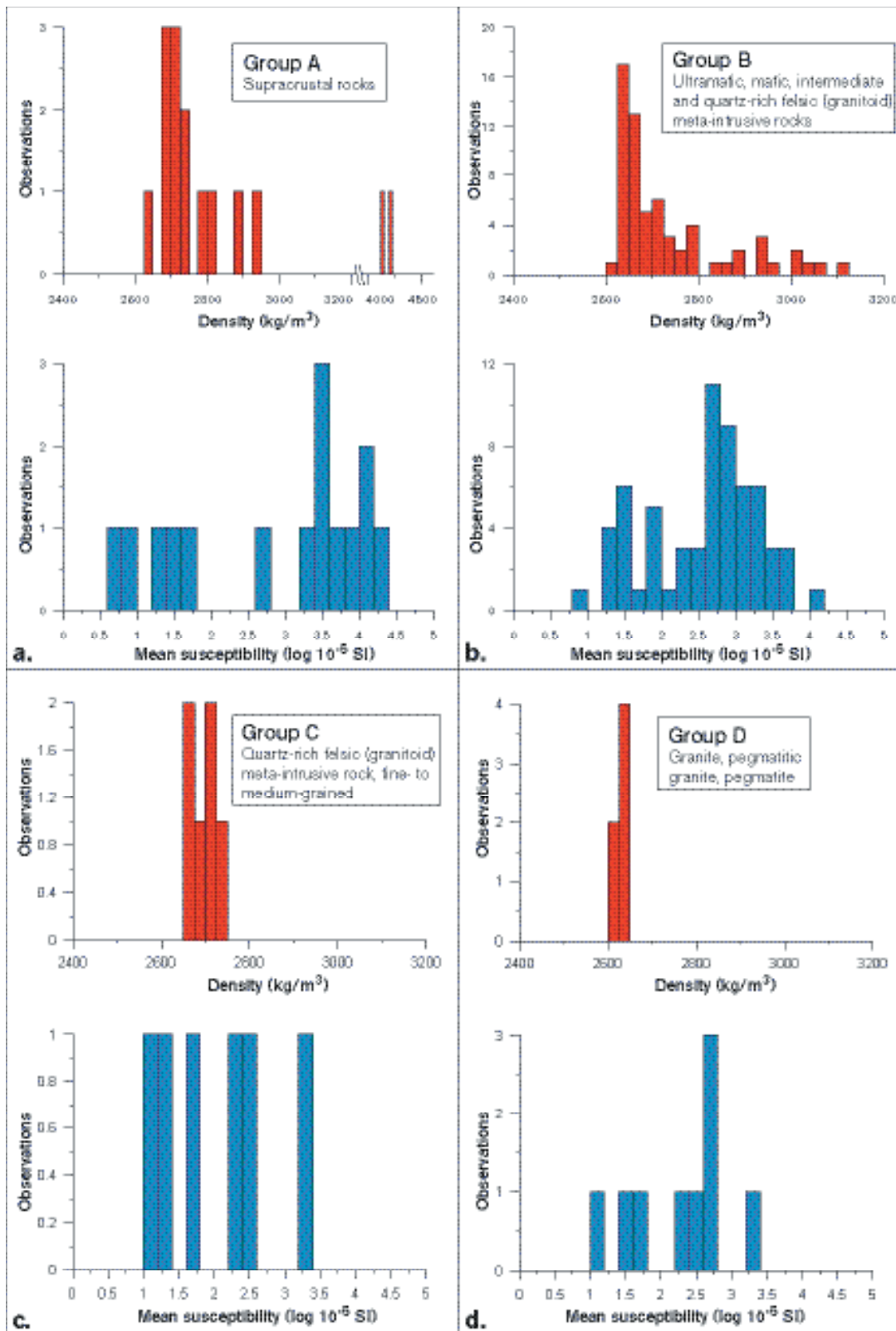
Figure 4-11. Histograms showing the distribution of density (red) and magnetic susceptibility (blue) values in the analysed samples in the different rock groups (modified after /Isaksson et al, 2004a/).

An important mineralogical feature of the felsic varieties is that they are quartz-rich, i.e. they belong to the group of felsic intrusive rocks referred to as granitoid. All recalculated quartz values on the QAPF plot are greater than 20% (Figure 4-10b). Three rock units that are medium-grained have been

separated on the geological map. Rocks with *tonalitic to granodioritic*, *granodioritic*, and *granitic (to granodioritic)* compositions dominate each of these units *(three different shades of brown colour in Figure 4-9)*. Biotite-bearing metagranite is the most conspicuous rock type in the candidate area at Forsmark (Figure 4-9). The average density of this rock is 2655 ± 11 kg/m³. A fourth unit, dominated by a rock that is *aplitic and granitic* in composition, has also been identified *(beige colour in Figure 4-9)*. This unit is prominent in the coastal area south and west of SFR (Figure 4-9).

Two concentrations of magnetic susceptibility values, with high and low values, respectively, appear to be present in the Group B intrusive rocks (Figure 4-11b). A more detailed discussion of the spread in the magnetic susceptibility data for the Group B rocks, including both laboratory and outcrop measurements, is presented in /Isaksson et al, 2004a/. The following key features are apparent:

• The concentration of low magnetic susceptibility values for the mafic and intermediate rocks.

• The presence of two concentrations of magnetic susceptibility values, at high and low values, in the metatonalites to metagranodiorites.

• The similar distribution pattern for magnetic susceptibility shown by the biotite-bearing metagranite (to metagranodiorite) and the aplitic metagranite, with a concentration at moderate to high values.
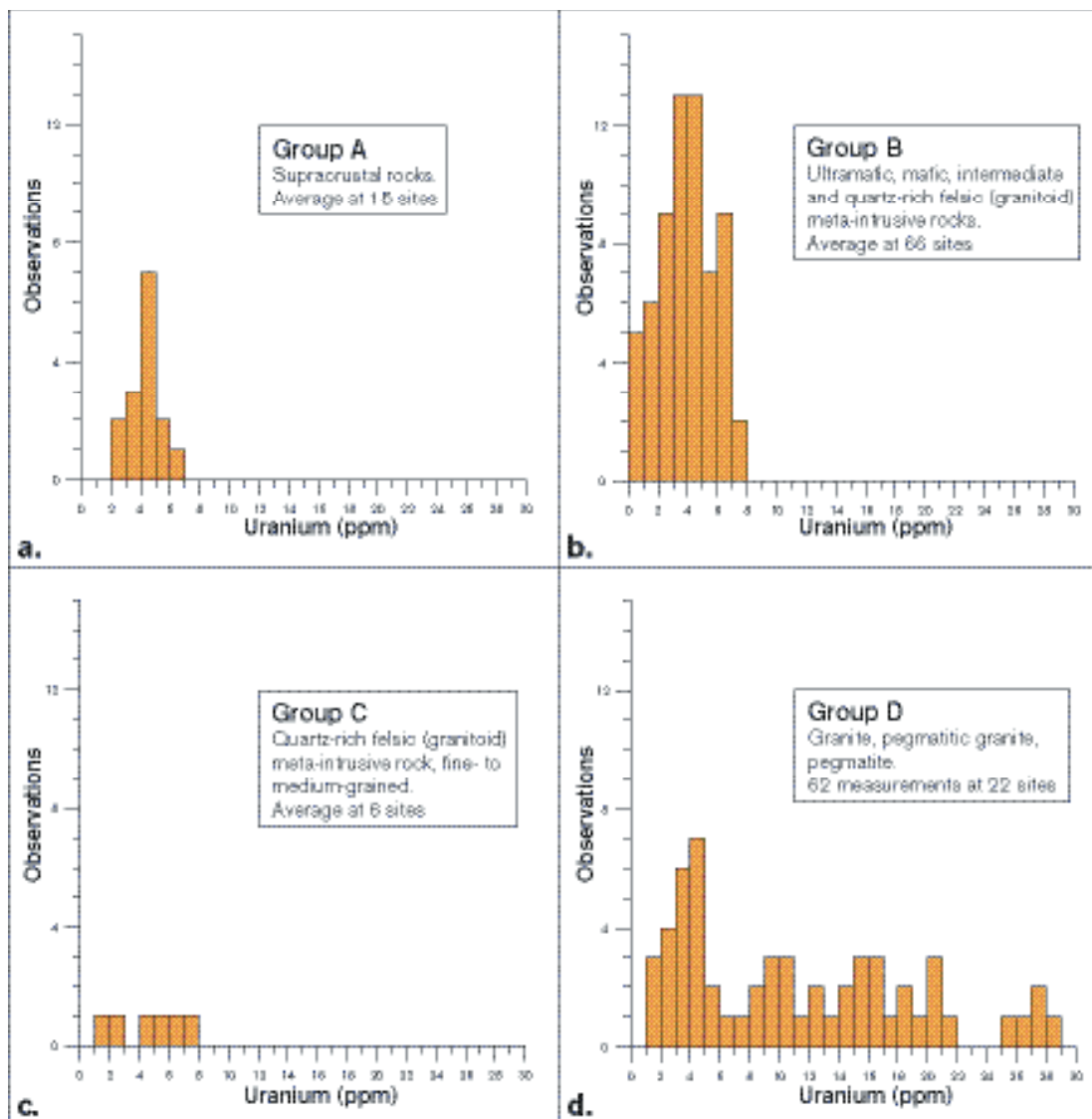
Figure 4-12. *Histograms showing the uranium content (ppm) for the in situ, gamma-ray spectrometry measurements in the different rock groups (modified after /Isaksson et al, 2004a/).*

The Group B plutonic rocks show a calc-alkaline trend and the felsic rocks are peraluminous (to metaluminous). The uranium values are not anomalous (Figure 4-12b). As for the volcanic rocks, the Group B rocks are enriched in large ion lithophile (LILE) relative to high field strength (HFSE) elements (Figure 4-13b and c). The felsic rocks, in particular, show distinctive depletions in the elements Nb and Ta relative to primordial mantle values (Figure 4-13c). The trace element compositions in these rocks indicate the influence of one or more source regions for these rocks that were affected, at some stage in their history, by subduction-related processes.

Some of the metagranites and amphibolites have been affected by an alteration that modified the relative contents of the alkali elements Na and K. Serpentine has formed after olivine in parts of the major ultramafic body in the southern part of the mapped area. Plagioclase feldspar in the intermediate and felsic members is commonly affected by saussuritization and/or sericitization. Epidote is also a common secondary mineral. Other secondary minerals include chlorite (after biotite), goethite (after pyrite), prehnite and calcite.

The Group B intrusive rocks belong to the early-tectonic suite of intrusive rocks that dominate large areas in the eastern part of central Sweden. These rocks show a range of U-Pb (zircon) ages in the time period c 1,903–1,840 million years. The Group B plutonic rocks formed during phase 1, during phase 2 or during both of these phases in the geological evolution in this part of Sweden (see Section 3.1).
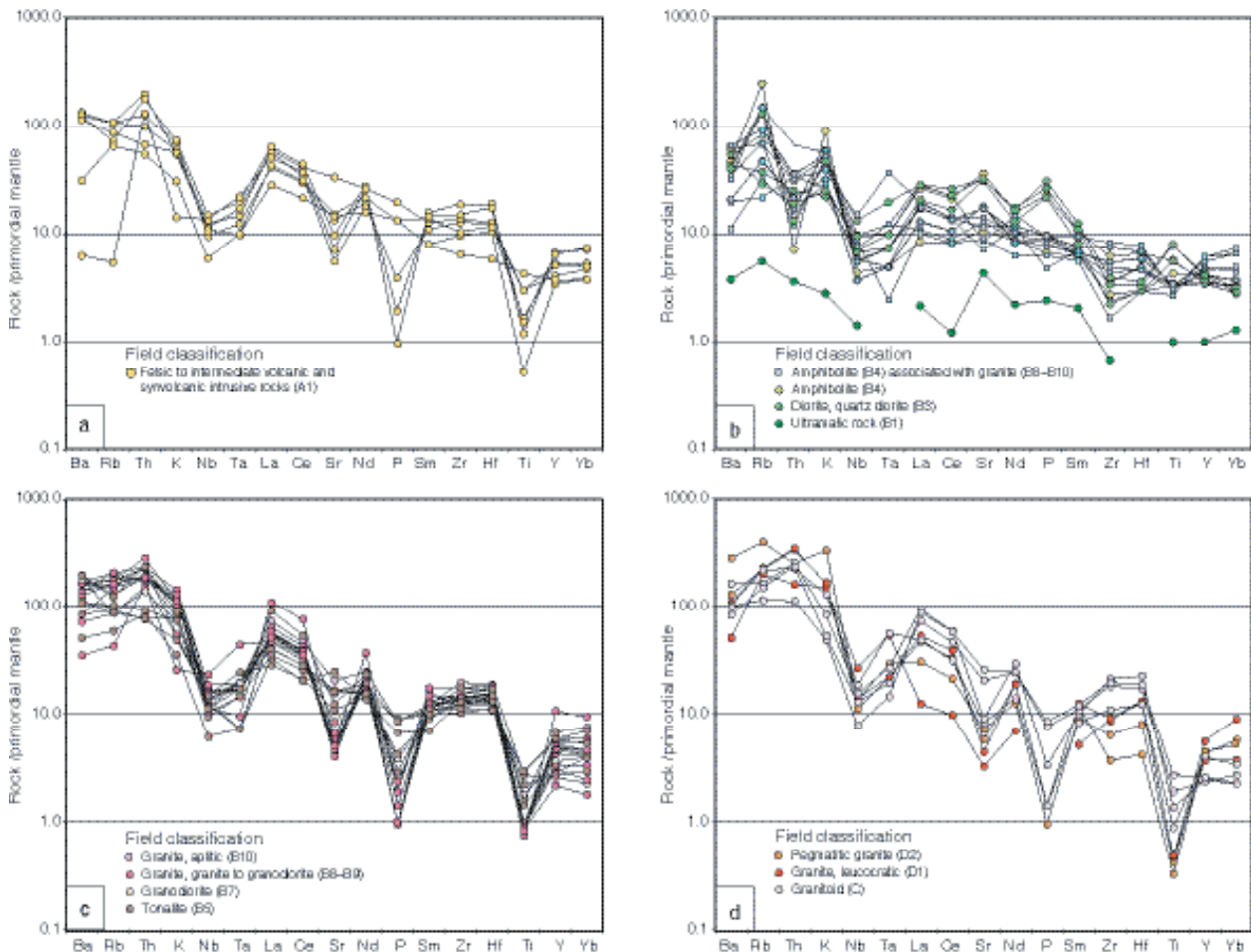
Figure 4-13. *Relationships between large ion lithophile (LILE, e.g. Ba, Rb) and high field strength (HFSE, e.g. Zr, Ti and Y) elements for the analysed samples in the different rock groups /after Stephens et al, 2003b/. The element values in each sample have been normalised against the respective values for primordial mantle /McDonough et al, 1992/.*

Fine- to medium-grained, felsic (quartz-rich) meta-intrusive rocks (Group C)

The intrusive rocks within this group are a subordinate component in the Forsmark area. Only a limited number of larger intrusive bodies, predominantly in the western part of the mapped area, are inferred to be present at the surface *(few small areas with a pale pinkish colour in Figure 4-9)*. Nevertheless, the rock type is a relatively common, subordinate component in outcrop.

As for the older felsic intrusive rocks, the Group C intrusive rocks are rich in quartz and belong to the granitoid group. They are distinguished from the Group B felsic intrusive rocks on the basis of their grain size and their field occurrence.

The Group C intrusive rocks are fine- to medium-grained and occur as smaller lens-shaped massifs, possible boudins or dyke-like bodies in the rocks belonging to both Groups A and B. They display a ductile deformational mineral fabric and have been affected by amphibolite-facies metamorphism. The mineral fabric is more commonly linear in character. At several places, the contacts of these bodies are discordant to a planar mineral fabric or an inferred tectonic banding in the adjacent host rocks. They intruded after at least some deformation had affected the rocks within Groups A and B but prior to later ductile deformation and metamorphism.

The Group C intrusive rocks show a compositional bias towards granodioritic and tonalitic compositions (Figure 4-10c). Their average density is $2,701 \pm 30$ kg/m^3. Magnetic susceptibility values are variable (Figure 4-11c). They are mineralogically and geochemically similar to the Group B felsic intrusive rocks and form a second generation of calc-alkaline intrusive rocks in the Forsmark area. In particular, the U contents (Figure 4-12c) and the element distribution pattern on the LILE/HFSE diagram (Figure 4-13d) are identical to those observed for the Group B felsic rocks. The secondary minerals are also similar to those observed in the Group B felsic rocks.

The composition and intrusion-deformation relationships are reminiscent of the igneous and tectonic development in, for example, the Askersund area in the southwestern part of the Bergslagen geological province /Wikström, 1996; Wikström and Karis, 1998/ or the Loos-Kårböle-Ljusdal area in the central part of Sweden /Delin, 1993, 1996; Delin and Persson, 1999/. Metagranitoids in these areas have yielded U-Pb (zircon) ages around c 1,850 and in the period c 1,870–1,840 million years, respectively. If this correlation is correct, then the Group C rocks formed during phase 2 of the geological evolution in this part of the Fennoscandian Shield (see Section 3.1).

Granite, pegmatitic granite and pegmatite (Group D)

The intrusive rocks in Group D are a common, yet subordinate component in outcrop. Only a limited number of larger intrusive bodies of pegmatitic granite are inferred to be present at the surface *(orange colour in Figure 4-9)*. They display variable time relationships to the rocks in Group C and, in places, it has proven difficult to separate the Group D granites from the Group C rocks with granitic composition.

The granites are fine- or medium-grained and generally show low contents of biotite. Aplites are included in this subgroup. All these rocks occur as minor bodies or dykes. Some of these dykes are zoned in character with a thin pegmatitic rim along the margins of the dyke. The granites are distinctly discordant to the banding and mineral fabric in the older rocks that belong to Groups A, B and C. They are inferred to form the youngest rocks in the area.

The term pegmatitic granite has been applied to those rocks where the grain size is highly variable and irregularly distributed, often from pegmatite to fine- to medium-grained, leucocratic granite to aplite, in a single body. Pegmatitic granite commonly occurs as irregular concentrations along the contacts to and as injections within the Group C rocks. These field relationships suggest that pegmatitic granite intruded close in time to or after intrusion of the Group C rocks.

Pegmatite occurs as discontinuous bands, lenses and segregations, as more irregular minor bodies and as dykes. These features display highly variable relationships to the ductile deformation in the rocks that belong to Groups A, B and C. Some pegmatites are tightly folded and concordant to the banding and mineral fabric in the host rocks. Other pegmatites show distinctly discordant relationships but are, nevertheless, commonly weakly folded. Different generations of pegmatite are inferred to be present.

The Group D rocks show low densities (< 2,635 kg/m^3) and variable magnetic susceptibilities (Figure 4-11c). The element distribution pattern on the LILE/HFSE diagram (Figure 4-13d) is once again similar to that observed for the Group B felsic rocks. By contrast, a distinctive geochemical feature of the Group D rocks is the more variable content of uranium (Figure 4-12d), in part with anomalously high values (> 16 ppm U). The pegmatites and pegmatitic granites that are rich in uranium and show high natural exposure rates are commonly situated southwest and west of the candidate area. Epidote, chlorite and a conspicuous saussuritization/sericitization of plagioclase feldspar form the main secondary minerals in the Group D rocks.

Bearing in mind a reservation for some of the pegmatites, the Group D intrusive rocks are inferred to belong to the late-tectonic suite of intrusive rocks in the Bergslagen area and its surroundings. These rocks display U-Pb (zircon) ages of c 1,850–1,750 million years. They are inferred to have formed during phase 2 of the geological evolution in central-eastern Sweden (see Section 3.1).

Bedrock inhomogeneity

Bedrock inhomogeneity can be assessed at different scales. Inspection of the bedrock geological map (Figure 4-9) reveals belts of inhomogeneous bedrock on the several hundred metres to kilometre scale especially southwest and west of the candidate area, and along the coast to the north of the candidate area.

Inhomogeneity at the outcrop scale has been documented in the bedrock-mapping programme. The subordinate rocks in each outcrop have been registered in the outcrop database in their relative order of importance at the outcrop. However, numerical data that estimate the volume of each rock type at outcrop are lacking. Bedrock inhomogeneity at outcrop scale is illustrated more schematically in the bedrock map database. For purposes of clarity, this information has not been included in Figure 4-9. The subordinate rock types in outcrop occur as:

• Xenoliths of predominantly supracrustal rocks within intrusive rocks.

• Amphibolite that occurs as enclaves in tonalite, and as dykes and irregular inclusions in the biotite-bearing metagranite (to metagranodiorite) and the aplitic metagranite.

• Dykes and minor intrusions of granite, aplite, pegmatitic granite and pegmatite.

• Bands and lenses of one rock type within another. The bands and lenses may be deformed inclusions, deformed dykes or both these possibilities.

The various inclusions, bands and lenses and the amphibolite dykes generally trend parallel or subparallel to the tectonic foliation, whereas the younger granite, aplite, pegmatitic granite and pegmatite dykes and minor intrusive bodies display a more varied orientation.

The medium-grained metagranite that dominates the candidate area contains subordinate contents of other rock types. These include dykes and irregular inclusions of amphibolite, minor intrusions of fine- to medium-grained metagranitoid (Group C), and dykes and minor intrusions of younger granite, aplite, pegmatitic granite and pegmatite (Group D). In the northwestern part of the candidate area, aplitic metagranite also locally intermingles with the medium-grained metagranite.

4.2.3 Lineament identification

Data and inferred lineaments

The identification of lineaments has been carried out at different times and using different sets of data in three separate areas (Figure 4-14):

• The area on the mainland.

• The sea area northeast of the candidate area, including the islands.

• The outboard area to the northeast under Öregrundsgrepen and on Gräsö.
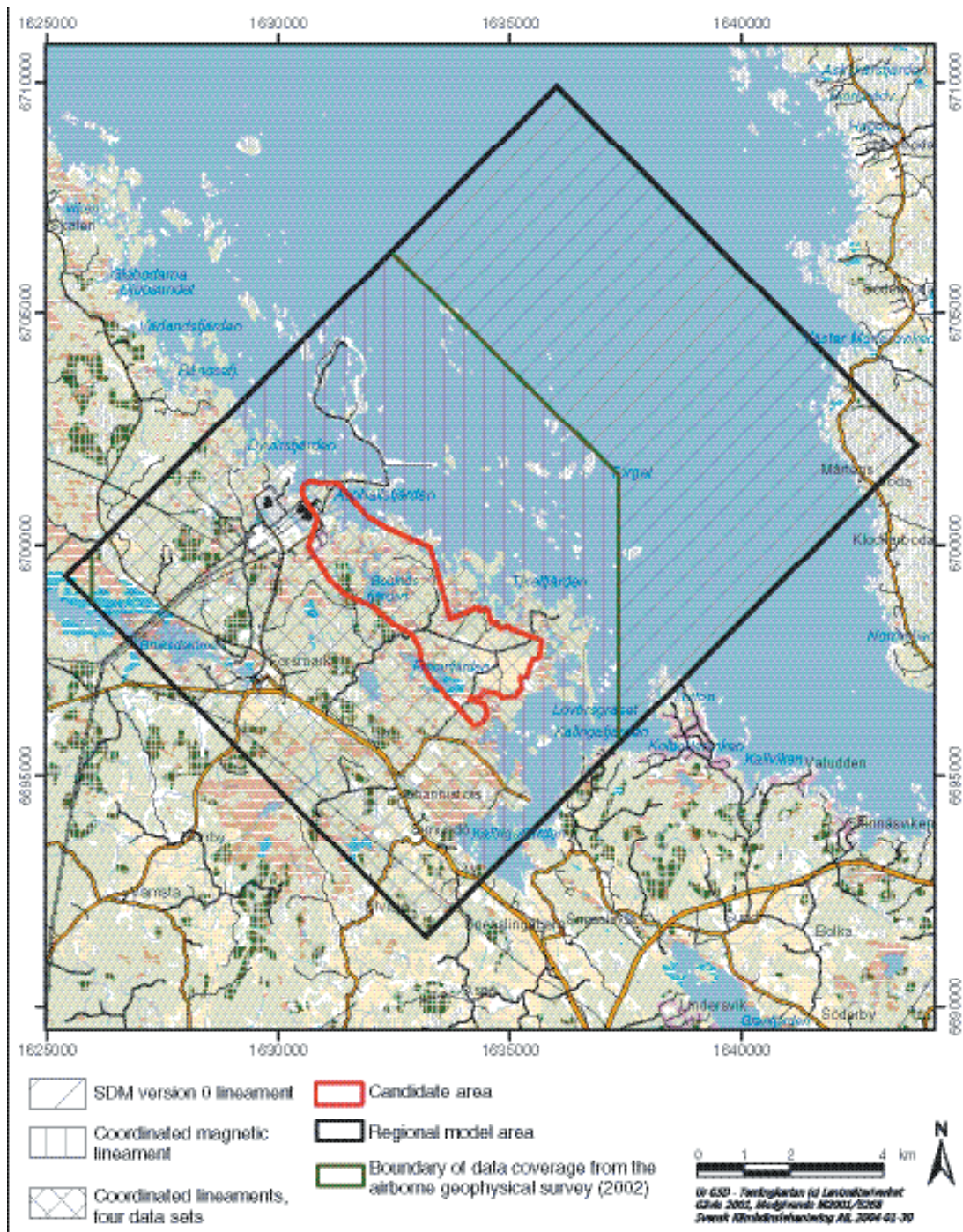
Figure 4-14. *Basis upon which lineaments have been identified in the regional model area.*

Lineaments in the *mainland area* have been identified on the basis of a coordinated interpretation of four sets of data, each of which has been interpreted separately /Isaksson et al, 2004b/. These lineaments are referred to as *coordinated lineaments* /Isaksson et al, 2004b/ and are based on:

- Lineaments interpreted from airborne, magnetic data /Isaksson et al, 2004b/.

- Lineaments interpreted from airborne, electromagnetic (EM) data /Isaksson et al, 2004b/.

- Lineaments interpreted from airborne, very low frequency electromagnetic (VLF) data /Isaksson et al, 2004b/.

- Lineaments interpreted from topographic data /Isaksson, 2003; Isaksson et al, 2004b/.

The airborne magnetic, EM and VLF data were obtained from helicopter measurements during 2002 /Rønning et al, 2003/. The flight line spacing of the airborne measurements was 50 m in a north-south direction over a larger area and 50 m in both north-south and east-west directions in a smaller domain that includes the candidate area (Figure 4-15). Tie lines were flown every 500 m in both directions. The normal ground clearance for the measuring instrument was c 30–60 m. Data were acquired at a measurement interval of 0.1 seconds (c 3 m spatial interval) for the magnetic and EM data, and 0.2 seconds (c 6 m) for the VLF data. No measurements were carried out over the nuclear power plants (Figure 4-15). There are also disturbances in the measurements along power lines and a DC-cable. The data coverage for the different methods is shown in Figure 4-15.

The airborne, geophysical data have been processed with a grid cell size of 10x10 m. Older airborne geophysical data that cover the Forsmark area were utilised in the areas where new airborne geophysical data are either absent or disturbed. The data processing and methodology used in connection with the interpretation work and the resulting three sets of lineaments derived from each data set are described in /Isaksson et al, 2004b/. Low magnetic lineaments that are discordant to the banding and tectonic foliation in the bedrock, and magnetic connections that occur as minima parallel to these structures are both included in the magnetic lineaments. A map of the airborne magnetics, based on the north-south survey, is displayed in Figure 4-16.

The topographic data were produced from aerial photographs taken at a height of 2,300 m and with a 0.2 m spatial resolution /Wiklund, 2002/. Both orthorectified, infrared aerial photographs and a digital terrain model have been used in the interpretation of topographic lineaments. The digital terrain model utilised an elevation grid cell size of 10x10 m and elevation contours with 1 m equidistance /Wiklund, 2002/. The data processing and methodology used in connection with the interpretation work and the resulting topographic lineaments are described in /Isaksson, 2003/ and /Isaksson et al, 2004b/. The topographic map, based on the digital terrain model for the area, is displayed in Figure 4-17.

The airborne EM and VLF data provide limited possibilities to recognise lineaments in the *sea area northeast of the candidate area*. Furthermore, new bathymetric data from the marine geological investigations were not available prior to May 2003. For these reasons, only the new airborne magnetic data have been used to interpret lineaments in this area. The lineaments in this area are referred to as *coordinated magnetic lineaments* /Isaksson et al, 2004b/.

In the *outboard area under Öregrundsgrepen and on Gräsö*, no new data have been generated in connection with the site investigation programme. For this reason, lineaments in this area have been adopted for modelling purposes (see Section 5.1.2) from the Site Descriptive Model version 0. The lineaments in this area are referred to as *version 0 lineaments*.

The following information was provided for each of the coordinated lineaments on the mainland and the coordinated magnetic lineaments in the sea area, northeast of the candidate area:

- The method or methods (magnetics, EM, VLF and topography) used to identify the lineament, arranged in order of priority.

- An estimate of uncertainty of the lineament, graded as low, medium and high. In effect, this attribute is an expert judgement concerning the degree of clarity of the lineament.

- An estimate of how well the lineament is defined in space. A value in the range 10–100 m with a general estimate at 20 m has been provided.
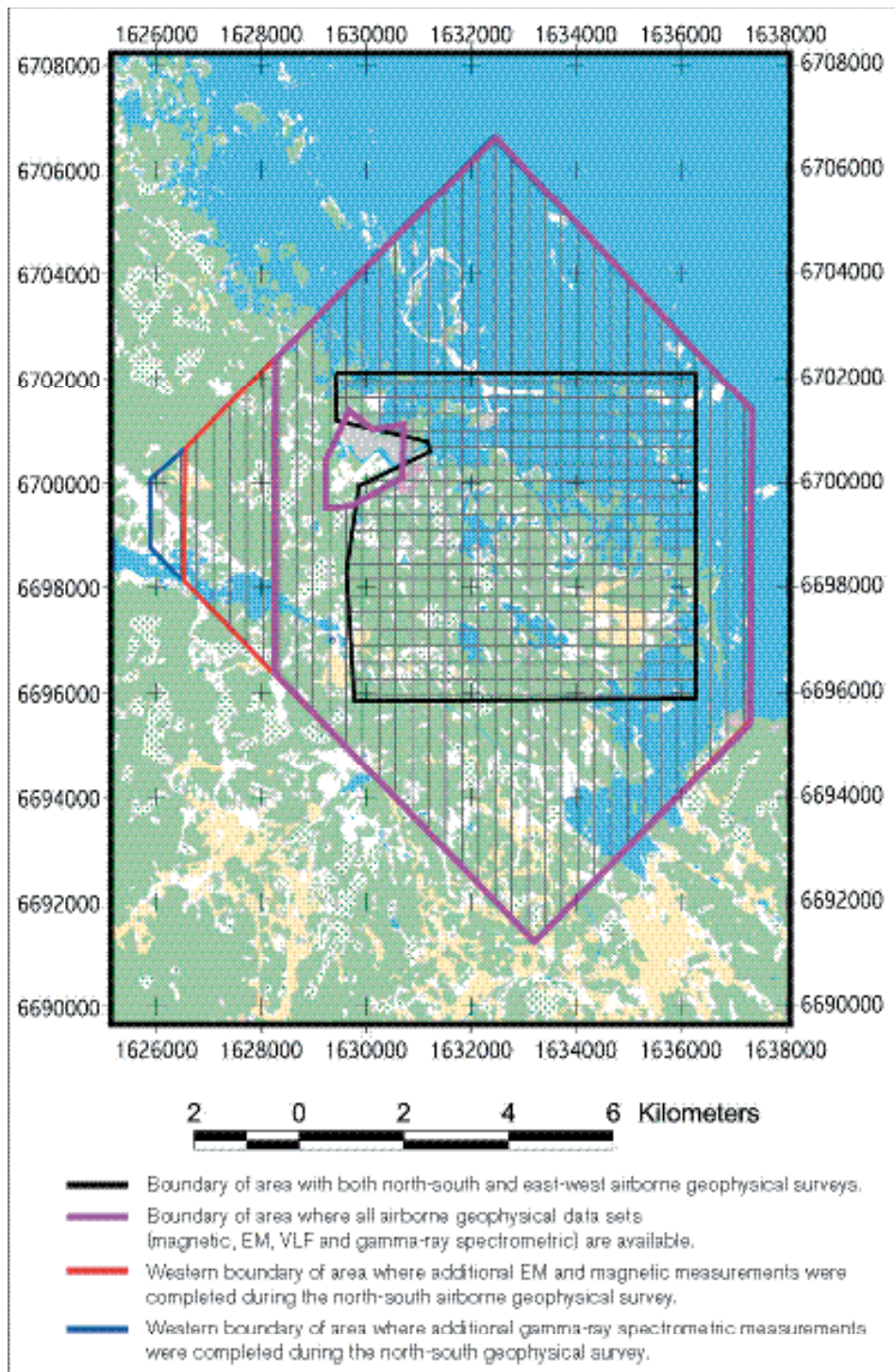
Figure 4-15. *Map showing airborne geophysical data coverage. No data were acquired in the vicinity of the nuclear power plants /after Isaksson et al, 2004b/.*
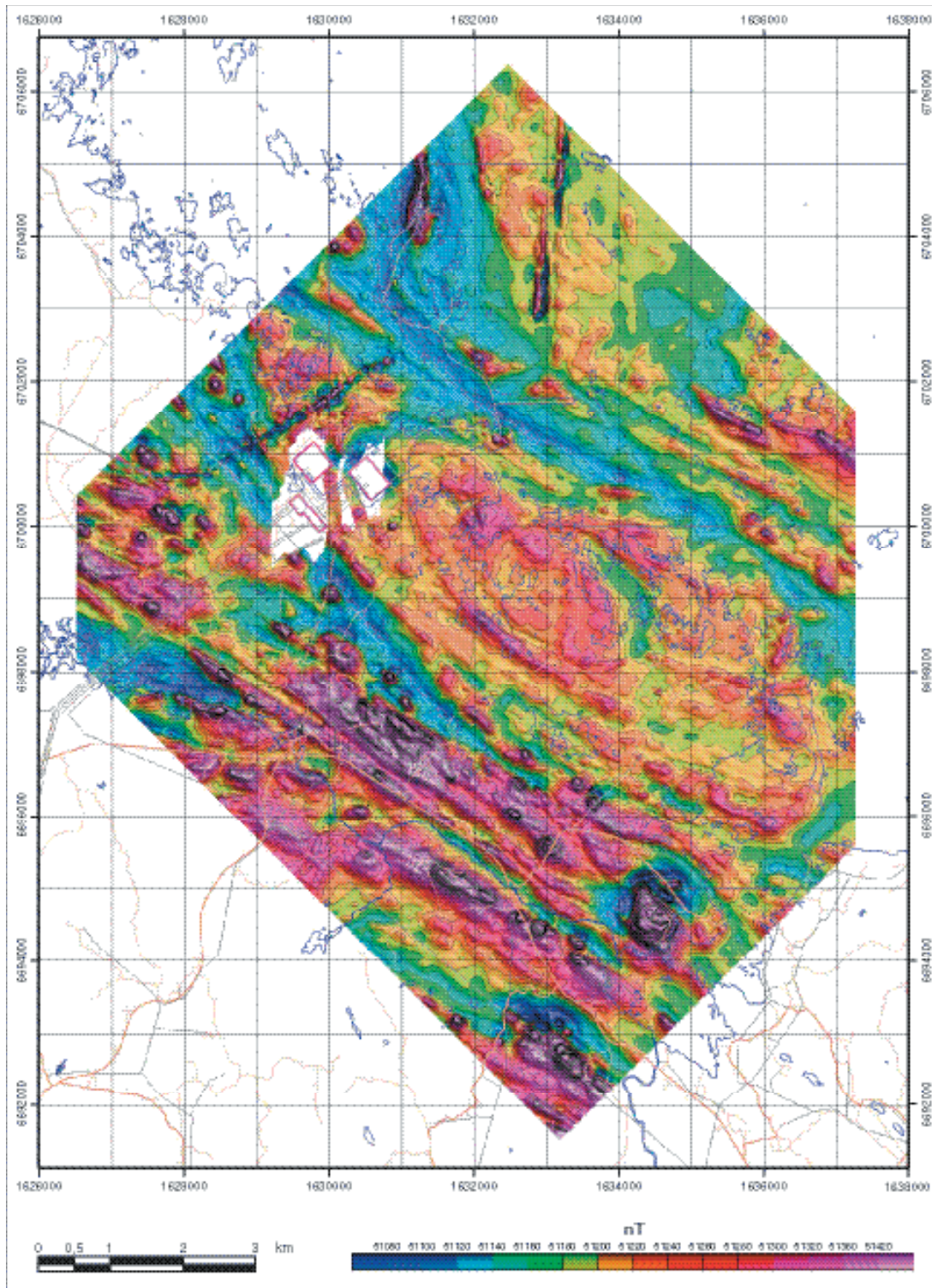
Figure 4-16. *Map of the magnetic total field that was derived from the results of the airborne (helicopter), geophysical survey in a north-south direction. The red-lilac end of the colour spectrum indicates strongly magnetic bedrock and the blue end of the spectrum indicates weakly magnetic bedrock. Data are lacking in the vicinity of the nuclear power plants and are disturbed by a DC-cable in the area northwest of the power plants and under Öregrundsgrepen northeast of the power plants (along coordinate grid line 1633000).*
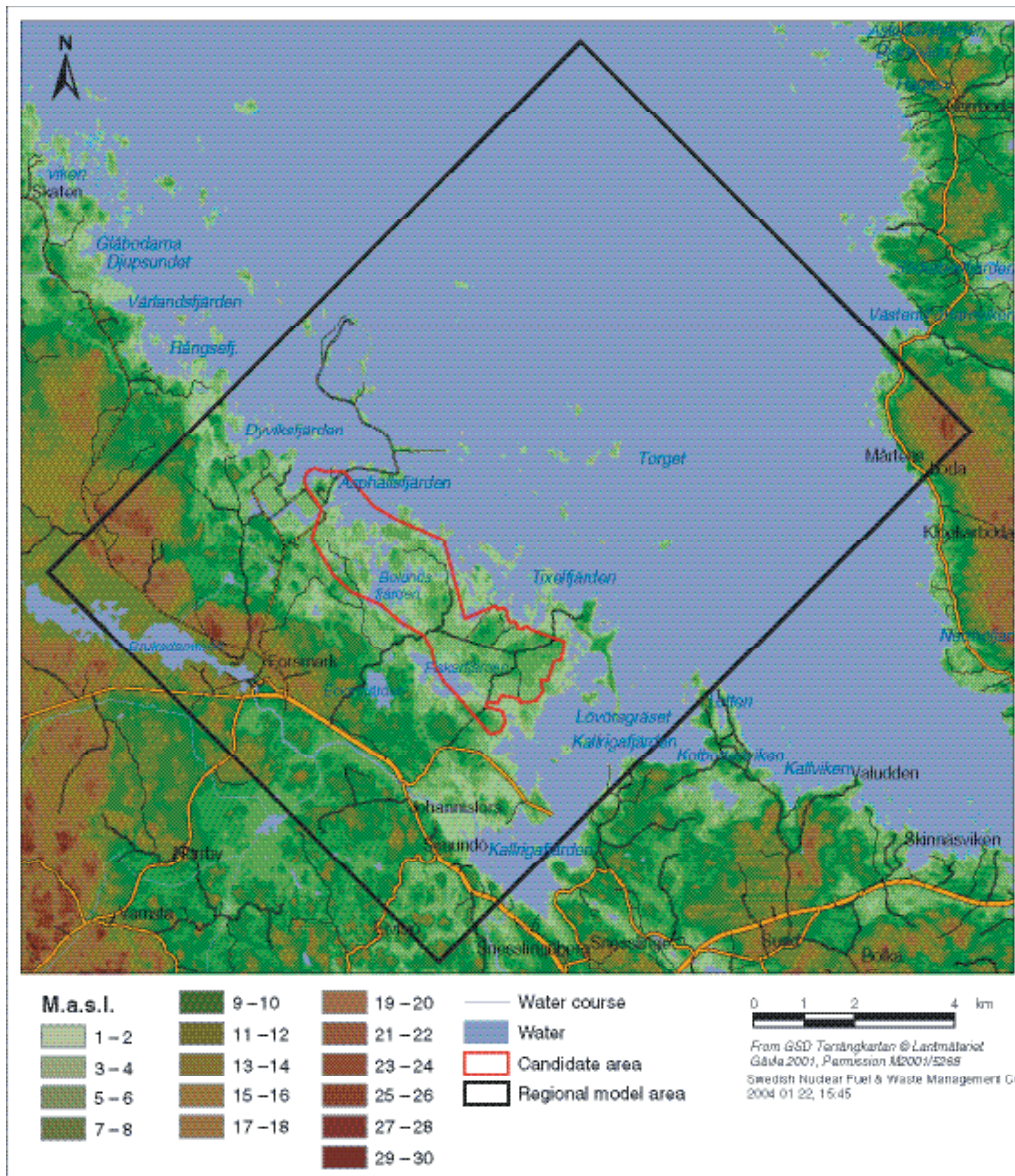
Figure 4-17. Topographic map of the Forsmark area based on data in /Wiklund, 2002/.

Evaluation

During the interpretation of the lineaments, an individual coordinated lineament has been defined until it did not prove possible to identify the lineament with the help of a particular method or if a new method was used to identify the lineament. At this point, the lineament was split and a new coordinated lineament defined with a new method ranking. This process has been adopted even though there is a high degree of confidence that the lineament continues. Since it is important to know the lengths of lineaments, it was judged necessary to link the various segments along what is judged with confidence to be the same lineament. These *linked lineaments* have been assigned the following attributes:

• ID-number according to SKB's recommendations (XFMxxxxxx).

• The character of the lineament (coordinated, coordinated magnetic, version 0).

• The number of original segments along the linked lineament.

• The property that has been used to identify the linked lineament (1=magnetics, 2=electrical conductivity based on combined EM and VLF, 3=topography). A weighted average has been calculated for each property, according to the length of each segment in the linked lineament.

- An estimate of uncertainty of the linked lineament, graded as 1=low, 2=medium and 3=high. In effect, this attribute is an expert judgement concerning the degree of clarity of the lineament. A weighted average has been calculated according to the length of each segment in the linked lineament.

- An overall assessment of the quality of the linked lineament. This assessment is based on both the number of properties (1 to 3) upon which the lineament has been identified and the degree of uncertainty (1 to 3). A weighted average, graded continuously from 1=low quality to 5=high quality, has been calculated according to the length of each segment in the linked lineament.

- The length of each linked lineament.

- The average trend of each linked lineament.

- An estimate of how well the linked lineament is defined in space. A value in the range 10–100 m with a general estimate at 20 m has been provided.

879 linked lineaments have been identified in the analysis of the airborne geophysical and topographic data in the regional model area (Figure 4-18). 851 of these lineaments have a unique identity number (first seven positions of the ID-number, XFMxxxx). 28 linked lineaments form separate segments along what is judged with confidence to be part of the same lineament. These segments have a different denomination in positions 8 and 9 in the ID-number. Approximately 700 lineaments are less than 1 km in length and only seven of the lineaments with a unique identity number are longer than 10 km. A statistical evaluation of the lineaments, including the recognition of orientation sets and their relationships to the various fracture sets, is provided in Section 5.1.6.
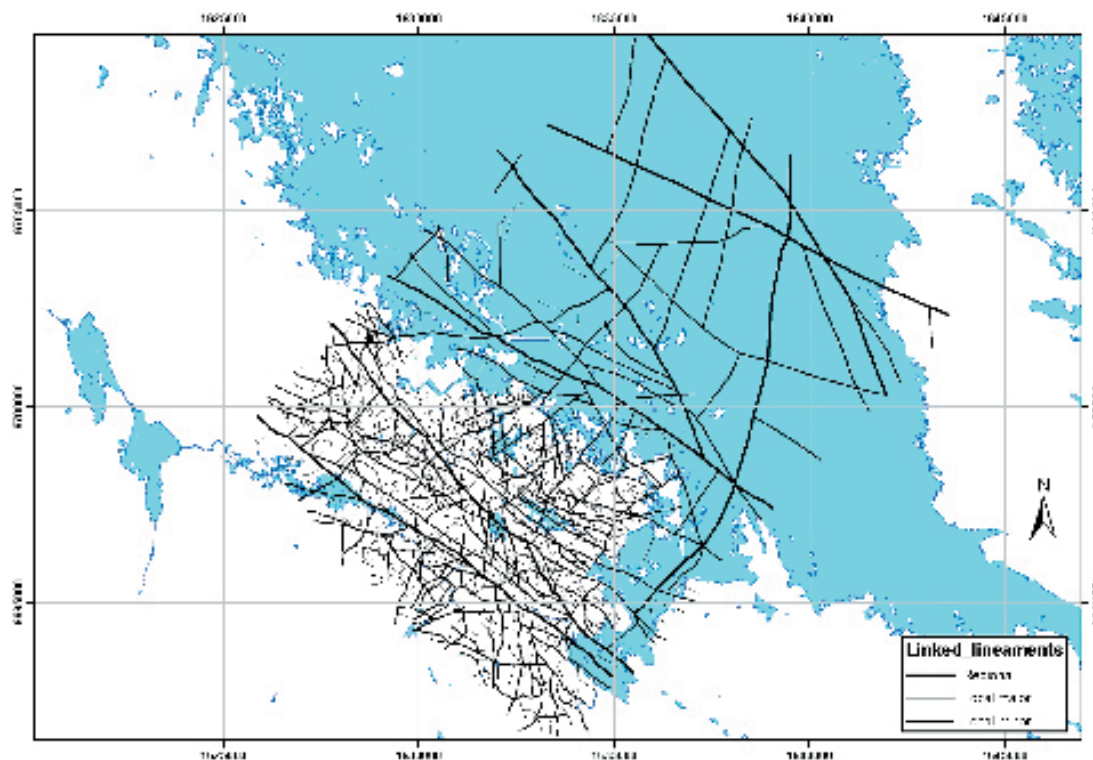
Figure 4-18. *Linked lineaments in the regional model area.*
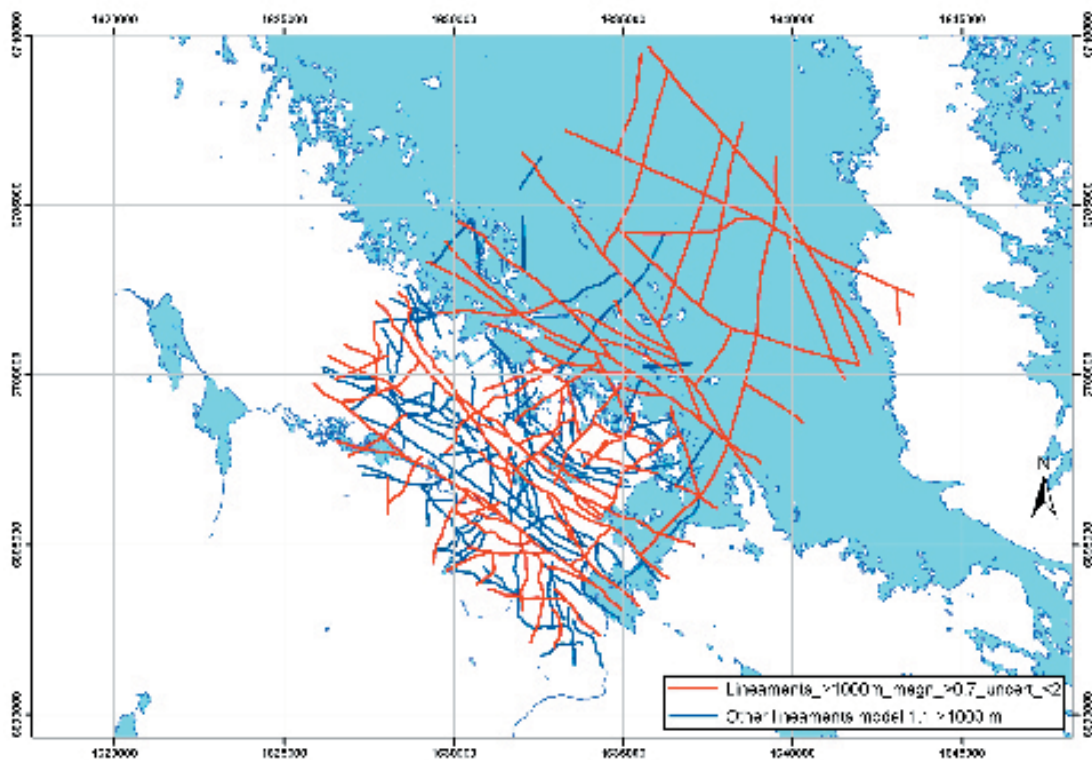
Figure 4-19. Regional and local major linked lineaments. The map separates lineaments that show both a high degree of clarity and are solely or predominantly defined by a low magnetic anomaly (red) from all the other linked lineaments in the same length class (blue).

Lineaments based on low magnetic anomalies are judged with confidence to be related to structural features in the bedrock. By contrast, it is more difficult to judge whether a lineament based on electrical conductivity or topographic data is related to structures in the bedrock or to features in the Quaternary cover. The majority of linked lineaments that are longer than 1 km show both an uncertainty rating that is < 2, and a method of identification that solely or strongly (≥ 70% along the length of the linked lineament) made use of the magnetic data (Figure 4-19). By contrast, nearly 60% of the lineaments that are shorter than 1 km are based solely on topographic data.

4.2.4 Ductile and brittle structures

Data

Raw data, which document the character and orientation of ductile and brittle structures at the surface, have been assembled during 2002, in connection with the bedrock-mapping programme at Forsmark. The data have been assembled essentially in the area between road 76 and the coast, including the candidate area, and consist of the following components (Figure 4-20):

- The measurements of ductile structures and bedrock contacts at 819 of the 1,054 outcrops (Figure 4-20a) that were mapped in connection with the field activities during 2002 /Stephens et al, 2003a/. These structural data were subsequently evaluated and interpreted in /Stephens et al, 2003b/.

- The laboratory measurements of the anisotropy of magnetic susceptibility (AMS) that were carried out on samples from 80 outcrops (Figure 4-8c) /Mattsson et al, 2003/. These data were subsequently evaluated and interpreted in /Isaksson et al, 2004a/.

- The documentation of minerals that fill fractures in 80 of the 1,054 outcrops referred to above /Stephens et al, 2003a/.

- The detailed mapping of fractures (including fracture fillings) that are longer than 50 cm in two cleaned outcrops at drillsites 2 and 3 (Figure 4-20b) /Hermanson et al, 2003/. These outcrops are c 600 m² in areal extent.

- The measurements of the frequency and orientation of fractures that are longer than 100 cm in 44 of the 1054 outcrops referred to above /Stephens et al, 2003a/. Fracture fillings were also noted in some of these outcrops. The 44 outcrops are located predominantly within the candidate area (Figure 4-20b) and the data were subsequently evaluated and interpreted in /Stephens et al, 2003b/.

This section focuses attention on the ductile structures, including the AMS values, and presents some evaluation of the brittle structures. A statistical evaluation of the character, orientation and intensity of fractures from the surface outcrops is included in Section 5.1.6.

Evaluation of ductile structures

The ductile structural data have been divided into three separate subareas (Figure 4-20a). Each of these subareas is judged to be homogeneous with respect to the character of the ductile deformation in the bedrock and they are referred to as subarea SW, subarea central and subarea NE. These sub-areas correspond to domains A, B and C, respectively, that were recognised during the Östhammar feasibility study /Bergman et al, 1998/. Subarea central includes the candidate area at Forsmark and forms part of a tectonic lens in which the ductile deformation is inferred to be generally lower relative to that in subareas SW and NE.

In each subarea, the poles to measured ductile planar structures, that are referred to as foliation, banding or combined foliation and banding in the outcrop database, have been plotted on the lower hemisphere of a Schmidt stereographic projection. The foliation corresponds to a planar grain-shape fabric. In the dominant felsic rocks that belong to Groups A and B, this fabric is defined by oriented grains of biotite and, locally, hornblende, as well as elongate aggregates of recrystallised quartz and feldspar.
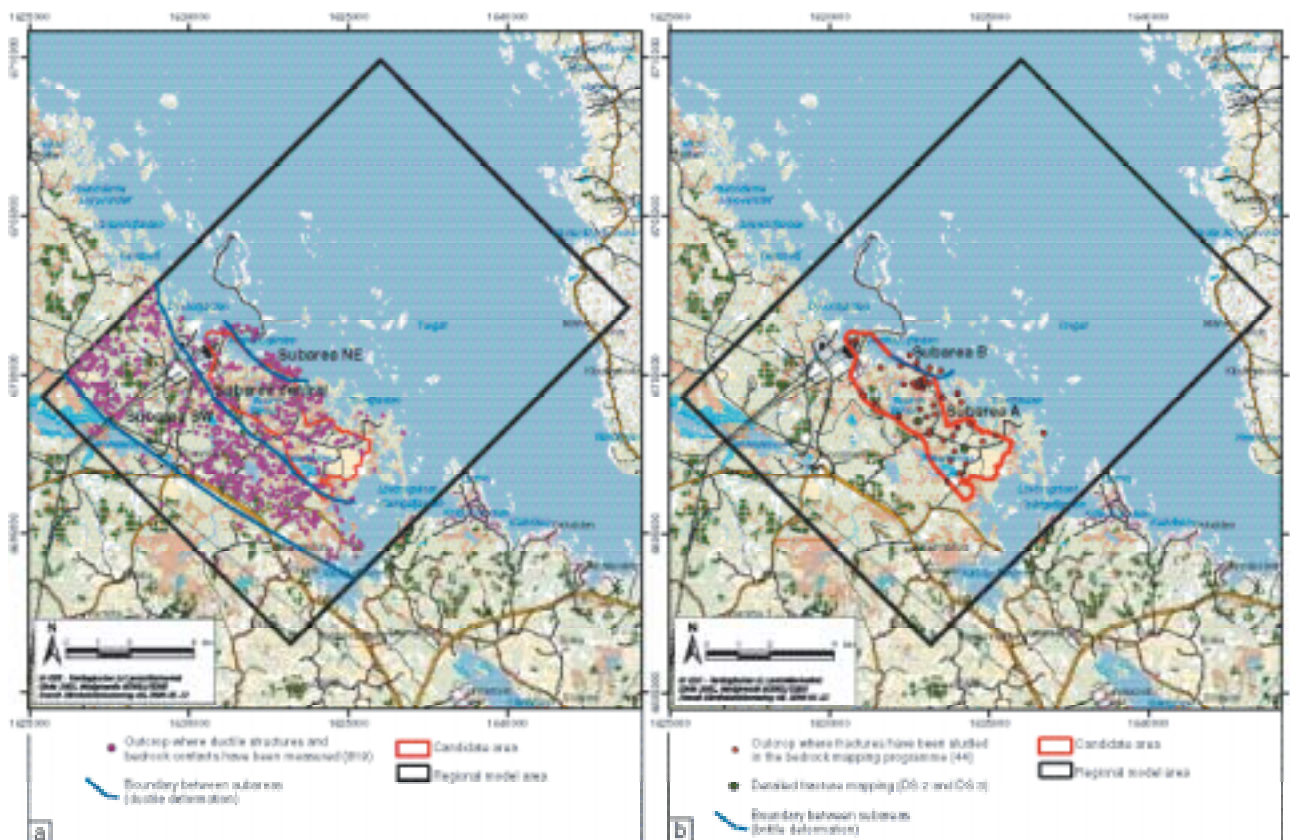
Figure 4-20. *Summary of surface field data used to assess the character and orientation of (a) ductile and (b) brittle structures in the regional model area. The boundaries to the various subareas, within which the ductile and brittle structural data have been assembled during the bedrock-mapping pro-gramme, are also shown.*

In each subarea, two types of measured ductile linear structures, that are referred to as mineral lineation and fold axis in the outcrop database, have been plotted on separate stereographic plots. The mineral lineation corresponds to a linear grain-shape fabric. Oriented hornblende crystals in the Group B mafic and intermediate rocks most conspicuously define this fabric. Oriented biotite grains and elongate aggregates of recrystallised quartz and feldspar also define the lineation in the felsic rocks that belong to Groups A to C. The mineral lineation is inferred to mark the direction of stretching during the ductile deformation. All the folds observed in the field deform a foliation or tectonic banding.

The anisotropy of magnetic susceptibility (AMS) measurements permit calculations of the mean directions of the principal AMS axes and the mean values of the principal susceptibilities $(K_1 \geq K_2 \geq K_3)$ for each sample locality. With the help of the mean values of the principal magnetic susceptibilities, estimates of the degree of anisotropy and the shape of the anisotropy ellipsoid can also be completed for each locality. The ellipsoid may be prolate (with a dominance of magnetic lineation), spherical, or oblate (with a dominance of magnetic foliation). The AMS values are inferred to reflect the regional ductile deformation in the bedrock samples /Isaksson et al, 2004a/.

The bedrock in subareas SW and NE generally shows a high level of ductile strain and strongly developed, ductile structures (SL tectonites). Exceptions to this general rule include several of the ultramafic, mafic and intermediate plutons (Figure 4-9) and two areas in the northwestern and southeastern marginal parts of subarea SW. These features are confirmed, at least in the southwestern area, by the higher degree of magnetic anisotropy (Figure 4-21a) and the oblate ellipsoid shape (Figure 4-21b) for the AMS values.

The ductile structures in subareas SW and NE display a highly regular orientation pattern. The planar structures strike SE or ESE and dip steeply to the SW or SSW, respectively (Figure 4-22a and b). The mineral lineation and fold axes plunge moderately to the SE in subarea SW (Figure 4-22b and c) and ESE in subarea NE (Figure 4-22e and f). Asymmetric structures in ductile high-strain zones in both these subareas indicate a dextral component of movement. Minor folds, which contain an intense, mineral stretching lineation along the fold axes, deform the planar fabric in the high-strain zones. An eye-shaped, tubular fold has been observed at one locality.
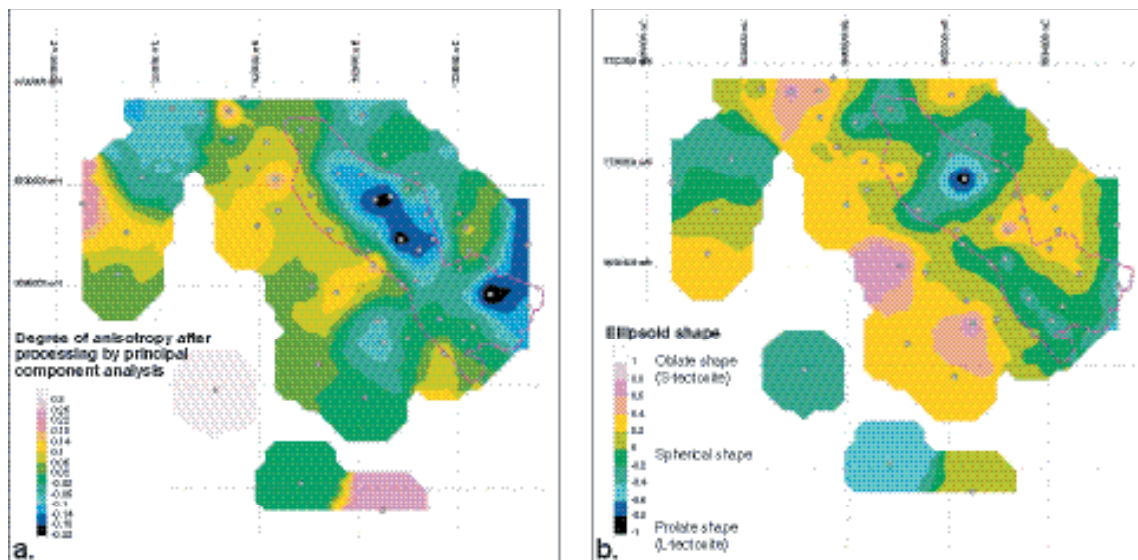
Figure 4-21. *Contoured diagrams that show a) the normalised degree of magnetic anisotropy and b) the ellipsoid shape parameter in the Forsmark area. Only the felsic Group B rocks are included and the 54 sample locations are shown with a grey dot /after Isaksson et al, 2004a/. It has been assumed that the degree of magnetic anisotropy is dependent on a linear combination of grain shape and volume susceptibility. On the basis of this assumption, a principal component analysis has been applied to the degree of magnetic anisotropy and the corresponding volume susceptibility values, in order to correct the former for the effects of the volume susceptibility. A more detailed discussion of this procedure is presented in /Isaksson et al, 2004a/.*
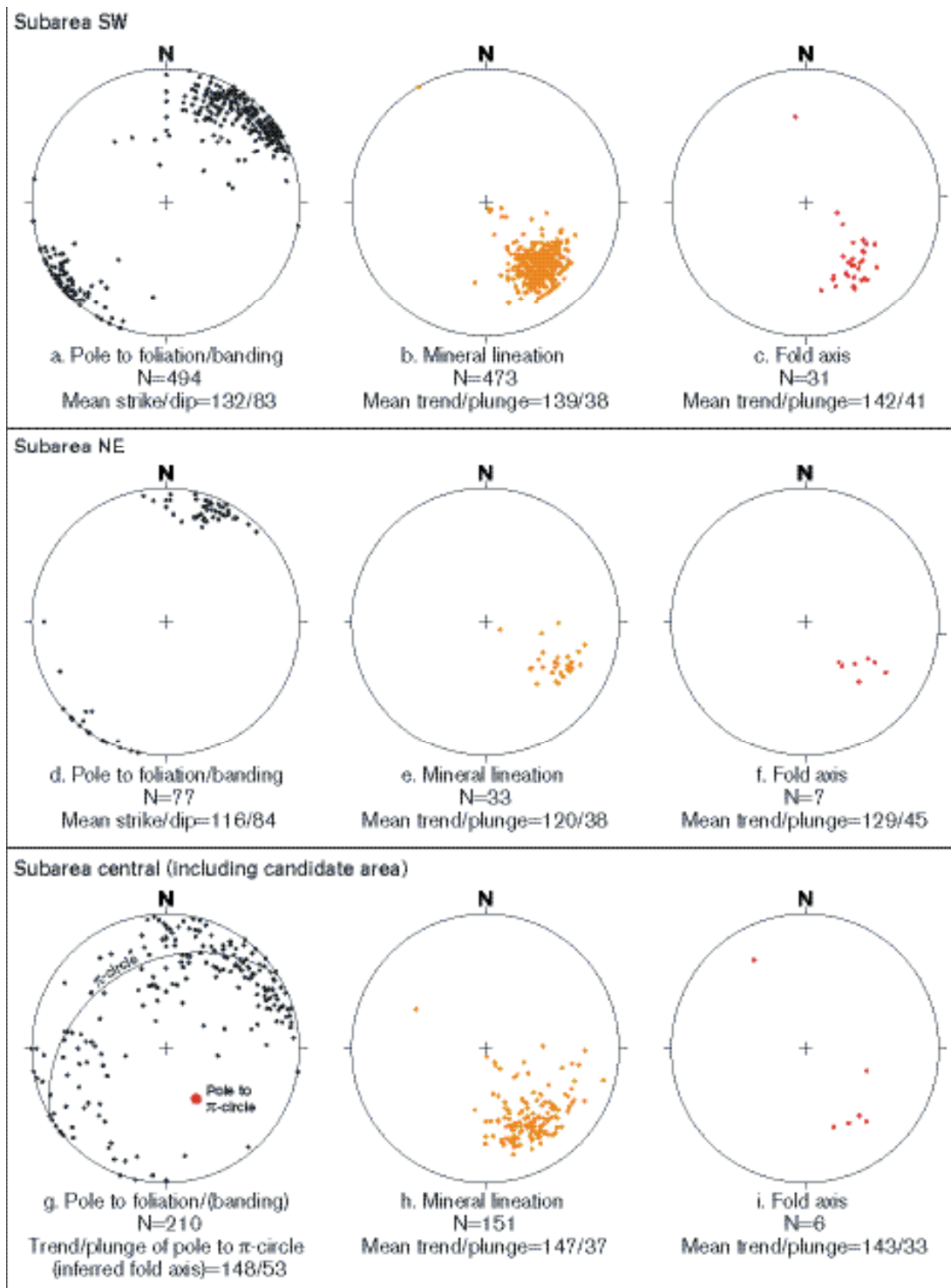
Figure 4-22. *Orientation of ductile structures in subareas SW, NE and central (including candidate area). All structures have been plotted on the lower hemisphere of a Schmidt stereographic plot. Poles to planes are plotted on a, d and g /after Stephens et al, 2003b/. The subareas are defined in Figure 4-20a.*

The bedrock in subarea central is inferred to show a low level of ductile deformation relative to that observed in the areas to the southwest and northeast. In general, a linear grain-shape fabric with subordinate, planar structures (LS tectonites) dominates this subarea. These features are confirmed by the lower degrees of magnetic anisotropy (Figure 4-21a) and, in general, a prolate to spherical ellipsoid shape (Figure 4-21b) for the AMS values.

Major folds, which formed after the development of the planar grain-shape fabric, dominate the structural framework in subarea central (Figure 4-9 and Figure 4-22g). These folds plunge moderately to the SE (Figure 4-22g), irrespective of whether they are antiformal or synformal in character. Both the fold axis inferred from the π-circle on the foliation plot (148/53) and the measured fold axes are parallel to the mineral stretching lineation (Figure 4-22g–i). These geometric features are reminiscent of oblique folds /Passchier and Trouw, 1998/ or tubular-shaped structures that are referred to as sheath folds /Cobbold and Quinquis, 1980/.

The minimum, principal AMS axes (poles to magnetic foliation) for the rocks in Groups A and B plot along a π-circle on the lower hemisphere of a Schmidt stereographic projection, with a strong cluster in the north-eastern part of the diagram (Figure 4-23). A fold geometry with an axis that plunges moderately to the SE is inferred. The inferred fold axis (135/47) is similar in orientation to the maximum, principal AMS axes (magnetic lineation) for these samples (Figure 4-23). This pattern, including the inferred fold axis orientation, is very similar to that indicated from the measured structural data.

The ductile deformation in the Forsmark area is characteristic of regions where planar grain-shape fabric development, mineral stretching lineation and folding are intimately related during strong, non-coaxial, progressive deformation. The tectonic lens in subarea central shows more prolate structures and lies in the hinge of an oblique or sheath fold that plunges to the SE. It is sandwiched between slabs of bedrock that show stronger ductile deformation and more oblate structures.

- Site mean, pole to magnetic foliation (N=66)
- Site mean, magnetic lineation (N=68)
- Pole to π-circle (inferred fold axis)
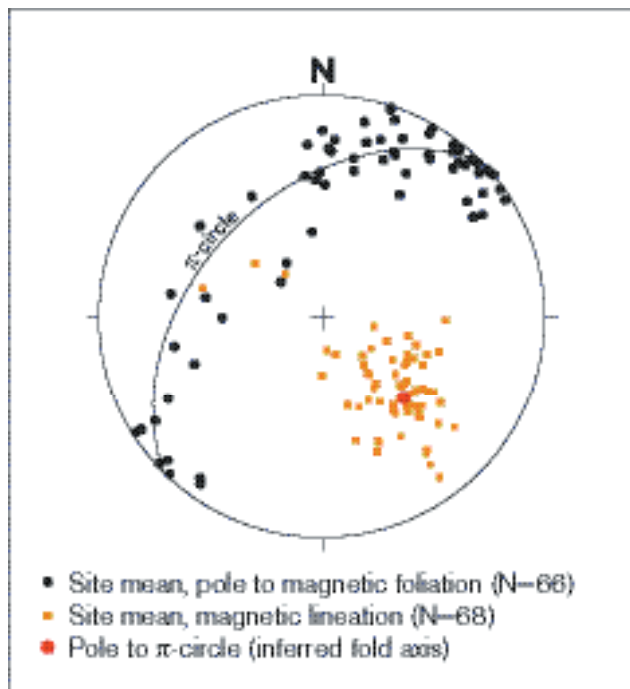
Figure 4-23. Orientation of the site mean values of magnetic foliation and magnetic lineation for the rocks in Groups A and B. The poles to the magnetic foliation define a π-circle, the pole to which is also shown. All structures have been plotted on the lower hemisphere of a Schmidt stereographic plot.

Evaluation of brittle structures

During the detailed fracture mapping at drillsites 2 and 3, fracture trace maps, that show fracture trace geometry, were produced for each outcrop (Figure 4-24). The assembled data include the 3D geometry of fracture traces and their associated geological parameters, including mineralogy, undulation, trace length and termination properties. The resolution of the trace data is from 50 cm length up to the maximum length of the cleaned outcrops. At drillsites 2 and 3, 986 and 1,235 fractures, respectively, were mapped. Scan line measurements were also completed at each outcrop along NS and EW directions, with a truncation length of 20 cm. The analysis of the data from the detailed mapping of fractures is presented in Section 5.1.6.

The simplified mapping of fractures, which was completed at 44 outcrops in connection with the bedrock-mapping programme, was carried out along two orthogonal lines with NS and EW directions. The location and orientation of fractures, with a truncation length of 100 cm, were recorded during this scan line mapping. In subarea A (Figure 4-20b), the frequency of fractures longer than 100 cm was generally 1 to 2 fractures/metre. Although there are considerably less data, it appears that the frequency of fractures longer than 100 cm increases in subarea B (Figure 4-20b) to values that are generally > 2 fractures/metre and locally up to 5 fractures/metre.

The orientation of more than eight hundred fractures have been measured in subarea A (N=834). The majority of these fractures are steeply dipping (Figure 4-25) but occasional, sub-horizontal fractures have also been encountered. Two major trends of steeply-dipping fractures with strike NE (dominant) and NW are prominent. A third subordinate trend is also apparent that is steeply-dipping and strikes NS.

The number of fractures measured in subarea B (N=263) is considerably less than that in subarea A. This seriously inhibits confident recognition of trends of fractures based on orientation. Virtually all fractures measured in subarea B are steeply dipping (Figure 4-25).
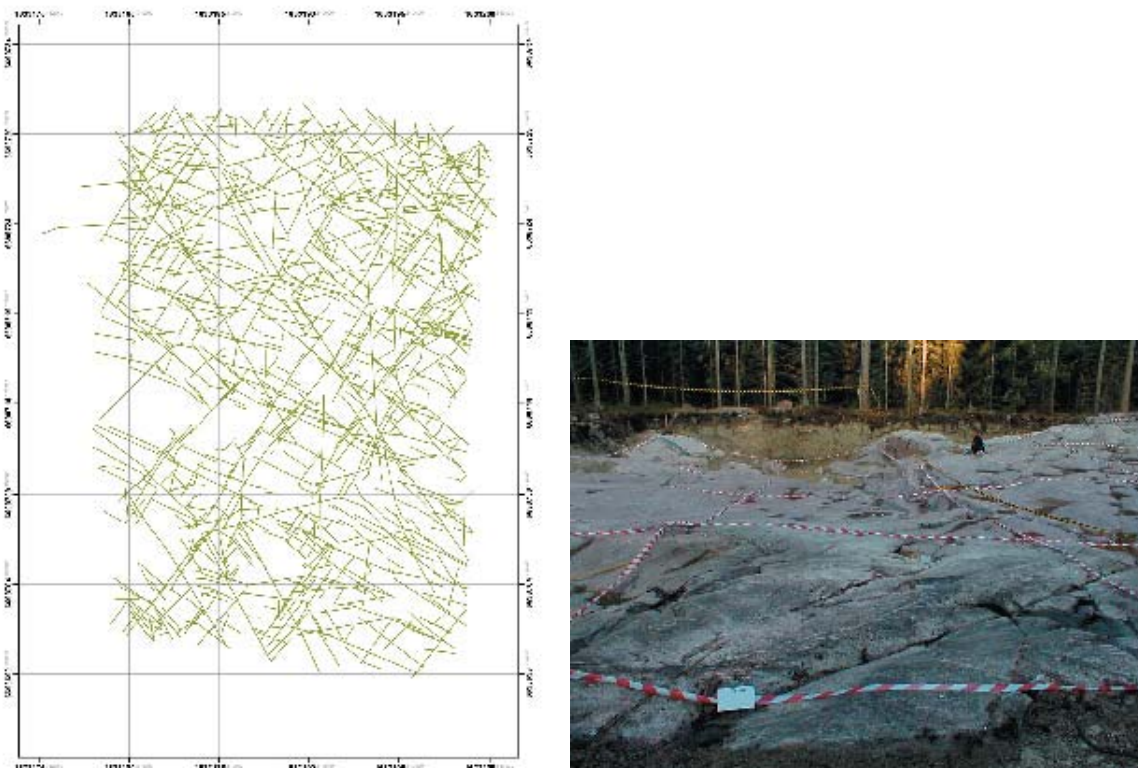
Figure 4-24. *Fracture trace map and view of outcrop at drillsite 2.*
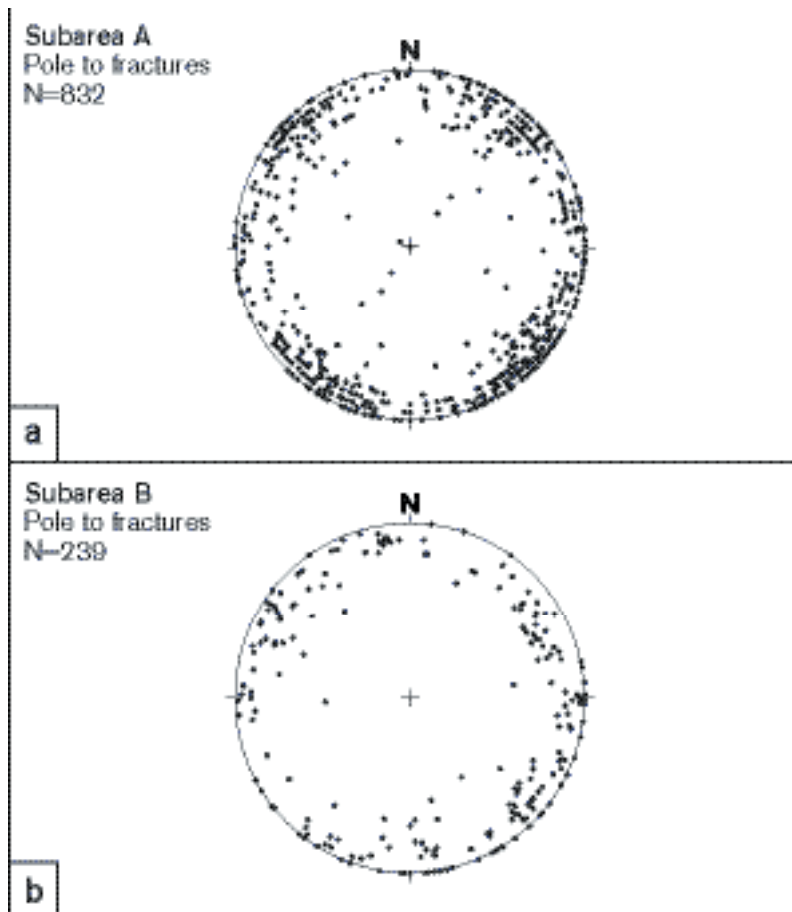
Figure 4-25. Orientation of fractures from 44 outcrops documented during the bedrock-mapping programme (after Stephens et al, 2003b/. Separate lower hemisphere, Schmidt stereographic plots of poles to fracture planes are shown for subarea A (upper) and subarea B (lower). The subareas are defined in Figure 4-20b.

Epidote and quartz are the dominant minerals that have been observed to fill fractures in the bedrock outcrops. Chlorite, hematite, pyrite and magnetite have also been observed. At several outcrops, a hard, reddish-coloured mineral has been documented which, locally, is inferred to be hematite-stained quartz. Larger segregations or veins of hydrothermal quartz, in places stained with hematite, are also present. Many fractures show a thin altered border zone which is also reddish and is inferred to be composed of tiny hematite grains.

There are insufficient data to assess the relationship between the occurrence of the different fracture-filling minerals and the orientation of the fractures. It is suggested that hydrothermal fluids, that were at temperatures corresponding to greenschist-facies metamorphic conditions, moved along the fractures that are filled with epidote.

Quartz, hematite-stained quartz, chlorite, calcite, a mineral that is inferred to belong to the zeolite group and one or more unidentified minerals have been documented during the detailed fracture mapping at drillsites 2 and 3.

4.2.5 Surface geophysics

Data

Two types of surface geophysical data have been acquired during the site investigation programme at Forsmark:

- Approximately 16 km of high resolution reflection seismic data along five separate, cross-cutting profiles, each of which varies in length from 2 to 5 km /Juhlin et al, 2002/. The shot and receiver spacing intervals along the profiles were 10 m (c 1,300 shot points) and a dynamite source that weighed 15 to 75 gm was employed. Most of the shots were also recorded on a stationary network of 11 Orion 3-component seismometers in order to provide a velocity model. The profiles are sited predominantly within the candidate area (Figure 4-26).

- Ground EM (slingram) and magnetic measurements at drillsites 1, 2 and 3 /Thunehed and Pitkänen, 2002/. Measurements were also carried out along a northeasterly continuation of one of the east-west profiles at drillsite 1. This extra profile extends c 600 m along the land strip that lies directly north of Bolundsfjärden (Figure 4-27). The survey was completed with a 10 m interval between the measurement points.

Gravity data have also been acquired during the site investigation programme /Aaro, 2003/. However, these data are of a broad regional character and have, as yet, not been interpreted. For these reasons, they have not been assessed and utilised in the present study.
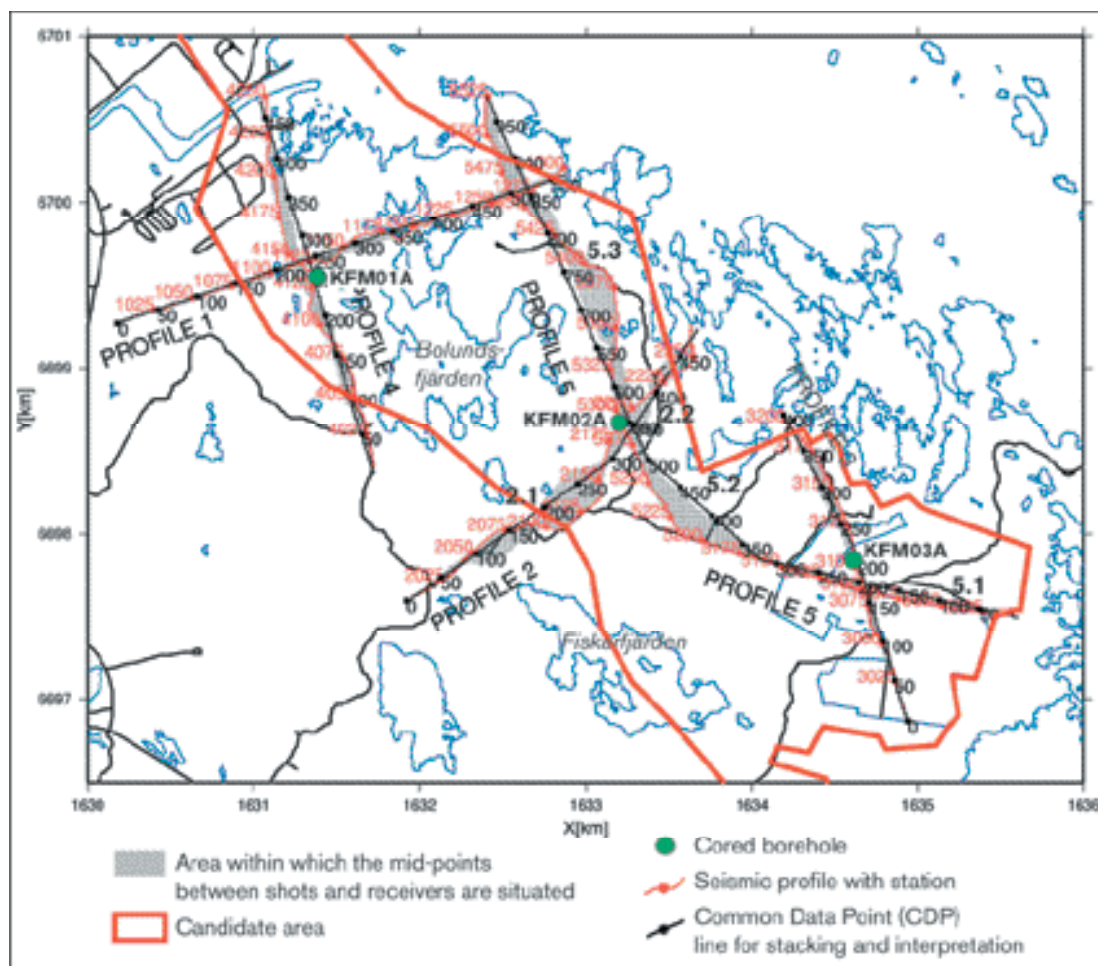
Figure 4-26. *Common Data Point (CDP) lines along which the reflection seismic data have been projected for stacking and interpretation /after Juhlin et al, 2002/. Lines 2 and 5 were split into separate linear segments and referred to as 2.1 and 2.2, and 5.1, 5.2 and 5.3, respectively, in /Cosma et al, 2003/.*
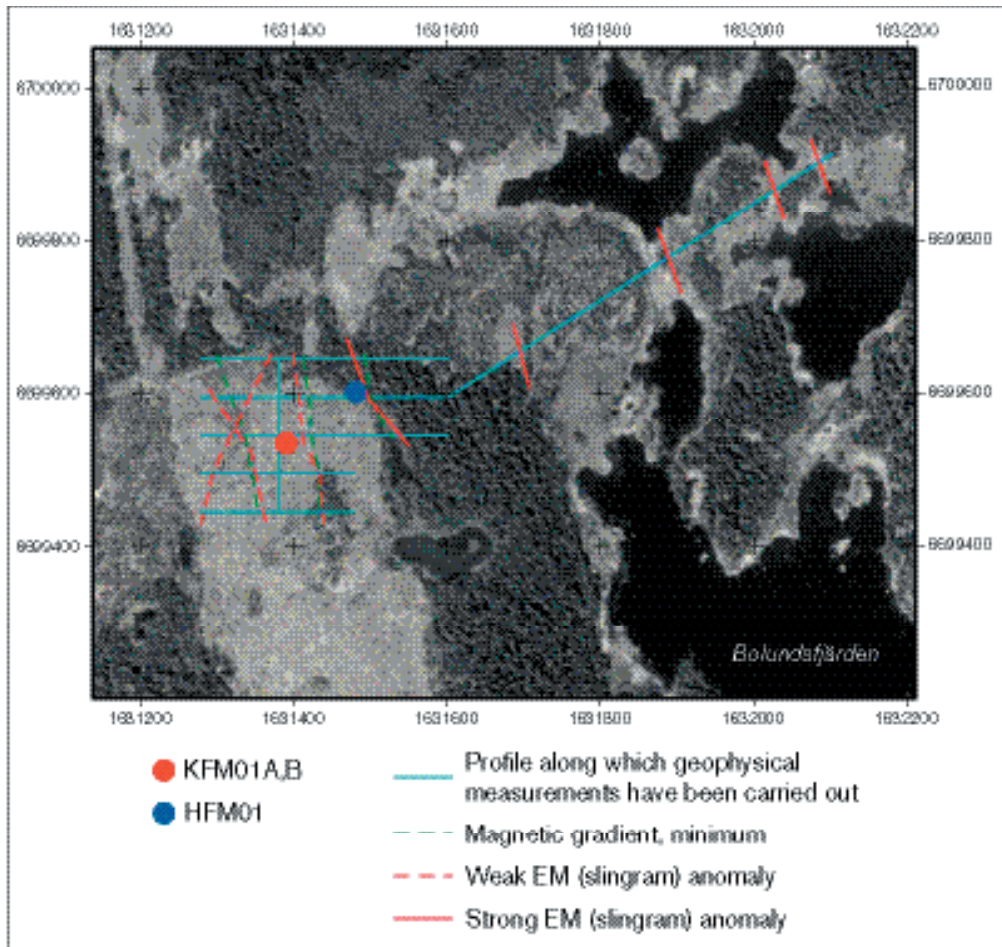
Figure 4-27. Ground EM (slingram) and magnetic measurements close to drillsite 1 /after Thunehed and Pitkänen, 2002/.

Considerable seismic refraction data are also available in the area around the nuclear power plants and in the vicinity of SFR and, locally, together with ground EM (slingram) and magnetic measurements, in other parts of the regional model area. Due to the incomplete character of the data in SKB's SICADA database, the absence of a complementary report and the limited time available for the present work, these older data were not assessed or utilised in the present site descriptive modelling procedure (see also Chapter 2). These data will be included in Site Descriptive Model version 1.2.

Evaluation

Reflection seismic data

The reflection seismic survey has been able to image reflectors in the bedrock down to depths of at least 3 km. There is a higher concentration of well-defined reflectors in the upper 2 km of bedrock in the southeastern part of the candidate area (Figure 4-28), relative to that observed in the northwestern part, closer to the nuclear power plants (Figure 4-29). Nevertheless, possibly the most conspicuous group of reflectors (referred to as A0–A1 in /Juhlin et al, 2002/) are seen in the results for profile 4, in the northwestern part of the candidate area (Figure 4-29).

Since measurements have been carried out along profiles that intersect each other and it has been possible to recognise the same reflector on two cross-cutting profiles, the strike and dip of 25 reflectors have been estimated (Table 4-5, Table 4-6 and Table 4-7). These reflectors were labelled in nine groups (A to I), according to their inferred orientation /Juhlin et al, 2002/. No orientation was provided for a limited number of reflectors that were observed in only one of the two cross-cutting profiles (e.g. reflector Y1 in Figure 4-29). Using the strikes and dips as well as a correlation between the results from different sets of cross-cutting profiles, the reflectors have been projected in both
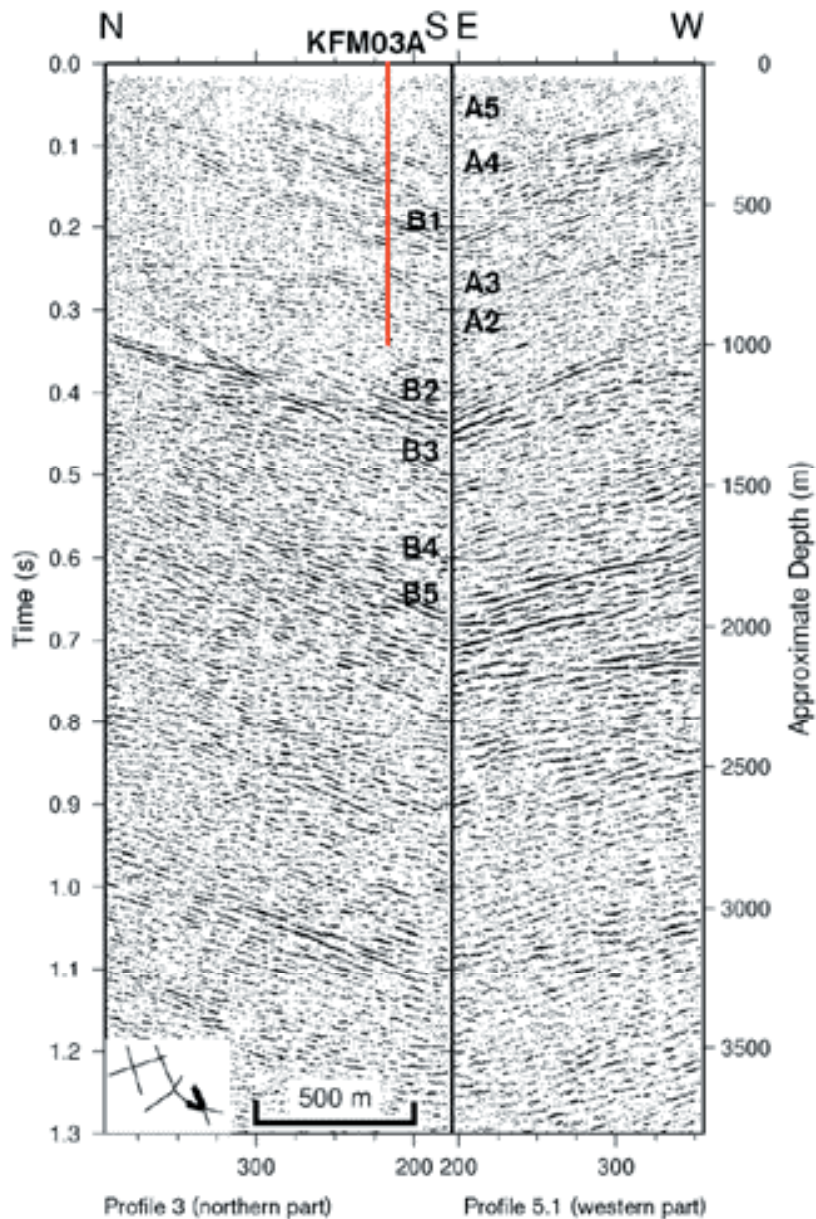
Figure 4-28. Correlation of stacks from profiles 3 and 5 at their crossing points, in the southeastern part of the candidate area. The location of each section is shown in the lower left-hand part of the two figures. The depth scale along the vertical axis is only valid for sub-horizontal reflectors. The numbers along the horizontal axis refer to the CDP line along which the data have been projected for stacking and interpretation /after Juhlin et al, 2002/. Only the reflectors in groups A, B and C (definite reflectors) are labelled.

strike and dip directions. Several reflectors have been projected up to the surface. In order to relate travel time values to approximate depth values, i.e. the distance at depth from the measuring line, an average velocity for the bedrock of 5,850 m/s has been adopted.

Several key questions emerge from an analysis of the seismic reflection data:

• How well-defined is an individual reflector? An assessment of the degree of clarity, and, thereby, some judgement concerning whether or not a reflector is present, is provided in /Juhlin et al, 2002/. Definite, probable or possible reflectors were recognised in this assessment. However, this exercise is subjective in character and is open to varied interpretations.
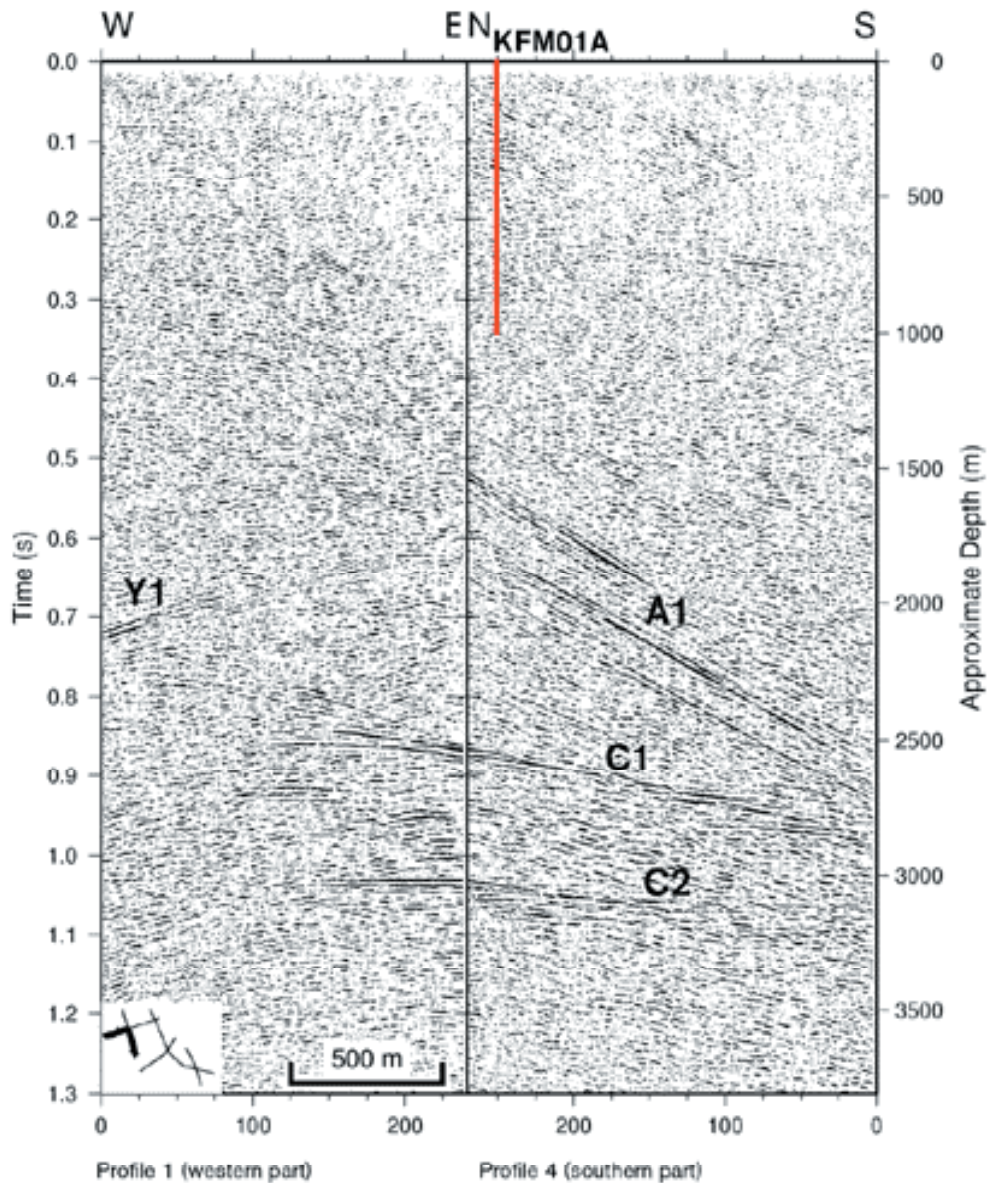
Figure 4-29. Correlation of stacks from profiles 1 and 4 at their crossing points, in the northwestern part of the candidate area. The location of each section is shown in the lower left-hand part of the two figures. The depth scale along the vertical axis is only valid for sub-horizontal reflectors. The numbers along the horizontal axis refer to the CDP line along which the data have been projected for stacking and interpretation /after Juhlin et al, 2002/. Only the reflectors in groups A, B and C (definite reflectors) are labelled.

- How well do reflectors match each other in the intersecting profiles and, by inference, how well-defined are the inferred dips?

- How well do the inferred reflectors connect together in the different pairs of intersecting profiles and, by consequence, how well-defined is the extension of the reflectors in both the strike and dip directions?

- How reliable is the adopted velocity model and, by consequence, the estimate of the depth at which the reflector is sited?

- What is the geological feature (or features) that is represented by an individual reflector?

Bearing in mind the potential significance of the seismic reflection data to determine regional or local major /Andersson et al, 2000/ deformation zones and the uncertainties raised by the questions listed above, it was judged necessary to complete an independent, new assessment of the interpretation of the primary data. This work /Cosma et al, 2003/ also aimed to place the reflectors in 3D space.

Apart from the reflectors in groups G, H and I, all the reflectors have been identified with confidence in the independent reassessment. Based on the judgements in both /Juhlin et al, 2002/ and /Cosma et al, 2003/, the reflectors in groups A, B and C are classified here as definite (Table 4-5), the reflectors in groups D, E and F are classified as probable or possible (Table 4-6), and the reflectors in groups G, H and I are classified as highly uncertain (Table 4-7).

The matching of seismic reflectors, both in two transecting profiles as well as between different pairs of transecting profiles, have been re-evaluated and the dips and strikes of all the reflectors in groups A to F have been recalculated (Table 4-5 and Table 4-6).

Table 4-5. Comparison of the orientation estimates for the seismic reflectors that have been classified as definite in /Juhlin et al, 2002/ and that have been recognised with confidence in /Cosma et al, 2003/. These reflectors are classified here as definite reflectors.

Definite reflectors					
Reflector ID	/Juhlin et al, 2002/		/Cosma et al, 2003/		
	Strike	Dip	Strike	Dip	Profile (relevant set of stations)
A1	075	45	082	50	1 (148–441)
			081	39	2.1 (35–247)
			081	39	4 (2–175)
			082	50	4 (238–436)
			081	45	4 (176–244)
			082	36	5.3 (258–480)
A2	080	22	094	25	2.2 (14–63)
			098	12	2.2 (69–86)
			094	24	5.3 (20–109)
			098	12	5.3 (114–141)
A3	065	25	065	25	5.3 (1–131)
			045	21	2.2 (1–160)
A4	065	25	061	26	3 (18–274)
			061	26	5.1 (1–319)
			061	26	5.2 (1–91)
A5	075	30	075	32	3 (1–177)
			074	32	5.1 (1–222)
A6	075	30	077	31	3 (1–68)
			077	31	5.1 (1–34)
B1	030	25	032	27	3 (1–333)
			032	27	5.1 (1–284)
B2	030	25	025	27	3 (65–286)
			025	27	5.1 (68–319)
B3	030	21	030	24	3 (179–402)
			030	24	5.1 (111–319)
B4	050	28	050	29	2.1 (243–325)
			050	29	2.2 (1–96)
			050	29	5.2 (1–179)
			050	29	5.3 (1–336)
B5	050	25	062	26	3 (54–287)
			062	26	5.1 (158–319)
			050	9	5.1 (1–146)
C1	015	20	038	18	1 (153–338)
			037	18	2.1 (1–161)
			037	18	4 (1–426)
C2	355	10	035	13	1 (241–492)
			035	13	2.1 (1–325)
			035	13	4 (83–276)
			072	8	4 (1–286)
			035	13	5.3(1–62)

Table 4-6. Comparison of the orientation estimates for the seismic reflectors that have been classified as probable or possible in /Juhlin et al, 2002/ and that have been recognised with confidence in /Cosma et al, 2003/. These reflectors are classified here as probable or possible reflectors.

Probable or possible reflectors					
Reflector ID	/Juhlin et al, 2002/		/Cosma et al, 2003/		
	Strike	Dip	Strike	Dip	Profile (relevant set of stations)
D1	320	65	062	36	5.1 (1–319)
			062	36	3 (122–400)
D2	120	50	040	30	5.1 (1–319)
			040	30	3 (1–402)
D3	320	65	037	28	5.1 (1–319)
			037	28	3 (1–402)
E1	270	9	297	12	2.1 (234–325)
			297	12	2.2 (1–39)
			297	12	5.2 (143–180)
			297	12	5.3 (1–92)
F1	020	20	023	18	2.2 (1–69)
			027	2	5.2 (145–178)
			020	18	5.3 (15–120)
			020	4	5.3 (120–220)

Table 4-7. Seismic reflectors that have been classified as probable or possible in /Juhlin et al, 2002/ and that have not been recognised with confidence by /Cosma et al, 2003/. These reflectors are classified here as highly uncertain reflectors.

Highly uncertain reflectors				
Reflector ID	/Juhlin et al, 2002/			/Cosma et al, 2003/
	Uncertainty	Strike	Dip	
G1	Possible	180	3	Not recognised with confidence
G2	Possible	180	3	Not recognised with confidence
G3	Possible	360	2	Not recognised with confidence
G4	Possible	360	2	Not recognised with confidence
H1	Probable	123	70	Not recognised with confidence
H2	Probable	123	70	Not recognised with confidence
I1	Probable	030	70	Not recognised with confidence

Apart from the reflectors in group D, there is good agreement with the estimates made in /Juhlin et al, 2002/. Refinements of the velocity model, which take account of the low velocity zone between c 0 m and 150 m, have been applied. In this way, errors in the estimate of the depth to the deeper (> 150 m) reflectors has been reduced to ± 12 m. The positions of the reflectors have subsequently been estimated in 3D space /Cosma et al, 2003/. Care has been taken to extend the reflectors in strike and dip directions only as far as the data from the different profiles permit.

The question raised in the evaluation that concerns the geological character of the seismic reflectors remains. It should be possible to address this question in more detail when geological data from especially the cored borehole KFM03A, in the southeastern part of the candidate area, are available. It is sufficient at this stage to state that the reflectors potentially represent deformation zones, along which the mechanical and/or compositional character of the bedrock has been sufficiently altered to cause distinctive anomalies in the seismic reflection data.

It is emphasized that care needs to be taken in the use of the reflectors in groups G, H and I. They were graded as probable or possible in /Juhlin et al, 2002/, but their existence was questioned in /Cosma et al, 2003/. Care is also recommended concerning the use of the reflectors in group D, bearing in mind the radically different interpretations of the orientation of these reflectors. There is also an inherent bias towards shallow-dipping structures in the reflection seismic data obtained from surface investigations.

Due mainly to the uncertainties in the interpretation of the geological feature (or features) to which the reflectors are coupled, the seismic reflectors in the Site Descriptive Model version 1.1 have been utilised as supportive rather than deterministic information. It is possible that the role of the inferred seismic reflectors will become more deterministic in character, when more borehole data along the intersections of the seismic profiles are available in the Site Descriptive Model version 1.2.

Ground EM and magnetic measurements

A conspicuous EM (slingram) anomaly with NNW trend was noted in the northeastern part of the area surveyed at drillsite 1 (Figure 4-27). Similar, strong EM anomalies were noted at four more locations along the continued east-west profile (Figure 4-27). A poor correlation with magnetic minima was noted for these anomalies. All these ground EM anomalies correspond to lineaments with NNW trend. The lineaments have been identified mainly on the basis of topographic and airborne EM data.

Two minor EM (slingram) anomalies with a north-south trend were identified at drillsite 2. These anomalies do not correspond to magnetic minima.

A distinctive EM (slingram) anomaly with northeasterly trend was identified in the northwestern part of the area surveyed at drillsite 3. Fine-grained, Quaternary deposits cover the area and this feature complicates the interpretation of the anomaly. However, the anomaly corresponds closely to a conspicuous lineament that has been identified on the basis of airborne magnetic and EM data as well as topographic data. Furthermore, both the ground EM (slingram) anomaly and the inferred lineament lie close to the inferred surface projection of seismic reflector A5.

4.3 Meteorology, hydrology, near surface hydrogeology and oceanography

The same meteorological, discharge and oceanographical data is used for model version 1.1 as for version 0. Existing data was compiled by /Lindell et al, 2000/ and /Larsson-McCann et al, 2002/. Figure 4-30 shows the locations of the observation stations of interest for the Forsmark area. All water chemical data are presented in Section 4.8.1.

4.3.1 Meteorological data

In Table 4-8 the meteorological stations of interest for the Forsmark area are presented.

Table 4-8. Existing meteorological data of interest for the Forsmark area /Larsson-McCann et al, 2002/.

Station no	Station name	Co-ordinates	RT90	Period	Information
10832	Örskär	671476	164097	1881–1995	No air pressure
10832	Örskär A	671475	164099		1995–
10815	Östhammar	668510	164176	1989	Only prec
10811	Risinge	667533	163423	1962–	Only temp, prec
10725	Lövsta	670070	161437	1925–	Only prec
10714	Films Kyrkby	668149	161626	1982–2000	
10714	Films Kyrkby A	668156	161629	2000–	
9753	Uppsala Flygplats	664306	159991	1949–	
307	Uppskedika V	668148	163416	1990–	Only during winter
320	Dannemora V	667855	161318	1990–	Only during winter
324	Gräsö V	670861	164362	2001–	
2994	Forsmark MAST	670029	163015	1992–1996	Raw data
2389	Forsmark biotest	670256	163118	1992–1998	Only wind, temp

Figure 4-30. *Meteorological, hydrological and oceanographical stations of interest for the Forsmark area /Larsson-McCann et al, 2002/.*

The short description below of the meteorological conditions at the Forsmark area is based on data compiled by /Lindell et al, 2000/ and /Larsson-McCann et al, 2002/. A more detailed description is given in these reports.

A wind rose from the station at Örskär, which is judged to be representative for the Forsmark area, is presented in Figure 4-31, together with a wind rose from Uppsala airport. Compared to the common pattern in southern Sweden, northerly winds are much more frequent. In winter, strong northerly winds often bring heavy snowfall.

In north-eastern Uppland, the precipitation maximum occurs some km inland from the coast. As an example, the mean annual precipitation in Lövsta, approximately 10 km inland, is 758 mm compared with 588 mm at Örskär (values corrected for wind losses etc by 15 and 21% for Lövsta and Örskär, respectively). The mean annual precipitation in the Forsmark area can be estimated to be 600–650 mm. 25–30% of the precipitation falls in the form of snow.

The average monthly mean temperature varies between –4°C in January–February and 15°C in July. The winters are slightly milder at the coast than inland and the mean annual temperature at Örskär is 5.5°C compared to 5.0°C at the more inland stations at Risinge and Films kyrkby. The vegetative period (daily mean temperature exceeding 5°C) is about 180 days.
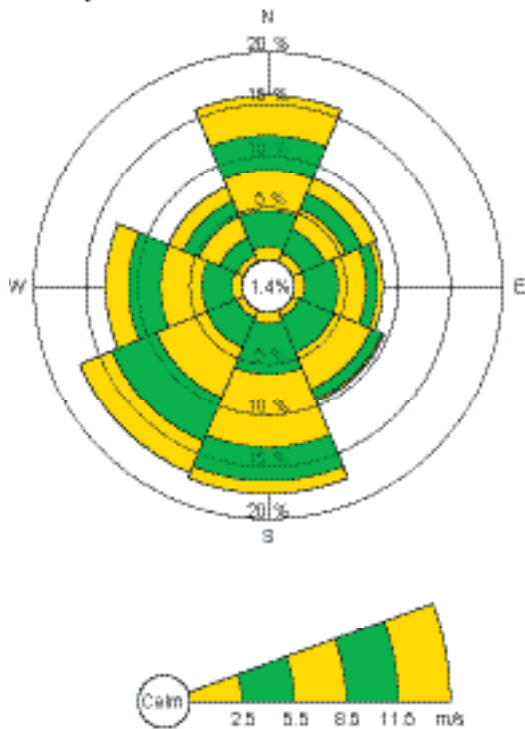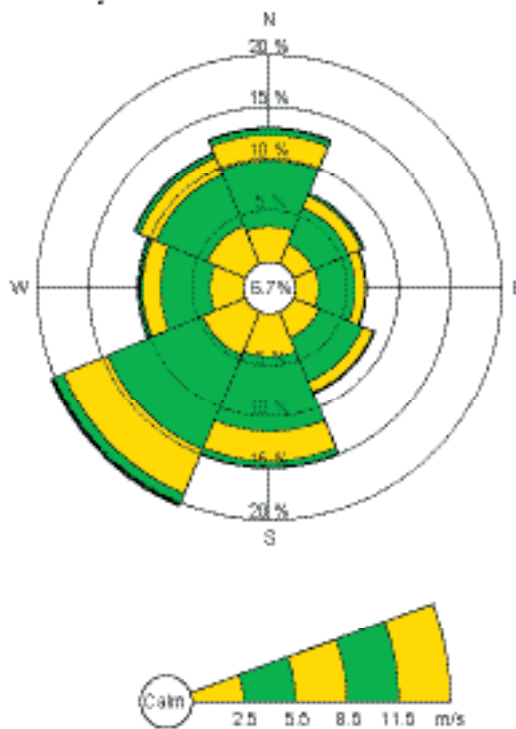
Figure 4-31. Wind rose from the SMHI-station at Örskär and Uppsala airport /Larsson-McCann et al, 2002/.

The annual sunshine time is 1,700–1,800 hours at the coast of north-eastern Uppland /SKB, 2002a/. Based on the synoptic observations at Örskär, the mean annual global radiation was calculated to 930 kWh/m^2, with the mean monthly values varying from 4 kWh/m^2 in December up to slightly more than 170 kWh/m^2 in June.

The ground is covered by snow about 120–130 days per year with an average annual maximum snow depth of approximately 50 cm.

Comments

Two meteorological stations were established in the candidate area during 2003. Precipitation, temperature, wind, humidity and global radiation are measured. Furthermore, snow depth and ground frost is measured at 3 locations.

4.3.2 Hydrological data

The new hydrological data available for model version 1.1 compared with version 0 include:

- Detailed delineation of catchment areas.
- Simple, sporadic discharge measurements in some water courses.

Regional discharge data

The hydrological stations in Uppland are shown in Figure 4-30 and in Table 4-9.

Table 4-9. Hydrological stations in Uppland /Larsson-McCann et al, 2002/.

Stn No	Name	River	Lake %[1]	Area km²	N	E	Period
50110	Vattholma	Fyrisån	5	294	665713	160736	1917–2000
910	Uvlunge	Vendelån	2.6	263	666663	160043	1917–1942
2299	Tärnsjö	Stalbobäcken	2	13.7	666859	156333	1975–2000
573	Gimo	Olandsån	3.2	587	667489	163287	1922–1932
1256	Fors	Olandsån	3.2	577	667170	163344	1931–1959
1053	Näs	Tämnarån	4.2	1176	670862	159995	1925–1971
1260	Odensfors	Tämnarån	6.3	772	668382	158822	1930–1950
	OL1	Olandsån	1.4	880.9	669252	163452	1962–2001
	FO1	Forsmarksån	4.6	375.5	669500	163249	1962–2001

[1] percentage of catchment area.

The station at Vattholma was chosen by /Larsson-McCann et al, 2002/ to be the main representative for the Forsmark area. The catchment area is 294 km² and the mean specific discharge is 7.5 L/s/km². Monthly discharge values for the Vattholma Station are shown in Figure 4-32. The precipitation gradient, with low precipitation close to the coast, means that the specific discharge in the Forsmark area will be considerably lower than the measured value at Vattholma. The specific discharge can be estimated to be approximately 6.5 L/s/km² (approximately 200 mm/year) /SGU, 1983/.
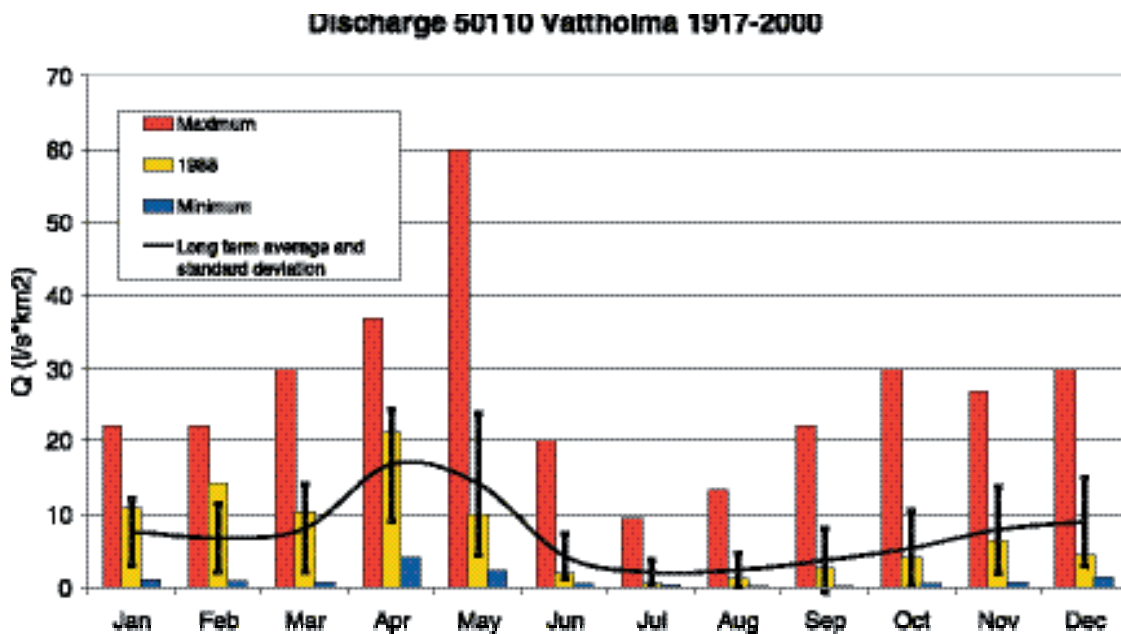
Figure 4-32. Monthly discharge at Vattholma. Maximum and minimum daily mean, long term average and standard deviation (L/s/km²). 1988 selected as a representative year /Larsson-McCann et al, 2002/.

Catchment areas

Based on maps, aerial photos and field checks, a detailed delineation of catchment areas has been made (Figure 4-33). In Table 4-10 data on size and land use of the catchment areas are presented. 25 "lake-centred" catchment areas have been delineated, varying in size from 0.03 km² to 8.67 km². Forest is dominating and covers between 50 and 96% of the areas of the catchments. Wetlands, both forest-covered and open, are frequent and cover more than 20% of the area in five of the catchments. Only in one catchment area agricultural land constitutes an important part of the total area (Bredviken with 27% agricultural land).

Data for the lakes are given in Table 4-11. Several of the lakes have levels that are close to the Baltic Sea level. During events of high sea levels, water from the Baltic Sea may intrude into these lakes. For example, sea water relatively frequent flows into Lake Bolundsfjärden (10).
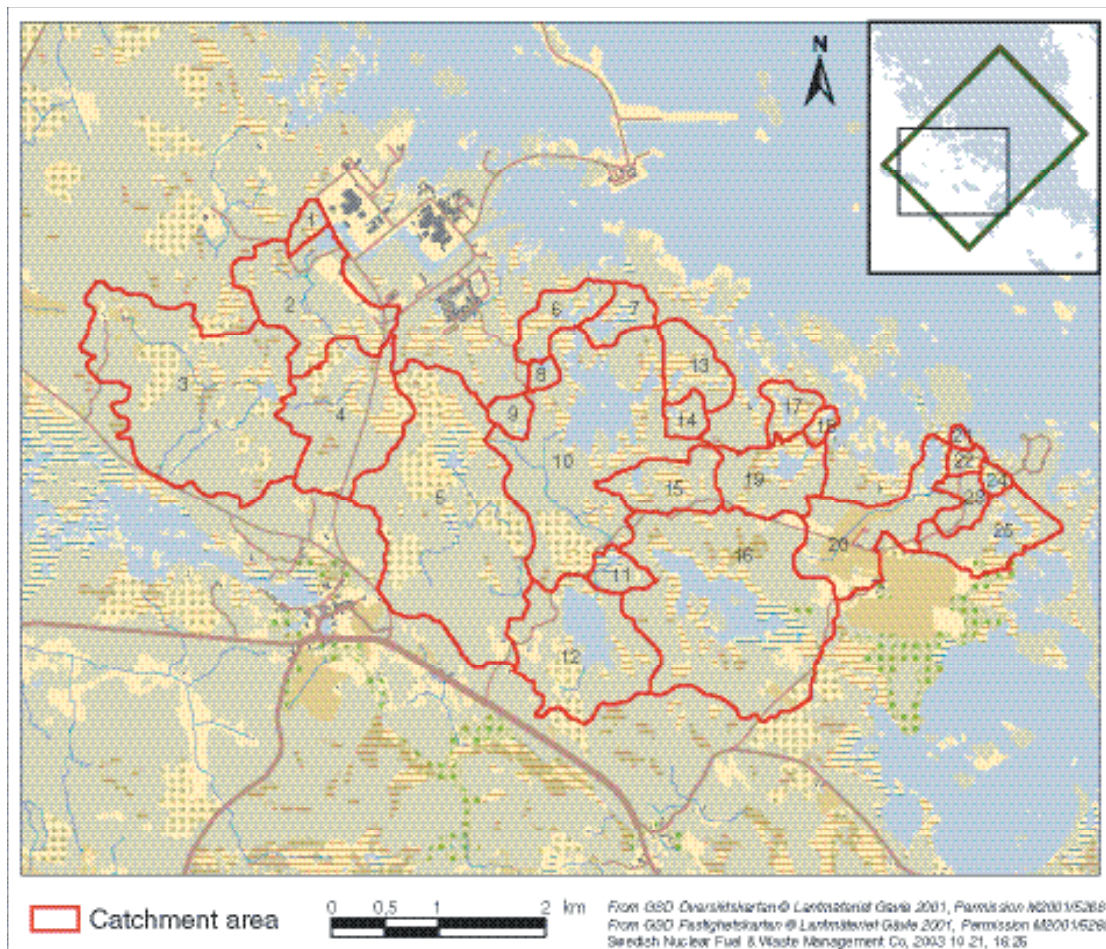
Figure 4-33. *Delineated catchment areas /SKB GIS, 2003/.*

Table 4-10. Size and land use of delineated catchment areas /SKB GIS, 2003/.

Number in Figure 4-33	Name	Catchment area (km²)	Forest (%)	Forest wet-land (%)	Clear-cut area (%)	Agric. land (%)	Open land wetland (%)	Other open land (%)	Water (%)
1	Gunnarsbo-Lillfjärden (norra)	0.1035	70.6	5.1			10.9	2.8	10.6
2 (incl. 1,3,4)	Gunnarsbo-Lillfjärden (södra)	5.1202	78.1	2.1	6.7	0.8	7.7	3.2	1.3
3	Gunnarsboträsket	2.7344	80.5	1.9	8.2	1.5	4.6	2.4	0.9
4 (incl. 3)	Labboträsket	3.9277	78.8	2.1	8.2	1.0	7.0	2.0	0.9
5	Gällsboträsket	2.8910	67.9	0.7	21.3		8.7	1.0	0.5
6 (incl. 5, 7, 8, 9, 10, 11, 12, 13, 14, 15)	Norra Bassängen	8.6682	67.1	0.6	10.6		11.4	1.1	9.1
7	Puttan	0.2488	60.2				26.6		13.2
8									
9	Kungsträsket	0.1257	93.0				5.4		1.6
10 (incl. 5, 9, 11, 12, 13, 14, 15)	Bolundsfjärden	8.0030	67.1	0.7	11.5		10.5	1.1	9.1
11 (incl. 12)	Stocksjön	1.4720	66.4	0.1	7.7		6.7	4.1	15.0
12	Eckarfjärden	1.2972	65.3	0.1	8.7		5.0	4.4	16.5
13	Graven	0.3917	71.7	0.6			23.9		3.8
14	Fräkengropen	0.1384	79.9				16.3		3.9
15	Vambörsfjärden	0.4837	74.5	0.7			20.0		4.8
16	Fiskarfjärden	2.9259	63.7	3.2	1.4	0.7	13.5	4.1	13.4
17	Tallsundet	0.2154	57.9	2.8			32.0		7.4
18		0.6898	64.2	3.6			22.8	0.3	9.1
19	Lillfjärden	0.6208	66.3	4.0			21.1	0.3	8.3
20	Bredviken	0.9439	49.2	0.8	1.4	26.9	3.4	11.4	6.9
21	Simpviken	0.0346	76.4				9.3		4.3
22		0.0771	82.7				15.4		2.0
23		0.1918	92.2	3.8			3.1		1.0
24 (incl. 22, 23)	Märrbadet	0.3372	81.0	2.2			13.2	0.1	3.6
25 (incl. 22, 23, 24)		0.8952	70.2	1.6			15.6	1.8	10.7

Table 4-11. Geometrical data for the lakes /SKB GIS, 2003/

No in Figure 4-33	Name	Elevation (masl)	Area (m²)	Max. depth (m)	Mean depth (m)	Volume (m³)
1	Gunnarsbo-Lillfjärden (norra)	1.64*	22870	0.90	0.30	6870
2	Gunnarsbo-Lillfjärden (södra)	1.60*	32870	2.22	0.70	23110
3	Gunnarsboträsket	5.81**	67080	1.29	0.51	34040
4	Labboträsket	3.56*	59390	1.07	0.27	15950
5	Gällsboträsket	1.91**	185760	1.51	0.17	32100
6	Norra Bassängen	0.56*	75460	0.88	0.31	23650
7	Puttan	0.63*	81810	1.29	0.37	30150
8		1.82*	9780	0.60	0.29	2860
9	Kungsträsket	2.60*	7600	0.54	0.20	1550
10	Bolundsfjärden	0.64*	609220	1.81	0.61	373950
11	Stocksjön	2.92*	36000	0.82	0.22	8030
12	Eckarfjärden	5.37*	282430	2.12	0.91	257340
13	Graven	0.65*	48260	0.35	0.12	5920
14	Fräkengropen	1.35*	19140	0.79	0.19	3660
15	Vambörsfjärden	1.14*	47400	0.98	0.43	20550
16	Fiskarfjärden	0.54**	751890	1.86	0.37	274450
17	Tallsundet	0.13	79230	0.80	0.23	18350
18						
19	Lillfjärden	−0.07*	160620	0.89	0.29	47030
20	Bredviken	−0.12*	97450	1.72	0.74	72010
21	Simpviken	−0.29*	34860	1.53	0.38	13320
22		0.38*	9600	0.81	0.24	2250
23		0.22*	6380	0.70	0.25	1620
24	Märrbadet	0.00*	23580	1.01	0.36	8500
25		−0.26*	162470	1.07	0.32	52570

* Water levels measured April 16–20, 2002   ** Water levels measured Oct 22–23, 2002

Simple discharge measurements

Connected to the surface water sampling, simple discharge measurements have been performed in running waters at eight locations since March 2002 (Figure 4-34) /Nilsson et al, 2003/.

The simple discharge measurements were performed 1–3 times per month. A 150 ml plastic bottle, 2/3 filled by water, was used as a float and the discharge was calculated from the observed flow velocity and the cross-sectional area.

The highest recorded discharge during the period March 2002–April 2003 was 175 L/s at PFM000068, March 18, 2003. This corresponds to a specific discharge of 31.5 L/s/km². It should be stressed that the measurements have been sparse and that higher discharges may very well have appeared. Furthermore, the period from March 2002 to April 2003 was quite dry compared with average conditions. All water courses were dry for a substantial part of the period /SKB SICADA, 2003/.

Comments

At four locations, permanent discharge measurement stations are planned (at PFM000066, 68, 69 and 70). At PFM000068, discharge measurement flumes were installed in December 2003. At the three other sites, installations are planned for summer 2004, based on the experience from measurements during winter conditions at PFM000068.
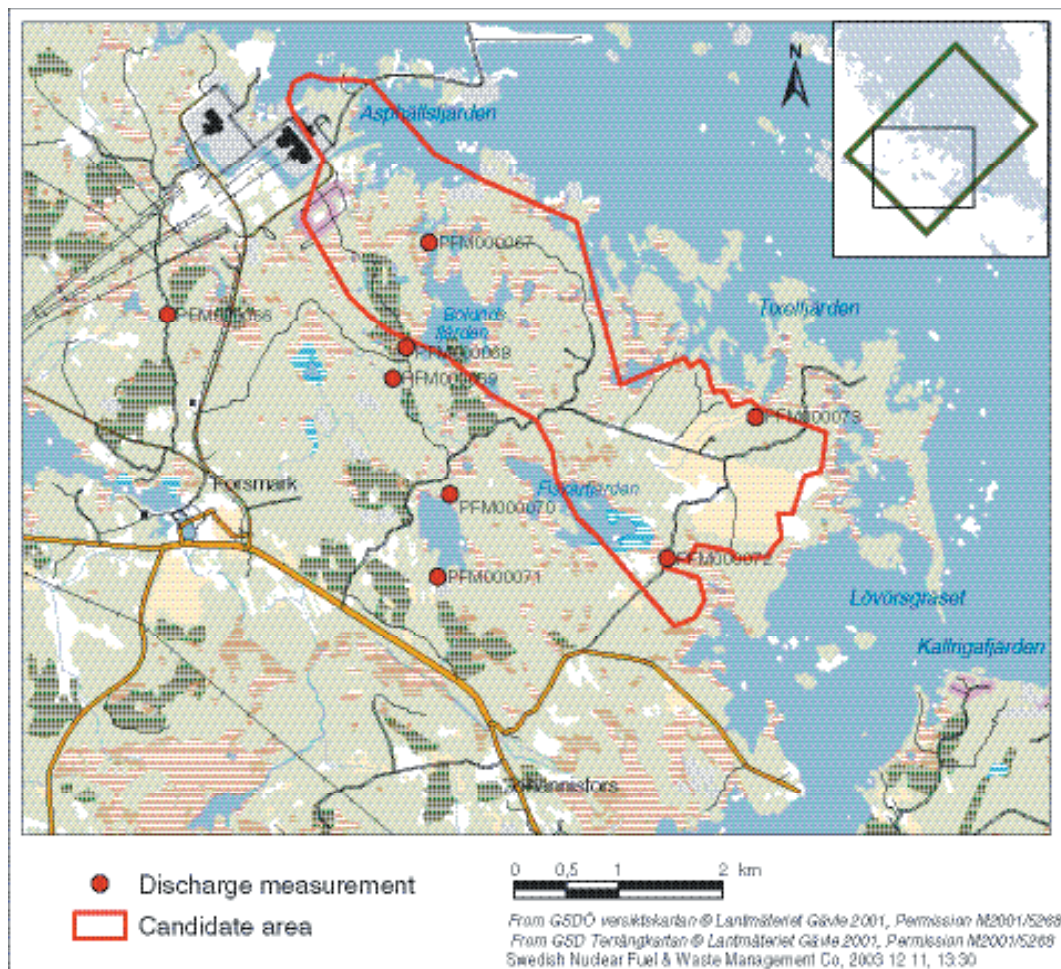
Figure 4-34. *Locations for simple discharge measurements.*

4.3.3 Hydrogeological data in Quaternary deposits

Slug tests for determination of hydraulic conductivity of the contact zone between the Quaternary deposits (till) and the bedrock have been performed in 36 monitoring wells /Werner and Johansson, 2003/. The monitoring wells had an inner diameter of 50 or 75 mm and the screens were 1 m long (in one borehole the screen was 0.5 m and in another one 2 m). The screens were placed in the till right above the bedrock contact or partly in till and partly in the bedrock /Johansson, 2003/. The depth from the ground surface to the bottom of the screens varied between 2.3 and 17.0 m.

A stainless steel slug was used to create the water-level displacement in the 50 mm wells, while a HDPE pipe filled with sand and a steel rod was used for the 75 mm wells. Diver® pressure transducers and loggers were used for registration of the water level changes. Both falling and rising head tests were performed.

The data from the tests were evaluated using three separate methods: the Cooper et al method, the Hvorslev method, and the Bouwer and Rice method /Butler, 1998/. For most wells a good to acceptable fit to the type curves of the Cooper et al method was obtained applying a fixed α (corresponding to a storativity (S) of 10^{-5}). In Figure 4-35, the hydraulic conductivities are shown. The data presented are all from the evaluation by the Cooper et al method and a fixed α. Figure 4-36 shows a histogram for the hydraulic conductivities.

The hydraulic conductivities varied between $5.62 \cdot 10^{-8}$ to $5.50 \cdot 10^{-4}$ m/s. The geometric mean was $1.18 \cdot 10^{-5}$ m/s (arithmetic mean $6.91\ 10^{-5}$ m/s, median $1.25 \cdot 10^{-5}$ m/s) and the standard deviation of log K was 1.00. Assuming log-normal distribution, the 95% confidence interval for the mean was $5.58 \cdot 10^{-6}$–$2.49 \cdot 10^{-5}$ m/s and the 95% confidence interval for a new observation was $1.32 \cdot 10^{-7}$–$1.05 \cdot 10^{-3}$ m/s.
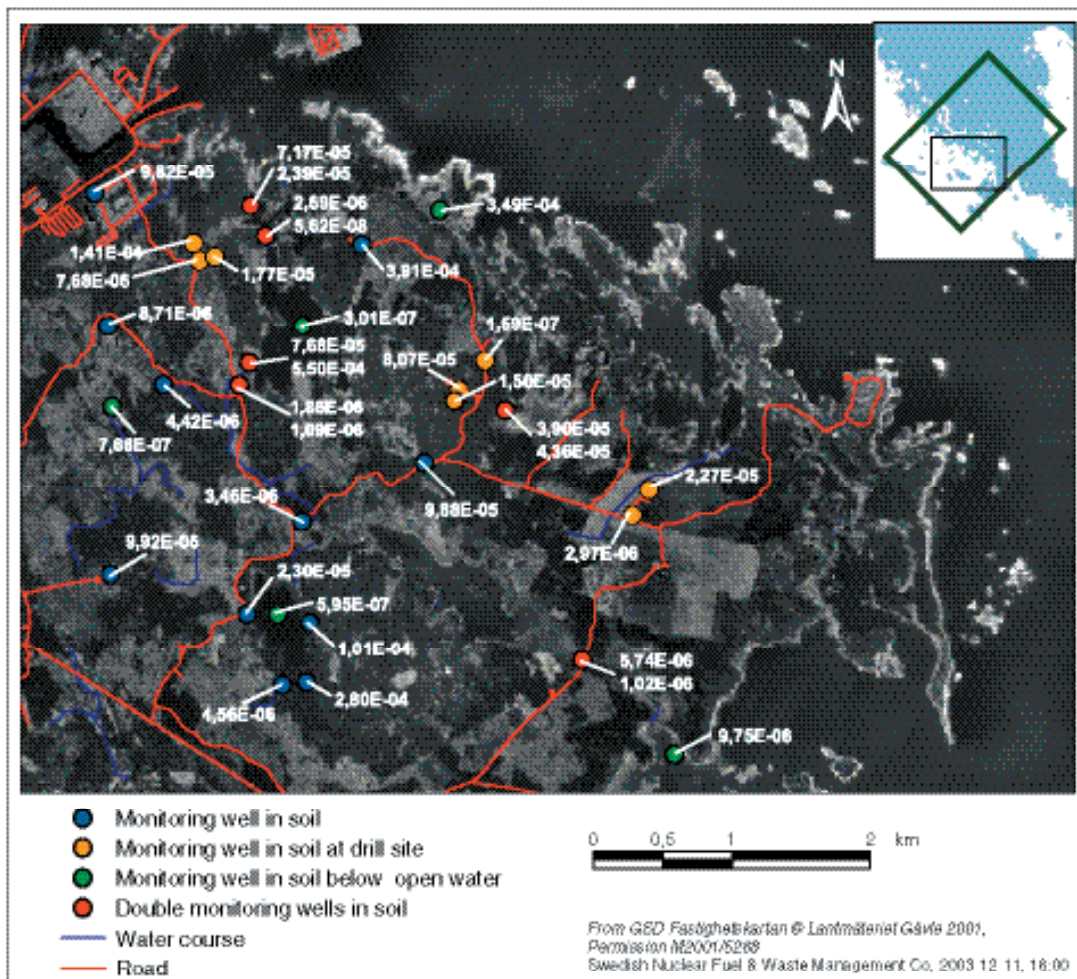
Figure 4-35. *Hydraulic conductivities obtained from slug tests evaluated by the Cooper et al method /Cooper et al, 1967/.*
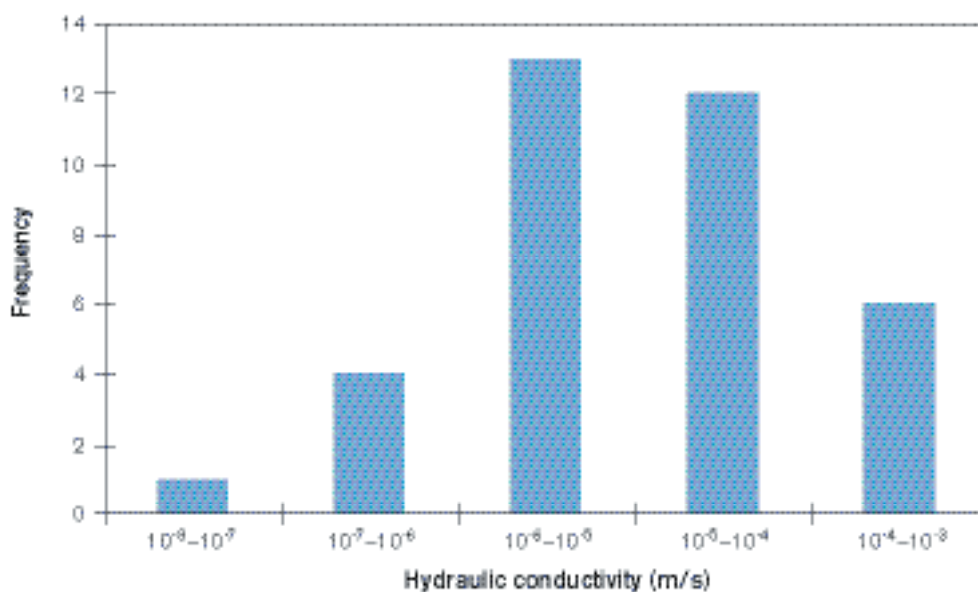
Figure 4-36. *Histogram for the hydraulic conductivities of the contact zone between the Quaternary deposits and the bedrock obtained from slug tests in 36 groundwater monitoring wells /Werner and Johansson, 2003/.*

4.3.4 Oceanography

In this report, the term oceanography includes the physics and chemistry of the open sea. Geology of the sea bed and biology of the sea, which are sometimes included in the term oceanography, are here treated under the geology and biology (biota) headings, respectively. Furthermore, data on physical and chemical parameters in shallow bays, collected in the surface water programme, are here treated in the hydrogoechemistry section.

No new site-specific oceanographic data were available at the data freeze. Previously available site-specific oceanographic data are presented in /Engqvist and Andrejev, 1999/, /Lindell et al, 2000/ and /Larsson-McCann et al, 2002/.

4.4 Geologic interpretation of borehole data

4.4.1 Geological and geophysical logs

Geological borehole data for model version 1.1 are available from:

- Core-drilled borehole KFM01A between c –100 m masl down to c –1,000 m masl.

- Percussion-drilled boreholes around drillsite 1; HFM01, HFM02, HFM03 and the first one hundred meters of KFM01A.

- Percussion-drilled boreholes HFM04 and HFM05 at drillsite 2.

- Percussion-drilled boreholes HFM06, HFM07 and HFM08 at drillsite 3.

The locations of the available boreholes are shown in Figure 4-37. The cored borehole KFM01A has been mapped using the BOREMAP /Petersson and Wägnerud, 2003/. There are no geophysical borehole logs available for KFM01A. Both geological (BIPS) interpretations and geophysical logs are available from the percussion-drilled holes /Gustafsson and Nilsson, 2003; Nilsson and Gustafsson, 2003; Nilsson and Aaltonen, 2003/. None of the geophysical logs from the percussion-drilled boreholes has been utilised in model version 1.1 because of poor data quality (HFM01, 02, 03; see /Gustafsson and Nilsson, 2003/) or because of time constraints.

The type of data that are available from the cored borehole KFM01A and from the percussion-drilled boreholes are shown in Table 4-12 and Table 4-13. An important piece of information from the hydraulic point of view is the division into open and sealed fractures.

Table 4-12. Available geological data from KFM01A.

Type of data	KFM01A, percussion-drilled section 0–100 m	KFM01A, core-drilled section 100–1000 m
Lithology (rock types)	0 to 100 m	102 to 1000 m
Fracture orientation	30 to 48 m	100 to 1000 m
Fracture mineralization		100 to 1000 m
Weathering		100 to 1000 m
Tectonization		100 to 1000 m
Core loss		100 to 1000 m
Crush		100 to 1000 m

Table 4-13. Available geological data from the percussion-drilled boreholes*.

Type of data	HFM01	HMF02	HFM03	HFM04	HFM05	HFM06	HFM07	HFM08
Lithology (rock types)	X	X	X	X	X	X	X	X
Fracture location	X	X	X	X	X	X	X	X
Fracture orientation	X	X	X	X	X	X	X	X
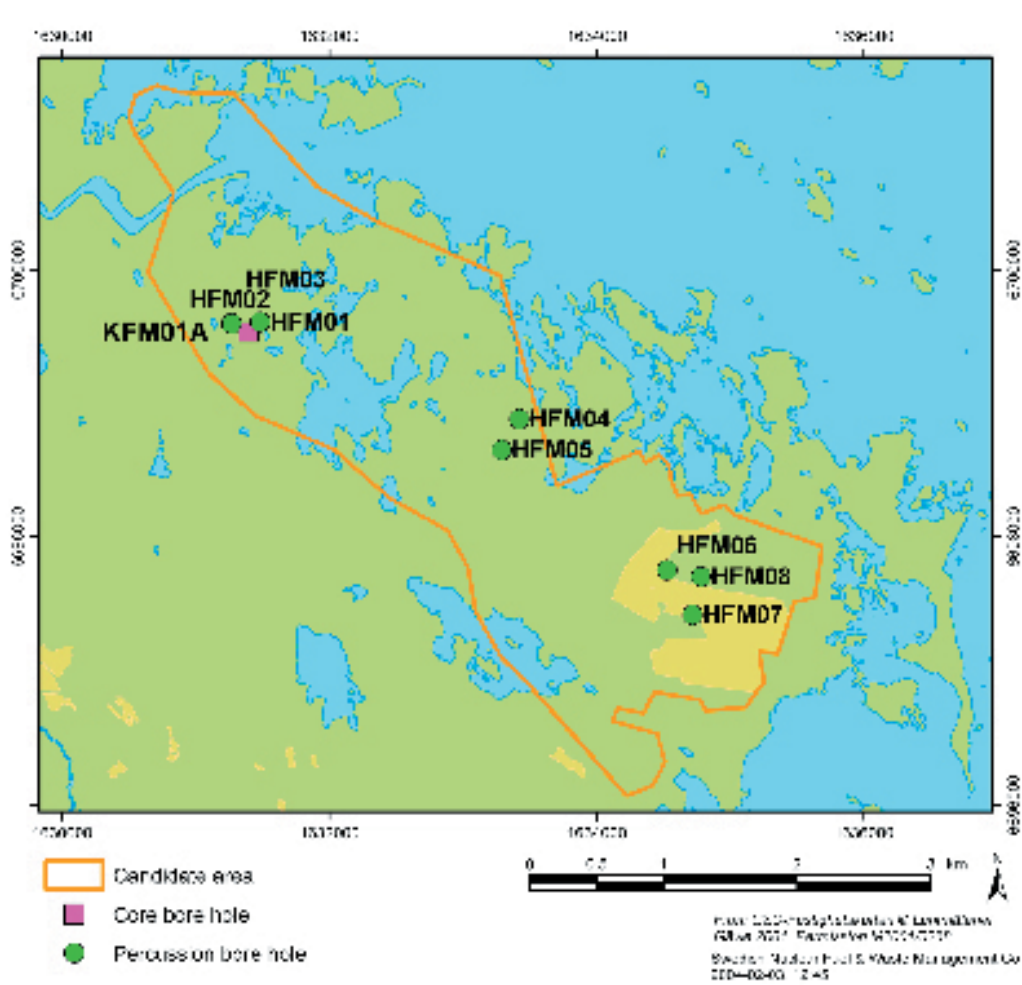
Figure 4-37. *Location of boreholes from which data are available for model version 1.1.*

4.4.2 Borehole rock types

The most abundant rock in KFM01A is a medium-grained, metamorphosed and reddish-grey to grey granite to granodioritic rock, which covers over 84% of the mapped core length, cf Table 4-14 and Figure 4-38. There are several subordinate rock types including finer grained metagranitoids (10%), pegmatites, amphibolites and minor bands, dykes or veins of leucogranitic material (5%). The more shallow percussion-drilled boreholes indicate the same pattern of lithology as in the deeper parts of KFM01A.

Table 4-14. Occurrence of rock types along the core-drilled part of KFM01A.

Rock name	Granite to granodiorite	Finer-grained granitoid	Pegmatite, pegmatitic granite	Amphibolite	Calc-silicate rock	Granite, commonly leucocratic
Rock ID	**101057**	**101051**	**101061**	**102017**	**108019**	**111058**
Total rock occurrence (m)	761.62	97.5	13.7	18.38	2	11.99
Part of total length (%)	84.14	10.77	1.51	2.03	0.22	1.32
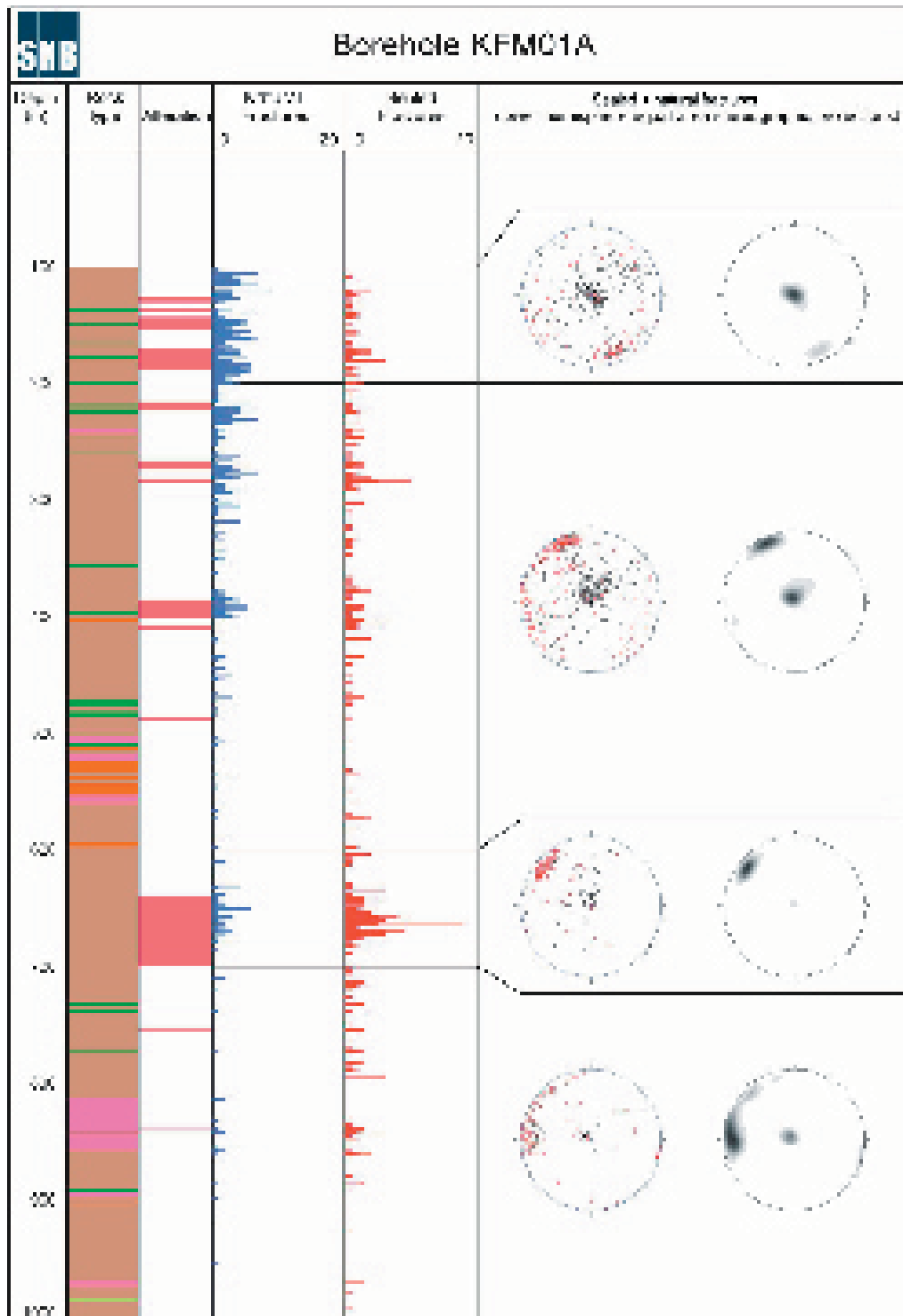
Figure 4-38. *Overview of KFM01A.*

The most abundant rock, granite to granodiorite, is deformed and shows a fairly constant foliation throughout the cored borehole length with a general orientation around 350/87 (right-hand rule), cf Figure 4-39. The ductile deformation of the rock is also visible in the orientation of the contacts between the fine grained, equigranular metagranitoids and the main rock mass with a parallel orientation to the foliation.
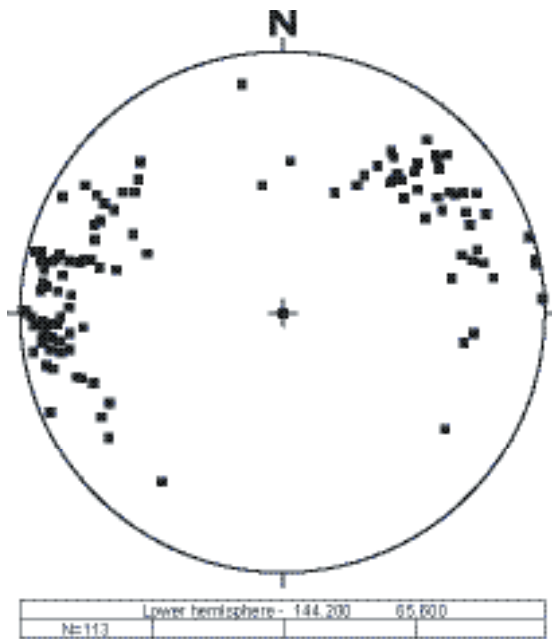
KFM01A poles to ductile foliation planes

Figure 4-39. *Lower hemisphere equal-area stereo plot of poles to ductile foliation planes in KFM01A, measured at depths between 100 m and 1,000 m.*

4.4.3 Borehole fractures

Fracture classification

The fracturing in boreholes has been classified in two fracture groups, *natural* and *sealed*, by the mapping geologists. The difference between these groups was not completely clear at the onset of the modelling and has caused considerable confusion. In a first analysis of borehole fractures, it was assumed that the group *sealed* fractures are not open and that *natural* fractures are open when observed in the core. It was further assumed that this classification does not incorporate fractures that were opened by the drilling.

The classification above does not provide reliable information on the real state of the fracture, i.e. whether it is truly open or sealed in the rock mass. However, the mapped fracture data contain other parameters that can be used to get closer to the true state of the fractures. Therefore, the measured fracture aperture was used to divide fractures into the groups open and sealed.

Aperture is measured from the BIPS image during the BOREMAP survey of the core. The BIPS image has a lower aperture detection limit of 1 mm. However, the geologist also has access to the core, which gives further possibilities to estimate smaller apertures. In percussion-drilled boreholes, the source of fracture information comes from the BIPS image solely, and the aperture limit is 1 mm.

As a working hypothesis, it was assumed that fractures with an aperture larger than 0 mm are classified as open and fractures with no aperture are classified as sealed. The relevance of this classification needs to be reassessed in further model versions when feed-back can be given from rock mechanical and hydrogeological interpretations.

The original data set of mapped fractures in each of the groups *natural* and *sealed* in the cored borehole KFM01A are given in Table 4-15. The results of the adapted classification of fractures into open and sealed in the cored borehole KFM01A, based on apertures, are shown in Table 4-16.

Table 4-15. Classification of fractures in KFM01A as delivered from SICADA, delivery 03_109.

Borehole	Section (borehole depth (m))	Fracture type	No of fractures
KFM01A	100–1000	Natural	818
KFM01A	100–1000	Sealed	699
KFM01A	100–1000	All	1517

Table 4-16. Fracture classification in the cored borehole KFM01A, based on measured aperture.

Borehole	Section (borehole depth (m))	Fracture type	No of fractures
KFM01A	100–1000	Open (aperture > 0 mm)	201
KFM01A	100–1000	Sealed (aperture = 0 mm)	1316
KFM01A	100–1000	All	1517

Data from the percussion boreholes are available in the form of open and sealed fractures, based on aperture on the BIPS images. However, this data set has not been thoroughly analysed in the model version 1.1 work and it is necessary to revisit these data in coming model versions. A preliminary data review is presented, but the fracture evaluation has mainly been performed on data from the cored borehole KFM01A.

Fracture orientations

The cored borehole KFM01A has large populations of gently dipping fractures and steeply dipping, NE striking fractures. The borehole fracturing is subject to sampling bias due to the near-vertical borehole orientation.

A bias correction, using a Terzhagi correction with a minimum bias angle of 15 degrees, enhances the presence of the steep fractures, striking mainly NE and NS, cf Figure 4-40. When dividing the population into open and sealed fractures, a stronger sub-horizontal set is visible in the open fracture data than in the sealed. There is also a sub-set of NE striking and steeply dipping fractures in the open fracture set, cf Figure 4-41a. The sealed fractures have, in principal, the same pattern as the open ones, but with a larger population of NE striking and steeply dipping fractures.
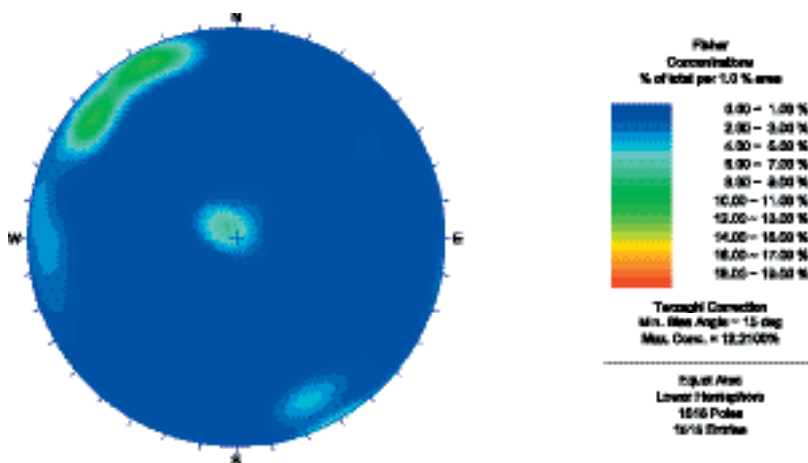
Figure 4-40. *Terzhagi corrected fracture orientations in the cored borehole KFM01A (borehole length 100 m to 1,000 m). Lower hemisphere equal area projection of poles to fracture planes.*
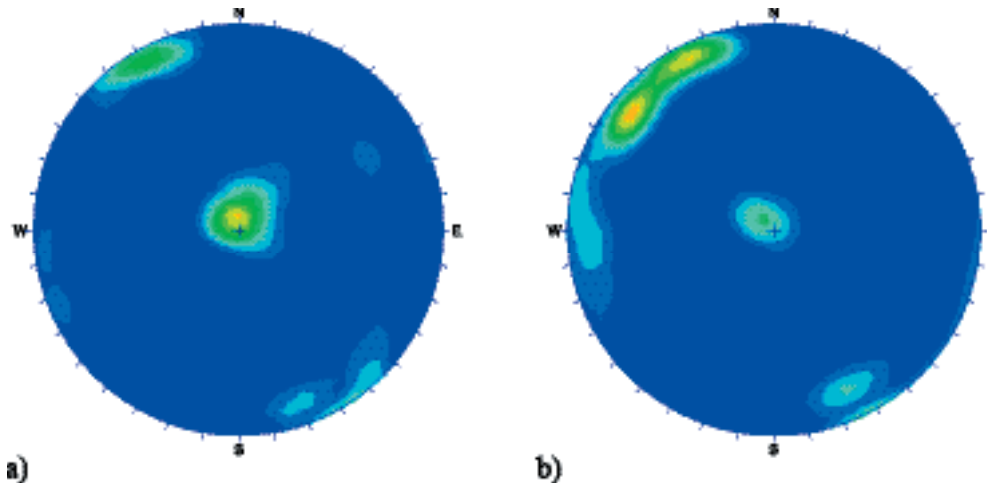
Figure 4-41. Terzhagi corrected (a) open (201) and (b) sealed (1,316) fracture orientations in the cored borehole KFM01A (borehole length 100 m to 1,000 m). Lower hemisphere equal area projection of poles to fracture planes.

The open fractures in the HFM01 to HFM03 percussion boreholes indicate a similar orientation pattern as the open fractures in the core-drilled borehole KFM01A. However, the sampled sealed fractures in the percussion holes are too few to make any interpretation meaningful.

The orientations of dominating fracture fillings have been briefly evaluated for model version 1.1. In general, laumontite, hematite and quartz all show a consistent NE striking and steeply dipping pattern throughout the borehole, with less than 5% of the fractures classified as open, cf Figure 4-42. Calcite filled fractures, cf Figure 4-43, have a sub-horizontal set of fractures in addition to the NE striking and steeply dipping pattern. There is no obvious difference between open and sealed fracture orientations when looking at the whole fracture sample at the same time. As will be seen later, fracture mineralogy is to some extent coupled to open and sealed fracture intervals in the borehole, but does not necessarily appear in different orientation sets for the two groups, open and sealed.
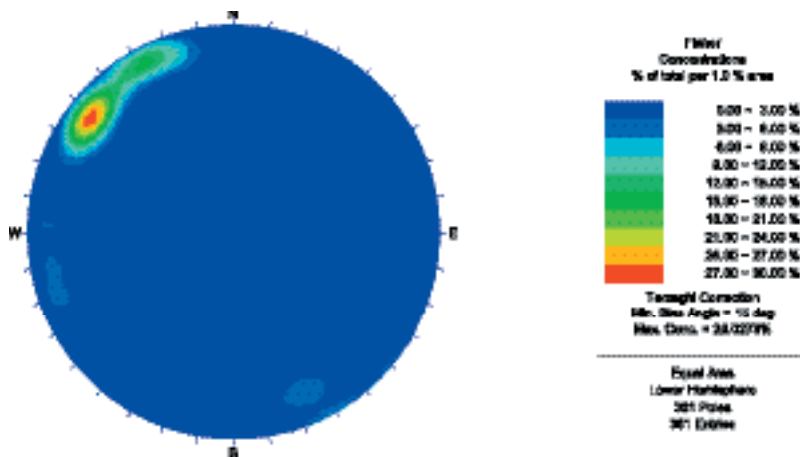
Figure 4-42. Orientations of Laumontite mineralization along the cored borehole KFM01A. Lower hemisphere equal area projection of poles to fracture planes.

122
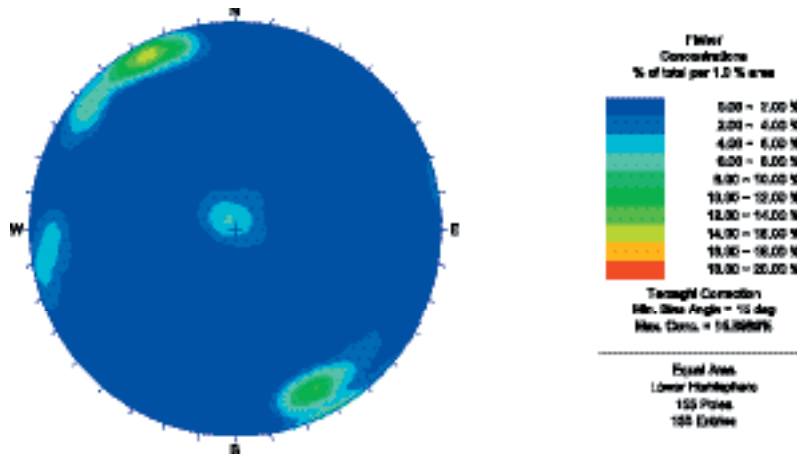
Figure 4-43. Orientations of Calcite mineralization along the cored borehole KFM01A. Lower hemisphere equal area projection of poles to fracture planes.

Fracture frequency

Open and sealed fractures in the core-drilled borehole KFM01A are shown in a normalised cumulative probability plot in Figure 4-44. The cumulative curve illustrates how the fracture frequency increases and decreases along the borehole length. Each of the curves show the relative cumulative proportion of fractures mapped along the length of the borehole. Each group of fractures (all, open and sealed) have been normalized to each sample size such that all curves start at a probability of 0 and end at a probability of 1. The change in frequency along KFM01A is similar for both sealed and open fractures, although the open fractures have a higher frequency than the sealed in the upper 400 m of the borehole (i.e. gentler slope of the curve in the diagram). More than 70% of all open fractures and almost 60% of the sealed fractures are found in the section c –100 to –400 masl in KFM01A.
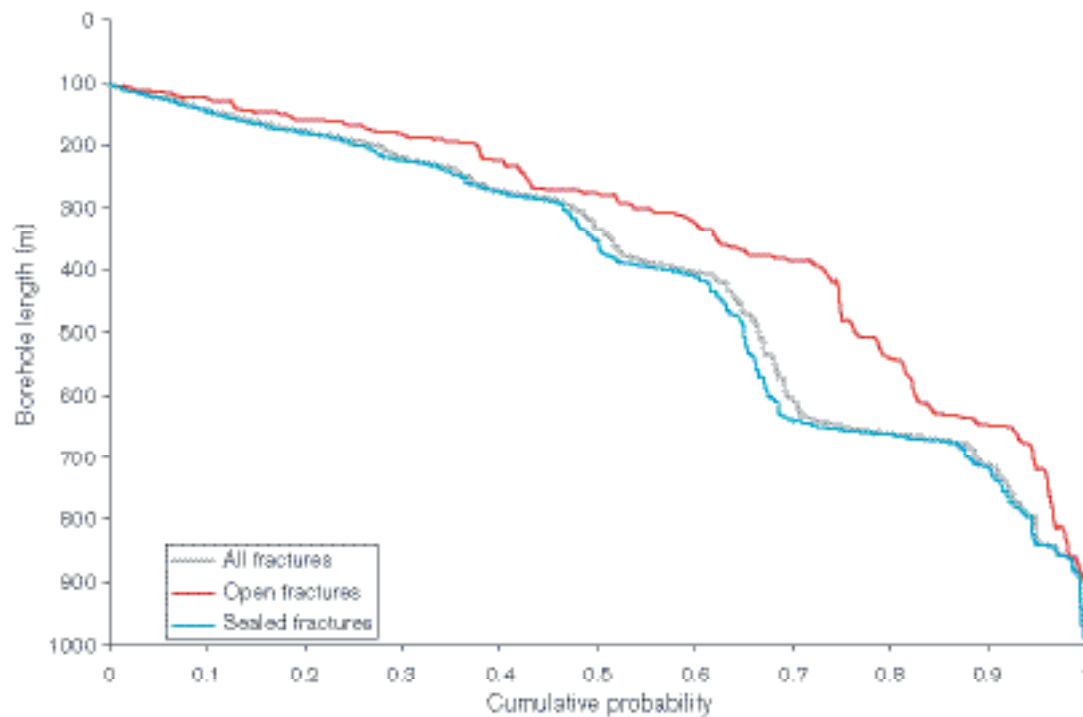
Figure 4-44. Open and sealed fracture frequency in KFM01A shown as a normalised cumulative probability plot.

Below –400 masl and down to approximately 650 m, there is a decrease in frequency of both classes of fractures (i.e. steeper slopes of the curves in the diagram). Between approximately 650 and 700 m, there is a sharp increase in the sealed fracturing and somewhat smaller increase in the open fractures. The open fracture frequency then decreases again below 700 m, followed by the sealed fractures.

The analysis of fracture mineralogy was based on the frequency of the most dominant fracture fillings only, using BOREMAP data from the core-drilled borehole KFM01A. No microscopic studies and analyses of the mineral assemblages were performed in model version 1.1. However, it is expected that such information will be incorporated in model version 1.2.

The most abundant fracture fillings, regardless of fracture classification, are chlorite, laumontite and hematite. However, the relative proportion of dominant fillings differs between open and sealed fractures. Open fractures are dominated by chlorite, unknown and calcite fillings, cf Figure 4-45. The unknown fillings are, in this study, interpreted as being either not possible to interpret by the mapping geologist, or so minute that it is not possible to see the mineralization.
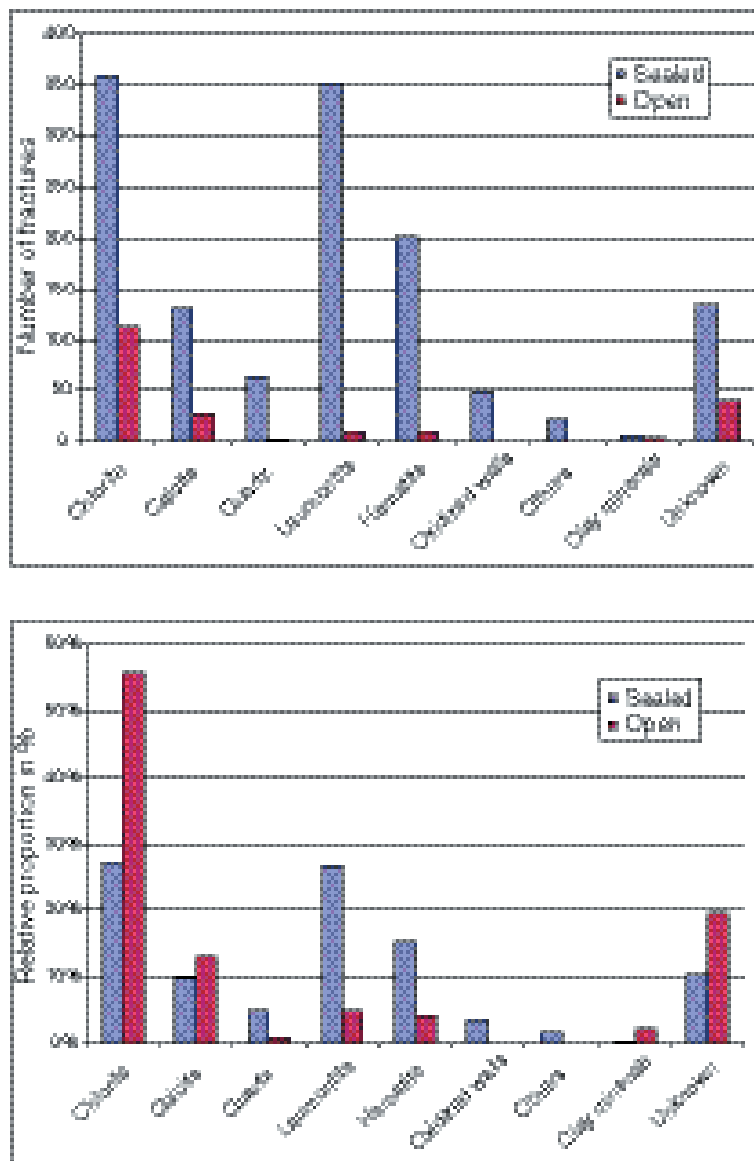
Figure 4-45. *Fracture frequency of dominant mineral fillings for open and sealed fractures. The actual numbers of fractures (upper) and the relative proportion of the open and sealed fillings (lower) are shown.*

Chlorite is the dominant mineral in over 55% of the open fractures. The sealed fractures have an equal proportion of chlorite- and laumontite-filled fractures, around 28% of each. Minerals such as epidote, pyrite, prehnite, iron hydroxides and biotite are lumped together under the denomination "others" and substitute less than 5% of the sealed fractures. These minerals are absent in the open fractures.

A cumulative probability analysis was also made of the dominant fracture mineral fillings and the result is shown in Figure 4-46. In all fractures, independent of their classification, chlorite and calcite follows a relatively even frequency down to 400 m in KFM01A, where the frequency of both decrease. Calcite filled fractures show a minor increase again in the densely fractured section between 650 m to 700 m, whereas chlorite (and hematite) filled fractures more follows the frequency trend of the whole fracture set.

Laumontite- and quartz-filled fractures, together with fractures that have oxidized walls, do not show a clear decrease in frequency below 400 m. Laumontite seems to be evenly distributed along the borehole, but shows a strong increase in the 650 m to 700 m interval as well as in other zones of high general fracture frequency. On the contrary, quartz-filled fractures and fractures with oxidized walls are less correlated to general zones of high fracture frequency, and are relatively evenly distributed along the borehole.

The fracture fillings in the open fracture sample, cf Figure 4-47, shows a similar pattern as the whole fracture sample, except that quartz-filled fractures and fractures with oxidized walls are either too few to be included in the plot or do not exist. Chlorite-filled fractures also dominate the open fractures. Calcite-filled fractures are common above 400 m, but are very few further down. Chlorite, hematite and laumontite all have a relative increase in fracture frequency around 650 m to 700 m. However, note that the data set for hematite and laumontite is very small.
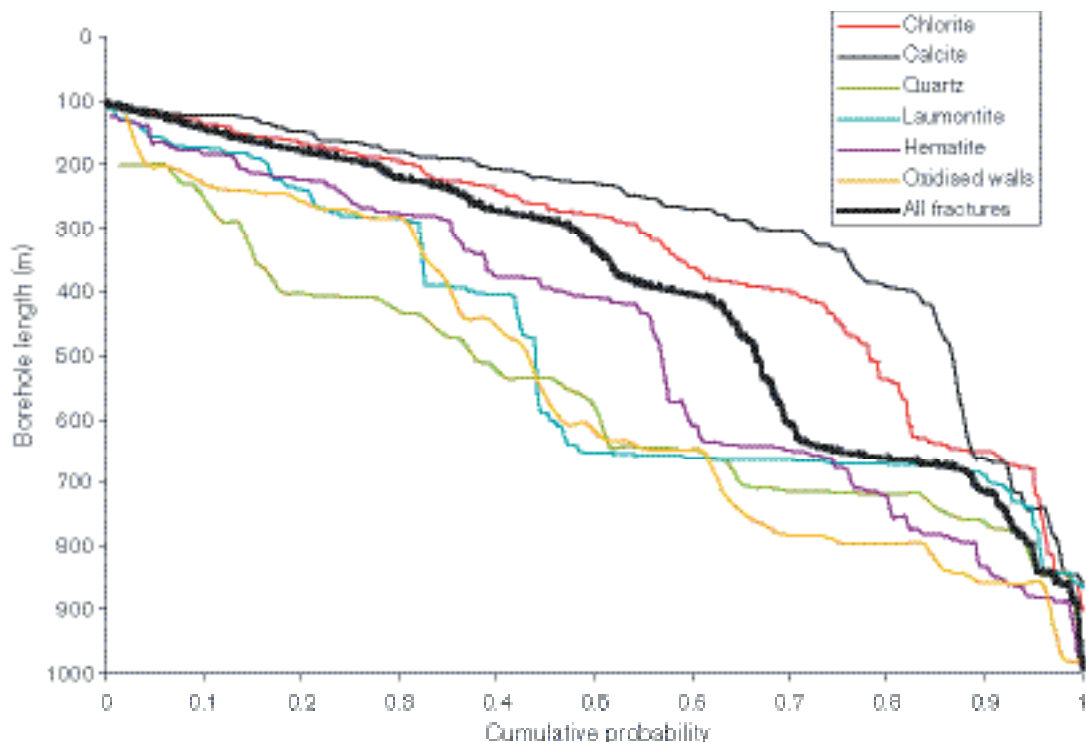
Figure 4-46. *Fracture frequency of dominant mineral fillings shown as a normalised cumulative probability plot. This plot includes all fractures regardless of classification in open or sealed fractures.*
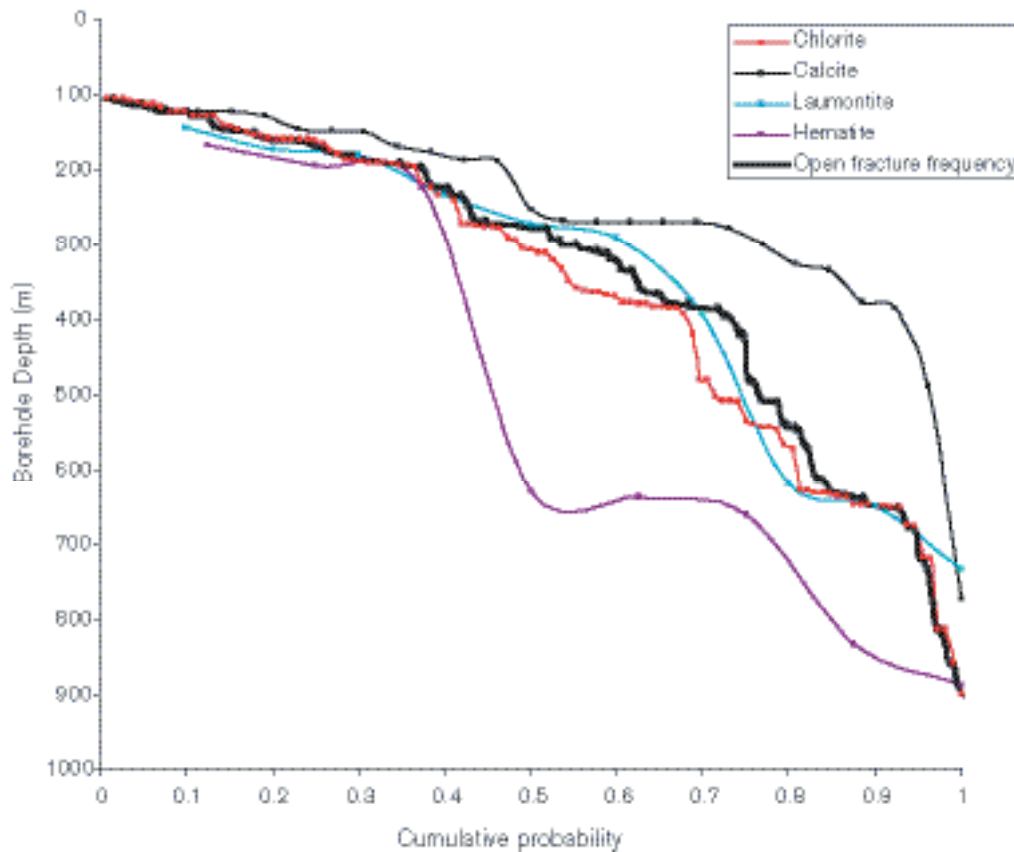
Figure 4-47. *Open fracture frequency of dominant mineral fillings shown as a normalised cumulative probability plot.*

4.4.4 Borehole radar

There are forty-two identified radar reflections in KFM01A, most of which occur in the interval between 100 m and 500 m depth. The radar information has not been analysed in detail in support of model version 1.1, but will be done so in coming model versions.

4.4.5 Single hole interpretation

Geological data from the cored borehole is important in the construction of the geological 3D models, since the borehole constitutes the only available direct data at depth in the candidate area. A simplified geological single-hole interpretation was made based on lithology and fracturing, using the same resolution as applied in the modelling of geological domains in the 3D model. The geological units used from the surface mapping have been treated in a similar way. This is explained in Chapter 5.

A more complete single-hole interpretation is expected to be performed for model version 1.2, provided that geophysical borehole data is available.

The lithology in KFM01A does not change with depth and is completely dominated by one single rock type. This is the same rock type as observed in large areas of the candidate area. As a working hypothesis, the lithology observed in KFM01A was considered as a single uniform lithology.

The frequency of open fractures in the upper 400 m of the borehole is higher compared with the lower 600 m, although the decrease with depth is gradual. Furthermore, the fracturing in the borehole is dominated by sub-horizontal fractures. The rock along the borehole wall does not show any distinct geological change with depth, such as change in rock type or degree of ductile deformation.

A statistical analysis of borehole fractures is presented in Section 5.1.6.

126

4.5 Hydrogeological interpretation of borehole data

4.5.1 Single-hole tests and borehole data.

Historical data

A large number of single-hole tests were conducted in the SFR area during the construction of the SFR repository. The hydraulic data from these single-hole tests were compiled and scrutinised by /Axelsson et al, 2002/. Based on their assessment, the data were incorporated in model version 1.1 to assign hydraulic properties to the fracture-zone segments. The values used and how they were used are described in Section 5.4.6.

The hydraulic data from the single-hole tests conducted in the deep, cored boreholes DBT-1 and DBT-3, located within the Forsmark reactor plant area, were not incorporated in model version 1.1 due to two limitations. First, the geological information from the two boreholes was not considered in the current structural model, which prohibited a joint quantitative analysis between hydrogeology and geology. Secondly, the hydraulic data from these boreholes were not accessible from the SICADA database at time of the data freeze for model version 1.1. However, the structural and hydraulic information reported by /Carlsson and Olsson, 1982/ was recognised qualitatively. For example, it was noted that the investigations conducted in the deep, cored borehole DBT-1 suggest that the bedrock is less conductive below c –320 masl and that the interpreted fracture zone intersecting DBT-1 at c –320 masl was not possible to investigate hydraulically due to, among other things, high flow rates.

Data freeze 1.1

Hydraulic tests in single holes, conducted in support of model version 1.1, were performed in the percussion-drilled boreholes HFM01–08 and in the cored borehole KFM01A. Hydraulic tests were also conducted in the pilot holes of the cored borehole KFM01A. The hydraulic tests conducted in the percussion and pilot boreholes were performed as open-hole pumping tests, whereas the difference-flow logging method was applied in the cored borehole using a test section length of five metres for the sequential measurements and one metre for the overlapping measurements. The size of the overlapping interval was 0.1 metre. The lengths of the pilot and percussion boreholes range between 26 and 222 m. The cored borehole KFM01A is c 1,000 m deep.

The drilling and the subsequent BIPS logging of the percussion drilled boreholes indicated an extensive fracturing in the superficial bedrock and a number of distinct, large sub-horizontal fractures/fracture zones at various depths. This information is consistent with the historical information from the excavations carried out in the reactor area /Carlsson, 1979/. The single-hole tests conducted in the percussion-drilled boreholes HFM01–08 and in the pilot hole of the cored borehole KFM01A /Ludvigson et al, 2003a,b; Källgården et al, 2003/ showed that the transmissivity of the most conductive fractures/fracture zones range between $5·10^{-5}$ and $1·10^{-3}$ m²/s.

/Carlsson, 1979/ showed that the extensively fractured, superficial bedrock in the reactor area was several metres thick and that the fracture apertures were generally quite large (see Figure 4-60 in Section 4.6.5). Interestingly, many of the most open fractures were found to be filled with fine-grained sediments. This information is consistent with observations made in some of the percussion-drilled boreholes in the candidate area. For instance, dry, sediment-filled fractures of large apertures were encountered between c 50 and 70 m below the ground surface during the percussion drilling of HFM07 and the pilot hole of KFM03A.

The sequential difference flow logging conducted in KFM01A indicated that the rock at drillsite 1 is very low-conductive below the casing shoe at c –100 masl. Out of a total of 179 five-metre long test sections, 22 test sections were found to yield water above the theoretical limit for sequential flow measurements, 0.1 mL/min (6 mL/h) /Rouhiainen and Pöllänen, 2003/. The corresponding theoretical transmissivity threshold for these measurements was c $1.5·10^{-10}$ m²/s in this particular borehole.

All the 22 conductive test sections were found above –400 masl, see Figure 4-48. The abrupt change in the transmissivity distribution in Figure 4-48 conforms to the observed decrease in the fracturing, see Figure 4-38. In Figure 4-49, the fracture frequencies along the length of KFM01A are plotted as continuous functions using a moving average of 30 m in increments of 0.1 m. The division of the fracturing into "open" and "sealed" fractures is discussed in Sections 4.4.3 and 4.5.3. The legend "all" is simply the sum of these two classes. The interpretation of the plotted frequencies in Figure 4-49 in terms of fracture zones and rock in between is discussed in Section 5.1. It is noted here that the distinct frequency peak at c –660 masl in Figure 4-49 is poorly conductive according to Figure 4-48.
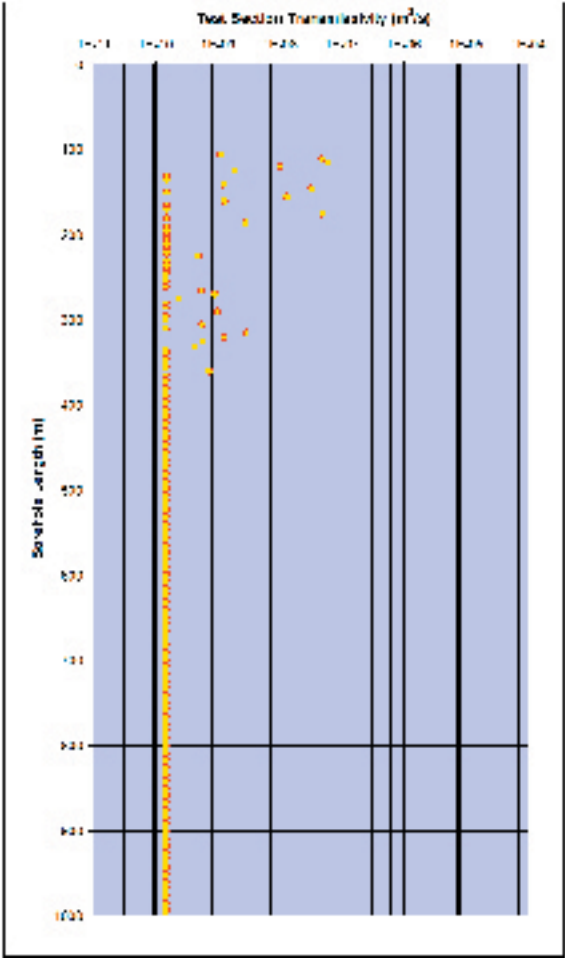
Figure 4-48. *Plot of the sequential difference flow logging conducted in KFM01A. The measurements and the interpretations are reported in /Rouhiainen and Pöllänen, 2003/. The theoretical threshold for the sequential test section transmissivity was $1.5 \cdot 10^{-10}$ m^2/s in this particular borehole.*
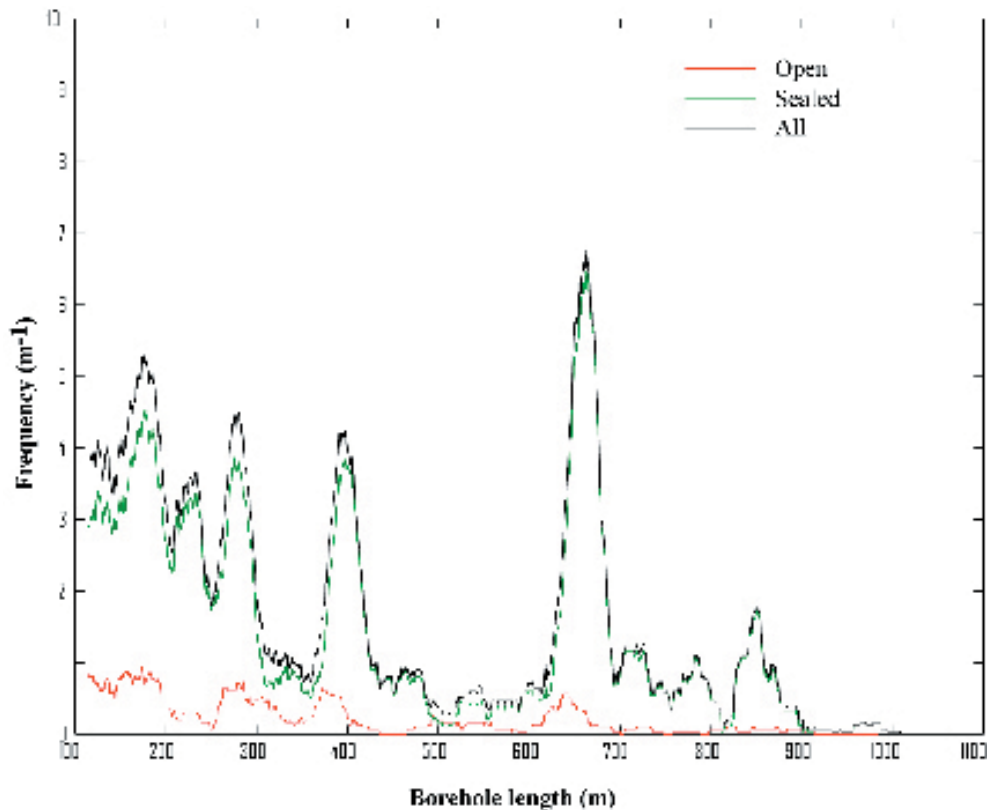
Figure 4-49. Plot of the fracture frequency observed in the cored borehole KFM01A. The frequencies were calculated by means of an overlapping moving average. The size of the moving average window was 30 m and the size of the incremental stepping was 0.1 m.

4.5.2 Interference tests

Historical data

Interference (cross-hole) tests were conducted in the SFR area during the construction of the SFR repository. Hydraulic data from these single-hole tests were compiled and scrutinised by /Axelsson et al, 2002/. Based on their assessment, the data were incorporated in model version 1.1 to assign hydraulic properties to the fracture zone segments. The values used and how they were used are described in Section 5.4.6.

Data freeze 1.1

During the percussion drilling, hydraulic responses were occasionally recorded in nearby percussion-drilled boreholes at all drillsites 1–3. However, regular hydraulic interference tests were not conducted in support of the version 1.1 site descriptive model, except for one test conducted at drillsite 1. This was and interference between the percussion-drilled boreholes HFM01 and HFM02 /Ludvigson and Jönsson, 2003/. The test was conducted twice in order to test the reciprocity principle and the possibility for hydraulic boundaries. The results support the geological interpretation of an extensive horizontal fracture zone at drillsite 1, the transmissivity of which was in agreement with the aforementioned transmissivity range (cf Section 4.5.1). In addition to the transmissivity, the storativity of the fracture zone was estimated to c $5 \cdot 10^{-5}$.

4.5.3 Conductive fractures

The interpretation of conductive fractures for model version 1.1 is strongly affected by the limited number of inflow points to the only cored borehole, KFM01A, from which data are available. Unfortunately, the geological classification of conductive fractures in the cored borehole KFM01A was not clear from the onset of the geological analysis. Section 4.4.3 explains the confusion and how the underlying principle for the classification was changed later on during the geological modelling. The effect of the changed geological classification of conductive fractures on the hydrogeological analysis and numerical modelling is explained in Section 5.4.6.

Results from the overlapping difference flow logging of KFM01A

Out of a total of 1,517 fractures in KFM01A, that were either open or sealed based on the changed aperture classification, 34 fractures only were found to yield water above the theoretical limit for quality-assured overlapping difference flow measurements, 0.5 mL/min (30 mL/h) /Rouhiainen and Pöllänen, 2003/. These 34 fractures were found between c –105 and –365 masl.

The corresponding transmissivity threshold for the overlapping difference flow measurements was c $7.5 \cdot 10^{-10}$ m²/s in this particular borehole. However, in practice it was found possible to extend the transmissivity threshold to $1.5 \cdot 10^{-10}$ m²/s.

Figure 4-50 shows two examples of BIPS images of flowing fractures observed in the cored borehole KFM01A. The identification of the conductive fractures in the drill core and in the BIPS images is an important piece of information for the conceptual modelling of hydraulic anisotropy and for the subsequent construction of discrete fracture network flow models. This information was not thoroughly analysed and ready for use in model version 1.1, but will be completed in subsequent model versions starting with version 1.2.
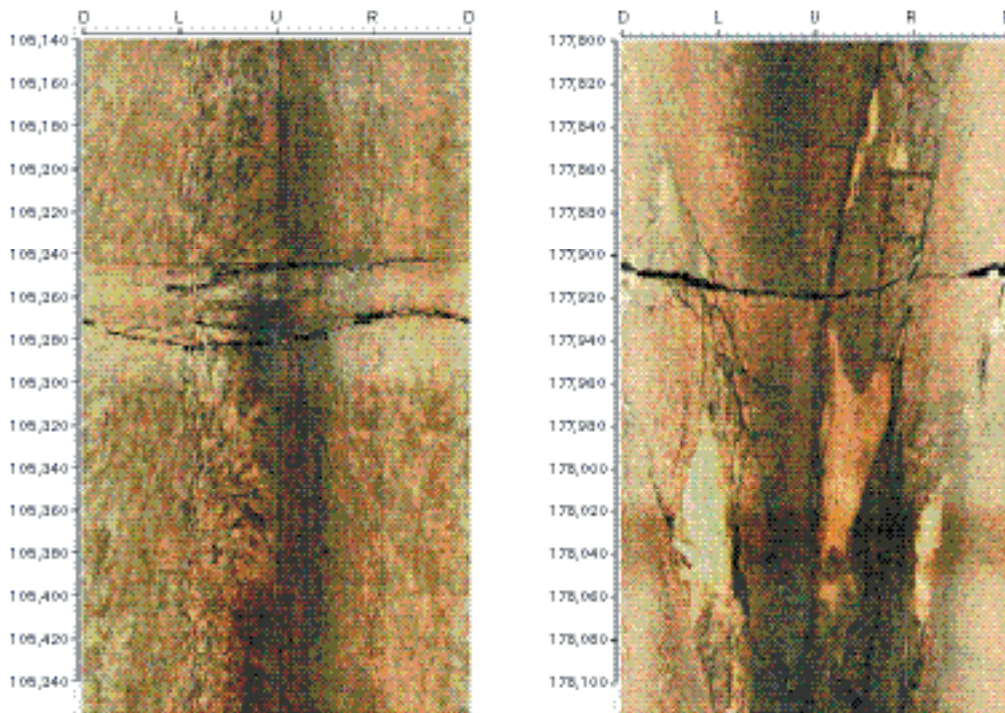
Figure 4-50. *Two examples of how flowing fractures observed in the cored borehole KFM01A may appear in the BIPS log. The fracture transmissivity is $1.1 \cdot 10^{-9}$ m²/s in the left image and $4.7 \cdot 10^{-8}$ m²/s in the right. Besides the position in the borehole the orientation can generally be obtained from the BIPS log.*

4.5.4 Hydrogeological evaluation

The qualitative information about the bedrock that are extracted from historical data and data freeze 1.1 may be summarised as follows:

- The documentation from the historical investigations shows that the superficial bedrock is extensively fractured and that the thickness varies in space. Available borehole logs indicate an average thickness of several metres, possibly more.

- High transmissivities were recorded in the percussion-drilled boreholes at all drillsites, which indicate that there may be several extensive fractures/fracture zones. The borehole information suggests that all of these fractures/fracture zones are either gently dipping or close to horizontal.

- Fracture infillings classified as fine-grained sediments of Quaternary origin were encountered at different depths within the candidate area. The mechanism behind these infillings is not fully understood. The encountered sediment-filled fracture/fracture zones were generally of low transmissivity according to the flow logging performed at the completion of the percussion drilling. According to the BIPS logs, some of the impervious fractures/fracture zones lacked fracture infillings, which suggests either a heterogeneous fracture aperture and/or a heterogeneously distributed infilling.

- The overlapping difference flow logging in the cored borehole KFM01A suggests that the bedrock in the Forsmark area may be very low-conductive at depth. This hypothesis is supported by the historical information reported from the cored borehole DBT-1, drilled in the reactor area. Compared to the hydrogeological experiences gained in the past from the investigations of the study sites (Kamlunge, Gideå, Svartboberget, Finnsjön, Fjällveden, Klipperås and Sternö) the sparse fracturing and low conductivity rock observed in the vicinity of KFM01A are considered exceptional.

4.6 Rock mechanics data evaluation

4.6.1 Stress measurements

No new stress information is available for the site descriptive model version 1.1. The previous model version /SKB, 2002a/ summarises the old in situ stress measurements from the area. Data originated from three methods: i) doorstopper, ii) overcoring, and iii) hydraulic fracturing. These methods are described for example in /Amadei and Stephansson, 1997/. In more detail, the data set consists of:

- Stress measurements for the discharge tunnel of Units #1 and #2 at a depth of 40–60 m (Doorstopper, 2D method).
- Stress measurements in deep boreholes by the former Swedish State Power Board to test and demonstrate the Borre Probe (overcoring, 3D method) for in situ stress measurements performed at depths between 10–501 m /Carlsson and Olsson, 1982/. The test site was located close to Unit #3 in boreholes DBT-1 and DBT-3.
- Stress measurements for the SFR facility using the Borre Probe (3D method) at a depth between 40 and 140 m.
- Stress measurements in the 500 m deep borehole close to Unit #3 to test equipment for hydraulic fracturing (2D method) /Stephansson and Ångman, 1984/.

The results give very consistent information of the orientation of the major principal stress /Carlsson and Christiansson, 1987; SKB 2002a/, but the knowledge of the stress magnitude versus depth is limited to the deep borehole behind Unit #3.

How the quality control of individual tests was carried out in the early days is not fully traceable, even though it is well understood that the quality requirements on the tests were already high. The Borre Probe was developed in the late Seventies as an up-to-date stress measurement method. In its first version, the strains prior to overcoring were recorded and then the communication cable was cut so that no observations during overcoring were collected. Since 1988, the Borre Probe is equipped with a downhole logger that continuously records the strains during overcoring. It is thus possible to perform quality control because problems such as influence of temperature increase during overcoring, creep in the bond, sudden failure of a strain gauge, etc can be identified by studying the strains during overcoring.

So far, there has been very limited possibility to do an independent and systematic analysis of the older overcoring results. However, a method and software tool based on numerical simulation has recently been developed in a co-operative project between Posiva and SKB /Hakala et al, 2003/. An application of this method is shown in Chapter 5, where considerations about the results also are included /Perman and Sjöberg, 2003/.

Drilling observations may also give indirect information on state of stress in the rock mass. It is well known that high stresses can cause core disking and/or borehole breakout. Core disking consists in fully developed cracks perpendicular to the core axis that occurs as the effect of the forces acting on the core during drilling and the release of the axial stress. Long before the core breaks, microcracking develops and can lead to failure of the core. The same phenomenon can affect the walls of the borehole producing borehole breakouts.

There is no significant evidence of core disking of the core from borehole KFM01A. The diameter of the borehole has not yet been logged, so there is no information on possible borehole breakout. To estimate if the core has been affected by the stress relaxation, P-wave velocity was measured perpendicularly to the core axis from borehole KFM01A /Tunbridge and Chryssanthakis, 2003/. The maximum and minimum principal P-wave velocities across the core could be determined with an accuracy of about ± 200 m/s. The results are presented in Figure 4-51. Here, the P-wave velocity shows a marked decrease for depths larger than about 500 m. This is an important indicator of high
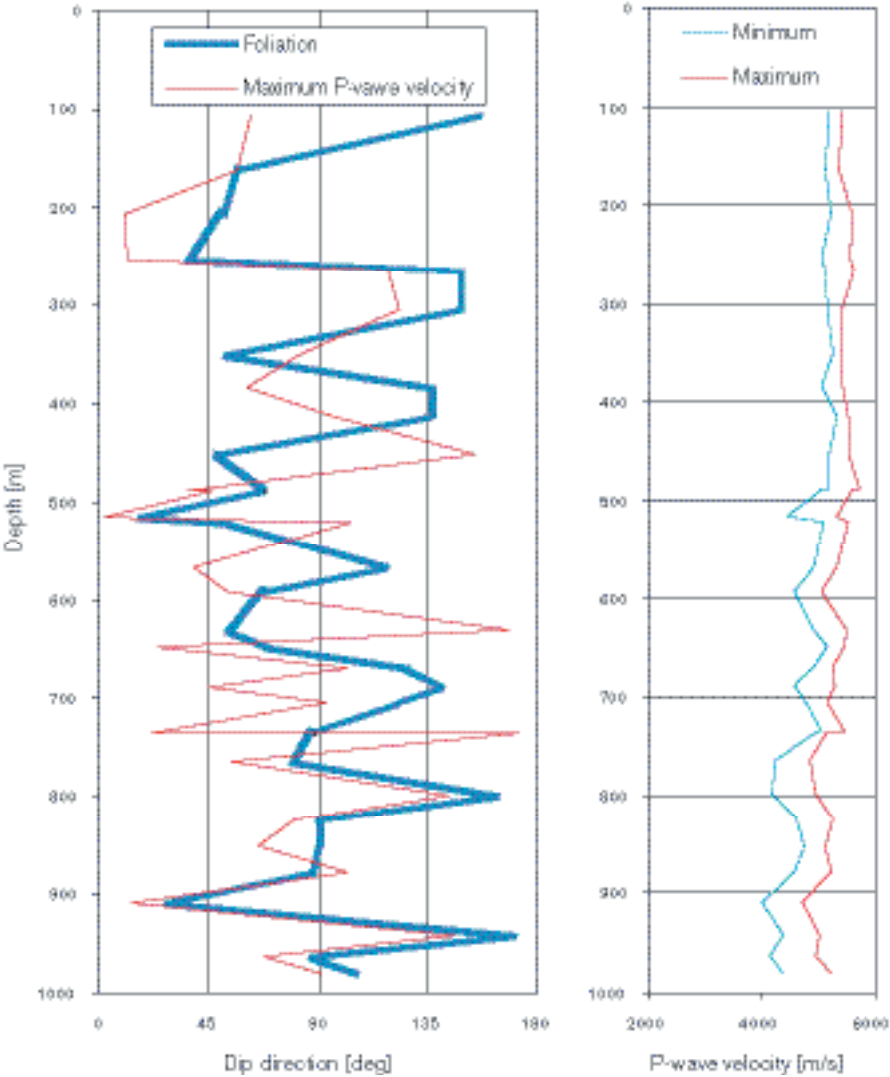
Figure 4-51. *Orientation and magnitude of the P-wave velocity measured perpendicular the core from borehole KFM01A. The orientation of the rock foliation and of the maximum velocity are shown in the same diagram. Note the decrease of the maximum and minimum velocity for depths larger than 500 m.*

rock stresses that will be used for building the stress model in Chapter 5. In fact, borehole cores affected by extensive microcracking due to stress relaxation exhibit lower P-wave velocity than undisturbed cores.

4.6.2 Mechanical tests

Most of the available results of mechanical tests were collected during the design and construction of the SFR repository for low and intermediate active nuclear waste. Samples were collected from boreholes KFR19, KFR20, KFR21, KFR22, KFR23, KFR24, KFR25 and KFR27 between the ground surface and a depth of about 250 m. The following tests were carried out between 1981 and 1985 on intact rock samples and rock joints /Hagkonsult, 1982a,b; Delin, 1983; Stille et al, 1985/: i) 88 uniaxial compressive tests; ii) 40 determinations of the Young's modulus and Poisson's ratio; iii) 162 point load tests at the site and 88 in the laboratory; iv) 17 determinations of the intact rock density; v) 11 shear tests on natural rock joints.

After the drilling of KFM01A, 41 tilt tests on rock joints were performed according to /Barton and Choubey, 1977/. Old and new data have been reviewed and stored in SICADA.

The test results show that the mechanical properties recorded are typical for Swedish host rock (Table 4-17). The uniaxial compressive strength of the rock is derived from the size-corrected Point Load Index $I_s(50)$. During the investigations for the SFR, it was observed that the values of the uniaxial compressive strength correlated well with the $I_s(50)$ when this was multiplied by a factor of 20. The point load tests in the laboratory were mainly carried out on dry samples. Two saturated samples showed a 14% lower uniaxial compressive strength than the dry samples. About one sample from every 8 m of core was taken for the point load tests performed in situ /Hagkonsult, 1982b/.

Table 4-17. Summary of the mechanical properties from uniaxial compressive tests and point-load tests /Hagkonsult, 1982b; Delin, 1983; Stille et al, 1985/.

Rock type	Mechanical property	Test no	Minimum	Average	Median	Maximum	Standard deviation
Gneiss	UCS [MPa]	61	119	248	262	322	52
	UCS* [MPa]	38	14	248	271	381	82
	UCS** [MPa]	28	106	243	239	350	53
	E [GPa]	17	60	78	77	93	7
	ν [–]	17	0.20	0.23	0.22	0.29	0.03
	Density [g/cm³]	9	2.64	2.65	2.64	2.67	0.01
Meta-volcanic rock	UCS [MPa]	22	31	118	127	212	57
	UCS* [MPa]	21	(4) 8	99	117	250	78
	UCS** [MPa]	12	50	143	134	256	62
	E [GPa]	4	55	80	81	101	23
	ν [–]	4	0.33	0.37	0.36	0.43	0.04
	Density [g/cm³]	4	2.86	2.89	2.89	2.91	0.02
Pegmatite	UCS [MPa]	18	80	148	151	198	28
	UCS* [MPa]	18	13	163	180	283	89
	UCS** [MPa]	16	66	179	184	274	60
	E [GPa]	9	41	70	75	83	13
	ν [–]	9	0.11	0.24	0.26	0.32	0.06
	Density [g/cm³]	4	2.63	2.63	2.63	2.64	0.01
Gneissic granite	UCS [MPa]	42	87	234	234	330	69
	UCS* [MPa]	20	13	276	298	360	66
	UCS** [MPa]	20	126	207	208	272	33
	E [GPa]	10	62	72	73	84	6
	ν [–]	10	0.17	0.21	0.22	0.23	0.02
	Density [g/cm³]		–	–	–	–	–
All rock types	UCS [MPa]	88	31	203	203	330	69
	UCS* [MPa]	162	(4) 8	212	241	381	106
	UCS** [MPa]	97	(4) 50	202	210	350	65
	E [GPa]	40	41	75	76	101	6
	ν [–]	40	0.11	0.24	0.23	0.43	0.02
	Density [g/cm³]	17	2.63	2.70	2.64	2.91	0.11

* Values obtained from the Size-corrected Point Load Index $I_S(50)$ performed in situ.

** Values obtained from the Size-corrected Point Load Index $I_S(50)$ performed in the laboratory.

The frictional parameters and the normal and shear stiffness of 11 samples of rock fractures were determined in the laboratory for assigned stress levels /Stille et al, 1985/. The results of the shear tests are presented for each of the five identified joint sets in Table 4-18. Furthermore, Table 4-19 summarises the results of tilt tests performed on fracture sampled from the core of borehole KFM01A /Chryssanthakis, 2003/. Each fracture set is characterised by a range of variation of the basic friction angle, Joint Roughness Coefficient (JRC) and Joint Compressive Strength (JCS) (upscaled to 100 cm) and the residual friction angle.

Table 4-18. Summary of the results of shear tests performed on rock joints /Stille et al, 1985/.

Fracture set	Normal stiffness [MPa/mm] for stress range 0.04–0.9 MPa	Shear stiffness [MPa/mm] at 1.6 MPa	Friction angle 1 [°]for stress range 0–0.5 MPa	Friction angle 2 [°]for stress range 0.5–1.5 MPa	Apparent cohesion [MPa] for stress range 0.5–1.5 MPa
Set EW	37	4.8	48	35	0.2
Set NW	29	4.4	51	37	0.4
Set NE	31	2.8	48	29	0.4
Set NS	24	2.7	48	30	0.3
Set SH	24	8.3	55	32	0.4
Random	25	10.4	54	38	0.5
All joints	32	5.4	51	35	0.4

Table 4-19. Summary of the results of tilt tests performed on rock joints /Chryssanthakis, 2003/.

Fracture set	Number of samples	Basic friction angle	JRC(100)	JCS(100)	Residual friction angle
Set EW	4	25–30	5–9	61–141	21–25
Set NW	1	29	7	105	24
Set NE	6	28–32	4–7	106–156	25–31
Set NS	4	24–31	4–8	93–126	20–29
Set SH	15	27–31	2–9	62–134	22–29
Random	10	24–31	4–9	65–136	20–30
All joints	40	29	6	102	25

4.6.3   Rock mechanical interpretation of borehole data

Characterisation based on BOREMAP data

Empirical methods have been assessed in a study for developing the methodology for rock mass characterisation /Andersson et al, 2002b; Röshoff et al, 2002/. Two empirical classification systems were selected for the purpose of mechanical property determination: the Rock Mass Rating (RMR) /Bieniawski, 1989/ and the Rock Quality Index (Q) /Barton et al, 1974/.

The characterisation of the rock mass with empirical methods is based on geomechanical data from BOREMAP-logging of borehole KFM01A. The geological parameters are: i) fracture frequency, ii) RQD for core lengths of 1 m, iii) rock type, iv) rock alteration, and v) structural features. The geological features of the fractures observed are: a) mineralization or infilling; b) roughness and surface features; c) alteration conditions; d) strike, dip, depth; e) width and aperture. A direct estimation of the Q-parameter Joint Alteration Number (J_a) was performed by the geologists. The information listed above is contained in SICADA.

In Figure 4-52, a summary of the borehole information about the open fractures is given for different depths. As can be observed, the total fracture frequency is moderate (i.e. 3–5 fractures/metre) down to a depth of 300 m. This observation is also supported by SFR data that give a fracture frequency of about 5 fractures/metre /Hagkonsult, 1982a/. For larger depth, the frequency drops significantly, with the exception of two locations at about 400 and 660 m, respectively. The background frequency
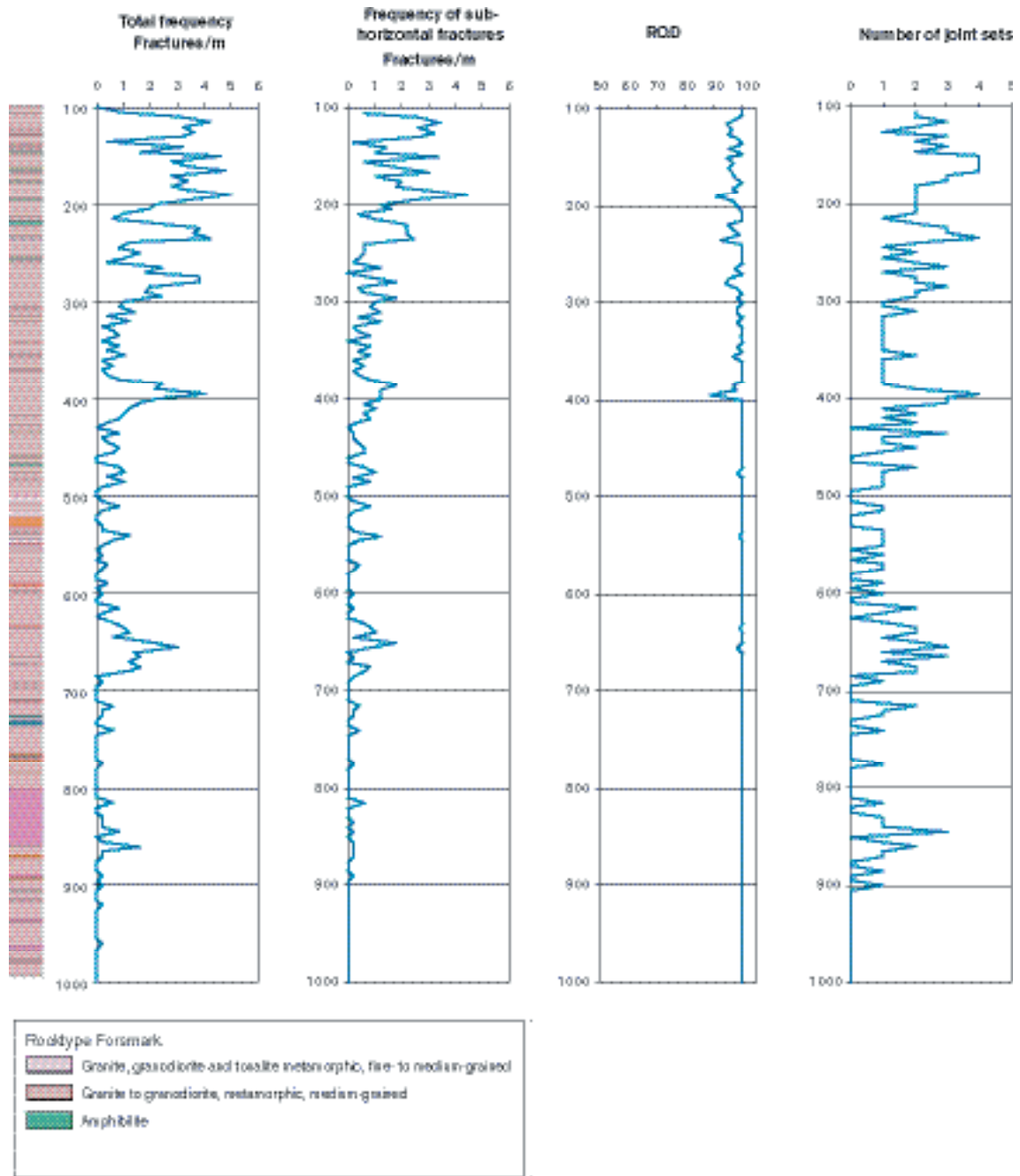
Figure 4-52. Variation of the total fracture frequency, frequency of the sub-horizontal fractures, RQD and number of joint sets with depth for borehole KFM01A. The values are averaged for each 5 m length of borehole.

below 300 m depth is less than 1 fracture per metre. A similar pattern can be seen on the frequency distribution of the sub-horizontal fractures. Whereas the high frequency in the upper 300 m of the core is mainly due to frequency of the sub-horizontal fractures, this does not seem to contribute to the peaks of the total frequency at 300 and 660 m. This can be explained by the fact that the two frequency peaks are primarily due to sub-vertical fractures. However, the bias due to preferential sampling of the sub-horizontal fractures by the vertical borehole cannot be completely avoided. As for the total fracture frequency, the RQD is slightly lower in the upper 400 m of the borehole. A very localised minimum can be observed at a depth of 400 m. For larger depths, RQD is with a few exceptions equal to 100.

The observation that the higher fracture frequencies at 400, 660 and, in some extent, at 860 m are mainly due to sub-vertical fractures is confirmed by the plot of the number of fracture sets observed at each depth. This diagram shows how many of the five recognised joint sets occur at different depths. It can be observed that the five fracture sets never appear at the same time for a particular depth. Three or four joint sets are observed frequently above 400 m depth and at the depths of 400, 660 and 840 m.

Some of the relations, most used in practice and tested, between RMR and Q and the mechanical properties of the rock mass are applied in Chapter 5 to determine the deformation modulus, Poisson's ratio, uniaxial compressive strength, cohesion and friction angle of the rock mass. In this application, RMR and Q are used for the "characterisation" of the rock mass. Thus, considerations about the shape and orientation of the excavation are neglected as well as technical considerations about stability and stress-related problems on the structures. In this report, the RMR and Q systems are applied to borehole sections of 5 m.

Parameterisation for RMR

The fracture length that gives a measure of the persistence and continuity of the fractures is largely unknown. Based on earlier experience at, this is estimated to be about 3 m in average. Results from compression tests on rock samples from borehole KFM01A are not yet available. Thus, the data in Section 4.6.2 are used to estimate the strength of the intact rock. Borehole KFM01A is observed to be mostly dry for its whole length which gives a rating for RMR equal to 15. RMR also requires a rating that takes into account the orientation of the excavation with respect to the fractures. For characterisation, this rating is chosen equal to 0 as suggested in /Andersson et al, 2002b/.

The ratings for RQD, fracture conditions, spacing and the resulting RMR values are shown in Figure 4-53 as a function of depth. Here, the best, average, most frequent and worse rating observable every 5 m of core length are plotted. These values indicate the possible local variation of RMR around the mean value plotted with a blue line. A slight increase of the RMR with depth is observed. Below 300 m, RMR classes the rock mass on average as "good rock" (RMR = 60–80). RMR seems to stabilise for depths larger than 400 m, and its values correspond on average to "very good rock" (RMR > 80). The difference between minimum and mean RMR value (about 10 points) seems to be quite constant and it is probably due to the stepwise way the classes of the ratings are assigned. On the other hand, the difference between mean and maximum RMR diminishes with depth down to 400 m (between 10 and 2 points), and then becomes almost constant.

Parameterisation for Q

The number of fracture sets for the Q-system is determined based on the number of fracture sets recognised in 5 m lengths of core. According to Figure 4-52, the number of fracture sets varies between zero and four. The Joint Water Reduction Factor Jw is assumed equal to 1, which is applicable to dry excavations or minor flow conditions. The Stress Reduction Factor for characterisation was suggested by /Barton, 2002/ as 5, 2.5, 1 and 0.5 for depth intervals from 0–5, 5–25, 25–250 and > 250 m.

Figure 4-54 shows the Joint Set Number, Joint Roughness Coefficient and Alteration Number as a function of depth. Between 200 and 300 m, Q seems to continuously diminish with depth. On average, the rock can be classified as "good". Between 300 and 400 m the values are scattered around a Q value of 100 ("very good rock"). For depths larger than 400 m, the difference between the minimum, maximum and mean Q value becomes negligible, with the exception of some more fractured zones at about 400, 480, 620, 650 and 860 m. Whereas the other fractured zones were already clearly visible from the plot of RQD and of the total fracture frequency, the zone at about 480 m seems to be due to the heavier alteration conditions and smoother fracture surfaces. On average, the rock below 400 m is classified as "extremely good rock" by the Q-system. As observed with RMR, Q suffers somewhat from the stepped way the input values are tabulated.
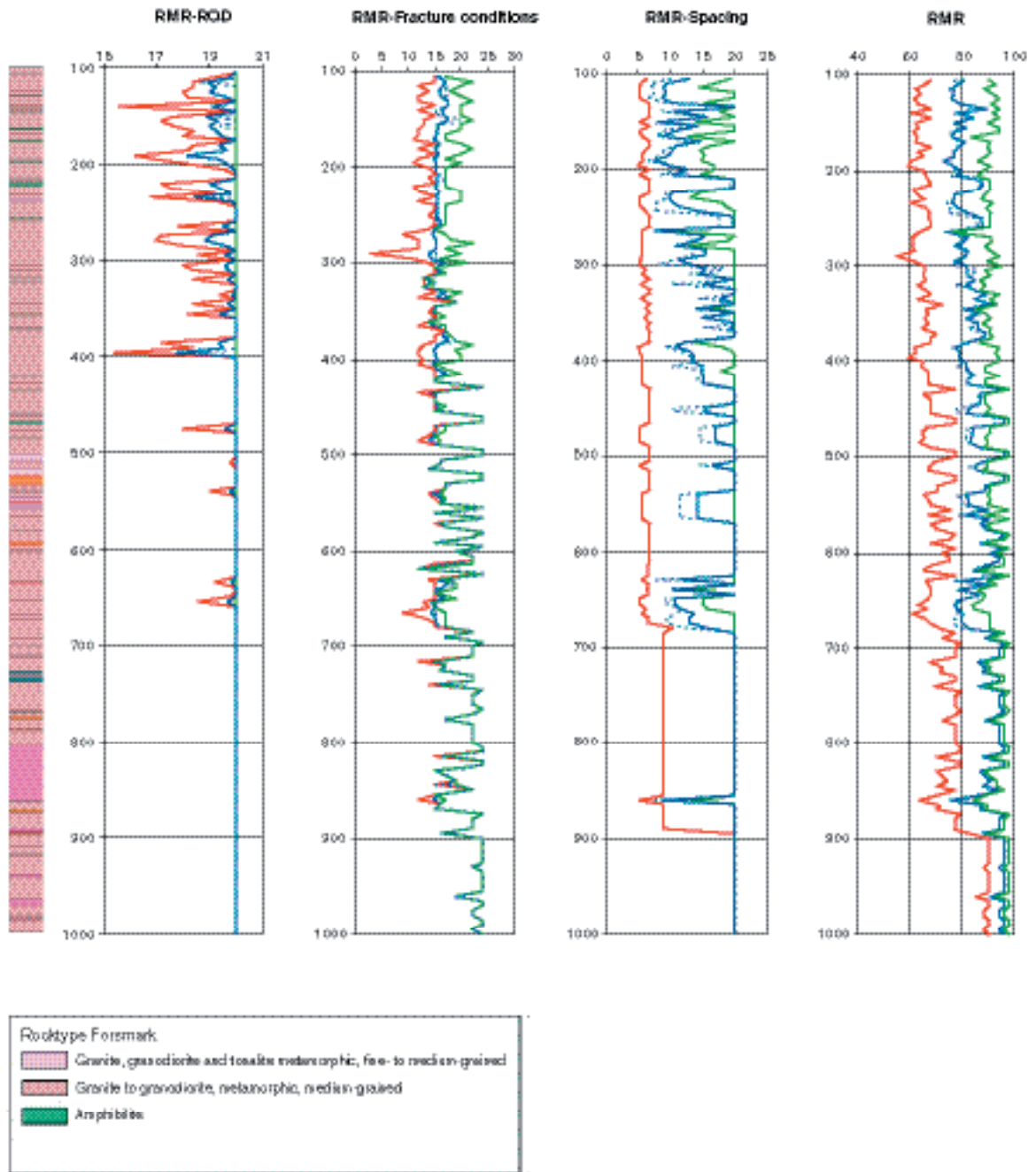
Figure 4-53. *RMR Ratings and RMR values from BOREMAP logging as a function of depth for borehole KFM01A. Minimum, average, most frequent and maximum values are plotted in red, blue, dashed blue and green, respectively. The values are given every 5 m.*

137
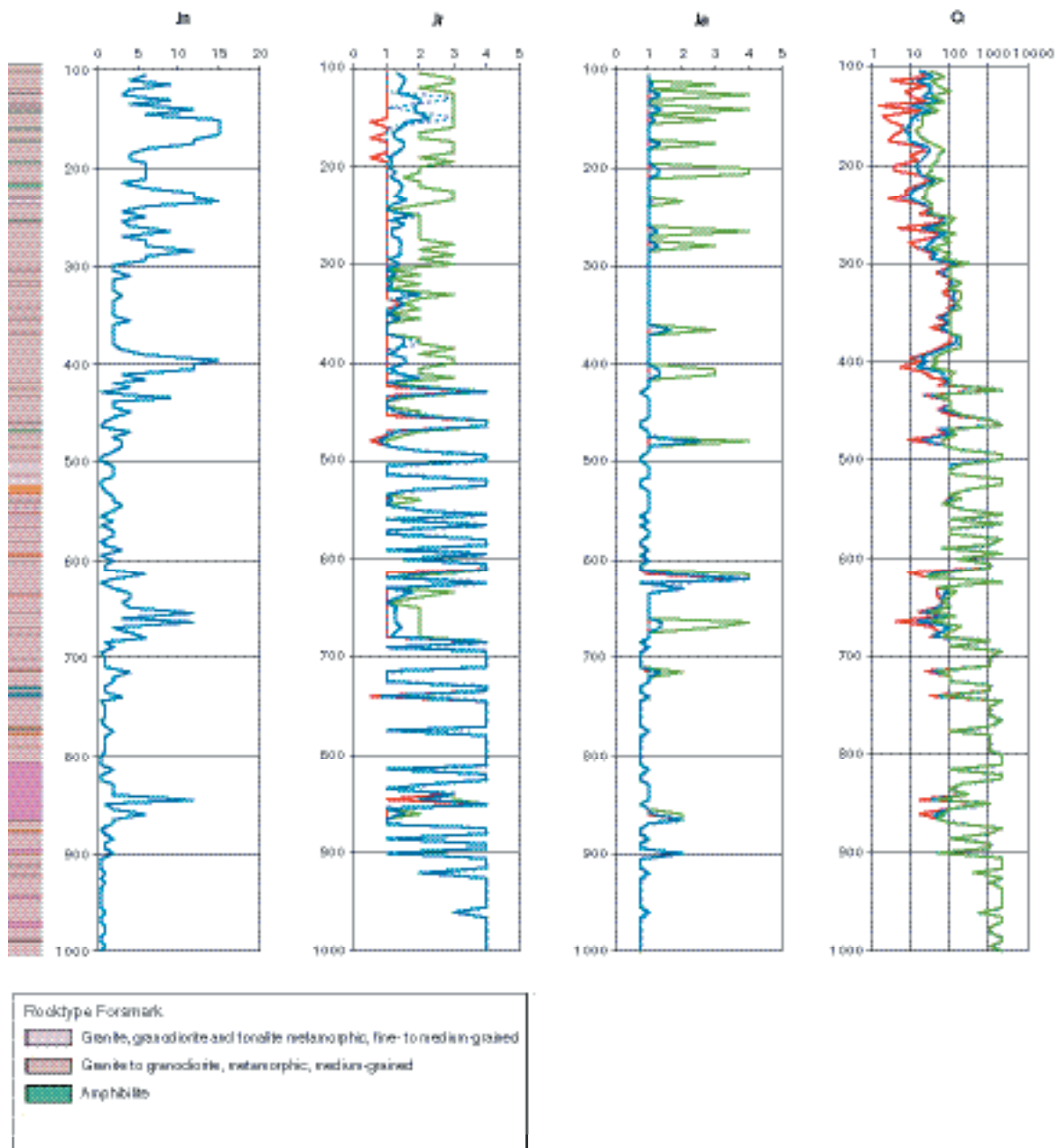
Figure 4-54. *Q inputs and Q values from BOREMAP logging as a function of depth for borehole KFM01A. Minimum, average, most frequent and maximum values are plotted in red, blue, dashed blue and green, respectively. The values are given every 5 m.*

Characterisation based on borehole Q-logging

An independent Q-logging of borehole KFM 01A was carried out with no access to BOREMAP data /Barton, 2003/. The logging was performed by the manually-recorded "histogram method" which allows direct storage of the parameters into histograms to facilitate further processing. The Q-logging identified four fractured zones that in average have Q of 14, ranging from 1 to 200 (Table 4-20). However, the overall quality of the core is very good to excellent with a mean Q of 48 and a most frequent value of Q of 100. The rock quality ranges between 2 and 2,130.

Table 4-20. Q index for the relatively fractured zones in borehole KFM01A /Barton, 2003/.

Depth interval [m]	$Q_{most\ frequent}$	Q_{mean}	$Q_{typ.min}$	$Q_{typ.max}$
166–199	16.7	10.9	1.0	100
295–297	22.0	11.5	1.8	75
385–407	20.9	19.0	2.7	200
651–683	37.8	19.0	2.3	200

138
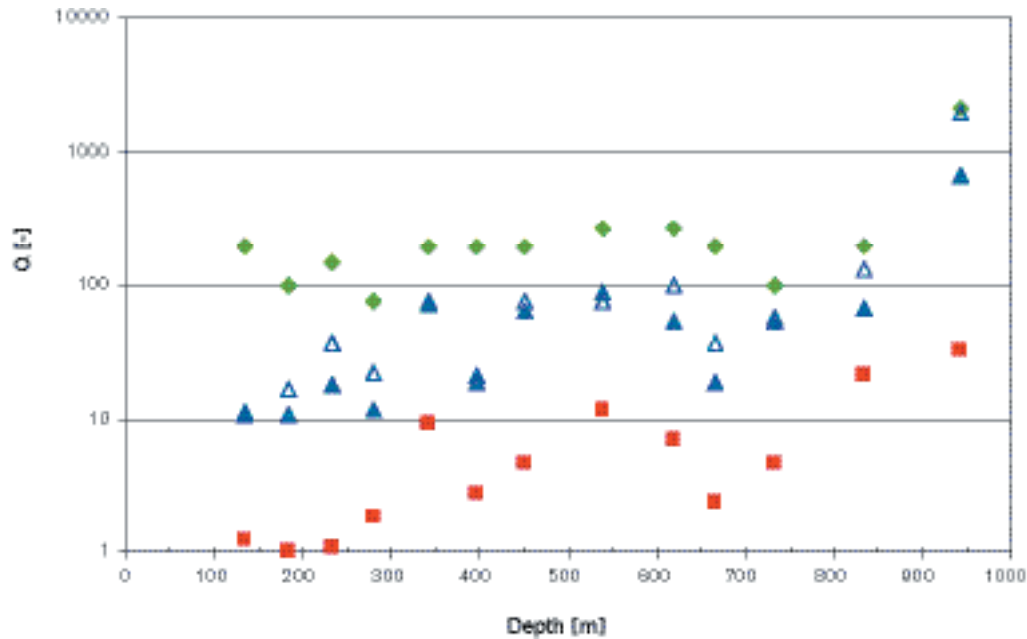
Figure 4-55. *Q obtained by direct Q-logging of the core from borehole KFM01A as a function of depth /Barton, 2003/. Minimum, average and maximum and frequent values are shown in red, blue, green and unfilled blue dots, respectively.*

4.6.4 Q-logging of surface exposures

An assessment of rock mass quality for the purpose of rock mass characterisation was recently done based on observations on outcrops and in the SFR access tunnels /Barton, 2003/. The locations are given in Figure 4-56.

Table 4-21 summarises the surface-mapped Q-values for mutual comparison of locations and rock formations, and shows results of an attempt of extrapolation to depth (i.e. 250–500 m) based on the preliminary and conservative assumption of maintained jointing frequency and properties with depth. J_w values may not need to be reduced with depth because the fracture connectivity is poor due to few joint sets. Boreholes in such kind of rock mass are likely to be dry. This can underestimate Q, judging from the Q-logging of the core of KFM01A /Barton, 2003/.

Table 4-21. A summary of surface logged mean Q-values in and close to the Forsmark candidate site, with attempted extrapolation to reference depths of 250 to 500 m, assuming unchanged jointing.

Rock domain	Surface locations	Comment regarding location	Weighted Q at the surface	Estimated Q at 250–500 m depth
29(a)	5, 6, 10, 11, 12, 13, 14	Nearer to contacts with foliated formations 17 and 32	11.6–16.6	43–58
29(b)	7, 8, 9 and 26, 27 (at KFM02/03)	Further from contacts with foliated formations 17 and 32	2.8–7.3	8.5–27
Q-logging of surface exposures	3, 4	–	10.1	37
17				
18	1, 2, 18	–	6.0–10.6	19–41
32	15, 16, 17	–	2.9–3.1	6–7
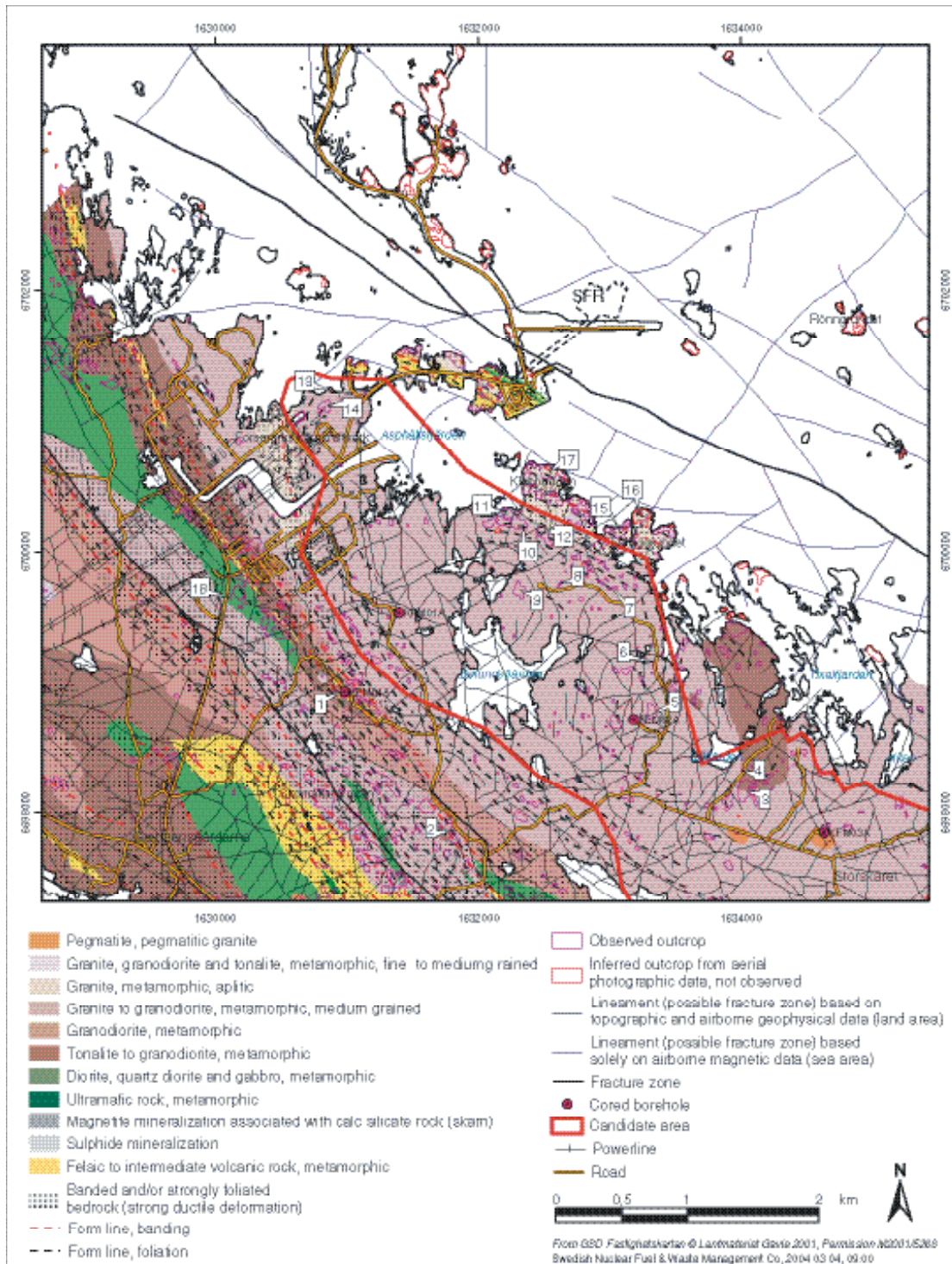
Figure 4-56. *Location of the Q-mapping.*

The locations 21, 19 and 22 in strongly-foliated "plastic deformation zones" gave the highest mean surface Q-values of 20, 26 and 40. A larger sample of Q-parameter observations in the SFR tunnels in the meta-granitoid (formation 33) gave mean near-surface Q-values of 4. In relation to the rock domains number 29 (central), 17 (lens), 18 (western border) and 32(eastern border) (see Figure 5-6 in Section 5.1.2), the logged locations gave the surface and depth-extrapolated trends shown in Table 4-21.

The survey of the surface exposure indicate that there are important rock mass quality contrasts between two rock formations inside domain 29, which are shown in graphic Q-parameter histogram format in Figure 4-57. Photographic examples of surface exposures from the two contrasting areas 29(a) – location 10 with Q equal to about 15 – and 29(b) – location 9 with Q equal to 4.7– are shown in Figure 4-58 and Figure 4-59. Dense forest and depressions in the terrain closer to the coastline, where formation 32 eventually becomes well exposed, suggest a much poorer, presumably more jointed rock mass quality at the edge of the more competent "plastic deformation zones".

Comparing BOREMAP logging, surface logging and direct core logging of Q

The overall Q-parameter statistics of KFM01A as obtained from Q-logging performed directly on the core show in general similar statistics as the Q-parameter interpretation from BOREMAP. Each of these methods of collecting rock joint parameter descriptions – in the form of ratings – has its sources or error, as each involve subjective judgement by the loggers. The Q-parameter data collected by both methods are experience-based estimates, as opposed to physically measured laboratory test results.
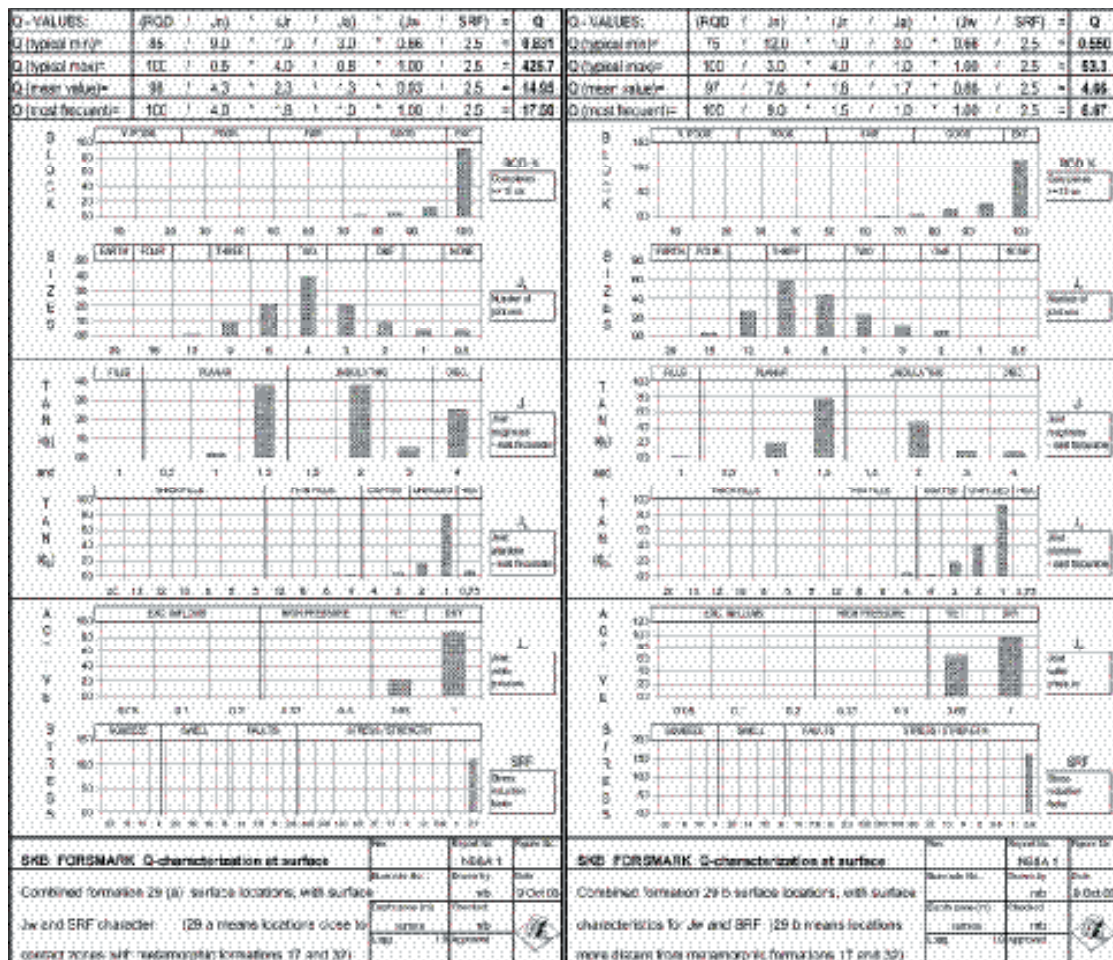
Figure 4-57. Q-parameter histograms for the solid type of outcrop shown in Figure 4-58 and the more broken outcrop surfaces shown in Figure 4-59.

Figure 4-58. *Example of 29a: view of #10 location.*

Figure 4-59. *Example of 29b: Front and side view of #9 location.*

The minimum, mean, maximum and frequent trends of BOREMAP derived Q-values have been compared to derive the common trends and differences. The comparison shows Q-values climbing steadily from the broad range of 1 to 100 in the first 100 to 300 m depth zones, eventually rising to the 100 to 1,000 range in most of the 400 to 1,000 m depth zone. In the core logging reported in /Barton, 2003/, the mean and the maximum values of Q did not generally rise to quite such high values, except in the deepest 800 to 1,000 m zone. The core-logged mean Q values generally were in the range 50 to 100, whereas the maximum Q values were generally in the 100 to 270 range. Such differences are to be expected when relying strongly on the borehole wall description for the BOREMAP Q-parameters.

We may speculate that if the degree of jointing expressed at the surface were to continue to a reference depth of 250 to 500 m we might then be seeing mean Q-values between 14 and 53. Broadly, similar trends are seen in the Q-logging and BOREMAP-derived Q-values as well, presented in this chapter.

4.6.5　Experiences from previous construction works

Previous construction works offer interesting information about the geology and rock mechanics in areas pertinent to the candidate site. During these works, the rock mass was investigated to determine geological structures and mechanical properties. Seismic investigations were also carried out giving some insights about the Singö Fault Zone. In the following sections a summary of the information collected at the power plants and at the SFR repository in Forsmark is given.

Construction of the power plants in Forsmark

Excavations were carried out for the construction of the power plants in Forsmark mainly during the later half of the Seventies. The works included excavations in the superficial rock mass for the three Units, the inlet channel for cooling water as well as two discharge tunnels. The works were carried out mainly in rock of Rock Group C and partially in rock of Rock Group C (see Section 4.2.2 and Figure 4-9). The discharge tunnels were driven through the Singö Fault Zone (ZFMNW0001).

The superficial rock mass has been described by /Carlsson, 1979/. Extensive sub-horizontal fracturing, often filled with sediments, is frequently observed (Figure 4-60). Systematic rock mass classification systems using any empirical method applied today were not available or applied during construction. As can be seen in Figure 4-60, the fracturing varies significantly as does the rock mass quality characterised with the empirical methods.

Figure 4-60. *View of excavations of Unit #3. Notice the sediment-filled horizontal fracture /Carlsson, 1979/. The rock mass is rather blocky with some more fractured zones. Generally, the fracture frequency at surface decreases within the depth of the excavations.*

The discharge tunnels are located at a maximum depth of approximately 75 m. The tunnels were driven through the major regional fault zone called the Singö Fault. In association with that structure, the rock is partly schistose. Long sections of the tunnel run, however, in very good rock conditions. Despite this, significant stability problems were experienced through the Singö Fault during construction of the tunnel serving Unit #3. A section of the tunnel from Units #1 and 2 is shown in Figure 4-61. Here, it can be noticed that the seismic velocity measured by surface refraction seismic ranges between 4.9 and 5.7 km/s in the granitic rock west of the Singö Fault (up to section 2/300). In the Singö Fault, the seismic velocity was reported in the range of 3.6–4.7 km/s. This reflects the variability of the stiffness of the rock mass that is further discussed in Chapter 5.

The records from the foundation of the power plants and the construction of the discharge tunnels indicate that the granitic rock in the area is partly heavily fractured close to the surface. Open and sediment filled fractures caused problems during excavation because the fracturing pattern is quite blocky. Alteration occurs but only in distinct zones. Already at some tens of meters depth, the rock mass is normally good for tunnelling. Some problems were experienced in the most significant fracture zone.
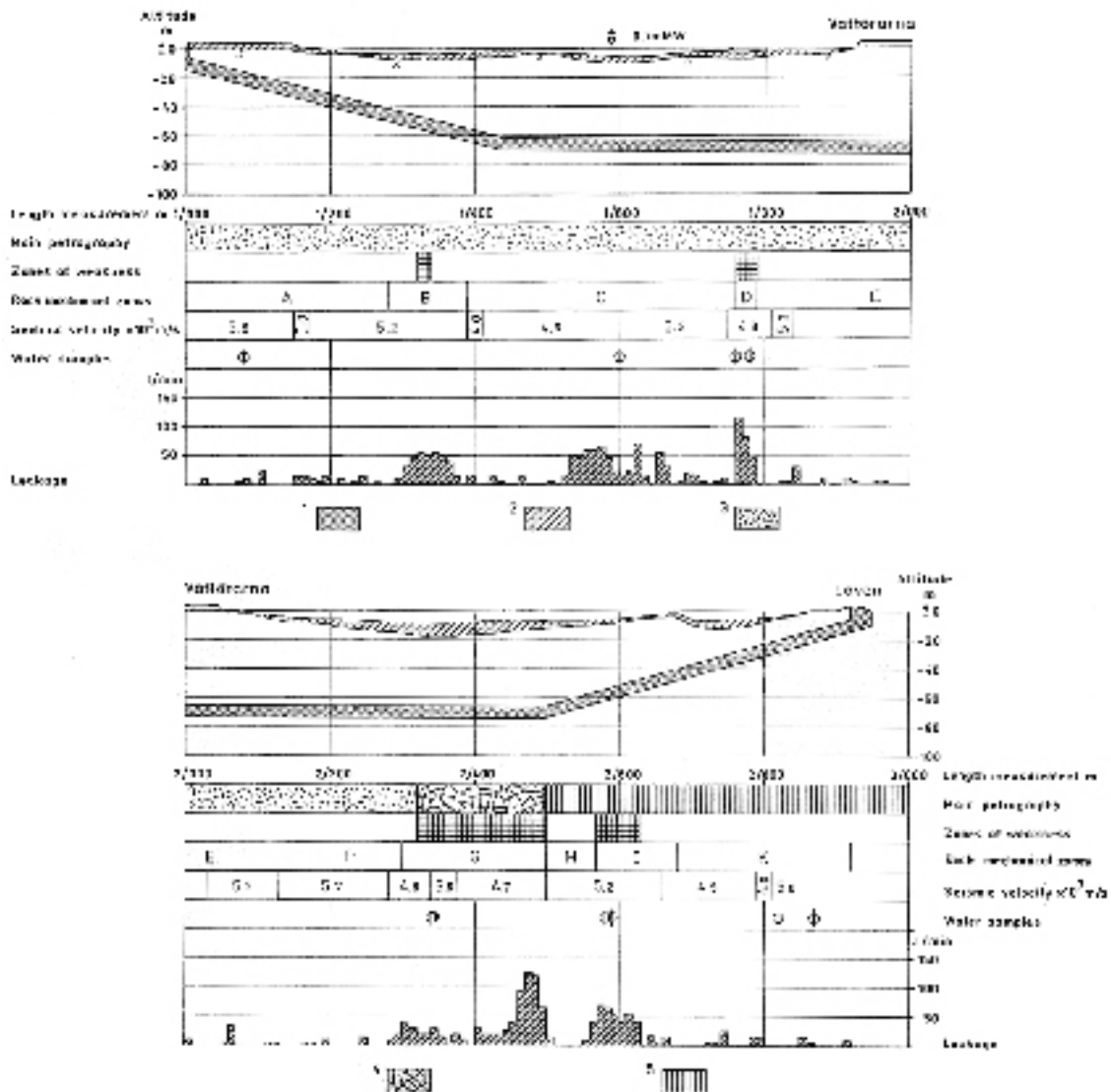
Figure 4-61. *Engineering geologist summary of the discharge tunnel from Unit # 1 and 2 /Carlsson and Olsson, 1982/.*

Construction of the SFR

Based on the partial data sets that were collected at the time, some authors have empirically characterised the rock mass at the Final Storage for Reactor Waste (SFR-1). The facility is located east of the Singö Fault Zone in a gneiss granite that can be assumed, from a rock mechanics point of view, to be similar to the Rock Group C. In these two studies /Hagkonsult, 1982a; Stille et al, 1985/, the RMR_{79} /Bieniawski, 1979/ and Q-system /Barton et al, 1974/ were applied for rock quality determination. The first study /Hagkonsult, 1982a/ (based on the analysis of borehole KFR21, KFR22, KFR23, KFR24, KFR25, KFR27) quantified the RMR_{79} between 69 and 83 (classes "good" to "very good" rock) with an average of 80. The second study by /Stille et al, 1985/ (that added data from borehole KFR19 and KFR20) resulted in slightly lower values of RMR_{79} (60–72) and Q (5–10) compared with the first study. This was explained by the higher fracture frequency observed in the additional data.

The two studies gave also estimations of the deformability and mechanical properties of the rock mass by means of relations with the empirical classification systems /Bieniawski, 1979; Hoek and Brown, 1980; Stille et al, 1982/. The first study concluded that the deformation modulus of the rock mass should vary between 35 and 65 GPa, with an average value of 45 GPa, while the Poisson's ration should be about 0.1. The cohesion and friction angle were estimated as 1.5 MPa and 45° respectively, and the uniaxial compressive strength of the rock mass was evaluated as 7 MPa. The second study updated the values of the deformation modulus and strength of the rock mass toward lower values. The deformation modulus was determined to be about 20–40 GPa and 2–43 GPa, using RMR_{79} and Q values, respectively. An average deformation modulus of 20 GPa and Poisson's ratio of 0.08 were assumed for the rock mass as a whole /Stille, 1986/. In terms of rock mass strength, the values obtained according to /Bieniawski, 1979/ were judged to be too low. Alternatively, /Hoek and Brown, 1980/ and /Stille et al, 1982/ methods were used, leading to a rock mass compressive strength varying between 5 and 29 MPa, with average values of 13 MPa and 8 MPa, respectively, with each method.

The rock mass parameters obtained in these two studies were also used as material properties for six different numerical calculations, by the FEM method, of the stability, support and deformation of the silo in SFR /Stille et al, 1985/.

Geological documentation during the tunnelling included sampling of mineral fillings in fractured zones and fracture fillings. In total, 13 clay samples were taken for x-ray spectrometer analyses. None of the samples contained swelling clays, but mixed layers of smectite – illite fillings were found.

4.7 Thermal properties data evaluation

4.7.1 Measurement of thermal properties

Method

There are different types of laboratory methods to determine thermal properties, see for example /Sundberg, 1988/. The recommended method for the site investigations is the TPS (transient plane source) method /SKB, 2001a; Sundberg, 2003a/. The TPS method is described in /Gustafsson, 1991/. With the method it is possible to measure the thermal conductivity and the thermal diffusivity simultaneously. From these results the heat capacity may be calculated.

Measurements on some samples from Forsmark have been made by SP (Swedish National Testing and Research Institute). The results are presented in /Adl-Zarrabi, 2003/. Some deviations from the prescriptions in SKB MD 191.001 were made in the measurement procedure. For example, only two measurements were made on each sample instead of five.

Results

Measurements have been made on 5 samples and the results are presented in Table 4-22. The thermal conductivity (λ) and the thermal diffusivity (κ) are measured directly with the TPS-method. The heat capacity is calculated from the equation $C = \lambda/\kappa$. The specific heat is calculated from the heat

capacity and the measured density. For each measurement two sub samples were used, one on each side of the sensor. The two sub samples were prepared perpendicular and parallel to the foliation. The produced results are a mean value of the thermal properties of the two sub samples.

For two of the samples (PFM001157 and 1164) the mean values of the individual sub measurements differ slightly from the values in the summary table in the report by /Adl-Zarrabi, 2003/. In Table 4-22 the results from the summary table is used. For one of the samples (PFM001157) the results from the two sub measurements differed by more than 3%.

Table 4-22. Results from TPS-measurements on rock samples from Forsmark /Adl-Zarrabi, 2003/. The table also translates ID in the report to ID in SICADA for available samples. Rock units are defined in Section 5.1.2.

Sample ID, in investigation report	ID, in SICADA database	Thermal conductivity W/(m·K)	Thermal diffusivity m²/s	Calculated heat capacity J/(m³·K)	Calculated specific heat J/(kg·K)	Rock type, according to report	Rock unit according to SKB
MBS020002B	PFM001157	2.94	$1.51 \cdot 10^{-6}$	$1.95 \cdot 10^6$	694	Metatonalite	101054
MBS020003B	PFM001158	2.28	$0.98 \cdot 10^{-6}$	$2.33 \cdot 10^6$	785	Metadiorite	101033
MBS020004B	PFM001159	3.51	$1.58 \cdot 10^{-6}$	$2.22 \cdot 10^6$	836	Metagranite	101057
MBS020007B	PFM001162	2.45	$1.27 \cdot 10^{-6}$	$1.93 \cdot 10^6$	696	Metatonalite	101054
MBS020009B	PFM001164	3.47	$1.82 \cdot 10^{-6}$	$1.90 \cdot 10^6$	715	Meta-granodiorite	101057

In order to investigate the influence of anisotropy in the rock, the samples were prepared parallel and perpendicular to the foliation. In the literature, the terms "parallel" and "perpendicular" is usually used in order to describe properties parallel and perpendicular to foliation respectively. However, in /Adl-Zarrabi, 2003/ it is indicated that the terms are used to describe if foliation is parallel or perpendicular to the sensor.

The measurements were made on each of the two sub samples together with insulation on the other side of the sensor. The result is a mean value of the thermal properties of the insulation and the sample and can only be used qualitatively and not quantitatively. The results are presented in Table 4-23 and are further evaluated in Chapter 5.

Table 4-23. Influence of anisotropy of samples. Results obtained with measurements on sample and insulation on each side of the sensor /Adl-Zarrabi, 2003/. The results can only be used as relative measures and not as material properties. The results are further discussed in Chapter 5.

ID in SICADA	Thermal conductivity "parallel" W/(m·K)	Thermal conductivity "perpendicular" W/(m·K)
PFM001157	1.35	1.61
PFM001158	1.28	1.13
PFM001159	2.07	1.67
PFM001162	1.21	1.24
PFM001164	1.76	1.76

In Table 4-24, the results of density and porosity measurements are presented. The measurements are made according to SKB MD 160.002.

Table 4-24. Mean values of density (wet) and porosity from sub samples (Adl-Zarrabi, 2003).

ID in SICADA	Density kg/m³	Porosity %
PFM001157	2809	0.40
PFM001158	2969	0.35
PFM001159	2656	0.48
PFM001162	2774	0.67
PFM001164	2659	0.49

4.7.2 Calculation of thermal properties from mineral composition

Method

The thermal conductivity of composite materials, such as rock, can be calculated from the mineral composition. In /Sundberg, 1988/, an overview of different approaches to the subject is given. For calculations of thermal conductivity of rock from mineral compositions, the self-consistent approximation (hereafter named SCA) of an n-phase material has been suggested /Sundberg, 1988, 2003a/.

Chemical and mineralogical composition are determined using the methods ICP, SEM and EDS /SKB, 2001a/. /Horai, 1971/, /Horai and Simmons, 1969/ and /Berman and Brown, 1985/ have determined values for the thermal conductivity and heat capacity of different minerals.

Mineral composition of samples

The mineral composition of surface samples from the Forsmark area has been investigated. The composition of 71 samples from the SICADA database has been used in order to calculate the thermal conductivity. The chemical composition of the plagioclase and olivine that influence the thermal properties is not known. Instead, assumed or typical values for the chemical composition are used. Correlations between individual samples and rock units have been studied in the geological model.

Results

The results of the SCA-calculations are presented in Table 4-25, divided into different rock units. The sampling was made by the geologist to investigate different variants of the rock units and not to get a mean mineral composition in proportion to the total mass of each rock unit. Therefore the mineral compositions, and the calculated thermal conductivities, are not necessarily representative to the rock units.

Table 4-25. Results of thermal conductivity of different rock units, calculated from the mineral composition from surface rock samples. The thermal conductivity is calculated with the SCA-method. Rock units with results in brackets are very uncertain, due to few samples and with minerals with unclear chemical composition. Please observe that the mean values only represent the mean of the rock samples and not necessarily the different rock units.

Rock unit	Mean value W/(m·K)	Stdev	Number of samples	Name
101004	(3.89)	–	1	Ultramafic rock, metamorphic
101033	(2.16)	0.275	2	Diorite, quartz diorite and gabbro, metamorphic
101054	2.93	0.391	15	Tonalite to granodiorite, metamorphic
101056	3.03	0.350	10	Granodiorite, metamorphic
101057	3.33	0.313	24	Granite to granodiorite, metamorphic, medium-grained
101058	3.01	0.355	7	Granite, metamorphic, aplitic
103076	2.79	0.423	12	Felsic to intermediate volcanic rock, metamorphic
			∑ 71	

4.7.3 Calculation of thermal properties from density measurements

Correlation has been found between thermal conductivity and density /Sundberg, 2003b/. The result is valid for the Äspö diorite and Ävrö granite type in a rather narrow density range. In the Forsmark investigation, there are few samples with determined thermal conductivity and density, and a potential correlation for actual rock types at Forsmark has not been investigated. Calculation of thermal properties from the density log in KFM01A based on these results is not meaningful at this stage of the investigation. Further, density determination from the density log seems to have a high uncertainty for KFM01A.

4.7.4 Thermal expansion of rock

No measurements have been made of thermal expansion on samples from the different rock units.

4.7.5 In situ temperature

The temperature has been logged in KFM01A. The result of the logging is presented in Figure 4-62, adjusted for borehole angle. At the 600 m level the temperature is about 13°C.

The temperature gradient has been calculated from the temperature logging results. In Figure 4-62, the mean gradient per 100 m is successively calculated versus depth. As shown in the figure, the gradient is increasing from about 11°C/km at the depth 400 m to about 14°C/km at about 900 m. At the end of the bore hole, the gradient is influenced by disturbances in the temperature measurement.
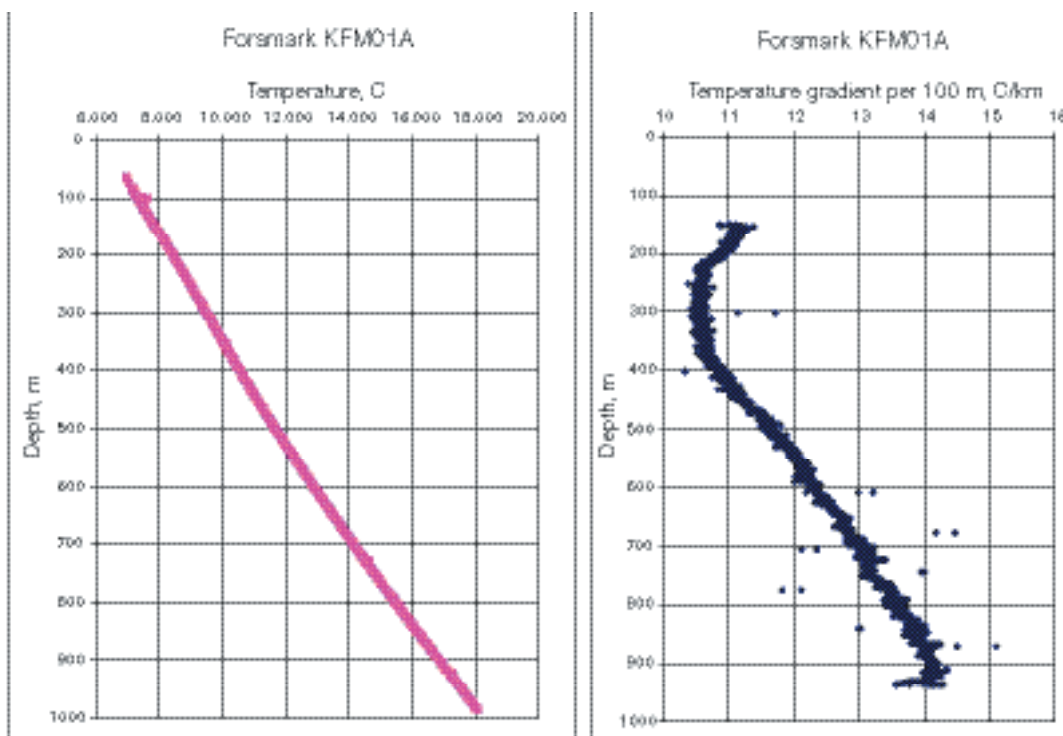
Figure 4-62. *Temperature (left) and temperature gradient (right) versus depth for borehole KFM01A. The temperature gradient is calculated per 100 m (approximately) and the corresponding depth is showed as the midpoint in each 100 m interval. The time between drilling and temperature logging is 6 months. The scatter in the temperature gradient is due to the method used to calculate the gradient.*

4.8   Hydrogeochemical data evaluation

The dataset available consists in total of 456 water samples /Laaksoharju et al, 2004/. Samples reflecting surface/near-surface conditions (precipitation, streams, lakes, sea water and shallow soil pipe waters) comprise a total of 422 samples. Of the remainder, 21 samples are from percussion-drilled boreholes and 13 samples from core-drilled boreholes; some of these borehole samples represent repeated sampling from the same isolated location. In conclusion, there is a heavy bias at this stage in the site characterisation to water samples from the surface and near-surface environments. Consequently, hydrochemical evaluation at greater depths is restricted to only a few borehole sampling points which are not as deep as expected repository levels.

The sampling locations at the Forsmark site are shown in Figure 4-63 and the sampling and analytical data have been reported by /Nilsson, 2003a,b,c/ and by /Nilsson et al, 2003/. In the total dataset, only 112 surface samples, five samples from percussion boreholes and two samples from the
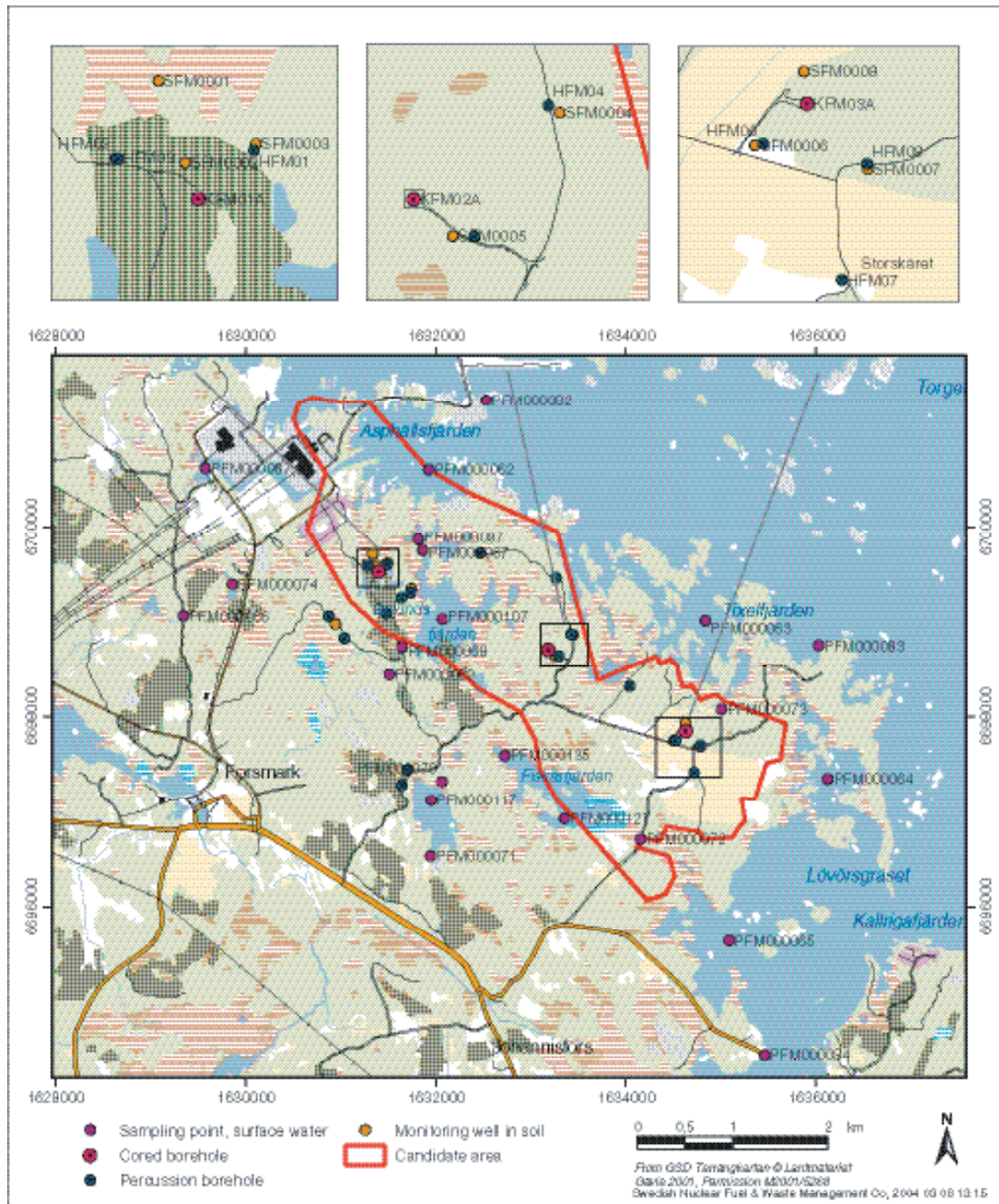
Figure 4-63. *The surface and groundwater sampling locations at the Forsmark site.*

149

core-drilled borehole were analysed for all the major elements, stable isotopes and tritium at the time of the "data freeze". This means that 26% of the samples could be used for more detailed evaluation concerning the origin of the water. How the dataset was used in the different models is listed in /Laaksoharju et al, 2004/.

4.8.1   Surface chemistry data

Surface and shallow water chemistry

Data on surface water chemistry has, together with some physical parameters, been collected biweekly to monthly of 8 stream, 6 lake and 3 sea sampling points from March 2002. The surface water programme is described in detail in /Nilsson et al, 2003/, together with a compilation of primary data. The stream and lake sampling points represent four different drainage areas in the local model area.

A total of 261 surface water samples were analysed sufficiently and could be used in the detailed evaluation. Analysed data include: major cations and anions (Na, K, Ca, Mg, Si, Cl, HCO_3^- SO_4^{2-}, S^{2-}), trace elements (Br, F, Fe, Mn, Li, Sr, DOC, N, PO_4^{3-}, U, Th, Sc, Rb, In, Cs, Ba, Tl, Y and REEs) and stable (^{18}O, ^2H, ^{13}C, ^{37}Cl, ^{34}S, ^{10}B) and radiogenic (^3H, ^{14}C, ^{226}Ra, ^{228}Ra, ^{222}Rn, ^{238}U, ^{235}U, ^{234}U, ^{232}Th, ^{230}Th and ^{228}Th) isotopes, but only for some samples. Additionally, for some samples there are nutrient and organic data including NH_4, NO_2, NO_3, N_{Tot}, P_{Tot}, PO_4, poP (particulate organic P), poN (particulate organic N), poC (particulate organic C), Chlorophyll A, Chlorophyll C, Pheopigment, TOC, DOC, DIC and O_2. Water temperature, pH, conductivity, salinity, turbidity and oxygen concentration values were determined in the field. There are no measured Eh values.

The current knowledge of the hydrogeochemistry of the near-surface groundwater in the Forsmark regional model area comes from an evaluation of water samples in shallow groundwater wells. The results are reported by /Ludvigson, 2002/ and are compiled in the Forsmark Site Descriptive Model version 0 /SKB, 2002a/.

Soil chemistry

No site-specific data on the chemistry of forest or agricultural soil are available for model version 1.1.

Radionuclides and organic pollutants in surface ecosystems

No site-specific data are available for version 1.1

4.8.2   Chemistry data sampled in boreholes

In the data evaluation, 45 groundwater samples have been used. The analytical program include: major cations and anions (Na, K, Ca, Mg, Si, Cl, HCO_3^- SO_4^{2-}, S^{2-}), trace elements (Br, F, Fe, Mn, Li, Sr, DOC, N, PO_4^{3-}, U, Th, Sc, Rb, In, Cs, Ba, Tl, Y and REEs) and stable (^{18}O, ^2H, ^{13}C, ^{37}Cl, ^{10}B, ^{34}S) and radiogenic (^3H, ^{226}Ra, ^{228}Ra, ^{222}Rn, ^{238}U, ^{235}U, ^{234}U, ^{232}Th, ^{230}Th and ^{228}Th) isotopes. Note: The samples were not analysed for all these elements at the time for the "data freeze" /see Laaksoharju et al, 2004/.

The different analytical results obtained with contrasting analytical techniques for Fe and S have been confirmed with speciation-solubility calculations and checking their effects on the charge balance. The values selected for modelling were those obtained by ion chromatography (SO_4^{2-}) and spectrophotometry (Fe) assuming that they have no colloidal contribution (as it could be with ICP measurements). The selected pH values correspond to laboratory measurements since no down-hole data were available. There is only one measured pairs of Eh and temperature values, which have been used in the detailed modelling of one borehole section.

4.8.3   Representativity of the data

By definition, a high quality sample is considered to be that which best reflects the undisturbed hydrological and geochemical in situ conditions for the sampled section. A low quality sample may include in situ, on-line, at-line, on-site or off-site errors such as contamination from tubes of varying compositions, air contamination, losses or uptake of CO_2, long storage times prior to analysis, analytical errors etc. The quality may also be influenced by the rationale in locating the borehole and selecting the sampling points. Some errors are easily avoided, others are difficult or impossible to avoid. Furthermore, chemical responses to these influences are sometimes, but not always, apparent.

A sampling and analytical protocol is established prior to a sampling campaign. This protocol is based on established sampling routines or special requirements associated with the sampling campaign. The sampling and analytical protocols used in the various sampling campaigns at Forsmark are described by /Nilsson, 2003a,b,c/ and by /Nilsson et al, 2003/. The analytical precision for the major components: Na, K, Ca, Mg, HCO_3, Cl and SO_4 were checked by ion-balance calculation, where the difference between the anions and cations was calculated. The charge balance calculated for 306 water samples (made both manually and through speciation-solubility calculations with PHREEQC) indicates that only seven samples show errors higher than 10%: four surface water samples, one sample from a percussion borehole (sample 4170 from 50.05 m depth in borehole HFM02) and two samples from soil pipes (sample 4220 from 5.75 m depth in borehole SFM0002 and sample 4221 from 11 m depth in borehole SFM0003).

The pre-sampling Chemac on-line monitoring data concerning pH, Eh, O_2, conductivity and temperature were not available to evaluate the quality and representativeness of the sampled groundwaters. Available information that could be used for this purpose were the percentage flushing water contents for boreholes KFM01A and KFM02. During the sampling period for borehole KFM01A at section 110.00–120.67 m, a flushing water content of 7.73% was recorded when sampling commenced; this decreased to less than 1% when the last 5 samples were taken from the same borehole section. From this evidence, only the first sample collected can be considered doubtful. Borehole KFM02, in contrast, recorded flushing water values of 43.47%, 20.3% and 89% from borehole sections 105.1–159.3 m, 250.00–291.45 m and 248.75–395.88 m respectively, during initial sampling. These high levels of flushing water contamination mean that great caution must be used when the groundwater data are evaluated, even to the extent of these data being omitted completely.

The drilling event is considered to be the major source of contamination of the formation groundwater. During drilling, large hydraulic pressure differences can occur due to uplifting/lowering of the equipment, pumping and injection of drilling fluids. These events can facilitate unwanted mixing and contamination of the groundwater in the fractures, or the cutting at the drilling head itself can change the hydraulic properties of the borehole fractures. Therefore, it is of major importance to analyse the drilling events in detail. From this information, not only the spiked drilling water can be traced, but also the major risk of contamination and disturbance from foreign water volumes can be directly identified. Too low or excessive extraction of water from a fracture zone prior to sampling can be calculated by applying the DIS (Drilling Impact Study) modelling /Gurban and Laaksoharju, 2002/.

Two sections in KFM01 were the subject of the DIS modelling: 110.1–120.67 m and 176.8–183.9 m. The modelling carried out for these fracture zones was based on the DIFF (differential flow meter logging) measurements and the main aim was to model the amount of the contamination (Figure 4-64) for each fracture zone. Unfortunately, for the first groundwater section sampled (110.1–120.67 m), the drilling data records were erroneous. The labelled water volume 'out' is higher than the labelled water volume 'in' and therefore the calculations could not be conducted. Thus, the DIS calculations were carried out for the second section in KFM01 (176.8–183.9 m) only. The DIS calculations showed that this section was contaminated with 2.9 m^3 water, of which a maximum of 19.4% consisted of drilling water. The actual results from the sampling showed 17.8% drilling water in the first sample. After removing 2 m^3 of water during sampling the remaining amount of drilling water was still around 4.8%. The DIS calculations indicate that by removing an additional 0.9 m^3 the contaminated water could have been removed from the section. In the future, the DIS calculations should be performed prior to sampling in order to support and guide the on-going sampling programme.
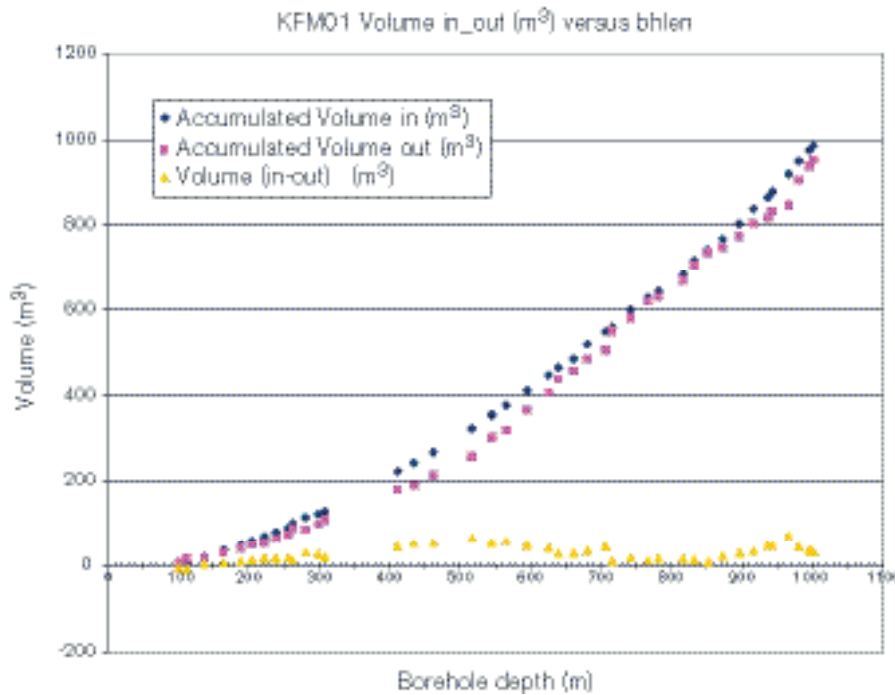
Figure 4-64. *Drilling water volume pumped in and out from KFM01 (176.8–183.9 m) during drilling.*

One fundamental question in modelling is whether the uncertainties lead to a risk of misunderstanding the information in the data. Generally the uncertainties from the analytical measurements are lower than the uncertainties caused by the modelling, but the variability during sampling is generally higher than the model uncertainties.

4.8.4 Explorative analysis

A commonly used approach in groundwater modelling is to start the evaluation by explorative analysis of different groundwater variables and properties. The degree of mixing, the type of reactions and the origin and evolution of the groundwater can be indicated by applying such analyses. It is also of major importance to relate, as much as possible, the groundwaters sampled to the near-vicinity geology and hydrogeology.

Because of either incomplete data or below detection or suspect values at the time of the 'data freeze', evaluation of, for example the radiogenic isotopes, ^{87}Sr, ^{10}B and REEs and other trace elements, have not been included in model version 1.1.

Evaluation of scatter plots

The hydrochemical data have been expressed in several X-Y plots to derive trends that may facilitate interpretation. Since chloride is generally conservative in normal groundwater systems, its use is appropriate to study hydrochemical evolution trends. When coupled to ions, ranging from conservative to non-conservative, it can provide information on mixing, dilution, sources/sinks etc. Therefore, many of the X-Y plots involve chloride as one of the variables. A preliminary evaluation of the various geochemical and isotopic trends apparent in the Forsmark groundwaters is described below. A more detailed evaluation of the major components and isotopes is given in /Laaksoharju et al, 2004/.

The laboratory analytical error in the data plotted is estimated to be ± 5% /cf Smellie et al, 2002/, which is illustrated in Figure 4-68. Note, however, that the very dilute surface and near-surface waters show a misleadingly small error when compared to the more highly mineralised borehole groundwaters.

At this juncture, it is useful to define 'Baltic Sea water' since it features prominently in many of the plotted data. As the plots reveal, some of the Baltic Sea data show a large spread to more dilute mixing compositions, and extreme examples exist where only small amounts of Cl are present. Whilst these diluted waters clearly do not represent typical Baltic Sea compositions in the Forsmark area, which average around ~ 2,600 mg/L Cl, they do represent some coastal Baltic Sea bay localities where there is a large fresh meteoric water input. According to /Samuelsson, 1996/, the salinity of the upper 50 m of open Baltic Sea equivalent to the latitude of Forsmark is ~ 3,000 mg/L Cl. Therefore, the Baltic Sea close to the Forsmark coast (~ 2,600 mg/L Cl) represents a somewhat diluted composition. However, since this diluted composition more accurately represents the 'Baltic Sea' composition at the site area, it should be used as the reference or end-member.

General comparison of Cl versus depth with other sites

A general depth comparison of the Forsmark chloride data has been made with the Laxemar (Oskarshamn) and Olkiluoto (Finland) datasets (Figure 4-65). It may be argued that such a comparison should be treated with caution since, particularly, Laxemar is geographically distant, represents a different hydrogeological regime and involves greater depths. Olkiluoto is at least also located at the coast and appears to have had a similar palaeo-evolution to the Forsmark region. However, the hydrogeochemistry at great depths (> 1,000 m) in the Fennoscandian basement probably shares general similarities to the other described sites, irrespective of geographic location and therefore Figure 4-65 can serve a useful purpose.

The Laxemar data show dilute groundwaters extending to a depth of around 1,000 m before a rapid increase in salinity occurs up to maximum values of around 47 g/L Cl at 1,700 m depth. Olkiluoto shows an initial sharp increase in chloride at around 150 m depth, which levels off at 5 g/L Cl and remains at that level to 450 m depth. From that depth, there is a relatively steady increase to maximum values of around 20 g/L Cl at 900 m depth (one maximum value of 44 g/L Cl was recorded). The Forsmark data show a close similarity to the initial Olkiluoto trends. It will be interesting to see if this levelling out at around 5 g/L Cl continues with increasing depth. An initial observation at this juncture is that the levelling out at 5 g/L Cl at Olkiluoto has been interpreted as possibly reflecting a Litorina seawater component. This may also be the case at Forsmark due to similarities in palaeo-evolution at the two sites.
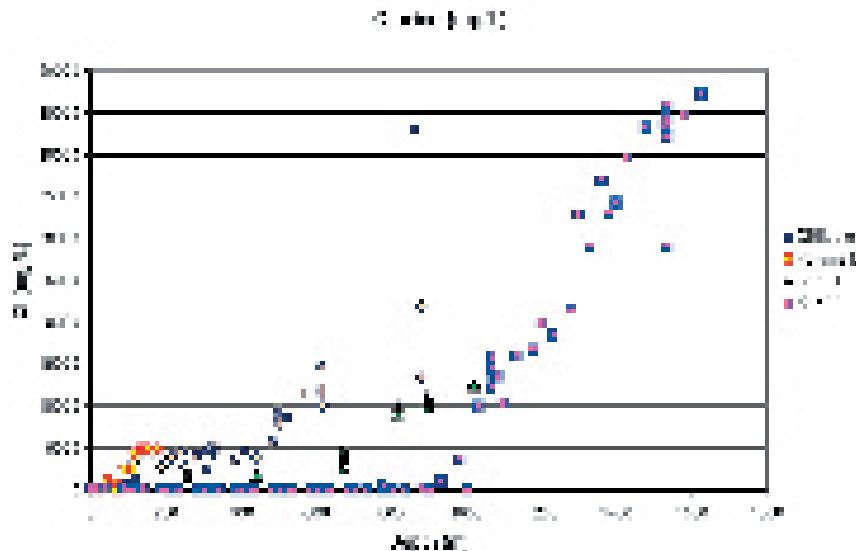
Figure 4-65. Depth comparison of chloride between the Forsmark site and the Laxemar (KLX01 and KLX02) and Olkiluoto localities.

153
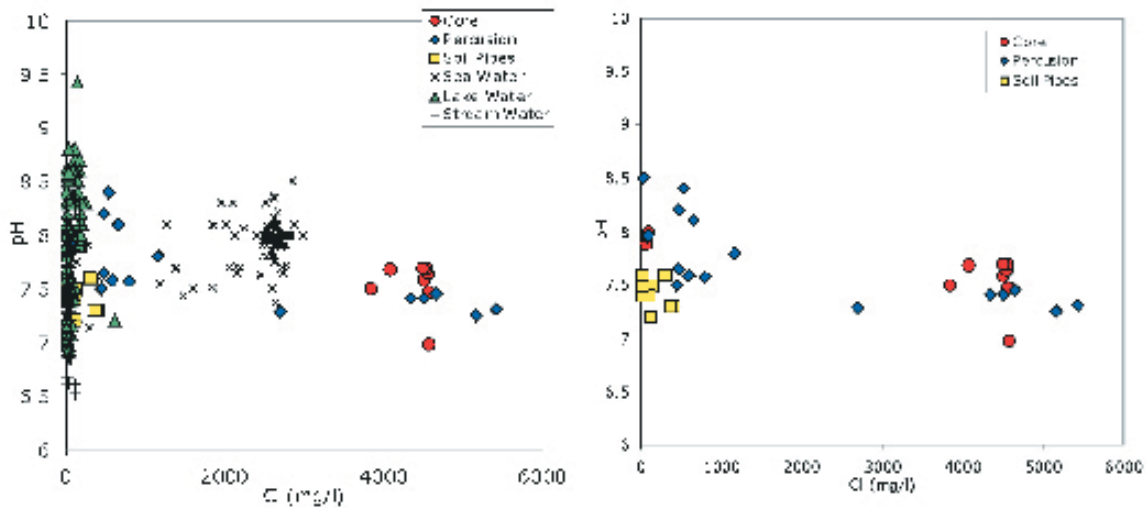
Figure 4-66. *pH versus chloride content (increasing with depth) in Forsmark waters.*

pH versus Cl

Superficial fresh waters show a wide range of pH values as a consequence of their multiple origins (Figure 4-66). The lowest values are lower than in any other water in the Forsmark area due to the influence of atmospheric and biogenic CO_2. However, pH can also exceed 9 in some superficial waters, such as lake waters, mainly due to photosynthetic activity.

Groundwater samples from cored boreholes and percussion boreholes show a slightly decreasing trend with chloride, obscured by the dispersion in pH values. Some of the less saline groundwaters have very high pH values, reflecting a superficial imprint. However, the broad scatter of pH values in these groundwaters, especially in the brackish and saline members, can be an artefact caused by the late measurement of pH in the laboratory instead of in situ. In /Laaksoharju et al, 2004/ the reader can find an analysis of the uncertainties associated with pH values.

Broadly speaking, the main features of the pH trend can be correlated with other Scandinavian sites with similar waters (e.g, Äspö and Olkiluoto; /Laaksoharju and Wallin, 1997; Pitkänen et al, 1999/), which also are affected by great uncertainties in pH /e.g. Pitkänen et al, 1999/.

Alkalinity versus Cl for all Forsmark data

Alkalinity (HCO_3^-) is, together with chloride and sulphate, the other major anion in the system being the most abundant in the non saline waters. Its concentration increases in the surface waters, as a result of e.g. calcite dissolution and the contribution of biogenic CO_2, up to equilibrium with calcite. Then, the HCO_3-concentration and salinity decreases dramatically with depth (Figure 4-67), but the solubility of calcite is increasing.
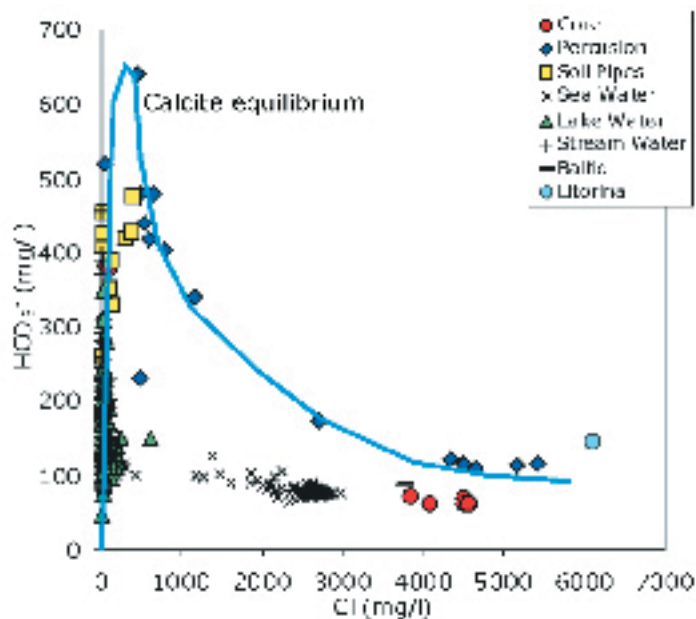
Figure 4-67. *Plot of alkalinity versus Cl for all Forsmark data.*

Mg versus Cl for all Forsmark data and comparison with other Swedish sites

Figure 4-68 shows two clear trends: a) an obvious modern Baltic Sea water dilution line, and b) a clear borehole saline dilution line distinct from (a).

The Baltic Sea values cluster around 2,600 mg/L Cl, which is recommended to represent the Baltic Sea end-member composition at the Forsmark site (see discussion above). The plotted data show a large spread to more dilute mixing compositions, and extreme examples exist where only small amounts of Cl are present. These dilute samples represent some coastal Baltic Sea bay localities where there is a large fresh meteoric water input.

The borehole data generally plot along a separate saline dilution line with some important exceptions. It is not the case for the KFM01A cored-borehole section at 110–120.67 m and for the percussion borehole HFM08 (0–93 m). HFM08 (0–93 m) shows some affiliation to the Baltic Sea water trend, whilst KFM01A shows a greater deviation from the rest of the borehole data by plotting even further away from a Baltic Sea influence. Of particular interest is the Mg and Cl difference between HFM08 (0–93 m) and HFM08 (0–143 m) which can be explained only by the greater sampling depth (some 50 m) in the latter. HFM08 (0–143 m) appears to have penetrated a horizon/pocket/lens of more highly saline water of marine origin where the Mg (~ 290 mg/L) and Cl (~ 5,300 mg/L) contents are approaching those estimated values for the Litorina Sea composition (Mg ~ 448 mg/L; Cl ~ 6,500 mg/L) as derived by /Pitkänen et al, 1999/. Mixing with a Litorina Sea component may explain the deviation of KFM01A (110–120.67 m), but a deeper, perhaps non-marine saline source, cannot be ruled out at this stage. The effect of possible Na/Mg exchange on the data has to be studied in future modelling.

A further comment on Figure 4-68 is the close association of some of the Soil Pipe samples to the modern Baltic Sea water dilution line; the other three samples show very little Cl but significant Mg. This may suggest: a) contact with an older marine water followed by cation exchange reactions and later flushing out of chloride, or b) simply water/rock interaction of recharge with minerals in the soil.

Comparing the Forsmark data with other Swedish sites (Figure 4-69), underlines the greater Mg contents (> 200 mg/L) associated with the sampled boreholes at Forsmark (e.g. KFR7A) when compared with, for example, the maximum content (~ 175 mg/L) at Äspö (borehole SA2240). This suggests that either Forsmark has better retained its high initial marine-derived Mg than the other Swedish sites, or indicates a greater influence from a later marine component (e.g. Litorina).

155
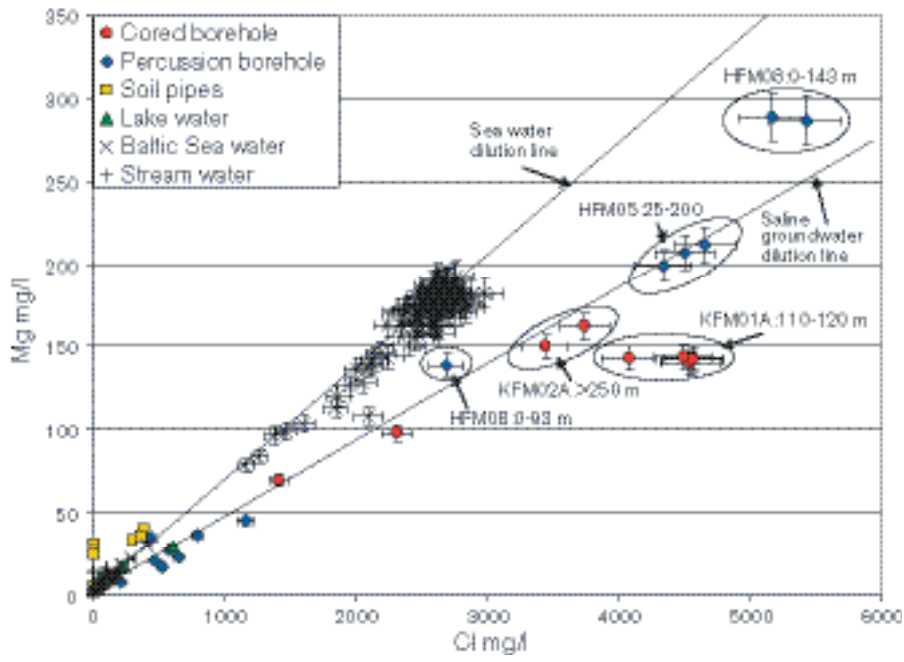
Figure 4-68. *Plot of Mg versus Cl for all Forsmark data showing analytical error bars (± 5%).*
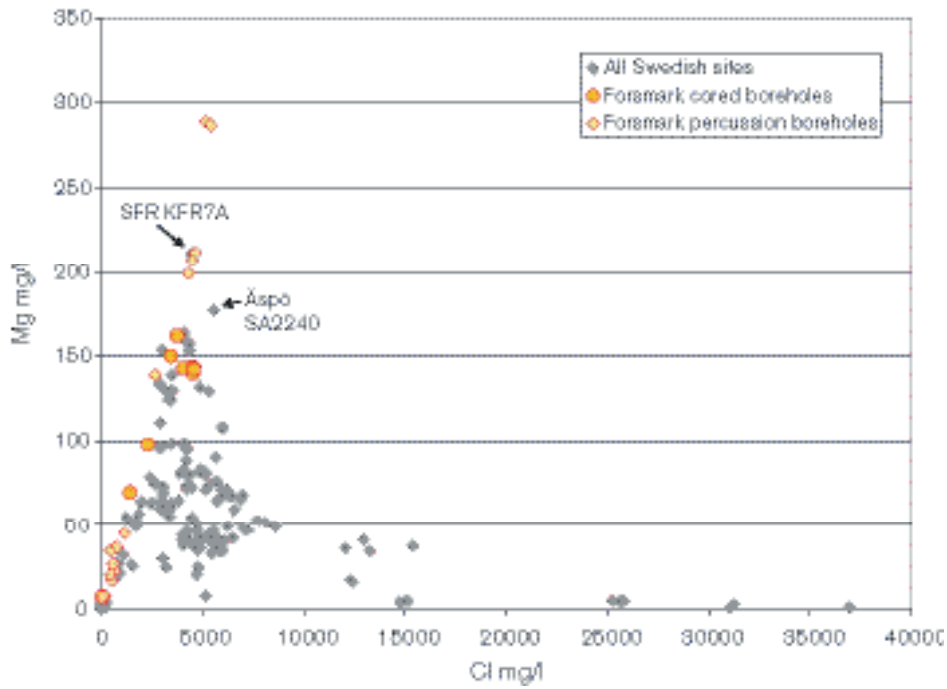
Figure 4-69. *Plot comparing all Forsmark Mg versus Cl data with other Swedish sites.*

Ca/Mg versus Br/Cl comparing all Forsmark data with other Fennoscandian sites

Plotting Ca/Mg versus Br/Cl (Figure 4-70) indicates those data of marine origin compared to a non-marine or a non-marine/marine mixing origin. For comparison, the Forsmark data are grouped with other Fennoscandian sites (Finnsjön, SFR, Simpevarp, Äspö, Laxemar, Olkiluoto and Stripa). The Yellow Knife-Thompson data have been included since they represent highly evolved basement brines in Canada where a significant marine component is unlikely.

The figure shows clearly the clustering of modern Baltic Sea water values. These can be compared to the other extreme, the Stripa groundwaters, which are considered to be more representative of a non-marine origin since this area was not transgressed by the Litorina Sea or subsequent marine transgressions /Nordstrom et al, 1985/. Between these two extremes fall the range of Finnsjön and Äspö groundwaters, considered to have a marine component of varying amount /Smellie and Wikberg, 1991; Laaksoharju et al, 1999b/, and the Olkiluoto groundwaters, which lean to a less marine component at greater depths /Pitkänen et al, 1999/. The Simpevarp cored-borehole ground-water data plot within the range of the Äspö samples. The Laxemar data, of deep basement origin, plot off the diagram, further emphasising their non-marine character.

Collectively, the Forsmark borehole groundwaters cluster towards a dominant marine component, more similar to the SFR than the Finnsjön groundwaters, although some Forsmark cored borehole samples do extend towards a slightly less marine component which is significant.

Na versus Cl for all Forsmark data

Sodium shows a positive correlation with chloride concentration, which reflects that mixing is the main process controlling Na contents. In Figure 4-71, two different trends can be seen: 1) an initial trend of weathering followed by mixing with a saline source, and 2) the deviation of groundwaters from the Baltic Sea water dilution line and from the line joining the origin with the Litorina end-member (Figure 4-71). This deviation can be interpreted as a smaller influence of the saline end-member or as a Na removal due to cation exchange reactions.
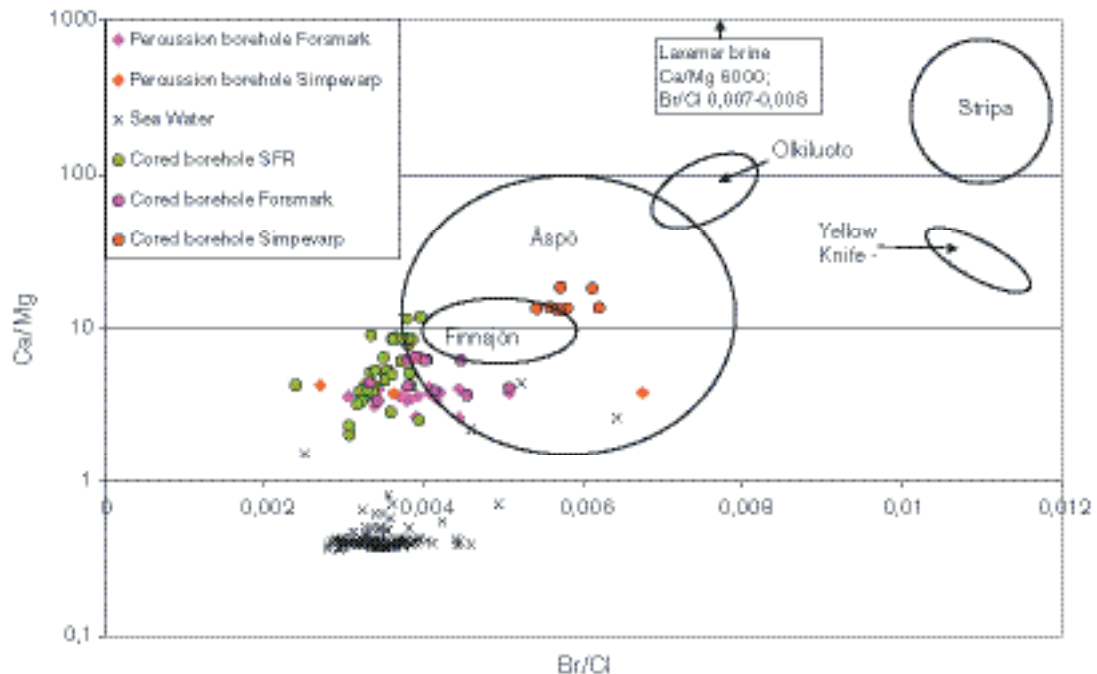
Figure 4-70. Plot comparing all Forsmark Ca/Mg versus Br/Cl data with other Fennoscandian sites and deep Canadian brines.
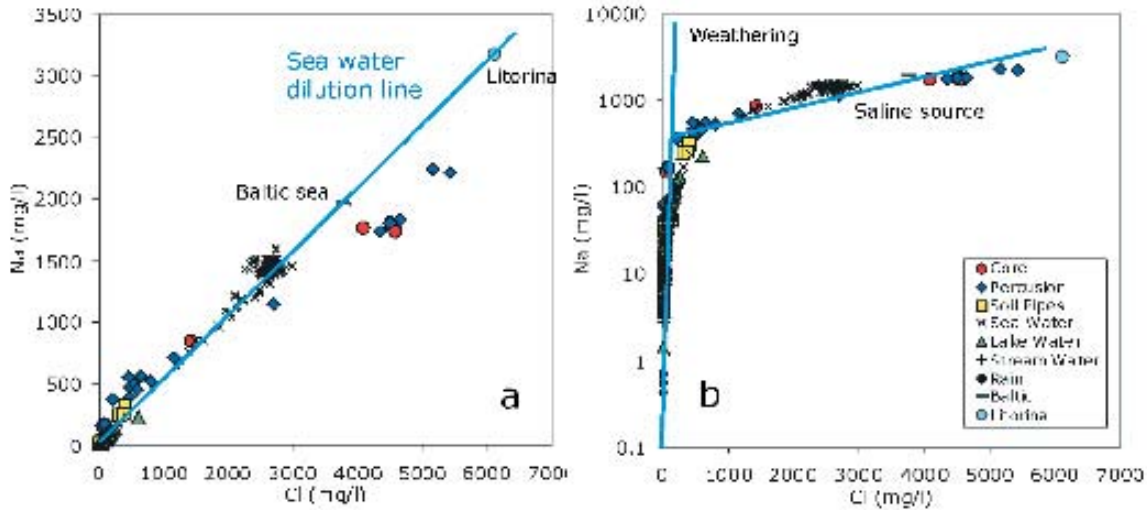
Figure 4-71. *Plot of Na versus Cl for all Forsmark data showing different trends in the data associated with different processes.*

Si versus Cl for all Forsmark data

The content of dissolved SiO_2 in surface waters indicates a typical trend of weathering, while in groundwaters it has a narrow range of variation indicative of a steady state (Figure 4-72). These two trends are commonly interpreted as the consequence of a re-equilibrium process as the residence time of waters increases and water-rock interaction becomes controlled by secondary fracture filling minerals. The general process evolves from an increase in dissolved SiO_2, by dissolution of silicates in surface waters and shallow groundwaters, to a progressive decrease, related to the participation of silica polymorphs and aluminosilicates in the control of dissolved silica, as the residence time of the waters increases.
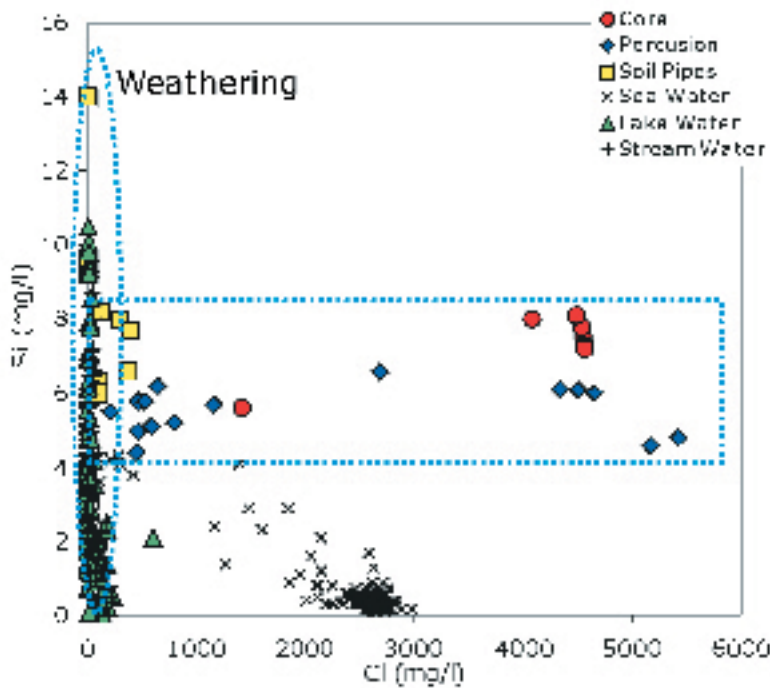
Figure 4-72. *Plot of Si versus Cl for all Forsmark data.*

δ¹⁸O versus Cl for all Forsmark data and comparison with the Finnsjön and SFR sites

Figure 4-73 shows a wide variation of $\delta^{18}O$ values at low chloride contents. This is thought to reflect a combination of seasonal fluctuations and mixing of local groundwater discharge (of varying residence times and recharge character) with modern Lake and Stream water sources. With only one exception, the Soil Pipe samples tend to cluster at lighter $\delta^{18}O$ values (–12 to –11‰ SMOW), which is close to the annual mean precipitation between –11 to –12‰ SMOW. The Baltic Sea water samples typically cluster around 2,600 mg/L Cl and –8‰ SMOW.

The borehole groundwater data show two concentrations; one high chloride (> 4,000 mg/L) with $\delta^{18}O$ values within the range of –12 to –10‰ SMOW (boreholes HFM05 and KFM01A) and one low chloride (< 1,500 mg/L) with $\delta^{18}O$ ranging from –12 to –9‰ SMOW. The latter represent mixing with more dilute, surface-derived waters.

The significance of these plotted distributions at Forsmark becomes more apparent when compared to data from the nearby Finnsjön and SFR sites (Figure 4-74). This figure shows two clear clusters representing present meteoric and present Baltic Sea waters, with a small degree of mixing between the two. The present Baltic Sea water dilution line intercepts the 'x' axis at approximately –11.7‰ SMOW, i.e. the average present-day recharge. The remaining data appear to be a scatter, but a dilution line linking a calculated Litorina Sea chloride content (6,500 mg/L) with fresh glacial meltwater ($\delta^{18}O$ = –25‰ SMOW) does suggest a degree of linear alignment of the SFR data, including some of the present Forsmark borehole data which earlier have been identified as potentially containing a significant Litorina Sea component. An increasing brine composition (i.e. more non-marine component) will plot more to the right of the Litorina Sea line, as shown by the deeper derived borehole groundwaters from Finnsjön. The scatter between the modern Baltic Sea, Litorina Sea and increasing brine components probably reflects variable mixing processes. Therefore, Figure 4-74 supports earlier suggestions that there are four main water types or end-members; present Meteoric, present Baltic Sea, an old Litorina Sea component and a deeper, more saline, increasingly non-marine component (Brine). Variable mixing between all four types is apparent.
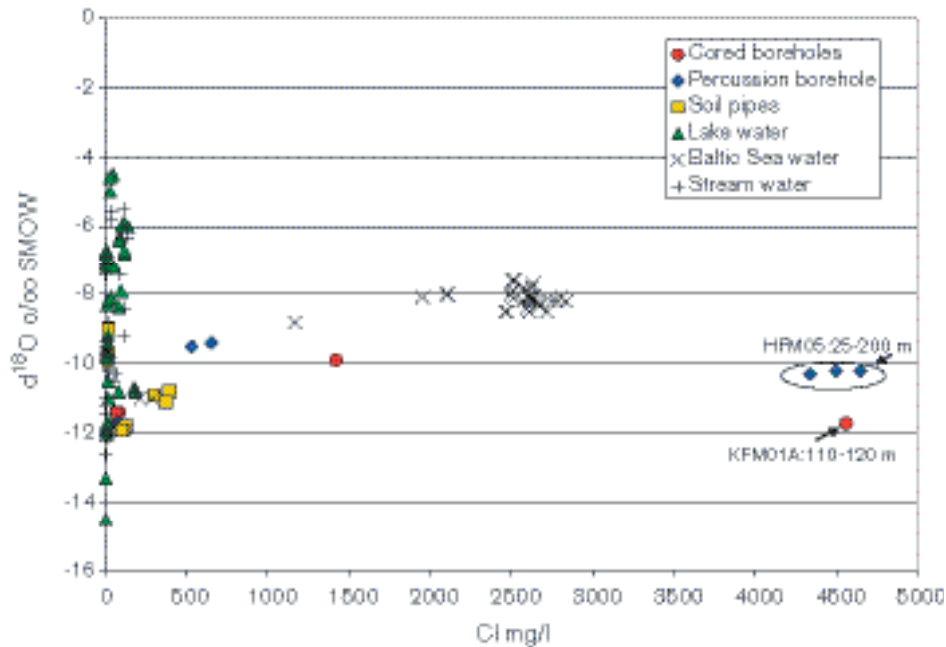
Figure 4-73. *Plot of $\delta^{18}O$ versus Cl for all Forsmark data.*
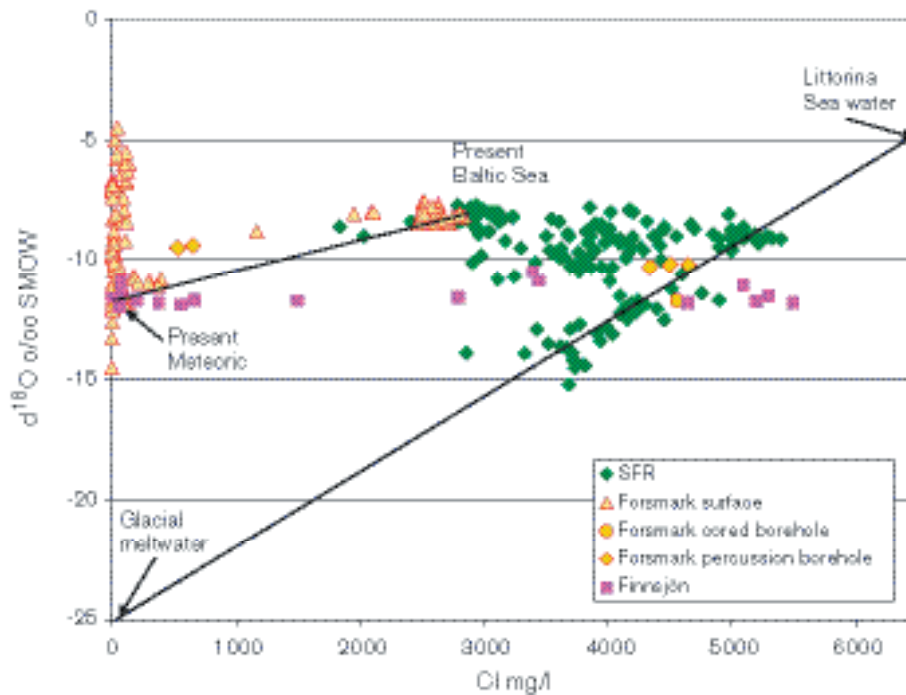
Figure 4-74. *Plot of $\delta^{18}O$ versus Cl comparing Forsmark with Finnsjön and SFR.*

A (significant?) in-mixing of a cool-climate meteoric water (e.g. glacial meltwater) is a probable explanation for the saline water with low $\delta^{18}O$ (< 13‰ SMOW) and chloride values around 3,500 mg/L. This 'Glacial' component therefore represents the fifth major water type or end-member.

$\delta^{18}O$ versus tritium for all Forsmark data

Figure 4-75 shows a wide range of $\delta^{18}O$ and tritium. The highest tritium value (~ 25 TU), compared to the present-day precipitation average of 10–15 TU, is associated with one of the Soil Pipe samples (SFM0003) and might be interpreted as reflecting a residual high bomb fall-out signature. Two Soil Pipe waters have very low tritium (below detection limit), which might suggest an area of groundwater recharge. Unfortunately, there are no corroborative ^{14}C data available for these samples.

The Lake and Stream water samples reflect modern waters of meteoric origin. Widespread mixing with waters/groundwaters from different sources has resulted in the observed scatter. Deeper borehole groundwaters (KFM01A; HFM01; HFM05) are older (> 5 TU); shallower borehole groundwaters (10–13 TU) have been influenced by variable mixing with waters that are younger and also with waters with a lighter $\delta^{18}O$ signature (present meteoric water).

Generally, the $\delta^{18}O$ ranges measured in the surface and near-surface waters may simply represent the seasonal range of present-day precipitation. Long-term seasonal precipitation records are not yet available to help resolve this issue.

The borehole groundwaters analysed record significant tritium (3–12 TU), indicating variable mixing (contamination?) with younger (years) meteoric waters (i.e. probably residual drilling water).
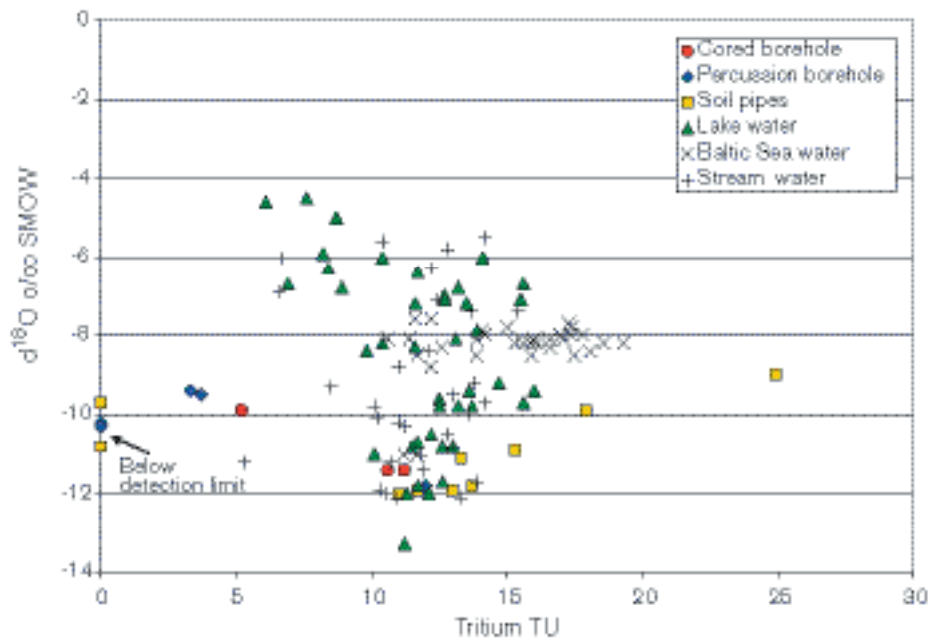
Figure 4-75. *Plot of $\delta^{18}O$ versus 3H for all Forsmark data.*

Water classification

The aim of water classification is to simplify the groundwater information. First the data set was divided into different salinity classes. Except for sea waters, most surface waters and some ground-waters from percussion boreholes are fresh, non-saline waters according to the classification used for Äspö groundwaters[1]. The rest of the groundwaters are brackish (Cl < 5,000 mg/L), except for two samples from percussion boreholes which are saline. Most surface waters are of Ca-HCO$_3$ or Na-Ca-HCO$_3$ type and, naturally, the sea water is of Na-Cl type. The deeper groundwaters are mainly of Na-Ca-Cl or Na-Cl-HCO$_3$ type. The results of the water type classification of the Forsmark samples are shown in Figure 4-76 and the results for all samples are listed in /Laaksoharju et al, 2004/. The linear correlation in the Ludwig-Langelier plot may indicate effects on the groundwater of processes such as ion exchange and weathering and of redox processes.

---

[1] The Äspö groundwaters were classified into three groups according to the site specific chloride concentrations /Laaksoharju and Wallin, 1997; Laaksoharju et al, 1999b/: non-saline groundwater (< 1,000 mg/L), brackish groundwater (1,000-5,000 mg/L) and saline groundwater (> 5,000 mg/L).
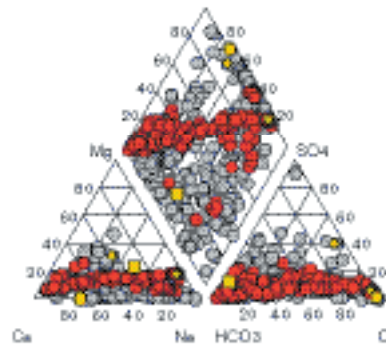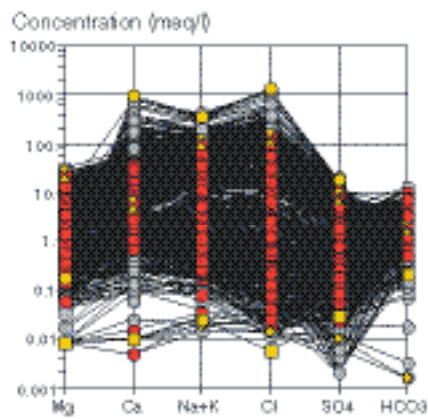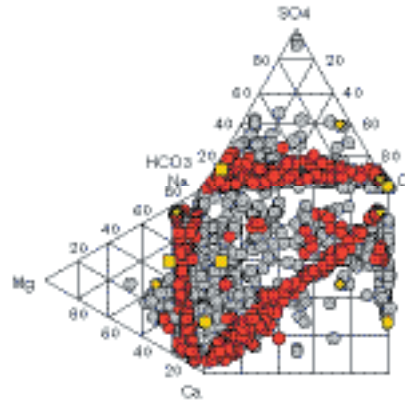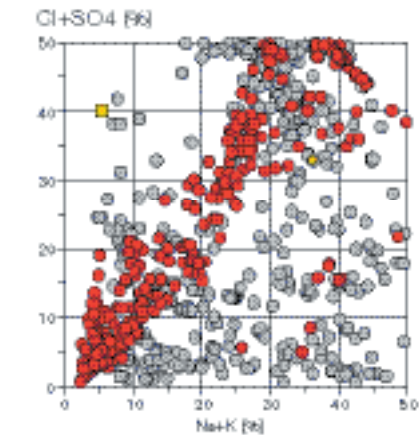
Figure 4-76. *Multicomponent plots used for classification of the groundwater data. From top left to top right to bottom left and bottom right: Ludwig-Langelier plot, Durov plot, Shoeller plot and Piper plot applied on all Forsmark data using AquaChem.*

162

4.9 Transport data evaluation

4.9.1 Transport data sampled on cores

No data from Forsmark are available for version 1.1. Therefore, sorption and diffusion data evaluated from measurements in samples from Finnsjön were utilised in the derivation of retention parameters for the rock (see Section 5.6)

4.9.2 Transport data sampled in boreholes

No data from Forsmark are available for version 1.1.

4.9.3 Joint transport, geological and hydrogeological evaluation of borehole data

No joint evaluation concerning transport properties has been made for version 1.1.

4.10 Biota data evaluation

This section gives a compilation of site-specific primary data concerning biota, e.g. producers, consumers and decomposers, as well as humans and human activities. Biota primary data may relate to both characterisation (e.g. species composition or habitat distribution) and processes (e.g. production or respiration).

Only primary data used for characterisation and modelling of ecosystems are presented in this section. All available data concerning objects and areas of environmental and/or cultural concern in the regional model area have been collected and compiled in the "accessibility map", which is a GIS-product describing the location and spatial distribution of these objects and areas (see Section 7.1.7).

4.10.1 Producers

Terrestrial producers

Vegetation mapping from satellite data of the Forsmark regional model area was conducted by /Boresjö Bronge and Wester, 2002/. Other site specific information has been presented by /Berggren and Kyläkorpi, 2002/, /Jerling et al, 2001/, /Jacobsson, 1978/ and /Svensson, 1988/. The vegetation map has been used together with some new information to produce models for standing crop biomass and production of the terrestrial vegetation in the Forsmark area. In order to arrive at a model of *standing crop biomass* and *production* of the terrestrial vegetation, a number of steps were undertaken;

1. Definition of habitat categories for the tree layer and for the bush, field and ground layers.

2. Assembly of the different habitat categories based on the vegetation map.

3. Production of habitat maps for these new tree, bush, field and ground layers, respectively.

4. Calculation of biomass and production values for the different habitat categories.

5. Assigning these values to the habitat categories in the maps.

As far as possible, site-specific data were used in the modelling process. However, since some of the information needed for the study has not been measured on the site, generic data were used for some calculations and some conversions of site-specific data into units necessary for the study. Table 4-26 shows the input data that were used for modelling of standing crop biomass and production in the different vegetation layers.

Table 4-26. Input data for modelling of biomass and production of terrestrial vegetation in the Forsmark regional model area.

Variable	Vegetation layer	Data source
Biomass	Tree layer	Forestry management plan, Sveaskog 1999
	Other layers	In situ studies of standing crop from bush, field, and ground layers /Fridriksson and Öhr, 2003/
	All layers	Generic data on dry weight and carbon content of biota /Jerling et al, 2001/
Primary production	Tree layer	Data obtained from the plots of the National Forest Survey,
	Other layers	In situ studies of standing crop from bush, field, and ground layers, /Fridriksson and Öhr, 2003/
	All layers	Generic data on dry weight and carbon content of biota /Jerling et al, 2001/

Aquatic producers

Limnic

No new site-specific data concerning primary producers in lakes and streams are available for model version 1.1. There exist some site-specific data from previous studies on primary producers in lakes in the area. The key data sources are found (or referred to) in /Brunberg and Blomqvist, 1998, 2000/ and /Brunberg et al, 2002/.

Marine

No new site-specific data concerning primary producers in the sea are available for model version 1.1. Previous available information on species composition and biomass of primary producers in the marine parts of the Forsmark area is compiled in /Kautsky et al, 1999/, /Kautsky, 2001/ and /Kumblad, 1999/.

4.10.2 Consumers

Terrestrial consumers

Terrestrial consumers in the Forsmark region are in model version 1.1 version represented by wild mammals and birds only, since no site-specific data are available for amphibians, reptiles or invertebrates /Berggren and Kyläkorpi, 2002/. Domestic animals like cattle, sheep and pigs will are addressed under the heading Humans and land use (Section 4.10.3).

Mammals

From late 2001 and to spring 2002, a study of wild mammals was conducted in the areas surrounding Forsmark /Cederlund et al, 2003/. The aim was to survey the main large mammals expected to be found in the Forsmark region, both terrestrial and aquatic. Selected species were: wolf, lynx, otter, marten, mink, red fox, wild boar, red deer, roe deer, moose, European hare and Mountain hare.

Birds

A survey of bird populations in the regional model area was performed during 2002 and the results are presented in /Green, 2003/. The survey continued during 2003, and thereafter a more thorough analysis of the results will be performed. Therefore, the results from the bird population survey have so far mainly been used for a qualitative characterisation of the bird fauna in Forsmark.

Aquatic consumers

Limnic

No new site-specific data concerning consumers in lakes or streams are available for model version 1.1. The results from standardised survey gill-net fishing in some lakes in the Forsmark area are compiled in /Brunberg and Blomqvist, 2000/.

Marine

No new site-specific data concerning consumers in the sea are available for model version 1.1. Previous studies on species composition and biomass of consumers in the coastal areas of Forsmark are compiled in /Kautsky et al, 1999/, /Kautsky, 2001/ and /Kumblad, 1999, 2001/.

4.10.3 Humans and land use

In order to arrive at an overall assessment of the human population and human activities in the model area, a wide range of various human-related statistics were acquired from Statistics Sweden. These statistics include survey data and time series on demography, labour, health, land use, agriculture etc. Beside this, some additional information was sampled from other sources, such as the National Board of Fisheries, the Swedish Association for Hunting and Wildlife Management, the County Administrative Board, and so on. The data sources used for the variables describing humans and land use are listed in Appendix 1, and a more thorough presentation of the data and results is given in /Miliander et al, 2004/.

5 Descriptive and quantitative modelling

The focus of this chapter is to describe the (3D) descriptive and quantitative modelling, i.e. how the already evaluated data from various sources (e.g. surface rock type distribution, lineament interpretation, single-hole interpretations, single-hole rock mechanics evaluations, evaluated data from hydraulic tests etc, as described in Chapter 4) are combined into an integrated description of the modelled volume. Important aspects of this modelling are formulation of hypotheses for extrapolation and interpolation, uncertainty evaluation including assessment of alternative hypotheses and cross disciplinary inter-comparisons. The resulting Site Descriptive Model is summarised in Chapter 7. The overall confidence in the Site Descriptive Model is assessed in Chapter 6.

5.1 Geological modelling

5.1.1 Quaternary deposits and other regoliths

The Quaternary cover forms the interface between the deeper geosphere and the surficial biosphere. Information on the spatial distribution and physical properties of the Quaternary deposits are therefore essential in order estimate the pathways and sinks for radionuclides and crucial base data for the model of near surface hydrology (cf Section 5.4). The surface distribution of the Quaternary deposits on land areas will be presented as a geological map. Future model versions will also aim at presenting a general stratigraphic distribution of the various types of glacial till. This information will be crucial not only for hydrogeological modelling, but also for the conceptual understanding of the glacial/post-glacial geological evolution of the Forsmark region. Lakes in general are considered to be discharge areas for groundwater, so the hydraulic properties of the lake sediments are of special interest. The spatial distribution of lake sediments will also be useful for modelling of future distribution of e.g. peatlands, essential information to project potential patterns of future land use.

Surface distribution

The spatial distribution of the upper layer of Quaternary deposits is descriptive in nature and based on field observations from the initiated site investigations /Sohlenius et al, 2003/ in combination with the initial geological map /Persson 1985, 1986/. No new 2D model (i.e. geological map) is available for model version 1.1.

Stratigraphy – Terrestrial Quaternary deposits

For model version 1.1, only point observations derived from corings are available (cf Section 4.2.1). Therefore, the model of the stratigraphic distribution of the glacial till is very simple, only including the depth to bedrock (cf Section 7.1.4). Stratigraphic variations within the till cover have not been included in the model.

Stratigraphy – Lake sediments

The model of the Quaternary deposits includes 3D models of the distribution of water laid sediment in Lake Eckarfjärden and Lake Bolundsfjärden (Section 7.1.4). The models aim of visualising the succession of sediment layers, and will be a useful contribution in the conceptual understanding of the surface hydrogeology as well as the ontogeny of the lakes. This model version is based on field classifications of the lithological units.

Model set-up

The geometrical models are built in a rectangular box enclosing the lake form. Since the lakes have a geographic extension in the order of c 1,000 m on the surface, and a maximum water-depth of only c 2 m, a scaling of the z-coordinates is needed. Therefore the z-axis has been expanded by a factor of 50. This gives the false impression of the lakes to be very deep and the littoral to be very steep.

The borehole measurements, which also have water depth recordings, are not sufficient to define the geometric shape of the lake. Therefore, the bathymetry and the shoreline of the lake were used /SKB GIS, 2003/. Furthermore, it was assumed that glacial till underlies the water-laid sediment.

There were in total 28 borehole samples available from Lake Eckarfjärden. 15 originated from /Bergström, 2001/ and 13 from the site investigations /Hedenström, 2003/. The boreholes were distributed unevenly over the lake area, concentrated along a central profile (Figure 5-1). There were in total 40 borehole samples available from Lake Bolundsfjärden, all originating from the site investigations. The samples where evenly distributed over the lake area, but mostly taken from the profundal regions (Figure 5-2).

Fabrication of additional samples Bolundsfjärden

The lake geometry of Lake Bolundsfjärden is shallow and quite complicated. Adjusting the sediment layers to the lake form was not possible with so few measuring points at hand. The measuring points can only give an impression of how the sediment layers are present in the measured points, and this knowledge had to be extrapolated throughout the lake bottom.

In order to model the surfaces so that they smoothly follow the data samples and the lake bottom geometry, and that they did not result in nesting that is not accounted for in the sample population, the sample information was spread out over the lake bottom. This was done by duplication of the existing samples. The duplicated samples were distributed around their original locations where each sample could be expected to be representative. When possible, the new fabricated sample was placed on the same bathymetric level as its original, but in some cases it was necessary to replenish data on other levels. In the latter case, the duplicated sample was lowered or raised to the appropriate level. In Figure 5-2, the total set of boreholes is shown.

The approach used is purely a modelling technique and one way to accomplish the additional points needed for the interpolation of the sediment layers. The method can, of course, give wrong results in some places, but the whole lake model has a general weakness of accuracy depending on the sparse sampling of the bottom.

A first analysis of the water depth from the borehole data set showed a consistent discrepancy of the borehole data, compared with the depth from the geographic bathymetry data files. In Lake Eckarfjärden, this discrepancy was estimated as 0.5 m, where the borehole data were deeper than the bathymetry. A possible source for this discrepancy is that the borehole measurements were taken during the winter when the lake was frozen and the characteristic bottom vegetation was not as dense as during the summer when the bathymetry was measured. To establish a consistent lake model, the borehole data were modified by 0.5 m. In Lake Bolundsfjärden, a correction of 0.2 m was applied.

Sediment layer analyses

The general stratigraphy in the boreholes was consistent. Nevertheless there are some inconsistencies in some layers, characterised by the absence of layers. However, the layer order is never altered. Especially the lower layers (glacial clay and post-glacial sand) are very consistent over the whole area in Lake Eckarfjärden. The layering is, of course, in some places very fine and intricate and therefore some simplifications are required.

Some of the layers in Lake Eckarfjärden are nested. This is the case in the layers of calcareous gyttja and algal gyttja; in some boreholes it has up to five consecutive alterations, yet elsewhere it has only one or two. This can partly be the result of the differences of measuring techniques between the different data sets, but also indicates a varying and heterogenic layer. In the model, these layers were represented as one clustered layer. Also the uppermost layers were clustered. This was made based on the observation of the consistent anomaly between the different data sets. After the simplifications, exclusions and clustering, seven layers above the till were identified. Some of the layers were sporadic whereas others were consistent over the whole lakes.

In Lake Eckarfjärden, a distinct correlation between the use of shallow boreholes and the absence of the lower layers of sand and clay was found. These layers are known to be quite consistent; therefore a need for data completion in the shallow boreholes was implied. This was performed by linear

Figure 5-1. *The location of the boreholes in Lake Eckarfjärden. The PFM and SFM points are from the site investigation while the one letter/digit points are from /Bergström, 2001/.*
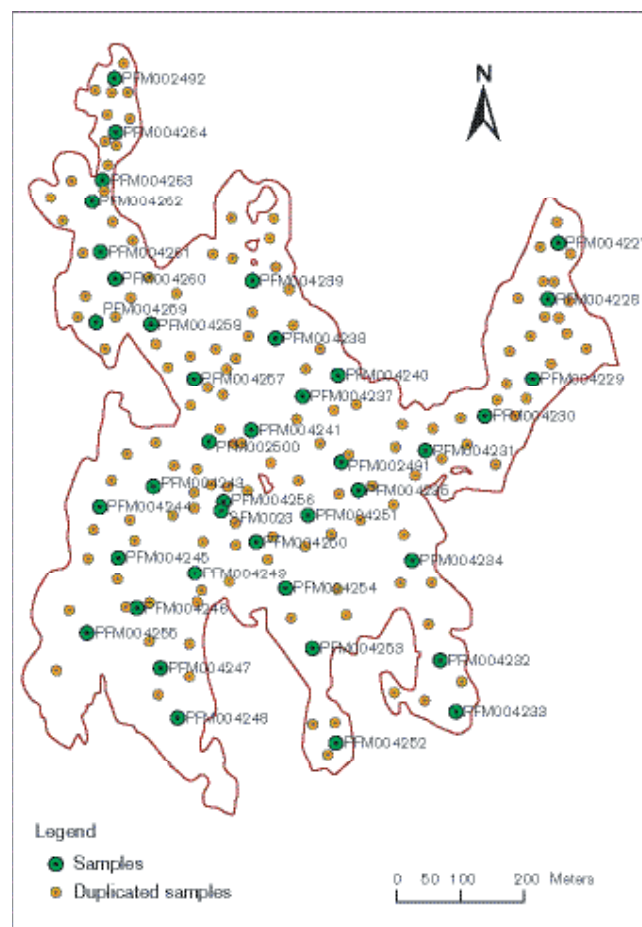
Figure 5-2. *The location of the boreholes in Lake Bolundsfjärden, green labels. The yellow labels indicate the position for the fabricated samples.*

interpolation between the surrounding boreholes, which were drilled deeper. The interpolation was made on all occasions when the lower layers were missing, except if the borehole was noted to be terminating against rock or boulders. In Lake Bolundsfjärden, all the boreholes except one terminated in the glacial till. Therefore, no completion of the layers was necessary.

Development of the 3D model

The modelling procedure can at its simplest be described as two steps:

1. Surface modelling, in which the surfaces representing the border between the different layers are created.

2. Block modelling, where the volumes are generated and sorted into appropriate classes.

In each model, a number of surfaces were created. The upper surface represents the bottom of the water volume, i.e. the actual bottom of the lake. Below this, each of the lithological units was represented by a surface indicating its lower limit.

The surface modelling was done in various ways depending on the complexity of the surface.

*   Surfaces with small variations in depth were best modelled by generating an even grid that was interpolated between the co-ordinates at the shoreline and those at the sampling points. These surfaces were splined and came out quite soft. The surfaces were mathematically quite complicated and consequently a low resolution of the grids was necessary. Therefore, the layers did not match the borehole data perfectly. At first, Krieging was used to avoid this, but this resulted in a very strange behaviour at places where the data density was low. Therefore, linear interpolation with a nearest neighbour fit was used. The parameters were individually adjusted in order to achieve each surface optimally.

*   Where the surfaces were more varying, i.e. great variations in depth were present over short distances, pure triangulation was used. This gives a more accurate model when it comes to the data fit, but the surfaces looked quite unnatural since it generated a lot of sharp edges and corners. This approach was avoided as far as possible, but in developing the Bolundsfjärden model it was necessary to use it on several occasions.

In order to get the sediment layer to end in a consecutive order from the shore towards the depth, the co-ordinates used for the interpolation of the layers at the shoreline were raised above the water surface level with some distance between each layer. This technique forced each layers to cross the bottom surface consecutively (Figure 5-3).
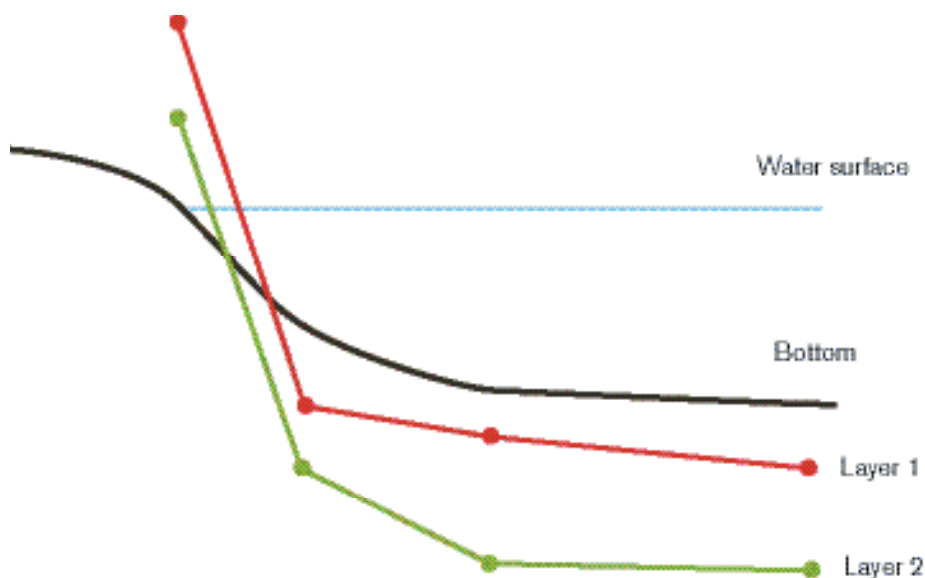
Figure 5-3. *Schematic figure, showing how the interpolated surfaces are forced to intercept the bottom in consecutive order. In the example, layer 1 represents algal-gyttja and layer 2 gyttja.*

Finally, a manual correction was performed on the surfaces. The layer order was controlled so that unwanted nesting was minimised. Especially in the narrow coves the interpolation was not flexible enough.

The block modelling was performed in RVS. The block generation followed a code where a separate block was generated for each volume that is completely cut off from the adjacent volumes by surfaces or the model boundary. The surfaces were imported and the blocks generated and sorted into the appropriate layers.

Two surfaces that lie very close to each other can sometimes be subjected to unwanted nesting. The reasons to this are that the spline functions in the various softwares used are hard to control entirely and that the rendering accuracy at a very detailed level not always is perfect. Especially, this nesting will occur when one goes from one software representation to another. Doing so was necessary at several occasions during the modelling procedure. Therefore, the blocks had to be sorted manually after they were generated and this caused some of the sediment bodies to be quite shattered. The 3D distribution of lake sediment is displayed in figures in Section 7.1.4.

5.1.2 Rock domain modelling – regional scale

Modelling assumptions and input from other models

No previous, three-dimensional model for the distribution of rock domains has been presented for the Forsmark site. During the work with the version 0 of the site descriptive model /SKB, 2002a/, the various rock units that had been recognised at the surface as well as the units with more intense ductile deformation were simply identified and located on the top surface of a three-dimensional block. No extrapolation to depth was carried out. Furthermore, few primary data were available to permit a detailed documentation of the properties of rock domains or rock types.

This section describes how a three-dimensional model for the rock domains at the Forsmark site has been constructed. The terms units and domains are used here according to the terminological guidelines in /Munier et al, 2003/. Rock units are defined on the basis of the composition and grain size of the dominant rock type or the degrees of bedrock inhomogeneity and ductile deformation. All these geological features are judged to have some relevance for the construction and long term safety of a repository. Rock domains are defined on the basis of an integration of these different geological criteria.

Since only one deep borehole (KFM01A) and eight relatively shallow percussion boreholes are available for model version 1.1, it is clear that the surface data are of primary importance for the construction of the rock domain model (see Section 4.2.2 and the evaluation of ductile structures in Section 4.2.4). A prime step in the modelling procedure has been the recognition of rock domains at the surface.

The modelling procedure has involved the use of eight rock units that have been distinguished on the basis of the composition and grain size of the dominant rock type and four rock units that show different degrees of bedrock inhomogeneity and ductile deformation (Table 5-1).

The following key assumptions have been adopted during the modelling procedure:

- The strike and dip of the planar ductile structures, banding and tectonic foliation (see Section 4.2.4), as measured at the surface, are assumed to provide an estimate of the strike and dip of the contacts between the major rock domains, i.e. those domains that can be followed at the surface over several kilometres.

- Since the contacts between the major rock domains are commonly estimated to be steeply dipping, all these domains are assumed to extend downwards to, at least, the base of the regional model volume (–2,100 m).

- The lenses of ultramafic, mafic and intermediate rocks at the surface (SKB codes 101033 and 101004) are assumed to trend downwards in the direction of the mineral stretching lineation (see Section 4.2.4) and to extend to, at least, the base of the regional model volume.

- The remaining lenses of smaller rock domains at the surface are assumed to trend downwards in the direction of the mineral stretching lineation (see Section 4.2.4) for a distance no longer than the distance that each domain can be followed at the surface.

These four assumptions form a basis for the construction of a single, geometric model for the three-dimensional distribution of rock domains in the regional model volume. This model is presented in connection with the description of the site (Section 7.2.1). It is important to keep in mind that the character and proportions of rock types along borehole KFM01A (see Section 4.4) are similar to those observed at the surface. These data confirm the extension of at least this rock domain to a depth of c 1,000 m.

Geometric modelling

Four working stages have been followed during the geometric modelling:

- Some simplification of the geological map that has been produced during the site investigation programme in the area between road 76 and the coast (Figure 4-9).

- Integration with the bedrock geological map that was used in the model version 0 work for the areas south of road 76 and northeast of the coast /SKB, 2002a/.

- Definition of the areal extension of thirty-four rock domains at the surface using the bedrock components defined above (Table 5-1).

- Downward projection of the thirty-four rock domains throughout the regional model volume.

Table 5-1. Bedrock components that have been used in the modelling procedure.

Rock units – composition and grain size of dominant rock type

Code (SKB)	Composition	Complementary characteristics		
111058	Granite		Fine- to medium-grained	SDM version 0 geological map. Inferred group D.
111051	Granitoid	Metamorphic		SDM version 0 geological map. Inferred group B.
101058	Granite	Metamorphic	Aplitic	Group B on SDM version 1.1 geological map
101057	Granite to granodiorite	Metamorphic	Medium-grained	Group B on SDM version 1.1 geological map
101054 and 101056 combined	Tonalite and granodiorite	Metamorphic		Group B on SDM version 1.1 geological map
101033 and 101004 combined	Diorite, quartz diorite, gabbro and ultramafic rock	Metamorphic		Group B on SDM version 1.1 geological map
103076	Felsic to intermediate volcanic rock	Metamorphic		Group A on SDM version 1.1 geological map
106000	Sedimentary rock	Metamorphic		SDM version 0 geological map. Inferred group A.

Rock units − degrees of inhomogeneity and ductile deformation

Rock unit	Degree of inhomogeneity	Degree of ductile deformation	
1	Inhomogeneous	Banded, foliated and lineated (BSL-tectonites).	Inferred higher degree of ductile deformation
2	Inhomogeneous	Lineated and weakly foliated (LS-tectonites).	Inferred lower degree of ductile deformation
3	Homogeneous	Foliated and lineated (SL-tectonites).	Inferred higher degree of ductile deformation
4	Homogeneous	Lineated and weakly foliated (LS-tectonites).	Inferred lower degree of ductile deformation

In order to carry out the modelling procedure effectively, it was necessary to simplify the new bedrock geological map of the area between road 76 and the coast (Figure 4-9). Minor rock units on the geological map were included in the modelling procedure as subordinate rock types within the adjacent major rock unit. This simplification included the two types of mineralisation, the Group C metagranitoid, and the Group D pegmatitic granite and pegmatite (Figure 4-9) as subordinate rocks within the adopted rock domains. Furthermore, the ultramafic rocks were modelled together with the metamorphosed gabbro, diorite and quartz diorite, and the metatonalite together with the metagrano-diorite. These changes reduced the eleven rock units on the geological map to five rock units in the modelling work.

The second stage in the modelling procedure involved an integration of the bedrock geological map that covers the area between road 76 and the coast, with the older compilation of the bedrock geology in the two areas south of road 76 and northeast of the coast /SKB, 2002a/. This procedure was necessary since the new bedrock-mapping programme was not complete when the model version 1.1 work initiated and did not cover the whole regional model area. Three rock types are present that define mappable rock units in the areas south of road 76 and northeast of the coast but are absent in the newly-mapped area. These include metasedimentary rock, metagranitoid (unspecified), and fine- to medium-grained granite. The fine- to medium-grained granite is possibly correlatable with the Group D granites that were recognised during the new bedrock-mapping programme.

The simplification and integration procedures of the surface data have yielded three important products:

- A geological map that shows the distribution of mappable rock units over the regional model area (Figure 5-4), each of which is dominated by one of the eight rock types defined in Table 5-1.

- A geological map that shows the variation in the degree of both bedrock inhomogeneity and ductile deformation over the regional model area (Figure 5-5). The four units displayed on this map are also defined in Table 5-1.

- A geological map that shows rock domains over the regional model area (Figure 5-6). They have been defined by identifying all the combinations in the two products described above. The rock domains are recognised with different numbers in Figure 5-6.

On this basis, thirty-four rock domains have been identified at the surface in the regional model volume. All these domains have subsequently been modelled at depth.

The fourth and final stage in the modelling work concerns the projection of the rock domains that have been recognised at the surface to a depth of –2,100 m, i.e. to the base of the regional model volume. The key assumptions adopted in this procedure have been summarised earlier. An important working component has been to define subareas that are structurally and lithologically homo-geneous.

The Schmidt stereographic plots for two representative subareas that show contrasting structural characteristics are presented here. The stereographic plots for all subareas are presented in Appendix 2. The data from the subarea defined by rock domains 29 and 34 (RFM029 and RFM034), that include a major part of the candidate area, indicate large-scale folding of the tectonic foliation with a fold axis that plunges moderately to the southeast, parallel to the mineral stretching lineation (Figure 5-7). The structural data from the subarea defined by rock domains RFM008, RFM018, RFM026 and RFM028 are considerably more homogeneous. The planar structures strike in a north-westerly direction and dip steeply to the southwest, and the linear structures plunge moderately to the southeast (Figure 5-8). This geometric configuration is also typical of the subarea that is situated immediately to the northeast of the candidate area and includes rock domain RFM021 (Appendix 2).

The mean values of both the strike and dip of banding and tectonic foliation, and the trend and plunge of the mineral stretching lineation have been estimated in the different subareas. These values have then been used to assist in the projection of the various rock domains at depth.
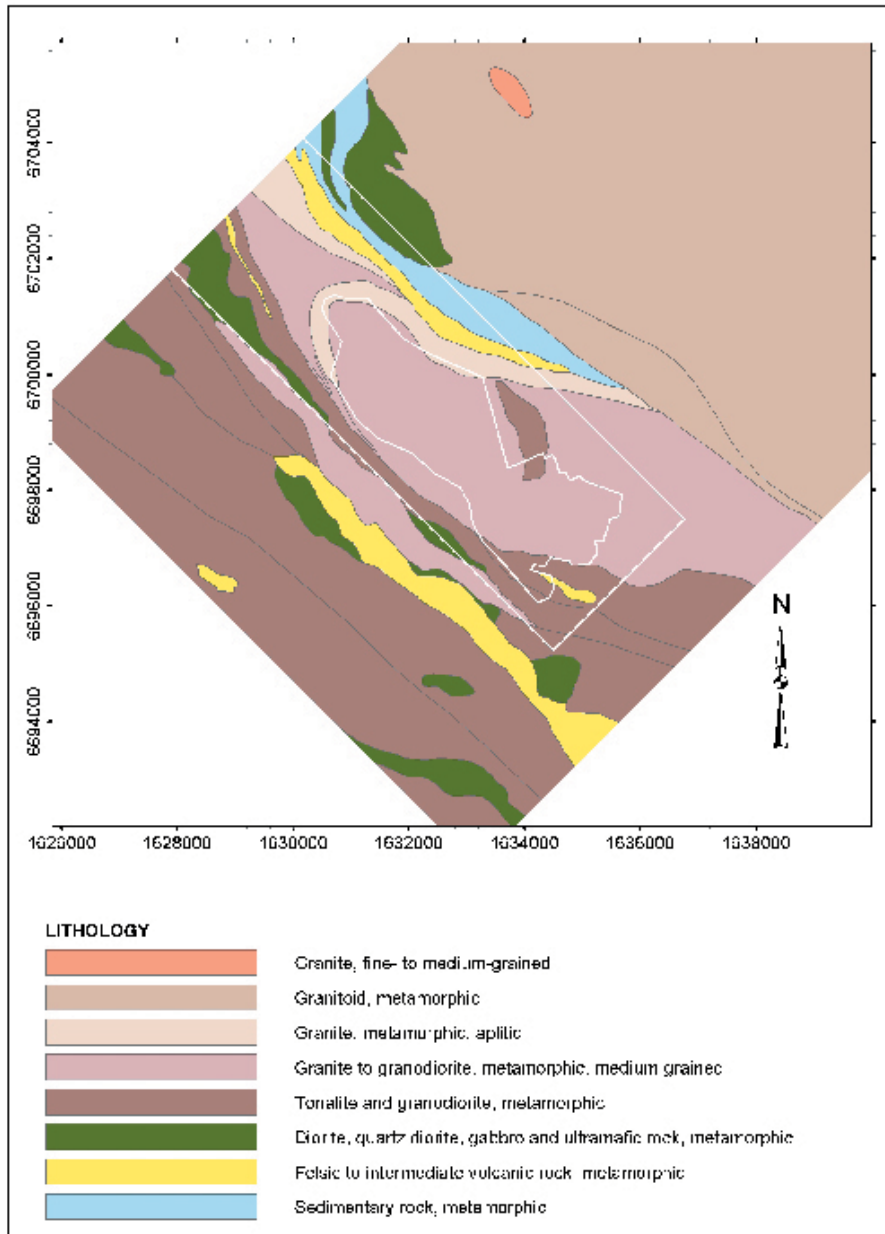
Figure 5-4. *Rock units defined by different dominant rock types. Surface view of the regional model volume.*
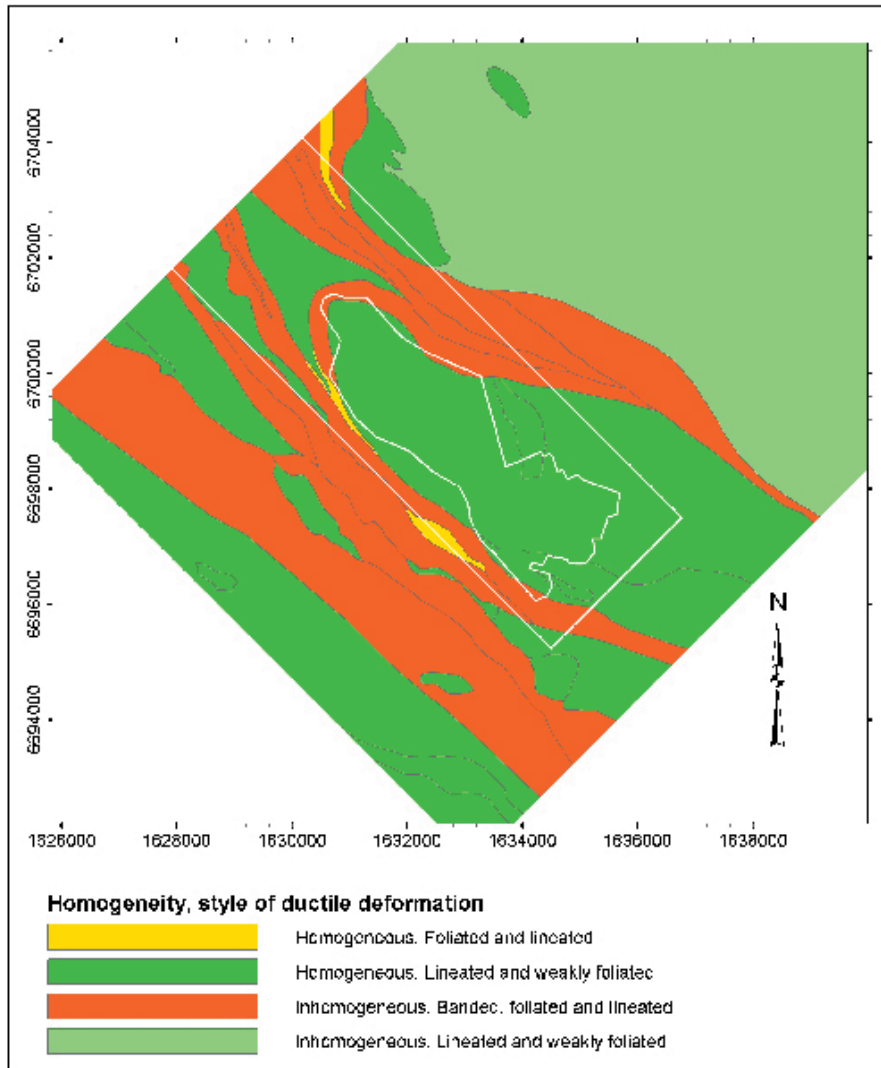
Figure 5-5. Rock units distinguished on the basis of degree of inhomogeneity and ductile deformation in the bedrock. Surface view of the regional model volume.
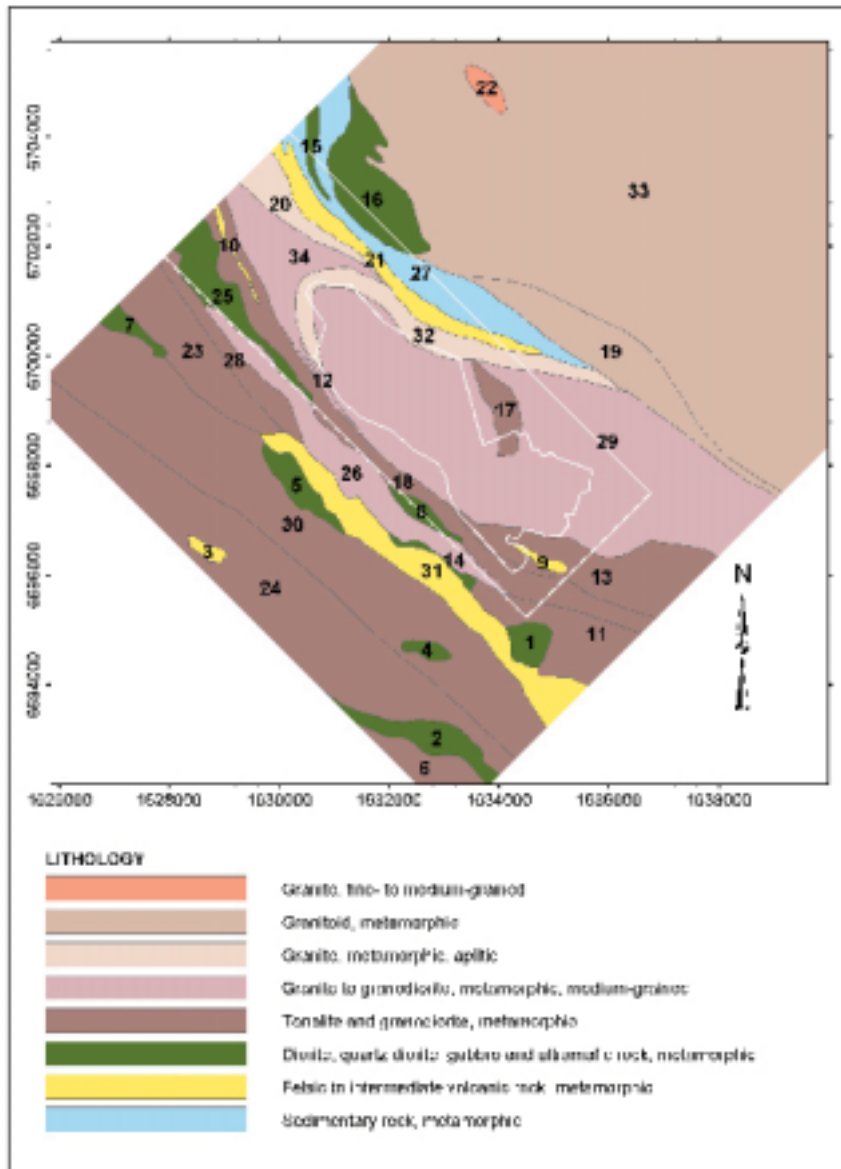
Figure 5-6. *Rock domains used in the modelling procedure numbered from 1 to 34. The colours show the rock units that were defined on the basis of dominant rock type. These units are identical to those shown in Figure 5-1. Surface view of the regional model volume.*
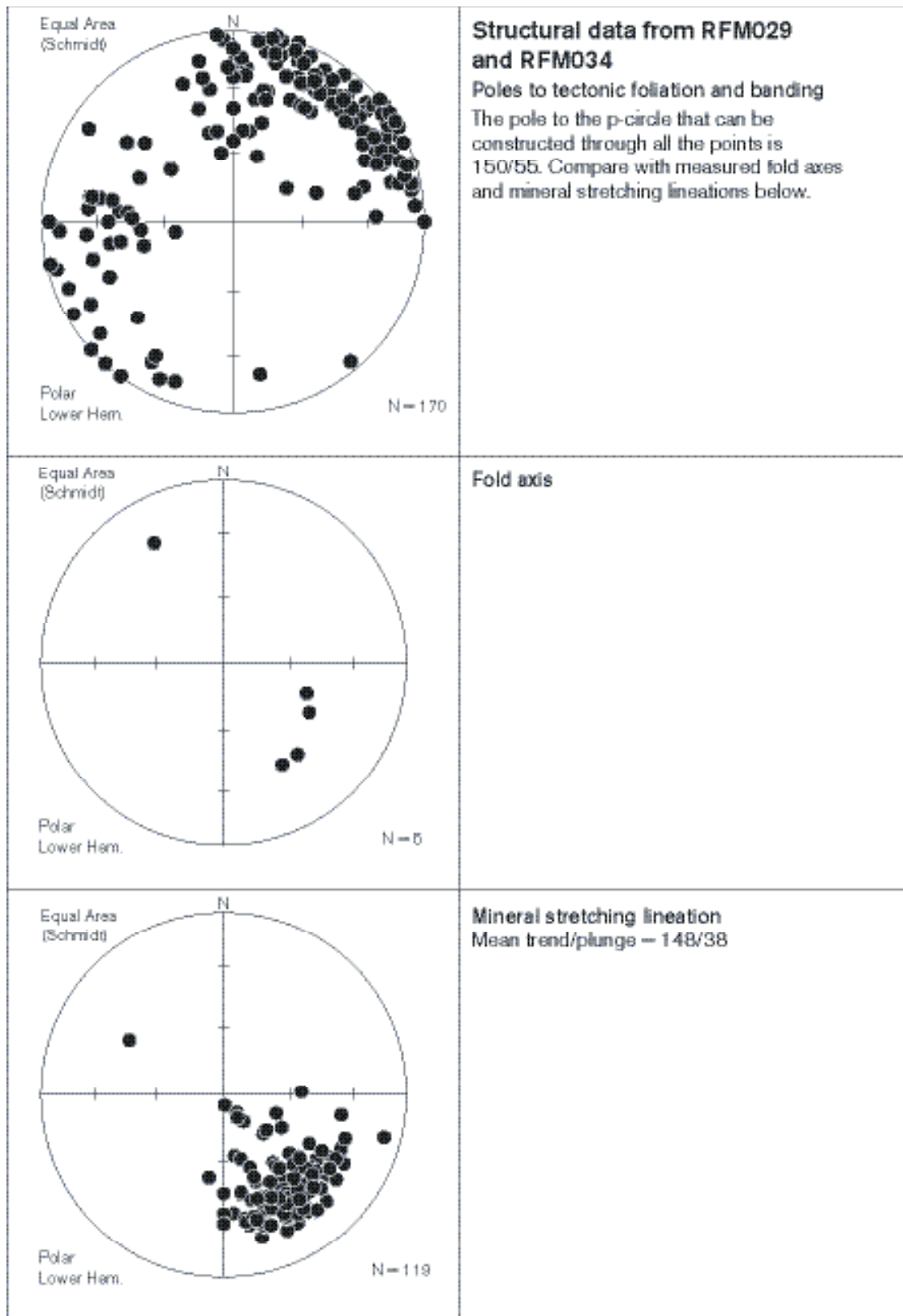
Figure 5-7. Lower hemisphere Schmidt stereographic plot of the ductile structures in the subarea defined by rock domains 29 and 34.

Structural data from RFM008, RFM018, RFM026 and RFM028
Poles to banding and tectonic foliation
Mean strike/dip = 139/86

Fold axis

Mineral stretching lineation
Mean trend/plunge = 140/39
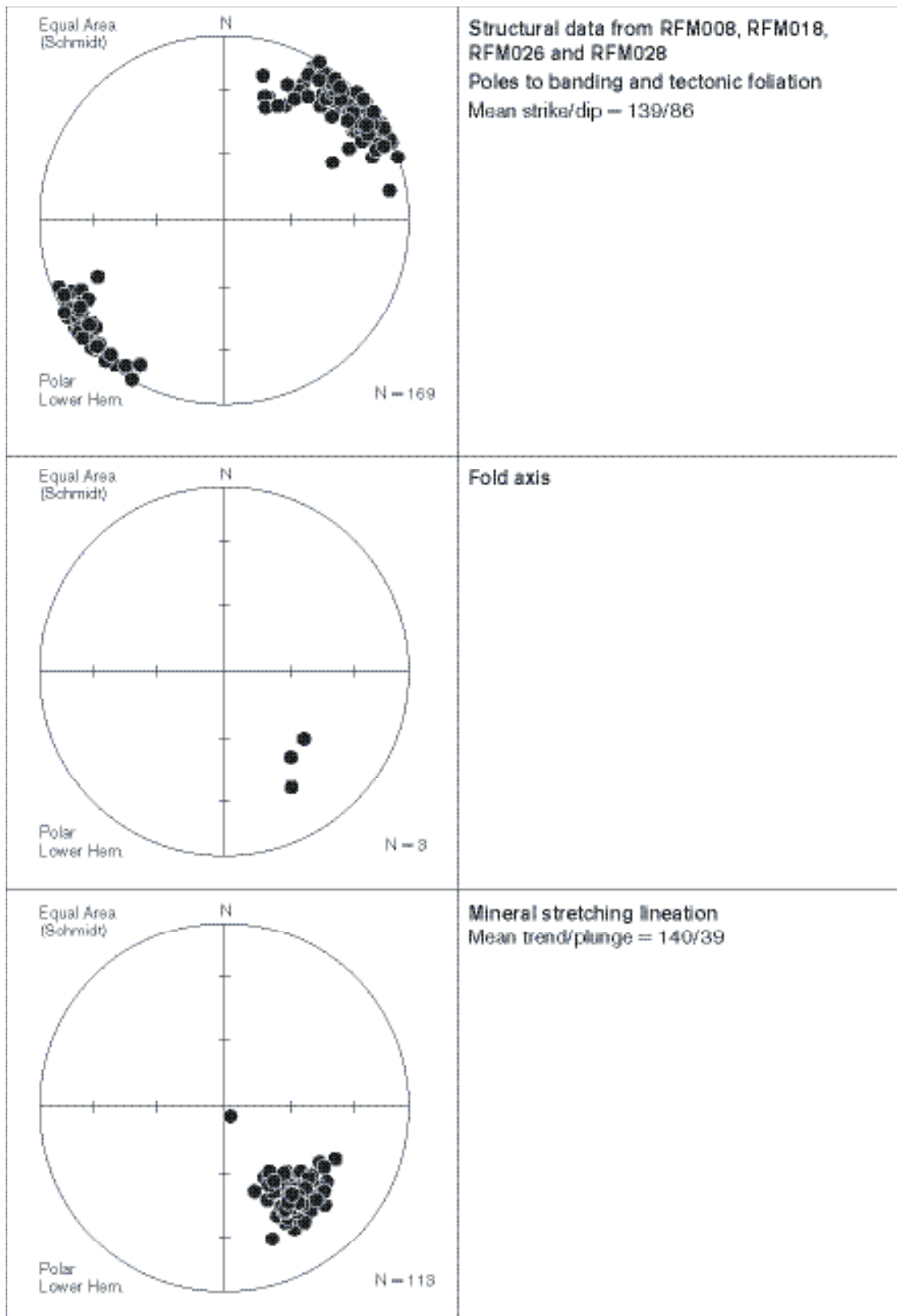
Figure 5-8. Lower hemisphere Schmidt stereographic plot of the ductile structures in the subarea defined by the rock domains 8, 18, 26 and 28.

Property assignments

Each rock domain has been assigned a list of properties (Table 5-2), including the dominant and subordinate rock types in the domain. Furthermore, the properties of the different rock types (Table 5-3) have also been defined. All these properties are presented in tabular format in the description of the site (Section 7.2.1).

For the rock domains that are situated partially or completely within the newly mapped area between road 76 and the coast, the properties of the rock domains (Table 5-2) have been extracted from the outcrop database (see Section 4.2.2). In rock domain RFM029, additional information on rock type is available in the data from borehole KFM01A and the eight percussion boreholes (see Section 4.4). Only limited information is available from the bedrock compilation work for the rock domains that are situated south of road 76 and northeast of the coast (see Section 4.2.2).

Table 5-2. Properties assigned to each rock domain.

Rock property
Rock domain ID (RFM***, according to the nomenclature recommended by SKB).
Volume.
Dominant rock type.
Subordinate rock types.
Degree of inhomogeneity.
Character of high-temperature alteration (metamorphism) in the dominant rock type.
Character of ductile deformation.
Classification of rock unit, 1–4 (see Table 5-1)
Low-temperature alteration around fractures (if data is available).
Fracture filling (if data is available).

A critical property is the composition and grain size of the different rock types in the various domains. In the domains that lie between road 76 and the coast, it has been possible to estimate qualitatively the relative amounts of the different rock types in each domain from the outcrop database (see Section 4.2.2). For example, in rock domain RFM029, the lithology that forms the dominant rock type in over 80% of the outcrops that have been studied (197) is a medium-grained, metamorphosed granite to granodiorite (Figure 5-9). In over 20 outcrops, this lithology is the only rock type that has been recorded (Figure 5-9). However, pegmatitic granite and pegmatite, amphibolite, metamorphosed aplitic granite, and various finer-grained, younger granitoids that show variable effects of metamorphism form common, yet subordinate rock types (Figure 5-9). Similar qualitative information concerning the proportions of dominant and subordinate rock types in most of the remaining rock domains are presented in Appendix 3. It has only been possible to estimate quantitatively the proportions of different rock types in rock domain RFM029 using the data from cored borehole KFM01A (see Section 4.4). These data conform well to the qualitative surface estimates.

The key properties that define the various rock types (Table 5-3) have been obtained from the petrographic, geochemical and petrophysical analyses of surface samples or, in the case of the gamma-ray spectrometric data, from the measurements carried out directly on the outcrop (see Section 4.2.2). Mean and standard deviation values as well as the number of samples analysed are provided for each property and rock type.
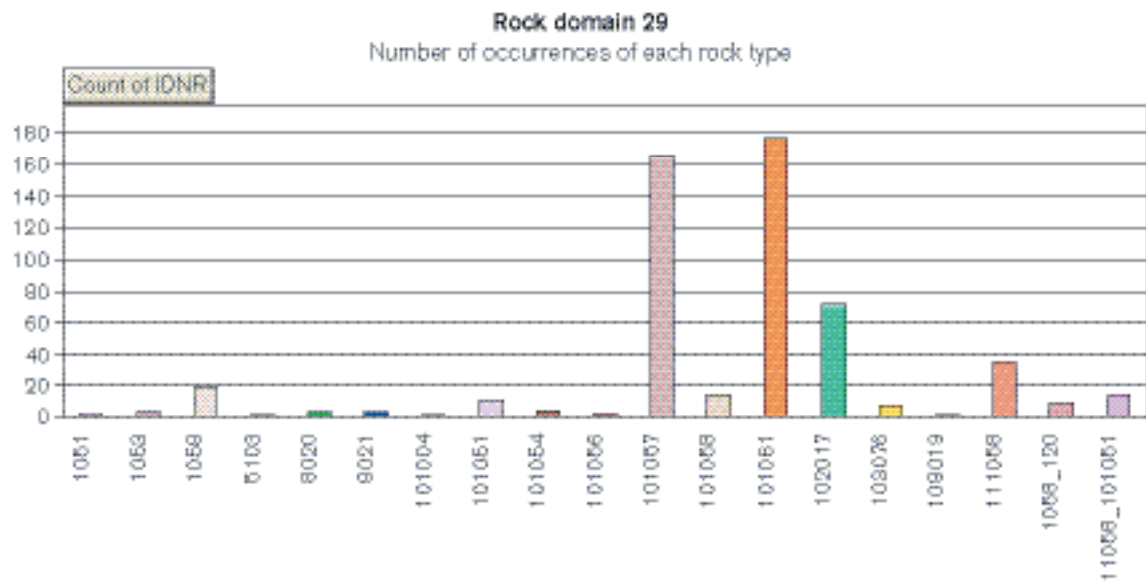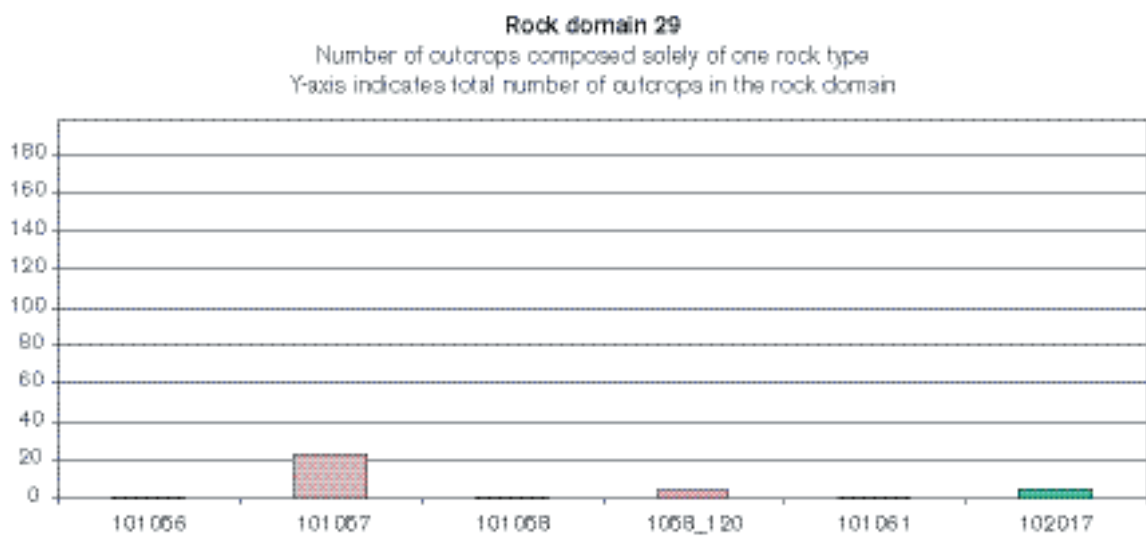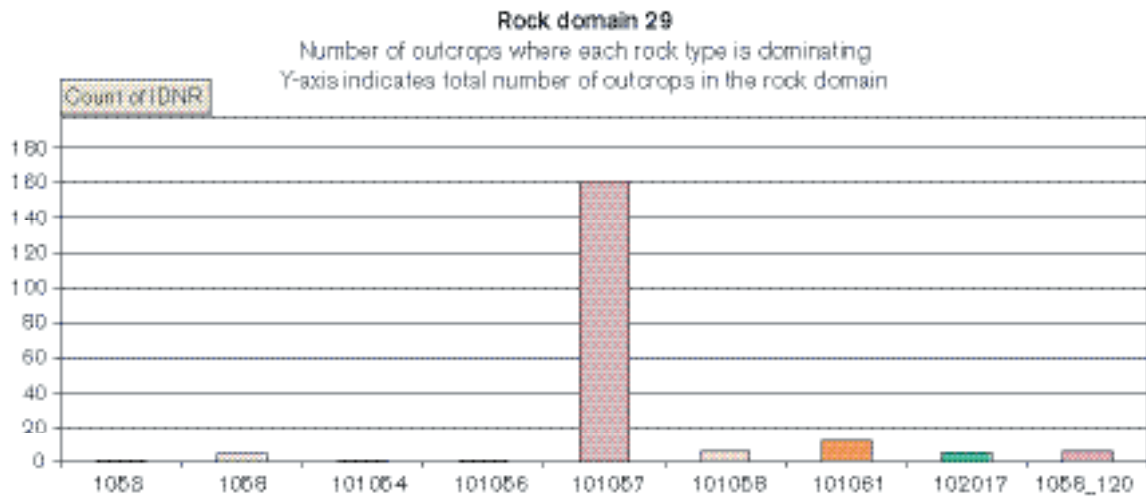
Figure 5-9. Qualitative assessment of dominant and subordinate rock types in rock domain RFM029 based on surface outcrop data. The translation of the rock codes to rock type is provided in Appendix 3.

Table 5-3. Properties assigned to each rock type.

Property
Rock code (according to the nomenclature recommended by SKB).
Rock name (classification according to IUGS/SGU).
QAPF values (%).
Grain size (classification according to SGU).
Age (million years).
Density (kg/m³).
Porosity (%).
Magnetic susceptibility (SI units).
Electrical resistivity in fresh water (ohm m)
Uranium content based on gamma-ray spectrometric measurements (ppm).
Uranium content based on geochemical measurements (ppm).
Natural exposure (microR/h).

Evaluation of uncertainty

The variation in the quality of the surface geological data over the regional model area (see Section 4.2.2) is an important source of uncertainty in the modelling procedure. This problem will reduce dramatically south of road 76 and in the coastal area northeast of the candidate area, when new data are available for version 1.2 of the site descriptive model. However, uncertainties under Öregrundsgrepen and in the areas between the islands close to the coast will remain throughout the site investigation programme.

In the land area, uncertainties concern the location of the boundaries between the rock units that have been defined on the basis of composition and grain size, and the rock units that have been defined on the basis of degree of inhomogeneity and degree of ductile deformation. High outcrop intensity and access to the new airborne, geophysical data (see Sections 4.2.2 and 4.2.3) are two factors that help to reduce the uncertainty in the drawing of these boundaries on, for example, the geological map. There also remains an uncertainty concerning the actual occurrence of a rock domain since, in some cases, data are completely absent, e.g. rock domain RFM033 under Öregrundsgrepen, or are limited in extent, e.g. rock domain RFM027.

Since the projection work has predominantly made use of structural data from surface outcrops, there remain considerable uncertainties concerning the extension of rock domains to a depth of –2,100 m. Compositional and structural data only exist at depth in one of the rock domains (RFM029), and only down to c 1,000 m. This problem will remain throughout the site investigation programme for most of the rock domains. Future reduction of this uncertainty may be obtained by modelling of airborne or ground geophysical data.

With the above considerations in mind, an expert judgement has been carried out to assess, at least qualitatively, the confidence in the occurrence and geometry of the thirty-four rock domains (Table 5-4). Confidence is generally expressed at three levels, "high", "medium" and "low". The confidence level referred to as "very low" has been used for the down-dip extension of the rock domains under Öregrundsgrepen.

Table 5-4. Table of confidence for the occurrence and geometry of rock domains.

Domain ID	Basis for interpretation	Confidence at the surface	Confidence to a depth of −2100 m
RFM001	Surface data (11 observed outcrops, airborne magnetic data), bedrock geological map, SDM version 1.1	High	Medium
RFM002	Bedrock geological map, SDM version 0	Medium	Low
RFM003	Bedrock geological map, SDM version 0	Medium	Low
RFM004	Bedrock geological map, SDM version 0	Medium	Low
RFM005	Surface data (21 observed outcrops, airborne magnetic data), bedrock geological map, SDM version 1.1	High	Medium
RFM006	Bedrock geological map, SDM version 0	Medium	Low
RFM007	Surface data (18 observed outcrops, airborne magnetic data), bedrock geological map, SDM version 1.1	High	Medium
RFM008	Surface data (14 observed outcrops, airborne magnetic data), bedrock geological map, SDM version 1.1	High	Medium
RFM009	Surface data (2 observed outcrops, airborne magnetic data), bedrock geological map, SDM version 1.1	High	Medium
RFM010	Surface data (6 observed outcrops, airborne magnetic data), bedrock geological map, SDM version 1.1	High	Medium
RFM011	Surface data (44 observed outcrops, airborne magnetic data), bedrock geological map, SDM version 1.1	High	Medium
RFM012	Surface data (8 observed outcrops, airborne magnetic data), bedrock geological map, SDM version 1.1	High	Medium
RFM013	Surface data (16 observed outcrops, airborne magnetic data), bedrock geological map, SDM version 1.1	High	Medium
RFM014	Surface data (11 observed outcrops, airborne magnetic data), bedrock geological map, SDM version 1.1	High	Medium
RFM015	Bedrock geological map, SDM version 0, shallow tunnel	Medium	Low
RFM016	Bedrock geological map, SDM version 0	Medium	Low
RFM017	Surface data (19 observed outcrops, airborne magnetic data), bedrock geological map, SDM version 1.1	High	Medium
RFM018	Surface data (74 observed outcrops, airborne magnetic data), bedrock geological map, SDM version 1.1	High	Medium
RFM019	Airborne magnetic data, bedrock geological map, SDM version 0	Low	Very low
RFM020	Bedrock geological map, SDM version 0, shallow tunnels	Medium	Low
RFM021	Surface data (13 observed outcrops, airborne magnetic data), bedrock geological maps, SDM versions 0 and 1.1, shallow tunnels	High	Medium
RFM022	Bedrock geological map, SDM version 0	Low	Very low
RFM023	Surface data (42 observed outcrops, airborne magnetic data), bedrock geological map, SDM version 1.1	High	Medium
RFM024	Bedrock geological map, SDM version 0	Medium	Low
RFM025	Surface data (38 observed outcrops, airborne magnetic data), bedrock geological map, SDM version 1.1	High	Medium
RFM026	Surface data (100 observed outcrops, airborne magnetic data), bedrock geological map, SDM version 1.1	High	Medium
RFM027	Bedrock geological map, SDM version 0, shallow tunnels	Medium	Low
RFM028	Surface data (15 observed outcrops, airborne magnetic data), bedrock geological map, SDM version 1.1	High	Medium
RFM029	Surface data (197 observed outcrops, airborne magnetic data), bedrock geological map, SDM version 1.1, cored borehole (down to 1001.49 m), eight percussion boreholes (down to 221.7 m)	High	High (down to 1000 m), medium (below 1000 m)

Domain ID	Basis for interpretation	Confidence at the surface	Confidence to a depth of −2100 m
RFM030	Surface data (214 observed outcrops, airborne magnetic data), bedrock geological map, SDM version 1.1	High	Medium
RFM031	Surface data (97 observed outcrops, airborne magnetic data), bedrock geological map, SDM version 1.1	High	Medium
RFM032	Surface data (55 observed outcrops, airborne magnetic data), bedrock geological map, SDM version 1.1, shallow tunnel	High	Medium
RFM033	Bedrock geological map, SDM version 0, shallow tunnels	Low (high at SFR)	Very low (medium at SFR)
RFM034	Surface data (12 observed outcrops, airborne magnetic data), bedrock geological map, SDM version 1.1, shallow tunnels	High	Medium

The information concerning the properties of the different rock domains (Table 5-2) once again emerges primarily from the surface outcrop data (see Section 4.2.2). Sub-surface data are only available in rock domain RFM029 (see Section 4.4). Although it has been possible to estimate from the surface data the relative importance of the different rock types in a specific domain, there remains, with the exception of rock domain RFM029, an uncertainty concerning the quantitative proportions of the different rock types. This feature is a basis for uncertainty in the characterisation of most of the rock domains, since there are difficulties to take account of the bedrock inhomogeneity in the domains.

Mean and standard deviation values of the properties of most rock types (Table 5-3), which were recognised during both the surface and borehole mapping activities, are available from the surface investigations (see Section 4.2.2). There remain uncertainties concerning the properties of the rock types referred to as "metamorphic sedimentary rock" (SKB code 106000), "metamorphic granitoid" (SKB code 111051) and "fine- to medium-grained granite" (SKB code 111058). No data are available for these rock types. On the basis of the model version 0 work /SKB, 2002a/, these rock types dominate in domain RFM027 (rock type 106000), domains RFM019 and RFM033 (rock type 111051) and domain RFM022 (rock type 111058).

5.1.3 Rock domain modelling – local scale

The three-dimensional models for the distribution of rock domains are identical on both regional and local scales. For this reason, no new information is included in this section.

5.1.4 Deterministic structural modelling – regional scale

Modelling assumptions and input from other models

The deterministic structural model on a regional scale has made use of:

- The regional structural model that was presented in version 0 of the site descriptive model /SKB, 2002a/.

- The structural models for SFR /Axelsson and Hansen, 1997; Holmén and Stigsson, 2001/.

- A variety of borehole and seismic reflection data that have been assembled in connection with the ongoing site investigation programme (see Sections 4.4 and 4.2.5, respectively).

- The identification of linked lineaments that has been completed during the ongoing site investigation programme (see Sections 4.2.3 and 4.2.5).

The regional structural model addresses the deformation zones that are inferred to be 1 km or longer in length, i.e. local major and regional deformation zones according to the terminology of /Andersson et al, 2000/.

All the regional deformation zones, which were recognised as highly probable to certain in the model version 0 /SKB, 2002a/, have been included in the structural model presented here. Information from tunnels and boreholes as well as ground geological and geophysical data have contributed, to variable extents, to the definition of these four zones (Table 5-5). The Eckarfjärden and Forsmark deformation zones locally display an anastomosing geometry at the surface. In these areas, minor splays from the main zone as well as the main zone itself envelop minor bedrock blocks with lens-like form. Four such splays are present along both zones. In each case, the main zone has been coded with the letter A and the splays with the letters B to E.

The positions of the model version 0 zones at the surface /SKB, 2002a/ have been redefined on the basis of the interpretation of the linked lineaments in the ongoing site investigation programme (see Section 4.2.3). These lineaments are based primarily on the airborne magnetic data. Since the interpretations of the new airborne geophysical and topographic data have provided a more precise siting of these zones on the surface and, thereby, their mean strike, there are some minor changes in these attributes relative to the SDM version 0. The dip of each zone in the structural model has been estimated (ZFMNW0001 and ZFMNW0002) or is assumed (ZFMNW0003 and ZFMNW0004) to be 90°. The adoption of this dip follows the site descriptive model version 0 /SKB, 2002a/.

Table 5-5. Summary of deformation zones which have been included in the deterministic structural model at the regional scale.

Zone ID, SDM version 1.1	Alternative name	Zone ID, SDM version 0	Basis for interpretation
Deformation zones modified from SDM version 0			
ZFMNW0001	Singö deformation zone	ZFM00001A0 (Singö fault zone)	Tunnels, boreholes, seismic refraction data, linked lineament based on airborne magnetic data.
ZFMNW0002		ZFM00002A0	Tunnel, linked lineament based on airborne magnetic data.
ZFMNW003A, B, C, D and E	Eckarfjärden deformation zone	ZFM00003A0	Ground geology, linked lineament based on airborne magnetic and electrical conductivity data in combination with topographic data.
ZFMNW004A, B, C, D and E	Forsmark deformation zone	ZFM00004A0	Ground geology and geophysics, linked lineament based on airborne magnetic and electrical conductivity data in combination with topographic data.
Deformation zones adopted from the structural models presented for SFR			
ZFMNE0869	Zone 3 (SFR)		Tunnels, boreholes, seismic refraction data.
ZFMNW0805	Zone 8 (SFR)		Boreholes, seismic refraction data, linked lineament based on airborne magnetic data.
ZFMNE0870	Zone 9 (SFR)		Tunnels, boreholes.
ZFMNE0871	Zone H2 (SFR)		Tunnels, boreholes.
Deformation zones based on borehole data, seismic reflection data and inferred linked lineaments, all acquired during the ongoing site investigation programme			
ZFMEW0865			Boreholes KFM01A, HFM01, HFM02.
ZFMNE0061			Borehole KFM01A, linked lineament based on airborne magnetic and electrical conductivity data in combination with topographic data.
ZFMNE0866			Boreholes HFM04, HFM05 and KFM02A.
ZFMNE0867			Boreholes HFM06, HFM08 and KFM03A, seismic reflection data (reflector A5).
ZFMNE0868			Borehole HFM07, seismic reflection data (reflector A6).
Possible deformation zones based solely on the interpretation of linked lineaments that was completed during the ongoing site investigation programme			
153 unspecified possible deformation zones in four orientation sets			

North of the Singö deformation zone (ZFMNW0001), in the vicinity of SFR, five deformation zones were included in the structural model (Figure 5-10) that was used in the SAFE project /Holmén and Stigsson, 2001/. Four of these zones were estimated to be longer than 1 km and, for this reason, have been included in the regional structural model presented here. All the zones from the area around SFR are based on data from shallow boreholes; tunnelling work and seismic refraction surveys have also provided important information (Table 5-5).

The zone identified here as ZFMNW0805 (Zone 8 in the older compilations at SFR) corresponds at the surface to a linked, low magnetic lineament that is at least 6 km in length. The strike of this zone is assumed to correspond to the trend of the linked lineament and the zone has been modelled with a dip of 90° following /Axelsson and Hansen, 1997/. Both zone ZFMNW0805 and zone ZFMNW0002 appear to be splays off the regionally more important Singö deformation zone (see Section 7.2.1).

The strike and dip of the shorter zones that strike in a northeasterly direction, ZFMNE0869 (Zone 3) and ZFMNE0870 (Zone 9), have been adopted directly from /Axelsson and Hansen, 1997/. It is assumed that these zones terminate southwards against the Singö deformation zone and northwards against zone ZFMNW0805, both of which strike in a northwesterly direction. The orientation of zone ZFMNE0871 (Zone H2) has been adopted directly from the SAFE model /Holmén and Stigsson, 2001/. This zone also strikes in a northeasterly direction. However, it differs from the other zones since it dips shallowly towards the southeast.

Five deformation zones have been modelled with the help of the seismic reflection data as well as the data from the cored borehole KFM01A and the eight percussion boreholes (see Sections 4.2.5 and 4.4, and Table 5-5). Four of these zones resemble zone ZFMNE0871 (Zone H2) at SFR, in that they are sub-horizontal (ZFMEW0865) or dip shallowly towards the southeast (ZFMNE0866, ZFMNE0867 and ZFMNE0868). The fifth zone strikes in a northeasterly direction but dips steeply towards the south-east (ZFMNE0061). It corresponds at the surface to a linked lineament that has been defined on the basis of airborne magnetic and electrical conductivity data in combination with topographic data.
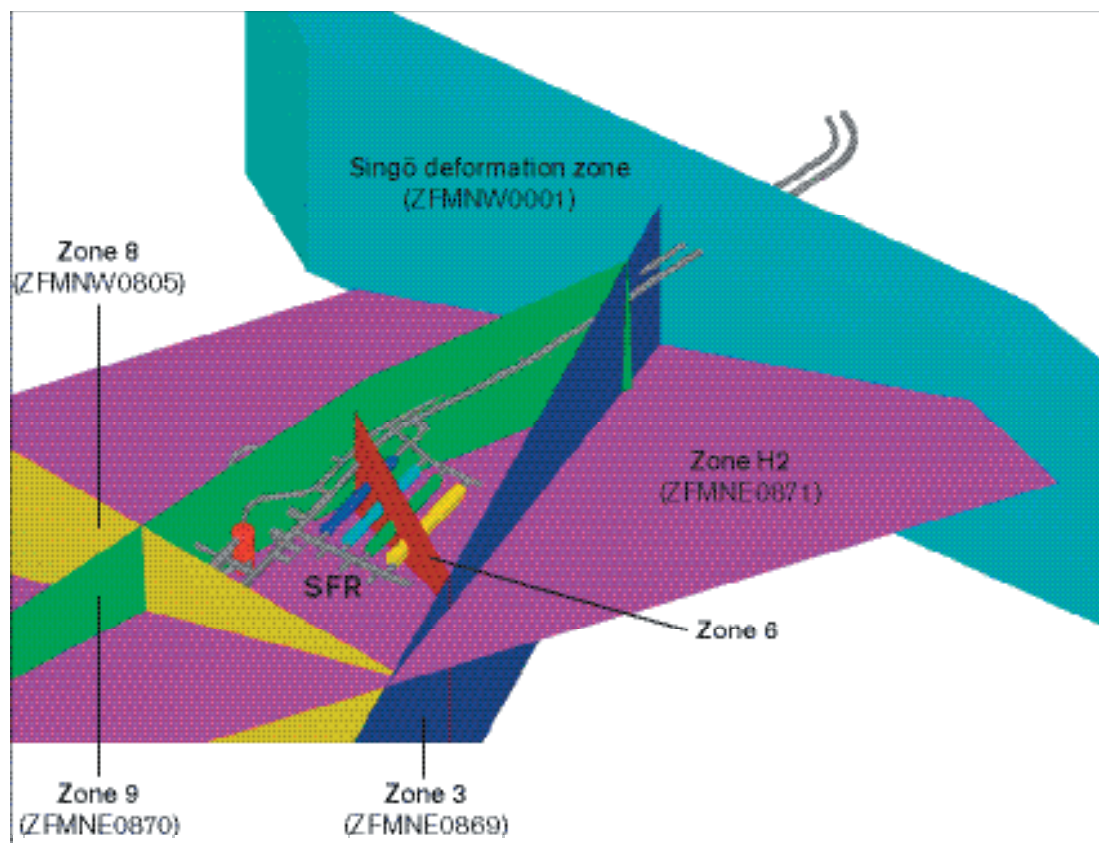
Figure 5-10. *Deformation zones within the structural model for the SFR area and the general layout of the tunnel system at SFR. Based on /Holmén and Stigsson, 2001/.*

There remains a clear possibility that one or more new deformation zones will be recognised in a later modelling phase, following completion of a single-hole interpretation of KFM01A. This work had not been carried out when the deadline for model version 1.1 had passed. This prediction essentially concerns the depth interval c 50–410 m in KFM01A.

The remaining 153 possible deformation zones included in the regional structural model correspond to the linked lineaments that are 1 km or more in length (see Section 4.2.3). Two of these zones (ZFMNW0017 and ZFMNW0025) locally display an anastomosing geometry at the surface with one or more blocks of bedrock with lens-like form, similar to that observed along ZFMNW0003 and ZFMNW0004. It is assumed that the strike of the possible deformation zones that have been inferred solely from linked lineaments corresponds to the trend of the corresponding lineament. All except zone ZFMNS0099 are assumed to dip at 90°. Since zone ZFMNS0099 failed to intersect borehole HFM01, it is assumed to dip steeply towards the east, away from drillsite 1.

A key question in the modelling procedure concerns the extension of the deformation zones at depth. Different assumptions have been adopted for the vertical or steep- dipping zones, on the one hand, and the sub-horizontal or gently dipping zones on the other.

It is assumed that the deformation zones that are vertical or steep-dipping, and can be recognised at the surface as a linked lineament, extend downwards for the same distance that they can be followed as a lineament at the surface. This assumption implies that the frequency of deformation zones decreases with depth. The assumption gains some merit when the results concerning the decreasing frequency of fractures at depth in KFM01A are borne in mind (see Section 4.4). Despite the restriction inherent in the assumption, a majority of the deformation zones in the structural model extend to the base of the regional model volume, since their surface length exceeds the depth of the model.

A base model for the sub-horizontal or shallow-dipping zones assumes that these zones extend only to the nearest inferred vertical or steep-dipping zone. For example, zone ZFMNE0871 (zone H2 at SFR) is assumed to be restricted to a relatively limited volume between the Singö deformation zone and the NW splay from the Singö zone (zone ZFMNW0805 or Zone 8 at SFR). In an alternative structural model, the sub-horizontal and shallow-dipping zones are extended to the boundaries of the regional model volume and form regionally far more extensive structures. The two models for the sub-horizontal or shallow-dipping zones provide two extreme concepts as a means to model these structures. The presentation of alternative models is justified, bearing in mind the historical debate that has taken place concerning alternative models for these structures (see summary in /SKB, 2002a/).

The base structural model and the alternative structural model for the sub-horizontal or shallow-dipping zones are presented in connection with the description of the site (Section 7.2.1).

Geometric modelling

An initial step in the modelling procedure made use of the evaluation of the seismic reflection data (see Section 4.2.5), and the results in /Cosma et al, 2003/, in order to place the various seismic reflectors in the regional model volume (Figure 5-11). The subsequent modelling work was executed by placing the following groups of deformation zones in the regional model volume, in the order indicated below:

- The regionally important deformation zones with northwesterly strike and vertical dips, and their associated splays, that have been included in older structural models.

- The local major fracture zones with northeasterly strike and vertical or steep southeasterly dips that have been included in the structural model for SFR or are supported by new borehole data.

- The possible deformation zones that have been inferred solely from the interpretation of linked lineaments.

- The fracture zones that are sub-horizontal or gently-dipping to the southeast and have been included in the structural model for SFR or are supported by new borehole data.

The modelling procedure has made use of the key assumptions concerning the dip and both the along-strike and down-dip extensions of a single deformation zone, that were outlined in the previous section. Both a base model and an alternative model for the extent of the sub-horizontal
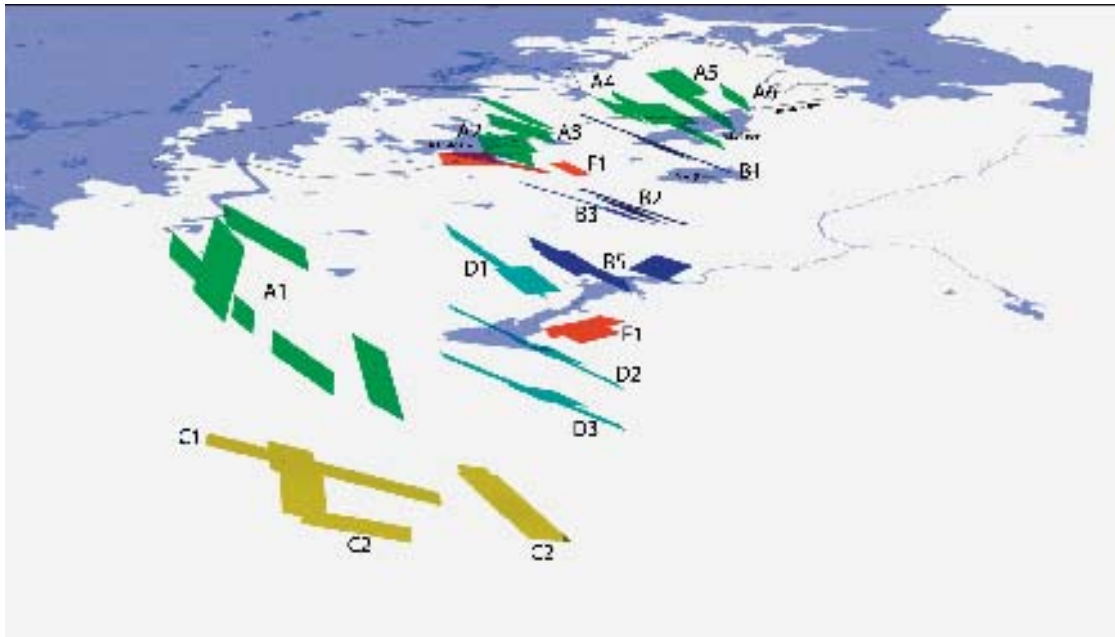
Figure 5-11. *Location of the seismic reflectors A–F in the regional model volume, following the recommendations in /Cosma et al, 2003/. The highly uncertain reflectors (G–I) and the reflectors with unknown, true strike and dip are not included. Note the dominant NE to ENE strike and moderate to gentle, southeasterly dips of the reflectors.*

and shallow-dipping zones are presented. The arguments for and the steering assumptions in these two models were presented in the previous section.

Deformation zones included in SFR and SDM version 0 models – NW strike and vertical dip

The regionally important deformation zones with northwesterly strike and vertical dips, and their associated splays with similar orientation, were recognised already during the SFR and SDM version 0 modelling episodes. They include zones ZFMNW0001, ZFMNW0002, ZFMNW003A–E, ZFMNW004A–E and ZFMNW0805 (equivalent to Zone 8 at SFR). They are complex structures, with both a ductile and brittle deformational history, that form boundary deformation zones both to the northeast and to the southwest of the candidate area. The strike of these zones has been estimated from the mean trend of the linked lineament to which the zone is coupled. Dips have been set at 90°. Bearing in mind the assumptions discussed earlier, these zones have been extended to the base of the regional model volume.

Fracture zones included in SFR models or supported by new borehole data – NE strike and vertical or steep dip to the southeast

Fracture zones ZFMNE0869 and ZFMNE0870 are situated northwest and southeast of SFR and are equivalent to Zones 3 and 9, respectively, at SFR. The strike and dip values used in the modelling procedure have been adopted from /Axelsson and Hansen, 1997/. The zones have been extended laterally as far as the Singö deformation zone in the south and zone ZFMNW0805 in the north. Thus, a concept in which the shorter zones with northeasterly strike are sandwiched between the regionally more important and more complex northwesterly zones has been adopted in the model.

The marked increase in both the frequency of sealed fractures and the degree of bedrock alteration in the depth interval c 640–680 m, in borehole KFM01A, suggest that a fracture zone intersects the borehole within this interval (ZFMNE0061). Furthermore, a narrow crush zone was mapped in the uppermost part of this depth interval and a radar image anomaly at c 650–674 m (Table 5-6). The orientation of the fractures at this borehole depth suggests that this structure strikes in a northeast direction and dips steeply towards the southeast. The results from the borehole radar investigations confirm the steeply dipping character of the zone.
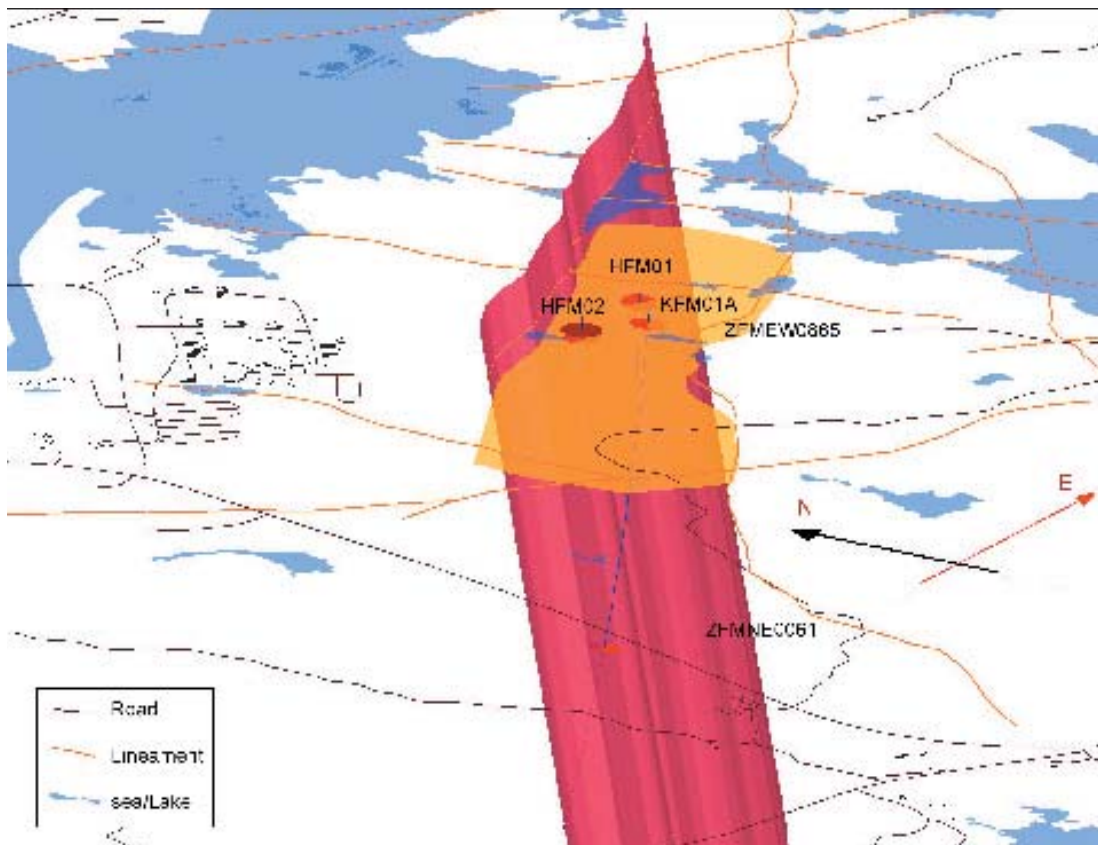
Figure 5-12. *Development of zones ZFMNE0061 and ZFMEW0865 at drillsite 1 based on the interpretation of borehole data at drillsite 1 and linked lineaments.*

In the modelling procedure, the fracture zone at this depth interval has been coupled to a linked lineament that lies northwest of drillsite 1 (Figure 5-12). This lineament has been identified on the basis of airborne magnetic and electrical conductivity data in combination with topographic data. It also displays a low, weighted uncertainty value (1.4). The strike of the fracture zone has been estimated from the trend of the lineament. By modelling a connection between the linked lineament and a fracture zone sited at c 665 m, the dip has been estimated to 81°SE.

The three zones described in this section belong to a group of fracture zones in the Forsmark area that are vertical or steeply dipping and are strongly discordant to the older northwesterly structural trend.

Possible deformation zones inferred solely from the interpretation of lineaments

153 possible deformation zones have been inferred solely from the interpretation of linked lineaments that are longer than 1 km. Only four of these zones are longer than 10 km. All the linked lineaments have been grouped into different orientation sets (Section 5.1.6). Lineaments with NW, NE and NS trends dominate; a fourth EW set has also been proposed. The strike of the possible deformation zones inferred from linked lineaments has been defined by the trend of the lineament at the surface. The projection of the zones at depth is based on the assumptions discussed earlier.

Fracture zones included in SFR models or supported by new borehole data – sub-horizontal or gently dipping to the south-east

The final stage in the modelling procedure has involved the inclusion of the fracture zones that are sub-horizontal (ZFMEW0865 at drillsite 1) or dip gently to the southeast (ZFMNE0871 that is equivalent to Zone H2 at SFR, ZFMNE0866 at drillsite 2, and ZFMNE0867 and ZFMNE0868 at drillsite 3). Only the details of the procedure used during the establishment of the base structural model are discussed below. An alternative structural model is presented for all the fracture zones

included in this section. This model allows each zone to continue both along the strike and in the dip direction to the margins of the regional model volume. The alternative model places a far stronger regional significance on these fracture zones relative to that envisaged in the base structural model.

The strike and dip of zone ZFMNE0871 has been adopted from the SAFE model for SFR /Holmén and Stigsson, 2001/. In the base model presented here, this zone has been terminated along the Singö deformation zone to the south and zone ZFMNW0805 to the north.

At drillsite 1, the same fracture zone (ZFMEW0865) is inferred to be present at more or less the same depth (c 40 m) in boreholes KFM01A, HFM01 and HFM02 (Table 5-6). The zone is indicated by the occurrence of crushed rocks and flat-lying, radar image anomalies in all boreholes, and an increase in fracture frequency in HFM01 and HFM02. On the basis of the three intersections, the strike and dip of this sub-horizontal zone have been calculated to be 266/01°. In the base structural model, zone ZFMEW0865 has been continued, in both the strike and dip directions, as far as the nearest vertical or steeply dipping deformation zones.

At drillsite 2, the same fracture zone (ZFMNE0866) is inferred to be present in HFM04 (c 62 m), HFM05 (c 154 m) and in the percussion-drilled part of KFM02A (c 80 m). Some increase in fracture frequency in HFM04 and HFM05, the presence of a crush zone in HFM05, and the occurrence of radar image anomalies in all the boreholes indicate the presence of a fracture zone (Table 5-6). With the help of the intersection points in the three boreholes, a strike and dip of 058/36° have been estimated.

Table 5-6. Basis for the interpretation of fracture zones from borehole data assembled during the site investigation programme. The feature used for the interpretation of the zone has been documented in all the relevant boreholes, if not otherwise stated.

Zone ID and borehole(s)	Basis for interpretation	Basis for calculation of strike and dip	Strike and dip
ZFMNE0061 (KFM01A)	• Increase of fracture frequency. • Crush zone. • Steep-dipping, radar image anomaly. • Bedrock alteration.	Correlation with linked lineament at surface. Strike estimated from trend of linked lineament. Dip estimated from modelling.	068/81°
ZFMEW0865 (KFM01A, HFM01 and HFM02)	• Increase of fracture frequency in HFM01 and HFM02. • Crush zones. • Flat-lying, radar image anomaly.	Zone inferred to intersect three different boreholes.	Sub-horizontal (266/01°)
ZFMNE0866 (HFM04, HFM05 and KFM02A)	• Some increase of fracture frequency in HFM04 and HFM05. • Crush zone in HFM05. • Radar image anomaly.	Zone inferred to intersect three different boreholes.	058/36°
ZFMNE0867 (HFM06, HFM08 and KFM03A)	• Increase of fracture frequency in HFM06 and HFM08. • Crush zones in HFM06. • Radar image anomaly in HFM06 and HFM08. • Correlation with seismic reflector A5.	Zone inferred to intersect three different boreholes.	055/20°
ZFMNE0868 (HFM07)	• Increase of fracture frequency. • Bedrock alteration. • Radar image anomalies. • Correlation with seismic reflector A6.	Orientation of seismic reflector A6.	077/30°

The surface projection of zone ZFMNE0866 corresponds approximately to a linked lineament that is < 1 km in length and lies northwest of drillsite 2. In the base structural model, zone ZFMNE0866 has been extended along its strike and dip to the nearest, vertically dipping deformation zones. On the basis of this modelling procedure, the zone is < 1 km in length and strictly a local minor zone. However, the zone has been included in the modelling procedure, bearing in mind the uncertainty in the assumptions used for the extension of these deformation zones.

At drillsite 3, the same fracture zone (ZFMNE0867) is inferred to be present in HFM06 (c 70 m), HFM08 (c 137 m) and in the percussion-drilled part of KFM03A (c 66 m). An increase in fracture frequency in HFM06 and HFM08, the presence of crushed rocks in HFM06, and the occurrence of radar image anomalies in the two percussion boreholes indicate the presence of a fracture zone (Table 5-6). Once again, the three intersection points have been used to calculate the orientation of the zone (055/20°). This zone can confidently be considered to correspond with the seismic reflector A5. It was estimated that reflector A5 should intersect borehole KFM03A at c 60 m depth /Juhlin et al, 2002/.

A marked increase in fracture frequency, a strong alteration of the bedrock, with the growth of hematite and chlorite, and several radar image anomalies all occur in the depth interval 55–67 m in borehole HFM07 (Table 5-6). During the modelling procedure, it was noted that seismic reflector A6 intersects HFM07 within this depth interval. On the basis of these observations, a fracture zone (ZFMNE0868) is inferred to be present within this depth interval and has been included in the modelling procedure. The strike and dip of seismic reflector A6 (077/31° following /Cosma et al, 2003/) have been used to estimate the orientation of this fracture zone.

In the base structural model, both fracture zones at drillsite 3 have been extended along-strike and down-dip to the nearest vertically dipping deformation zones.

Property assignments

Key properties, and numerical estimates for the uncertainty in some of these parameters, have been assigned to each of the thirteen deformation zones based on a variety of geological and geophysical information (Table 5-7). The properties of the deformation zones are presented in tabular format in the description of the site (Section 7.2.1).

The properties of the four deformation zones that were classified as highly probable to certain in the SDM version 0 have been extracted primarily from /SKB, 2002a/. The strike and length of all four deformation zones as well as several properties along the Eckarfjärden zone are based on the inter-pretation of linked lineaments (see Section 4.2.3) and an examination of outcrop data (see Section 4.2.4), respectively. Since an estimate of the total length of these deformation zones was completed during the model version 0 work /SKB, 2002a/, the total length of these regionally important zones, and their associated splays, is also provided here.

The properties of the four deformation zones that were recognised earlier in the structural models at SFR have been extracted primarily from the data tabulated in /Axelsson and Hansen, 1997/. One exception concerns the strike and minimum length of zone ZFMNW0805 (equivalent to Zone 8 at SFR), that has been estimated with the help of the interpretation of linked lineaments (see Section 4.2.3). A minimum length is provided since this zone extends along strike to the northwestern margin of the regional model area. Its continuation to the northwest has not been defined. Secondly, the orientation of zone ZFMNE0871 (equivalent to Zone H2 at SFR) has been adopted from the SAFE model for SFR /Holmén and Stigsson, 2001/. The length of this zone refers to the estimate in the base structural model.

The properties of the five fracture zones that have been identified primarily from the ongoing drilling programme have been assembled from the data that has emerged from the examination of the respec-tive boreholes (see Section 4.4). One exception includes the orientation and length of the steeply dipping zone that passes through KFM01A (ZFMNE0061). These features have been determined by using both the interpretation of linked lineaments and the borehole data (see Sections 4.2.3 and 4.4). Secondly, the orientation of zone ZFMNE0868 has been adopted from the orientation of seismic reflector A6 /Cosma et al, 2003/. The length of the four zones that are sub-horizontal or gently dipping to the southeast refers to the estimate in the base structural model.

Table 5-7. Properties assigned to the thirteen deformation zones along which there are, to variable extents, confirmatory geological and geophysical data.

Property	Comment
Deformation zone ID	ZFM******, in two places with additional letter A, B, C, D and E (according to the nomenclature recommended by SKB).
Position	With numerical estimate of uncertainty.
Strike and dip	With numerical estimate of uncertainty.
Width	With numerical estimate of uncertainty.
Length	With numerical estimate of uncertainty.
Ductile deformation	Indicated if present along the zone.
Brittle deformation	Indicated if present along the zone.
Alteration	Indicated if present along the zone.
Fracture orientation	In places, with numerical estimate of uncertainty.
Fracture frequency	With numerical estimate of uncertainty.
Fracture filling.	Mineral composition.

There are few data available at the present time that concern the properties (including numerical estimates of uncertainty) of the possible deformation zones, that are based solely on the interpretation of linked lineaments (Table 5-8). The data that are available are presented for each orientation set – NW, NE, NS and EW – in the description of the site (Section 7.2.1). Both the NW and NS orientation sets are divided into two subsets that include the regional and local major deformation zones, respectively.

An estimate of the mean value of the strike and dip of the possible deformation zones for each of these sets (or subsets) is provided on the basis of the statistical analysis of fractures and lineaments in the DFN model (see Section 5.1.6). The estimate of width is based solely on a comparison with the thirteen deformation zones where more data are available. In essence, this estimate is an assumption. The indication of ductile deformation along the orientation set with NW strike and the absence of such deformation along the remaining orientation sets is based on the general experience from the field investigations at the surface.

Table 5-8. Properties assigned to the 153 possible deformation zones that are based solely on the interpretation of linked lineaments.

Property	Comment
Orientation set	Each zone within the set is identified with a ZFM****** code, in two places with additional letters A and B or A, B and C (according to the nomenclature recommended by SKB).
Position	With numerical estimate of uncertainty.
Strike and dip	With numerical estimate of uncertainty. Statistical analysis.
Width	With numerical estimate of uncertainty. Assumption – no data available.
Length subset	Regional (> 10 km) or local major (1–10 km).
Ductile deformation	Indicated if present along the zone.
Brittle deformation	Indicated if present along the zone.

Evaluation of uncertainty

An expert judgement concerning the level of confidence for the occurrence of the various deformation zones is provided in Table 5-9. 13 deformation zones are allocated a high confidence of occurrence. Two of these zones (ZFMNW003 and ZFMNW004) each consist of one longer and four shorter segments. The different segments have been distinguished using letters (A–E). 71 deformation zones are allocated a medium confidence of occurrence. ZFMNW017 consists of a longer segment with two shorter segments and ZFMNW025 consists of one longer and one shorter segment. Once again, the different segments have been distinguished using letters (A–C and A–B, respectively). 76 deformation zones are allocated a low confidence of occurrence and 6 deformation zones are allocated a very low confidence of occurrence. In summary, there are 166 deformation zones that consist of 177 zone segments.

All the thirteen zones that are based, at least in part, on confirmatory geological and geophysical data are included in the deformation zones with a high confidence of occurrence. Since there is considerable uncertainty concerning the interpretation of the geological significance of the linked lineaments, the 153 deformation zones that are based solely on the interpretation of these lineaments are judged to have a lower degree of confidence. Strictly, they form a group of possible deformation zones. For the reasons outlined in the evaluation of the primary data (see Section 4.2.3), both the character and the clarity of the linked lineaments are used to assess the confidence level of the respective, possible deformation zones that have been identified from these lineaments.

The linked lineaments that are based solely or strongly on the airborne magnetic data (low magnetic anomaly ≥ 70% along the total length of the lineament) and that show a weighted uncertainty index that is < 2, are judged with medium confidence to represent deformation zones. In summary, these zones are based on the more distinctive, low-magnetic lineaments. By contrast, the linked lineaments that are based solely or strongly on the airborne magnetic data but show a weighted uncertainty index ≥ 2 or are based, to a less extent, on the airborne magnetic data (< 70% along the total length of the lineament), are judged with low confidence to represent deformation zones. Six of the 153 deformation zones are based solely on either topographic or electrical conductivity data. The confidence level for the occurrence of deformation zones along these linked lineaments is judged to be very low.

Table 5-9. Table of confidence for the occurrence of deformation zones.

Zone ID		Basis for interpretation	Confidence
ZFMNW0001 (Singö deformation zone)		Airborne geophysics (magnetic 100% along the length, low uncertainty), seismic refraction data, tunnels, boreholes	High
ZFMNW0002 (splay from Singö deformation zone through tunnel 3)		Airborne geophysics (magnetic 100% along the length, low uncertainty), tunnel	High
ZFMNW003A, B, C, D, E (Eckarfjärden deformation zone)		Airborne geophysics (magnetic 100% along the length, electrical data, low uncertainty), topography, ground geology	High
ZFMNW004A, B, C, D, E (Forsmark deformation zone)		Airborne geophysics (magnetic 100% along the length, electrical data, low uncertainty), topography, ground geology, ground geophysics	High
ZFMNE0869 (Zone 3, SFR)		Seismic refraction data, tunnels, boreholes	High
ZFMNW0805 (Zone 8, SFR)		Airborne geophysics (magnetic 100% along the length, low to medium uncertainty), seismic refraction data, boreholes	High
ZFMNE0870 (Zone 9, SFR)		Tunnels, boreholes	High
ZFMNE0871 (Zone H2, SFR)		Tunnels, boreholes	High
ZFMEW0865 (40 m level in KFM01A)		Three boreholes	High
ZFMNE0061 (656–674 m level in KFM01A)		Airborne geophysics (magnetic 100% along the length, electrical data, low uncertainty), topography, borehole	High
ZFMNE0866 (62 m level in HFM04)		Three boreholes, seismic reflection data	High
ZFMNE0867 (70 m level in HFM06)		Three boreholes, seismic reflection data	High
ZFMNE0868 (55–67 m level in HFM07)		Borehole, seismic reflection data	High
NE set of possible deformation zones		Airborne geophysics (magnetic ≥ 70% along the length ± electrical, *low to medium* uncertainty) ± topography	Medium
ZFMNE0060	ZFMNE0071		
ZFMNE0062	ZFMNE0072		
ZFMNE0063	ZFMNE0075		
ZFMNE0064	ZFMNE0076		
ZFMNE0065	ZFMNE0081		
ZFMNE0066	ZFMNE0082		
ZFMNE0067	ZFMNE0084		
ZFMNE0068	ZFMNE0086		
ZFMNE0070	ZFMNE0087		
	ZFMNE0850		

Zone ID		Basis for interpretation	Confidence
NE set of possible deformation zones		Airborne geophysics (magnetic < 70% along the length ± electrical) ± topography	Low
ZFMNE0069	ZFMNE0120	or	
ZFMNE0073	ZFMNE0128	Airborne geophysics (magnetic ≥ 70% along the length ± electrical, *medium to high* uncertainty) ± topography	
ZFMNE0074	ZFMNE0135		
ZFMNE0077	ZFMNE0138		
ZFMNE0078	ZFMNE0807		
ZFMNE0079	ZFMNE0808		
ZFMNE0080	ZFMNE0817		
ZFMNE0083	ZFMNE0825		
ZFMNE0088	ZFMNE0827		
ZFMNE0097	ZFMNE0829		
ZFMNE0103	ZFMNE0846		
NE set of possible deformation zones		Topography	Very low
ZFMNE0091			
NW set of possible deformation zones		Airborne geophysics (magnetic ≥ 70% along the length ± electrical, *low to medium* uncertainty) ± topography	Medium
ZFMNW0016	ZFMNW0044		
ZFMNW017A	ZFMNW0050		
ZFMNW017B	ZFMNW0806		
ZFMNW017C	ZFMNW0809		
ZFMNW0018	ZFMNW0813		
ZFMNW0019	ZFMNW0832		
ZFMNW0020	ZFMNW0835		
ZFMNW0022	ZFMNW0836		
ZFMNW025A	ZFMNW0837		
ZFMNW025B	ZFMNW0851		
ZFMNW0027	ZFMNW0852		
ZFMNW0032	ZFMNW0853		
ZFMNW0034	ZFMNW0854		
ZFMNW0040	ZFMNW0856		
NW set of possible deformation zones		Airborne geophysics (magnetic < 70% along the length ± electrical) ± topography	Low
ZFMNW0021	ZFMNW0046	or	
ZFMNW0024	ZFMNW0047	Airborne geophysics (magnetic ≥ 70% along the length ± electrical, *medium to high* uncertainty) ± topography	
ZFMNW0026	ZFMNW0051		
ZFMNW0028	ZFMNW0056		
ZFMNW0029	ZFMNW0085		
ZFMNW0031	ZFMNW0118		
ZFMNW0033	ZFMNW0136		
ZFMNW0035	ZFMNW0139		
ZFMNW0036	ZFMNW0140		
ZFMNW0042	ZFMNW0289		
ZFMNW0045			
NW set of possible deformation zones		Topography	Very low
ZFMNE0041			
NW set of possible deformation zones		Airborne geophysics (electrical data)	Very low
ZFMNE0048			

Zone ID		Basis for interpretation	Confidence
NS set of possible deformation zones		Airborne geophysics (magnetic ≥ 70% along the length ± electrical, *low to medium* uncertainty) ± topography	Medium
ZFMNS0005	ZFMNS0126		
ZFMNS0089	ZFMNS0823		
ZFMNS0093	ZFMNS0828		
ZFMNS0101	ZFMNS0857		
ZFMNS0107	ZFMNS0858		
ZFMNS0108	ZFMNS0859		
ZFMNS0115	ZFMNS0860		
ZFMNS0117	ZFMNS0861		
NS set of possible deformation zones		Airborne geophysics (magnetic < 70% along the length ± electrical) ± topography	Low
ZFMNS0043	ZFMNS0111	or	
ZFMNS0090	ZFMNS0112	Airborne geophysics (magnetic ≥ 70% along the length ± electrical, *medium to high* uncertainty) ± topography	
ZFMNS0092	ZFMNS0113		
ZFMNS0095	ZFMNS0114		
ZFMNS0096	ZFMNS0116		
ZFMNS0098	ZFMNS0119		
ZFMNS0100	ZFMNS0124		
ZFMNS0102	ZFMNS0125		
ZFMNS0104	ZFMNS0127		
ZFMNS0105	ZFMNS0843		
ZFMNS0106	ZFMNS0848		
ZFMNS0109			
NS set of possible deformation zones		Topography	Very low
ZFMNS0030	ZFMNS0099		
ZFMNS0094			
EW set of possible deformation zones		Airborne geophysics (magnetic ≥ 70% along the length ± electrical, *low to medium* uncertainty) ± topography	Medium
ZFMEW0023	ZFMEW0059		
ZFMEW0049	ZFMEW0137		
ZFMEW0052	ZFMEW0815		
ZFMEW0054	ZFMEW0816		
ZFMEW0055	ZFMEW0862		
ZFMEW0058			
EW set of possible deformation zones		Airborne geophysics (magnetic < 70% along the length ± electrical) ± topography	Low
ZFMEW0037	ZFMEW0110	or	
ZFMEW0038	ZFMEW0121	Airborne geophysics (magnetic ≥ 70% along the length ± electrical, *medium to high* uncertainty) ± topography	
ZFMEW0039	ZFMEW0122		
ZFMEW0053	ZFMEW0123		
ZFMEW0057	ZFMEW0838		

The most important uncertainties in the properties of virtually all the deformation zones concern their dip, their along-strike continuity and their down-dip extension. In the present model, the dip of most of the deformation zones is assumed to be 90°. Since there is little control on the dip of most of the zones, presentation of a variety of alternative models for their geometry has not been considered to be a viable solution at this stage. A base model and an alternative model have only been presented for the along-strike continuity and down-dip extension of the established, sub-horizontal and shallow-dipping deformation zones, in order to illustrate, in a conceptual manner, the uncertainty in these properties.

Quantitative estimates of the uncertainty in the position, orientation, width and length of the thirteen deformation zones with high confidence of occurrence are provided in the tabulation of the properties of these zones in the site description (Section 7.2.1). Similar estimates of the uncertainty in the

orientation and frequency of fractures along these zones have been given for some of the zones. A quantitative estimate of the uncertainty in the position of the possible deformation zones, which are based solely on the interpretation of linked lineaments, is also available in the various property tables (Section 7.2.1).

Finally, there remains a conceptual uncertainty concerning the interpretation of the geological significance of the seismic reflectors. It is possible that the reflectors represent deformation zones, compositional changes in the bedrock, that do not have any relationship to deformation zones, or a combination of these features. The results at drillsite 3 indicate that reflectors A5 and A6, at least, do represent fracture zones. However, no simple, unconstrained correlation between seismic reflector and fracture zone has been carried out in model version 1.1. It is anticipated that this question will be resolved when especially KFM03A is mapped, and the results of the mapping are carefully correlated with the results of the reflection seismic work.

5.1.5   Deterministic structural modelling – local scale

The deterministic structural models on both local and regional scales are identical. No new information is included in this section.

5.1.6   Stochastic DFN modelling – local scale

Discrete Fracture Network (DFN) model

Fractures play an important role in understanding the rock mechanics as well as the flow and transport properties in the rock mass. The possibilities of deterministically modelling the geometry and properties of a large number of individual fractures are extremely limited. Hence, a statistical treatment is used to describe the fracture systems in the rock mass. The fracture statistics in this section are aimed at providing input for DFN (discrete fracture network) models.

In order to create a fracture network model, the following minimum amount of information is required:

- orientation of the fractures,

- size distribution in three-dimensions of the fractures,

- fracture termination,

- fracture intensity, and

- spatial distribution of the fractures.

A number of assumptions are made in order to evaluate the three-dimensional geometric properties of the fracture network.

It is attractive if fractures with the same orientation can be sorted into fracture sets. Orientation does not need to be the only property defining sets; size, termination, fillings and other properties can identify sets as well. On the basis of borehole logs and fracture trace maps (outcrop fracture maps or lineament maps), the distribution of orientations of fractures or larger features are assigned.

It is assumed that fractures are planar objects of any shapes. The size of a fracture refers to the equivalent radius of a circle with the same area as the fracture. Fracture mappings on outcrops are used together with lineament maps to determine the distribution of fracture radii that gives the best match to the observed trace length data. The analysis takes into account censoring, truncation and sampling bias of fracture traces. As a result of the analysis, the fracture radius distributions are given in the form of probability density functions of the following types: Exponential, Lognormal, Normal of Log, Uniform, Power Law or can be given a constant value.

The geometry of fracture trace maps can present different aspects that are not necessarily dependent on the fracture size or orientation. This aspect mainly depends on the spatial distribution of fracture traces within a given surface. Fractures can be heavily clustered or regularly dispersed over the surface. A spatial analysis of a trace map permits to characterise the clustering of fractures.

Fracture intensity in a three dimensional volume is most conveniently described by the fracture area per unit volume, in this report denoted P_{32}. This parameter can be assessed by simulation of synthetic fractures, which are sampled from outcrops and boreholes similar to the source of real fracture data.

The analysis behind the derivation of the parameters in the DFN-model is described in the following subsections.

Forsmark DFN model volume

No previous DFN model has been presented for the Forsmark site. The model version 0 /SKB, 2002a/, only contains a model for surface geology and for deformation zones.

A new DFN model has been developed for the rock mass in the local model domain at Forsmark. The DFN analysis involves using fracture statistics presented in Sections 4.2.4 and 4.4.3 and the results of the three-dimensional rock domain modelling described in Section 5.1.2.

The DFN model is limited to stochastic fractures with a maximum size of 1 km (circular radius of 500 m). This is the lower bound for the deterministic deformation zone model presented in Section 5.1.4. The DFN model described in this section is based on geometrical and geological data only.

Data sources for the DFN analysis

Data from three different sources have been used to assess the statistics for the DFN model:

- The portion of the lineament map that is located on land, cf Figure 5-13.
- Detailed fracture maps from drillsite 2 and drillsite 3.
- KFM01A borehole data.

Qualitative supportive information has also been drawn from selected fracture mappings from the bedrock mapping program.
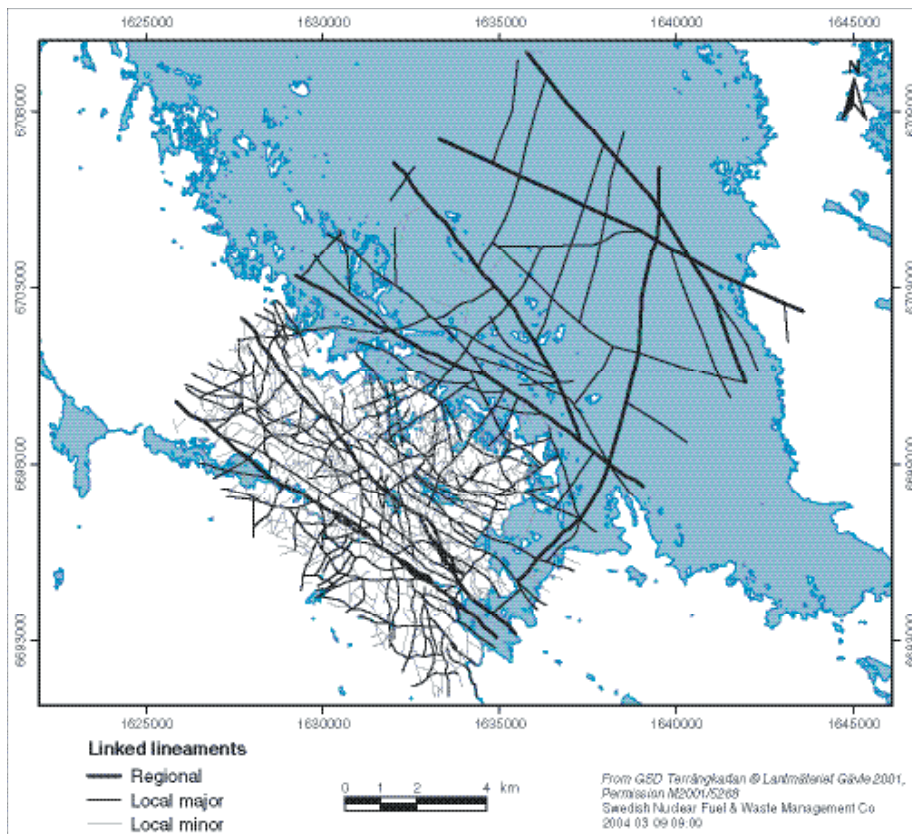
Figure 5-13. *The lineaments on land.*

The interpretation of lineaments is based on remote sensing technique, as described in Section 4.2.3, and involves indications from topography, magnetics, EM and VLF signals. However, these signals show a signature of sometimes very complex deformation history. A deformation zone typically consists of a series of individual rupture events that initiate from the tips of previous ruptures. Often these series of ruptures maintain approximately the same strike, although individual segment lengths may vary depending upon the amount of energy available for fracture propagation. The geological deformation history during the growth of the deformation history may be very different and thus showing a mixture of geophysical signals along different parts of the zone. The lineament map presented in Section 4.2.1 is an effort to combine these different signals into a map of geophysical or topographic anomalies.

In this study, it is assumed that the interpreted lineaments represent the intersection of deformation zones with the ground surface. It is also assumed that each straight segment of a lineament is representative to individual rupture lengths of a much larger deformation zone, and that they can be analysed as individual, but related traces that define the surface extent of deformation zones.

The other source of surface fracture data comes from detailed outcrop maps at drillsites 2 and 3, as described in Section 4.2.4. The fracture traces on these maps are divided into open and sealed fractures, according to the notation in the mapping database. This division is based on the observation of the mapping geologist and contains no information about aperture.

The analysed borehole data comes from the core-drilled borehole KFM01A, section 100 m to approximately 1,000 m length. Fracture data in the borehole have been divided into open and sealed fractures based on aperture, as described in Section 4.4.3.

Fracture orientation sets

The three data sets (lineament, outcrop traces and borehole intersections) provide information at three different resolutions; lineaments span from hundreds to thousands of metres, the traces from 0.5 m to tens of metres and borehole intercepts show details with a resolution of centimetres.

Considerations in the orientation analysis are as follows:

- Lineaments contain trace length and strike information, but no dip.

- Outcrop traces contain precise information about trace length, strike and dip as well as information about fracture type (open, sealed).

- Borehole data contain strike and dip as well as a classification of fracture type based on aperture (open, sealed).

- Surface data (lineaments and outcrops) are sampled on sub-horizontal planes.

- Borehole data are sampled along a nearly vertical scan-line.

Lineament orientations

The orientation of lineaments is presented in a rose diagram in Figure 5-14. Four dominant orientation sets can be seen in the lineaments; sets trending NS, NE, NW and EW. Each set can be defined by specifying a strike sector, which encloses lineaments that appear to belong to one orientation set. Table 5-10 presents strike sectors for each of the four orientation sets, based on visual observations of the rose diagram and of the lineament map. The EW lineament set is minute plotted together with the other lineament sets and does not show up until the lineament traces are separated in trace maps for each set.

Figure 5-15 and Figure 5-16 illustrate the lineament orientation sets based on these sector definitions.
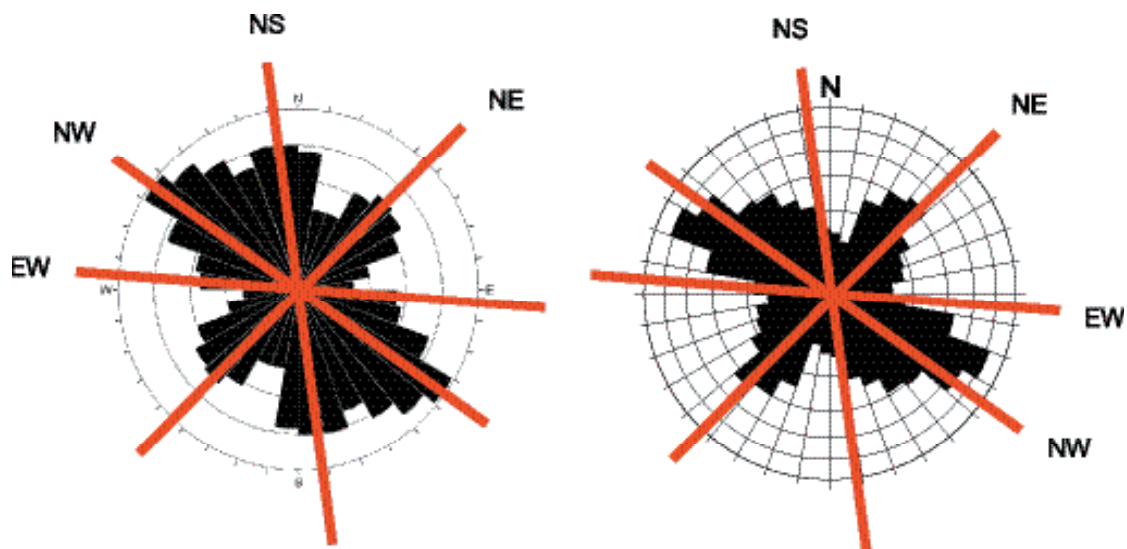
Figure 5-14. *Rose diagram of lineaments on land (left) and drillsites 2 and 3 (right).*

Table 5-10. Definition of lineament trend sectors based on the rose diagram in Figure 5-14 (left).

Set	Sector 1	Sector 2 (sector 1 + 180°)
NS	335° – 20°	155° – 200°
NE	20° – 80°	200° – 260°
NW	110° – 155°	290° – 335°
EW	80° – 110°	260° – 290°
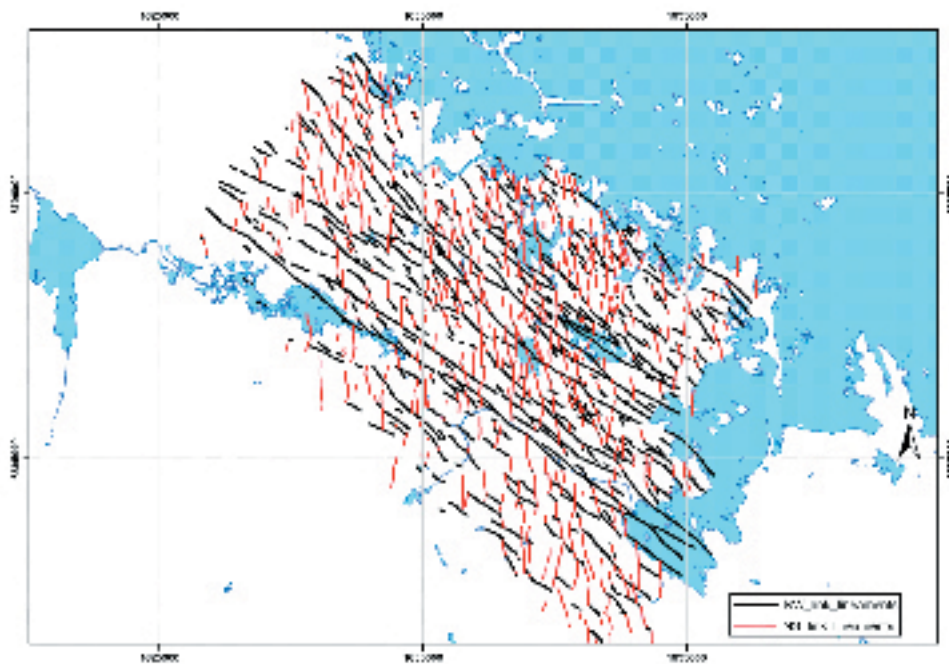
Figure 5-15. *The NW and NS orientation sets of lineaments.*
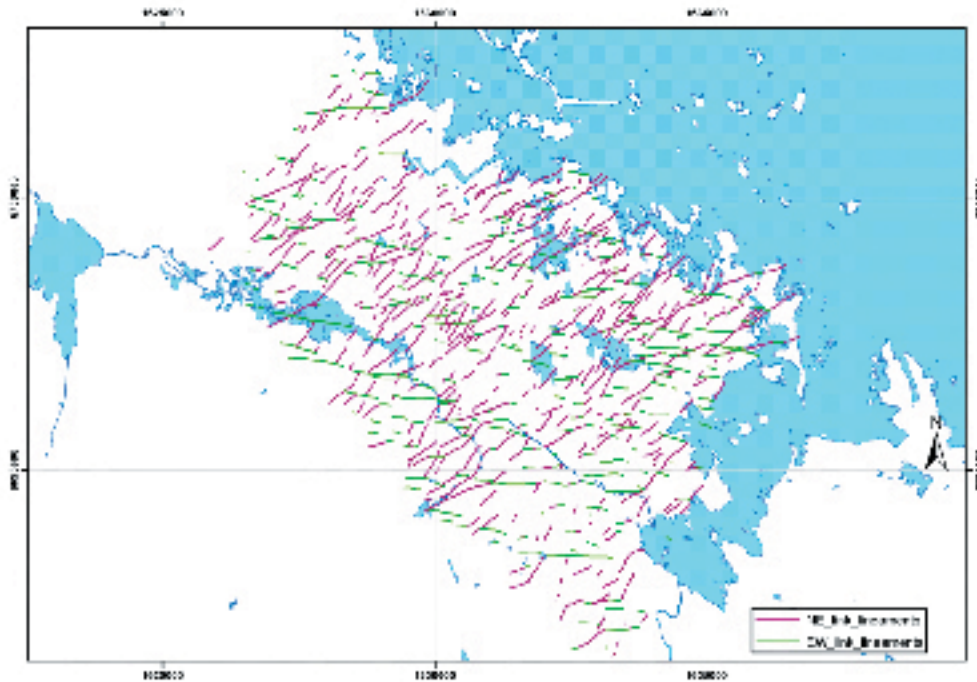
Figure 5-16. *The NE and EW orientation sets of lineaments.*

Fracture outcrop orientations

The fracture orientation data from drillsites 2 and 3 both show similar orientation sets. They are located in the same rock domain, in the centre part of the tectonic lens at Forsmark. As a working hypothesis in model version 1.1, it was assumed that the fracturing at the two outcrops is comparable to each other and that they can be combined and presented in a rose diagram (Figure 5-14 right).

The identified orientation sets for the lineaments have been super-positioned on top of the outcrop rose diagram. The detailed fracture maps show similar orientation sets as the lineaments, but slightly rotated compared to the lineament sets. However, this slight rotation does not seem to be sufficient enough to suggest that the outcrop and lineament orientations should be given different orientations or that they are genetically unrelated.

One reason for this small discrepancy may be local perturbations in the stress field during fracturing. The lineament map covers several kilometres, whereas the outcrops cover several tens of metres. On a small scale, the orientation of fractures can be affected by local geological structural variations, or that one or both outcrops are close to larger zones that may affect the fracture orientations. This has not been considered further in this analysis, but needs to be re-assessed in future DFN analyses of the Forsmark site.

As a working hypothesis for model version 1.1, the two data sources are interpreted as showing the same (sub-vertical) orientation sets. This assumption makes it possible to deduce fracture dip from outcrops, since this information is not available from lineament data.

The Terzhagi corrected, lower hemisphere plots, shown in Figure 5-17, illustrate the outcrop fracture orientations of open and sealed fractures at drillsite 2. The orientation sets for open and sealed fractures are essentially the same, apart from an additional sub-horizontal fracture set in the open fracture data. The sub-horizontal set of fractures has about the same proportion of open fractures and sealed fractures. The steep sets are dominated by sealed fractures. The open fractures constitute approximately 26% of all mapped fractures at drillsite 2.

Fractures at drillsite 2 were then divided into the defined strike sectors with the additional definition of a sub-horizontal set of fractures dipping less than 45 degrees. These results are shown in Figure 5-18.
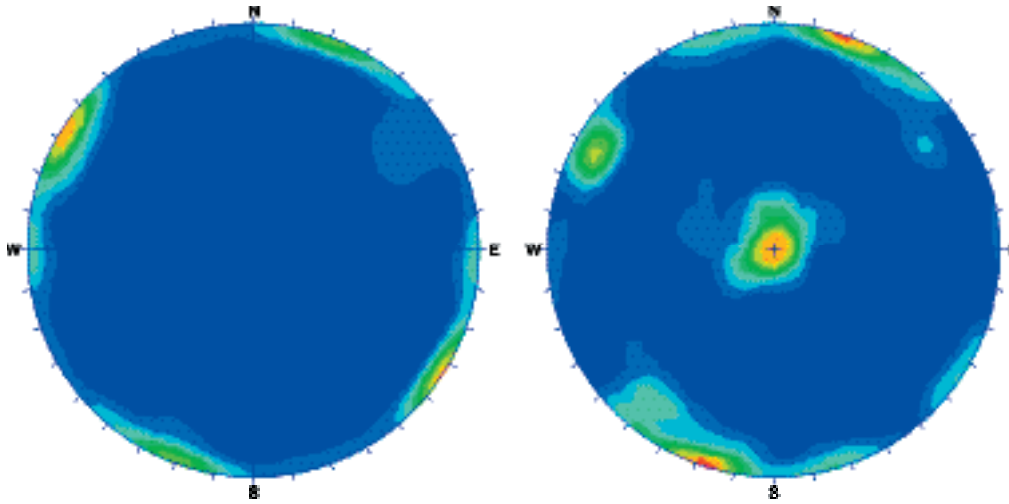
Figure 5-17. *734 sealed (left) and 252 open (right) fractures at drillsite 2. Lower hemisphere equal area projections. Data is corrected for orientation bias.*
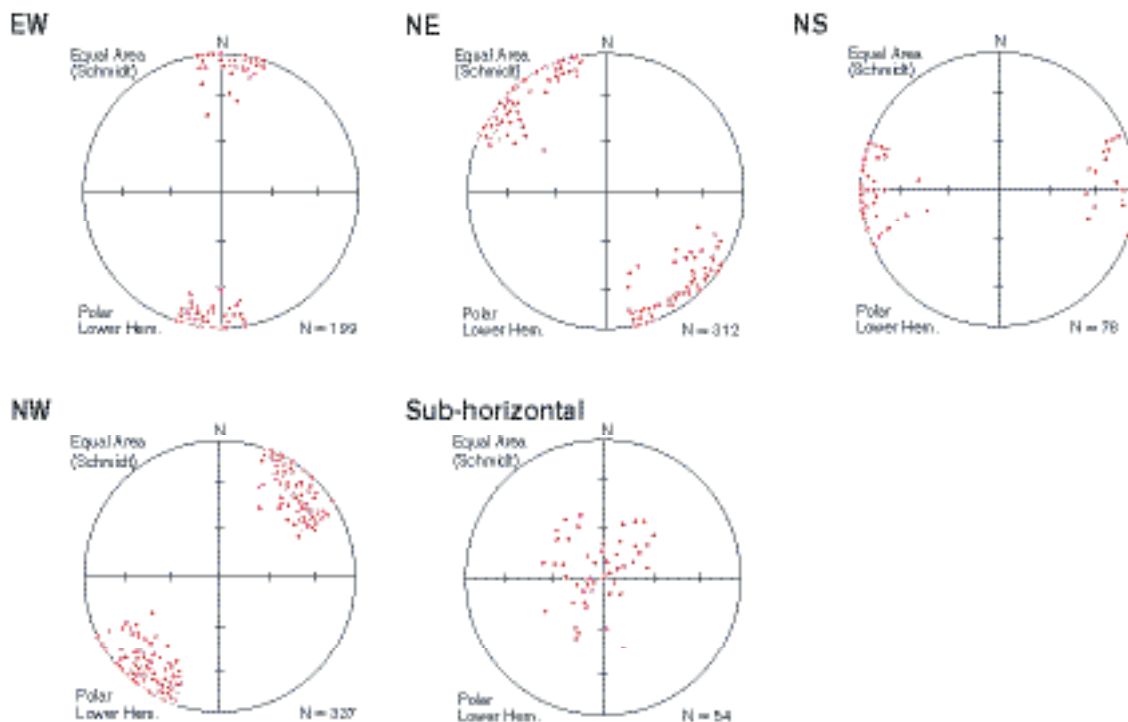
Figure 5-18. *Poles of all fractures mapped on drillsite 2 assigned to their respective sectors.*

Drillsite 3 shows a similar orientation pattern as drillsite 2. However, the amount of mapped open fractures on drillsite 3 is only 4% (44) of all the mapped fractures (1,235), which is clearly different from drillsite 2. Open fractures are predominantly sub-horizontal, cf Figure 5-19. The sealed fractures are dominated by steep fracture sets, but have a relatively minor set of sub-horizontal fractures.

In total, sub-horizontal fractures are relatively sparse in both outcrops and constitute c 5% (116) of the total fracture sample (2,221). One reason could be that a sub-horizontal fracture is less likely to intersect an outcrop surface that is horizontal. The portion of open fractures that are sub-horizontal at both drillsites is somewhat higher, c 18% (53) of the open fracture sample (296).
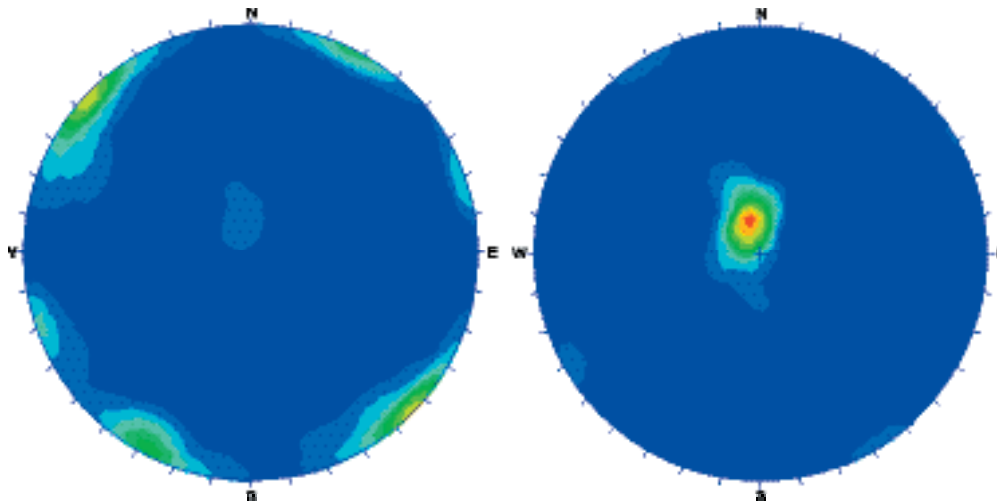
Figure 5-19. 1191 sealed (left) and 44 open (right) fractures at drillsite 3. Lower hemisphere equal area projections. Data are corrected for orientation bias.

Data on sub-horizontal fractures from the drillsites were considered to be too few to provide a sufficient data set to analyse for model version 1.1. The steep fracture sets provide data that have considerably larger sample sizes. Therefore, data from borehole KFM01A were used to characterise the orientation distribution of the sub-horizontal set. This will be discussed further below.

The steep sets identified at drillsite 2 and 3 by sector definitions were statistically quantified using a Fisher distribution. Other types of distributions were not tested in the derivation of model version 1.1. The reason for choosing a Fisher distribution, as a working hypothesis, is that previous studies of the crystalline rock of southeastern Sweden generally recognized Fisher distributed orientations, see for example /LaPointe et al, 1995/. A Fisher distribution is defined by its mean pole orientation trend and plunge and its dispersion parameter K.

The results of the analysis of the orientation of the steeply dipping sets of fractures mapped on drillsite 2 and 3 are given in Table 5-11. The steeply dipping, open fracture sets have similar mean poles as the sealed fracture sets. But, as the numbers of open fractures are few, the Fisher dispersion factor is lower. For this study, however, both open and sealed fractures were considered to have the same Fisher distribution parameters.

Table 5-11. Fisher distributions of the fracture poles (mean trend and plunge, dispersion) for steeply dipping sets at drillsites 2 and 3, divided by sector.

	EW	NW	NE	NS
Mean pole (tr, pl) in degrees	187.7, 3.0	216.0, 2.5	313.9, 1.3	265.5, 2.4
Fisher K	37.3	22.8	19.7	21.0

Borehole fracture orientations

The core-drilled borehole KFM01A is dominated by a sub-horizontal fracture set, with fractures dipping less than 45 degrees, and a steeply dipping, NE striking set, cf Figure 4-41. Approximately 40% of the fracture sample falls within the sub-horizontal fracture sector.

The borehole has a relatively small proportion of open fractures; 13% of the whole sample. The open fractures orientations are dominated by the sub-horizontal set (nearly 70% of the open fracture sample), but also contains a smaller proportion of steep, predominantly NE striking fractures.

The borehole fracture sample has similar orientation sets as those observed at the surface, although it is dominated by sub-horizontal and NE striking sets. The same sector definitions as are used for surface data are presented in Table 5-12.

The NE and NS fracture sets have relatively large numbers of fractures and show similar dispersion factors as the surface sets. The EW and NW sets are sparse in the borehole. For this study, both open and sealed fractures were considered to have the same Fisher distribution parameters.

Table 5-12. Fisher distributions of the fracture poles (mean trend and plunge, dispersion) for steeply dipping sets in the core drilled borehole KFM01A, divided by sector.

	EW	NW	NE	NS	Sub-horizontal
Number of fractures	34	89	592	191	609
Mean pole (tr, pl) in degrees	4.1, 1.5	49.2, 3.5	323.1, 5.6	264.4, 7.7	330.2, 79.3
Fisher K	10.7	10.1	17.4	19.3	11.8

Fracture termination

Some or all of the fracture sets may have formed at different times. Relative chronology can often be inferred by evaluating the terminations of one set upon another. The reason that terminations can be used in this way is that a propagating fracture often terminates against an existing open, or partially open, fracture due to the mechanics of the fracturing process. Thus, if one set consistently terminates against another set, the terminating set is probably relatively younger.

In model version 1.1, only lineaments have been analyzed for termination properties. Termination pattern of outcrop traces and their relation to lineament terminations are equally important to understand and needs to be assessed in the next model versions.

In order to determine the order of origin for the lineaments, the number of terminations of each lineament set against each other set was counted. The oldest set should have a low proportion of terminations against the other sets. The second oldest should have a dominating proportion of its terminations against the older set, and so forth.

Following these assumptions, the determined order of origin was: NW, NS, NE and EW. Table 5-13 shows the results of the termination analysis. It cannot be excluded that the pattern of terminations indicates a sequence of fracturing where lineaments in one set have formed in several time periods.

Table 5-13. The percentage of terminations, of each fracture set in the top row, that terminates against each fracture set in the left column. The last column shows the summarized percent-units of terminations against each set.

Fracture sets	NS	EW	NW	NE	Sum of terminations
NS	x	51	33	30	114
EW	25	x	8	5	38
NW	41	19	x	65	125
NE	34	31	59	x	124
Total no of terminations	100	100	100	100	400

Fracture size evaluation

The size of fractures of a discrete fracture network (DFN) model relates here to the radius of disc-shaped, two-dimensional objects. However, this radius cannot be observed directly in the field. Only fracture traces can be observed in the field, i.e. the intersection between a rock surface and the fracture surface. This is illustrated in Figure 5-20.

The fracture that creates a trace on an outcrop is referred to as the 'parent' fracture. The evaluation of fracture size distribution is made in two steps: (1) characterisation of the distribution of the trace length, followed by (2) estimation of the parent fracture population's radius distribution from the trace length distribution.
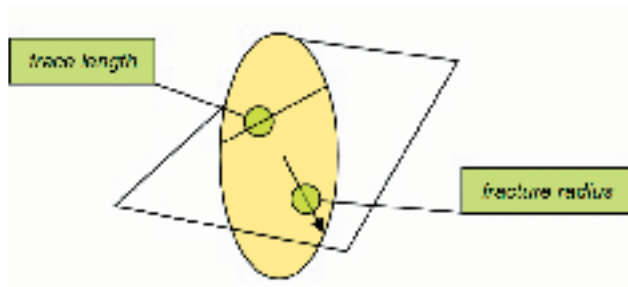
Figure 5-20. *Difference between trace length and fracture radius.*

Data on sub-horizontal fracture traces from the surface were too sparse for a fracture size evaluation. The evaluation of size distribution was therefore limited to sub-vertical fractures. The size of sub-horizontal fractures remains an unconstrained parameter in this preliminary model and needs to be re-assessed in future model versions.

Information about lineament lengths is available from the lineament map for large scale features, and about fracture trace lengths from the mapping at drillsites 2 and 3. The drillsites are large enough to provide information about features with trace lengths up to c 30 m only. In the same way, the lineament map is not detailed enough to provide information about features shorter than c 200 m, although a few linear segments of the lineaments are shorter. However, fractures in the largely unmeasured scale range between c 30 m and c 200 m play an important role in flow and transport models and must be captured in the fracture model. Data on the size and frequency of fractures in this critical scale range are inferred by area-normalization of the lineament and outcrop trace-length data.

In this study it is assumed that, for a given orientation set, fractures observed on outcrops and lineaments are samples from the same population. This assumption may need to be re-evaluated in later model stages, but serves as a first hand hypothesis of how fracturing has occurred in the Forsmark region.

Figure 5-21 shows the number of fractures on different scales normalized by dividing the number of fractures by observation area. This type of plot makes it possible to compare fractures on different scales. The ordinate axis expresses the probability of occurrence. That is, by fitting a straight line to each pair of orientation sets (NS lineaments – NS outcrop traces etc) the probability that a fracture trace is greater than a value X_0 can be calculated as:

$$N_{normalized}^{fractures} = N^{fractures} \frac{lineament\ area}{\sum outcrop\ area} \tag{5.1}$$

$$P[X > x] = (x_0 / x)^{D_{trace}} \tag{5.2}$$

Expression 5-2 is called the complementary cumulative density function (CCDF) and the power-law exponent (D_{trace}) can be estimated from the slope of the straight line in Figure 5-21. $X_{0,\ trace}$ is the value of X for which the probability equals 1.

For each sub-vertical orientation set a plot similar to Figure 5-21 was used to calculate values of the power-law exponents and its corresponding $X_{0,\ trace}$ value. Table 5-14 shows the results of this evaluation based on trace lengths from drillsites 2 and 3 and the lineament map.

Table 5-14. Trace length statistics estimated from graphs.

Set	EW	NW	NE	NS
x_0 [m]	0.33	0.72	0.74	0.52
D	1.82	1.86	1.97	2.05
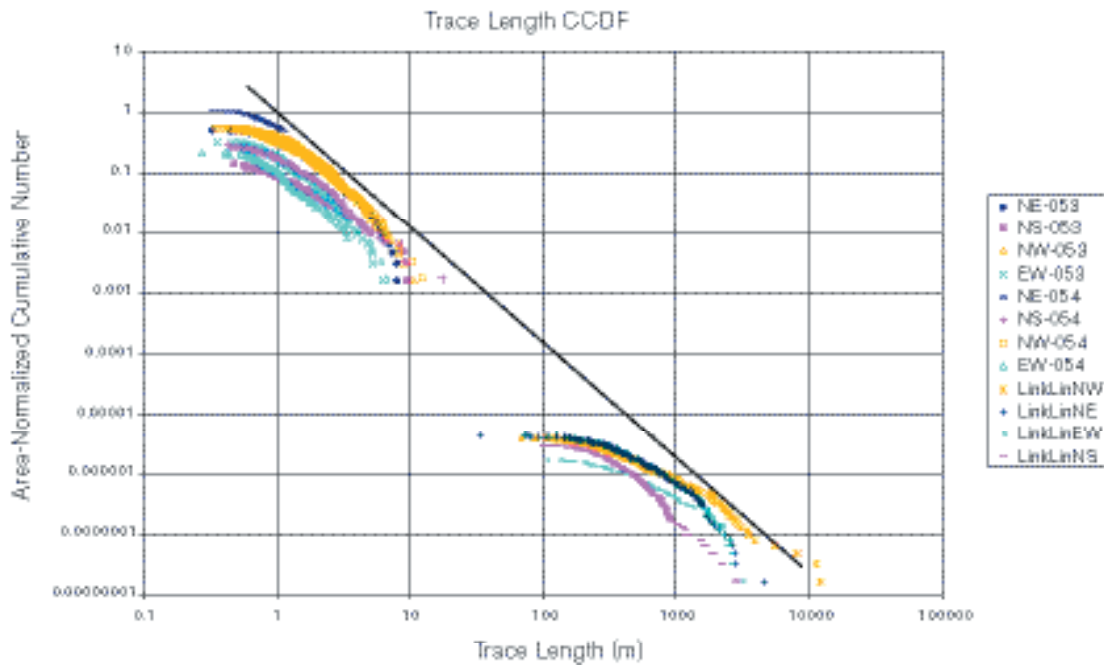
Figure 5-21. *Complementary Cumulative Density Function (CCDF) of the trace lengths of the four sub-vertical fracture groups observed on the lineament map, and from fracture mapping at drillsites 2 and 3. The plot is area normalized.*

Once the CCDF for each fracture group has been evaluated, the probability density function (PDF) of the trace lengths can be derived.

The CCDF presented above corresponds to the following frequency function as:

$$P(X=x) = D_{trace}/x_{0, trace} \cdot (x_{0, trace} / x)^{D_{trace}+1} \tag{5.3}$$

where $D_{trace}+1$ is the slope of the power law exponent of the PDF.

The main characteristic of the power law is that it predicts a high probability of occurrence for small trace lengths and a low probability for large trace length.

Table 5-15 shows the parameters of the power-law PDF of trace lengths for the four sub-vertical sets.

Table 5-15. Trace length statistics estimated from graphs (Power law distribution).

Set	EW	NW	NE	NS
x_0 [m]	0.33	0.72	0.74	0.52
exponent = D+1	2.82	2.86	2.97	3.05

Fracture size distribution of the parent population

If the assumed power-law form of the observed PDF for trace lengths is correct, it implies that the underlying 3D fracture radius distribution also follows a power-law distribution. However, the parameters that characterise the power-law distribution for trace lengths cannot be used directly to estimate the size distribution of the parent population, since the trace lengths are a truncated form of the parent population. Truncation and bias effects must be accounted for when transferring the parameters of the function from trace lengths to the parent population. Truncation of trace length data is related to the orientation of the scan line or surface relative to the orientation of fracture sets, and to the edges of the mapping domain. Bias can be introduced in that larger fractures have a higher probability of intersecting the surface than do smaller ones.

The power-law function presents some specific characteristics useful in deriving parameters of trace lengths for the parent population. With an assumption on the shape of the fractures, the size distribution of the fractures intersecting a trace plane can be related to the size distribution of the observed trace lengths. Furthermore, the size distribution of the parent population can be derived from the size distribution of the intersecting fractures. /LaPointe, 2002/ present the mathematical solutions for the calculation of the size distribution of the parent population from the distribution obtained on trace lengths, assuming circular fractures and a fractal fracture system. The following equations are applied to estimate the radius size distribution of the parent population from the size distribution of fractures intersecting a trace plane to the size distribution of parent population:

$$D_{parent} = D_{trace} + 1 \qquad (5.4)$$

$$x_{0,\,parent} = x_{0,\,trace} \cdot 2/\pi \qquad (5.5)$$

D_{parent} and $x_{0,\,parent}$ are the power-law exponent and minimum radius for the parent fracture radius distribution, respectively. Table 5-16 lists the estimated parameter values for the sub-vertical sets.

Table 5-16. Fracture radius distribution parameters of the parent fracture populations.

Set	EW	NW	NE	NS
x_0 [m]	0.21	0.46	0.47	0.33
exponent	3.82	3.86	3.97	4.05

The probability density function (PDF) of the fracture radius is defined as:

$$P(X=x) = D_{parent}/x_{0,parent} \cdot (x_{0,parent} / x)^{D_{parent}+1} \qquad (5.6)$$

The lineaments form the upper bound for this size estimation, and there is no information on whether they are brittle fracture zones or ductile shear zones. Fractures from outcrops form the lower bound, and they have been divided into open and sealed fractures. However, as working hypothesis, it is assumed that open and sealed fractures have the same size distributions. Future investigations of fracturing in larger outcrop windows may help to better define if open fractures have size distributions that are significantly different from sealed fractures.

Fracture intensity

The fracture intensity is defined as the amount of fracture area per unit volume of rock, P_{32} (m^2/m^3) /Dershowitz and Herda, 1992/. This parameter cannot be assessed in the field. It can be estimated on the basis of a linear correlation with P_{10} (m^{-1}), which is defined as the number of fractures per metre (along a scan line or a borehole) or P_{21} (m^{-1}), which is defined as the amount of fracture trace length per unit area.

The advantage of using P_{32} to specify intensity is that this parameter is independent of the orientation and size distribution of fractures and also of the rock volume under consideration. To determine P_{32}, a DFN model is generated from an assumed P_{32}, referred to as the simulation intensity, or $P_{32,sim}$. Then, sampling boreholes or fracture maps are subsequently simulated in the model by placing a borehole or surface into the DFN model with the same geometry as the observation boreholes or outcrops.

Next, the simulated $P_{10,sim}$ or $P_{21,sim}$ are checked against $P_{10,obs}$ or $P_{21,obs}$ obtained from the field data. The relation between the simulated and observed data is a constant of proportionality that is only a function of borehole (or outcrop) orientation and fracture orientations. Thus, the ratio of the observed to simulated values determines the constant of proportionality, which can then be used to calculate the true P_{32} by multiplying P_{32sim} by this constant.

The intensity analysis is divided into two phases. First, the intensity of sub-vertical fractures mapped at drillsites 2 and 3 are analysed. Secondly, the sub-horizontal intensity is analysed based on the fracturing in the core-drilled borehole KFM01A. Sub-vertical fractures are defined as fractures with a dip larger than 45 degrees. Sub-horizontal fractures are defined as fractures with a dip of 45 degrees and less.

Intensity of sub-vertical fractures

The analysis of P_{32} was carried out by simulating a DFN model based on the four sets of fractures as defined previously. The parameters used to simulate fracture size distribution are given in Table 5-16. The values for $P_{21,obs}$ were obtained separately from the fracture mapping at drillsites 2 and 3 for each set. The values of $P_{21,sim}$ were obtained separately from simulated fracture mappings on a horizontal surface of 100 m by 100 m.

First, the intensity analysis was based on all sub-vertical fractures observed on drillsites 2 and 3. The derived P_{32} data obtained from these simulations are shown in Table 5-17.

Table 5-17. P_{32} summary table of all sub-vertical fractures on drillsites 2 and 3.

Drillsite 2	NE	NW	NS	EW	total
Total trace length [m]	544.31	639.89	146.14	282.12	1612.46
$P_{21,obs}$	0.84	0.99	0.23	0.44	2.50
P_{32}	0.80	0.97	0.21	0.43	2.42
Drillsite 3	**NE**	**NW**	**NS**	**EW**	**total**
Total trace length [m]	868.31	518.56	284.66	137.69	1809.22
$P_{21,obs}$	1.46	0.87	0.48	0.23	3.04
P_{32}	1.36	0.83	0.44	0.23	2.86
mean P_{32}	1.13	0.89	0.35	0.34	2.71

The equivalent mean P_{32} for all sub-vertical fractures is 2.71 m²/m³, which can be compared to other values determined in Äspö. /Stigsson et al, 2001/ reported a global value of 3.41 m²/m³ in the prototype repository domain of Äspö Hard Rock Laboratory. /Hermanson and Stigsson, 1998/ computed a global P_{32} for small and large fractures of 2.75 m²/m³ in the Zedex tunnel domain in the same laboratory.

Secondly, the intensity analysis was based on open sub-vertical fractures observed on drillsites 2 and 3. The derived P_{32} data obtained from these simulations are shown in Table 5-18.

The equivalent mean P_{32} for open sub-vertical fractures is 0.40 m²/m³, which can be compared to other values determined in Äspö. /Follin and Hermanson, 1996/ reported a conductive fracture frequency of 0.47 m²/m³ at the TBM tunnel in the Äspö HRL.

Table 5-18. P_{32} summary table of open sub-vertical fractures on drillsites 2 and 3.

Drillsite 2	NE	NW	NS	EW	total
Total trace length [m]	140.43	197.82	37.94	84.91	461.10
$P_{21,obs}$	0.22	0.31	0.06	0.13	0.71
P_{32}	0.21	0.29	0.06	0.13	0.70
Drillsite 3	**NE**	**NW**	**NS**	**EW**	**total**
Total trace length [m]	18.04	28.81	10.00	2.82	59.67
$P_{21,obs}$	0.03	0.05	0.02	0.00	0.10
P_{32}	0.03	0.05	0.02	0.00	0.10
mean P_{32}	0.12	0.17	0.04	0.07	0.40

Intensity of sub-horizontal fractures

The fracture frequency in KFM01A shows that over 70% of *all* open fractures and slightly less than 60% of all sealed fractures are found in the section 100 m to 400 m (Figure 4-44). The lower 600 m of the borehole is thus substantially less fractured. The open and sealed *sub-horizontal* fracture frequency along the borehole shows a similar pattern, although of a more gradual change, see Figure 5-22.
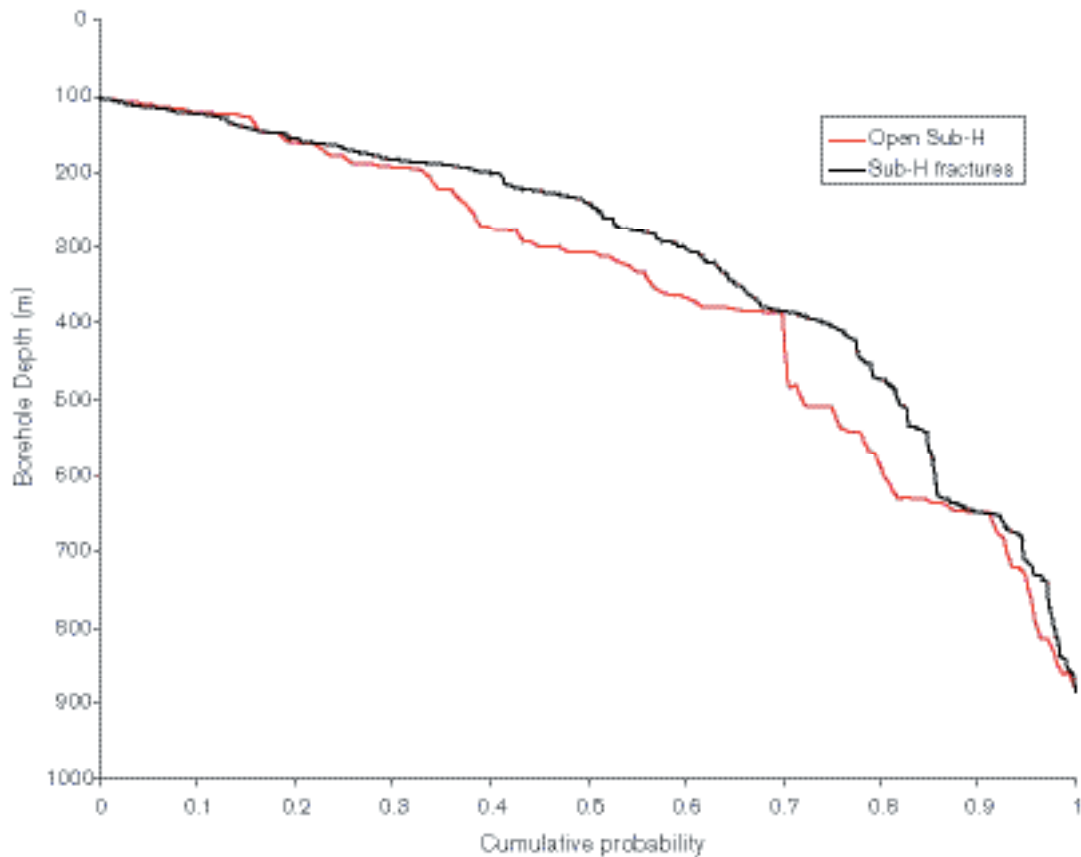
Figure 5-22. *Sub-horizontal fracture frequency of (a) all fractures, (b) open fractures, in KFM01A shown as a normalised cumulative probability plot.*

The fracture frequency of sealed and open fractures in the upper section between 100 m and 400 m in the borehole is shown in Table 5-19. The fracture frequency below 400 m depth in the borehole is shown in Table 5-20. The sealed fracture frequency decreases with c 24% below 400 m and the open fracture frequency decreases with over 60%. It can also be concluded that the major decrease occurs in the NW and the sub-horizontal fracture sets. The open sub-horizontal fracture frequency decreases with c 56% below 400 m borehole depth. However, the sub-vertical NW set generally shows a low frequency in the whole borehole and is thus more sensitive to a change in frequency. The NE sub-vertical set, on the other hand, shows an increase in frequency below 400 m borehole depth. This may in part be due to the fact that the section between 650 and 700 m borehole depth (Zone ZFMNE0061) has been included in the frequency analysis. In general, the results show that sub-vertical fracturing in the borehole does not follow the same decrease below 400 m borehole depth as the sub-horizontal fractures.

Because the sub-vertical fracture frequency has been estimated from surface data, it is also likely that this intensity is more correlated to the upper part of KFM01A than to the lower. Therefore, the section between 100 m and 400 m in KFM01A is used for the analysis of the sub-horizontal fracture intensity. However, it is presently not known if the surface observations are representative for the sub-vertical fracture data, since the fracture data from the first 100 m of the borehole are less reliable. This needs to be re-assessed in future model versions when near-surface core-drilled borehole data become available.

The reason for the change of fracture frequency at depth is presently not known and needs to be re-assessed in the next model version. Gently dipping deformation zones in the upper 50 m of rock in the Forsmark area are known from the construction of the power plant /Carlsson, 1979/. There are also indications of several gently dipping fracture zones in the upper 300 m at drillsites 1, 2 and 3 (see Section 5.1.4).

Table 5-19. Fracture frequency in KFM01A in the section 100 m to 400 m.

Set	Sealed (m^{-1})	Open (m^{-1})	All (m^{-1})
NE	0.79	0.10	0.89
NS	0.21	0.03	0.25
NW	0.21	0.03	0.24
EW	0.08	0.01	0.09
Sub-Horizontal	1.19	0.32	1.51
Total	2.48	0.49	2.97

Table 5-20. Fracture frequency in KFM01A in the section 400 m to 1000 m.

Set	Sealed (m^{-1})	Open (m^{-1})	All (m^{-1})
NE	1.06	0.03	1.09
NS	0.38	0.01	0.39
NW	0.06	0.00	0.06
EW	0.02	0.00	0.02
Sub-Horizontal	0.39	0.14	0.52
Total	1.90	0.18	2.08

The derivation of the sub-horizontal P_{32} was carried out by simulating a DFN model based on the sub-horizontal set along a simulated borehole that has the same orientation as KFM01A. Since the size distribution of this set is unknown, it was, as a working hypothesis, assumed that it had the same size distribution as the NS sub-vertical set. This assumption cannot presently be verified and will have to be re-assessed in the next model version. However, as previously discussed, the value of P_{32} is independent of the size distribution, so the lack of constraint for the size parameters for the sub-horizontal fractures produces no additional uncertainty in the P_{32} value.

The derived P_{32} value for all sub-horizontal fractures is 1.63 m^{-1}. The fracture frequency for sub-horizontal fractures below 400 m borehole depth is c 34% of the fracture frequency for all sub-horizontal fractures, cf Table 5-20 and Table 5-23. The P_{32} for all sub-horizontal fractures below 400 m borehole depth is thus equal to 0.56 m^{-1}.

The derived P_{32} value for open sub-horizontal fractures is 0.34 m^{-1}. The fracture frequency for open sub-horizontal fractures below 400 m borehole depth is c 44% of the fracture frequency above 400 m borehole depth. The P_{32} for open sub-horizontal fractures below 400 m borehole depth is thus equal to 0.15 m^{-1}.

If a corresponding analysis is made for the group of fractures that are classified as natural fractures (see Section 4.4.3, Table 4-15) it will result in other fracture intensities for sub-vertical and sub-horizontal fractures. This approach is presented as an alternative interpretation of one specific type of fracture classification and illustrates the impact it has on fracture intensities in a DFN model. It also illustrates that it is necessary to better understand the mapped fracture data in future model versions as well as to correlate the geological classifications with other information such as flow logs and the outcome of the hydrogeological and rock mechanics models.

Statistics for *natural* fractures can only be given for the sub-horizontal fracture set, since the sub-vertical fractures are deduced from surface data which have not been classified using the SICADA terminology of *natural* fractures.

A derived P_{32} value for the sub-horizontal set of *natural* fractures is 1.23 m^{-1}. The fracture frequency for sub-horizontal *natural* fractures below 400 m depth is c 13% of the fracture frequency of all sub-horizontal *natural* fractures. P_{32} below 400 m is equal to 0.15 (13% of 1.23), cf Table 5-21 and Table 5-22.

Table 5-21. Fracture frequency for *natural* fractures in KFM01A in the section 100 m to 400 m, (the concept of natural fractures is explained in Section 4.4.3).

Set	Natural fractures (m⁻¹)
NW	0.13
NS	0.11
NE	0.35
EW	0.04
Sub-H	1.43
Total	2.07

Table 5-22. Fracture frequency for *natural* fractures in KFM01A in the section 400 m to 1000 m, (the concept of natural fractures is explained in Section 4.4.3).

Set	Natural fractures (m⁻¹)
NW	0.01
NS	0.04
NE	0.05
EW	0.01
Sub-H	0.18
Total	0.27

Spatial model

The way fractures are located in space and their size distribution defines which geometrical conceptual model to use for generating a DFN model. This was assessed through a Box fractal dimension calculation. The distribution of fractures is evaluated by counting the amount of fractures or fracture centres in a stepwise increasing reference domain size. This computation is processed with the geoFractal software /LaPointe et al, 2000/. There are two main methods of counting the fractures: the first method counts the fracture trace centre-point and the second uses multiple random points along the fracture trace. When using the fracture centre-point option, a series of concentric circles is generated around a single point, and for each circle the number of fracture centres in each circle is counted. The number of fracture centres is plotted against the circle radius on a log-log graph. The slope of the regression line defines the box dimension. The random-points option is very similar, except that one or several random points are selected along the trace. These methods are appropriate for determining the spatial model for generation of fractures in a DFN.

By definition, the values range from 1 to 2 for outcrops and lineament data. A box dimension of 1 identifies a fracture pattern with fractures that are grouped and almost aligned in space. A box dimension of 2 represents a random fracture pattern that follows a Poisson distribution in space.

The box dimension was calculated for the local and regional corrected lineaments data by applying the fracture centres option. The calculated box dimension of 1.6 suggests that the fracture pattern is somewhat clustered, and the rock mass is divided into blocks of non-uniform size (Figure 5-23). Despite the low degree of clustering, a Poissonian model was adopted for the spatial representation of stochastic fractures. However, it is recognized that the spatial model needs further analysis in future model versions since there are indications that other spatial models than a Poissonian can be applicable.
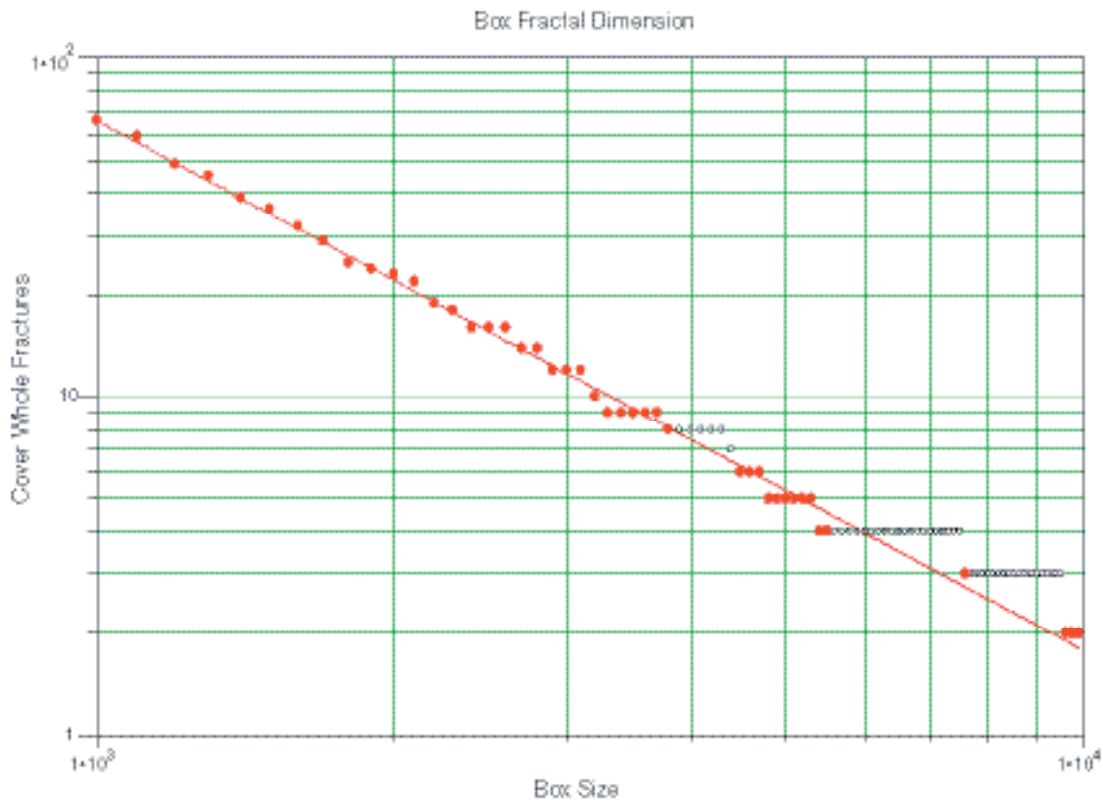
Figure 5-23. *Box fractal analysis of the linked-lineament map showing a box fractal dimension of 1.6.*

Summary DFN statistics

Table 5-23, Table 5-24 and Table 5-25 show a summary of the evaluated fracture statistics for *all, open* and *natural* fractures, respectively. These tables are appropriate for implementation of parameter values in a DFN model. However, these parameters only describe the geometry of the observed fracture distributions. Therefore, a re-evaluation together with other appropriated data may be needed before applying the model in flow and transport or rock mechanics simulations. Note also that the tables present truncated size distributions with a maximum radius of 500 m. The truncation level adopted within a DFN model will, for example, affect intensity of fracturing.

Generating a DFN model based on the data in Table 5-23 will produce a large number of fractures in the local model domain due to the power-law assumption of fracture sizes.

Figure 5-24 illustrates how P_{32} for each orientation set changes by truncating the minimum radius in the data in Table 5-23. The upper bound of 1 km (circular radius of 500 m) is a censoring, which will affect the fracture intensity in the model very moderately. Truncating the minimum allowed size affects the fracture intensity substantially. The truncation level needs to be set by other complementary investigations. For example, a hydrogeological approach is presented in Section 5.4 where a transmissivity distribution is derived based upon these geometric properties and groundwater flow logs.

210

Table 5-23. Summary DFN statistics for *all* fractures. Size distributions censored at a maximum radius of 500 m.

Parameter	Value	Comments
NE		
Orientation (Mean pole trend and plunge, dispersion	313.9, 1.3, K = 19.7	Fisher model
Intensity (P_{32} [m²/m³])	1.13	All fractures
Size	Exp = 3.97, x_0 = 0.47	
NW		
Orientation (Mean pole trend and plunge, dispersion	216.0, 2.5, K = 22.8	Fisher model
Intensity (P_{32} [m²/m³])	0.89	All fractures
Size	Exp = 3.86, x_0 = 0.46	
NS		
Orientation (Mean pole trend and plunge, dispersion	265.5, 2.4, K = 21.0	Fisher model
Intensity (P_{32} [m²/m³])	0.35	All fractures
Size	Exp = 4.05, x_0 = 0.33	
EW		
Orientation (Mean pole trend and plunge, dispersion	187.9, 3.0, K = 37.3	Fisher model
Intensity (P_{32} [m²/m³])	0.34	All fractures
Size	Exp = 3.82, x_0 = 0.21	
Sub-horizontal		
Orientation (Mean pole trend and plunge, dispersion	330.2, 79.3, K = 11.8	Fisher model
Intensity (P_{32} [m²/m³])	1.63	All fractures –100 to –400 m
Intensity (P_{32} [m²/m³])	0.56	All fractures –400 to –1000 m
Size	Exponent = 4.05, x_0 = 0.33	Adopted from the NS set

Table 5-24. Summary DFN statistics for *open* fractures. Size distributions censored at a maximum radius of 500 m.

Parameter	Value	Comments
NE		
Orientation (Mean pole trend and plunge, dispersion	313.9, 1.3, K = 19.7	Fisher model
Intensity (P_{32} [m²/m³])	0.12	Open fractures
Size	Exp = 3.97, x_0 = 0.47	
NW		
Orientation (Mean pole trend and plunge, dispersion	216.0, 2.5, K = 22.8	Fisher model
Intensity (P_{32} [m²/m³])	0.17	Open fractures
Size	Exp = 3.86, x_0 = 0.46	
NS		
Orientation (Mean pole trend and plunge, dispersion	265.5, 2.4, K = 21.0	Fisher model
Intensity (P_{32} [m²/m³])	0.04	Open fractures
Size	Exp = 4.05, x_0 = 0.33	
EW		
Orientation (Mean pole trend and plunge, dispersion	187.9, 3.0, K = 37.3	Fisher model
Intensity (P_{32} [m²/m³])	0.07	Open fractures
Size	Exp = 3.82, x_0 = 0.21	
Sub-horizontal		
Orientation (Mean pole trend and plunge, dispersion	330.2, 79.3, K = 11.8	Fisher model
Intensity (P_{32} [m²/m³])	0.34	Open fractures –100 to –400 m
Intensity (P_{32} [m²/m³])	0.15	Open fractures –400 to –1000 m
Size	Exp = 4.05, x_0 = 0.33	Adopted from the NS set

Table 5-25. Summary DFN statistics for natural fractures (sub-horizontal set). Size distributions censored at a maximum radius of 500 m.

Parameter	Value	Comments
NE		
Orientation (Mean pole trend and plunge, dispersion	313.9, 1.3, K = 19.7	Fisher model
Intensity (P_{32} [m²/m³])	1.13	All fractures
Size	Exp = 3.97, x_0 = 0.47	
NW		
Orientation (Mean pole trend and plunge, dispersion	216.0, 2.5, K = 22.8	Fisher model
Intensity (P_{32} [m²/m³])	0.89	All fractures
Size	Exp = 3.86, x_0 = 0.46	
NS		
Orientation (Mean pole trend and plunge, dispersion	265.5, 2.4, K = 21.0	Fisher model
Intensity (P_{32} [m²/m³])	0.35	All fractures
Size	Exp = 4.05, x_0 = 0.33	
EW		
Orientation (Mean pole trend and plunge, dispersion	187.9, 3.0, K = 37.3	Fisher model
Intensity (P_{32} [m²/m³])	0.34	All fractures
Size	Exp = 3.82, x_0 = 0.21	
Sub-horizontal		
Orientation (Mean pole trend and plunge, dispersion	330.2, 79.3, K = 11.8	Fisher model
Intensity (P_{32} [m²/m³])	1.23	Natural fractures –100 to –400 m
Intensity (P_{32} [m²/m³])	0.15	Natural fractures –400 to –1000 m
Size	Exp = 4.05, x_0 = 0.33	Adopted from the NS set
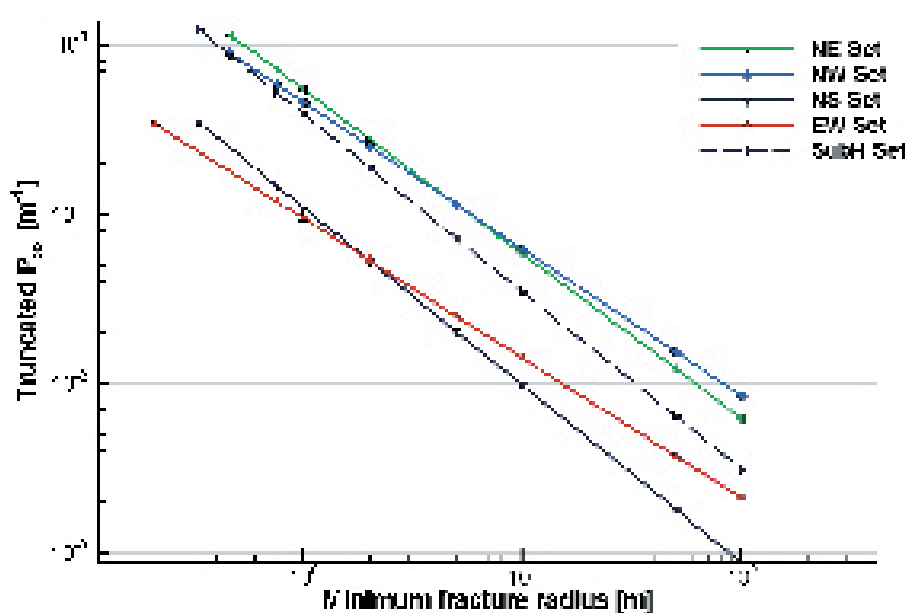
Figure 5-24. *Relation of truncated size distributions (minimum radius) and P_{32}, for the five orientation sets used in the Forsmark DFN model version 1.1.*

DFN properties in other domains in the local model volume

The entire data set presented above is derived from rock domain 29, except for parts of the lineament map which covers a larger area. Thus, the evaluated fracture statistics are in essence valid only for the fracturing in the central part of the tectonic lens at the Forsmark site. This part of the rock mass resides inside rock domain 29, which is considered homogeneous with regards to lithology and deformation.

Orientation sets outside rock domain 29 are not well known. The lineaments indicate that similar orientations occur in other domains, but with different intensities. In addition, there is no reliable source of information about the fracture size distribution outside of rock domain 29.

As a very early working hypothesis, it is proposed that orientation and size properties for each observed fracture set is valid also outside rock domain 29. If lineaments reflect the orientations and sizes of fractures also in other rock domains, then the intensity of lineaments may reflect how fractured these domains are.

The area of the Forsmark site that is covered by the lineament map is larger than rock domain 29. The lineament intensity varies over the Forsmark area and different rock domains show different lineament intensities. In addition to the lineament data, there are 44 scan-line outcrops, partly outside of the lineament coverage, that can give indications of fracture intensities along the more deformed rock domains around the tectonic lens of Forsmark.

The hypothesis of lineament intensity controlled fracturing is built on these assumptions:

- The lineament areal intensity P_{21} of a rock domain is proportional to the discontinuity volumetric intensity P_{32} of this rock domain.

- The ratio between the areal intensities P_{21} of two rock domains is equal to the ratio of the volumetric intensities P_{32} of these rock domains.

Based on these two assumptions, it is possible to calculate the volumetric intensity for any rock domains where the linked-lineament intensity is known by applying the following relationship:

$$\frac{P_{21 \text{ lineament, rock domain } 1}}{P_{21 \text{ lineament, rock domain } 2}} = \frac{P_{32 \text{ rock domain } 1}}{P_{32 \text{ rock domain } 2}} \tag{5.7}$$

If we consider that 'rock domain 1' is the Forsmark rock domain 29, then $P_{21 \text{ lineament}}$ and P_{32} are known. Rock domain 2 can be any other rock domain within the local model. Its $P_{21 \text{ lineament}}$ is also known from the lineament map.

The evaluation of the $P_{21 \text{ lineament}}$ from the lineament map is carried out by a grid analysis as follows:

1. Apply a grid over the linked lineament maps. The grid cells have a dimension of 200 m x 200 m. The grid covers the totality of the linked lineaments.

2. Within each grid cell, a value of P_{21} is calculated for each sub-vertical fracture set.

3. Grid cells contained within each rock domain and their P_{21} values are identified for each sub-vertical fracture set.

4. For each rock domain, an average value of P_{21} of lineaments is calculated for each sub-vertical fracture set.

The grid analysis provides a single average value of the linked lineament P_{21} for every rock domain in the local model as shown in Figure 5-25.

Figure 5-25 shows that the areal lineament intensity is absent or only partially available for some rock domains. Qualitative assessment of fracture data from scan-line mappings was used to fill some of the gaps. However, if no data were available in a rock domain, it was assumed to have the same DFN properties as a geologically similar domain nearby, i.e. a domain following the same classification for rock domains as is given in Section 5.1.2.
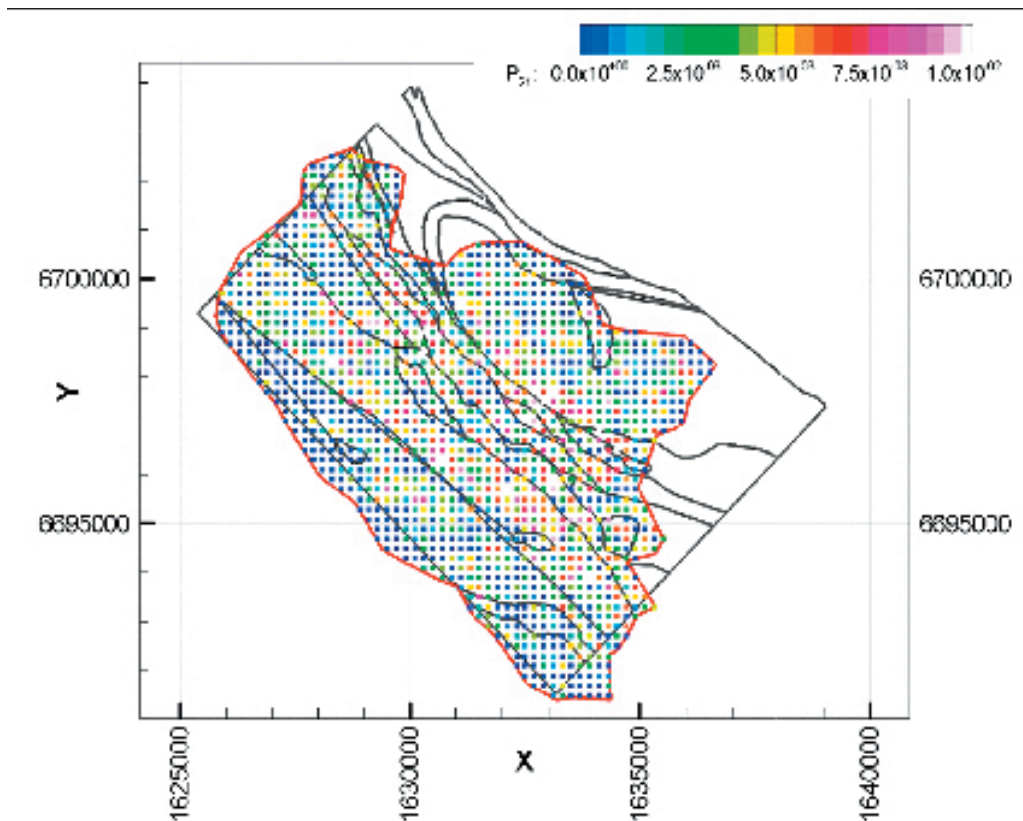
Figure 5-25. *Grid cells and their P_{21} values for a given fracture set over the local model linked lineaments. The black lines represent the rock domains at the surface.*

Table 5-26, shows which rock domains that are inside the local model domain in whole or in parts. Rock domains that have similar fracture intensities (for each set) are grouped from 1 to 8, each group with their specific fracture intensities.

Table 5-26. List of rock domains inside the local model volume and the grouping of these rock domains into DFN types.

Group	Rock domain
1	29–34
2	8, 11, 15, 16, 18, 20, 21, 25, 27, 32
3	9
4	10
5	12
6	13
7	17

Figure 5-26 shows the calculated results of $P_{21, \text{any rock domain}}/P_{21, \text{rock domain 29}}$ for the NW set. Fracturing in the rock domains 18 and 8, both located along the western edge of the tectonic lens, is generally higher than in rock domains inside the lens. Figure 5-27 illustrates how P_{32} for fracture sets NE, NS and EW increases or decreases in the different rock domain groups as given in Table 5-26.

214
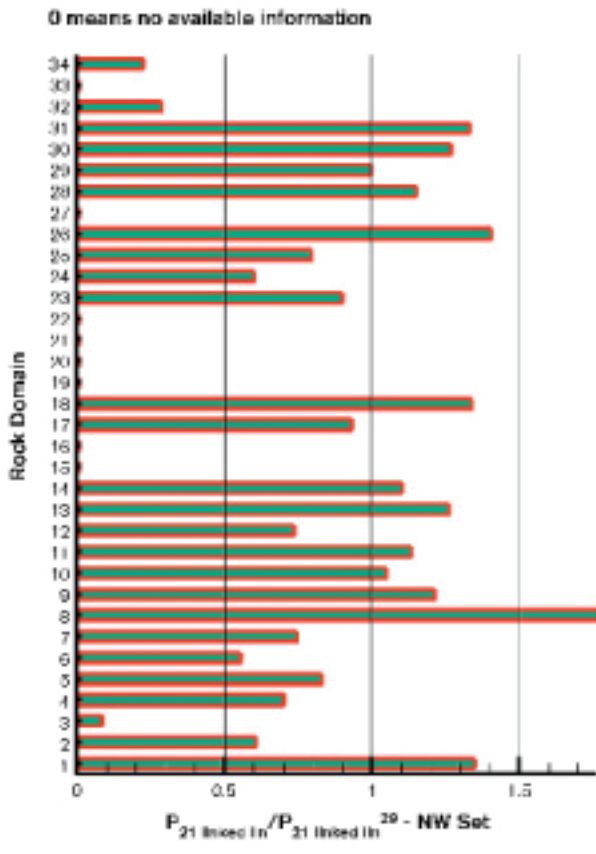
Figure 5-26. *Calculated $P_{21,\ any\ rock\ domain}/P_{21,\ rock\ domain\ 29}$ of the NW set for each rock domain in the local model domain.*
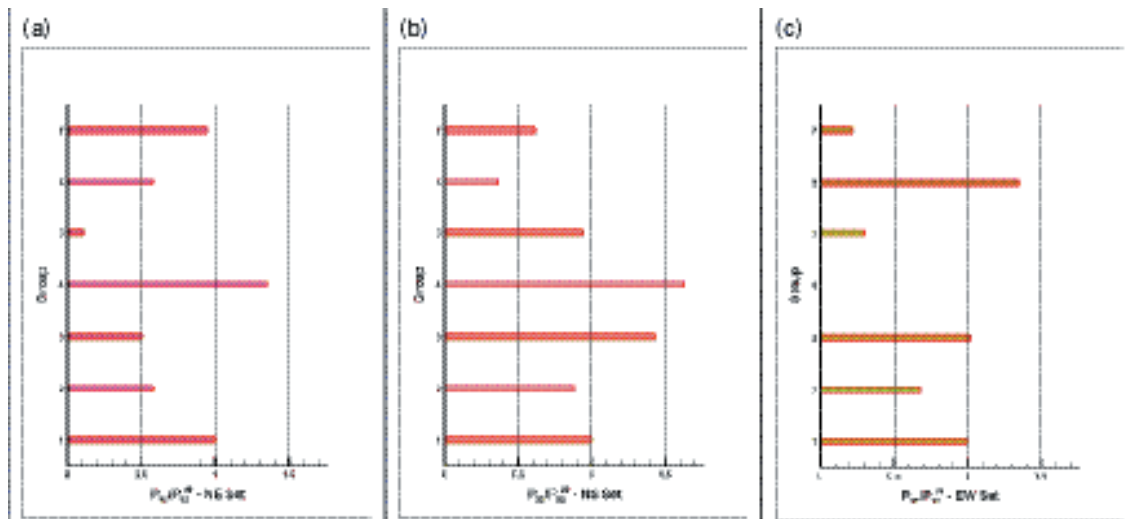
Figure 5-27. *Calculated $P_{32,\ group}/P_{32,\ rock\ domain\ 29}$, for (a) NE set, (b) NS set and (c) EW sets.*

215

Evaluation of uncertainties in the DFN model

The DFN statistical analysis presents a hypothesis where fracturing on different scales follows the same orientation and size distributions. The analysis follows the approach that the orientation sets observed at lineament scale can be transferred to outcrop scale. The results show that this assumption does not fit perfectly to the data and further re-evaluation in future model versions is needed. In particular, results show that other properties than orientation may need to be tested in order to better understand the fracture network properties. However, the chosen approach serves the purpose of answering some basic fracture behaviour at Forsmark.

The entire data set that has been used for the statistical analysis comes from rock domain 29, which covers most of the local model area. Rock domain 29 is located inside a large tectonic lens that may have substantially different fracture patterns in its more deformed boundaries. Therefore, the fracture distributions are valid in rock domain 29 only. The lineament intensity analysis carried out in order to extrapolate DFN properties to other rock domains shows several uncertainties and the results can only be viewed as indicative at most.

The statistics are derived from surface data of different resolution that are more or less limited to sub-vertical fracturing. Surface data on sub-horizontal fracturing are sparse and instead borehole data have been utilised.

There are uncertainties regarding how well the surface fracturing reflects the fracturing at depth. The sub-vertical borehole data from KFM01A confirm that the orientation sets for sub-vertical fractures are similar at the surface and at depth, although the data sample from the borehole is limited.

The classification of fractures into open and sealed needs to be re-assessed based on other supportive information from hydrogeology and rock mechanics. Aperture may seem to be a valid qualifier for open fractures, but are also difficult to appreciate as the resolution of the BIPS system limits precise mapping. Any aperture that is measured from the core only must be considered as highly uncertain. The classification of *natural* and *sealed* fractures was the original way data was delivered from SICADA, and has later been re-defined into the newer classification based on aperture. A DFN model based on *natural* fractures is provided as an alternative way to interpret data. This alternative shows that different geological interpretations give quite different DFN models.

The size distributions derived from surface data are not possible to verify at depth unless fracture information from tunnels or shafts are available. The SFR tunnels may provide such information that can be addressed in future model versions. Also, the size distribution for sub-horizontal fractures is unconstrained as there are limited data available.

Likewise, the estimation of fracture intensity is based on the assumption that sub-vertical fractures have the same intensity throughout the model depth as measured on the surface outcrops. However, this assumption may over-represent steep fractures in the model, since previous studies /e.g. Carlsson, 1979/ and the borehole information show increased fracturing near the surface. But without very precise information, it is not possible to correlate the surface fracturing to the fracturing at depth. Currently, the first 100 m of the KFM01A borehole does not present detailed and reliable information about the fracturing since this part is percussion drilled.

The fracture frequency, especially of the sub-horizontal fractures, is dropping at depths larger than 400 m without any other geological change in the rock. This effect has previously been identified at more shallow depths during the construction of the power plant /Carlsson, 1979/. The reason for this is not well known and it will be a challenge for further investigation in future model versions. There is also an even more dramatic decrease of transmissive structures below 400 m of depth.

The spatial model analysis of the fracturing shows that the fracture system does not perfectly follow a Poissonian distribution, but are somewhat clustered. This analysis was based on lineaments only. The same analysis needs to be performed for outcrop fractures in future model versions. The clustering effect has not been accounted for and a Baecher (Poissonian) spatial model has been adopted as a working hypothesis. This assumption may have an important effect on the connectivity of the DFN model and needs to be investigated further.

All these uncertainties in fracture orientation, size, intensity and spatial model of both sub-vertical and sub-horizontal fractures will be necessary to revisit in future model versions as new borehole data and other supportive data become available from the site.

5.2 Rock mechanics modelling

In this section, the various rock mechanics aspects of the present site model are drawn together from a variety of sources. Both historic and recent local construction experiences are of importance, when only one borehole forms the backbone of presently reported, sub-surface exploration. A more 'distributed' aspect of the several km^2 of the candidate site is the existence of logging data from selected surface exposures carried out to get a first estimate of the areal distribution of rock qualities and empirically derived parameters.

The conceptual rock mechanics model of the bedrock, within the presently understood geological and hydrogeological framework of the candidate site, is influenced by the variations seen across surface exposures and local construction sites (the nuclear power plant foundations) and by the variations seen down boreholes KFM01A and B.

The variations in fracture frequency and the sometimes occurring variations in intact rock strength have a combined effect on the stiffness or deformability of the rock mass. In turn, this usually affects the rock stresses measured at selected locations, helping to explain where stresses are more aniso-tropic and larger or smaller in magnitude. Often, this logic is tested by unexpected trends, which may give a clue to requirements for supplementary and more distributed testing in the future. The possible influence of significant pore pressure or its suspected 'absence' in dry parts of the rock mass, adds to the uncertainty at the present stage of the site investigations.

5.2.1 Modelling assumptions and input from other models

The rock mechanics modelling relies to a large extent on geological information /Andersson et al, 2002b/. This information provides the basis for considering how representative the rock mechanics parameters are when they have been sampled at certain points in the rock mass but are used to characterise one or several large rock units. The main objective of the interaction between the geologists and the rock mechanics modellers is to ensure the good understanding of the geological site model and to guarantee the compatibility of the rock mechanics characterisation with the geological representation.

The main modelling assumption in this study is that rock mechanics properties are distributed according to the rock domains presented in Section 5.1.2. However, the data presented in Chapter 4 mainly concern rock domains 29 and 33. In lack of other information, the mechanical properties of the rock domains were assigned values based on data from the SFR repository in Unit 33.

The available data are clearly a fairly thin basis on which to construct a rock mechanics model and can be summarised as: i) the nuclear power plant excavations at the northern end of the candidate formation; ii) a fairly poor areal distribution of available surface exposures (mostly E and NE of the candidate site) and; iii) one presently reported sub-vertical borehole. Thanks to a well-mapped geology and to distinctive formations, the present 'points and line' sampling, from which rock mass properties are estimated, can, with some confidence, be extrapolated to larger areas and volumes of the rock mass.

The 'points and line' samples have been described with a consistent descriptive framework of rock mass characterization techniques, namely the Q-system /Barton et al, 1974; Barton, 2002/ (and in the case of the borehole) also with RMR /Bieniawski, 1989/. Some of the input data for these quantita-tive methods have been obtained from direct measurement. RQD, intact rock strength, rock stress, fracture roughness, fracture wall compressive strength, fracture orientations and their grouping in sets, have each been measured directly. Supplementary data for evaluating the remaining rock mass characterization parameters of Q and RMR have been obtained by use of experienced judgement within the fields of rock engineering, geology, mineralogy and hydrogeology.

Because most of the information is collected on generally good rock, primarily from rock domain 29, there is limited geological information available from the other rock domains and fracture zones. Thus, their mechanical properties can only be estimated based on experience from previous construction projects summarised in Section 4.6.5. However, the present geological understanding gives possibilities to assess the homogeneity of the rock mass outside fracture zones based on the following questions:

- How complex is the lithological distribution?

- What could be extracted from fracture statistics?

- How good is our knowledge on fracture distribution and density?

5.2.2 Conceptual model of the bedrock with potential alternatives

The rock domain model in Section 5.1.2 presents a distribution of rock types in the model volume of the site. Variations within each rock unit as well as dikes and veins occur. Nevertheless, geographical grouping of lithological units has been possible, showing areas and potential volumes with similar chemical and structural composition. It can be assumed that the mechanical properties within each lithological unit may group into classes with a certain distribution. The primary uncertainties are related to the actual variations within the dominant rock type, and the extent of other rock types within the domain (variants, dikes, veins). Because the rock domain model points out possible similarities between the candidate area and areas of previous construction, it is assumed that old data from rock mechanics testing of core specimens (see Section 4.6.2) are of relevance for this model version.

The fracture statistics presented in Section 5.1.6 show an overall distribution that is similar to what has been recorded during construction in the area (Power Plant Unit #3 and SFR, Figure 5-28). The records show fracture sets orientated vertically in the directions NW-SE (foliation in the area), NE-SW and E-W. A sub-horizontal set is also present. The records also indicate less dominant fracture sets orientated vertically in NNW-SSE directions and trending E-W, dipping 25–40° towards south /Carlsson and Christiansson, 1987/. So far, limited information on facture infillings that can be compared with older data is available. It is therefore assumed that the fracture characteristics recorded earlier in the nearby construction areas of Unit #3 and SFR are applicable for the site investigation area. From the construction areas it is known that:

- Fracture density can be significantly higher close to the surface, compared to only some metres depth.

- When sediment-filled horizontal fractures occur in the superficial rock mass, there is often a higher fracture density above the opened fracture.
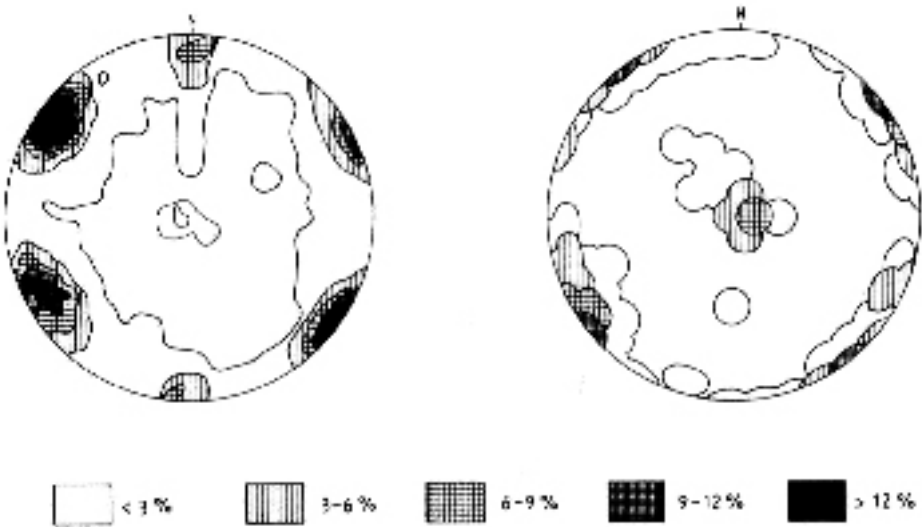
Figure 5-28. Fracture statistics from Power Plant Unit #3 (left) and SFR /Carlsson and Christiansson, 1987/.

- Many of the fracture sets show a variable density. Relatively more fractured areas caused by fracture clustering are often found, at least down to 150 m depth.

- Large volumes outside the fractured zones display low fracture density. For example, in the deep borehole DBT-1 close to Power Plant Unit #3, a frequency in the range of 1.0–1.8 fractures per metre was reported between 350 and 500 m depth /Carlsson and Olsson, 1982/.

The current data gives limited information on fracturing with depth. The fracture distribution in the borehole KFM01A displays low fracture frequency below 400 m, except for some relatively more fractured sections. This can be a bias caused by the limited data sample and the actual borehole orientation at depth. However, there is no geological information available that contradicts an assumption that the rock mass at larger depth could be, from a rock mechanics point of view, equal to or better than the "average rock" in which underground constructions have been carried out before.

5.2.3 State of stress

The stress model predicts the in situ stress magnitudes in Forsmark and is based on the limited data available at data freeze 1.1 in terms of study of the lineaments, stress measurements and analysis of the core conditions. Due to the lack of new data, a deeper understanding of the distribution and properties of lineaments has not yet been obtained. Numerical modelling of the possible state of stress and of the effect of lineaments is still needed /Andersson et al, 2002b/. Old measurements indicate high stresses in the Forsmark region. However, the re-evaluation of old rock stress data by /Perman and Sjöberg, 2003/ reduces somewhat the expectation for high stresses at depth. The results from their transient strain analysis performed on data from borehole DBT-1 and DBT-3 are summarised in Figure 5-29.

Transient strain analysis

Given the lack of clear trends of the rock stress with depth, /Perman and Sjöberg, 2003/ found it difficult to state which of the stress measurements were less reliable. Nevertheless, an attempt was made to discard apparent data outliers. The remaining stress data were analysed by linear fitting of the trends with depth, which results in the following relations for the vertical and horizontal stress components:

$$\sigma_v = 0.127z$$

$$\sigma_H = 0.113z$$

$$\sigma_h = 0.069z$$

where all stresses are in MPa and z is the depth below ground surface in metres.

The obtained stress gradients are relatively high, and may be considered an upper limit of the stress gradient. The present analysis assumes a zero intercept of the major horizontal principal stress at the ground surface (Figure 5-29). If a different intercept is assumed, the stress gradients would be lower. However, the former model version based on all available stress data from the site estimated excessive major horizontal principal stresses of about 4 MPa close to ground surface.

Other indicators on state of stress

There is no significant core disking in borehole KFM01A. However, the decrease in P-wave velocity along the borehole below approximately 550 m (Figure 4-51) indicates a slight influence of the stresses on the sampled core due to microcracking caused by stress relief. Once strength properties of the rock are determined, it may be possible to assess the magnitude of the stress.

In a previous stress model, /Carlsson and Christiansson, 1987/ concluded that there was agreement between the orientation of the major principal stress and the dominant foliation/schistosity trending NW-SE. Because the structural orientations are similar in the model area, it can be assumed that the stresses are rather evenly orientated in the area. The possible local influence on the state of stress caused by fracture zones has not yet been assessed due to lack of structural information.
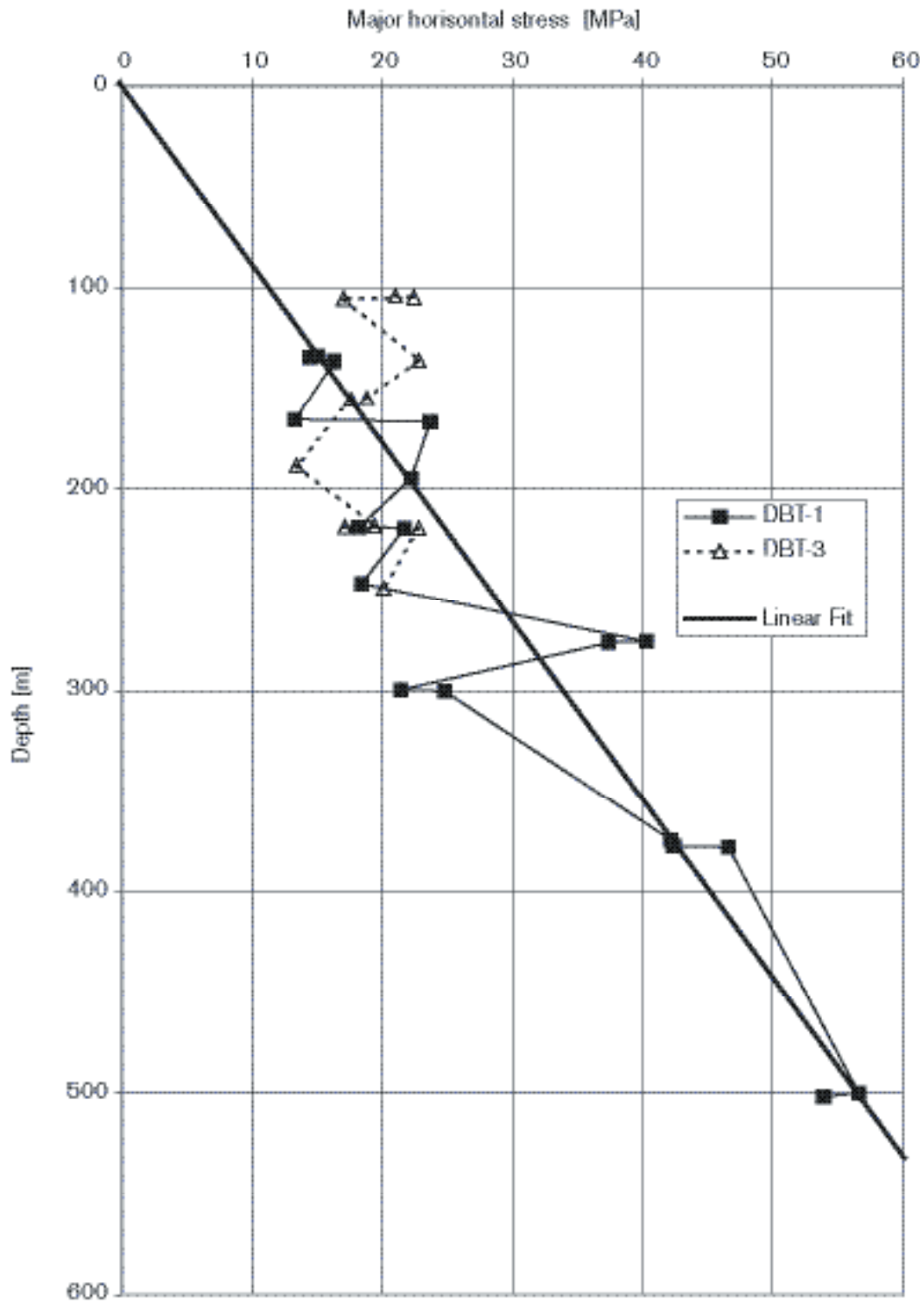
Figure 5-29. *Maximum principal stress based on overcoring technique in DBT-1 and DBT-3 /SKB, 2002a/. The re-evaluation of overcoring results is also shown as a linear fit /Perman and Sjöberg, 2003/*

The linear fit of stress versus depth diagrams presented by /Perman and Sjöberg, 2003/ is a simplification compared to earlier interpretations /Carlsson and Olsson, 1982; Carlsson and Christiansson, 1987; Christiansson and Martin, 2001/. Earlier works were focused more on the "stress jump" under a possible sub-vertical fracture zone located at 320 m in borehole DBT-1. No similar structure was found in the borehole KFM01A, so the possible extrapolation of the older hypothesises towards the south from the older boreholes is, so far, very uncertain. On the other hand, the first drillings (core and percussion drilling) at the site show a significant frequency of horizontal fractures close to the surface in association with high transmissivity. The possibility that these conditions are produced by high stresses has to be further explored in later model versions. The current interpretation of the stress state at the site is given in Chapter 7.

5.2.4 Mechanical properties

The analysis of the primary data of fracture frequency and orientation, number of fracture sets and RQD summarised in Figures 4-38 and 4-52 suggests the need of a finer sectioning of borehole KFM01A into homogeneous sections compared to that proposed in Figure 4-38. From a rock mechanics point of view, this implies that the borehole is divided into 9 sections. This decision was taken to highlight the difference between fractured rock and background rock mass of higher quality that otherwise would be hidden by averaging processes.

There is not yet any geophysical logging available from the borehole, thus a full "single hole interpretation" of the geo-mechanical conditions is not available for model version 1.1. However, the RMR and Q-loggings confirm the presence of poorer rock in association with the fractured sections in the borehole (Figure 4-52 to 4-54), one of which agrees with the zone NE0061 resulting from the geological modelling that would cross the borehole at 664 m depth. According to the geological model, borehole KFM01A is completely drilled through rock domain 29.

Empirical estimates using BOREMAP data from KFM01A

As illustrated in Section 4.6, two empirical classification systems were used by /Lanaro, 2004/ for the purpose of determine the mechanical properties of the rock mass along borehole KFM01A: the Rock Mass Rating (RMR) /Bieniawski, 1989/ and the Rock Quality Index (Q) /Barton et al, 1974/. The methodology for empirical evaluation of the mechanical properties of the rock mass suggests the use of certain relations between RMR and Q and the following mechanical properties of the rock mass: i) deformation modulus; ii) Poisson's ratio; iii) uniaxial compressive strength; iv) cohesion, and v) friction angle /see Andersson et al, 2002b; Röshoff et al, 2002/.

Deformation modulus of the rock mass

The deformation modulus is calculated, from RMR, according to the relation provided by /Serafim and Pereira, 1983/. For each 5 m core section, different values of the RMR-ratings and Q-indexes can be assigned based on the geological information. Assuming for a section the average ratings and indexes, the mean deformation modulus Emm of rock mass can be determined (Figure 5-30). The variation of the mean with depth will mirror the spatial variability of the parameters. If instead of the mean RMR-ratings and Q-indexes, the minimum and the maximum are respectively combined in the most favourable and unfavourable fashion, the possible minimum and maximum values of the deformation modulus can be obtained as plotted in Figure 5-30. These extreme values are used for the discussion of the uncertainty in the deformation modulus determination.

In Figure 5-30, the E_m obtained from RMR does not experience the same sharp variations as E_m obtained from Qc does. Moreover, it can be observed that both methods tend to give values larger than the Young's modulus of the intact rock, which is used as cut-off value. The mean E_m from RMR varies between 45 and 75 GPa (Table 5-27), whereas the mean E_m from Qc extends from 25 to 75 GPa (Table 5-28). However, even if independently obtained, the mean values from the two methods seem to agree rather well as shown in Figure 5-30 (right), especially for the sections of lower rock quality.
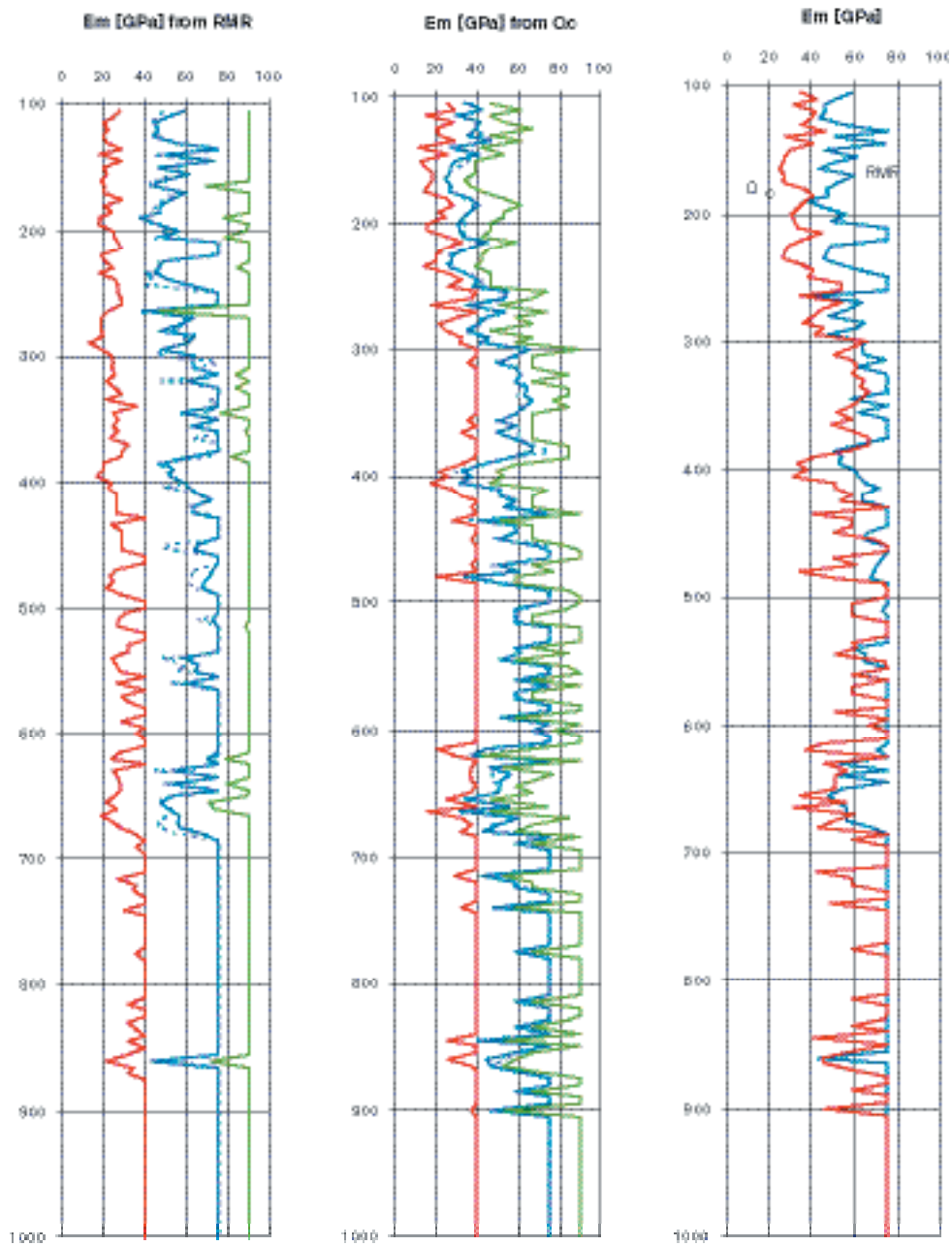
Figure 5-30. *Variation with depth of the deformation modulus of the rock mass obtained from RMR and Qc, respectively /Lanaro, 2004/. Minimum, average, most frequent and maximum values are plotted in red, blue, dashed blue and green, respectively. The third diagram compares the mean values of the deformation modulus obtained with the two methods. The values are given every 5 m.*

222

Table 5-27. Statistics of the mean deformation modulus of the rock mass, Emm, obtained from RMR for certain intervals of core length /Lanaro, 2004/. Inside each interval, Emm is determined every 5 m.

Depth [m]	Emm minimum [GPa]	Emm mean [GPa]	Emm frequent [GPa]	Emm maximum [GPa]	Emm standard deviation [GPa]
105–155	44	55.2	50.7	75	11
155–200	37.4	48.7	47.6	59.8	6.6
200–265	39.3	61	63.1	75	14.4
265–300	47.4	57.9	61.1	64.3	7.5
300–385	49.9	68.9	75	75	8.1
385–410	52	58.4	59.2	65.2	5.5
410–650	52.3	71.1	75	75	6.5
650–685	47.3	58.7	56.4	75	9.5
685–1000	42.9	74.5	75	75	4

Table 5-28. Statistics of the mean deformation modulus of the rock mass Emm obtained from Qc for certain intervals of core length /Lanaro, 2004/. Inside each interval, Em is determined every 5 m.

Depth [m]	Emm minimum [GPa]	Emm mean [GPa]	Emm frequent [GPa]	Emm maximum [GPa]	Emm standard deviation [GPa]
105–155	27.3	35.9	35.2	46.4	6.5
155–200	24.8	31.3	30.4	40.2	5.6
200–265	26.4	37.1	34.3	54.3	9
265–300	35.8	46.7	44.6	65.4	9.9
300–385	49.3	59.4	58.5	66.9	5.5
385–410	31.1	38.8	37.2	51.1	7.9
410–650	34.2	61.6	58.5	75	12.1
650–685	31.2	49.7	50	75	15.3
685–1000	40.5	69.7	75	75	10

Poisson's ratio of the rock mass

The Poisson's ratio of the rock mass can been related to the Poisson's ratio of the intact rock by means of the ratio between the deformation modulus of the rock mass and that of the intact rock. Thus, the calculated values strongly depend on the quality of the obtained deformation modulus of the rock mass. In Table 5-29, an estimation of the Poisson's ratio is given for 9 borehole sections. These are determined according to the mean values of the deformation modulus obtained from RMR and Qc.

Table 5-29. Estimates of the Poisson's ratio of the rock mass based on the mean rock mass deformation moduli obtained from RMR and Qc values.

Depth [m]	ν from Em-RMR	ν from Em-Qc
105–155	0.18	0.11
155–200	0.16	0.10
200–265	0.20	0.12
265–300	0.19	0.15
300–385	0.22	0.19
385–410	0.19	0.12
410–650	0.23	0.20
650–685	0.19	0.16
685–1000	0.24	0.22

Uniaxial compressive strength of the rock mass

The uniaxial compressive strength of the rock mass can be calculated from the values of RMR by means of the Hoek and Brown's criterion /Hoek and Brown, 1997/. For comparison with the values obtained from RMR, Q_c could also be assimilated to a compressive strength parameter. However, in this case some physical limits have to be assumed when Q_c becomes larger than the values of uniaxial compressive strength of the intact rock in Figure 5-31.
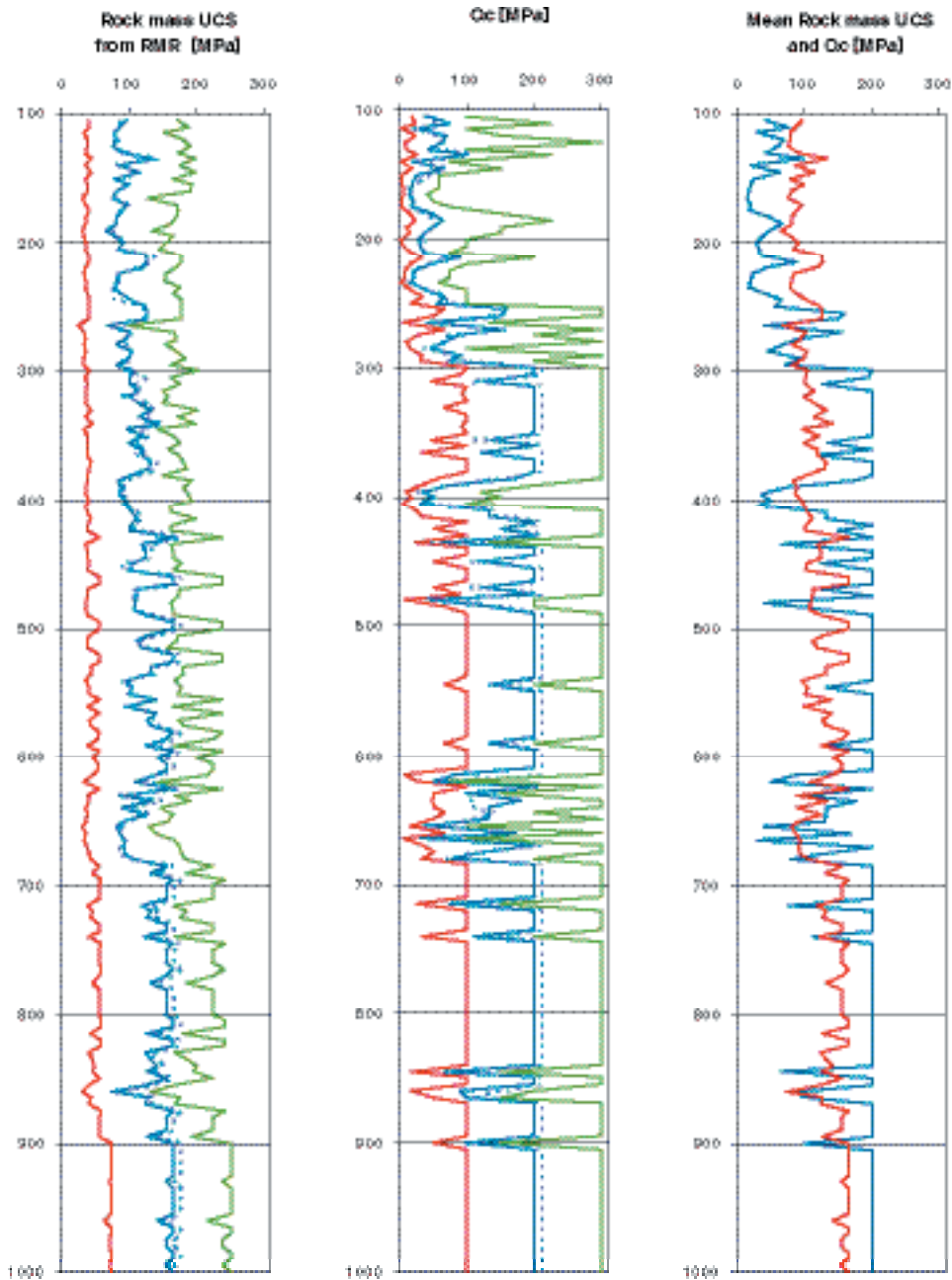
Figure 5-31. *Variation of the uniaxial compressive strength of the rock mass and of Qc with depth. Minimum, mean, most frequent and maximum values are shown in red, blue, dashed blue and green, respectively. In the third diagram, the mean values of UCS and Qc are compared. The values are given for 5 m core length.*

Cohesion and friction of the rock mass

The strength of the rock mass can be quantified in terms of equivalent cohesion and friction angle for a certain level of confinement. By linear approximation of Hoek and Brown's criterion /Hoek and Brown,1997/, the strength of the rock mass can be described in terms of equivalent cohesion c' and friction angle ϕ'. Another set of equations is provided together with Q for evaluating the "frictional and cohesive components" FC and CC of the rock mass /Barton, 2002/.

The values of the rock mass friction angle and cohesion from RMR in Figure 5-32 are obtained for confining pressure between 10 and 30 MPa. The friction angle slightly decreases in average with depth from about 36° to 32°. On the other hand, the rock mass cohesion increases on average with depth from about 20 MPa to up to 48 MPa due to the effect of the increasing rock quality. The
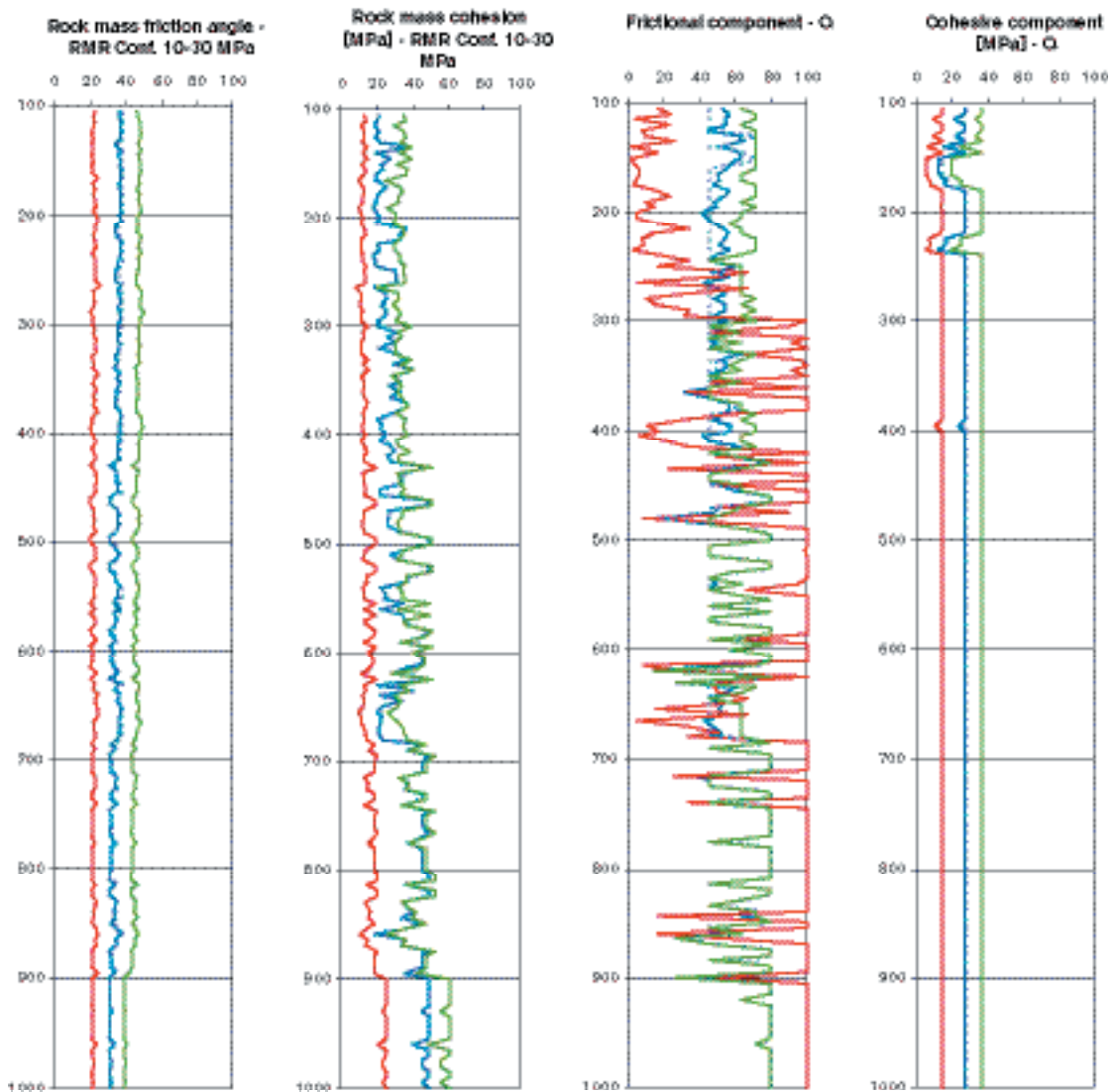
Figure 5-32. *Variation of the rock mass friction angle and cohesion from RMR, and frictional and cohesive components from Qc for borehole KFM01A under stress confinement /Lanaro, 2004/. The minimum, mean, most frequent and maximum values for each 5 m of borehole length are shown in red, blue, dashed blue and green lines, respectively.*

frictional component, which should apply for low stress confinement, spans from about 45° to 70°, with very sudden variations. The cohesive component is almost constant with depth at about 27 MPa, which corresponds to the cohesion of the intact rock for the specified stress level.

Empirical estimates using surface information

The results of surface logging presented in Section 4.6 are summarised in Table 5-30. Based on present levels of data collection, the more jointed areas in rock domain 29 (termed 29b) resemble the character of the relatively more fractured zones in the core. The more massive rock seen in north-eastern outcrops, closer to the plastic deformation formation (rock domain 32), resembles the 'back-ground' character of the generally quite massive core.

Table 5-30. A summary of surface logged mean Q-values in and close to the Forsmark candidate area, with attempted extrapolation to reference depths of 250 to 500 m, assuming unchanged jointing /Barton, 2004/. Depth (or stress) increases have a positive effect on E_{mass}, while porosity has a negative effect. /Barton, 2002/.

Formation/Depth (Surface/Core)	Ranges of Q_{min}	Maximum Q_c-range (σ_c = 220–310 MPa) ($Q_c = Q_x \sigma_c/100$)	E_{mass} (GPa)
29(a) surface	11.6 to 16.6	25.5 to 51.5	29–37
Estimation for 29(a) 250–500 m (*)	43 to 58	94.6 to 179.8	61–79
29(b) surface	2.8 to 7.3	6.2 to 22.6	18–28
Estimation for 29(b) 250–500 m (*)	8.5 to 27	18.7 to 83.7	46–63
17 surface	10.1		
Estimation for 17 250–500 m (*)	37		
18 surface	6.0–10.6		
Estimation for 18 250–500 m (*)	19–41		
32 surface	2.9–3.1		
Estimation for 32 250–500 m (*)	6–7		
KFM01A–B massive 300–400 m (*)	73.0	160.6 to 226.3	74–79
KFM01A–B massive (iv) 400–500 m(*)	65.3	143.7 to 202.4	74–83
KFM01A–B fracture zone FZ 2, 265–297 m (*)	11.5	to 35.7	50– 54
KFM01A–B fracture zone FZ 3, 385–407m (*)	19.0	41.8 to 58.9	56–58

* There is an approximate depth correction for E_{mass} and V_P.

Empirical estimates using data from Q-logging of KFM01A–B

The deformation modulus of the rock mass is determined according to /Barton, 2002/. Some depth corrections to take into account porosity and P-wave velocity have also been applied /Barton, 2002/. The depth corrections result in a 10–30% increase of the tabulated estimates of the deformation modulus compared to the uncorrected ones (Table 5-31).
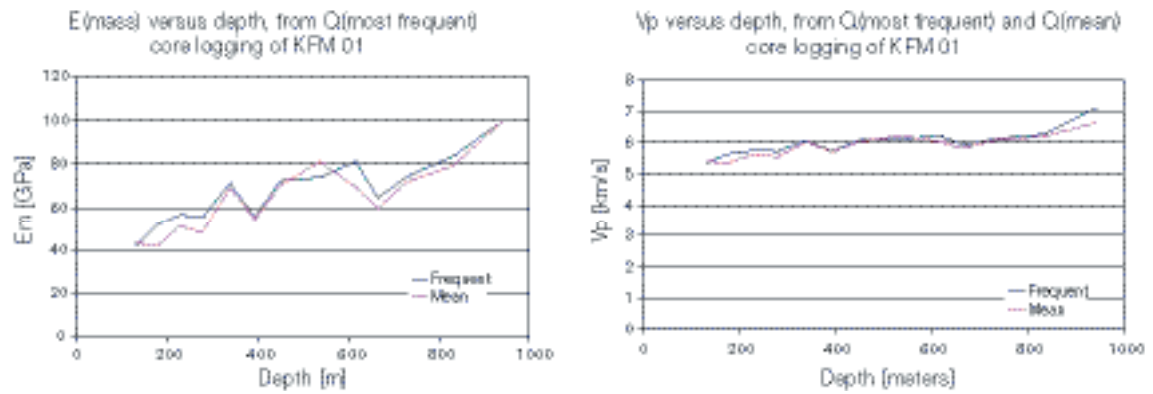
Figure 5-33. *Variation of the deformation modulus of the rock mass and the expected P-wave seismic velocity Vp obtained from direct Q-core logging of borehole KFM01A with depth /Barton, 2003/.*

Table 5-31. Deformation modulus of the rock mass Em obtained from direct core Q-logging of borehole KFM01A. A cut-off is applied to keep the values of Em below 100 GPa /Barton, 2003/.

Depth [m]	Em most frequent [GPa]	Em mean [GPa]
134	42	43
183	52.1	42.3
232	56.7	50.9
281	55.4	48.2
341	71.3	69.2
396	55.8	54.5
452	72.4	70.3
541	74.1	81.3
618	81.3	69.7
667	64.6	59.8
734	74.7	72.4
834	83.8	79.4
943	100	100

Comparison of deformation modulus from different methods

The ranges of variation of the mean deformation modulus in Table 5-27, Table 5-28 and Table 5-31 are also plotted in Figure 5-34. It can be noticed that the mean value of the deformation modulus increases with depth independent of the method used for its calculation. In the same fashion, the deformation modulus increases for the sections of borehole with lower fracture frequency and higher RQD. The values obtained through Qc are in general lower than those obtained from RMR, which experiences smaller variation between the section with better and poorer rock. The figure shows that the range of variation of the deformation modulus is wider for the values calculated from Qc. However, considering the slight methodological differences of the BOREMAP logging compared to the direct Q-logging performed on the core, the results show a very good agreement and support each other.

As an illustrative example, the results from BOREMAP logging and direct Q-logging are presented together in Figure 5-35. It is noticeable that all depth intervals show a more or less bi-modal distribution; one group that clusters close to the assessed average for the intact rock, which is used for cut-off, and the other group with a lower average. The first group represents sections with very low fracture frequency.
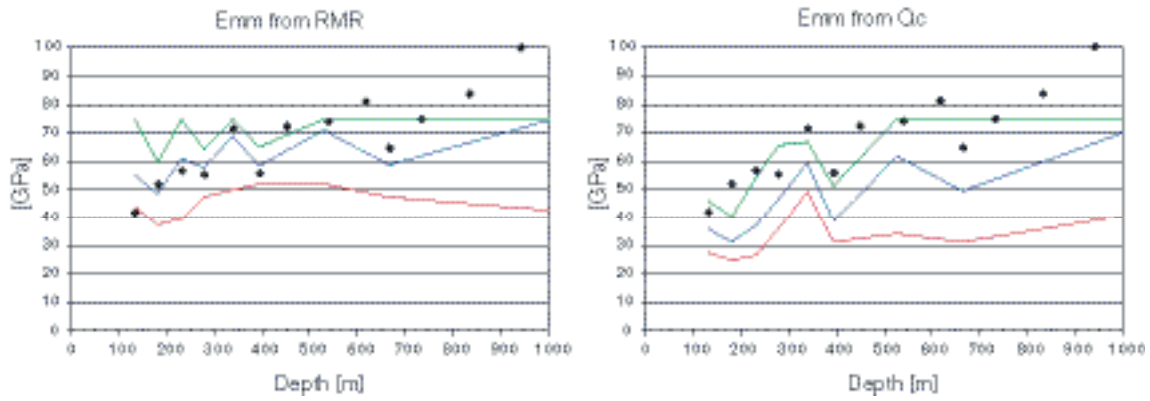
Figure 5-34. *Range of variation of the mean deformation modulus Emm obtained from RMR and Qc logging of BOREMAP /Lanaro, 2004/ (coloured lines) compared to direct Q-logging data /Barton, 2003/ (black rhombi). The ranges for nine core sections and data are given in Table 5-27 and Table 5-28.*
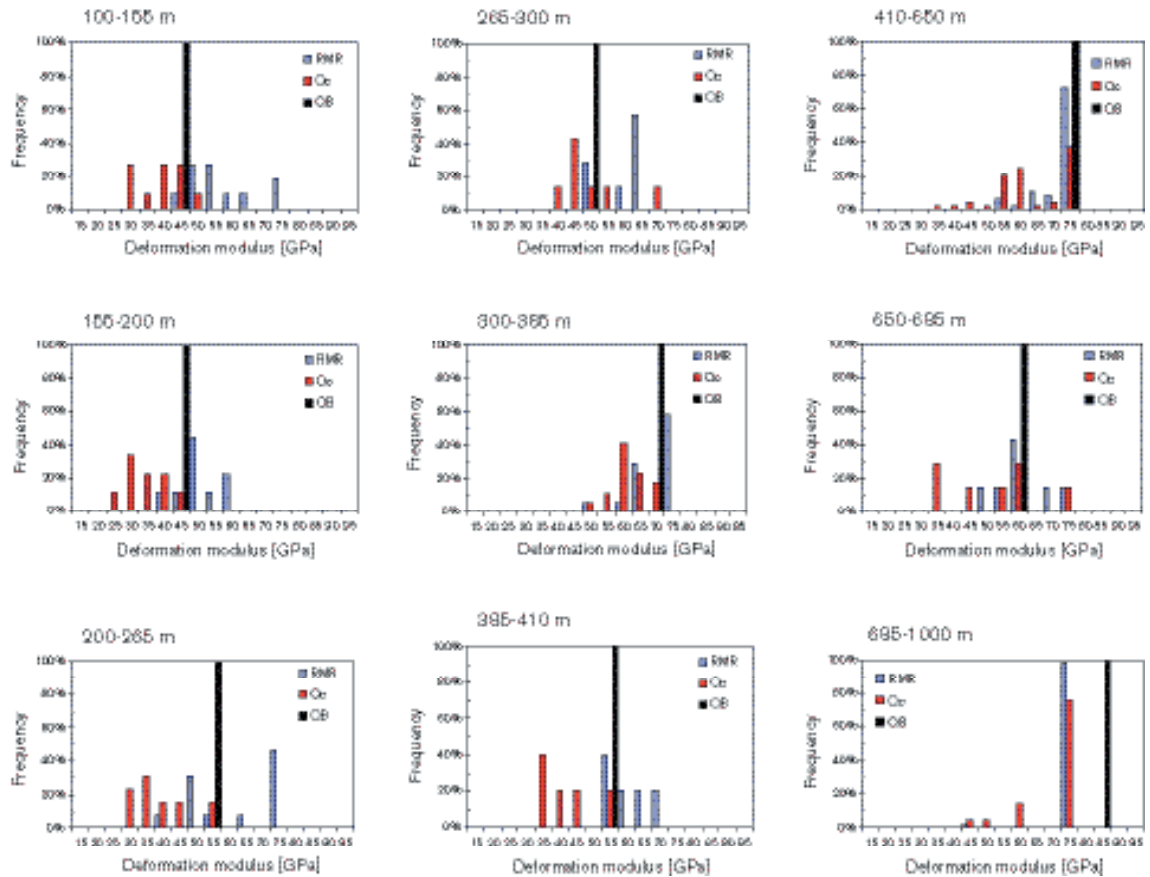
Figure 5-35. *Histograms of the mean deformation modulus Em from RMR and Qc from BOREMAP-logging /Lanaro, 2004/ and from direct Q-logging (QB) /Barton, 2003/) at different depths.*

228

Evaluation of data from the power plants and SFR

The documentation of the discharge tunnel from Power Plant Units # 1 and #2 (Figure 4-61) did not contain test results on the rock mechanics properties. Based on the measured seismic velocities, the rock mass Young's modulus can be estimated by means of empirical relations given by /Barton, 2002/ to be: i) within 20–50 GPa in the average granite west of the regional Singö fault zone, ii) 3–10 GPa within the Singö fault zone and iii) 15–30 GPa in minor fractured zones in the granite, as well as in the gneissic rock east of the Singö fault zone. As reported in Section 4.6.5, the deformation modulus of the rock mass at SFR had been estimated to be about 20–40 GPa and 2–43 GPa, depending on the use of RMR_{79} /Bieniawski, 1979/ or the Q-system /Barton et al, 1974/ values. An average deformation modulus of 20 GPa and Poisson's ratio of 0.08 were assumed. These data concern the silo dome at some 70–90 m depth and agree reasonable well with estimates from the discharge tunnel located at a similar depth.

Estimation of the mechanical properties of the rock domains

Section 5.2.4 offers a summary of all the performed determinations of the rock mechanics properties of the rock mass. All borehole data available concern rock domain 29, while surface and tunnel mapping give sparse information on rock domains 17, 18, 32 and 33 (Table 5-30). Due to the scattering of this information, only the evaluation of mechanical properties of rock domain 29 is presented in Chapter 7. The parameters for this domain are inferred based on the comparison of the results from BOREMAP logging, Q-core logging, surface Q mapping and earlier estimation of the mechanical parameters from construction works in Forsmark. However, expert judgement has been a major input of the parameter determination mainly due to the scarce information with respect to the spatial geological variability.

The conclusions of the rock mechanics interpretation of the data available are summarised as follow:

* There is a general influence of depth on the fracture frequency that mirrors into increasing values of the mechanical properties of the rock mass with depth. A sharp difference can be observed for the rock above and below the depth of 400 m where, for example, the estimated compressive strength of the rock mass increases from about 50 MPa to over 150 MPa at depth.

* Surface mapping suggests the presence of an edge zone around rock domain 29 characterised by poorer rock quality than the more competent central core zone.

* Homogeneous rock mass is often characterised by prevalent good rock quality, and localised clustering of fractures that reduces the quality. This is shown for rock domain 29 in Figure 5-35 where the deformation modulus is on average high at all depths (45–80 GPa) with some minimum values of 25 GPa.

* The most remarkable feature at depth can be observed between 600 and 700 m depth, where a minor deformation zone is likely to be present (NE0061).

* The poorest rock in the investigated boreholes and areas occurs at the Singö Fault Zone (ZFMNW0001) where the deformation modulus was estimated to be about 3–10 MPa. These values could be used as an estimation of the properties of the deformation zones in the Site Descriptive Model version 1.1.

* As Figure 5-35 shows, the empirical methods adopted seem to be rather consistent with each other and strengthen the property estimations given in this section.

5.2.5 Evaluation of uncertainties

Confidence of the rock quality from BOREMAP logging

When applying the empirical classification systems for characterisation of the rock mass, the uncertainties in the geological and rock mechanics data become reflected in the uncertainties of the Q-indexes and RMR-ratings and thus in the final Q and RMR values. The uncertainty on a single parameter can vary depending on the acquisition technique, subjective interpretation or size of the sample population. However, uncertainty can also derive from the way the values of the indexes and ratings are combined. One cannot exclude that the representative value of Q or RMR for a certain section of borehole may result from the most unfavourable combination of the values of each index

or rating. In addition, the empirical systems used were not originally developed for characterisation purposes. Additional uncertainties are to be related to the origin of the empirical formula for determine rock quality and derived mechanical properties.

On top of the uncertainties regarding the characterisation methods, the fact that borehole KFM01A and B, the surveyed outcrops and the experiences from earlier excavation works may not be representative of all the rock mass at the site also affects the uncertainty of the rock mechanics model. For example, an estimation of the properties of the fracture zones can only be provided by excavation logging through the Singö Fault Zone, by the minor fractured zones intercepted by borehole KFM01A and B and identified on the surface. In the following sections, more specific considerations are made for the main tools of the rock mechanics analysis. These considerations are the background of the parameters given in Chapter 7 as representative for the rock mass at the site.

Uncertainties in the stress model

It is difficult to state, with certainty, which of the reported measurements is reliable. There are few clear trends in the data, even when cross-correlating the different analyzed parameters. An attempt has, however, been made to discard some of the measurements to arrive at probable estimates on the measured stress state. Only the vertical and horizontal stress components were considered in this task. Some measurements were discarded based on quality criteria and hypotheses. The amount of unexplained strain is high for nearly all measurements in DBT-1 and DBT-3. The error values are particularly high for measurements below 250 m depth.

Uncertainty in RMR and Q determination

The uncertainty on Q and RMR values can be correlated to the maximum and minimum occurring value of each Q-index or RMR-rating used for the BOREMAP logging of borehole KFM01A. This means that, for every borehole section, the range of possible variation of the indexes and ratings was identified based on the raw data (see Figure 4-53 and Figure 4-54). In this way, a range of physically possible values of Q and RMR is obtained and, based on them, a range of possible mechanical properties.

Uncertainty in the assessment from surface mapping

The outcrop assessment as a base for estimating rock mass quality with depth assumes that the surface is to a realistic degree representative to the deeper seated rock mass. An alternative interpretation, whose origin is derived from examination of the nuclear power plant excavations and interpretations given at that time by /Carlsson, 1979/ is that late-glacial sub-horizontal, sediment-filled major discontinuities underlay some areas of the candidate site (Figure 4-60). Photographs of the power plant excavations, and the experience of exceptionally high permeabilities in certain locations in the upper 40–50 m, at least in the vicinity of borehole KFM01A, have a certain consistency. The sub-horizontal features under discussion, perfectly exposed in some walls of the power plant foundations and also found in the fist boreholes, cause significant difficulties in extrapolating empirical characterisation from surface exposures to depth.

With this conceptual model for certain areas of the candidate site, the four to six fracture set trends mapped at some cleaned drill-site locations (e.g. drillsites 2 and 3) could perhaps be explained by late-glacial fracturing of 'rock mass pavements' that could have occurred above assumed major, debris-filled, hydraulically-fractured discontinuities. How widespread this alternative model is in reality is not known.

Uncertainty in deformation modulus determination

The uncertainty intervals for the deformation modulus calculated from Qc are much smaller than those calculated from RMR (Figure 5-30). In most cases, the maximum possible deformation modulus suggested from the RMR based method is the maximum physically possible value of 90 GPa. On the other hand, even if the deformation modulus from RMR is larger than that from Qc, the minimum possible deformation modulus obtained from RMR is approximately as large as that obtained from Qc. This indicates that RMR is more sensitive than Qc to effects of the uncertainty as to the indexes and ratings, and spatial variability. The estimation of the deformation modulus from

BOREMAP logging and Q-logging seems to give the same results in terms of mean values, except for the deepest sections where the deformation modulus from Q-logging was allowed to reach values of 100 GPa.

5.3   Thermal properties modelling

5.3.1   Modelling assumptions and input from other models

Components of the Thermal Site Descriptive Model

The temperature and temperature distribution are central for design of the repository and also have an influence on the rock mechanical stability, the groundwater flow, biological activity and chemical reactions.

The thermal site descriptive model should include the temperature distribution, boundary conditions and the thermal properties of the rock mass. The boundary conditions are described by geothermal heat flow, and by temperature and climatic conditions at the ground surface. The prediction should focus on variations in rock mass properties, for intact rock as well as different kinds of discontinuities, on a canister deposition scale of 1–10 m, and the boundary conditions /Sundberg, 2003a/.

The thermal site descriptive model contains the following parts:

- Geometrical framework.
- Property distribution.
- Spatial distribution.
- Description of uncertainties.

Required prediction range

The required prediction range depends on the purpose of the modelling. The properties in the model need only be predicted within the appropriate range of uncertainty. The demands on the prediction range of a property are for example lower for the modelling of natural temperature conditions than for the design distance between canisters. The demands are also dependent on the absolute level of the thermal properties. The requirements on the prediction range are higher if the level of a property is close to the suitability indicator for the siting of a repository. The suitability indicators and criteria are defined in /Andersson et al, 2000/. /Andersson, 2003/ discusses the assessment of uncertainty in the site descriptive modelling.

If the thermal conductivity is so low that it may influence the distance between the canisters and the size of the investigation area, the demands on accuracy of the model and the property distribution are higher. In practice, this means that the investigation programme becomes more extensive.

Interaction with other disciplines

The site descriptive model consists of models produced in a number of disciplines. These models are developed jointly and iteratively, and refined versions are produced at the different stages of the site investigation. The geological model and, to a minor extent, the hydrogeological model contain valuable information for the development of the thermal model. Especially, the geometrical framework and rock type description/distribution is of interest.

5.3.2   Thermal property modelling

Model domains

The different rock domains are evaluated in Section 5.1.2. In Figure 5-36, these rock domains are illustrated together with locations of samples for thermal properties analysis (calculation from modal analysis and measurement).
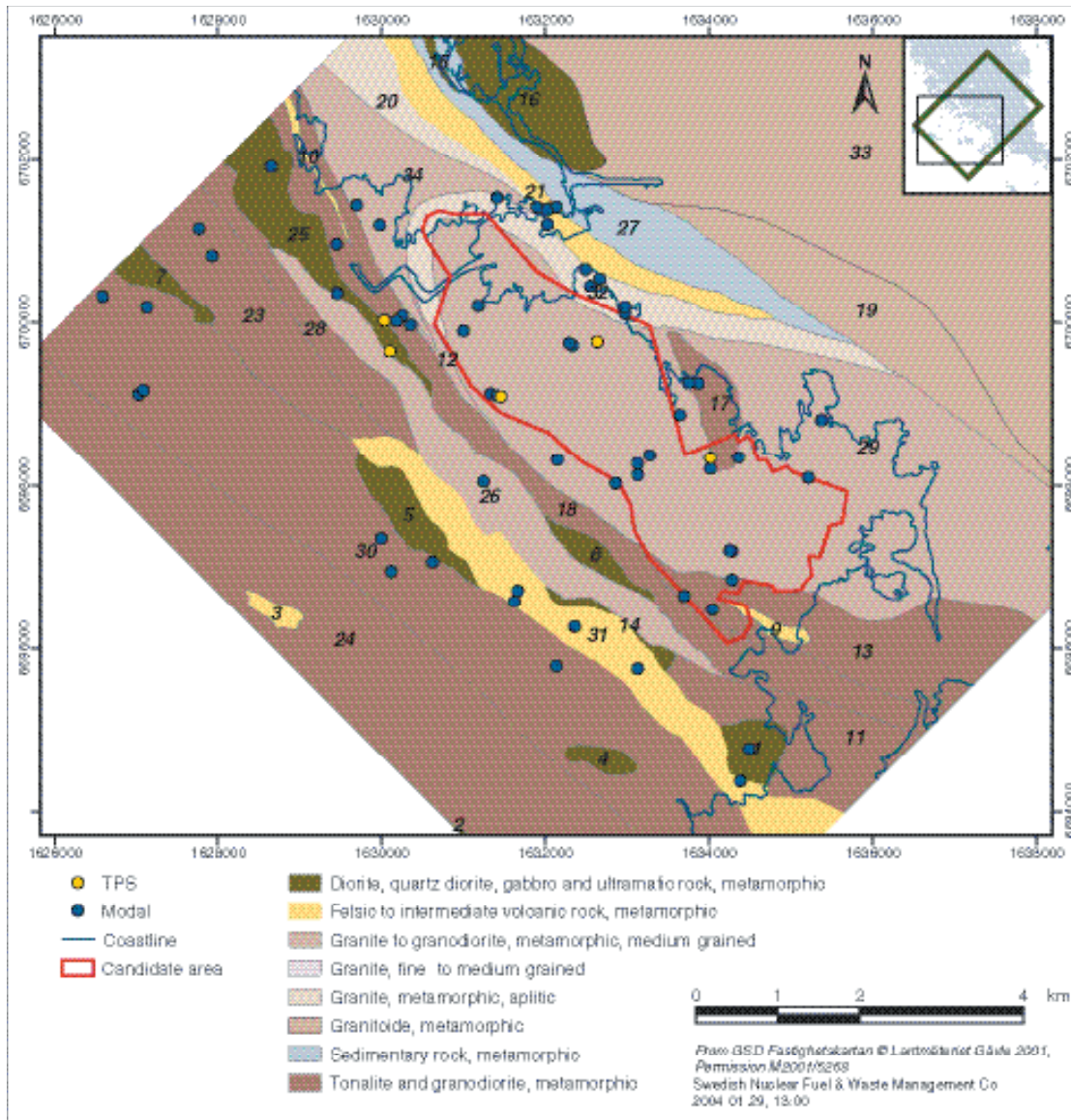
Figure 5-36. *Rock domains together with the location of samples for measurement and calculation of thermal properties.*

Thermal properties for model domains

In Table 5-32 the thermal properties for different rock domains are summarised, based on calculations from modal analysis with the SCA method. For some of the domains, the results are quite uncertain and may be seen as indications only, primarily due to few samples but also because of uncertainties in chemical composition and thermal data for some minerals. The sampling has not been made in order to be representative for the different rock units or rock domains. Therefore, the mineral compositions and the calculated thermal conductivities are not necessarily representative to the rock domains.

Table 5-32. Thermal conductivity of samples from different rock domains, calculated from the mineralogical compositions with the SCA-method. Rock domains with few samples are very uncertain. Please observe that the mean values only represent the mean of the rock samples and not necessarily the different rock domains.

Rock domain	Thermal conductivity (SCA) W/(m·K)		Number of samples
	Mean value	Stdev	
1	(3.89)	–	1
9	(3.64)	–	1
13	2.98	0.286	3
17	2.73	0.216	6
18	3.04	0.314	4
21	2.70	0.578	3
23	(2.64)	0.242	2
25	(2.16)	0.275	2
26	(3.46)	0.011	2
29	3.35	0.322	20
30	3.02	0.350	8
31	2.83	0.389	7
32	3.04	0.335	8
34	3.02	0.574	4
All samples	3.06		71

Domain 29 and domain 17 dominate the candidate area and are therefore further evaluated below.

Rock domain 29

Statistical tests were performed to decide if the data from domain 29 follow a normal or a lognormal distribution. Figure 5-37 indicates that the data from domain 29 are not normally distributed. A test for normally distributed data (Anderson-Darling test) results in a p-value of only 0.03, i.e. the assumption of a normal distribution can be rejected at a 5% α-level. The p-value for test of log-normality is even lower. However, these results are highly influenced by the outlier in the lower left corner of the graphs in Figure 5-37. Generally, outliers can have one of three causes /Helsel and Hirsch, 1991/:

- a measurement or recording error,

- an observation from a population not similar to that of most of the data,

- a rare event from a single population that is quite skewed.

The outlier in Figure 5-37 is probably a result of the second cause. In contrast to the other observations, the outlier is an Amphibolite and from experience it is known that values of thermal conductivity (SCA) for this type of rock are highly uncertain due to differences in chemical composition. The outlier is therefore excluded from the analysis.

When the outlier is excluded, data will fit both a normal distribution and a lognormal distribution, according to Figure 5-38 (these hypotheses cannot be rejected). Smaller Anderson-Darling values indicate that the distribution fits the data better and consequently a lognormal distribution models the data slightly better than a normal distribution.

In Table 5-33, the mean thermal conductivity is estimated, together with the 90% confidence interval for the mean. The first method used (Methods of Moments, MM) is the traditionally used method for normally distributed data. The second method is the Minimum Variance Unbiased Estimator (MVU) for lognormally distributed data, as described by /Gilbert, 1987/. The corresponding confidence interval is estimated by Land's statistically exact method /Gilbert, 1987/. The third method used is the Maximum Likelihood (ML) method, as implemented in the statistical software package Minitab.
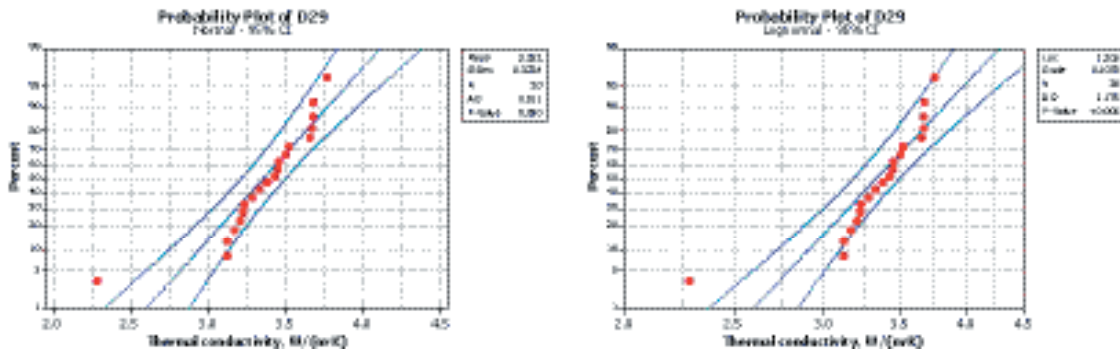
Figure 5-37. *Normal and lognormal probability plots of all data from rock domain 29 with 95% confidence intervals.*
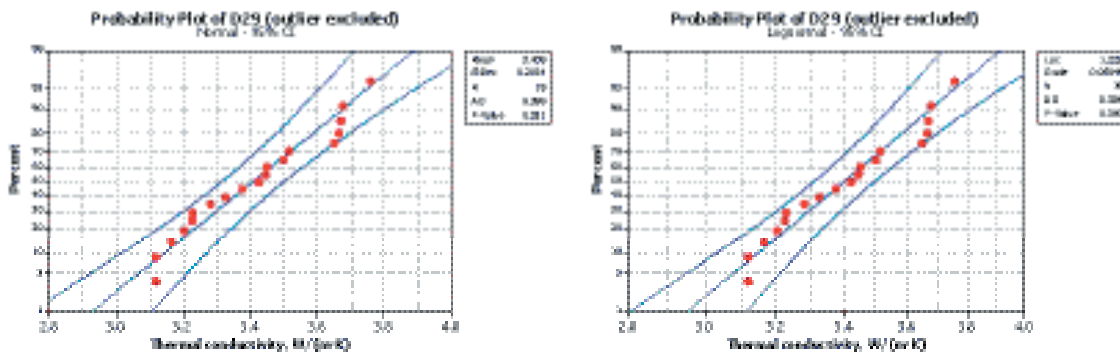
Figure 5-38. *Normal and Lognormal probability plots of data from rock domain 29 with 95% confidence intervals (outlier excluded).*

Table 5-33. Estimation of mean and confidence intervals for the mean (rock domain 29). Three different methods are used. Values in parenthesis include the outlier. All units in W/(m·K).

Method	Estimation of mean value	90% confidence limits for the mean value	
		Lower	Upper
MM	3.41 (3.35)	3.33 (3.23)	3.49 (3.48)
MVU	3.41 (3.35)	3.33 (3.22)	3.49 (3.50)
ML	3.41 (3.35)	3.33 (3.23)	3.49 (3.49)

As illustrated in Table 5-33, the three methods give almost identical results.

Rock domain 17

Only six data points are available from Domain 17. Similar to domain 29, test of normality and lognormality were performed. The Anderson-Darling test indicates that a lognormal distribution fits the data best (Figure 5-39). A lognormal distribution was therefore used to model the data.
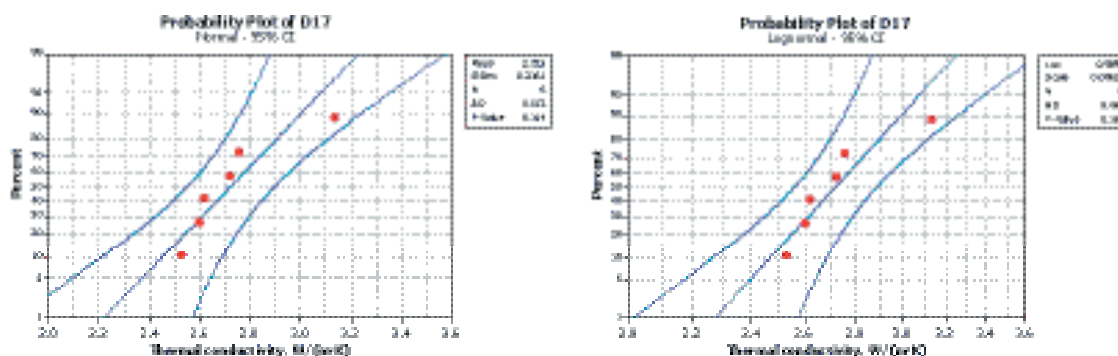
Figure 5-39. Normal and lognormal probability plots of data from rock domain 17 with 95% confidence intervals.

Mean and confidence intervals for the mean was estimated with the same methods as for domain 29, see Table 5-34. The three methods give similar results.

Table 5-34. Estimation of mean and confidence intervals for the mean (rock domain 17). Three different methods were used. All units in W/(m·K).

Method	Estimation of mean value	90% confidence limits for the mean	
		Lower	Upper
MM	2.72	2.55	2.90
MVU	2.72	2.56	2.91
ML	2.72	2.60	2.85

Monte Carlo simulation

The two models for rock domains 17 and 29 are visualised in Figure 5-40. Both domains are modelled by lognormal distributions. The variance is similar for both distributions but the mean is different.

Note that the distributions in Figure 5-40 only are valid at the SCA scale, i.e. at the mm-cm scale. If the distributions are to be applied at a different scale, a transformation to the appropriate scale must first be performed.

The two distributions have been combined to illustrate the thermal conductivities that can be expected in borehole KFM01A with the simplified assumption that the composition can be represented as a combination of domain 29 (90%) and domain 17 (10%). In reality, 90% of the core consists of metagranite represented by samples from domain 29 and a complicated mixture of other rock types in the remaining part /Petersson and Wägnerud, 2003/. Monte Carlo (MC) simulation was performed to create a distribution reflecting the expected thermal conductivities in the borehole (Figure 5-41). The distribution was created by 100,000 MC simulation runs.

The distribution in Figure 5-41 is the distribution of thermal conductivity values that can be expected in the borehole with the following assumptions:

- The SCA data for both rock domains (17 and 29) are representative for the borehole.

- 10% of the rock in the borehole consists of rock types represented by rock domain 17 and 90% belong to rock types represented by rock domain 29.

- The scale of measurement is the same as the scale for the SCA data presented above.

The influence of the original distributions in Figure 5-40 is clearly visible in Figure 5-41. The 95% confidence interval for the thermal conductivity data (simulated distribution) is 2.58–3.82 W/(m·K). The mean of the simulated distribution is 3.34 W/(m·K), see Table 5-35. The table indicates that 90% of all thermal conductivity values will exceed 2.98 W/(m·K), i.e. the 10% percentile.
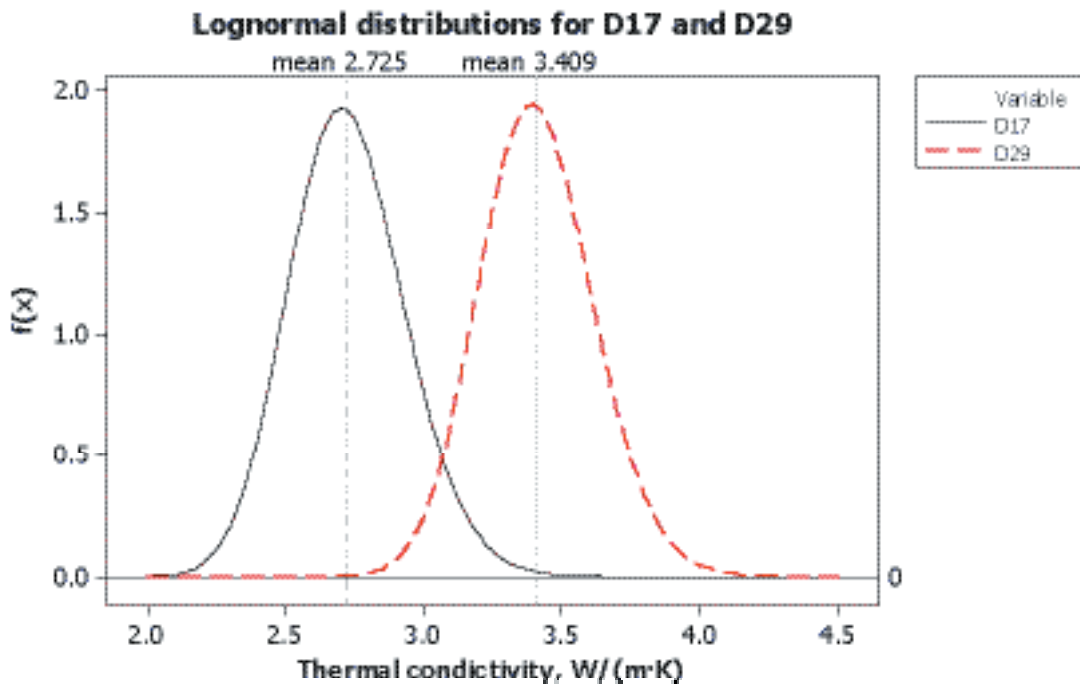
Figure 5-40. *Lognormal probability distributions fitted to data from rock domains 17 and 29.*
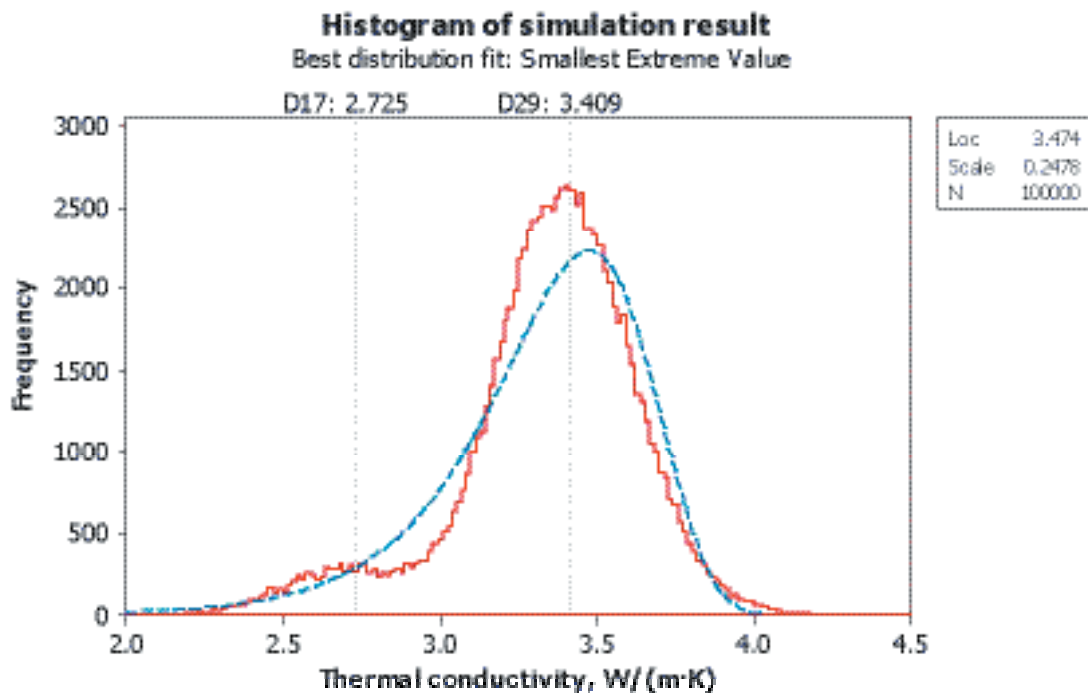
Figure 5-41. *The expected distribution of thermal conductivities (red line) in KFM01A if the rock type distribution is simplified (10% of the rock belong to domain 17 and 90% to domain 29). The blue line is the best fitted distribution.*

236

The Smallest Extreme Value distribution exhibits the best fit to the simulated distribution in Figure 5-41, of the available parametric distributions.

In the actual case, with only two simple distributions, the Monte Carlo simulation is not necessary and only illustrates a possible evaluation method.

Table 5-35. Percentiles and mean for the simulated distribution of thermal conductivities in a borehole. All units in W/(m·K).

Distribution	Percentiles			Mean (median)	Percentiles		
	2.5%	5%	10%		90%	95%	97.5%
Simulated distribution	2.58	2.72	2.98	3.34 (3.37)	3.66	3.74	3.82
Fitted distribution (model)	2.56	2.74	2.92	3.33 (3.38)	3.68	3.75	3.80

5.3.3 Influence of anisotropy

Thermal conductivity, parallel and perpendicular to the sensor, was evaluated from the TPS-measurement described in Section 4.7. The values for the rock were determined approximately by weighting of the measurement result and the thermal conductivity of the insulation (0.04 W/(m·K)).

However, the thermal influence on the TPS measurement has the shape of an ellipsoid-sphere. Measurements made with the sensor parallel or perpendicular to the foliation therefore result in data combining both these two directions. It is possible to evaluate both principal directions with the TPS-method but a special measurement and evaluation technique is necessary. Thus, the values in Table 5-36 comprise a combination of the two directions and do not represent the extreme values.

Measurements with the sensor perpendicular to the foliation should normally give higher values than with the sensor parallel to the foliation because of the initial cylindrical heat flow perpendicular to the sensor. In Table 5-36 one of the five samples gives a significant higher value with the sensor perpendicular to the foliation, which is the opposite that expected. An explanation needs a closer investigation of samples and the details in the measurement technique.

Table 5-36. Influence of anisotropy. Approximately values on thermal conductivity, on samples with foliation parallel and perpendicular to the sensor. The values are evaluated from TPS-measurements made by /Adl-Zarrabi, 2003/, see also text. The measurement result in each direction is influenced by thermal transport in the other direction, see also text.

Sample ID	Thermal conductivity with sensor perpendicular to foliation, $\lambda\parallel$ W/(m·K)	Thermal conductivity with sensor parallel to foliation, $\lambda_\perp$ W/(m·K)	Mean value of thermal conductivity W/(m·K)	Anisotropy factor $\lambda\parallel/\lambda_\perp$
MBS020002B	3.18	2.66	2.92	1.20
MBS020003B	2.22	2.52	2.37	0.88
MBS020004B	3.30	4.10	3.70	0.80
MBS020007B	2.44	2.38	2.41	1.03
MBS020009B	3.52	3.48	3.50	1.01

Anisotropic properties may occur in lineated or foliated rocks (Figure 5-42). In rock domain 29 a lineation, with a moderate plunge towards SE, dominates. The thermal effect of this lineation was not investigated.

Figure 5-42. *Bore core from KFM01A, 778.36–789.75 m. The figure illustrates the geological struc-tures in the rock, such as foliation.*

5.3.4   Comparison between measurements and calculations

Comparisons were made between thermal conductivity determinations by measurements and calcula-tions with the SCA-method on available samples. The results are presented in Table 5-37 and show individual discrepancies, but the mean difference is low. Earlier comparisons indicated that calcula-tions with the SCA-method produced lower values than measured, in the interval 5–8% /Sundberg, 2003b/. No correction was made in the SCA-data above, due to lack of comparable samples.

Table 5-37. Comparison between calculated thermal conductivity with the SCA-method and measured with the TPS-method. Not exact same samples have been used for the different determinations.

		SCA W/ (m·K)	TPS W/ (m·K)	Difference %
PFM001159A	Granite	3.44	3.51	1.9
PFM001159B	Granite	3.20	3.51	8.8
PFM001162A	Tonalite	2.62	2.45	–6.8
PFM001164A	Granodiorite-granite	3.66	3.47	–5.6
				–0.4

5.3.5   Temperature

At the 600 m level the temperature is about 13°C. The temperature gradient increases from about 11°C/km at the depth 400 m to about 14°C/km at about 900 m. The explanation of this could be changes in the thermal conductivity (lower thermal conductivity gives higher gradient at a constant heat flow) or climate changes (changes in the last 200–300 years can be measured down to about 250 m). If changes in thermal rock conductivity are the reason, the actual change in temperature gradient indicates a reduction in thermal conductivity by about 30% at lower depths.

Important climate events are for example a period with lower temperature about 300 years ago and when the candidate area emerged from the sea (about 500 years ago, see also Section 3.2).

The influence of the rock properties and from climate changes on the temperature distribution in boreholes will be further analysed in the next model version.

5.3.6 Evaluation of uncertainties

General uncertainties are described in the thermal site descriptive model /Sundberg, 2003a/. Here only uncertainties connected to the actual data are mentioned.

Measurement of thermal properties

- Uncertainties in measurement techniques. The technique used to determine thermal conductivity perpendicular and parallel to the rock foliation has large uncertainties and was not developed for that purpose. It is possible to evaluate both principal directions with the TPS-method but a special measurement and evaluation technique is necessary. These uncertainties may also influence the determined mean values for the samples. There are also uncertainties in the used terminology. An overhaul of the SKB MD 191.001 is recommended.

- Small number of samples. The small number of measurements for each rock unit gives uncertainties in measured values and low accuracy in the comparison with calculated values.

- Lack of data concerning thermal properties at elevated temperature.

Modelling from mineral content

- Uncertainties in the chemical composition of primarily plagioclase in the investigation area.

- Uncertainties in the representativeness of calculated thermal conductivities for different rock units and domains.

Assigning thermal properties to the rock mass

In this model version, the uncertainties are high for all aspects of this area, as listed in the thermal site descriptive model /Sundberg, 2003a/. However, a general uncertainty is the small-scale variation in thermal properties for rock units and in the up scaling to a larger volume. No attempt to assign thermal properties to fracture zones has been made.

The rock units and domains seem to have anisotropic thermal properties. However, at this stage it is not possible to quantify them.

5.4 Hydrogeological modelling

5.4.1 Systems approach, basic assumptions and input from other models

The hydrogeological model of the Forsmark area is based on four different sources of information. The four sources are: (*i*) mapping of Quaternary deposits and bedrock geology (rock type, lineaments and deformation zones) (*ii*) meteorological and hydrological investigations, (*iii*) hydraulic borehole investigations and monitoring, and (*iv*) hydrogeological interpretation and analysis. The model may be described by means of parameters, which detail:

- the geometric and hydraulic properties of the Quaternary deposits and the crystalline bedrock, and

- the hydrological processes that govern the hydraulic interplay between surface water and groundwater, including groundwater flow at repository depth.

Figure 5-43 illustrates schematically SKB's systems approach to hydrogeological modelling of groundwater flow. The division into three hydraulic domains (soil, rock and conductors) constitutes the basis for the numerical simulations carried out in support for the site descriptive model version 1.1.

Hydrogeological model
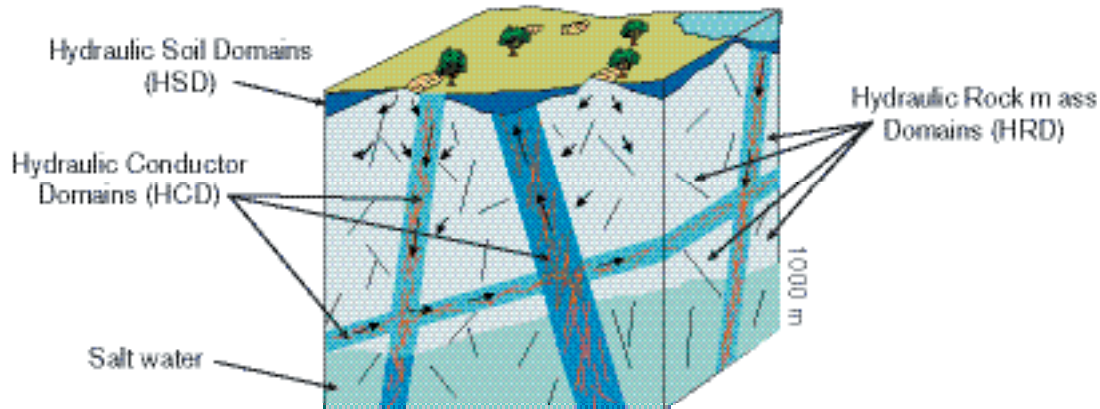
Figure 5-43. *The Quaternary deposits and the crystalline bedrock are divided into separate hydraulic domains representing the Quaternary deposits (Soil, HSD) and the Rock volumes (HRD) between major fracture zones (conductors, HCD). Within each domain the hydraulic properties are represented by mean values or by spatially distributed statistical distributions. Modified after /Rhén et al, 2003/.*

From a hydrogeological perspective, the geological data and interpretations constitute the basis for the geometrical modelling of the different hydraulic domains. Thus, the investigations and documentation of the bedrock geology, the Quaternary deposits and their underlying references provide input to:

- The geometry of deterministic fracture (deformation) zones and (HCD) and the bedrock in between (HRD).

- The distribution of Quaternary deposits (HSD), including genesis, composition, stratification, thickness and depth.

Likewise, the investigations and documentation of the present-day meteorology, hydrology and near-surface hydrogeology together with the shoreline displacement during Holocene constitute the basis for the version 1.1 hydrological process modelling. This information provides input to:

- The present-day interpretation of drainage areas, as well as mapping of springs, wetlands and streams, surveying of land use such as ditching and dam projects, water supply resources, nature conservation areas, etc.

- Mean estimates of the present-day precipitation and runoff, heads and flows in watercourses.

- An assessment of the relative impact of local topography, shore level displacement, variable-density groundwater flow and inferred fracture zones for the definition of initial and boundary conditions and the numerical simulation of present-day (and future) recharge and discharge areas of groundwater flow.

The documentation of hydraulic borehole investigations and monitoring are of interest for the definition of hydraulic properties of the different hydraulic domains. There are basically two main sources of information for the bedrock hydrogeology:

- Hydraulic tests and hydrogeological monitoring in boreholes conducted within the Forsmark candidate area.

- Hydraulic tests and other hydrogeological observations in boreholes drilled in the proximity to the Forsmark candidate area, in particular, the Forsmark power plant and to the final repository for reactor waste, SFR.

The current knowledge about the hydraulic properties of the Quaternary deposits is based on slug tests conducted in a large number of groundwater monitoring wells.

5.4.2   Hydrology and near-surface hydrogeology

Background

No quantitative surface hydrological modelling is performed in model version 1.1. In the quantitative modelling of the hydrogeology, the Quaternary deposits are treated in a simplified way as a layer of constant thickness and homogeneous hydraulic properties.

The description below will form the preliminary conceptual basis for the distributed quantitative surface water and near surface hydrogeology models to be developed for later model versions. Very few measured data within the area were available for version 1.1 and the description and the figures given below, with exception of the hydraulic conductivities for the contact zone between the Quaternary deposits and the bedrock, are based on expert judgment, and generic and regional data. The description and the figures presented are meant to be used as a starting point for the development of the quantitative models and will be successively revised and substituted by site-specific data.

Physiographic data

From the description of the topography and Quaternary deposits of the Forsmark area in Chapters 4 and 5 it can be concluded that the area is characterized by a low relief with a small-scale topography and relatively shallow Quaternary deposits. Almost the entire area is below 20 masl. The Quaternary deposits are less than 20 m thick and rock outcrops are frequent. Till is the dominating soil. Sandy, silty till appears in the northern part of the area whereas clayey tills are common in the southern part. Forest covers most of the area and wetlands are frequent.

Annual precipitation is relatively low, 600–650 mm, and the specific runoff is approximately 200 mm. Since spring 2003, two meteorological stations have provided site-specific data. These data can together with land use, vegetation and geological maps of Quaternary deposits be used for modeling of actual evapotranspiration in future quantitative model versions.

Infiltration

The infiltration capacity exceeds rainfall and snowmelt intensity with few exceptions. Unsaturated (Hortonian) overland flow may appear over short distances on agricultural land covered by clayey till and on frozen ground where the soil water content was high during freezing. Also on outcropping bedrock unsaturated overland flow may appear but just over very short distances before water meets open fractures or the contact zone between bedrock and soil. Initially, unsaturated overland flow can be assumed to be negligible in the quantitative hydrological modelling, and the groundwater recharge in recharge areas can be set equal to the specific discharge, i.e. approximately 200 mm/year. Saturated overland flow appears in discharge areas where the groundwater level reaches the ground level.

Recharge and discharge areas

The division of the landscape into groundwater recharge and discharge areas is fundamental. The small-scale topography means that many small catchments will be formed with local, shallow groundwater flow systems in the Quaternary deposits. Groundwater levels are shallow. Usually < 3 m below ground in recharge areas and < 1 m in discharge areas. The annual groundwater level fluctuation can be assumed to be 2–3 m in recharge areas and about 1 m in discharge areas. Sea water level fluctuations may have a major influence on the absolute groundwater levels and the groundwater level fluctuations in the low-lying parts of the area.

The flat terrain and the shallow groundwater levels mean that the extension of the recharge and discharge areas may vary during the year. Furthermore, the shallow groundwater levels mean that there will be a strong interaction between, evapotranspiration, soil moisture and groundwater. The evapotranspiration will influence the groundwater level and its recession during summer by indirect or direct root water uptake from the groundwater zone /Johansson, 1986, 1987a,b/.

Groundwater flow and runoff generation

To describe the groundwater flow and the runoff generation process it is feasible to distinguish between processes in recharge areas, and unsaturated and saturated discharge areas.

In recharge areas, the soil water deficit has to be restored before any major groundwater recharge takes place. By-pass flow in different types of macropores may take place but can be assumed to be insignificant from a quantitative point of view, perhaps with exception of areas covered by clayey till where relatively frequent and deep fractures have been observed. However, from a contaminant transport perspective, preferential flowpaths can be of critical importance.

In the upper approximately one meter of the Quaternary deposits, the hydraulic conductivity and effective porosity are much higher than further down in the profile /Lundin, 1982; Johansson, 1986, 1987a,b; Espeby, 1989/. This is mainly due to soil forming processes, probably with ground frost as the single most important process. However, wave washing also means that the till at exposed locations is coarser at the soil surface and at some locations coarse out-washed material has been deposited, cf PFM0030 in Figure 7-4). The hydraulic conductivity in the upper one meter can typically be 10^{-5}–10^{-4} m/s. The effective porosity typically varies between 10 and 20%.

Below the depth strongly influenced by the soil forming processes, the hydraulic conductivity and the effective porosity of the till will be much lower. Depending on the type of till the hydraulic conductivities typically varies between 10^{-8} and 10^{-6} m/s, with the lower values for the clayey till. The effective porosity is typically 2–5%.

The hydraulic conductivity values of the till/bedrock contact zone, measured in the area, are quite high with a geometric mean of $1.18\cdot10^{-5}$ m/s (standard deviation of log K 1.00). Assuming a log-normal distribution, the 95% confidence interval of a new observation is $1.32\cdot10^{-7}$–$1.05\cdot10^{-3}$ m/s. The cause of these relatively high hydraulic conductivities is not clear. The preliminary evaluation does not show any obvious correlation with the rough soil classification in the field or with field notes of fractured rock at the contact. A re-evaluation will be made when grain size distribution analyses are available. Several indications are, however, available of heavily fractured rock at shallow depths in the area.

The described permeability and storage characteristics of the soil profile mean that very little water needs to be added to raise the groundwater table below approximately one meters depth. A ground-water recharge of 10 mm will give 20 to 50 cm increase in groundwater level. In periods of abundant groundwater recharge the groundwater level in most recharge areas reaches the shallow part of the soil profile where the hydraulic permeability is much higher and a significant lateral groundwater flow will take place. However, the transmissivity of this upper layer is so high that the groundwater level does not reach much closer to the ground surface than 0.75–1 m in typical recharge areas.

In discharge areas, defined as areas where the groundwater flow has an upward component, by definition no groundwater recharge takes place. However, not all discharge areas are saturated up to the ground surface, but water flows sub-horizontally in the uppermost most permeable part of the soil profile. In unsaturated discharge areas, the soil water deficit is usually very small and these areas respond quickly on rainfall and snowmelt.

The lakes are assumed to be important discharge areas. The hydraulic contact with the groundwater zone is highly dependent on the hydraulic conductivity of bottom sediments. Borings in the lake sediments shows relatively thick sediments of gyttja and thin layers of clay at most locations. However, especially in Lake Bolundsfjärden, exposed coarse-grained deposits indicate good hydraulic contact at some locations. Comparison of lake water levels and the groundwater levels in the Quaternary deposits below and close to the lake can give information on recharge-discharge conditions and the permeability of the bottom sediments. In the future work, it is essential to perform hydraulic tests for evaluation of the hydraulic conductivity of the sediments.

The flat terrain means that the extension of recharge and discharge areas may vary during the year. Conceptually it is important to understand if some of the lakes act as recharge areas during periods of the year.

The creeks are also considered as important discharge areas, however, they are dry during parts of the year.

The wetlands can either be in direct contact with the groundwater zone and constitute typical discharge areas, or be separate systems with tight bottom layers and little or no hydraulic contact with the groundwater zone. Information needs to be gathered to clarify the hydraulic contact between groundwater and major wetlands.

By use of oxygen-18 as a tracer, information can be obtained of the runoff generation process as well of groundwater reservoir volumes /Lindström and Rodhe, 1986; Johansson, 1987a; Rodhe, 1987/. /Rodhe, 1987/ studied the runoff generation process by oxygen-18 in several small Swedish catchment areas. The results showed that also in peak runoff events groundwater (pre-event water) often constitutes the dominating fraction of the discharge. The infiltrating water pushes the "old" water down to form the peak runoff. Also, in an area with shallow Quaternary deposits, like the Forsmark area, the total reservoir volume in till is larger than the annual groundwater recharge. The water stored in a 3 m thick saturated till profile corresponds to 3–4 years of groundwater recharge. In traditional hydrological linear reservoir modelling the active storage used is usually much smaller than the total storage. However, in hydrochemical and contaminant transport modelling the total storage is also of major interest.

The vertical distribution of the hydraulic conductivity of the till will have a major influence on the size of the "active storage", the mean transit time, and the transit time distribution of the water in the soil and groundwater zone. Based on existing knowledge it seems reasonable to initially work with a 3-layer model of the Quaternary deposits: (i) a upper layer of one meter thickness with a hydraulic conductivity of 10^{-5}–10^{-4} m/s and an effective porosity of 10–20%, (ii) a second layer down to approximately 1.0 m above the bedrock contact with a hydraulic conductivity of 10^{-8}–10^{-6} m/s depending of the grain size distribution of the till, and an effective porosity of 2–5%, and (iii) a third layer down to the bedrock with a hydraulic conductivity of 10^{-8}–10^{-4} m/s and effective porosity of 2–5%.

Quantitative modelling in version 1.1

The hydrogeological conditions of the Quaternary deposits were approximated in the numerical groundwater simulations. A continuous top layer with constant material properties across the entire model domain was assumed. The reason for this simplification is twofold; lack of spatially distributed data and insufficient time for a reasonable analysis of how to scale existing data to fit a mesh discretisation of 100 m. Figure 5-44 illustrates the spatial distribution of existing points where the thickness of the Quaternary deposits is known. The thickness of the Quaternary deposits is uncertain in all areas except where the bedrock is outcropping (blue points) and where there are boreholes (red). Given the site investigation data mentioned previously in this section, the simplified top layer was assigned a constant thickness of three (3) metres, a constant hydraulic conductivity of $1.5 \cdot 10^{-5}$ m/s and a constant kinematic porosity of 5% in the numerical groundwater simulation model.

Comments

No decision has yet been taken regarding the type of surface hydrological and near surface hydrogeological models to be used and how to couple these models to the hydrogeological model of the bedrock. However, to answer the questions of interest for the environmental assessment and the risk analysis, the model has to be distributed. The area to be covered by a detailed surface-near surface model has not yet been decided. The area for which detailed delineation of catchments area has been performed, with exception of some small areas in the northeast, seems feasible as a starting point (see Figure 4-33).

The distributed hydrological model to be developed should be based on the existing digital terrain model. The groundwater divides of shallow groundwater flow in the Quaternary deposits can be assumed to follow the topography. Major challenges in the future work will be to define adequate spatial and temporal resolution, details of process descriptions, and integration with the hydrogeological model of the deeper groundwater in terms of recharge and discharge.
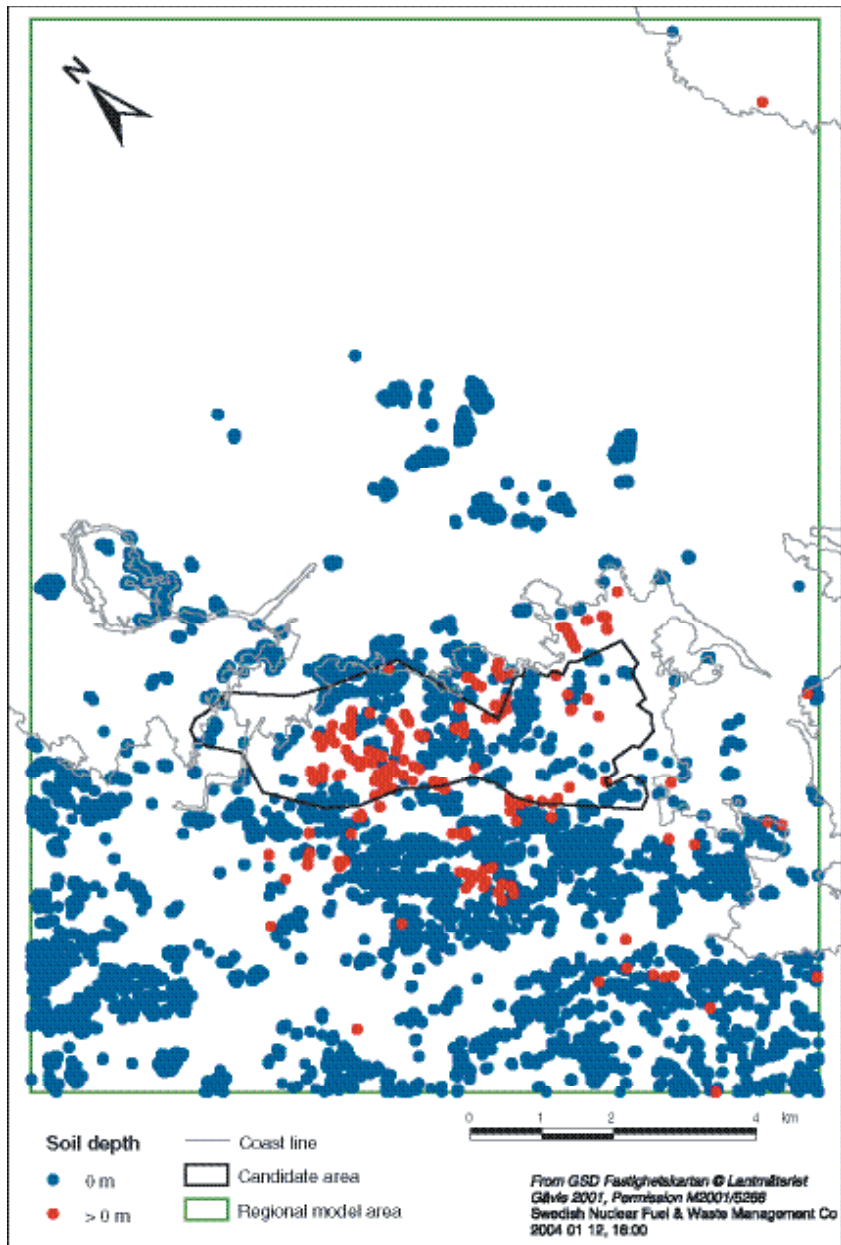
Figure 5-44. *Map of outcropping bedrock (blue) and boreholes with known thicknesses of the Quaternary deposits (red).*

5.4.3 Oceanography

In the numerical groundwater simulations the oceanographic conditions on the top surface of the model domain were approximated by assuming spatial and temporal varying Dirichlet conditions for both pressure and salt at all times between 8,000 BC and 2,000 AD.

5.4.4 Conceptual model of the bedrock

The Regional Model Domain has its bottom surface at –2,100 masl and the horizontal dimensions are 15 km by 11 km. The visualisation in Figure 5-45 shows the model domain in a perspective view with the physical dimensions to scale. The top surface follows the topography and bathymetry as defined for the version 0 site descriptive model /Brydsten, 1999a/. Below the thin layer of porous Quaternary deposits (HSD) the bedrock is fractured consisting of Hydraulic Conductor Domains (HCD) and Hydraulic Rock Domains (HRD), cf SKB's systems approach shown in Figure 5-43.
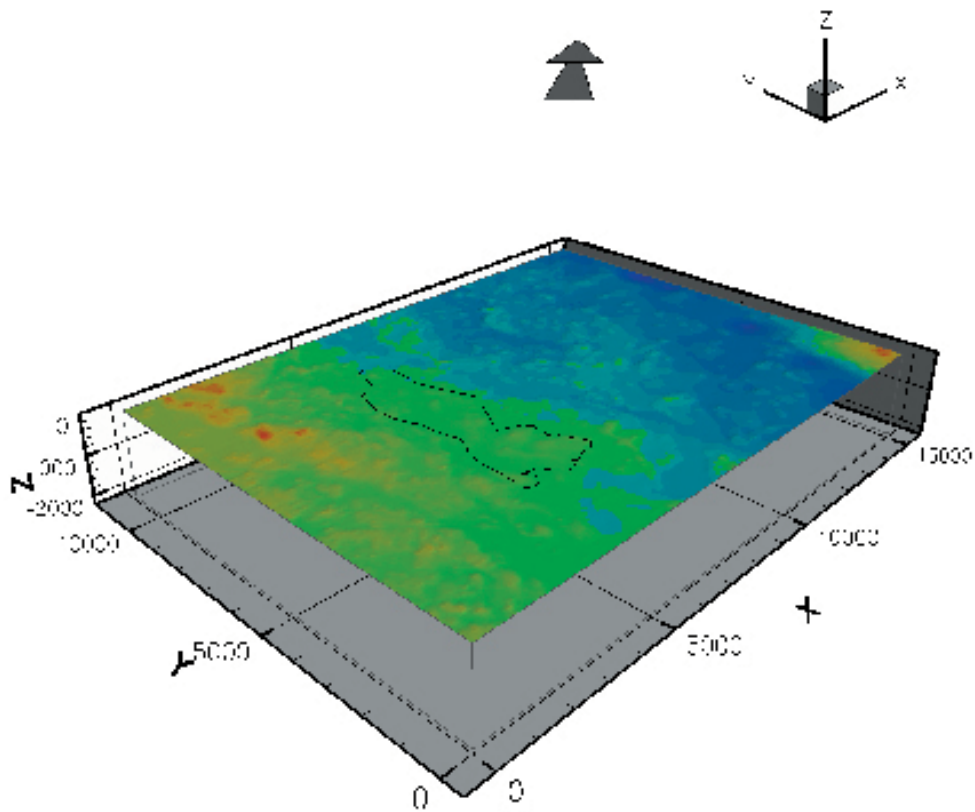
Figure 5-45. *The Regional Model Domain as defined in model versions 0 and 1.1. The colours illustrate the topgraphy.*

The 166 fracture zones defined in Section 5.1.4 constitute the primary input for the division of the bedrock into HCDs and HRDs (Figure 5-46). Geometrically, the fracture zones split into 177 fracture zone segments (cf Table 5-9). The segments are of varying size and confidence level. The trace length threshold was set to one kilometre and the penetration depth was assumed no greater than the trace length. These constraints are not precise by any means, but should be considered as working hypotheses. Moreover, the interpretations of hydraulic tests conducted in boreholes intersecting one or more of these segments constitute the basis for assigning hydraulic properties to all segments, including those not intersected by boreholes. In conclusion, some fracture zone segments are more certain than others, both geologically and hydraulically.

245
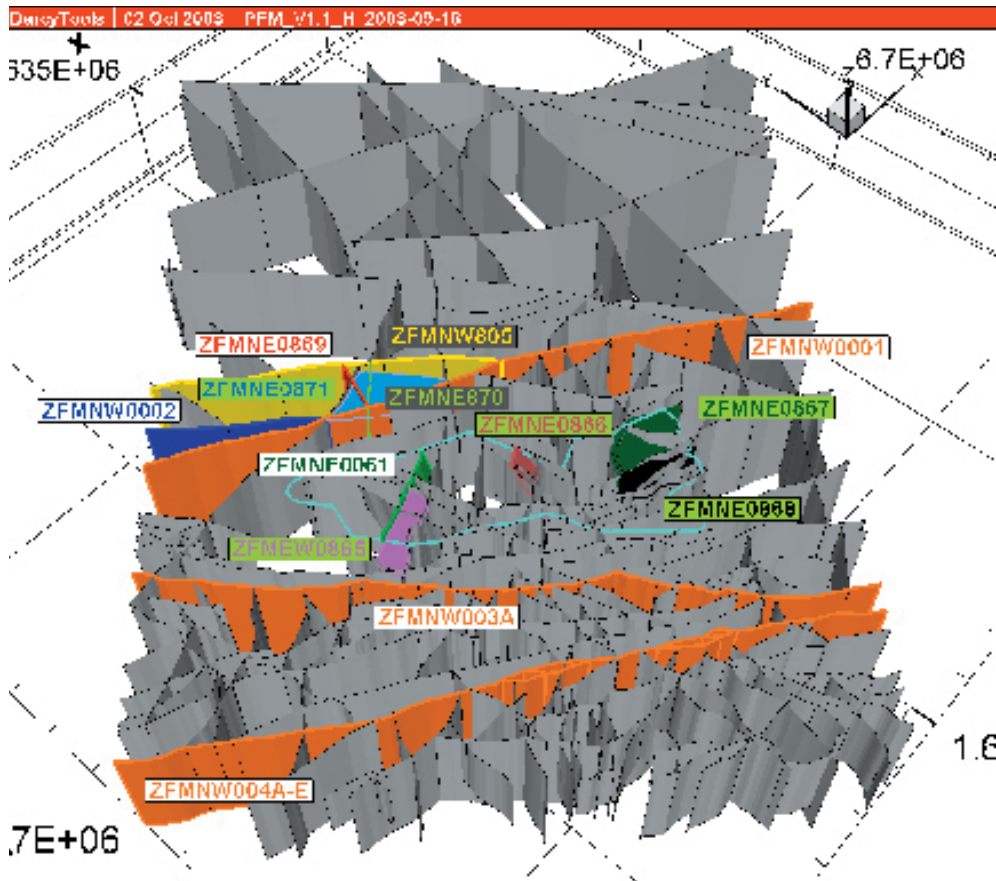
Figure 5-46. *Visualisation of the inferred fracture zones for model version 1.l. The total number of fracture zones is 166. The fracture zones consist of 177 segments out of which 21 are of a high-confidence level. Grey coloured fracture zones segments are of medium or low confidence, whereas bright coloured segments are of high confidence. The latter have ID tags attached to them. The turquoise line in the centre indicates the location of the Forsmark candidate area.*

The 177 fracture zone segments were used "as are" in the hydrogeological modelling regardless of their confidence level. That is, each fracture zone segment was treated as a conductor without uncertainty. Alternative geometric interpretations were not treated at this point, but potential ideas for alternatives exist. These will be formed, tested and scrutinised when more data from the site investigations become available, starting with model version 1.2. Figure 5-47 shows a vivid, however hypothetical, example of a variant with very extensive sub-horizontal fracture zones.

5.4.5 Assignment of hydraulic properties to the HCD

Some of the high-confidence fracture zones were investigated hydraulically in conjunction with the construction of the SFR, whereas others were identified and investigated hydraulically for the first time during the site investigation phase 1.1.

The high-confidence fracture zones investigated hydraulically in conjunction with the construction of the SFR are ZFMNW0001–2, ZFMNW0805, and ZFMNE0869–871. The thickness and transmissivity values available for these fracture zones are reported in /Axelsson et al, 2002/ and /SKB, 2002a/.

The high-confidence fracture zones investigated hydraulically during the site investigation phase 1.1 are ZFMNW003A–E, ZFMNE0061, ZFMNE0866–868, and ZFMEW0865. The thickness and transmissivity values available for these fracture zones are reported in /Rouhiainen and Pöllänen, 2003/, /Ludvigson et al, 2003a/, /Ludvigson et al, 2003b/, /Ludvigson and Jönsson, 2003/ and /Källgården et al, 2003/.
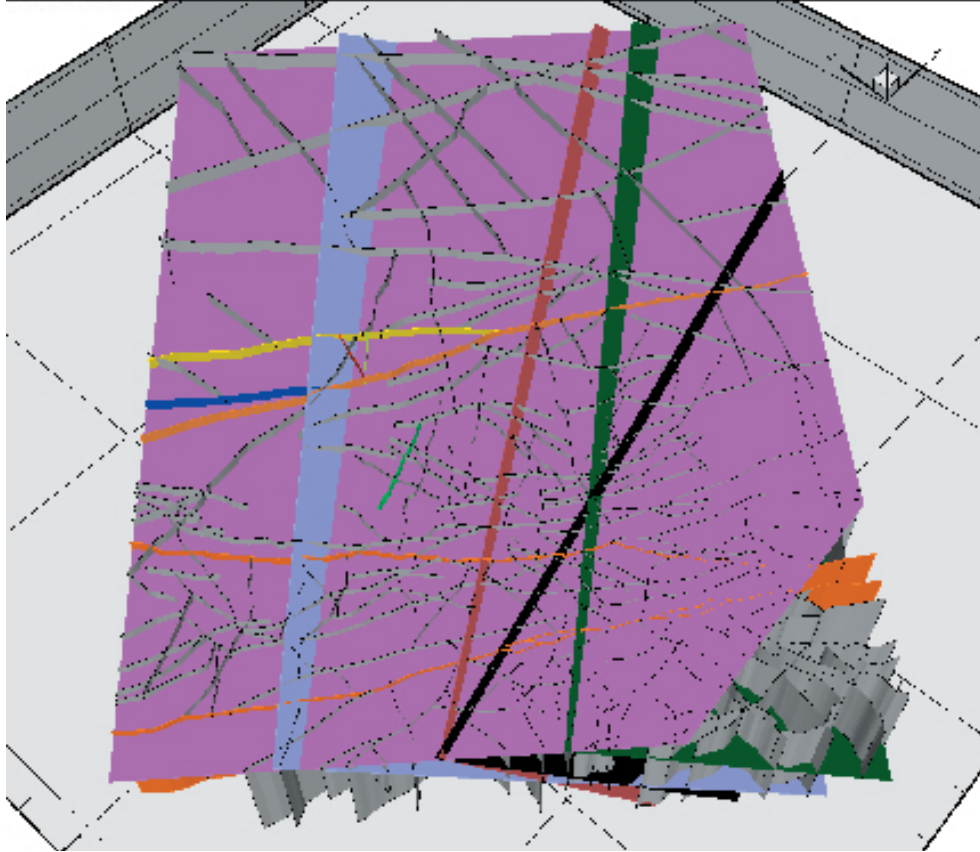
Figure 5-47. *Visualisation of a hypothetical variant of the fracture zone model shown in Figure 5-46. The extensions of the sub-horizontal fracture zone segments were not limited by the nearest vertical fracture zone segments but extrapolated until they reached the regional model domain.*

The thickness and the transmissivity of the remaining high-confidence zone, ZFMNW004A–E, was not investigated. However, it is by far one of the largest fracture zones in the region and commonly referred to as the Forsmark Fault Zone. Its geological history and strike resemble that of the Singö (ZFMNW0001–2) and the Eckarfjärden (ZFMNW003A–E) deformation zones.

Table 5-38 summarises the hydraulic properties of the HCDs treated in model version 1.1. The high-confidence fracture zones that were investigated hydraulically have been assigned transmissivity values in accordance with the reported results. Where several data exist intermediate values were adopted. The transmissivity assigned to the Forsmark Fault Zone mimics the values of the Singö and the Eckarfjärden deformation zones.

The hydraulic properties of all medium and low confidence HCDs are by definition unknown. In order not to exaggerate their hydraulic impact, intermediate hydraulic properties were assigned for version 1.1, at least compared to the values available from the testing of the high-confidence fracture zones. No sensitivity analyses were carried out at this point as a means of testing their hydraulic property uncertainty.

The database is very limited concerning fracture zone specific storativity. The only value available stems from the short-distance hydraulic interference test conducted at drillsite 1 /Ludvigson and Jönsson, 2003/. The storativity of the tested fracture zone ZFMEW0865 was evaluated to be of the order $5 \cdot 10^{-5}$. The deduced specific storativity of ZFMEW0865, obtained by dividing the storativity by the hydraulic thickness, was provisionally assigned to all fracture zones, being deterministic or stochastic, see Table 5-38 and Table 5-40. For the numerical simulations performed in support of the palaeo-hydrogeological discussion the uncertainty associated with this assumption is unimportant. This will be discussed in detail later on in this section.

Likewise, the database for the kinematic porosity is also very limited. The values given in Table 5-38 have no reference to data from Forsmark. The values proposed in Table 5-38 constitute a reasonable estimation compared to data reported from tests conducted at Äspö /Rhén et al, 1997b/.

Table 5-38. Summary of the property settings of the HCDs as used in the numerical simulations.

Name of HCD RVS ID	Geological confidence High/Med./Low	Transmissivity m^2/s	Hydraulic thickness m	Specific storativity m^{-1}	Kinematic porosity –
ZFMEW0865	High	$5.0 \cdot 10^{-5}$	2	$2.5 \cdot 10^{-5}$	$5.0 \cdot 10^{-3}$
ZFMNE0866	High	$5.0 \cdot 10^{-5}$	2	$2.5 \cdot 10^{-5}$	$5.0 \cdot 10^{-3}$
ZFMNE0867	High	$5.0 \cdot 10^{-5}$	2	$2.5 \cdot 10^{-5}$	$5.0 \cdot 10^{-3}$
ZFMNE0868	High	$1.5 \cdot 10^{-10}$	10	$2.5 \cdot 10^{-5}$	$5.0 \cdot 10^{-4}$
ZFMNE0871	High	$2.0 \cdot 10^{-6}$	10	$2.5 \cdot 10^{-5}$	$5.0 \cdot 10^{-4}$
ZFMNE0869	High	$2.0 \cdot 10^{-5}$	7	$2.5 \cdot 10^{-5}$	$1.0 \cdot 10^{-3}$
ZFMNE0870	High	$2.0 \cdot 10^{-7}$	5	$2.5 \cdot 10^{-5}$	$5.0 \cdot 10^{-4}$
ZFMNW004A-E	High	$2.4 \cdot 10^{-5}$	30	$2.5 \cdot 10^{-5}$	$1.0 \cdot 10^{-3}$
ZFMNW003A-E	High	$2.4 \cdot 10^{-5}$	30	$2.5 \cdot 10^{-5}$	$1.0 \cdot 10^{-3}$
ZFMNE0061	High	$1.5 \cdot 10^{-10}$	10	$2.5 \cdot 10^{-5}$	$5.0 \cdot 10^{-4}$
ZFMNW0001	High	$2.4 \cdot 10^{-5}$	30	$2.5 \cdot 10^{-5}$	$1.0 \cdot 10^{-3}$
ZFMNW0002	High	$2.4 \cdot 10^{-5}$	30	$2.5 \cdot 10^{-5}$	$1.0 \cdot 10^{-3}$
ZFMNW0805	High	$8.0 \cdot 10^{-6}$	10	$2.5 \cdot 10^{-5}$	$5.0 \cdot 10^{-4}$
ZFM*	Medium/Low	$7.0 \cdot 10^{-7}$	10	$2.5 \cdot 10^{-5}$	$5.0 \cdot 10^{-4}$

5.4.6   Assignment of hydraulic properties to the HRD

Groundwater flow through the Hydraulic Rock Domains is governed by the geometric and hydraulic properties of the fractures between the Hydraulic Conductor Domains. The geometric and hydraulic properties of this fracturing are commonly described statistically. Section 5.1.6 treats the statistics for the following geometric properties: *orientation*, *size*, *termination, intensity* and *spatial distribution*. The present section treats the statistics of the fracture transmissivity.

The working hypothesis used for model version 1.1 attempts to couple the interpreted fracture transmissivities in KFM01A to the power-law size distribution inferred from outcrop fractures and linked lineaments. In order to couple fracture transmissivity measured in a borehole to fracture size the following information is needed:

• the statistical distribution for the fracture transmissivity of all fractures of interest, and

• a method for transferring the inferred size distribution from outcrops fractures and linked lineaments in the vertical direction.

Concerning the realism of this working hypothesis it is important to remember that the hydraulic data available come from a single borehole solely, and that only a minor portion of this borehole was found to be more conductive than the measurement threshold of the testing equipment used (cf Section 4.5.3). That is, the interpretation of conductive fractures for model version 1.1 is strongly affected by the limited number of inflow points and their non-uniform occurrence in the only cored borehole available, KFM01A.

Comment on the geological classification of conductive fractures

Besides the measurement threshold, the geological classification of conductive fractures also has a strong impact on the deduced fracture transmissivity distribution. Section 4.3.3 describes how the geological classification of conductive fractures was made and how the underlying principle for the classification was changed later during the geological modelling. The results from the discrete fracture network modelling are given in Section 5.1.6.

Unfortunately, the late change in the geological classification of conductive fractures was not possible to address in the numerical modelling. However, its effect on the deduced transmissivity distribution was evaluated. In order to make the presentation of the numerical modelling readable, the deduction of the fracture transmissivity distribution is presented for both the initial and the changed geological classification of conductive fractures.

The initial geological classification of conductive fractures was based on a classification of *natural* fractures, where all natural cuts in the drill core were tacitly assumed to represent conductive fractures. In contrast, *sealed* fractures were considered non-conductive.

The geological classification of conductive fractures adopted later on was based on fracture aperture, where an *open* fracture had an aperture > 0 mm and a *sealed* fracture had an aperture = 0. Unfortunately, the difference in the two geological classifications is not self-evident from the wording alone. The reason for the changed classification was that a large number of the natural fractures were found to have no visible apertures and that a few fractures, previously classified as sealed, were found to have one or more tiny holes in the sealing fabric, i.e. they were not perfectly sealed despite the name of the classification.

According to Table 4-15 in Section 4.4.3, 1,517 fractures were found in the cored borehole KFM01A. 818 of these were classified as natural and 699 as sealed. However, if aperture is selected as a criterion for the classification of potentially conductive fractures, Table 4-16 shows that there were 201 open fractures (aperture > 0 mm) and 1 316 sealed fractures (aperture = 0 mm).

It is obvious that it makes a significant difference if the analysis of the frequency of conductive fractures (CFF) is based on 818 fractures instead of 201 fractures. However, it should be noted that the geological classification of potentially conductive fractures based on aperture solely is a working hypothesis and that there are many assumptions (uncertainties) inherent in this classification. Indeed, a fracture that was mapped as sealed may have an aperture > 0 elsewhere. The occurrence of tiny holes in an otherwise sealing fabric may be considered a pertinent example of this conceptual complexity.

Model version 1.1 treats large-scale phenomena mainly, which means that channelling within individual fractures was not possible to address thoroughly at this stage of the modelling. Notwithstanding, model version 1.1 may still be considered of value for a discussion of this matter since a coupling between fracture transmissivity and fracture size was attempted.

The changed geological classification of open fractures also affected the outcrop traces. In the initial geological classification, all traces were assumed to be conductive. In the updated geological classification, outcrop traces mapped as open by the field geologist were considered conductive. Table 5-39 summarises how the initially inferred fracture intensity P_{32} was affected by the changed geological classification of conductive fractures. It is noted once more that the numerical simulations presented later on in this section were based on the intensities inferred from the initial geological classification.

Table 5-39. Comparison of inferred fracture intensities P_{32} (m²/m³) between the initial and changed geological classifications of conductive fractures.

Geological classification	NE-set	NW-set	NS-set	EW-set	Sub-H-set	Sum
Initial (–100) – (–400) m	1.13	0.89	0.35	0.34	1.23	3.94
Initial (–400) – (–1000) m	0.15	0.12	0.05	0.04	0.15	0.51
Changed (–100) – (–400) m	0.12	0.17	0.04	0.07	0.34	0.74
Changed (–400) – (–1000) m	0.04	0.06	0.00	0.00	0.15	0.24

Table 5-39 shows "untruncated" intensities, $P_{32}[L \geq L_0]$. These were truncated in the numerical simulations to match the window between the smallest fracture zone size, 1,000 m, and the resolution of the discretisation mesh, i.e. 100 m. For the truncation the following equation was used

$$P_{32}[L_{min}, L_{max}] = P_{32}[L \geq L_0] (L_{max}^{[2-k_L]} - L_{min}^{[2-k_L]})/(-L_0^{[2-k_L]}) \qquad (5.8)$$

where k_L is the slope of the parent fracture size distribution plotted in a CCDF plot. For model version 1.1, different values of the truncated fracture intensity were used above and below (–400) masl.

Joint interpretation based on the initial geological classification of conductive fractures

There were 623 natural fractures in KFM01A between c (–100) and (–400) masl and 195 below c (–400) masl. 34 of the 623 natural fractures were found to be more conductive than the transmissivity threshold at $1.5 \cdot 10^{-10}$ m²/s.

Figure 5-48 shows a log-log plot of the complementary cumulative density function (CCDF) of the transmissivity of all natural fractures between c (–100) and (–400) masl in KFM01A. The fracture transmissivities above the measurement threshold may be fitted to a straight line, thus indicating that field data may conform to a power-law distribution. The values of m_T and k_T deduced from the difference flow logging in KFM01A between c (–100) and (–400) masl are $m_T = 1.06 \cdot 10^{-12}$ m²/s and $k_T = 0.545$.

Figure 5-49 shows that the data also can be fitted to a log-normal distribution with a common log arithmetic mean of c –13.5 and a common log standard deviation of c 3.1. For model version 1.1 it was decided to work with the power-law distribution shown in Figure 5-48.

Joint interpretation based on the changed geological classification of conductive fractures

For the sake of comparison the statistical analysis of the fracture transmissivity was repeated later on as the results of the changed geological classification of conductive fracture was available. The repeated analysis gave the following results:

There were 147 open fractures in KFM01A between c (–100) and (–400) masl and 54 below c (–400) masl. 34 of the 147 open fractures were found to be more conductive than the transmissivity threshold at $1.5 \cdot 10^{-10}$ m²/s.

Figure 5-50 shows a log-log plot of the CCDF of the transmissivity of all open fractures between c (–100) and (–400) masl in KFM01A. The fracture transmissivities above the measurement threshold may be fitted to a straight line, thus indicating that field data may conform to a power-law distribution. The values of m_T and k_T deduced from the difference flow logging in KFM01A between c (–100) and (–400) masl are $m_T = 1.74 \cdot 10^{-11}$ m²/s and $k_T = 0.545$.
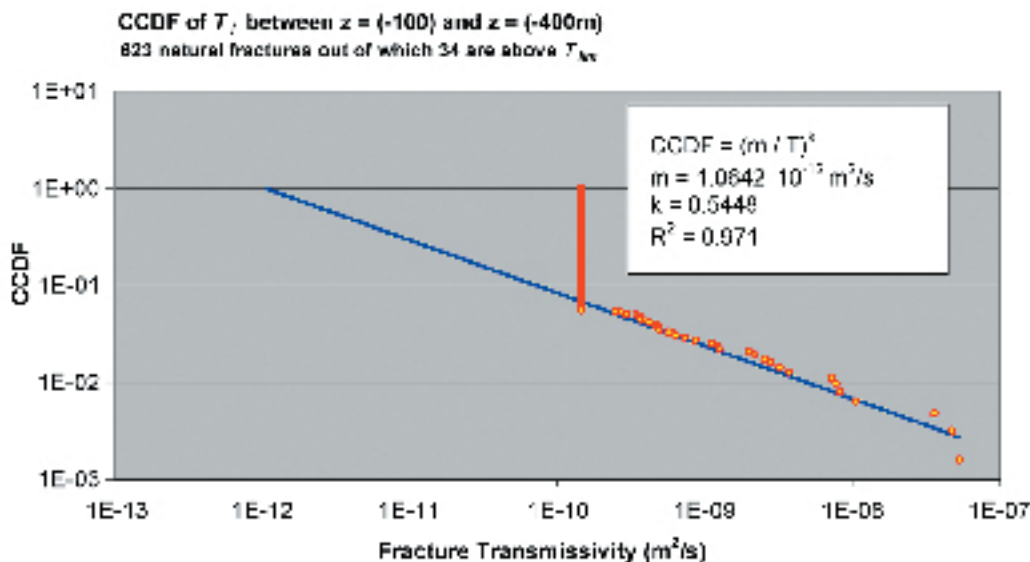
Figure 5-48. *Complementary cumulative density function (CCDF) plot of all fracture transmissivities between c (–100) and (–400) masl in KFM01A.*
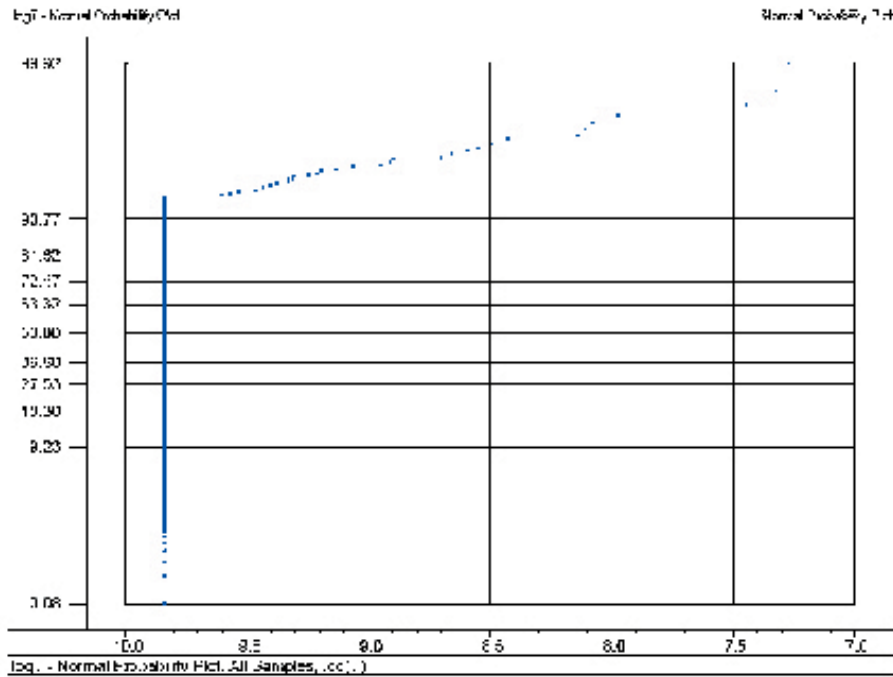
Figure 5-49. *Log-normal probability plot of all fracture transmissivities between c (–100) and (–400) masl in KFM01A.*

Fracture transmissivity

The attempted coupling between fracture transmissivity (T) and fracture size (L) for model version 1.1 is based on the working hypothesis that available data from data freeze 1.1 can be fitted to power-law distributions. By assuming that the CCDF for fracture transmissivity (T) is positively correlated with the CCDF for fracture size (L), i.e.

$$P(T \geq T_1) = P(L \geq L_1) \tag{5.9}$$

the following relationship between T and L is obtained:

$$T = a L^b \tag{5.10}$$

Equation (5.10) is obtained by recognising that Equation (5.9) can be written as

$$(m_T/T)^{k_T} = (m_L/L)^{k_L} \tag{5.11}$$

keeping in mind the equation of the CCDF for a power-law distribution.

A separation of terms yields that:

$$a = (m_T / m_L^{\,b}) \tag{5.12}$$

$$b = k_L / k_T \tag{5.13}$$

The values of m_T and k_T deduced from the difference flow logging in KFM01A between (–100) and (–400) masl are shown in Figure 5-48 for the initial geological classification and in Figure 5-50 for the changed classification. The values of m_L and k_L were estimated by means of numerical simulation using the method described below.

The values of m_L and k_L were estimated by means of numerical simulation using the method described below.

The DFN parameters representing the natural fracturing in KFM01A between (–100) – (–400) masl

were used to generate a 3D fracture network realisation. The sizes of the generated fractures were explored by introducing a scanline into the realisation mimicking the 300-m long borehole interval, see Figure 5-51. Figure 5-52 shows the CCDF for these fractures and the deduced values of m_L and k_L; $m_L = 0.352$ m and $k_L = 0.976$.

The values of m_T, m_L, k_T, and k_L derived for the initial geological classification (Figure 5-48) were inserted into Equations (5.12) and (5.13) and the calculated values of a and b rendered

$$T = 2.47 \cdot 10^{-12}\ L^{1.791} \tag{5.14}$$

The uncertainty in the calculated values of a and b in Equation (5.14) was not examined by means of Monte Carlo simulation due to lack of time. Furthermore, no attempt was made distinguish between different fracture sets.

Repeating the calculations above using the values of m_T, m_L, k_T, and k_L derived for the changed geological classification (Figure 5-50) rendered

$$T = 1.13 \cdot 10^{-10}\ L^{1.791} \tag{5.15}$$

In conclusion, the changed geological classification results in a much sparser fracturing than does the initial geological classification, see Table 5-39. However, the transmissivity of changed fracturing is much higher, see Figure 5-53.

The coupling between fracture transmissivity and size expressed by Equation (5.10) leads to a flow system that on each scale of consideration is governed by the *largest* feature on that scale. The rationale for such a model is of course that large features are the main contributors to the fracture network connectivity. Moreover, large features are generally both wider and thicker than small features. The Äspö Task Force considered a coupling between fracture transmissivity and size similar to Equation (5.10) in their specifications for Task 6 /Dershowitz et al, 2003/.
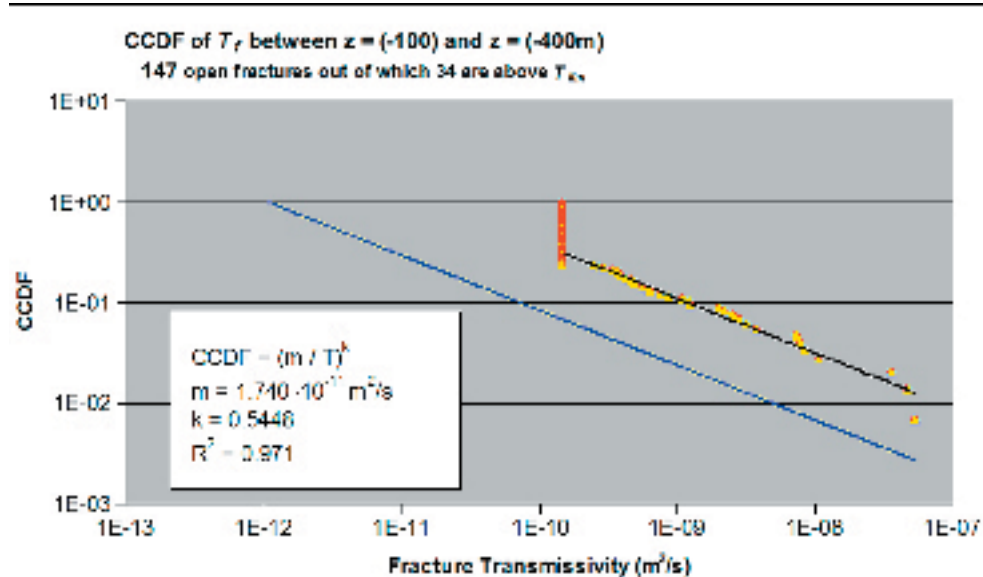
Figure 5-50. *Complementary cumulative density function (CCDF) plot of all fracture transmissivities based on open fractures between c (–100) – (–400) masl in KFM01A. The blue line represents the position of the data fit for all natural fractures shown in Figure 5-48.*
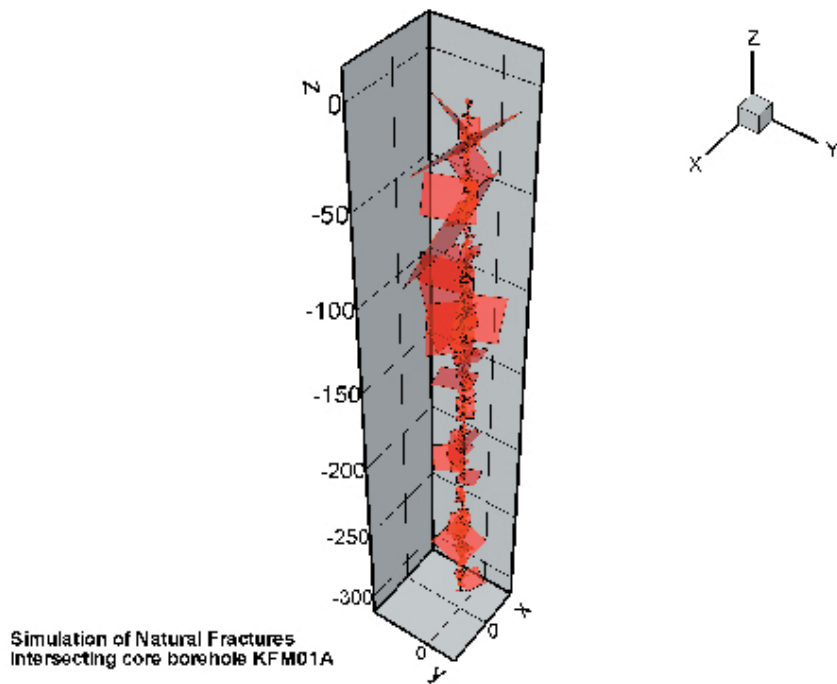
Figure 5-51. *Visualisation of a numerical simulation of fractures intersecting a 300 m long borehole interval. The DFN parameters representing the natural fracturing in KFM01A between (–100) and (–400) masl were used to generate the underpinning 3D fracture network realisation.*
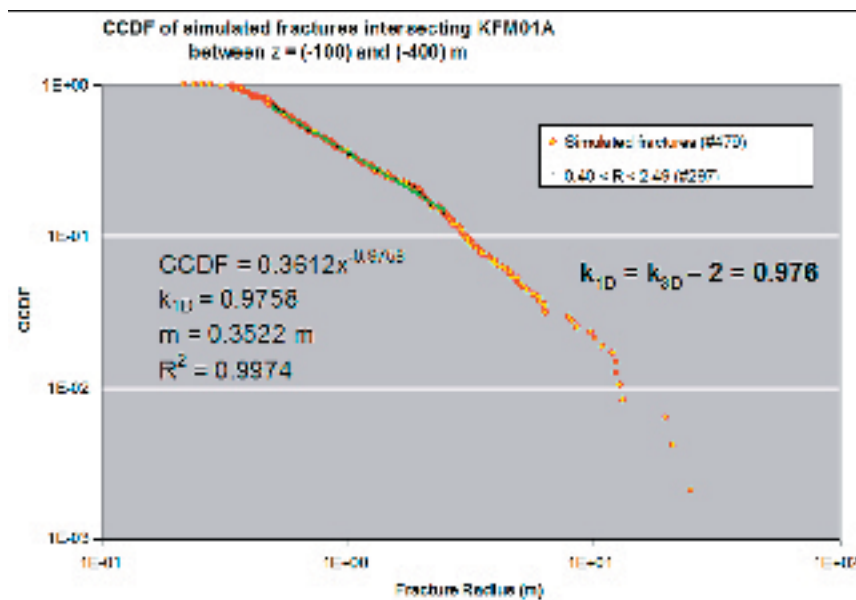
Figure 5-52. *Plot of the complementary cumulative density function (CCDF) of a numerical simulation of fractures intersecting a 300 m long borehole interval.*

253
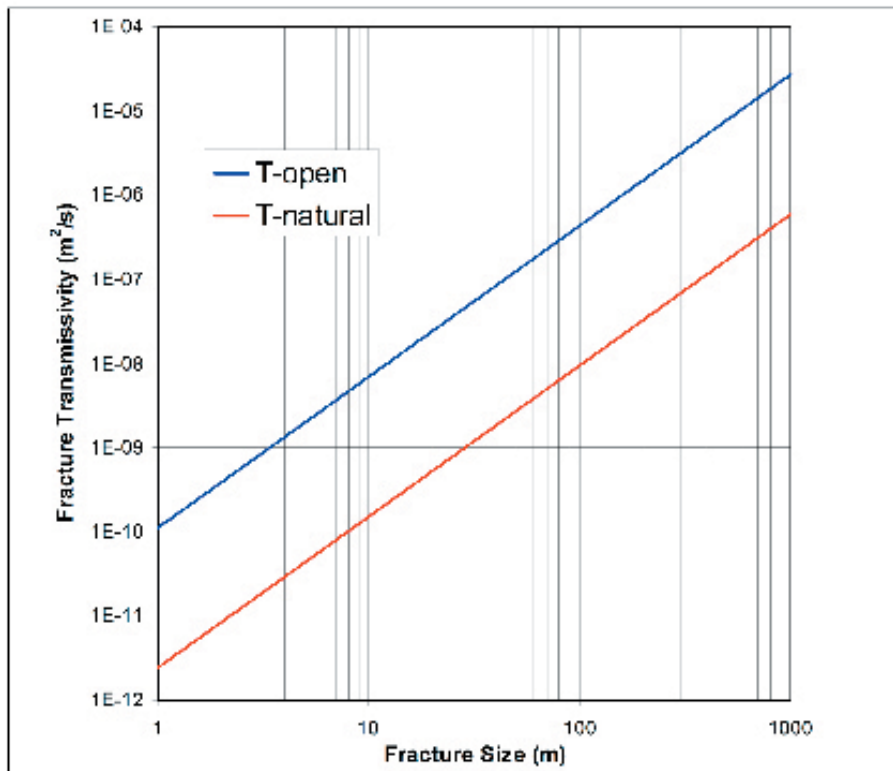
Figure 5-53. *Plot of the deduced relationships between fracture transmissivity versus fracture size. The difference between the two graphs is due to differences in the geological classification of conductive fractures.*

The coupling between fracture transmissivity values from overlapping measurements with the difference flowlogging and a geological classification of conductive fractures described above is innovative in the sense that it has not been used elsewhere. The difference between Equations (5.14) and (5.15) clearly shows that uncertainties in the geological classification has a very strong impact on the result as does the measurement threshold of the difference flow logging equipment. Consequently, the novel approach used in model version 1.1 needs to be scrutinised and tested with more data.

In theory, other relationships between fracture transmissivity and size may exist, including no relationship at all. To our current understanding, however, no relationship whatsoever between fracture transmissivity and size means a much more resistant flow system than a coupled flow system as expressed by Equation (5.10). As more data become available from the site investigations in Forsmark, it will be fruitful to test other types of models as well as the uncertainty in Equation (5.10).

Other hydraulic properties

Besides fracture transmissivity, the main hydraulic properties of interest for groundwater flow modelling are the fracture storativity and kinematic porosity. There are generally very few experimental data to support a discussion about magnitudes. It is often assumed that these entities are positively correlated with the transmissivity, but with a much smaller range of variability. Whereas transmissivity often varies several orders of magnitude, storativity and kinematic porosity are assumed to vary within one or, at the most, two orders of magnitude /Ahlbom et al, 1992; Rhén et al, 1997b/.

Table 5-40 shows the hydraulic properties used to characterise the groundwater flow system contained in the Hydraulic Rock Domains, i.e. the flowing fractures between the Hydraulic Conductor Domains. The stochastic fracturing is set to treat features between 100–1,000 m of size. The lower size limit was more or less due to computational constraints, whereas the upper size limit coincides with aforementioned threshold used in identification of fracture zone segments.

Table 5-40. Summary of the property settings of the HCDs as used in the numerical simulations.

Fracture size m	Geological confidence Determ./Stoch.	Transmissivity m²/s	Hydraulic thickness m	Specific storativity m⁻¹	Kinematic porosity –
100–1,000	Stochastic	$(0.094–5.8)\cdot10^{-8}$	0.5–2.0	$2.5\cdot10^{-5}$	$(0.2–1)\cdot10^{-4}$

5.4.7 Comments on the joint structural-hydrogeological model

Figure 5-54 visualises an example simulation of how a combination of deterministic fracture zones (HCDs) and the conductive stochastic fracturing in the Regional Model Domain may look like. The visualisation is based on the fracture statistics presented in Section 5.1.6 except for fracture intensity, which was based on the initial geological classification of conductive fractures, see Table 5-39. The stochastic fracturing was set to vary in size between 100 m and 1,000 m following the power-law size distribution inferred for model version 1.1.
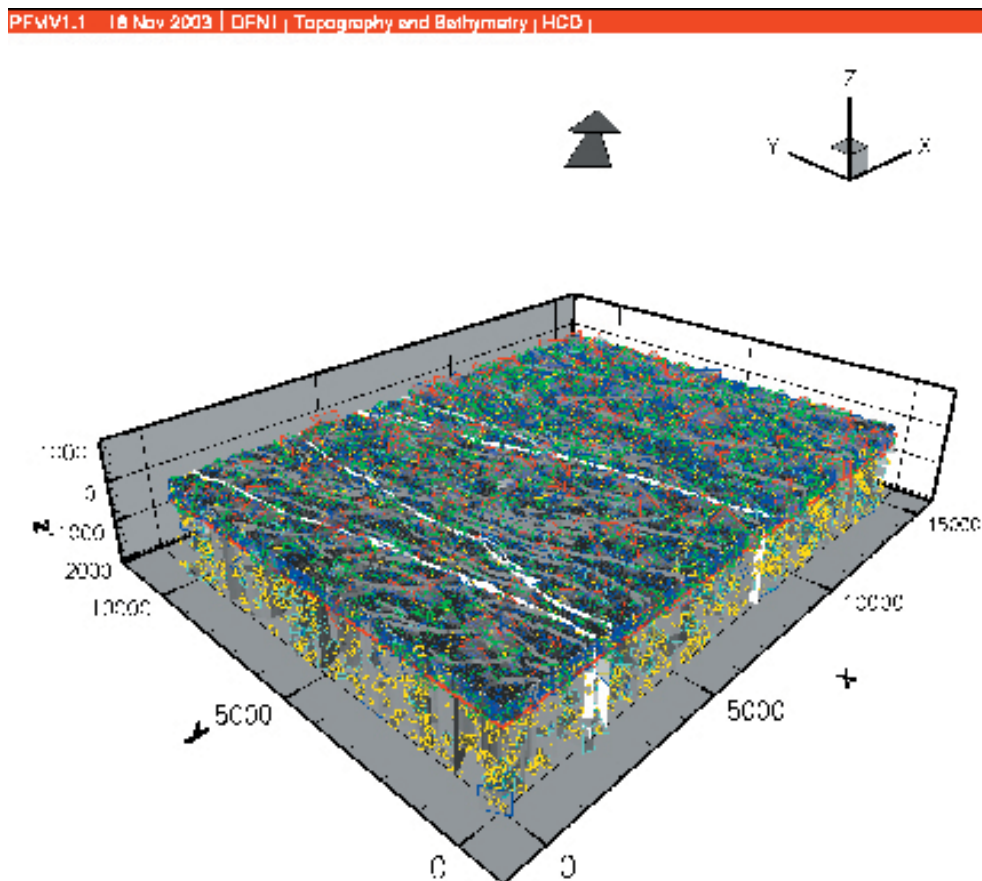
Figure 5-54. Example simulation showing a stochastic fracture network realisation between the 177 HCDs. Below the red line at (–400) masl the fracture intensity is considerably less than the intensity above this level, see Table 5-39. The simulation is based on an extrapolation of the statistics inferred from one borehole only.

The example simulation was based on an extrapolation of the statistics inferred from one borehole only. If there is a change in the fracture intensity versus depth as depicted by the data from KFM01A, the example simulation visualises that large volumes of rock at repository depth are intersected by very few fractures which are greater than 100 m. For the given size range the intensities described in Table 5-39 give rise to approximately 86,000 fractures in the rock volume above (–400) masl and 14,000 fractures below. For a uniform mesh discretisation of 100 m these numbers indicate that on the average every grid cell above (–400) masl is intersected by at least one stochastic fracture, whereas only two grid cells out of ten below (–400) masl are intersected by at least one stochastic fracture. The 100-m mesh discretisation used in the numerical simulations together with the 177 HCDs fracture zones to scale is visualised in Figure 5-55.

Figure 5-54 shows that the fracturing of the 100-m cells is very sparse when it comes to features greater than 100 m in size. On top of this geological interpretation, the transmissivity to size relationship shown in Figure 5-53 indicates that the features less than 100 m in size are of pretty low transmissivity. The changed geological classification of conductive fractures makes the situation even more extreme. On one hand, Figure 5-53 implies that the changed fracture transmissivity is c 40–50 times greater, but on the other hand, Table 5-39 states that the changed fracture intensity between (–100) and (–400) masl is 87% lower and that the changed fracture intensity below (–400) masl is 53% lower.
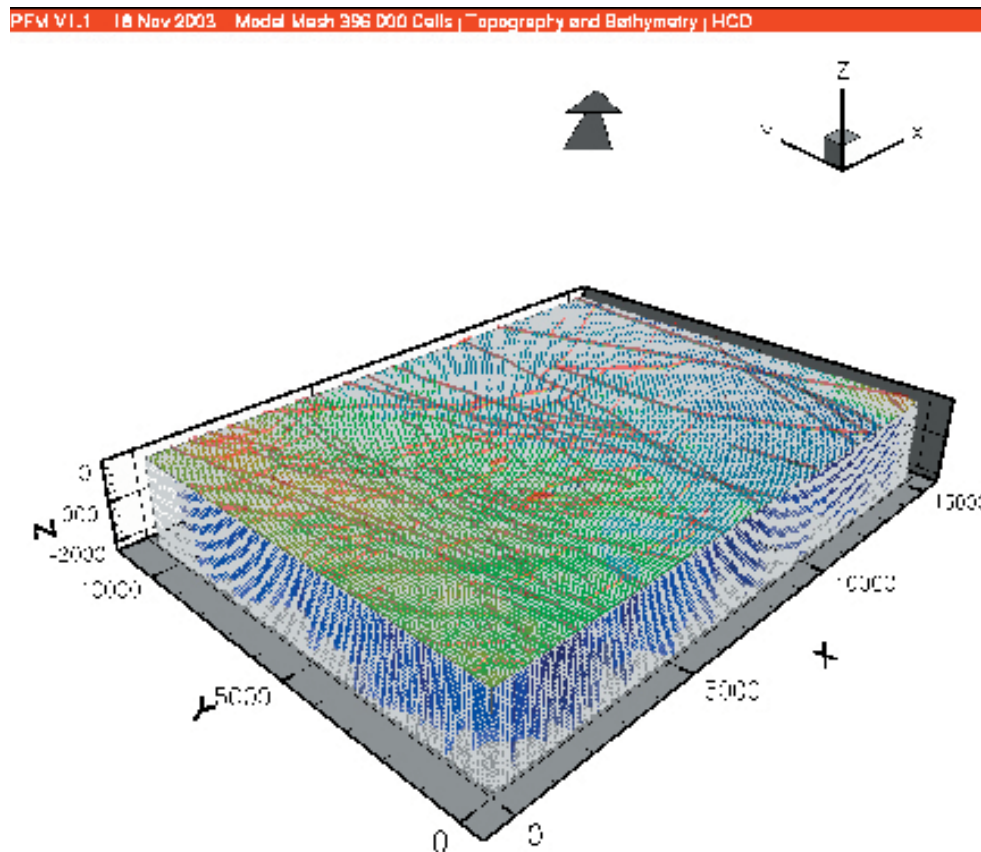
Figure 5-55. *Visualisation of the 100-m mesh discretisation used in the numerical simulations together with the 177 HCDs fracture zones to scale.*

Regardless of the geological classification used, the discussion above suggests that the hydrogeological model formed for model version 1.1 is very discrete. That is, the stochastic fracturing of the HRDs between the HCDs will not contribute significantly to the connectivity of the advective flow system. If the changed geological classification of conductive fractures is considered more correct than the initial, the situation becomes very extreme, suggesting an essentially binary flow system consisting of large volumes of low-conductive rock between a limited number of large features of high transmissivity. In the latter kind of model, the geometry and transmissivity of the deterministic fracture zones become very important.

The groundwater storage not readily accessible to advective flow, constitutes, more or less, an immobile volume of groundwater accessible mainly through diffusion processes. The larger the immobile volume, the longer the "initial" groundwater conditions in the bedrock between the flowing fractures will be preserved. There are no data from data freeze 1.1 to support a quantitative discussion of this situation. However, provided that the joint structural-hydrogeological model inferred for model version 1.1 is not completely incorrect, the numerical modelling of variable-density groundwater flow and mass (salt) transport on a detailed scale needs some data support from the site accompanied by sensitivity tests.

In model version 1.1, the assignment of sub-grid material properties was based on expert judgments rather than precise data. The equivalent hydraulic conductivity of the bedrock intersected by features of less than 100 m was assumed to be homogeneous and isotropic, with a magnitude of $1 \cdot 10^{-12}$ m/s. The kinematic porosity was set to $1 \cdot 10^{-5}$ and the immobile porosity to $1 \cdot 10^{-4}$. Hence, the mobile volume of groundwater in a 100-m cube of background bedrock was set to 10 m^3, whereas the immobile volume was set to 100 m^3. The motivation for using a ratio of ten between the immobile to mobile porosities comes from the experience of the multi-rate diffusion modelling of non-sorbing tracer experiments (uranine) conducted by the Äspö Task Force. In these tracer experiments the, so called, capacity ratio parameter of the multi-rated model was found to be of this order of magnitude /Svensson and Follin, 2003/.

5.4.8   Initial and boundary conditions for the numerical modelling

The information contained in Figure 3-10 and Figure 5-56 below constitutes a basis for a discussion of initial and boundary conditions for the version 1.1 site descriptive model. The graph in Figure 3-10 shows the development of the salinity in the Baltic Sea during Holocene and the graph in Figure 5-56 shows a plot of the shoreline displacement process at Forsmark during the same period. The map in Figure 5-57 shows the shoreline in Forsmark at 0 AD.

According to Figure 5-56, a suitable starting point for a hydrogeological modelling of the Forsmark area is c 8,000 BC. At this point in time the surface water conditions in the Baltic region were governed by the freshwater Ancylus Lake. The groundwater composition, on the other hand, is more or less unknown at depth at this point in time. The working hypothesis used for model version 1.1 assumed an initial condition where fresh groundwater rests on top of a more saline groundwater. The depth to and origin of the saline groundwater is probably complex but given the information available from Olkiluoto and Laxemar one may advocate that a major source for the salinity is old groundwater of brine type. The previous marine period, the Yoldia Sea, was considered to have had little, if any, impact on the subsurface hydrological conditions /Westman et al, 1999/.

There are no data in the data freeze for version 1.1 that reveal the current chemical situation at depth in KFM01A, but there are a few data from the uppermost part of the bedrock, see Figure 5-58. The deep data from Olkiluoto and Laxemar, also shown in Figure 5-58, suggest that the current groundwater salinities at these two sites are moderate down to several hundreds of metres below the sea level. The salinities then rapidly increase and reach a value of circa ten percent by weight at a depth of about two kilometres.

A comparison between the Olkiluoto and Laxemar salinity profiles shown in Figure 5-58 is of great interest to Forsmark. Like Forsmark, Olkiluoto was covered by seawater until quite recently, c 900 AD, whereas the flushing of Laxemar started already at c 3,500 BC.
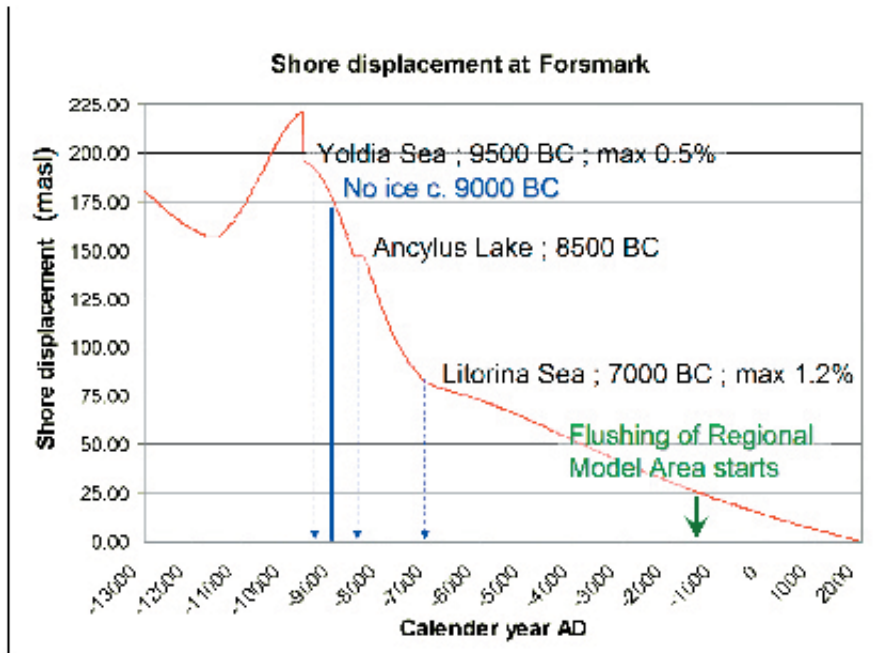
Figure 5-56. *The shoreline displacement process at Forsmark during Holocene. Modified after /Påsse, 1996/.*
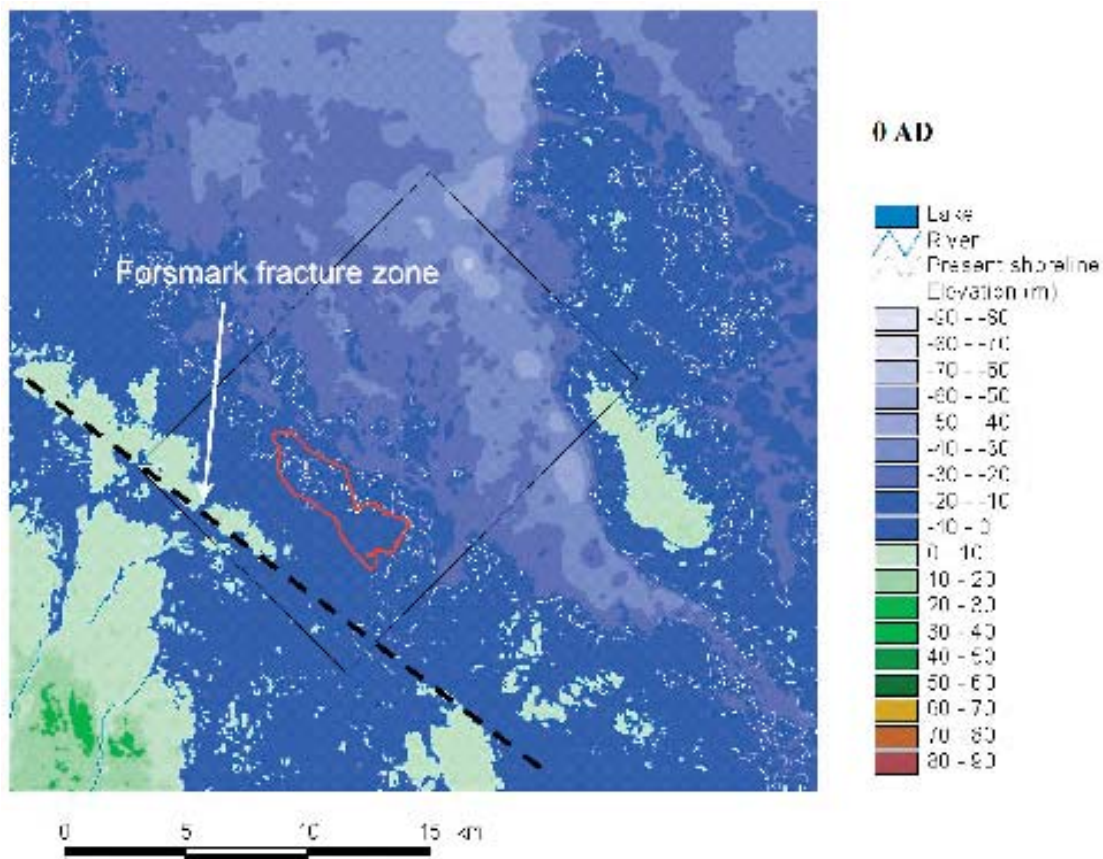
Figure 5-57. *Visualisation of the shoreline in the Forsmark area at 0 AD. The black-lined rectangle represents the Forsmark regional model area and the red-lined polygon the Forsmark candidate area.*
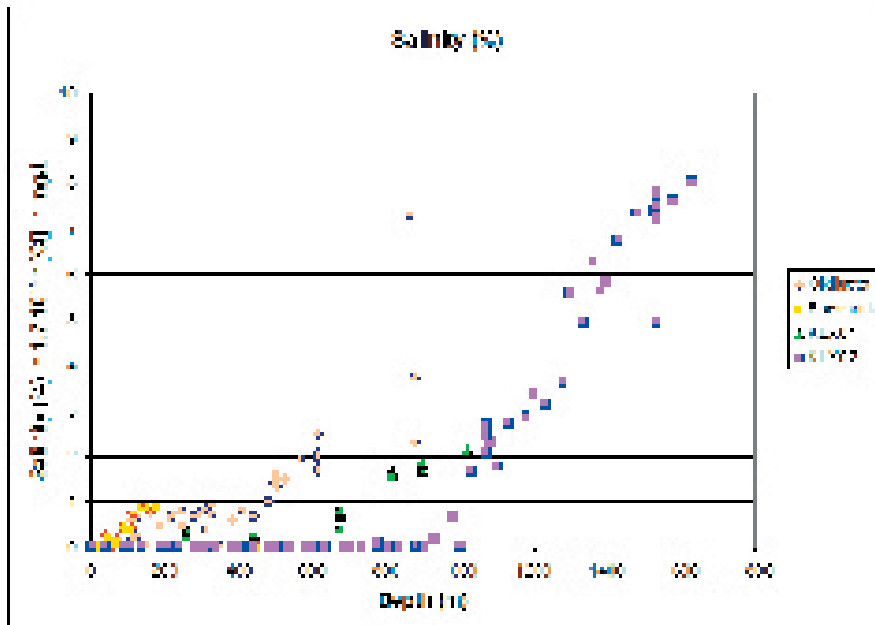
Figure 5-58. *Plot showing the chloride content in groundwater versus depth. The plot shows data from Forsmark, Olkiluoto and Laxemar (two boreholes)*

The working hypothesis used in the hydrogeological modelling for model version 1.1 assumed a value of circa ten percent by weight for the salinity at the end of the last glaciation period, i.e. 8,000 BC, and that this value still prevails. The main incentives for this boundary condition are, among other things, a flat topography, low fracture intensity at depth and the density of saline groundwater of ten percent salinity.

Concerning the initial groundwater composition versus depth at 8,000 BC, the working hypothesis used for model version 1.1 was a freshwater system down to –500 masl. Below this level, the salinity was assumed to increase linearly up to ten percent by weight at –2,100 masl.

The hydrological conditions on the top surface of the regional model domain were simplified by assuming spatially and temporally varying Dirichlet conditions for both pressure and salt at all times between 8,000 BC and 2,000 AD. From a hydrological point of view it may be advocated that the subsequent outcropping of ground surface associated with the shoreline displacement should be associated with a Neumann condition, i.e. infiltration, instead of a specified pressure and concentration, fixing a fresh groundwater table to the topographic relief. However, given the simplified representation of the Quaternary deposits, cf Section 5.4.2, a Dirichlet condition was considered sufficient for the model version 1.1. As the information about the Quaternary deposits improves, by means of more data points and/or a better spatial analysis (interpolation) of existing data, a Neumann condition for flow is likely to be adopted as a part of the development of a refined top layer description in forthcoming numerical simulation models.

The hydrological boundary conditions on the lateral (vertical) sides and the bottom side of the regional model domain are more or less uncertain. Since none of the lateral sides coincides with a major surface water divide they must be considered artificial boundaries rather than physical. The regional topographic gradient is quite consistent and parallel to the longest dimension of the model domain. This condition allows for a common simplification often used in numerical modelling, i.e. the parallel groundwater flow outside the lateral sides is assumed not to interact with the flow inside the model domain, hence no-flow boundaries are assigned.

Concerning the artificial upstream boundary a different situation prevails. Between the artificial upstream boundary and the border of the Forsmark candidate area there exists both a regional fracture zone and a major surface water divide. The regional fracture zone is the Forsmark Fault zone. The major surface water divide is located between the Forsmark Fault zone and the border of

259

the Forsmark candidate area. The divide reroutes all surface runoff from northern Uppland, crossing the artificial upstream boundary, towards the bay in the Baltic Sea to the southeast of the Forsmark candidate area (Kallrigafjärden). The working hypothesis used for version 1.1 is a case where both the Forsmark Fault Zone and the major surface water divide contribute to a situation where the (natural) groundwater flow system below the candidate area is separated from the (natural) groundwater flow crossing the artificial upstream boundary. Although this hypothesis remains to be tested, it is advocated here that a no-flow upstream boundary is a reasonable assumption for model version 1.1. Among the uncertainties, one should mention the potential impact of hydraulic anisotropy and the potential occurrence of large extensive fracture zones.

The assumption of a no-flow downstream artificial boundary is less problematic as it is located far from the Forsmark candidate area and quite close to a bathymetric low in the Baltic Sea.

Finally, as a consequence of the high salinity at depth, the bottom of the model domain was considered to be a no-flow boundary and sufficiently far away from the part of the model domain of interest. After all, the deepest boreholes that will be drilled during the site investigations will only reach c 50% of the model depth.

Two studies have been carried out which support the adopted hydraulic boundary conditions /Follin and Svensson, 2003; Holmén et al, 2003/. The major conclusion from these two studies is the strong impact of local topographic gradients, which easily exceeds the potential role of the regional topographic gradient.

No particular sensitivity analyses of the boundary conditions used were carried out for model version 1.1 as a means of testing the uncertainties, e.g. with regards to hydraulic anisotropy. It should be noted, however, that the concept of hydraulic anisotropy indeed also is a geometric matter, where a large input comes from the DFN modelling. Sensitivity analyses are likely to be performed in due time as a part of the development of more elaborated site descriptive model versions.

5.4.9 Simulation/calibration against hydraulic tests

No hydraulic interference tests applicable for simulation and calibration were conducted. The aforementioned interference test conducted at drillsite 1 is a short-distance hydraulic interference test only /Ludvigson and Jönsson, 2003/.

5.4.10 Example simulation of past evolution

In preparation of the delivery of the geological model version1.1, preliminary numerical simulations were executed using the fracture zone segments and hydraulic properties presented in the version 0 site descriptive model /SKB, 2002a/. The main objective of the preliminary simulations was to study the past hydrogeological (palaeo-hydrogeological) evolution, using different material properties for a homogeneous substratum fully saturated with freshwater at 8,000 BC. In the numerical simulations conducted subsequent to the delivery of the geological model version 1.1, some of the palaeo-hydrogeological simulations were performed a second time using a DFN-based derivation of the material properties in combination with the initial boundary conditions described in Section 5.4.6.

The preliminary numerical simulation demonstrated, among other things, that the classic formulation of the mass balance equation for groundwater flow is not applicable "as is" to the particular problem of interest. To our understanding the shoreline displacement process does not create an elastic release of groundwater when the sea water depth changes. That is, the change in sea water depth causes a change in the total pressure rather than just a change in the pore pressure. The erratic effect of incorporating an elastic release of groundwater becomes noticeable for values of the specific storativity greater than $1 \cdot 10^{-6}$ m^{-1}. This was concluded by means of numerical simulations. As a consequence it was decided to set the specific storativity to zero in all palaeo-hydrogeological simulations.

The role of the initial conditions and the shoreline displacement process, the boundary conditions of which are specified on the top side of the model domain, is exemplified in Figure 5-59. In this figure, the mobile salinity for a vertical cross section is shown at two different time slices. The profile is located in the centre of the model domain and runs parallel to the longest dimension. At c 7,000 BC the Litorina Sea begins to intrude the glacial freshwater system due to its greater density. The continuing upheaval of the sea bottom and subsequent outcropping of land results in a flushing of the terrestrial parts beginning at c 1,500 BC. The extent of the flushing depends also on the ratio between the immobile porosity and the flow (kinematic) porosity, see Figure 5-60.
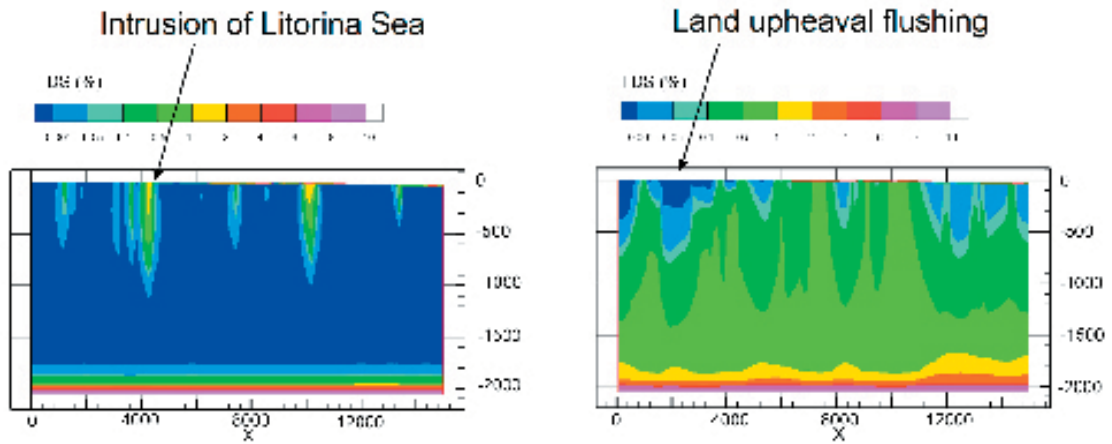
Figure 5-59. Visualisation of the simulated Litorina Sea intrusion and the subsequent flushing of meteoric water due to land upheaval.
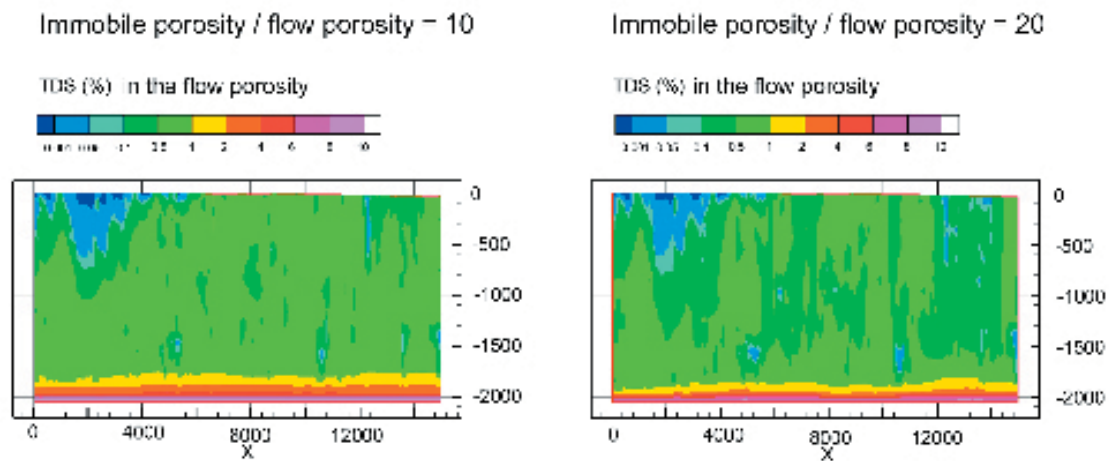
Figure 5-60. Visualisation of the role of the ratio between the immobile porosity to the flow (kinematic) porosity.

5.4.11 Example simulation of present-day flow conditions

Figure 5-61 shows an example simulation of the present-day distribution of the vertical component of the Darcy flux field using the structural and hydraulic data available for model version 1.1. The left image shows the flux field at (–500) masl and the right image shows the flux fields at (–1,000) masl. The colour range between yellow and blue represents downward fluxes, whereas the colour range between orange and purple represents upward fluxes. The thin black lines represent the trace lines of vertical HCDs. The striped polygons represent the orthographic projections of sub-horizontal HCDs. The contour of the Forsmark candidate area is also shown. The differences in the flux field versus depth and between HCDs and HRDs show that the present-day hydrogeological conditions are not at steady state.

Figure 5-62 visualises the accompanying present-day distribution of mobile salinity. The legend levels are chosen such that the different salinity concentrations of interest can be identified in the image, e.g. 1.2% corresponds to the maximum salinity of Litorina Sea water, 0.6% to Baltic Sea water, etc. The black lines within the Forsmark candidate area represent the three cored boreholes KFM01A–3A.

The spatially varying distribution of mobile salinity is a consequence of the shoreline displacement process and the changing sea water conditions. Figure 5-63 shows the results of solving five different advection-dispersion equations in parallel to the variable-density formulation, one a-d equation for each of following "water types": Old saline groundwater of brine type, Glacial melt water, Litorina Sea water, Baltic Sea water and Meteoric water. At each point in the flow system the sum of the fractional concentrations of these five water types is one (100%). The vertical cross-section is parallel to the longest dimension of the model domain and runs through the cored borehole in centre of Figure 5-62 i.e. KFM02A.
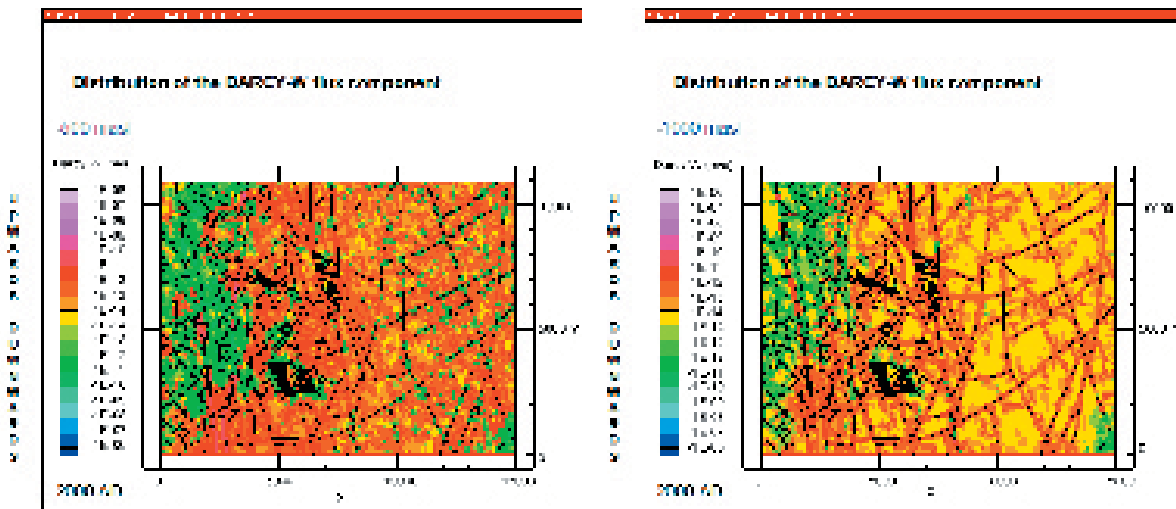
Figure 5-61. *Example simulation of the present-day distribution of the vertical component of the Darcy flux field. The left image shows the flux field at (–500) masl and the right image shows the flux fields at (–1,000) masl. The legend levels are chosen such that yellow – green – blue represent downward fluxes and orange – red – purple represent upward fluxes.*
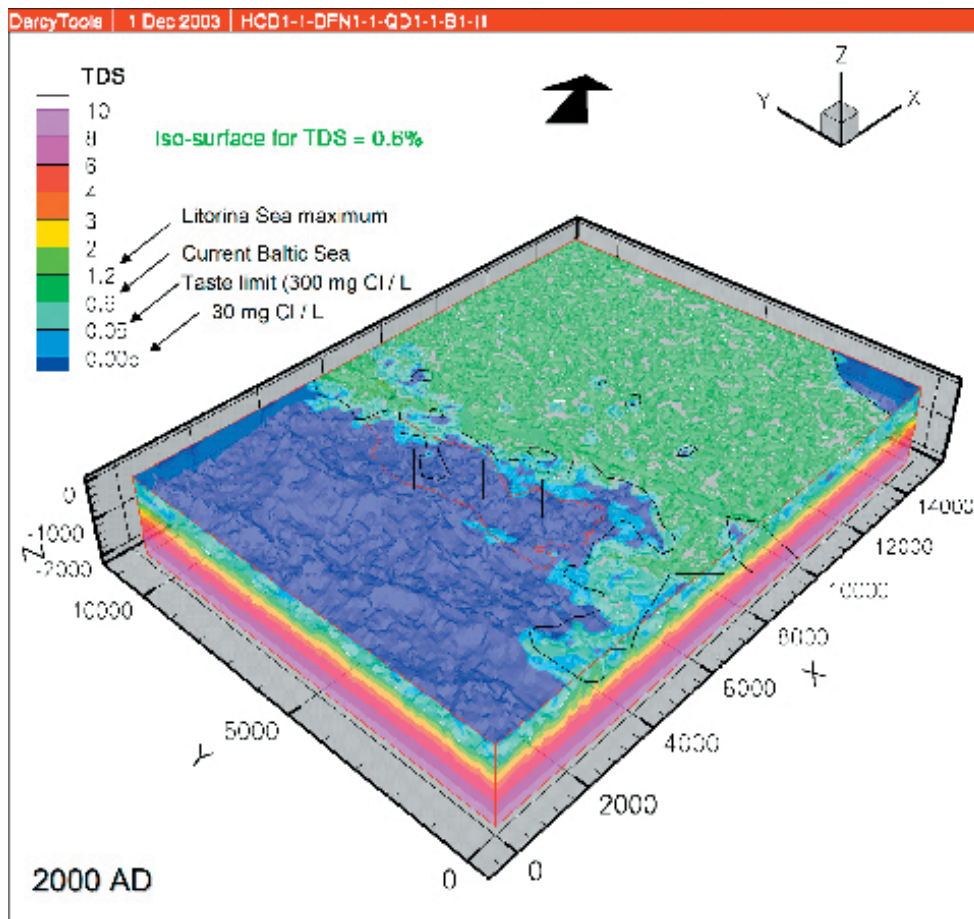
Figure 5-62. Visualisation of the present-day distribution of mobile salinity. Initial conditions as specified in Section 5.4.8. Structures and hydraulic properties according to the specifications for model version 1.1.

5.4.12 Evaluation of hydrogeological uncertainties

Model version 1.1 is the first step towards a realistic site description of the *in situ* conditions at Forsmark. Some of the uncertainties described above are due to lack of data and will be resolved in due time, whereas others will always be, more or less, a part of any site description, regardless of the extent of the investigations. The latter condition is obvious for two reasons:

* large areas are far from the target area and will never be investigated, and

* the number of boreholes in the target area must be limited due to, among other things, physical reasons.

It is within this framework that numerical hydrogeological modelling comes into play as a tool for analysing the impact of both parameter heterogeneity and various conceptual uncertainties. For the development of future model versions more and/or better data concerning the following hydrogeological issues are particularly emphasised:

HCD

* The structural geological model of the target area; in particular, the occurrence and extensions of sub-horizontal deformation zones.

* The hydraulic signature and potential differences between deformation zones of varying geological confidence.
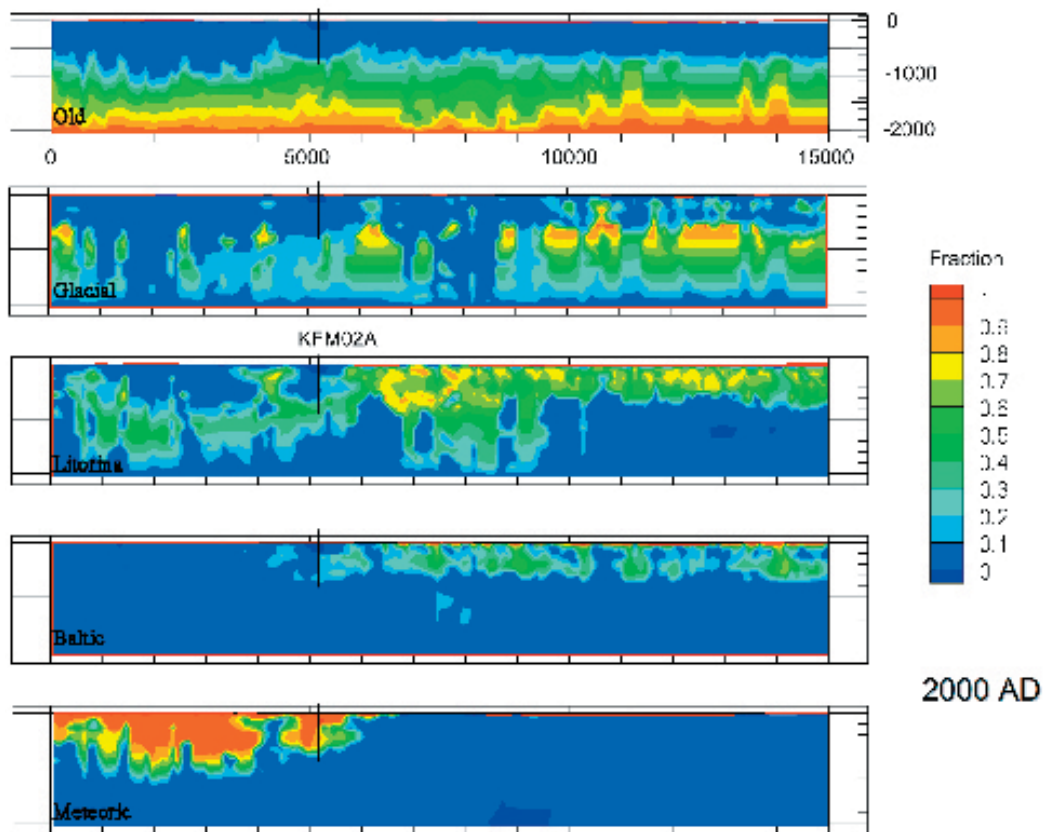
Figure 5-63. Visualisation of the present-day distribution of mobile salinity in terms of five different water types: Old saline groundwater of brine type, Glacial melt water, Litorina Sea water, Baltic Sea water and Meteoric water. At each point in the flow system the sum of the relative concentrations add to 100%. Initial conditions are as specified in section 5.4.7. Structures and hydraulic properties are according to the specifications for the version 1.1 site descriptive model.

HRD

*   The geological fracture network description; in particular, surface variability, the coupling between surface and depth data, and the geological classification of conductive fractures.

*   The database for the deduction of fracture transmissivity; in particular, the motives for assigning set-specific differences (geometric anisotropy).

HSD

*   The spatial variability of the thickness of the Quaternary deposits, i.e. bedrock topography.

*   The database for assigning hydrogeological properties to the Quaternary deposits.

*   Observations of seasonal variations in the groundwater table, which describe the role of evapotranspiration.

Hydrogeochemistry

*   The description of groundwater salinity versus depth in the kinematic fracture system.

*   The description of groundwater salinity in the immobile, low-conductive rock.

*   Evidence for discharging deep groundwater.

5.5   Hydrogeochemical modelling

The main objectives of the hydrogeochemical modelling are to describe the chemistry and distribution of the groundwater in the bedrock and overburden and the processes involved in its origin and evolution. The SKB hydrogeochemistry programme /Smellie et al, 2002/ is intended to fulfil two basic requirements: 1) to provide representative and quality assured data for use as input parameter values in calculating long-term repository safety, and 2) to understand the present undisturbed hydrogeochemical conditions and how these conditions will change in the future. Parameter values for safety analysis include pH, Eh, S, SO_4, HCO_3, PO_4 and TDS (mainly cations), together with colloids, fulvic and humic acids, other organics, bacteria and nitrogen. These values will be used to characterise the groundwater environment at, above and below repository depths. When the hydrogeochemical environment has been fully characterised, this knowledge, together with an understanding of the past and present groundwater evolution, should provide the basis for predicting future changes. The site investigations and the modelling will therefore provide important source material for safety analyses and the environmental impact assessment for the Forsmark site. The data evaluation and modelling becomes a complex and time-consuming process when the information has to be decoded. Manual evaluation, expert judgment and mathematical modelling must normally be combined when evaluating groundwater information. A schematic presentation of how a site evaluation/modelling is performed and its components are shown in Figure 5-64 and described in detail by /Smellie et al, 2002/.
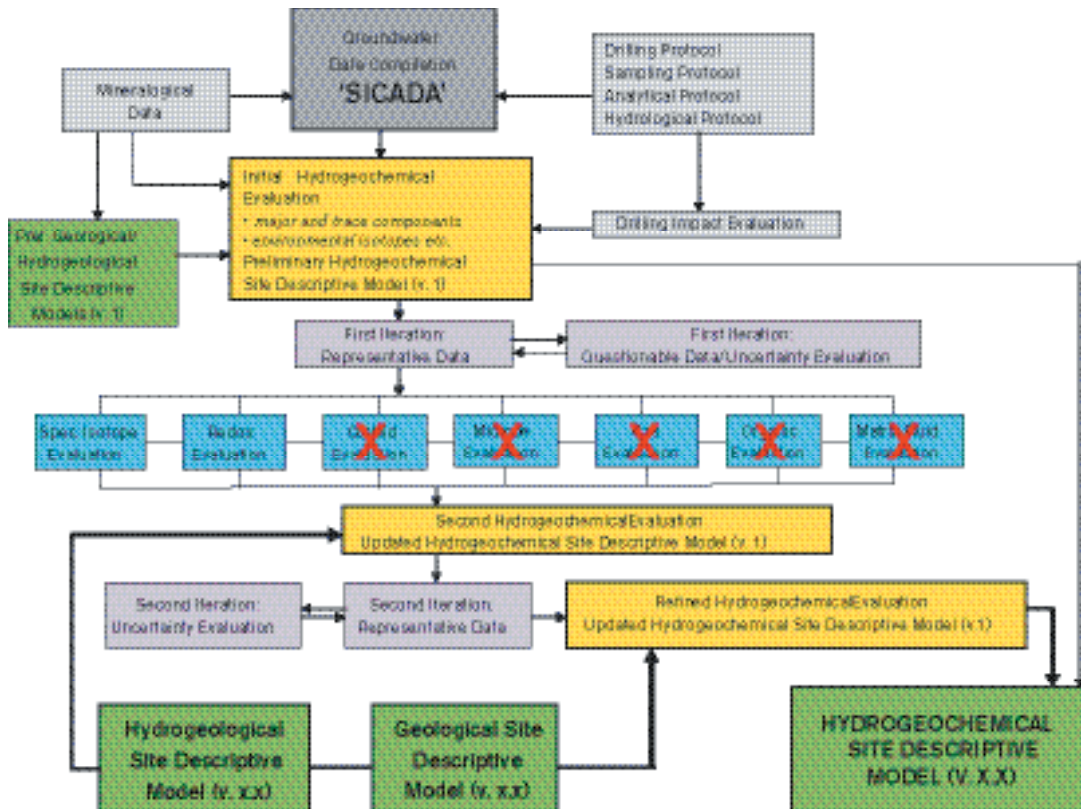
Figure 5-64. *The evaluation and modelling steps used in this report. The crossed over evaluation steps were not performed due to lack of data /after Smellie et al, 2002/.*

For the groundwater chemical calculations and simulations the following standard tools were used.

For evaluation and explorative analyses of the groundwater:

- AquaChem: Aqueous geochemical data analysis, plotting and modelling tool (Waterloo Hydrogeologic).

Mathematical simulation tools:

- PHREEQC with the database WATEQ4F: Chemical speciation and saturation index calculations, reaction path, advective-transport and inverse modelling /Parkhurst and Appelo, 1999/.
- M3: Mixing and Mass balance modelling /Laaksoharju et al, 1999a/.

Visualisation/animation:

- TECPLOT: 2D/3D interpolation, visualisation and animation tool (Amtec Engineering Inc).

5.5.1 Modelling assumptions and input from models

Hydrogeochemical modelling involves the integration of different geoscientific disciplines such as geology and hydrogeology. This information is used as background information, supportive information or as independent information when models are constructed or compared. The following sections describe how geological information was used in the modelling and how speciation, mass-balance, coupled modelling and mixing modelling was carried out.

Geological information is used in hydrogeochemical modelling as direct input in mass-balance modelling, but also to judge the feasibility of the results from, for example, saturation index modelling. For this particular modelling exercise, geological data were summarised, the information was reviewed and the relevant rock types, fracture minerals and mineral alterations were identified /see Laaksoharju et al, 2004/.

The underlying geostructural model provides important information of water-conducting fractures, which is used for the understanding and modelling of the hydrodynamics. The cutting plane used for visualisation of groundwater properties is generally selected with respect to the geological model. The results from the modelling are generally presented by using 2D/3D visualisation tools. Unfortunately, the lack of data from the depth at Forsmark precludes a 3D interpolation and production of a 2D cutting plane for this model version.

5.5.2 Conceptual model with potential alternatives

Because of the lack of data from depth few alternative models were tested. Those tested included different reference waters and local and regional models, and various modelling tools and approaches were applied on the data set.

5.5.3 Speciation, mass-balance and coupled modelling

Speciation modelling

Speciation-solubility modelling has been carried out with PHREEQC /Parkhurst and Appelo, 1999/ and the WATEQ4F thermodynamic database.

In this type of calculations, starting from the concentration of a set of elements in a water sample and other relevant parameters (temperature, pH, Eh, total or carbonate alkalinity, and, in some cases, density) the concentration and activity of all the relevant species in the system and the saturation indices (SI) with respect to a predefined set of minerals is computed. It is a purely thermodynamic calculation where it is assumed that all dissolved species are in mutual homogeneous equilibrium. This approach defines the proximity of a solution to equilibrium with a relevant phase through a saturation index defined as:

$$SI = \log \frac{IAP}{K(T)} \qquad (5.16)$$

where *IAP* is the ionic activity product and $K(T)$ is the equilibrium constant of the dissolution-precipitation reaction of the relevant phase. A positive value indicates that thermodynamically a mineral can precipitate a negative value that it can dissolve. A value close to zero indicates that the mineral is not reacting. The saturation index indicates the potential for the process, not the rate at which the process will proceed. From the results, conclusions concerning possible major reactions taking place and indirect indications of the dynamics of the system can be drawn.

The calculations were used to investigate the processes that control water composition at Forsmark. The procedure only deals with plausible minerals in the system, i.e. those that can reach equilibrium with the groundwater. Therefore, clearly undersaturated mineral phases are not included in this description. In addition, only mineral phases actually identified from the Forsmark site were considered.

The following description is divided into two main parts, one addressing the state of non-redox elements and phases and the other focussing on the redox state of the system.

Carbonate system

A pH sensitivity analysis /Laaksoharju et al, 2004/ showed that laboratory pH values could have been affected by CO_2 degassing. Because there are no pH values from down-hole continuous logging to compare with, it is difficult to assess the likelihood of the results and therefore this uncertainty will propagate into the speciation-solubility calculations.

Calcite saturation states indicate that surface and subsurface waters can be either undersaturated or oversaturated with respect to calcite, but most groundwater samples are near equilibrium (Figure 5-65a), considering the commonly accepted ± 0.5 uncertainty in the SI of this mineral when uncertainties in pH are evaluated /Pitkänen et al, 1998, 1999/. The computed P_{CO2} values show a roughly decreasing trend with depth (Figure 5-65b), but with scatter. P_{CO2} and SI scatter are mainly attributable to the above-commented uncertainties in pH, which are propagated to P_{CO2} and calcite SI values during calculations.

Trends of alkalinity, pH and saturation state of calcite are apparently related to water-rock interaction processes (dissolution-precipitation of fracture filling calcite and silicate hydrolysis) in agreement with the model for the Stripa groundwaters /Nordstrom et al, 1989/ and verified in other Swedish and Finnish sites.

The measured initial steep rise in alkalinity (Figure 4-67) and pH affecting superficial waters is related to weathering of the bedrock, causing calcite dissolution and hydrolysis of silicates. Calcite reaches saturation (or oversaturation) at the alkalinity peak and the subsequent depletion in alkalinity can be attributed to calcite precipitation. This precipitation process is induced by calcium enrichment in groundwaters associated with mixing with a saline source.

The pH usually increases slightly beyond the alkalinity peak. As calcite precipitation produces a decrease in pH, it has been assumed that the pH increase is associated with the effect of silicate hydrolysis (as consuming proton reactions) deep in the bedrock. Because the trend observed in the Forsmark groundwaters is a pH decrease, there is apparently minor or no silicate hydrolysis compensation. An additional reason could be kinetic constrains on aluminium silicate weathering reactions due to the relatively short residence time of the surface water /pers comm, J Bruno, 2004/. Nevertheless, this pH decreasing pattern in Forsmark can be magnified (with respect to other Scandinavian sites) by the high alkalinity peak developed in the more recent superficial waters. The existence of older recharge groundwaters with lower pH and/or uncertainties in pH measurements (i.e. actual pH lower than measured pH due to degassing) would modify the interpretation of the pH pattern.
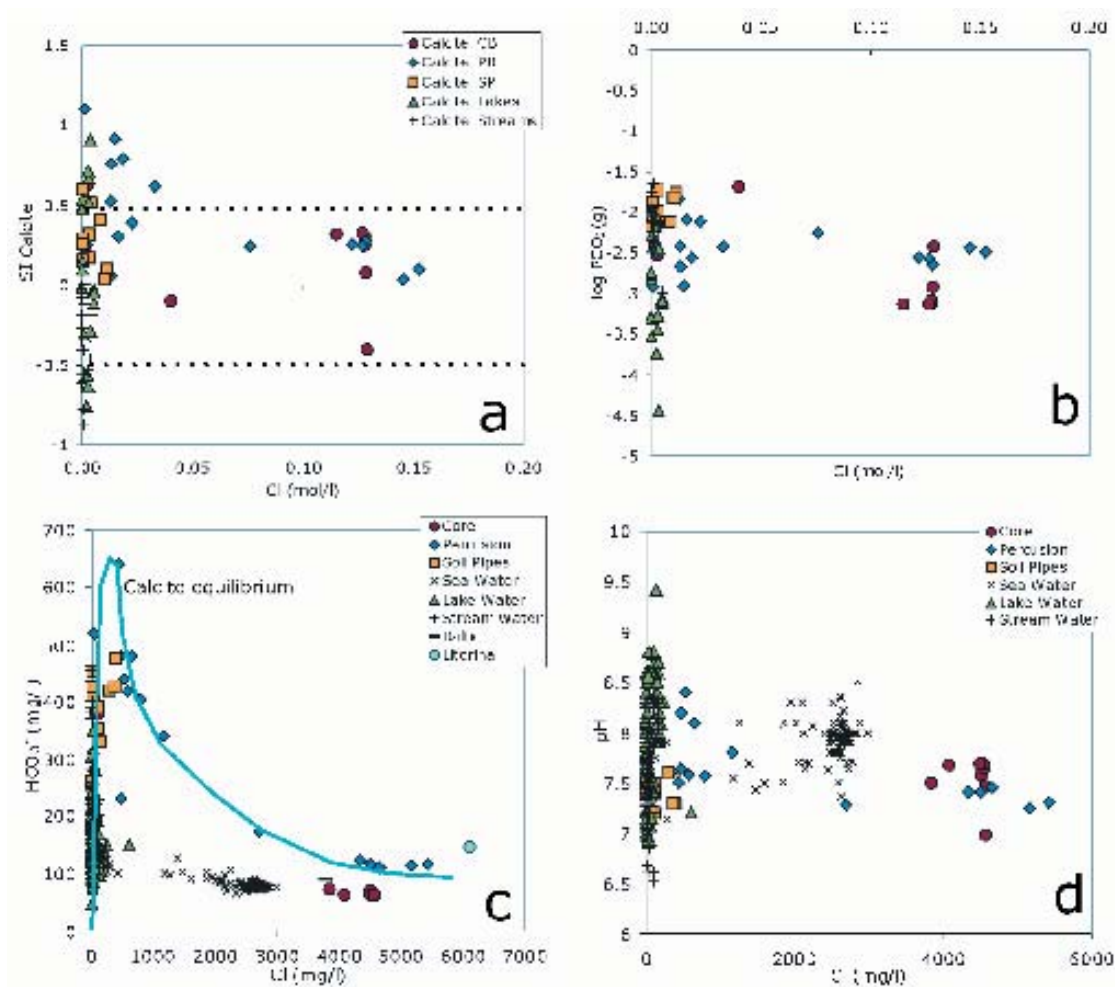
Figure 5-65. *Evolution of the carbonate system in Forsmark waters. (a) and (b) calculated calcite saturation index and partial pressure of CO_2 against chloride;(c) and (d) Alkalinity and pH against chloride. The dotted lines in figure (a) represent the uncertainty associated with SI calculations.*

Silica system

The weathering of rock-forming minerals is the main source of dissolved silica. Superficial waters have a variable degree of saturation with respect to silica phases (quartz and chalcedony). This is compatible with the weathering hypothesis.

Superficial waters are oversaturated with respect to quartz and close to equilibrium with chalcedony (Figure 5-66). Saturation indices of these phases are relatively constant and independent of the chloride content of the waters. This suggests that the groundwater has already reached a stationary state associated with the formation of aluminosilicates or secondary silica phases like chalcedony, which control the concentration of dissolved silica.

The lack of dissolved aluminium data for Forsmark groundwaters precludes the calculation of speciation-solubility diagrams for aluminosilicates (Figure 5-67). Therefore, activity diagrams were used to study the stability of silicate minerals in the system. The accuracy of these diagrams depends on pH and they are therefore affected by the uncertainties in the pH measurements at Forsmark. Uncertainties in the equilibrium constants of the aluminosilicates (especially phillosilicates) also affect the conclusions drawn from these diagrams. This last source of uncertainty has been partially removed by considering multiple equilibrium constants for the same phase. Nevertheless, the conclusions are preliminary.
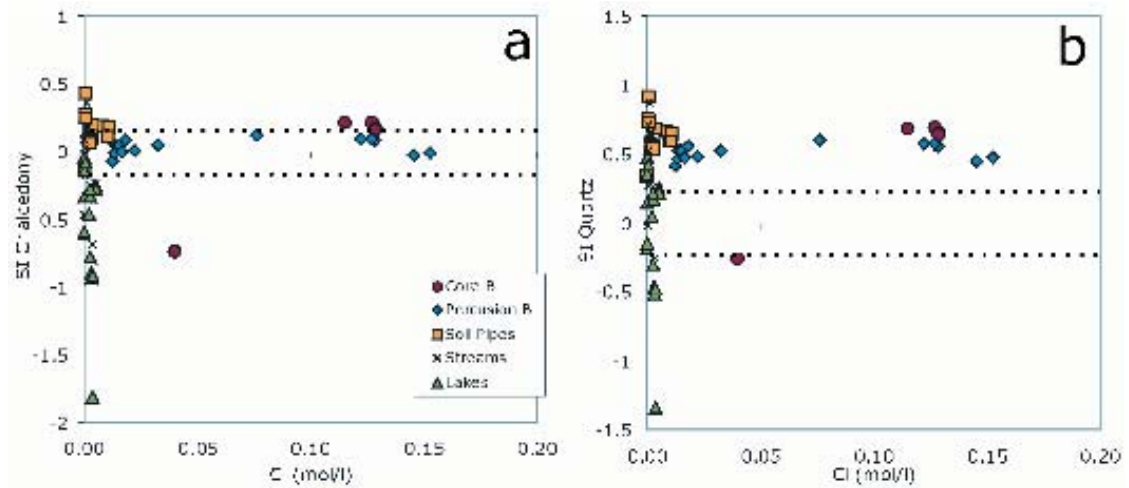
Figure 5-66. *Saturation indices of chalcedony and quartz as a function of Cl. The dotted lines represent the uncertainty associated with SI calculations /Deutsch et al, 1982/.*
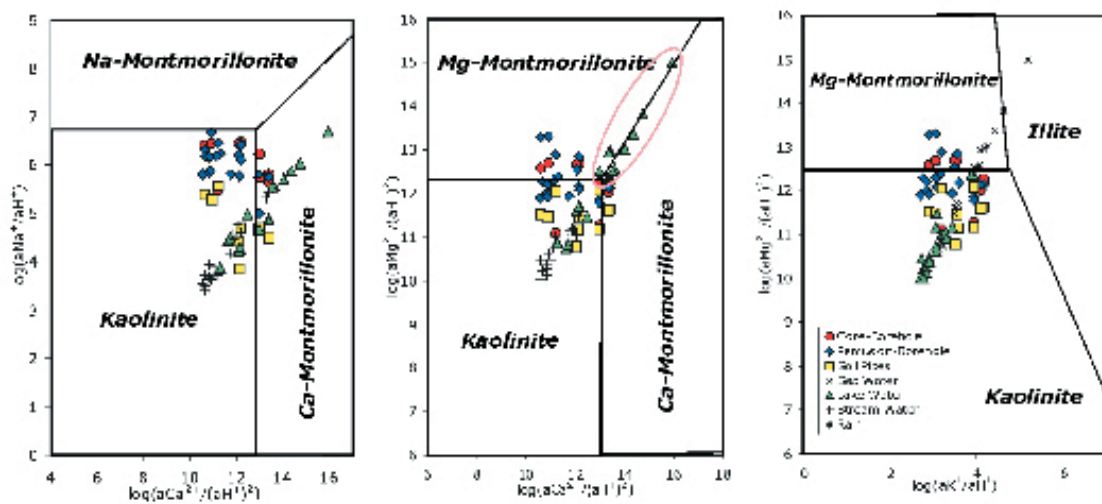
Figure 5-67. *Aqueous activity diagrams for some aluminosilicate minerals at 7°C, 1 bar. The field boundaries were calculated with data from /Helgeson, 1969/ and a logarithmic silica activity of −4.*

Most groundwaters are in or near the stability field of Montmorillonite, but with no clear trend. Locally, both Mg-montmorillonite and Ca-montmorillonite are favoured and Mg-Ca or Ca-Mg exchange reactions are possible. Mg/Na exchange processes may play an important role in the Lake waters. Some groundwaters fall in or near the Ca-montmorillonite stability field and accordingly Na would be released to solution.

Figure 5-68 shows three additional stability diagrams for other mineral phases identified as filling fracture minerals in the KFM01A borehole: adularia, albite, prehnite, laumontite and chlorite. The diagrams are based on data calculated at 15°C by /Grimaud et al, 1990/ for the Stripa groundwaters and show that most groundwaters are near or in the albite stability field. Samples along the boundary with adularia indicate equilibrium between albite and adularia. Also, more saline groundwaters define a trend towards equilibrium with chlorite. The Lake water data appear to be in equilibrium with laumontite, which has been identified in the fracture mineralogy of the bedrock.

269
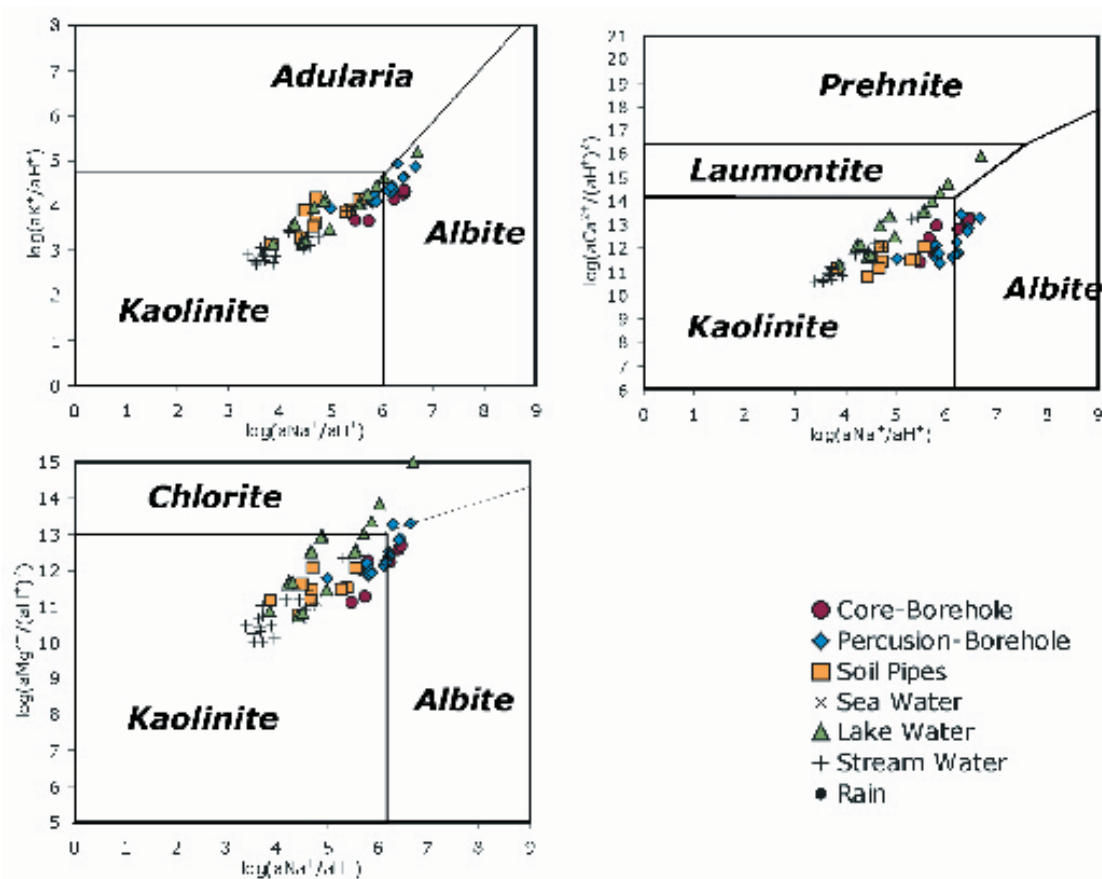
Figure 5-68. *Aqueous activity diagrams for some aluminosilicate minerals at 15°C, 1 bar. The field boundaries have been calculated from the data of /Grimaud et al, 1990/.*

Finally, Figure 5-69 includes illite. Diagram (a) was used in the Cigar Lake natural analogue study /Cramer and Smellie, 1994/, and is based on data from /Helgeson, 1969/ and /Helgeson et al, 1978/. Diagram (b) was constructed with data from /Garrels, 1984/. Both diagrams suggest that illite plays an important role in controlling the groundwater system, although the available mineralogical data indicate that the abundance of illite in fracture fillings is low. This, however, may be an underestimation due to the loss of soft and fine grained material during drilling.

Cation exchange processes are probably more important than clay mineral recrystallisation during short-term water-rock interactions at low temperature, but in waters with long residence times these exchange processes may cause irreversible changes in clay minerals as the solubility diagrams suggest /Pitkänen et al, 1999/.

Redox pairs calculations

The available analytical data (dissolved Fe^{2+}, total Fe, total sulphide and sulphate concentrations) allow a standard redox pair calculation for KFM01A waters at 115.33 m depth (brackish waters) only. Preliminary values of in situ temperature (7°C) and Eh (–180 mV) are available for borehole KFM01A at the same depth and were used as reference values in the calculations.

The analysed samples (#4480, 4481, 4484, 4520, 4524 and 4538) showed a fairly homogeneous chemical composition, as expected from samples taken from the same depth. pH values were also rather constant, between 7.47 and 7.69, except for sample 4525 which had an anomalously low pH value (6.98) and was omitted from the data set. In the calculations, pH was varied between 7.4 and 7.7 to take into account the actual uncertainty in this parameter. This range includes the pH value calculated assuming equilibrium with calcite /see Laaksoharju et al, 2004/.

270
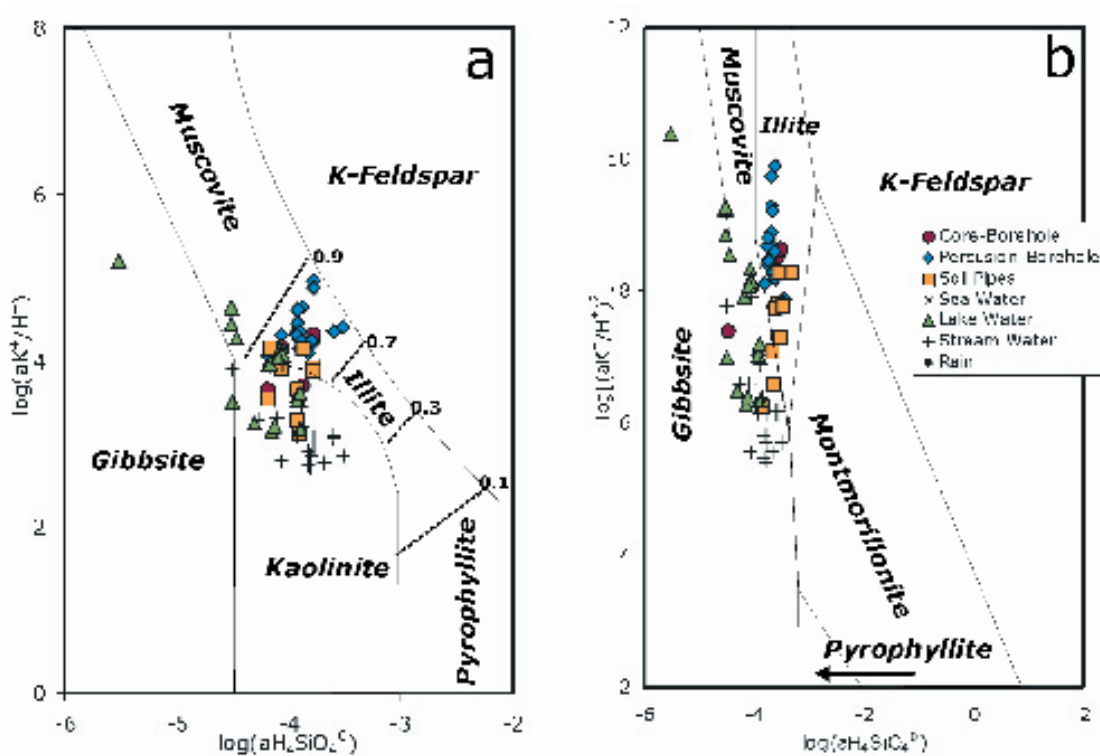
Figure 5-69. Aqueous activity diagrams for some aluminosilicate minerals at 25°C, 1 bar, including illite. The field boundaries have been calculated with data from /Helgeson, 1969/ and /Helgeson et al, 1978/ in graph (a) and from /Garrels, 1984/ in graph (b). In graph (a) the illite field is contoured to show the stability of different illite fractions in I/S.

Previous studies in "granitic" groundwaters from Sweden and Finland /Nordstrom and Puigdomenech, 1989; Smellie and Laaksoharju, 1992; Grenthe et al, 1992; Glynn and Voss, 1999; Bruno et al, 1999/ have found that the iron and sulphur redox pairs/buffers are the most reliable couples to estimate the redox state. In this system, the selected redox couples are dissolved Fe^{3+}/Fe^{2+} and SO_4^{2-}/S^{2-} and the heterogeneous $Fe(OH)_3/Fe^{2+}$, pyrrhotite/SO_4^{2-} and pyrite/SO_4^{2-} couples. Results using the Fe^{3+}-clay/Fe^{2+}-clay redox pair, as proposed by /Banwart, 1999/, were also tested. Using the method suggested by /Grenthe et al, 1992/ with the calibration for $Fe(OH)_{3(s)}/Fe^{2+}$ redox pair, both with and without activity correction /Glynn and Voss, 1999/, provided too low Eh values compared with the measured ones and with the rest of the redox pairs (Figure 5-70).

An alternative approach to the computation of the redox potential with the $Fe(OH)_{3(s)}/Fe^{2+}$ pair is that of /Bruno et al, 1999/. They used thermodynamic data for two end members, crystalline and amorphous $Fe(OH)_3$ (Figure 5-70). Using the thermodynamic data from /Bruno et al, 1999/ for amorphous $Fe(OH)_3$, the redox potential calculated by the $Fe(OH)_{3(s)}/Fe^{2+}$ would match the electrochemical measurement.

The potential calculated with the SO_4^{2-}/S^{2-} pair is between –194 and –210 mV and very close to the measured Eh in the borehole. Redox potentials calculated with the pyrrhotite/SO_4^{2-} redox pair (used by /Bruno et al, 1999/ in the Palmottu system) are around –220 mV, very similar to the values provided by the SO_4^{2-}/S^{2-} couple and close to the measured Eh of –180 mV. Calculated redox potentials assuming equilibrium with pyrite (pyrite/SO_4^{2-} couple) are also similar.

The Fe^{3+}-clay/Fe^{2+}-clay redox pair proposed by /Banwart, 1999/ is based on the reversible one-electron transfer between oxidised and reduced smectites. For this reaction, the conditional redox potential (Eh, V) as a function of pH at 10°C is defined by the equation:

Eh = 0.280–0.056 pH

271
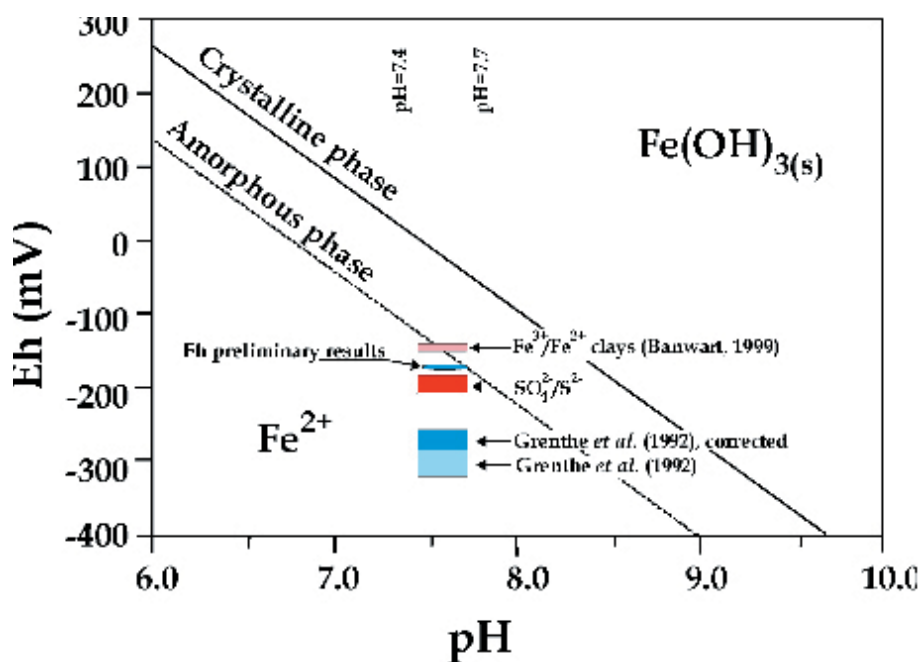
Figure 5-70. *Eh-pH diagram with Fe(OH)$_{3(s)}$/Fe^{2+} phase boundaries for crystalline (log K=3) and amorphous (log K = 5) Fe(OH)$_3$ phases. The diagram has been drawn using data from the Palmottu Natural Analogue study /Bruno et al, 1999/ assuming a concentration of Fe^{2+} = 3·10^{-5} M. The vertical lines bracket the uncertainty in pH of the samples. Also shown are the Eh values obtained with the /Grenthe et al, 1992/ calibration of the Fe(OH)$_{3(s)}$/Fe^{2+} pair (blue squares); the Eh values deduced from the SO$_4$$^{2-}$/S^{2-} and Fe^{3+}-clay/Fe^{2+}-clay pairs (red areas); and the potentiometric value measured in the borehole (blue ellipse).*

The results obtained applying this pair, between –138 and –150 mV, are also consistent with the measured values.

The above results suggest that the redox state of the brackish waters from the shallow depth interval (centred at 115.33 m) in borehole KFM01A could be buffered by the presence of iron oxides and hydroxides and by redox reactions among phyllosilicates. The lack of specific mineralogical data precludes a definitive confirmation of this conclusion.

Nevertheless, the good match between sulphur redox-pairs and between those and electrochemical Eh values, points to sulphide minerals as redox buffers. This buffering action, together with the presence of dissolved sulphides, suggests the development of an anoxic-sulphidic state, mediated by sulphate reducing bacteria (SRB). Typical precipitation of sulphide minerals, associated with the sulphidic environment, is suggested by the equilibrium between these waters and several monosulphide phases (e.g. pyrrhotite and amorphous FeS), as deduced from speciation-solubility calculations /see Laaksoharju et al, 2004/.

Microbial analysis and δ^{34}S isotopic data are not available for KFM01A waters. However, brackish waters from similar depths and setting in borehole HFM05 show high δ^{34}S values, between 24.5 and 24.6‰ CDT, substantially higher than the values found in shallower bicarbonate waters from borehole KFM02A (14–16‰ CDT). These elevated values suggest the existence of a microbially-catalysed reduction of dissolved sulphate. The presence of SRB has been reported at similar depths in studies at sites of the Finnish Programme /Figure 5.5.3.H; Haveman et al, 1998; Snellman et al, 1998, Pitkänen et al, 1998, 1999/.

The absence of key analytical data (Fe-concentration, sulphide, methane) for the rest of the samples in the area rules out a better characterisation of the sequence of redox conditions developed at depth.

Mass balance and mixing calculations

The inverse approach via mass balance and mixing calculations by using PHREEQC /Parkhurst and Appelo, 1999/ to track the hydrogeochemical evolution of the Forsmark area is handicapped by the few groundwater samples used to carry out the study, the absence of key analytical data, the scarcity of mineralogical data and the, so far, rather rudimentary hydrogeological model. Consequently, the results summarised in this section should be understood as preliminary, based only on: a) general premises with respect to the type of waters and reactive phases involved, and b) the inter-comparison with analogous systems (i.e. similar water end-members).

The evolution paths used in the calculations have been selected taking into account only the most general groundwater hydrogeochemical characteristics and its apparent age. Based on this, two water types were identified: fresh waters with a bicarbonate imprint and low residence times (tritium values above detection limit), and brackish-marine waters with Cl contents up to 6,000 mg/L and longer residence times (tritium values below detection limit).

For the analysis of the evolution of the *first water type* (fresh water), which has an *a priori* important water-rock interaction component, simple mass balance calculations with no mixing (to assess the reaction processes occurring between two water samples joined by a hypothetical flow line) and binary mixing with mass balance (to assess the mixing proportions of two water samples and the reaction processes necessary to explain the chemistry of a third water sample) were performed. For the analysis of the *second water type* (brackish-marine water), only multiple-mixing and mass balance calculations were carried out. The goal of these calculations was to explain, using hetero-geneous reactions between solid phases and the water, the chemistry of a water sample which is the product of the mixing of five or six groundwater end-members. For the calculations with PHREEQC the following chemical and isotopic data were used: Cl, HCO_3^-, SO_4^{2-}, SiO_2, Ca, Mg, Na, K, Fe, S^{2-}, $\delta^{18}O$ and δ^2H.

Model results for fresh, non-saline waters

From the modelling it was concluded that Ca-Na-HCO_3 waters are little evolved geochemically, with a chemistry totally controlled by water-rock interaction processes. Na-HCO_3-Cl waters have a longer residence time and therefore mass transfer processes are more significant. Alternatively, these waters can be explained as a mixing process with a minority marine end-member. Finally, Na-Cl-HCO_3 waters are clearly influenced by a marine component.

The modelling results indicate that water-rock interaction is the main process responsible for the chemistry of the Ca-Na-HCO_3 and Na-HCO_3-Cl waters in this group of fresh and non-saline waters. However, an increasing contribution of mixing with a marine end-member could explain the observed Cl increase in the more evolved Na-Cl-HCO_3 waters. The reactions that explain the water chemistry are similar in the three cases, the only change being the amount of mass transfer. Decomposition of organic matter, dissolution of calcite, plagioclase, biotite, and sulphides, precipita-tion of phyllosilicates (mainly smectites and montmorillonites), and Na-Ca ionic exchange are the main mass transfer processes encountered in most calculations. Smectite may be present in the near-surface fractures, but this has not been possible to confirm yet. In future modelling, the effects of Na/Ca and Mg/Na ion exchange reactions will be tested.

Model results for brackish-saline waters

The water end members most frequently used in analogous systems were also selected for the multiple mixing and mass balance calculations carried out for the Forsmark waters with PHREEQC. These water end members are: Rain 60, Litorina, Sea Sediment, Glacial Meltwater and Brine. In the M3 calculations for Forsmark, the end member Lake Water was also included (see below).

Modelling results for brackish groundwaters (Cl ≈ 4,500 mg/l) indicate the presence of two dominant end members, Litorina and Glacial Meltwater (with nearly the same proportions) in the mix that produces these waters. The most saline groundwater considered in the calculations (Cl ≈ 6,000 mg/l) is dominated by the Litorina end member (> 80%).

Feasible reactions associated to these mixing models include dissolution of plagioclase and biotite, precipitation of calcite and illite and ionic exchange processes (mainly Na-Ca). The quasi-conserva-tive behaviour of sulphate in the mixing and the lack of suitable isotopic data preclude a precise description of sulphate-reduction processes.

M3 modelling

A further modelling approach, which is useful in helping judge the origin, mixing and major reactions influencing groundwater samples, is the M3 modelling concept (Multivariate Mixing and Mass-balance calculations) detailed in /Laaksoharju et al, 1995/ and /Laaksoharju et al, 1999a/.

Introduction and model description

In M3 modelling, the assumption is that the groundwater composition is always a result of mixing and reactions. M3 modelling uses a statistical method to analyse variations in groundwater compositions so that the mixing components, their proportions, and chemical reactions are revealed. The method estimates the contribution to hydrochemical variations by mixing of groundwater masses in a flow system by comparing groundwater compositions to identified reference waters. Subsequently, contributions to variations in non-conservative solutes from reactions can be calculated.

The M3 method consists of 4 steps where the first step is a standard principal component analysis (PCA), selection of reference waters, followed by calculations of mixing proportions, and finally mass balance calculations (for more details see /Laaksoharju et al, 1999a; Laaksoharju, 1999/). The PCA applied to Forsmark data and all Nordic Sites data is illustrated in Figure 5-71. 118 samples from the Forsmark site were used in the calculations. The numerical values are given in /Laaksoharju et al, 2004/.

The reference waters used in the M3 modelling have been identified from previous site investigations (e.g. Äspö and Laxemar) and also from the evaluation of the Forsmark primary data set in Chapter 4 (for groundwater analytical data see Table 5-41):

- **Brine water:** Represents the sampled deep brine type (Cl = 47,000 mg/L) of water found in KLX02: 1,631–1,681 m /Laaksoharju et al, 1995/. An old age for the Brine is suggested by the measured ^{36}Cl values indicating a minimum residence time of 1.5 Ma for the Cl component /Laaksoharju and Wallin, 1997/.

- **Glacial water:** Represents a possible melt-water composition from the last glaciation > 13,000 BP. Modern sampled glacial melt water from Norway was used for the major elements and the δ^{18}O isotope value (−21‰ SMOW) was based on measured values of δ^{18}O in calcite surface deposits /Tullborg and Larson, 1984/. The δ^2H value (−158‰ SMOW) is a modelled value based on the equation ($\delta H = 8 \times \delta^{18}O + 10$) for the meteoric water line.

- **Litorina Sea:** Represents old marine water and its calculated composition has been based on /Pitkänen et al, 1999/.

- **Forsmark Lake water:** Corresponds to summer precipitation affected by evaporation indicated by high δ^{18}O values and a slight evaporation modification of the deuterium value.

- **Sea sediment:** Represents marine water affected by microbial sulphate reduction.

- **Precipitation:** Corresponds to infiltrating meteoric water (the origin can be rain or snow) from 1960. Sampled modern meteoric water with a modelled high tritium (2,000 TU) content was used to represent precipitation from that period.

Table 5-41. Groundwater analytical or modelled data* used as reference waters in the M3 regional modelling for Forsmark.

	Cl (mg/L)	Na (mg/L)	K (mg/L)	Ca (mg/L)	Mg (mg/L)	HCO$_3$ (mg/L)	SO$_4$ (mg/L)	^{3}H (TU)	δ^2H ‰	δ^{18}O ‰
Brine	47200	8500	45.5	19300	2.12	14.1	906	4.2	−44.9	−8.9
Glacial	0.5	0.17	0.4	0.18	0.1	0.12	0.5	0	−158*	−21*
Litorina sea*	6500	3674	134	151	448	93	890	0	−38	−4.7
Sea Sediment	4920	2300	29	730	233	1200	36	14	−50.4	−7.3
Precipitation	0.23	0.4	0.29	0.24	0.1	12.2	1.4	2000*	−80	−10.5
Forsmark Lake water	45.8	21	3.21	30.3	5.9	110	16.18	7.6	−44.3	−4.5
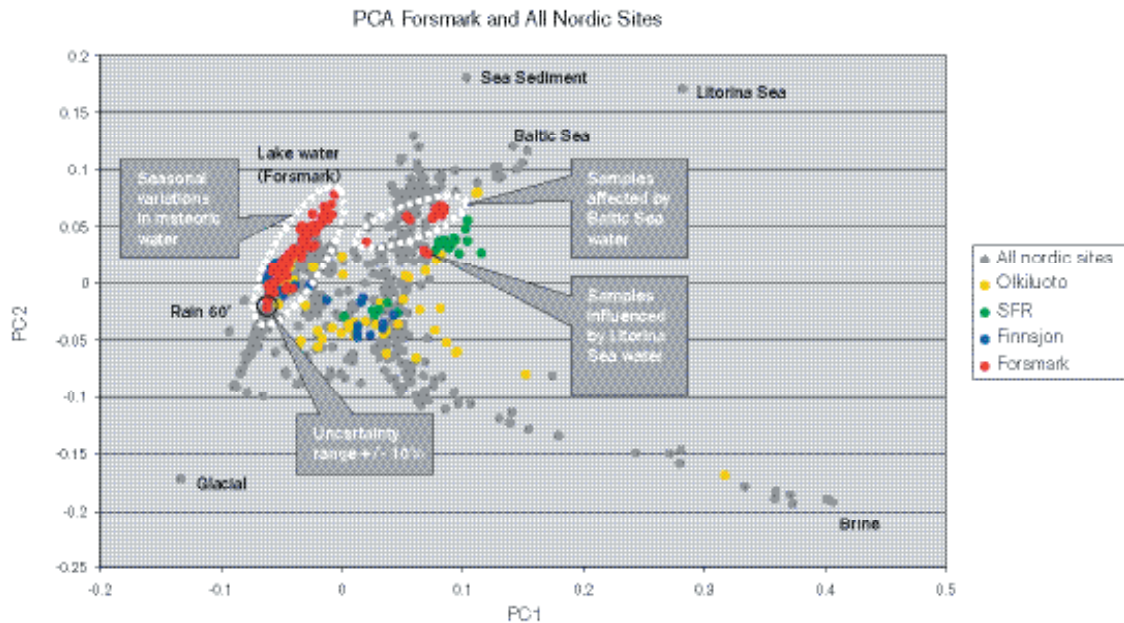
Figure 5-71. *This figure shows the principal components analysis and the location of the identified reference waters. (Variance: First principal component: 0.42236, First and second principal components: 0.6764, First, second and third principal components: 0.78329). The figure shows also the Forsmark data in relation to Nordic samples (e.g. Finnsjön, SFR and Olkiluoto data are indicated). The Lake water (Forsmark), Sea sediment, Marine (Litorina), Brine, Glacial and Rain 60' reference waters were used as reference waters for the modelling The model uncertainty of ± 10% is shown as an error circle for one sample (in black); the analytical uncertainty is ± 5% and represents therefore half the size of the circle.*

Based on past experience (e.g. Äspö and Laxemar sites), the following six reactions have been considered in the M3 modelling:

Organic decomposition: This reaction is detected in the unsaturated zone associated with Meteoric water. This process consumes oxygen and adds reducing capacity to the groundwater according to the reaction: $O_2 + CH_2O \rightarrow CO_2 + H_2O$. M3 reports a gain of HCO_3 as a result of this reaction.

Organic redox reactions: An important redox reaction is reduction of iron III minerals through oxidation of organic matter: $4Fe(III) + CH_2O + H_2O \rightarrow 4Fe^{2+} + 4H^+ + CO_2$. M3 reports a gain of Fe and HCO_3 as a result of this reaction. This reaction takes place in the shallow part of the bedrock associated with influx of Meteoric water.

Inorganic redox reaction: An example of an important inorganic redox reaction is sulphide oxidation in the soil and the fracture minerals containing pyrite according to the reaction: $HS^- + 2O_2 \rightarrow SO_4^{2-} + H^+$. M3 reports a gain of SO_4 as a result of this reaction. This reaction takes place in the shallow part of the bedrock associated with influx of Meteoric water.

Dissolution and precipitation of calcite: There is generally dissolution of calcite in the upper part and precipitation in the lower part of the bedrock according to the reaction: $CO_2 + CaCO_3 \rightarrow Ca^{2+} + 2HCO_3^-$. M3 reports a gain or a loss of Ca and HCO_3 as a result of this reaction. This reaction can take place in any groundwater type.

Ion exchange: Cation exchange with Na/Ca is a common reaction in groundwater according to the reaction: $Na_2X_{(s)} + Ca^{2+} \rightarrow CaX_{(s)} + 2Na^+$, where X is a solid substrate such as a clay mineral. M3 reports a change in the Na/Ca ratios as a result of this reaction. This reaction can take place in any groundwater type.

Sulphate reduction: Microbes can reduce sulphate to sulphide using organic substances in natural groundwater as reducing agents according to the reaction: $SO_4^{2-} + 2(CH_2O) + OH^- \rightarrow HS^- + 2HCO_3^- + H_2O$. This reaction is of importance since it may cause corrosion of the copper capsules. Vigorous sulphate reduction is generally detected in association with marine sediments that provide the organic material and the favourable salinity interval for the microbes. M3 reports a loss of SO_4 and a gain of HCO_3 as a result of this reaction. This reaction modifies the seawater composition by increasing the HCO_3 content and decreasing the SO_4 content.

Model results

The modelling indicates two water types, one dominated by meteoric water and the other affected by marine water. The surface meteoric type shows seasonal variations. Some of the samples show possible influences from Litorina Sea water. The deviation calculations in the M3 mixing calculations show potential for organic decomposition/calcite dissolution in the shallow water. Closer to the coast the influence of marine water is detected but also at depth. Indications of ion exchange and sulphate reduction have been modelled.

These M3 results essentially support the initial evaluation of primary data in Chapter 4 and the other modelled results described above in this section.

Model uncertainties

The following factors can cause uncertainties in M3 calculations:

- Input hydrochemical data errors, originating from sampling errors caused by the effects from drilling, borehole activities, extensive pumping, hydraulic short-circuiting of the borehole and uplifting of water, which changes the in situ pH and Eh conditions of the sample, or as analytical errors.

- Conceptual errors such as wrong general assumptions, selecting wrong type/number of end-members and mixing samples that are not mixed.

- Methodological errors such as oversimplification, bias or non-linearity in the model, and the systematic uncertainty which is attributable to the use of the centre point to create a solution for the mixing model.

An example of a conceptual error is the assumption that the groundwater composition is a good tracer for the flow system. The water composition is not necessarily a tracer of mixing directly related to flow since there is not a point source for this composition as there is when labelled water is used in a tracer test.

Uncertainty in mixing calculations is smaller near the boundary of the PCA polygon and larger near the centre. The uncertainties have been handled in M3 by calculating an uncertainty of 0.1 mixing units (with a confidence interval of 90%) and stating that a mixing portion < 10% is under the detection limit of the method /Laaksoharju et al, 1999b/.

Visualisation of the groundwater properties

The 3D/2D visualisation of the Forsmark Cl values was performed with the Tecplot code. Figure 5-72 shows the 3D and the 2D visualisation of Cl at the 118 sampling points (values used in M3 calculations) in Forsmark. The few samples from depth did not allow any 3D interpolation of the Cl distribution or of the results of the M3 mixing calculations.
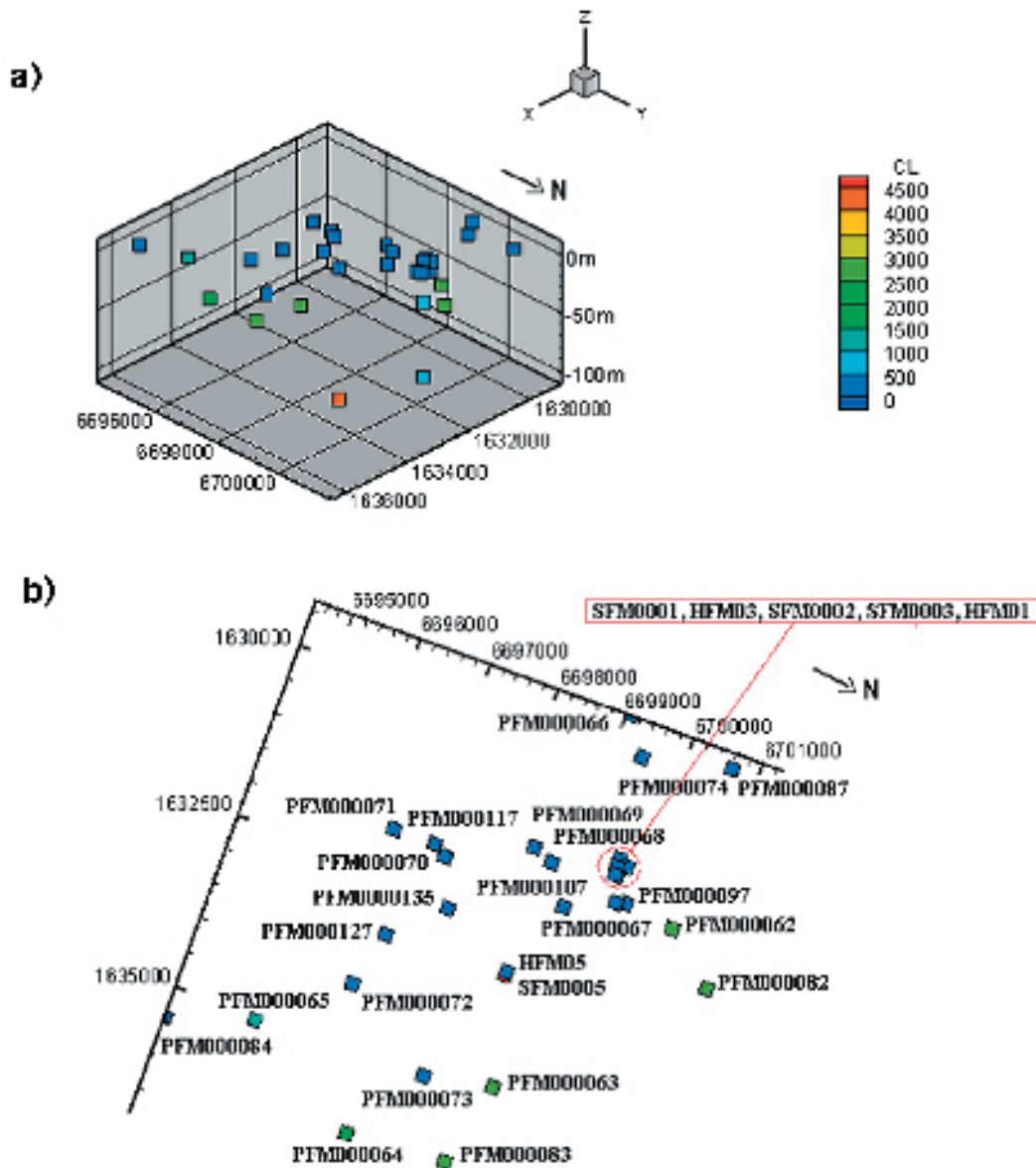
Figure 5-72. 3D (Figure a) and 2D (Figure b) visualisation of the Cl distribution and sampling points in Forsmark. The x, y, z coordinates represent the Easting, Northing and elevation of the mid sampling section of the location of the sampling points, and are expressed in metres.

5.5.4   Comparison between hydrogeological and hydrogeochemical model

Since hydrogeology and hydrogeochemistry deal with the same geological and hydrodynamic media when describing the bedrock groundwater properties, these two disciplines should be able to complement each other when modelling the groundwater system in question. Testing such an integrated modelling approach was the focus of a SKB project (Task 5) based on the Äspö HRL /Wikberg, 1998; Svensson et al, 2002; Rhén and Smellie, 2003/. The advantages with such an approach were identified as follows:

• Hydrogeological models will be constrained by a new data set. If, as an example, the model cannot produce any Meteoric water at a certain depth and the hydro-geochemical data indicates that there is a certain fraction of this water type at this depth, then the model has to be revised.

277

- Hydrogeochemical models generally focus on the effects of reactions on the obtained ground-water rather than on the effects of transport. An integrated modelling approach can describe flow directions and hence help to understand the origin of the groundwater. The turnover time of the groundwater system can indicate the age of the groundwater and it can indicate the reactions that are kinetically favoured. The obtained groundwater chemistry is a result of reactions and transport. Therefore only an integrated description can be used to correctly describe the measurements.

- By comparing two independent modelling approaches, a consistency check can be made. As a result, a better confidence in processes being active, geometrical description and material properties can be gained.

Major recent developments in hydrogeological modelling of the site (see Section 5.4) represents further progress since the TASK#5 exercise /Rhén and Smellie, 2003/. The present modelling should further facilitate future comparison and integration between hydrochemistry and hydrogeology. The hydrogeological model can provide predictions of the salinity in the connected rock matrix, in the flowing groundwater and dynamic predictions in time for the different water types (meteoric, marine, glacial, and brine) see e.g. Figure 5-63 in Section 5.4.11. Furthermore, the hydrogeological model can, independently from chemistry, predict these salinity features at any point of the modelled rock volume, and the predictions can be checked by direct hydrochemical measurements or calculations. Planned measurements of the connected pore water chemistry can be used in validation and comparison of the models. The mixing proportions from the hydrogeological model can in the future, for example, be directly compared with the mixing calculations from the hydrochemical modelling or, conversely, the hydrochemical model can be used to predict the chemistry which results from only transport which, in turn, can be compared with that obtained from reactions. The modelling will increase the understanding of transport, mixing and reactions and will also provide a tool for predicting future chemical changes due to climate changes.

5.5.5 Evaluation of uncertainties

At every phase of the hydrogeochemical investigation programme – drilling, sampling, analysis, evaluation, modelling – uncertainties are introduced, which have to be accounted for, addressed fully and clearly documented to provide confidence in the end result, whether it will be the site descriptive model or repository safety analysis and design /Smellie et al, 2002/. Handling the uncertainties involved in constructing a site descriptive model has been documented in detail by /Andersson et al, 2001, 2002a/. The uncertainties can be conceptual uncertainties, data uncertainties, spatial variability of data, chosen scale, degree of confidence in the selected model, and error, precision, accuracy and bias in the predictions. Some of the uncertainties recognised during the Äspö HRL modelling exercise are discussed below.

The following data uncertainties have been estimated, calculated or modelled for the data and models used for the Äspö Model Domain:

- disturbances from drilling; may be $\pm$ 10–70%,

- effects from drilling during sampling; is < 5%,

- sampling; may be $\pm$ 10%,

- influence associated with the uplifting of water; may be $\pm$ 10%,

- sample handling and preparation; may be $\pm$ 5%,

- analytical error associated with laboratory measurements; is $\pm$ 5%,

- mean groundwater variability during groundwater sampling (first/last sample); is about 25%,

- the M3 model uncertainty; is $\pm$ 0.1 units within 90% confidence interval.

Conceptual errors can occur from, for example, the palaeo-hydrogeological conceptual model. The influences and occurrences of old water end-members in the bedrock can only be indicated by using certain element or isotopic signatures. Therefore, the uncertainty is generally increasing with the age of the end-member. The relevance of an end-member participating in the groundwater formation can be tested by introducing alternative end-member compositions or by using hydrodynamic modelling to test if old water types can reside in the bedrock during prevailing hydrogeological conditions.

Uncertainties in the PHREEQC code are due to analytical uncertainties and uncertainties concerning the thermodynamic data bases (in speciation-solubility calculations). Care and expert knowledge is also required in order to select mineral phases that are realistic (even better if they have been positively identified) for the systems being modelled. The errors can be addressed by using sensitivity analyses, predictive models, alternative models and descriptions. Such analysis was regarded to be outside the scope of the model version 1.1 work due to lack of groundwater data.

The uncertainty due to 3D interpolation and visualisation depends on various issues, i.e. data quality, distribution, model uncertainties, assumptions and limitations introduced. Therefore, the uncertainties are often site specific and some of them can be tested, such as the effect of 2D/3D interpolations. The site specific uncertainties can be tested by using quantified uncertainties, alternative models, and comparison with independent models, such as hydrogeological simulations. Because of the lack of groundwater data from Forsmark available for model version 1.1 it was not possible to carry out any of these tests.

The discrepancies between different modelling approaches can be due to the differences in the boundary conditions used in the models or in the assumptions made. The discrepancies between models should be used as an important validation and confidence building opportunity to guide further modelling efforts.

5.6 Transport property modelling

5.6.1 Modelling assumptions and input from other models

The modelling procedure for Transport property modelling is described in /Berglund and Selroos, 2004/. The guidelines report describes the different steps in the workflow, namely i) identification, acquisition and control of input data, ii) evaluation of primary data, iii) three-dimensional modelling, iv) Overall confidence assessment, and v) documentation and data deliveries. The first two steps result in a Retardation model, i.e. an identification and parameterization of typical materials and layers (type structures). The three-dimensional modelling associates the defined type structures with specific units in the geological site-descriptive model.

As described in Section 4.9, no site-specific transport data are available from either laboratory or in situ measurements. Instead, the retardation model is based on generic information. Also, only the intact rock (matrix) is considered in the present version. Both the Geology and Hydrochemistry disciplines provide information that is relevant when assigning properties to this simplified retardation model.

The description of transport properties also involves numerical modelling using the hydrogeological description of the site. Specifically, flow-related transport properties, such as the transport resistance (F-factor) and travel time from depth to surface, are assessed for different parts of the local model domain. Combining the retardation model with the flow-related transport parameters provides the means for assessing solute transport characteristics of the site. The steps described above are visualised in Figure 5-73.
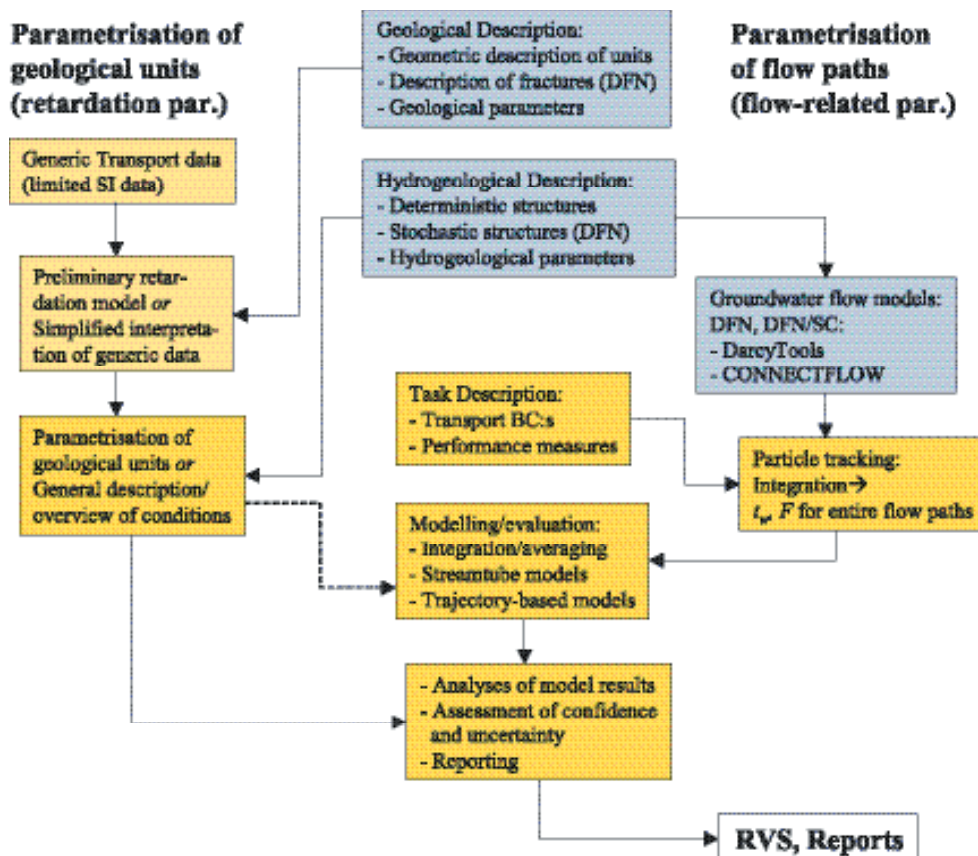
Figure 5-73. *Guideline for transport modelling steps during early stages of site investigations.*

5.6.2 Conceptual model with potential alternatives

The conceptual model is based on a description of solute transport in discretely fractured rock. Solutes (including radionuclides) are transported in fractures containing mobile water. Solutes may be transported by diffusion into the immobile parts of the rock matrix, and subsequently be adsorbed on the inner surfaces of the rock matrix. Also, reactions on the fracture surfaces may take place. The model of the host rock may thus be divided into different rock domains (depending on retardation properties, i.e. mainly mineralogical composition) and flow paths. Also the flow paths may have different retardation properties.

The retention processes considered are matrix diffusion and instantaneous linear sorption.

No alternative of this conceptual model is addressed within model version 1.1.

5.6.3 Transport properties of the rock domains

The main transport properties of the rock domain are diffusivities (D_e), sorption coefficients (K_d) and porosities /Widestrand et al, 2003/. As stated in Section 4.9, no site-specific measurements exist. Instead, an attempt has been made to relate site-specific data from the near-by site Finnsjön to Forsmark. Specifically, based on the rock domain model (see Section 5.1.2), existing diffusivity measurements from Finnsjön pertaining to a similar geological and mineralogical environment as rock domain 29 in Forsmark have been compiled. The candidate area in Forsmark is mainly made up of rock domain 29, see Section 5.1.2 for more details.

The rock properties controlling matrix diffusion can be expressed through the formation factor $f=D_e/D_w$ where D_e is the effective diffusivity of a radionuclide, and D_w is the corresponding free-water diffusivity. The formation factor incorporates effects such as tortuosity and constrictivity of the matrix pore system. The relation between porosity and formation factor has been assessed for the data population from Finnsjön, see Figure 5-74.

The selected samples are all based on the work by /Gidlund et al, 1990/ and correspond to medium-grained metamorfic granite/granodiorite. All values are from one single borehole from a depth of 224.68–224.75 m.

The porosity of rock domain 29 in Forsmark is $0.44 \pm 0.06\%$. Hence, values from /Gidlund et al, 1990/ that are close to this value $(0.53 \pm 0.06)\%$ were chosen for comparison, see Figure 5-74. The resulting formation factor is $(1.1 \pm 0.6) \cdot 10^{-5}$. This value can be compared to the corresponding value used in SR 97 /Ohlsson and Neretnieks, 1997/, which was $4.2 \cdot 10^{-5}$; i.e. approximately a factor four higher. It is argued that the three values chosen in Figure 5-74 best resemble the corresponding properties at Forsmark.

The obtained result thus indicates that diffusivities at Forsmark may be somewhat lower than at Finnsjön. However, the different stress conditions at the two sites may imply that it is problematic to transfer results between the two sites. Also, if one were to use the correlation based on all values in /Gidlund et al, 1990/, see Figure 5-74, a higher formation factor would be obtained. Based on the limited data and prevailing uncertainties, it is argued that there is no firm evidence at present to assume diffusivity values for the Forsmark site other than those used in SR 97 /Ohlsson and Neretnieks, 1997/. It should be noted that all diffusivity values discussed above pertain to the intact rock; diffusivities of possible alteration zones or gouge material in the fractures have not been addressed in model version 1.1.

Concerning K_d-values, no attempt was made in version 1.1 to relate Finnsjön-data to Forsmark. This is primarily due to the lack of certainty concerning the biotite content in the main rock types of rock domain 29. Biotite content has been shown to be of importance for sorption of radionuclides on rock surfaces /Byegård et al, 1998/.
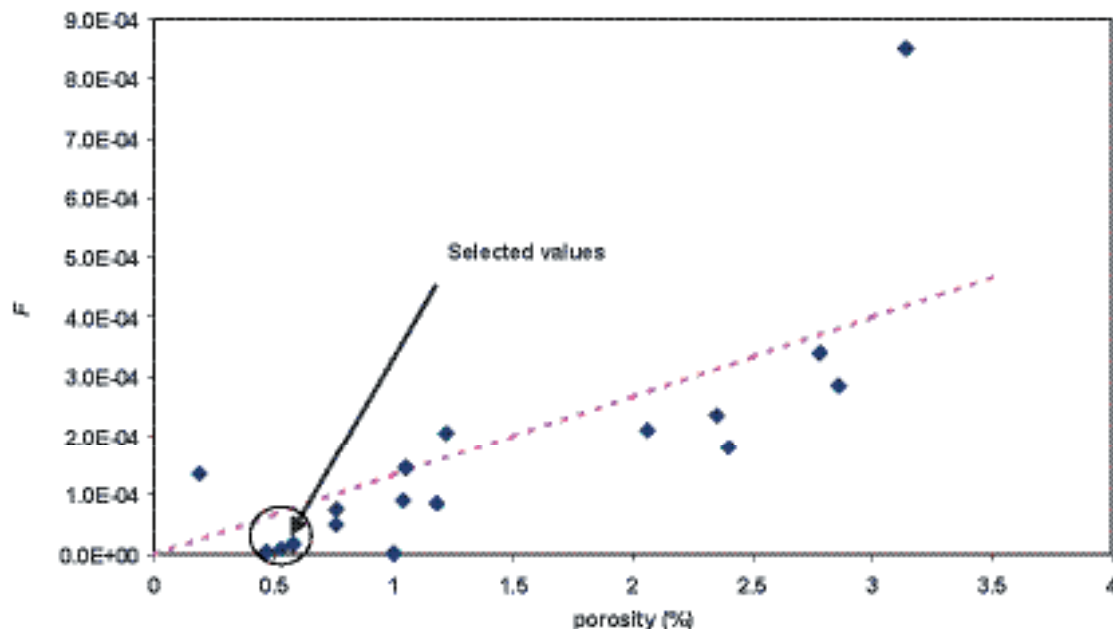
Figure 5-74. *Correlation between porosity and formation factor (f) for samples from Finnsjön.*

5.6.4 Transport properties of flow paths

The evaluated transport properties of flow paths are transport resistance (F-factor) and advective travel time. The transport resistance is defined in a continuum framework as $F=\Sigma a_r L/q$ where summation is made along the whole flow path and a_r is the flow-wetted surface per volume of rock, L is the flow path length, and q the Darcy velocity. In a discrete framework, the transport resistance is typically defined as $F=\Sigma 2WL/Q$ where summation again is made over the individual segments of the flow path, W is the path width, and Q the volumetric flow rate. The transport resistance, together with radionuclide retention properties, largely governs radionuclide transport.

The transport resistance has been estimated by releasing particles in the hydrogeological models. The particle trajectories as calculated by DarcyTools are shown in Figure 5-75. The methodology for calculating the F-factor in DarcyTools is described in /Svensson et al, 2004/. Three particles were released at 500 m depth in the model, one at each existing borehole (note that only data from one borehole have been used for setting up the model, and that the boreholes are not hydraulically included in the model). The three locations sample different parts of the candidate region. The particle trajectories are shown in Figure 5-75.

It is clearly seen in Figure 5-75 that the flow paths from the two starting positions with low Y coordinate tend to move up-wards more directly than the flow path from the third starting position. This flow path tends to be longer, and also move out further from the candidate area. The corresponding F-factors are given in Figure 5-76.
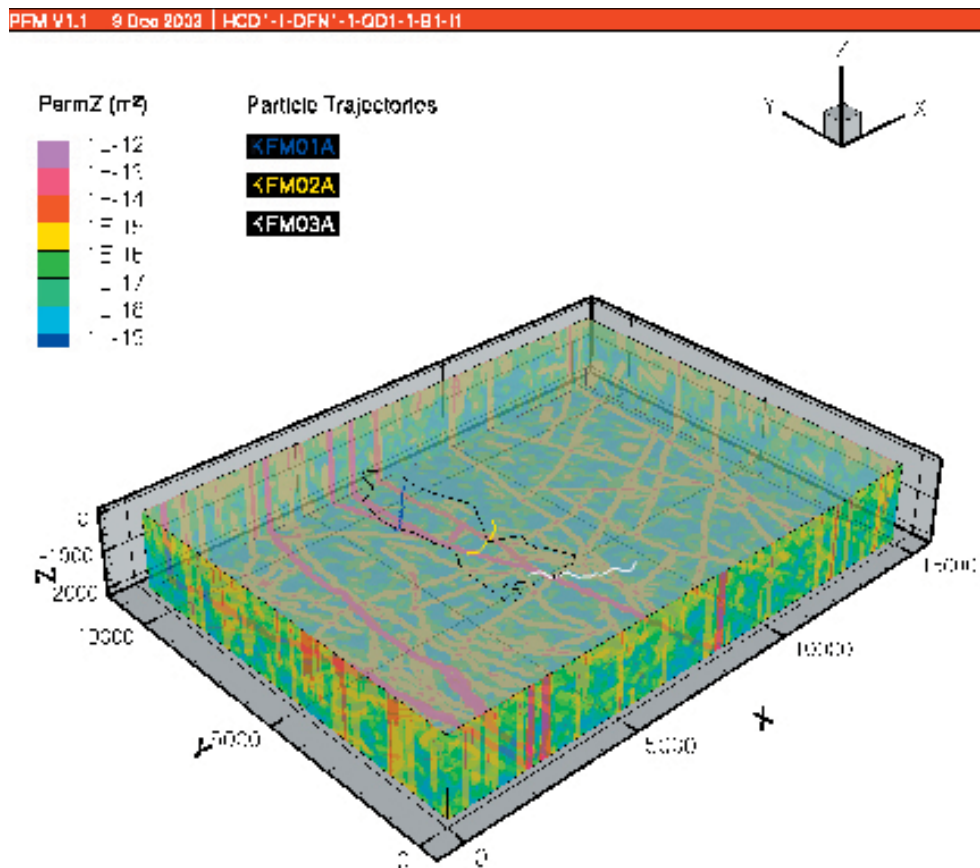
Figure 5-75. *Particle trajectories for particles released at 500 m depth at boreholes KFM01A, 02A and 03A.*
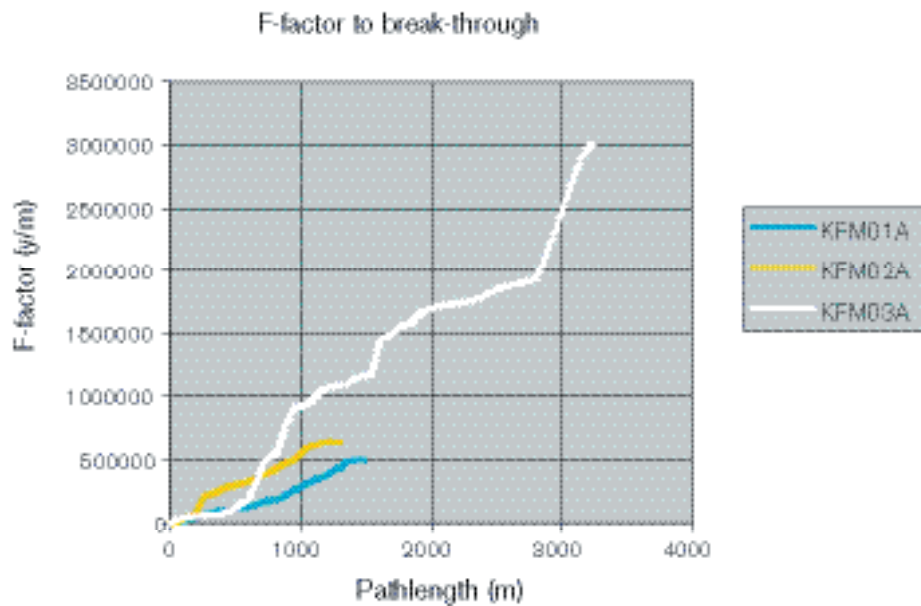
Figure 5-76. *Transport resistance as a function of flow path length for three particles.*

It is seen that the values of the F-factor range from approximately $5 \cdot 10^5$ year/m to $3 \cdot 10^6$ year/m. These values are considered good relative to the suitability indicator of $F > 1 \cdot 10^4$ year/m as expressed in /Andersson et al, 2000/. However, the limited data set used for the modelling may imply a bias towards low permeable conditions resulting in high values of the transport resistance.

5.6.5 Evaluation of uncertainties

The main uncertainty lies in the fact that no site-specific data on retention properties exist. Concerning the flow-related transport parameters, i.e. mainly the transport resistance, the obtained values are uncertain due to the underlying uncertainty in the groundwater flow models (e.g. transmissivity (conductivity) distribution, P_{32} values, boundary conditions). For the flow-related transport parameters, the uncertainties could be evaluated to a certain extent by running different variants. This has not been done within model version 1.1.

The large span in transport resistance obtained using only three particles indicates that the spread due to spatial variability and different flow conditions may be large when the full candidate area is considered.

Issues not considered in the present version, which also by their very nature add to the overall uncertainty, include the following:

- Are there regions with lower porosities than the one measured in rock unit 29? If so, this could have an adverse effect on effective diffusivity?

- Is there evidence of rock alteration that may indicate certain processes of relevance for radionuclide retention?

- Are there indications of water chemistry that may imply reduced potential for radionuclide retention?

- Are there indications of rock structures with potentially low transport resistance?

These issues need to be addressed in coming versions.

5.7 Ecosystem property description and modelling

5.7.1 Modelling assumptions and input from other models

According to the definition used in this report, the ecosystem starts at the surface of the deep bed-rock. This means that any Quaternary deposits and other regoliths, together with surface water and the biotic components, are included in the surface ecosystem. The abiotic parts of the ecosystem are described elsewhere in this report; the deposits in Section 5.1.1, the hydrology in Section 5.4.2, and the chemistry in Section 5.5. The surface ecosystem will be described using a large number of properties which, when combined, will constitute the ecosystem site descriptive model /cf Löfgren and Lindborg, 2003/. The surface ecosystem is divided into different subsystems based on the presence of system-specific processes and properties, and also on the collection, measurement and calculation of data that may differ between different subsystems. Accordingly, we end up with the three different subsystems: (1) the terrestrial system which includes all land and wetland areas, (2) the limnic system, i.e. lakes and rivers, and (3) the marine system, constituted by the sea and brackish waters.

The budgets of organic and inorganic matter will be described within the different subsystems, where matter is recycled between organisms in the food web and the physical environment. Matter may also be accumulated within the subsystem, e.g. as peat, and thereby leaving the circulation until some kind of disturbance occurs to release it to circulation again. Moreover, the different subsystems all interact with one another to some degree. For example, the terrestrial environment around a lake acts as a catchment area for rainwater and affects the lake through the runoff of water to the lake. The discharge area in the near-shore marine system is affected by the output from the lake and from the near-shore parts of the terrestrial system. Hydrological processes in the landscape are considered essential to the connectivity of the different subsystems. The landscape is therefore divided into functional units defined by catchment areas that are constructed from surface water divides in the landscape. The flows of matter in the landscape are considered to be hydrologically driven in this descriptive ecosystem model.

Since many of the started investigations not are finished yet, no budgets of matter transport are developed for version 1.1 of the site descriptive model. Accordingly, no overall ecosystem model will be developed until budgets of matter have been described both within and between the different subsystems.

5.7.2 Biota

Producers

Terrestrial producers – biomass

Tree layer

Biomass of the tree layer in the model area was calculated using information from the local Forestry Management Plan, where data on standing crop was available. The basis for the geometrical resolution was the vegetation map of the area (see Section 7.1.5). Since this map did not cover the lower left and right corners of the model area, vegetation data from the Terrain Type Classification (a coarse classification performed by Satellus (a company within Lantmäteriet) from satellite photos with lower resolution than what was used for the Vegetation map) was used to make the map spatially complete.

Biomass data were not available for all the different vegetation types as given in the vegetation map. Therefore, the vegetation types from the vegetation map were aggregated to five different classes; old (> 30 yr) coniferous forests, young (≤ 30 yr) coniferous forests, deciduous (> 70% deciduous trees) forests, no forests and water bodies. The latter two classes have no tree layer. The first three classes were assigned values of biomass, calculated from the local Forestry Management Plan. This value only gives the biomass of the stems, and therefore the biomass of the bark, pins, needles and roots had to be added. Calculations were made using data from the National Forest Survey /cf Berggren and Kyläkorpi, 2002/. These calculations showed that the stem weight in old coniferous trees and deciduous trees in this area is 64% of the total above-ground weight, and the corresponding value for young coniferous trees is 60%. In addition, the weight of the root system had to be added.

This information was obtained from /Lundmark, 1986/ which showed that trees above-ground parts on average are 85% of their total weight.

After these calculations the data on total tree weight was complete. This weight was then converted into dry weight by using the factor 0.42 /Jerling et al, 2001/ and thereafter to carbon content by using the factor 0.5 /Jerling et al, 2001/.

Shrub, field and ground layers

Biomass of the shrub-, field- and ground layers in the model area was calculated using the input data from /Fridriksson and Öhr, 2003/. In this study, the actual amount of carbon was measured in six different vegetation types; harvested areas, grazing areas, sea shores, wetlands, *Pinus* dominated areas and *Picea* dominated areas. For each of these vegetation types, six sample plots were assessed and measured with regards to carbon content.

The basis for geometrical resolution was again the vegetation map and, again, data from the Terrain Type Classification was used to fill out the map. The different vegetation types were aggregated to the six types studied in /Fridriksson and Öhr, 2003/. Thereafter, the average values of biomass dry weight in the different layers were calculated. These weight values were then translated to carbon content using the factor 0.453 in accordance with /Fridriksson and Öhr, 2003/.

For the categories arable land, mixed forest and deciduous forest, no *in situ* measurements of biomass have been conducted. Therefore, the deciduous forest was assigned the same value as grazing area and the mixed forest was assigned the same value as *Picea* forest. The biomass of the arable land was calculated based on the standard yield figures of barley, which is the main crop cultivated in the area /Berggren and Kyläkorpi, 2002/. To the standard yield of 312.5 g barley/m^2 /Berggren and Kyläkorpi, 2002/ were added generic values of threshing loss, straw yield and root production. The total figure was then translated to carbon content using the factor 0.453 in accordance with /Fridriksson and Öhr, 2003/. The categories bare rock, water and hard surfaces were assigned zero values; i.e. no terrestrial biomass was assumed to exist here.

The calculated biomasses for the different vegetation types within the separate layers are shown in Table 5-42 and the combined figures for the layers and for the total regional model area are shown Table 5-43.

Terrestrial producers – production

Tree layer

Production of the tree layer was calculated using data from the National Forest Survey. A previous cut-out of 520 sample sites covering a relatively large area including and surrounding the model area /Berggren and Kyläkorpi, 2002/ was used in order to obtain mean values with an acceptable level of statistical certainty.

In the present estimation of production, stem growth was calculated for the same plots as described above. Average values were used for the five different classes; old (> 30 yr) coniferous forests, young (≤ 30 yr) coniferous forests, deciduous (> 70% deciduous trees) forests, no forests and water bodies. In addition to stem growth, bark, pin, needle and root growth were added as for biomass calculations described above, assuming that all parts of the trees grow in a linear mode. Thereby, tree layer production values were arrived at for the three different vegetation types.

Shrub, field and ground layers

For the six different vegetation types studied in /Fridriksson and Öhr, 2003/, data on dry weight was divided into green and non-green categories. In order to arrive at production values, it was assumed that all green vegetation fractions constitute the yearly production. However, as stated in /Chapin III et al, 2002/, the green biomass only reflects 40% of the total production, so this value was used to increase the green fraction figure. These weight values were then translated to carbon content using the factor 0.453 in accordance with /Fridriksson and Öhr, 2003/.

For the categories arable land, mixed forest and deciduous forest, no *in situ* measurements of bio-mass have been conducted. Therefore, the deciduous forest was assigned the same value as grazing area and the mixed forest was assigned the same value as *Picea* forest.

The production of the arable land was assumed to be the same as the standing crop biomass, i.e. the calculations were performed in the same way as described above. The categories bare rock, water and hard surfaces were assigned zero values; i.e. no terrestrial production occurs here.

The calculated production for the different vegetation types within the separate layers are shown in Table 5-42 and the combined figures for the layers and for the total regional model area are shown Table 5-43.

The calculated values for biomass and production per vegetation type were used to produce biomass and production maps for the tree layer and for the shrub, field and ground layers in the Forsmark regional model area. These maps were finally converted to 10-m grids (Figure 5-77).

Table 5-42. Calculated biomass and production for different vegetation types in the Forsmark regional model area.

	Vegetation type	Biomass (kgC/m^2)	Production (kgC/m^2/yr)
Tree layer	Old coniferous forest	7.89	0.24
	Young coniferous forest	0.67	0.08
	Deciduous forest	3.60	0.24
	No forest layer	0.00	0.00
	Surface water	0.00	0.00
Other layers	Harvested area	0.69	1.13
	Grazing area	0.19	0.35
	Sea shore	0.25	0.25
	Wetlands	0.57	0.61
	Pinus forest	0.73	0.73
	Picea forest	0.59	1.04
	Arable land	0.30	0.30
	Mixed forest	0.59	1.04
	Deciduous forest	0.19	0.35
	Rocky area	0.00	0.00
	Surface water	0.00	0.00
	Hard surface area	0.00	0.00

Table 5-43. Calculated biomass and production within vegetation layers and totally for the terrestrial vegetation in the Forsmark regional model area. Mean values are based on the total land area in the regional model area.

	Total biomass (kg C)	Total production (kg C/yr)	Mean biomass (kg C/m^2)	Mean production (kg C/m^2/yr)
Tree layer	171 287 541	6 967 973	2.98	0.12
Other layers	30 997 428	44 192 043	0.54	0.77
Total	202 284 969	51 160 016	3.52	0.89
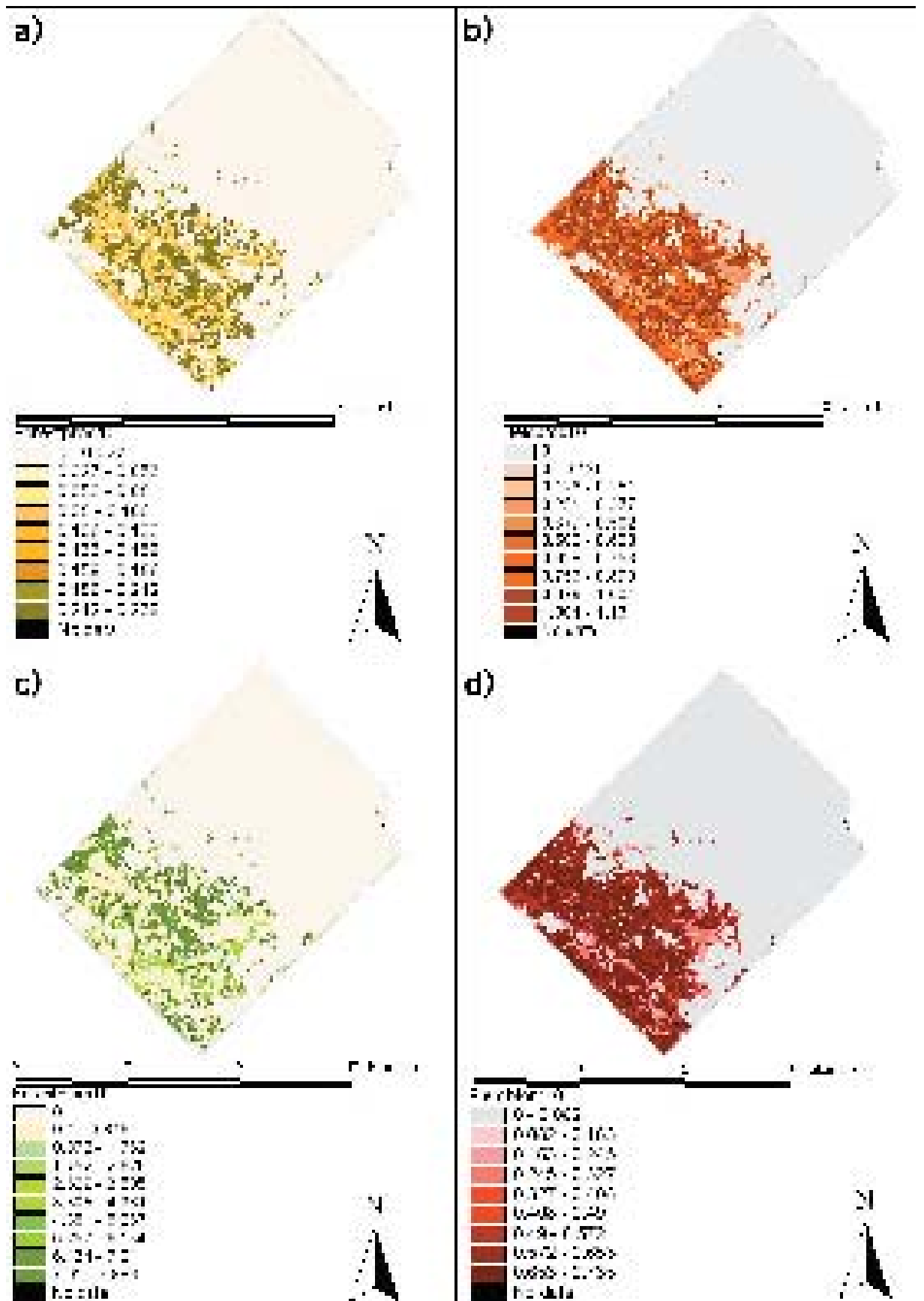
Figure 5-77. Grid maps illustrating a) tree layer production, b) shrub, field and ground layer production, c) tree layer biomass, and d) shrub, field and ground layer biomass, in the Forsmark regional model area.

Aquatic producers – limnic

Microphytobenthos

No new site-specific data are available for the Site Descriptive Model version 1.1.

Plankton

No new site-specific data are available for the Site Descriptive Model version 1.1.

Macrophytes

No new site-specific data are available for the Site Descriptive Model version 1.1.

Aquatic producers – marine

Microphytobenthos

No new site-specific data are available for the Site Descriptive Model version 1.1.

Plankton

No new site-specific data are available for the Site Descriptive Model version 1.1.

Macrophytes

No new site-specific data are available for the Site Descriptive Model version 1.1.

Consumers

Terrestrial consumers

No site-specific biomass data for terrestrial consumers, i.e. mammals or birds, are available for the Site Descriptive Model version 1.1. However, data on population abundances for a major part of the birds and mammals in the Forsmark regional model area have been collected during 2001–2002 /Cederlund et al, 2003; Green, 2003/, but investigations are not completed and quantitative analyses of the results remains to be done. Moreover, a significant part of the terrestrial biomass of consumers in the Forsmark region is probably that of domestic animals /Berggren and Kyläkorpi, 2002/ (cf Humans and land use 5.7.3).

Mammals

Not all of the 12 selected species were found in the regional model area, but may be found in other surveys to come (see Table 5-44). The most common mammal species was roe deer (59 deer/10 km^2) /Cederlund et al, 2003/. Moose was also common, but less than expected from earlier studies (0.7 moose/km^2). European and mountain hare were fairly low in abundance (4.4 hare/km^2), compared to other regions. Other observed mammals were badger, fox, marten, mink, otter and wild boar.

Table 5-44. Estimated abundances of mammal species in the Forsmark regional model area /Cederlund et al, 2003/.

Species	Animals per km²
Badger	Observed
Beaver	No obs.
European / Mountain hare	0.44
Fox	Observed
Lynx	0.02
Marten	Observed
Mink	Observed
Moose	0.7
Otter	Observed
Red deer	No obs.
Roe deer	5.9
Wild Boar	Observed
Wolf	No obs.

Birds

The number of bird species was quite high compared to surrounding regions in Uppland /Green, 2003/. In total, 125 species were found in the regional model area, and 25 of these are noted in the Red List as threatened bird species in Sweden. Some 83% of the documented individuals (totally 6,658) were birds associated with land, whereas 17% were birds associated with marine environments.

Mean number of individuals noted per km during line transect surveys was 57.0, including all bird species. The dominating species are listed in Table 5-45. The most common species on land were Willow Warbler and Chaffinch, and the most common species at sea were Cormorant and Greylag Goose. A major part of the nesting species was small birds, associated with the open or semi-open landscape. Other common bird species associated with marine environments, e.g. Cormorant, Canada Goose, Greylag Goose and Black-headed Gull, were only registered as number of observed individuals and not as individuals per line transect unit.

Since no quantitative data is available for the Site Descriptive Model version 1.1, the total biomass for each species has not been calculated. It is important to notice that the numerically most common species are quite small, and a calculation of total biomass for each species might give quite a different picture than the relative abundance estimates based on numbers. For detailed information on each species found in Forsmark, see /Green, 2003/.

Table 5-45. The ten most common nesting species in the Forsmark regional area, presented as the total number of birds registered and the number of birds per km during line transect surveys /Green, 2003/.

Species English (Swedish)	Latin	Total number	Abundance (n/km)
Willow Warbler (*Lövsångare*)	*Phylloscopus trochilus*	1213	12.51
Chaffinch (*Bofink*)	*Fringilla coelebs*	1153	11.89
Robin (*Rödhake*)	*Erithacus rubecula*	361	3.72
Siskin (*Grönsiska*)	*Carduelis spinus*	333	3.43
Blackbird (*Koltrast*)	*Turdus merula*	251	2.59
Song Thrush (*Taltrast*)	*Turdus philomelos*	165	1.70
Tree Pipit (*Trädpiplärka*)	*Anthus trivialis*	151	1.56
Great Tit (*Talgoxe*)	*Parus major*	139	1.43
Yellowhammer (*Gulsparv*)	*Emberiza citrinella*	124	1.28
Wren (*Gärdsmyg*)	*Troglodytes troglodytes*	100	1.03

Aquatic consumers – limnic

Invertebrates

No new site-specific data are available for the Site Descriptive Model version 1.1.

Fish

No new site-specific data are available for the Site Descriptive Model version 1.1.

Aquatic consumers – marine

Invertebrates

No new site-specific data are available for the Site Descriptive Model version 1.1.

Fish

No new site-specific data are available for the Site Descriptive Model version 1.1.

Mammals

No new site-specific data are available for the Site Descriptive Model version 1.1.

5.7.3 Humans and land use

Since much of the data was available on the parish level, this level of resolution was used to describe the situation in the Forsmark model area. The Forsmark parish is very similar in size to the model area and covers some 90% of its land area. When calculating a figure per square kilometre, a land area of 94.2 km² has been used. That figure has been obtained from Statistics Sweden, *www.scb.se,* and their register over Parish areas, dated 1 Jan 2000.

Some of the data, that were only available on another level of spatial resolution, had to be recalculated into the frame of the model area. The calculated figures for the variables describing humans and land use are given in Appendix 1, and a more thorough presentation of the data and results is given in /Miliander et al, 2004/.

The results of the study can be summarised as follows;

- The Forsmark area is very scarcely populated.

- The main employment sector is within electricity supply. There is a clear net daily in-migration to the employer (the Forsmark nuclear power plant).

- The land use is dominated by forestry; wood extraction is the only significant outflow of biomass from the area.

- The dominating leisure activity, by far, is hunting. Besides this, the area is only extensively used for leisure. This is probably a result of both the scarce population and the areas relative inaccessibility and distance from major urban areas;

- The agriculture in the area is limited in extent and the major crop is barley.

5.7.4 Development of the ecosystem model

No overall ecosystem model has been produced for the Site Descriptive Model version 1.1.

5.7.5 Evaluation of uncertainties

Data uncertainties and conceptual uncertainties

The site investigation programme concerning surface ecosystems is not designed to produce batches of completed investigations for each data freeze. Consequently, some investigations that have started are only partly completed and therefore not evaluated for the Site Descriptive Model version 1.1, while some other investigations are not evaluated due to lack of complementary data which are needed for a thorough evaluation and for modelling purposes. Therefore, data uncertainty caused by temporal and/or spatial variability, together with lack of data, is for the present high for many of the properties used to describe the ecosystem entities /cf Löfgren and Lindborg, 2003/. Table 5-46 shows a subjective estimation of the combined uncertainties for all properties used to describe a specific ecosystem entity, based on what is judged necessary for a complete Site Descriptive Model. If, instead, the degree of uncertainty was expressed in absolute terms, it would certainly differ between the different properties used to describe an ecosystem entity. For some properties, a "high" uncertainty may be adequate for the purpose of a site descriptive model, whereas it is necessary to attain a "low" uncertainty for other properties /see Lindborg and Kautsky, 2000/ for a discussion on the necessary temporal and spatial resolution for different properties).

Table 5-46. Estimation of data uncertainties (caused by temporal and spatial variability) and conceptual uncertainties, for properties within different ecosystem entities. High/low denotes a subjective and combined valuation for all properties used to describe the specific ecosystem entity, based on what is judged necessary for a complete Site Descriptive Model.

Ecosystem entity	Data uncertainties		Conceptual uncertainties
	Temporal	Spatial	
Abiotic			
Atmosphere	High	High	Low
Hydrology	High	High	High
Regolith	Not applicable	High	High
Biotic			
Terrestrial			
Producers	High	Low	Low
Consumers	High	High	Low
Human	Low	Low	Low
Limnic			
Producers	High	High	Low
Consumers	High	High	Low
Human	Low	Low	Low
Marine			
Producers	High	High	Low
Consumers	High	High	Low
Human	Low	Low	Low
Historical development	High	High	High

Ecosystem model uncertainties

No overall ecosystem model has been produced for version 1.1 of the Forsmark site descriptive model.

6 Overall confidence assessment

The Site Descriptive Modelling involves uncertainties and it is necessary to assess the confidence in the modelling. Based on the integrated strategy report /Andersson, 2003/ procedures (protocols) have been developed for assessing the overall confidence in the modelling. These protocols concern whether all data are considered and understood, uncertainties and potential for alternative interpretations, consistency between disciplines, and consistency with understanding of past evolution as well as comparisons with previous model versions. These protocols have been used in a technical auditing exercise as a part of the overall modelling work. This chapter reports the conclusions reached after this auditing.

6.1 How much uncertainty is acceptable?

A site descriptive model will always contain uncertainties, but a complete understanding of the site is not needed. As set out in the geoscientific programme for investigation and evaluation of sites /SKB, 2000b/ the site investigations should continue until the reliability of the site description has reached such a level that the body of data for safety assessment and repository engineering is sufficient, or until the body of data shows that the rock does not satisfy the requirements. Even if the Construction and Detailed Investigation Phase does not imply potential radiological hazards, it would still be required that no essential safety issues may remain, which could not be solved by local adaptation of layout and design.

During the Site Investigation there are several planned occasions when Safety Assessment will be able to provide organised feedback as regards the sufficiency of the site investigations. The SR-Can project /SKB, 2003/ will deliver its first interim report in mid 2004. In late 2004 or early 2005, Preliminary Safety Evaluations /SKB, 2002c/ of the investigated sites will follow. Quantitative feedback from Safety Assessment could thus not be obtained before these studies, but the type of feedback to be obtained can still be assessed in relation to its potential impact on decisions on the site investigation programme. The Safety Assessment planning suggests that only certain site properties are really important for assessing the safety. Generally, these are connected to the requirements already stated in /Andersson et al, 2000/. Consequently, there is a need to ensure that the site modelling is able to produce qualified uncertainty estimates of these properties.

According to current thoughts within Engineering there are essentially three design issues to be addressed during the Site Investigation phase:

- Is there enough space?
- What is the degree of utilisation (i.e. a subset of the space issue)?
- Are critical passages properly assessed?

The overriding issue whether there is enough space for the repository may be divided into determining the generally available space and the degree of utilisation within this generally available space. The factors controlling the generally available space are the regional and local major deformation zones. Deposition tunnels must not be placed closer than a certain respect distance from such zones. Working definitions of respect distances exist, but there is still some refinement work going on regarding what should be appropriate respect distances, see e.g. /SKB, 2002c/.

The repository layout is not only controlled by the regional and local major deformation zones. For example, deposition holes connected to large fractures or high inflows will not be used and the thermal rock properties affect the minimum allowable distances between deposition tunnels and deposition holes. During site investigations, this is handled in the design by estimating a "degree of utilisation" for the deposition panels already adjusted to the regional and local major deformation zones. Final selection of deposition holes and tunnels will be made locally, underground, during the construction and detailed investigation phase. Distribution of inflow to the deposition tunnels is an important aspect of the degree of utilisation. Apart from water, other factors affect the degree of

utilisation. This includes heat conductivity and rock mechanics properties affecting bedrock stability and rock burst.

For the engineering planning and selection of the surface access point it is necessary to identify and characterise potentially difficult passages (i.e. deformation zones) in the rock. However, the information needed would be quite detailed, which means that the overall site description will be used to identify potential access locations. At these locations there will be a need to drill some additional exploration boreholes in order to assess the actual critical passages. There is no need to assess critical passages in the entire model domain.

6.2 Are all data considered and understood?

The method of interpretation is the key to the confidence assessment. A similar and unbiased treatment of all different data and interpretations that explains several different observations enhances confidence.

6.2.1 Auditing protocol

A protocol has been developed for checking the use of data sources. It concerns:

- Data that have been used for the current model version (by referring to tables in Chapter 2).

- Available data that have not been used and what is the reason for their omission (e.g. not relevant, poor quality, lack of time, …).

- If applicable – What would have been the impact of considering the non-used data?

- The data and interpretation types and indicating how accuracy is established for these, e.g. by specified procedure, QA, etc.

- Estimating the potential for inaccuracy and the significance of the inaccuracy, by using the terms 'high', 'medium', 'low' and 'none' to describe these.

- If biased data are being produced, can these be corrected for the bias?

- To what extent are interpretations supported by more than one observation or set of observations.

Table 6-1 lists the answers to these questions for the bedrock and Table 6-2 for the near-surface descriptions. In version 1.1, this audit only concerned data from the site, and not "generic data" (like thermodynamic data used in the hydrogeochemical calculations) and basic geoscientific knowledge. Later versions may expand the scope of this uncertainty evaluation. Also, it may seem odd to explore for bias. If the method of correction is known, it can be applied and the data are no longer biased. However, auditing is relevant in order to retrospectively identify biases that need to be corrected and in flagging un-quantified biases.

Table 6-1. Protocol for use of available data and potential biases in the bedrock description.

Question	Geology	Roch mechanics and Thermal	Hydrogeology	Hydrogeochemistry	Transport
Which data have been used for the current model version (refer to tables in Chapter 2 of the report).	All data that have been used in the version 1.1 SDM are listed in Table 2-1 and referred to under the relevant section in Chapter 4. Even the older structural models from SFR have been included in version 1.1 SDM.	All data that have been used in the version 1.1 SDM are listed in Tables 2-2 and 2-3 and referred to under the relevant section in Chapter 4.	See Table 2-4. *Historical data*: SKB R-02-14: SFR – Evaluation of hydrogeology. *Version 0 data*: SKB R-02-32: Forsmark SDM V0. *Version 1.1 data*: SKB P-03-28: Difference flow logging of KFM01A. SKB P-03-33: Pumping tests and flow logging at DS1. SKB P-03-34: Pumping tests and flow logging at DS2. SKB P-03-35: Interference tests at DS1. SKB P-03-36: Pumping tests and flow logging at DS3.	See Table 2-5. KFM01A – Complete chemical characterization (class 4 and 5), Uranine analyses. KFM02A – Uranine analyses. Percussion drilled parts of KFM01A and 2A – Class 3 + isotopes. HFM01–08 – Class 3 + isotopes. SFM01–08 – Class 5. Precipitation – Class 5. Surface sampling – Class 3–5 + biosupplements. Other available data: SFR-data. Finnsjön-data.	A memo on site specfic diffusion and sorption data for Finnsjön and Äspö, by J Byegård. The rock domain model produced by Geology (specifically file Rock_properties_v1.1.xls). The flow-related transport parameters obtained from Hydrogeology.
If available data have not been used – what is the reason for their omission (e.g. not relevant, poor quality, lack of time, …).	Geophysical data reported in P-03-39 (HFM01, HFM02, HFM03 and the percussion-drilled part of KFM01A) have not been used due to some questionmarks concerning data quality. Regional gravity data reported in P-03-42 have not been used. There was insufficient time to complete the interpretation of these data by a geophysicist. A new assessment of older geological and geophysical data from the Forsmark nuclear reactor sites has not been carried out due to the incomplete character of the data submitted on 2003-04-30, the absence of a complementary report and the limited time available for the completion of the SDM version 1.1.	Old data from tunneling through the major fault zone (the Singö zone) are available in various sources, but not fully compiled and evaluated in terms of estimated mechanical properties of the rock mass in the Singö line. Especially convergence measurements in the fault during construction of the SFR ought to allow for a systematic back analysis.	Available hydrogeological data have been used in accordance with the status of the structural model. However, concerning historical hydrogeological data from the deep core boreholes in the reactor area (DBT1 and 3) available data have been used for the conceptual modeling mainly since the data were not digitized and ready for use within SDM V1.1.	SFR-data: Used for comparison and for conceptual model, not relevant for modelling due to different hydrogeology. Finnsjön-data: Used for comparison and for conceptual model. Many observations excluded from modelling due to no reported analyses at data freeze.	Conductive Fracture Frequency from borehole KFM01A has not been used to estimate flow-wetted surface for crude estimate of F-factor.

Question	Geology	Roch mechanics and Thermal	Hydrogeology	Hydrogeochemistry	Transport
(If applicable) What would have been the impact of considering the non-used data?	Geophysical data from HFM01, HFM02, HFM03 and the percussion-drilled part of KFM01A. There would have been more data available to help in the identification of rock types and possible deformation zones in these boreholes. Regional gravity data. Probably subordinate impact. The data are only of broad regional significance. Older data from Forsmark nuclear reactor sites. There would have been more data available for use in the geological model.	The use of convergence measurements from SFR (Singö falt zone and SFR) would decrease the uncertainties in state of stress and deformation modulus at these locations of the SDM.	Provided that the non-used historical data are of interest and of sufficient quality the information gained would contribute to the parameterisation of the conceptual model in areas outside the Candidate area.	Better description of spatial processes (more observations).	The impact is limited, since we believe the estimates produced by the groundwater flow models are better.
List the data and interpretation types and indicate how accuracy is established for these, e.g. by specified procedure, QA, etc (essentially just refer to tables in Chapter 2 and procedures in Chapter 4 in the report).	The data used are listed in Table 2-1. Reference to individual P-reports is strongly recommended. The evaluation of these data is provided in Chapter 4 (Sections 4.2.2 to 4.2.5, 4.4.1 and 4.6).	The borehole and core logs from KFM01A are used to derive the empirical rock mechanics properties for the purpose of characterisation according to /Andersson et al, 2002b/ and /Röshoff et al, 2002/. The outcome of Q-index are independently determined by /Barton, 2003/ and /Lanaro, 2004/ for the same borehole. Other derived mechanical properties of the rock mass are independently obtained by applying the RMR and Q-system. The old overcoring data from borehole DBT-1 and DBT-3 /Carlsson and Olsson, 1982/, have been assessed using transient strain analysis /Perman and Sjöberg, 2003/.	The interpretation of hydraulic tests presented in the data reports listed above follows standard QA procedures. The hydraulic tests focus mainly on the transmissivity. These interpretations have been considered "as are".	Surface water data: QA established. (+– 5–10% in analyses). GW data: QA established (+– 5–10%).	No interpretation of raw data done other than trying to scale Finnsjön-data to Forsmark. This is described in Section 5.6 of the SDM report.

Question	Geology	Roch mechanics and Thermal	Hydrogeology	Hydrogeochemistry	Transport
In the list above, estimate the potential for inaccuracy. Use the terms 'high', 'medium', 'low' and 'none' to describe these.	Radar and BIPS logging in boreholes. Low.	The deformation moduls obtained from RMR och Q is estimated to have a medium accuracy. This derives from i) the high accuracy of the oriented RQD, fracture fillings; ii) the mean accuracy of the fracture orientation, spacing and set; iii) low accuracy of fracture length, stresses and water conditions. Furthermore, the site and material dependency of the empirical relations between RMR och Q and mechanical properties for the rock mass lead to some uncertainties. The extension of the rock volume on which the determination is performed might also influence the resulting mechanical properties.	The interpretation of the hydraulic tests is generally considered to be of high quality (low inaccuracy). Possible sources of uncertainty are spatial heterogeneity and different kinds of drilling disturbances. Of particular interest is the occurrence of sediments in near surface fractures/ fracture zones. Due to lack of data about the occurrence of this phenomenon it is not possible to be conclusive about its impact on the modelling. The potential for a high inaccuracy cannot be discarded.	Low potential for inaccuracy, low significance of inaccuracy (sensitivity analyses will be performed).	Not relevant.
	Geophysical logging in the eight percussion boreholes. High to low. Some problems with measurements at drill site 1.				
	Boremap mapping of boreholes. Low.				
	Bedrock mapping at the surface, including detailed fracture mapping. Low.				
	Modal and geochemical analyses. Low.				
	Petrophysical analyses and in situ, gamma-ray spectrometry measurements. Low.				
	High-resolution reflection data. Low.				
	Airborne geophysical data. Low.				
	Topographic data. Low.	Re-evaluation of stress magnitudes has a higher confidence compared to previous SDM /SKB, 2002a/. The overall confidence in overcoring under high stress is uncertain due to the risk for microcracking and non-elastic strains /Martin and Christiansson, 1991/, /Christiansson and Hudson, 2003/. The old over-coring data should be further scrutinized in parallel with the future overcoring results. For high stresses, overcoring results should be evaluated together with data from other methods, mainly hydraulic fracturing. Until further data have been collected and evaluated the confidence in stress information at depth should be regarded as low.			
	Ground geophysical data. Low.				
	Regional gravity data. Low.				
		Thermal conductivity is still mainly derived from modal analyse information. Few observations with the TPS method indicate relatively good agreement. For this reason is the accuracy estimated to be "medium".			

Question	Geology	Roch mechanics and Thermal	Hydrogeology	Hydrogeochemistry	Transport
If biased data are being produced, can these be corrected for the bias?	There are far more lineaments and, thereby, inferred deformation zones on land than in the sea area to the northeast. This reflects the use of four data types on land in the lineament interpretation and the use of one or, in places, two data sets in the sea area. This bias will be reduced in model version 1.2, when further processing of the aiborne EM data as well as detailed bathymetric data will be available. Since focus in the deterministic structural model has been placed on lineaments that are both distinctive and are based solely or strongly on magnetic data, it is judged that this bias is not a major problem. A second bias concerns the fracture data from boreholes. All these boreholes are steep and the longest of these boreholes (KFM01A) is oriented to the northwest. Both these features introduce a bias in especially the orientation of fractures. The emphasis on flat-lying fractures and the low frequency of fractures with NW strike may be two results of this bias. This problem can be tackled with the help of a Terzaghi orientation correction and will be reduced more significantly when data from inclined boreholes in different orientations are evaluated in later model versions. Mapping of fractures at the surface will produce a bias towards steeply-dipping fractures. Some correction can be applied with the help of a Terzaghi orientation correction. Reflection seismic data from the surface focuses attention on the occurrence of flat-lying structures. VSP data from boreholes should help to rectify this imbalance.	Biases due to the limited extension of the investigated surface areas and to the linear sampling of the borehole have to be considered. Some corrections on spacing and fracture set determination are already applied. The mechanical properties of the intact rock and of the fractures can also be affected by sampling biases. This results in a tendency of overrepresent samples of relatively good quality. An increased number of randomly chosen test samples would decrease this uncertainty. The bias of sampling preferentially fractures sub-parallel to the borehole affects the evaluation of the fracture mechanical properties. In general, these biases will reduce as soon as other unaligned boreholes will be considered. Bias on non-elastic strains during overcoring can only be assessed by comparing to results from other methods, primarely hydraulic fracturing and hydraulic fracturing of pre-existing fractures (HTPF).	It is recognised that cored borehole KFM01A has a window effect in the fracture statistics due to its orientation. Hence, the structural model of the rock between the fracture zones is biased. This effect can be addressed by incorporating more boreholes with other orientations.	Biased data (uneven data coverage and erroneous data) can be corrected by use of generic data and back-calculations.	No, we can't correct for bias since we have no site-specific information. The main bias is that we assume that the porosity-formation factor correlation from Finnsjön is valid for Forsmark even if the stress conditions are different.

Question	Geology	Roch mechanics and Thermal	Hydrogeology	Hydrogeochemistry	Transport
To what extent are interpretations supported by more than one observation or set of observations? (list all examples). (or give reference to sections of the report where this is stated).	Composition of rock type based on surface data (Section 4.2.2). Distribution of rock units at the surface (Section 4.2.2). Character and, especially, orientation of ductile structures in the bedrock (Sections 4.2.4 and 4.4.1). Character and orientation of fractures from surface and borehole data (Sections 4.2.4, 4.4.1 and, especially, 4.6). Character of rock domain 29 in the rock domain model based on surface and borehole data (Section 5.1.2). Recognition of deformation zones with a high degree of confidence in the deterministic structural model (Section 5.1.4.) Occurrence and orientation of lineaments and, by consequence, deformation zones with a medium or lower degree of confidence in the deterministic structural model (Sections 4.2.3 and 5.1.4). Stochastic model of fractures (Section 5.1.6).	Deformation modulus of the rock mass is assessed based on indicators from old tunnelling, two independent empirical characterisations of KFM01A and surface surveying. The results seem to support each other, even if the variation span sometimes is wide. The other mechanical properties of the rock mass are always obtained by the two independent methods RMR and Q, respectively (Section 4.6.3 and 5.2.4). Measured stress orientation agree with foliation (see Section 5.2.3). Thermal conductivity based on modal analyses and limited TPS measurements.	Hydraulic responses during drilling have been observed in nearby boreholes at all three drillsites, see P-03-33–36.	E.g. redox conditions at depth, process description at depth. Interpretation of major components is supported by other measurements such as redox, minor components, gas analyses, isotopes, etc.	Not relevant, we only have one observation for the D_e estimate. For the flow-related transport properties we have results from two codes, but the assumptions are similar for both codes.

Table 6-2. Protocol for use of available data and potential biases in the description of the near surface.

Question	Hydrochemistry	Hydrology	Quaternary Deposits	Ecosystems
Which data have been used for the current model version (refer to tables in Chapter 2 of the report).	See Hydrogeo-chemistry in Table 6-1	Meteorology: Version 0 data: R-99-70, TR-02-02, R-02-32. Surface hydrology: Version 0 data: TR-02-02, R-02-32, SICADA – FM Fieldnote 169: Sporadic simple runoff measurements SICADA – FM Field note 115: Catchment areas. Near surface hydrogeology: P-03-65: Slug tests in 36 monitoring wells, P-03-64: GW levels (single measurements). Oceanography: Version 0 data.	Surface based data: Mapping of QD (P-03-11), Outcrop map, Geological map, version 0, Neotectonic movements. Stratigraphical data: Mapping of QD (P-03-14), Marine and lacustrine sediments (P-03-24, R-01-12), Analytical data from HFM01–08, SFM001–SFM008 (P-03-14), Stratigraphic descriptions from HFM01–08, (only in SICADA) and SFM0009–0049 + PFM002461–65, 002472–74 (P-03-64). (For references and more, detail, see Table 2-6 in Chapter 2).	Terrestrial vegetation models: – Vegetation map version 0 – R-02-08 – Biomass inventory P-03-80. Terrestrial fauna description: – Bird inventory – Mammal inventory – R-00-20 ("Naturvärden i Forsmarksområdet"). Aquatic vegetation description, limnic: – Vatten i Uppsala län, SKB R-99-68, TR-00-02. Aquatic vegetation description, marine: – SKB R-99-69, R-01-27, TR-01-15. Aquatic fauna description, limnic: – SKB R-02-08, TR-00-02. Aquatic fauna description, marine: – SKB R-99-69, R-02-08.
If available data have not been used – what is the reason for their omission (e.g. not relevant, poor quality, lack of time, …)		–		SKB P-03-81 "Vegetation inventory" not used. Reason: lack of time, important complementary data are not available. SKB P-03-27 "Surface water chemistry" not used. Reason: lack of time, important complementary data are not available.
(If applicable) What would have been the impact of considering the non-used data?				Vegetation map could have been validated by use of SKB P-03-81. A better characterization of surface waters by use of SKB P-03-27.

Question	Hydrochemistry	Hydrology	Quaternary Deposits	Ecosystems
List the data and interpretation types and indicate how accuracy is established for these, e.g. by specified procedure, QA, etc (essentially just refer to tables in Chapter 2 and procedures in Chapter 4 in the report.	See Hydrogeo-chemistry in Table 6-1.	Meteorology: SMHI standard. Surface hydrology: Catchment areas checked in the field, runoff outside model area according to SMHI standard. Near surface hydrogeology: According to standard methods described in MD + AP. Oceanography: Scientific status.	Field classification and sampling according to standard methods described in MD, calibration between experts. Laboratory analyses according to standard methods described in MD.	Terrestrial vegetation models: – Vegetation map – not validated yet – R-02-08 – unknown quality – SKB P-03-81 ("Vegetationsinventering") – unknown data quality – Biomass inventory P-03-80 – statistical description of accuracy available. Terrestrial fauna description: – Bird inventory – unknown data quality – Mammal inventory – statistical description of accuracy available. Aquatic vegetation description, limnic: – Vatten i Uppsala län, SKB R-99-68, TR-00-02 – scientific report status. Aquatic vegetation description, marine: – SKB R-99-69, R-01-27, TR-01-15 – scientific report status. Aquatic fauna description, limnic: – SKB R-02-08, TR-00-02 – scientific report status. Aquatic fauna description, marine: – SKB R-99-69, R-02-08 – scientific report status.
In the list above, estimate the potential for inaccuracy and the significance of the inaccuracy. Use the terms 'high', 'medium', 'low' and 'none' to describe these.		Meteorology: All stations outside regional model area: high inaccuracy, medium significance. Surface hydrology: Catchment areas: low inaccuracy, low significance; runoff: medium/high inaccuracy, high significance. Near surface hydrogeology: Slug tests: medium inaccuracy, medium significance; gw levels: high inaccuracy, high significance (no temporal variation). Oceanography: –	Field classification depends on expert judgments – low potential for inaccuracy (but difficult to quantify), low significance of inaccuracy. Laboratory analyses – low potential for inaccuracy, medium significance of inaccuracy.	The potential for inaccuracy is high for all data listed above due to lack of complementary data (e.g. flow logging for transport modelling), non-validated data or submodels (e.g. vegetation map), and lack of property data (e.g. vegetation biomass). The significance of inaccuracy is low for this model version since many investigations are not completed and synthesized for version 1.1. Complementary data will be produced for later, complete versions of the SDM.

Question	Hydrochemistry	Hydrology	Quaternary Deposits	Ecosystems
If biased data are being produced, can these be corrected for the bias?		Meteorology: precipitation data – standard correction for measurement errors. Surface hydrology: regional runoff in rel large catchments – generic information on variations in small areas, influence of topography, land use etc. Near surface hydrogeology: Slug test only in the contact between bedrock and QD, no representation of variation in depth, correction by expert judgment; gw level measurements: concentrated to topographic depressions and no temporal variation, correction by expert judgment. Oceanography: –	Stratigraphical data concentrated to infrastructure and to topographic depressions. Available data cover most QD types and more data will be available to v1.2	–
To what extent are interpretations supported by more than one observation or set of observations? (list all examples) (or give reference to sections of the report where this is stated).		Meteorology: Several observation stations outside regional model area. Surface hydrology: Catchment areas checked in the field; runoff: several observation stations outside regional model area. Near surface hydrogeology: Slug test: both falling and rising head, several evaluation methods. Oceanography: –	Field classification compared to laboratory analyses.	–

6.2.2 Observations

The answers to the auditing protocol on the use of data sources as expressed in Table 6-1 and Table 6-2 suggest the following overall observations.

Use of data

The database for the modelling is well defined and is listed in the tables of Chapter 2.

Generally all data available at the time of the data freeze 1.1 and as listed in the tables of Chapter 2 have been considered for the modelling. The main exception is that some "old data", i.e. data from the construction of the nuclear power plants or the SFR, are still underused. The main reason for this is that the transfer and auditing of these old data into a quality assured format had not been completed at the time of the data freeze for version 1.1.

Evidently, the old data may contain highly useful information, and in particular as some of it covers the area and volume presently covered by the power plants where new measurement would be very difficult or even impossible. Consequently, these data must be considered in coming versions of the Forsmark Site Descriptive Model.

Accuracy

Accuracy in field data and interpretation has been established using well-defined procedures as is explained in detail in Chapter 4 of this report. The potential for inaccuracy stemming from the field data is assessed and is in general judged to be a minor source of uncertainty in the resulting model description. Some important deviations from this general conclusion include *the overall confidence in overcoring under high stress magnitudes*, and the occurrence of *sediments in near surface fractures/fracture zones* as further explained in Table 6-1. These issues, in particular, need further scrutiny in coming model versions.

Bias

There are biases in the version 1.1 data. Important examples include:

- Varying spatial coverage of surface geophysics over sea and land and at the nuclear power plant – affects e.g. lineament interpretation such that more lineaments are identified in the well covered areas. In coming data freezes spatial coverage will be improved, but it is also necessary to keep the varying spatial coverage in mind when assessing uncertainties – uncertainties will be higher in areas with poor spatial coverage.

- The information data gap between lineaments and detailed exposure mapping.

- There is only one deep borehole which implies that most of the deep bedrock is not explored. More boreholes from different parts of the explored volume would reduce this bias.

- There are different directional biases in the data due to i) a single direction for the (only) deep borehole, ii) the surface data fracture mapping and iii) the higher sensitivity for sub-horizontal features in the reflection seismics. This bias affects both fracture statistics and the hydrogeological interpretation. Partly directional bias can be handled through bias correction techniques, like Therzagi correction, but would generally require information from bore holes from different directions. Such holes will also provide data in subsequent data freezes.

There is also "bias" stemming from little or no data from the site and where instead data from other sites are used as analogues. For example, it is assumed that the porosity-formation factor correlation from Finnsjön is valid for Forsmark even if the stress conditions are different. Such biases will be handled by assessing more data from the site itself.

Multiple evidence

Several interpretations, including *composition of rock types, orientation of structures, hydraulic responses, interpretation of major components of the groundwater, or means of exploring near surface hydrogeology* are supported by more than one observation or set of observations. The value of these multiple observations (and sometimes lack thereof) should be considered in the uncertainty evaluation.

6.2.3 Overall assessment

In general, it appears that most available data have analysed and treated according to good practices and that inaccuracy and biases are understood and accounted for in the subsequent modelling. The overriding issue affecting confidence in models based on version 1.1 data freeze is the bias and uncertainty resulting from varying spatial coverage of data and very few and unidirectional deep borehole data. These biases will evidently be improved in coming model versions.

6.3 Uncertainties and potential for alternative interpretations?

Small estimated uncertainties and inability to produce many different alternative interpretations from the same database are indications of confidence – although not strict proof. A related issue is whether new measurements or other tests could resolve uncertainties or separate between alternatives and thereby enhance confidence. However, it needs to be remembered that the aim of the Site Investigations is not to reduce uncertainties to insignificant levels. The uncertainties need only be resolved to the extent they significantly affect the ability to make conclusive safety and engineering assessments in support of the license application for the deep repository.

6.3.1 Auditing protocol

The Site Descriptive Models represent the characterization of a natural rock mass, and hence uncertainty is an inherent aspect of the Model development. There are conceptual uncertainties, and other types of uncertainty: data uncertainty, spatial variation, temporal variation, applicability of database information, measurement error, modelling error, etc. In some cases, we are dealing with unresolved scientific issues, which are decided by consensus. Furthermore, some uncertainties are more important than others.

The uncertainties need to be identified and the cause for uncertainty should be established. An associated issue is to what extent uncertainties are related to the information density (not only from boreholes) both laterally and vertically. Specifically, confidence in the description could be high even if there are few measurements if geological understanding is high (e.g. if there is a homogenous and evident geology), but could also be low, even with a 'wealth' of data, if the geological understanding is poor.

There is also the distinction between what is uncertain at an absolute level and what is uncertain in terms of the potential for alternative interpretations. We need to be able to state the potential for alternative explanations and later consider how to conduct diagnostic tests to establish the most likely interpretation. Where alternative interpretations cannot be eliminated, they may be carried through to performance assessment, to determine whether they are prejudicial to performance.

Thus a common philosophy is required for addressing uncertainty and the implementation needs to be audited. There is a need to consider how uncertainties can be identified through uncertainty elicitation. A protocol has thus been developed for checking this. It concerns:

- The main uncertainty areas and the subject items in these areas.
- Whether and how the uncertainties can be expressed numerically.
- Whether uncertainties are quantified.
- To what extent uncertainties are related to the information density?
- Whether uncertainty can be addressed by alternative interpretations, if so the lines of reasoning for producing alternatives and list (or provide reference to) alternatives produced.
- If there are measurements or other tests, which could separate between alternatives and enhance confidence.

Table 6-3 lists the answers to these questions for the bedrock and Table 6-4 for the near-surface descriptions.

Table 6-3. Protocol for assessing uncertainty in the bedrock description.

Question	Geology	Roch mechanics and Thermal	Hydrogeology	Hydrogeochemistry	Transport
List the main uncertainty areas and the subject items in these areas.	**Rock domains** 1. The quality of surface data south of road 76 and, especially, in the sea area to the northeast of the candidate area. This problem will reduce dramatically when new data are available for the SDM version 1.2. However, the problem will remain under Öregrundsgrepen. 2. The location of the boundaries between rock units that show different degrees of inhomogeneity and of ductile deformation. See also comment above. 3. The extension of rock domain boundaries at depth, especially outside the local model volume where data at depth are absent. The problem outside the local model volume will almost certainly remain in future model versions. 4. The properties of various rock types that make up the rock domains. This is not a source of major uncertainty and will be reduced when more data are available for the SDM version 1.2. 5. The proportions of various rock types in each rock domain, especially outside the local model volume. This problem will reduce inside the local model volume when more borehole data are available. It will almost certainly remain outside the local model volume in future model versions.	The rock domain model is used to establish domains with similar mechanical and thermal properties. The geological sampling provides several variants from the dominant rock types and fracture sets. However, the distribution of such variants could not be completely assessed. Small volumes of anomalous rock variants within a lithological unit may bias the estimate of intact rock mechanical properties and thermal conductivity based on modal analysis, because data are used without any possibility to weight with respect to the amount of occurrence. Future descriptions on the lithological distributions within the rock units would help to increase a general understanding of the lithological variations within the domains. With a certain degree of confidence, the mechanical properties of competent rock mass can be provided for further design and safety assessment. There is no new stress information, but the geological information on structures and lineations strengthen the earlier prediction of trend of the major principal stress. In addition to the rock stress, the deformability of fracture zones is a main uncertainty topic. The values are required as input to the numerical modelling.	All assumptions made in the structural model are directly transferred to the hydrogeological model. In particular, there is an uncertainty in the interpretation of lineaments as fracture zones (confidence level) and in the assignment of penetration depths. Generally, the hydraulic DFN model and resulting connectivity is highly uncertain. For example: 1. The interpretation of rock fracture intensity. 2. Assumed correlation between T and size. 3. The current rock fracture model assumes that the intensity of features of different sizes in different directions varies as power law distributions, with a unique slope for each fracture set. This interpretation is not speculative by any means, but the data analysis needs to be strengthened. 4. The current assumption is that the T-distributions are the same for all five fracture sets.	Spatial variability at depth. Temporal variability in surface streams. Model uncertainties.	Main uncertainty is that we have no site-specific data on retention properties. Concerning the flow-related transport parameters, i.e. transport resistance, the obtained values are uncertain due to uncertainty in groundwater flow models (e.g. transmissivity (conductivity) distribution, P_{32} values, boundary conditions).

Question	Geology	Roch mechanics and Thermal	Hydrogeology	Hydrogeochemistry	Transport
	Deterministic structural model 1. Presence of undetected zones 2. The geological feature (features) that gives (give) rise to the seismic reflectors. 3. The geological feature (features) that is (are) represented in the inferred lineaments. A key question is: Do they always represent deformation zones in the bedrock? 4. The position at the surface and, especially, the length, dip, width and extension at depth of the deformation zones that have been inferred from lineaments. Two points are of high uncertainty – the continuity and the dip of these inferred deformation zones. 5. The extension in both the strike and dip directions of the flat-lying deformation zones that are present in the model volumes. A key question is: How continuous are these structures? Stochastic model of fractures 1. The interpretation that fractures and lineaments can be coupled to the same statistical distributions for orientation, size and intensity. 2. The orientation, size and intensity of fractures that are longer than that documented in connection with the detailed fracture mapping at the surface and shorter than that inferred to be represented by lineaments. 3. The variability of geometric properties of fracturing at depth. 4. The variability of fracturing in rock domains outside RD29.		The current status concerning the groundwater salinity is poorly known at depth. This in turn makes it difficult to test the importance of the initial hydrogeological condition (paleohydrogeology). The current elevation model is not correct in the vicinity of the shoreline. The error is in the bathymetric data between 0 and –3 masl.		

Question	Geology	Roch mechanics and Thermal	Hydrogeology	Hydrogeochemistry	Transport
With reference to the list above, explain whether the uncertainties can be expressed numerically and how this could be done.	The properties of rock types that make up the rock domains. Mean and standard deviation values for analytical results are provided. See table for the properties of different rock types (Sections 5.1.2 and 7.2.1). The proportions of rock types in each rock domain. Make use of borehole data. Estimate only carried out in RD29 (Sections 5.1.2 and 7.2.1). The position, orientation, width and length of deformation zones with high confidence (see below) that are based on borehole, tunnel and specific surface data. Use available data from boreholes, tunnels etc. See tables for the properties of deformation zones (Sections 5.1.4 and 7.2.1). The position of deformation zones that are based on the interpretation of lineaments. Use the quality of both the airborne geophysical and topographic data available for the interpretation work and the scale at which this work has been carried out. See tables for the properties of deformation zones (Sections 5.1.4 and 7.2.1). The orientation of deformation zones that are based on the interpretation of lineaments. An estimate can be made from the statistical analysis of lineaments and fractures. See tables for the properties of deformation zones (Sections 5.1.4 and 7.2.1). The properties of trace lengths of lineaments and fractures in outcrop data can be approximated with a powerlaw law distribution (Section 4.6.2). Other statistical distributions may work (such as log normal approximation) but do not give new information to the "black hole" between the outcrop data and the lineament interpretation.	The estimation of the rock mass deformability (especially for deformation zones) was achieved through the application of independent characterisation schemes incorporating the geometrical and mechanical parameters from further site investigations. The influence that the different uncertainties have on the rock mechanics modelling and associated state of stress can also be established through sensitivity analyses by means of numerical modelling. The state of stress can be modelled to explain relative variations in different volumes of the tectonic model.	The uncertainties are in the interpretations as such (i.e. qualitative) and suffer from lack of data or bias in the data available. Some of the settings/assumptions can be tested by means of exploration simulations although there is no obvious answer to compare the solutions with, e.g. the paleohydrogical problem.	Spatial variability and temporal variability can be estimated by expert judgement. Model uncertainties are known.	For the flow-related transport parameters, the uncertainties could be evaluated by running different variants. There has been no time within version 1.1 to assess variants.

Question	Geology	Roch mechanics and Thermal	Hydrogeology	Hydrogeochemistry	Transport
	Except for identified deterministic zone intercepts, the borehole fracture data have currently been treated as one data set, where orientation is expressed as statistical distributions with standard deviation values. The fracturing in KFM01A can be analysed in sections at different depths to evaluate if the variability in intensity and orientation changes with depth. The variability of fracturing in other rock domains than RD29 cannot be analysed without more data in these rock domains.				
Are uncertainties actually quantified? If so provide reference to where in the SDM-report this information is stated. (Answer can be combined with answer to previous question).	Note. The numerical estimates of uncertainties that are provided in the text have been listed above (question 2). An assessment of the level of confidence for various features in the geological model has been estimated. Four levels of confidence have been used, i.e. high, medium, low and very low. The level of confidence has been provided for the following features in the geological model: 1. The occurrence and geometry of rock domains both at the surface and to a depth of 2,100 m (Section 5.1.2). 2. The assignment of the properties of rock domains (Sections 5.1.2 and 7.2.1). 3. The occurrence of deformation zones (Section 5.1.4). 4. The assignment of the properties of deformation zones (Sections 5.1.4 and 7.2.1). 5. Fracture orientation sets (Section 5.1.6). 6. Fracture size distributions (Section 5.1.6). 7. Fracture intensity (Section 5.1.6). 8. Fracture spatial distribution (Section 5.1.6).	The ranges of the mechanical properties, thermal properties and of the rock stresses provided in Chapter 7 give a measure of the combined effect of uncertainty and spatial variability. No deeper analyses have been carried out in version 1.1.	See the previous answer. The current uncertainties are not actually quantified in version 1.1.	Spatial variability is site specific. Spatial variability cannot be described in ISI. Temporal variability?? Model uncertainties are specified in the GW-chemistry method report.	Uncertainties are not quantified numerically. However, variability in F-factor due to heterogeneity (spatial variability) is assessed.

Question	Geology	Roch mechanics and Thermal	Hydrogeology	Hydrogeochemistry	Transport
To what extent are uncertainties related to the information density? (consider wealth of data in relation to overall "understanding").	Surface data for the lithological model are lacking south of road 76 and, especially, in the sea area to the northeast of the candidate area. This uncertainty will be reduced when more data are available during SDM version 1.2. The identification of lineaments has been carried out differently in the area on the mainland, in the sea area northeast of the candidate area (including the islands) and in the outboard area to the northeast under Öregrundsgrepen and on Gräsö. These differences are related to the density of available data and will be reduced during SDM version 1.2. Since no airborne geophysical measurements were carried out over the nuclear power plants and the topography is disturbed by all the building activities, there is a distinctive absence of new data in this area. Furthermore, there are disturbances in the airborne geophysical measurements along power lines and a DC-cable. These features affect the identification of lineaments in these areas. A closer assessment of historical data is planned for SDM version 1.2. This should reduce the effects of this data deficiency. There is major lack of data at depth in model SDM version 1.1. This will be amended in future model versions as borehole data increases in importance relative to surface data.	To high degreee – and also due to lack of information from stress measurements and laboratory testing.	A better spatial spreading of the boreholes and, in particular, more measurements at depth (including salinity data) will clearly reduce some of the current uncertainties.	Mostly related to this.	Not relevant for retention parameters since we lack data. For F-factor, estimated values are uncertain due to the fact that groundwater flow models are primarily based on data from one borehole (i.e. low information density).

Question	Geology	Roch mechanics and Thermal	Hydrogeology	Hydrogeochemistry	Transport
Can (is) uncertainty (be) addressed by alternative interpretations? If so, what are the lines of reasoning for producing alternatives in your discipline?	The following uncertainties can be addressed by alternative interpretations: **Extension of flat-lying fracture zones.** Three alternatives are possible. Alternative 1 extends these zones to the nearest inferred, steeply-dipping or vertical zone. Alternative 2 extends the flat-lying deformation zones to the margins of the regional model area. A third alternative, that lies between these two extremes, extends the flat-lying deformation zones to the nearest regional deformation zone. **Dip of deformation zones inferred from lineaments.** Alternative 1 assumes that these zones dip 90°. Alternative 2 assumes that the zones with NW, N-S and E-W strike dip 90° but the zones with NE strike dip gently to the southeast, in the same manner as the seismic reflectors. **Fracture intensity at depth.** Two alternatives are possible. Alternative 1 assumes that the fractures show the same intensity at depth. Alternative 2, inspired by the results from one cored borehole, reduces the fracture intensity at 400 m. **Uncertainty in the identification of lineaments.** Carry out an independent interpretation of the airborne geophysical and topographic data, possibly within a limited area, to check the reproducibility of the lineament interpretation.	What concerns rock mechanics, two empirical methods have been applied by different operators resulting in independent determinations. However, at this stage, the main problem is the lack of measurement information and possibly a comparison with results from numerical modelling.	Yes, uncertainty can be addressed by alternative interpretations. The obvious alternative interpretation at this point is to reduce the number of lineaments treated as vertical fracture zone segments. Secondly, the impact of at least one sub-horizontal fracture zone should be tested by means of exploration simulation. The power-law relationship between T and L ($T = a \cdot L^b$) used in the current DFN setup can be tested with other values of a and b or, indeed, no correlation whatsoever. The current setting $a = 2.47 \cdot 10^{-12}$ m²/s and $b = 1.791$ is not extreme by any means. For example, the setting used in SKB TR-02-19 was $a = 1 \cdot 10^{-12}$ m²/s and $b = 2$.	Alternative models will be constructed and model comparison with hydrogeological models and models based on generic data. Hypotheses for alternative models of the bedrock hydrogeochemistry concern reasons for groundwater composition, i.e. as a result of: i) mixing and reactions, ii) only reactions, iii) only mixing or iv) alternative end-members.	Same as for hydrogeology concerning F-factor. However, no alternative interpretations are assessed within version 1.1.

Question	Geology	Roch mechanics and Thermal	Hydrogeology	Hydrogeochemistry	Transport
(If applicable) list (or provide reference to) actual alternatives produced.	Two alternatives for the extension of flat-lying deformation zones are presented in the deterministic structural model. These correspond to the extreme alternatives 1 and 2 that were defined above (under 1). Since the uncertainties concerning the interpretation of the seismic reflectors remain (until the geological data from especially KFM03A are assessed and compared with the interpretation of the reflectors) all the deformation zones inferred solely with the help of lineaments have been given a dip of 90°. This corresponds to alternative 1 above (under 2). Two alternatives for the fracture intensity at depth are presented in the stochastic model of fractures. These alternatives correspond to the two alternatives that were defined above (under 3). No alternative interpretation of lineaments is available for the SDM version 1.1.	RMR and Q-systems were applied to determine the rock mass properties. In next model version, numerical modelling will flank the empirical determinations.	No alternatives have actually been evaluated in version 1.1.	Only initial evaluation in v1.1. Model version 0, model for SFR can also be seen as alternatives.	No alternatives.
Are there measurements or other tests, which could separate between alternatives and enhance confidence?	More borehole data are necessary to constrain the various alternatives for the continuity and dip of deformation zones. VSP investigations in boreholes may help to confirm the presence of steeply-dipping deformation zones.	Back calculations of available convergence measurements could provide and independent determination of the deformability of fracture zones similar to the Singö Fault Zone. Hard rock pressiometer tests might confirm the estimation of the rock mass deformation modulus in certain accessible areas. Independent determinations of the rock mass stresses (e.g. by means of overcoring and hydraulic fracturing) would improve the actual knowledge and maybe support alternative interpretations of the stress state.	The best way to calibrate a numerical model is to match simulations to interference tests. Given the many constraints listed above it is obvious that there is no point in making a calibration of the version 1.1 model. No major interference tests will be conducted within the version 1.2 data freeze. A few minor ones will probable be available. For version 1.2 it is important to compare the V1.1 findings between T and L with data from other cored boreholes, i.e. KFM02A and 3A.	New borehole data and samples from the rock matrix.	No alternatives discussed.

Table 6-4. Protocol for assessing uncertainty in the description of the near surface.

Question	Hydrochemistry	Hydrology	Quaternary Deposits	Ecosystems
List the main uncertainty areas and the subject items in these areas.	See Hydrogeo-chemistry in Table 6-3	Representativity of SMHI data outside the area. Spatial variability in precipitation and runoff. Spatial variability of conductivity in Quaternary deposits (QD).	Spatial variability, esp. in regional model area (e.g. QD mapping only in minor parts of local model area).	Transport of matter (runoff, concentration of main constituents). Biomass, production, decomposition in aquatic systems (flora and fauna). Description of regolith metabolism.
With reference to the list above, explain whether the uncertainties can be expressed numerically and how this could be done.		Uncertainty in transmissivity can be expressed in numerical terms for the contact zone QD/Bedrock. Other spatial variability can be estimated by expert judgment.	–	This will not be done in version 1.1. By using reference literature. By using reference literature.
Are uncertainties actually quantified? If so provide reference to where in the SDM-report this information is stated. (Answer can be combined with answer to previous question).		For conductivities of the contact zone QD/Bedrock, see Section 5.4.2.	–	No.
To what extent are uncertainties related to the information density? (consider wealth of data in relation to overall "understanding").		Uncertainties of the conductivity of the contact zone QD/Bedrock will not be very much reduced by additional measurements. For the other uncertainties lack of data is a major source of uncertainty.	Strongly related to info density (inhomogeneities in QD), extra-/interpolations depends on understanding.	Uncertainties are strongly related to info density, in that we need site-specific data for estimation of uncertainty.
Can (is) uncertainty (be) addressed by alternative interpretations? If so, what are the lines of reasoning for producing alternatives in your discipline?		In version 1.1 only conceptual modelling is performed. In future quantitative modelling, different modelling approaches can be used and sensitivity analyses and/or stochastic approaches can be applied to analyse uncertainties and their influence on predictions.	Spatial variability, esp. in regional model area (e.g. QD mapping only in minor parts of local model area).	No.
(If applicable) list (or provide reference to) actual alternatives produced.		–	–	–
Are there measurements or other tests, which could separate between alternatives and enhance confidence?		Conductivity data from slug tests can be compared with conductivity data retrieved from soil size distributions when these are available.		No.

6.3.2 Main uncertainties

Bedrock Geological Model

As already identified in Chapter 5 and as listed in Table 6-3 the main uncertainties in the version 1.1 *bedrock geological* model concern:

- Varying spatial support for the lithological description – especially outside rock domain RD29.

- The extension of rock domain boundaries at depth, especially outside the local model volume.

- Properties of various rock types that make up the rock domains and the proportions of various rock types in each rock domain, especially outside the local model volume.

- Presence of undetected zones.

- What are the features giving rise to the seismic reflectors and what features are represented in the inferred lineaments, do they always represent deformation zones in the bedrock?

- The position at the surface and, especially, the length, dip, width and extension at depth of the deformation zones that have been inferred from lineaments.

- The extension in both the strike and dip directions of the flat-lying deformation zones that are present in the model volumes. How continuous are these structures?

- Representativity of surface fractures for DFN-model and in particular the interpretation that fractures and lineaments can be coupled to the same statistical distributions for orientation, size and intensity.

- The DFN-size distribution in the range 50–500 m, i.e. the orientation, size and intensity of fractures that are longer than that documented in connection with the detailed fracture mapping at the surface and shorter than that inferred to be represented by lineaments.

- The variability of geometric properties of fracturing at depth.

- The variability of fracturing in rock domains outside RD29.

Many of these uncertainties are described by statistical distributions or at least by indication of confidence (for details see Table 6-3). Remaining uncertainties are left unresolved or as input to alternative hypotheses. Generally, much of the uncertainty is related to the information density and will thus be reduced in later model versions.

Rock mechanics and thermal

As already identified in Chapter 5 the main uncertainties in the version 1.1 *rock mechanics* and *thermal* model concern:

- Uncertainty in the rock type distribution in the rock domains (see above).

- Small volumes of anomalous rock variants within a lithological unit may bias the estimate of thermal conductivity based on modal analysis, because data are used without any possibility to weight with respect to the amount of occurrence. Future descriptions on the lithological distributions within the rock units would help to increase a general understanding of the lithological variations within the domains.

- Stress distribution at depth (no data in version 1.1).

- Deformability modulus values for fracture zones.

In version 1.1 these uncertainties are left un-quantified, since there is little reason to resolve these issues further until there are actual rock mechanics and thermal data from boreholes in the candidate area. Such data as are expected in version 1.2 combined with and integrated assessment of the structural geology and hydrogeology will allow for a more meaningful assessment of uncertainty and confidence in the rock mechanics.

Hydrogeology

As already identified in Chapter 5 the main uncertainties in the version 1.1 *hydrogeological* model concern:

- Uncertainty in top boundary conditions – e.g. minor errors in the current elevation model which is not correct in the vicinity of the shoreline.

- All assumptions made in the structural model are directly transferred to the hydrogeological model. In particular, there is an uncertainty in the interpretation of lineaments as fracture zones (confidence level) and in the assignment of penetration depths. Another uncertainty affecting the hydrogeology is in the interpretation of rock fracture size and orientation distribution and intensity variation with depth.

- Transmissivity distribution in deformation zones and the potential relation between deformation zone properties and the transmissivity assignment. This is certainly a conceptual issue that will need to be explored further.

- Lack of hydraulic measurements (in version 1.1) to support interpretations on anisotropy and spatial distribution.

- Fracture transmissivity correlation to fracture size. The current rock fracture model assumes that the intensity of features of different sizes in different directions varies as power law distributions, with a unique slope for each fracture set.

- (Lack of) fracture transmissivity correlation to depth and fracture orientation. The current assumption is that the T-distributions are the same for all five fracture sets and with no depth dependence. The observed "rock mass" depth variation and anisotropy is obtained indirectly from the orientation and depth variation of the fracturing.

- For version 1.1 the distribution of groundwater salinity is poorly known at depth. This in turn makes it difficult to test the importance of the initial hydrogeological condition (paleohydrogeology).

The current uncertainties are not actually quantified in version 1.1, since they originate from the interpretations as such (i.e. are qualitative) and suffer from lack of data or bias in the data available. Some of the settings/assumptions can be tested by means of exploration simulations although there is no obvious answer to compare the solutions with, e.g. the paleohydrogical problem. More hydraulic data, especially cross-hole tests and additional support for the geological model to be obtained in later data freezes, would allow a more meaningful quantification of the uncertainties.

Hydrogeochemistry

As already identified in Chapter 5 the main uncertainties in the version 1.1 *hydrogeochemical* model concern:

- Spatial variability at depth.

- Temporal variability in surface streams.

- "Model uncertainties".

Spatial variability and temporal variability can be estimated by expert judgement, but the spatial variability at depth cannot be meaningfully quantified before there are data available from the depth. In version 1.1 these uncertainties are left unresolved or as input to alternative hypothesis. The geochemical model uncertainties are specified in the methodology report /Smellie at al, 2002/.

Bedrock transport properties

As already identified in Chapter 5 the main uncertainties in the version 1.1 model of the *bedrock transport properties* concern:

- Lack of site-specific data (in version 1.1) on retention properties.

- Resulting uncertainties in the flow-related transport parameters, i.e. transport resistance, due to uncertainty in groundwater flow models (see above).

In version 1.1 uncertainties are not quantified numerically. For the flow-related transport parameters, the uncertainties could be evaluated by running different variants. However, variability in F-factor due to heterogeneity (spatial variability) is assessed.

Surface and near surface

As already identified in Chapter 5 the main uncertainties in the version 1.1 model of the *surface properties and ecosystems* concern:

- Representativity of hydrology data outside the model area.

- Spatial variability in precipitation and runoff.

- Spatial variability of the Quaternary deposits, including their hydraulic conductivity, especially in the regional model area (e.g. mapping only in minor parts of local model area).

- Transport of matter (runoff, concentration of main constituents).

- Biomass, production, decomposition in aquatic systems (flora and fauna).

- Description of metabolism of biomass in the Quaternary deposits.

The uncertainty in conductivities of the contact zone between Quaternary deposits and bedrock is assessed, see Section 5.4.4. Uncertainties in ecosystems will not be quantified in version 1.1, but could be done based on reference literature.

6.3.3 Alternatives

As discussed by /Andersson, 2003/ alternatives may both concern:

- alternative geometrical framework (e.g. the geometry of deformation zones and rock domains), and

- alternative descriptions (models such as DFN or SC – or parameter values) within the same geometrical framework.

Alternative model generation should be seen as a means for model development in general and as a means of exploring confidence in particular conceptualisations. At least in early stages, when there is little information, it is evident that there will be several different possible interpretations of the data, but this may not necessitate that all possible alternatives are propagated through the entire analysis to Safety Assessment. Combining all potential alternatives with all their permutations leads to an exponential growth of calculation cases – variant explosion – and a structured and motivated approach for omitting alternatives at early stages is a necessity.

In particular, relative to model version 1.1 it is evident that new data from later data freezes may result in considerable changes in later model versions. Spending efforts in completing various alternative models would thus be rather pointless. Instead, it is judged more fruitful to consider alternative hypotheses, which may continue to generate alternatives in later model versions. Nevertheless, a few alternatives have been developed in version 1.1.

Bedrock Geological Model

As further explained in Table 6-3, identified hypotheses for alternative models of the bedrock geology concern:

- Extension of flat-lying fracture zones.

- Dip of deformation zones inferred from lineaments.

- Fracture intensity at depth.

- Uncertainty in the identification of lineaments.

Of these hypotheses the following alternatives are presented for the version 1.1 model:

- Two alternatives for the extension of flat-lying deformation zones are presented in the deterministic structural model.

- Two alternatives for the fracture intensity at depth are presented in the stochastic model of fractures.

Due to lack of data it has not been judged meaningful to present alternatives for lineament interpretation or for the dip of the deformation zones. As explained in Table 6-3, there are various possibilities to explore these alternatives and alternative hypotheses using new data to be obtained in coming data freezes.

Rock mechanics and thermal

It has not been judged meaningful to discuss alternative models of rock mechanics and thermal properties in version 1.1.

Hydrogeological model

As further explained in Table 6-3, identified hypotheses for alternative models of the bedrock hydrogeology concern:

- Alternatives in the geological model (extent of sub-horizontal zones and depth decrease of fracture intensity). The obvious alternative interpretation at this point is to reduce the number of lineaments treated as vertical fracture zone segments. Secondly, the impact of at least one sub-horizontal fracture zone should be tested by means of exploration simulation.

- The power-law relationship between T and L ($T = a \cdot L^b$) used in the current DFN setup can be tested with other values of a and b or, indeed, no correlation whatsoever. Assignment of T (or K) based on measured data is a critical conceptual issue that will be explored further.

- T correlated to fracture orientation (and stress field).

However, none of these hypotheses have actually been explored further in version 1.1, but, as explained in Table 6-3, there are various possibilities to explore these alternative hypotheses using new data to be obtained in coming data freezes.

Hydrogeochemical model

As further explained in Table 6-3 identified hypotheses for alternative models of the bedrock hydrogeochemistry concern reasons for groundwater composition, i.e. as a result of:

- mixing and reactions,

- only reactions,

- only mixing, or

- alternative end-members.

However, in version 1.1 there has only been initial testing of these alternative hypotheses. Obviously, available descriptions of the groundwater composition as given in version 0 and at the SFR could also be considered as alternatives for 1.1.

Bedrock Transport Properties

The alternatives for hydrogeology would also result in alternative descriptions of the flow-related transport properties (the F-factor). However, it has not been judged meaningful to further discuss alternative models of the bedrock transport properties in version 1.1.

Surface and Near Surface

In version 1.1 only conceptual modelling of the surface hydrology is performed. In later quantitative modelling, sensitivity analyses and/or stochastic approaches can be applied to analyse uncertainties and their influence on predictions. As regards ecosystems alternative models are not judged a meaningful approach. The objective of the ecosystem modelling is much more to describe the current day situation, than to be used for predictive modelling in the future, where it is fully understood that uncertainties will be large.

6.3.4 Overall assessment

Evidently there is much uncertainty in the version 1.1 Site Descriptive Model, but main uncertainties are identified, some are also quantified and others are left as input to alternative hypotheses. However, since a main reason for uncertainty in version 1.1 is the lack of data and poor data density and as much more data are expected in coming data freezes it has not been judged meaningful to carry the uncertainty quantification or the alternative model generation too far. These efforts would anyway soon be outdated, whereas the types of uncertainties and alternative hypotheses identified are judged to be very useful input to the uncertainty and alternative model assessment in coming model versions.

6.4 Consistency between disciplines

Another prerequisite for confidence is consistency (i.e. no conflicts) between the different discipline model interpretations.

6.4.1 Actually considered interactions

As a first step in assessing the consistency between disciplines the modelling group has documented the interactions considered within the framework of an interaction matrix. Table 6-5 provides an overview of these interactions and Table 6-6 lists them in full.

As can be seen from the tables many inter disciplinary interactions are considered. Examples are given below.

Bedrock Geology and Rock Mechanics

Bedrock Geology on Rock Mechanics: There are several qualitative uses of the bedrock geological model in the rock mechanics model. The assessed spatial distribution of rock mechanics properties is based on the provided lithological domains, i.e. it is assumed that the properties are constant within each rock domain. The DFN model can be used for assessing rock mass properties as outlined in the rock mechanics methodology report /Andersson et al, 2002b/, although this was not done in version 1.1. The structural model is mainly used for estimating the variability of state of stress. Clearly, there are more potential for couplings. In particular, the structural model can be used for simulating the stress distribution as envisaged in the rock mechanics methodology report /Andersson et al, 2002b/. Also the description of fracture zones and fractures properties could be used to infer rock mechanics properties.

Rock Mechanics on Bedrock Geology There are also several qualitative uses of the rock mechanics model in assessing the reasonableness of the bedrock geological model. The overall stress orientations are reasonable in relation to the orientation of the fracture sets. Depth increase of rock stress provides a rationale for potential reduction in fracture intensity with depth. Also the lithological description of the rock domains is reasonable in relation to rock stresses.

Bedrock geology and hydrogeology

Bedrock geology on hydrogeology: Foremost, the geometry of deformation zones and fractures (deterministic and stochastic DFN) is directly transferred to the hydrogeological model. Indirectly, also the rock domain description is used as it motivates the spatial distribution of the DFN-model. Furthermore, the geological characterisation of individual deformation zones and of the fracture sets should affect the transmissivity assignment, but this was not really considered in version 1.1 (see also Section 6.3).

Hydrogeology on bedrock geology: The potential for high transmissivity in some zones (intersection borehole KFM01) has increased attention to describe the geometry of potential sub-horizontal zones. Generally, high transmissivity (or flow) in a borehole is a strong indicator of a zone (along with other zone indicators), but not the only indicator. There are zones without hydraulic significance. The observation of very low transmissivity at depth has inspired the hypothesis of low fracture intensity at depth.

Table 6-5. Summary of interactions considered in version 1.1. Note, an absence of a yes only indicates that the interaction was not considered – not that there is no interaction. (There is a clockwise interaction convention in the matrix, e.g. influence of geology on rock mechanics is located in Box 1,2, whereas the influence of rock mechanics on geology is located in Box 2,1).

Bedrock Geology	Yes	Yes	Yes	Yes	Yes	—	Yes	Later	—
Yes	Rock Mechanics (in the bedrock)	Yes	Yes	—	Yes	—	—	Later	—
Yes	—	Thermal (in the bedrock)	—	—	—	—	—	—	—
Yes	Yes	—	Hydrogeology (in the bedrock)	Yes	Yes	—	Later	—	—
—	—	—	Yes	Hydrogeochemistry (in the bedrock)	Yes	Yes	—	—	—
Later	—	—	Yes	Yes	Transport properties (in the bedrock)	—	—	—	—
—	—	—	—	Yes	—	Hydrochemistry (surface and near surface)	Yes	Later	Yes
—	—	—	Yes	—	—	Later	Hydrology (surface and near surface)	Later	Yes
Yes	Later	—	Yes	Later	—	Later	Yes	Quaternary deposits and topography	Yes
—	—	—	—	—	—	Yes	Yes	Later	Ecosystems

Table 6-6. Interactions between disciplines that were considered.

Bedrock Geology	Spatial distribution of properties based on lithological (rock) domains. DFN model used for assessing rock mass quality. Structural model helps to estimate the variability of state of stress. The description of fracture zones and fractures is used to assess fracture and fracture zone mechanical properties.	Spatial distribution of thermal properties based on the lithological domains. Mineral composition of rock types used to assign thermal properties (+ measurement from SFR samples in similar rock types). Potentially discussion on thermal gradient due to natural radiation.	Fracture zone and DFN geometry used as is in the hydro-geological model. (Rock domain model indirectly as this motivates the spatial distribution of DFN- properties). Fracture zone properties affects assignment of T but in version 1.1 this is only made qualita-tively. Identification of different fracture sets and fracture zones with potentially different hydraulic properties.	Fracture mineralogy, structural geology.	Indirectly via hydro-model (see below). Rock domain model used to assess spatial distribution of retention properties (De, Kd, porosity.) and to assess homogeneity within rock domains. Fracture zone description used in the same way. Qualitative assessment of fracture minerals.	—		(Direction of glacial movements – consistency check)	—
Stress orientations in relation to fracture sets. Rationale for potential reduction in fracture intensity with depth. Reasonable-ness of rock domainl model in relation to rock stresses.	**Rock Mechanics (in the bedrock)**	Assessment of stress impact on rock samples (porosity effect) for thermal properties (not really in version 1.1).	No explicit inclusion of MH coupling. However, T values in e.g. Eckarfjärden zone and Forsmark zone assumed analogous to Singö zone, partly based on stress and deformation history arguments. Anisotropy for different fracture orientation through differences in intensity (see geological model). (Direct effect on T could be a future hypothesis).	—	Consider stress impact on "intact" rock samples for porosity measurements.	—	—	(Boulder size – consistency check).	—

Affect classification on rock domains (mineral composition of rock types to be "grouped together").	—	**Thermal (in the bedrock)**	Nothing. (It is also assumed that thermal gradient is of little importance for flow compared to e.g. salinity effects).	—	—	—	—	—	—	—
The potential for high T in some zones has increased attention to describe some of the 13 best known zones. High T (or flow) in a borehole is a strong indicator of a zone (along with other zone indicators), but not the only indicator. There are zones without hydraulic significance. Observation of low T at depth has inspired the hypothesis of low fracture intensity at depth.	Existence of high conductive sub-horizontal zones suggests high horizontal stresses. Water pressure reduces the rock stress to effective stress. $\sigma' = \sigma - p$	—	**Hydrogeology (in the bedrock)**	Simulation of past salinity evolution, predicted salinity distribution and possibility to compare predicted and measured.	H-model used to calculate flow distribution, flow paths, F-values, tw and discharge areas.	—	(Discharge – coupling between bedrock and ecosystems)!!	—	—	—
—	—	—	Hypothesis of paleo evolution. Present day salinity distribution "calibration target" for simulation. (Would also need distribution in rock matrix).	**Hydrogeo-chemistry (in the bedrock)**	GW composition (Eh, pH, salinity etc) and assessment of which processes (mixing) could affect it in the future. (Note, an assess-ment is needed, not just interpolation between measured points).	GW composition (for conclusions concerning discharge).	—	—	—	—

(In future versions possibly affect division into rock domains).	—	—	Consistency check as regards porosities used in paleo-simulations.	Indirectly through the paleo-analyses in hydro.	**Transport properties (in the bedrock)**	—	—	—	—
—	—	—	—	Reference water in mixing calculations.	—	**Hydro-chemistry (surface and near surface)**	Chemical comp. for flow paths etc.	(Chemical comp. for RN-transport (K_d)).	Chemical comp. for comparison with biotic data and transport of C, N, P.
—	—	—	Recharge and discharge boundary condition. Meteorological data.	—	—	(Runoff) (Precipitation)	**Hydrology (surface and near surface)**	(Influence soil forming processes – consistency check).	Water balance calculations (Runoff for transport of C, N, P).
Lineaments based on topography of minor relevance since topography and rock over surface poorly correlated at Forsmark. Assessment on where there are outcrops.	Not in version 1.1 (Later assessment – neo-tectonics based on glacial geological model. Glacial isostacy).	—	Basis for derivation of recharge/discharge. Water divides etc. Paleo-evolution including shore-level displacement.	(Paleo evolution)	—	(QD affects chemical composition – consistency check)	Basis for derivation of hydraulic properties. Topography and bathymetry.	**Quaternary deposits and topography**	Topography and bathymetry! (QD for comparison with biotic data).
—	—	—	—	—	—	Biotic processes for interpretation of chemical data.	(Vegetation map for evapo-transpiration).	(Biotic data for comparison with QD).	**Ecosystems**

321

Rock Mechanics and Hydrogeology

There has been no explicit inclusion of MH or HM coupling. However, transmissivity values in e.g. the Eckarfjärden zone and the Forsmark zone are assumed analogous to the Singö zone, partly based on stress and deformation history arguments. In coming versions, anisotropy and depth dependence of transmissivity related to the stress field are worth considering.

Hydrogeology and Hydrogeochemistry

The simulation of past salinity evolution makes is possible to compare the hydrogeological model predictions with the predictions made in hydrogeochemistry and thus enhance understanding of the hydrogeochemical evolutionary processes. Conversely, the hydrogeochemical description of the current salinity distribution provides a "calibration target" for simulation (but the salinity distribution in the rock matrix would also be "needed"). Ultimately, the aim is to make the hydrogeology and hydrogeochemistry descriptions mutually consistent.

Quaternary deposits and Bedrock Geology

The main link between Quaternary Deposits/Topography and Geology is through the lineament interpretation. However, at Forsmark it was found out that lineaments based only on topography are of minor relevance, since topography and the surface of the bedrock are poorly correlated.

6.4.2   Overall assessment

It can generally be observed that numerous interdisciplinary interactions are considered in the site descriptive modelling. In particular, all disciplines share the geometric framework of the bedrock geological model. Furthermore, there is an effort to make the bedrock geology, rock mechanics and hydrogeology consistent in a qualitative sense. However, no attempts were made, mainly due to lack of deep data, to quantitatively explore implications from e.g. rock mechanics, hydrogeological or hydrogeochemical measurements on the geological description. Such evaluations are expected in coming model versions. Finally, the "paleohydrological" simulations demonstrate the aim to make the hydrogeology and hydrogeochemistry descriptions mutually consistent.

In later model versions the auditing may be extended to also ask for the interactions that ought to be considered. Then a more definite assessment regarding interdisciplinary consistency could be made. Furthermore, more quantitative analyses may be warranted, but this does not imply a need to apply coupled THM codes. The direct THM coupling, see e.g. /Andersson, 2004/, need only be considered in case there is significant change of the THM-state. It is probably sufficient to explore whether the final results (i.e. what is observed today) is qualitatively in agreement with known coupled processes.

6.5   Consistency with understanding of past evolution

For confidence it is essential that the naturally ongoing processes considered as important can explain – or at least not contradict – the model descriptions. The distribution of the groundwater compositions should, for example, be reasonable in relation to rock type distribution, fracture minerals, current and past groundwater flow and other past changes. Such 'paleohydrogeologic' arguments may provide important contributions to confidence even if they may not be developed into 'proofs'.

Table 6-7 lists how the current model is judged to be consistent with the overall understanding of the past evolution of the sites as outlined in Chapter 3. The answers generally suggest that the model as presented is in agreement with current understanding of the past evolution. However, the overall hydrogeochemical understanding of the site is restricted to processes taking place at the surface and down to a depth of 200 m. The confidence in this description is high since independent model approaches were utilised in the work. The origin and the post glacial evolution of the water are fairly well understood. The confidence concerning the spatial variation is low due to few observations at depth. The ongoing sampling programme will provide better spatial information and will increase this confidence.

Table 6-7. Consistency with past evolution

Site Descriptive Model (SDM) Technical Audit: Consistency with past evolution	
Assess consistency as regards crystalline bedrock from c 1,900 million years to the Quaternary.	Geological model is consistent with the regional geological evolutionary model and there are no new data in 1.1 which would necessitate an update of this evolutionary model.
	The overall stress model is the same as in version 0 and builds on the tectonic evolutionary model. There are no data for 1.1.
	It would be potentially interesting, i.e. not done in 1.1, to couple the geologic evolution and the formation of the different fracture sets (the order of formation could be determined) with hydrogeochemical indications (e.g. fracture minerals) of age. However, such studies performed at Äspö were rather inconclusive, but could nevertheless provide some insights into the validity of the conceptual model for groundwater flow and hydrogeochemical development.
Assess consistency as regards evolution during the Quaternary period.	In 1.1 there is no information (in support or against) to be used for assessing potential "neo-tectonic" movements. (Such information may potentially be available in later data freezes).
	Groundwater flow and salinity transport simulations cover the period from the melting of the last glaciation, but not alterations before that. Instead, the simulations have explored the impact of various assumptions on initial conditions, properties, events and boundary conditions over the last 10,000 years.
	In general, analysing the impact of potential changes during the Quaternary period on the current day groundwater flow and distribution of groundwater composition will affect and support the conceptual GW model.
Assess consistency as regards surface and ground water evolution.	The interaction is described concerning processes and origin of various water types (e.g. meteoric water, glacial melt water, Litorina water, brine, …
Assess consistency as regards Historical development of the surface ecosystems.	Not assessed in version 1.1.

6.6 Comparison with previous model versions

Another indication of confidence is to what extent measurement results from later stages of the investigation compare well with previous predictions. This will also be important for discussing the potential benefit of additional measurements. Clearly, if new data compare well with a previous prediction, the need for additional data may diminish.

6.6.1 Auditing Protocol

The Protocol developed for comparison with previous model version (i.e. version 0, /SKB, 2002a/) concerns:

- changes compared to previous model version,

- whether there were any "surprises" connected to these changes, and

- whether changes are significant or only concern details.

Table 6-8 lists the answers to these questions.

6.6.2 Assessment

As can be seen from Table 6-8 there are two types of changes in version 1.1 compared to version 0 /SKB, 2002a/. One concerns additional features/content of the model and the other concerns changes in the understanding of the site.

Compared to version 0 there are considerable additional features in the version 1.1, especially in the geological description and in the description of the near surface. This is natural since there is a considerable increase in data compared to the data available for version 0. This "added feature" aspect is also expected to continue for version 1.2, but will possibly "level off" in later model versions.

In terms of actual changes of the understanding of the site there are no really big surprises, even if some findings were more extreme than initially expected. It was expected that the site should be quite tight, but the very low fracture intensity and very tight rock below 400 m in borehole KFM01A

Table 6-8. Comparison with previous model version.

Site Descriptive Model (SDM) Technical Audit: Previous model version	
List changes compared to previous model version (i.e. version 0).	Additional/updated features: • Geological model based on more sub-surface information and much higher resolution surface data. A DFN-model has been developed. • A first thermal model. • Strength information from SFR. Empirical classification (Q) by depth at KFM01A and outcrop assessment. • Hydrogeological simulations including past evolution. New structure model input. New topography, data from depth (KFM01A). • Hydrogeochemical model based on a more detailed process description and better description of the distribution of the meteoric/Sea water. • A first crude transport model exists. • Additional information regarding stratigraphic distribution of glacial till and water-laid sediment Changes in the description: • Certain existence of highly fractured sub-horizontal zones. • Depth decrease of fracture intensity.
Address whether there were any "surprises" connected to these changes.	No really big surprises. However, • Low fracture intensity in KFM01A and very tight rock below 400 m – slight deviation from generic understanding of the Fennoscandian crystalline basement. • Variability in depth of Quaternary deposits and that peat covers less area than expected.
Address whether changes are significant or only concern details.	Updated process understanding of the surface water. This has significantly improved the understanding of the hydrogeochemical processes in the near-surface.

was more extreme than expected. Also the variability in depth of Quaternary deposits and that it was fairly uncorrelated to the bedrock surface variability was not fully expected. These findings suggest that the overall understanding of the Forsmark site may be more an issue than in general in the Fennoscandian crystalline basement.

6.7 Overall assessment

This chapter demonstrate that the overall confidence of the version 1.1 Site Descriptive Model of the Forsmark site is indeed assessed. Clearly, the methodology for confidence assessment will be updated in coming model versions. In summary the confidence assessment concludes that:

• Most available data have been analysed, treated according to good practices and inaccuracy and biases are understood and accounted for in the subsequent modelling.

• There is much uncertainty in the version 1.1 of the site descriptive model, but main uncertainties are identified, some are also quantified and others are left as input to alternative hypotheses. These hypotheses, if not resolved, would provide a starting point for formulating alternative models in version 1.2.

• Numerous interdisciplinary interactions are considered and good cross-discipline understanding of the interactions has been established.

• The model as presented is in general agreement with current understanding of the past evolution.

• Compared to version 0 there are considerable additional features in the version 1.1, especially in the geological description and in the description of the near surface.

• In terms of changes in the understanding of the site there are no really big surprises, even if some findings, like the very tight rock at depth, possibly are more extreme than initially expected.

The overriding issue affecting confidence in models based on version 1.1 data freeze is the bias and uncertainty resulting from varying spatial coverage of data and very few and unidirectional deep borehole data. These biases will evidently be reduced in coming model versions.

7 Resulting description of the Forsmark site

7.1 Surface properties and ecosystem

7.1.1 Climate

The mean annual precipitation in the Forsmark area is 600–650 mm. There is a relative strong gradient in the precipitation from the coast and inland, with a value of 588 mm at the meteorological station at Örskär, an island approximately 20 km northeast of Forsmark, compared with 758 mm at Lövsta, situated approximately 10 km inland. 25–30% of the precipitation falls as snow and the ground is covered by snow about 120–130 days per year. Maximum snow depth is approximately 50 cm.

The mean annual temperature is 5–6°C, with a mean monthly maximum of 15°C in July and a minimum of –4°C in January-February. The vegetation period is about 180 days per year (mean daily temperature > 5°C).

The mean annual potential evapotranspiration is approximately 500 mm.

7.1.2 Hydrology and near surface hydrogeology

Preliminary conceptual model

The Forsmark area is characterised by a low relief with a small-scale topography and relatively shallow Quaternary deposits. This means that many small catchments with shallow groundwater flow systems are formed. From regional data, the specific discharge can be estimated to approximately 200 mm/year (approximately 6.5 L/s/km^2). The infiltration capacity exceeds the rainfall and snow melt intensity with few exceptions and unsaturated overland flow is scarce and only appears over short distances. In recharge areas, the groundwater recharge can, as a first estimate, be set equal to the specific discharge. Groundwater levels are shallow. In recharge areas usually < 3 m below ground and in discharge areas < 1 m. The annual groundwater level fluctuations are assumed to be 2–3 m in recharge areas and < 1 m in discharge areas. Sea level fluctuations may have a major influence on groundwater levels in low-lying parts of the area.

The flat terrain and the shallow groundwater levels mean that the extension of the recharge and discharge areas may vary considerably during the year. Furthermore, the shallow groundwater levels mean that there will be a strong interaction between evapotranspiration, soil moisture and ground-water which will influence the groundwater level and its recession during summer. It is important to keep in mind that the mainly vertical water flow caused by evapotranspiration is twice as much as the lateral runoff.

The Quaternary deposits, totally dominated by till, are less than 20 m thick and outcropping rock is frequent. From a hydrogeological point of view, the till can as a first assumption be divided into three layers with significant difference in hydraulic properties. The upper one metre, strongly influence by soil forming processes, has a relatively high hydraulic conductivity and effective porosity (10^{-5}–10^{-4} m/s and 10–20%, respectively). Below approximately one metre depth, the hydraulic conductivity as well as the effective porosity are substantially lower. Depending on the grain size distribution the hydraulic conductivity typically can be assumed to vary between 10^{-8} and 10^{-6} m/s. The lower values are associated with the clayey till that appears frequently in the southern part of the area. Typical effective porosities are 2–5%. The performed slug-test gave relatively high hydraulic conductivities for the contact zone between the till and the bedrock. The geometric mean was $1.18 \cdot 10^{-5}$ m/s (standard deviation log K 1.00, 95% confidence interval for a new observation $1.32 \cdot 10^{-7}$–$1.05 \cdot 10^{-3}$ m/s). The cause of these relatively high hydraulic conductivities is not clear. Several indications are, however, available of heavily fractured rock at shallow depths in the area.

The described permeability and storage characteristics of the till profile means that very little water has to be added to get a considerable rise in the groundwater level. In periods of abundant recharge, the groundwater level will reach the uppermost, more permeable part of the profile in most recharge

areas. Relatively fast lateral groundwater flow will appear and contribute to surface water discharge. In unsaturated discharge areas, the response to input from precipitation or snow melt will be even more rapid since the groundwater level is shallow and the soil water deficit small.

The lakes are assumed to be important discharge areas. The actual discharge heavily depends on the permeability of the bottom sediments of the lakes. Also the creeks are considered to be important discharge areas, however, unsaturated during parts of the year. The wetlands can either be in direct contact with the groundwater zone and constitute typical discharge areas or be separate systems with little or no contact with the groundwater zone.

Based on the description above it is obvious that only a small fraction of the total groundwater recharge will eventually reach below the uppermost permeable part of the bedrock, probably < 10%.

A distributed model is necessary for the forthcoming quantitative modelling of the surface hydrology and the near-surface hydrogeology to answer the questions raised in the environmental impact assessment and the safety analysis. Major questions to be addressed are:

- Area necessary to cover by detailed surface – near surface modelling.

- Details of process description.

- Spatial and temporal resolution.

- Quantification of groundwater recharge at levels below the contact zone of the Quaternary deposits and the bedrock

- Handling of groundwater discharge from the bedrock aquifer

Sensitivity analyses and/or stochastic methods will have to be applied. Discharge measurements, analyses of chemical and isotopic composition of water as well as measurements of vertical groundwater potentials will be important for the study of surface water – groundwater interactions.

Catchment areas

25 "lake-centred" catchment areas have been delineated, varying in size from 0.03 km^2 to 8.67 km^2 (see Figure 4-33 and Table 4-10). Forest is dominant and covers between 50 and 96% of the areas of the catchments. Wetlands, both forest-covered and open, are frequent and cover more than 20% of the area in five of the catchments. Only in one catchment area does agricultural land constitute an important part of the total area (Bredviken with 27% agricultural land).

Lakes

According to /Brunberg and Blomqvist, 2000/, three main types of lake ecosystems can be identified in the coastal areas of northern Uppland:

1) *Oligotrophic hardwater lakes* are to a large extent surrounded by mires. Inflow as well as outflow of water is often diffuse, via the surrounding mire. The lakes are small and shallow, with nutrient-poor and highly alkaline water. Three habitats have been identified within the lakes; i) the pelagic zone, characterised by low production of biota, ii) the presumably moderately productive emergent macrophyte zone, dominated by *Sphagnum* and *Phragmites*, and iii) the light-exposed soft-bottom zone with *Chara* meadows and an unusually rich and presumably highly productive microbial sediment community. In later stages of the lake ontogeny, *Sphagnum* becomes more and more dominant in the system, which successively turns acidic. The final stage is likely to be a raised bog ecosystem with autonomous hydrological functioning.

2) *Brownwater lakes* are typically found within the main part of the river Forsmarksån and are characterised by a high water flow from the upper parts of the drainage area, which is dominated by mires. Their lake water is highly stained by allochthonous organic carbon imported from the catchment area. Also in this lake type a *Sphagnum*-littoral successively develops, and in a mature lake three habitats can be identified; i) the pelagic zone, most likely the dominant habitat in terms of production of organisms and in which bacterioplankton dominates the mobilisation of energy while phytoplankton are restricted by low light availability, ii) the emergent macrophyte zone, and iii) the profundal zone. Due to the characteristically short water renewal time, sedimentation processes are

of relatively small importance and most of the carbon imported and produced is lost through the outlet. Production at higher trophic levels (e.g. benthic fauna and fish) within the brownwater lake type is very limited.

3) *Deep eutrophic lakes* are characterised by a limited drainage area, a large lake volume and a slow turnover time of the water. All five habitats that optimally can be found in lakes are represented in this lake type: i) the pelagial, ii) the emergent macrophyte-dominated littoral zone, iii) the wind-exposed littoral zone, iv) the light-exposed soft-bottom zone and, v) the profundal zone. Traditionally, the pelagial has been regarded as the dominant habitat in terms of mobilisation of carbon energy in the system. However, the productivity in the littoral habitats together may be just as important as the pelagial. As a result of the long turnover time of the water, most of the production of carbon is retained within the lake basin and sedimentation to the profundal zone is the main retention process.

The Forsmark regional model area contains more than 20 more or less permanent pools of water which could be characterized as lakes. However, only three of these lakes, Lake Fiskarfjärden, Lake Bolundsfjärden and Lake Eckarfjärden, are larger than 0.2 km², and most of them are considerably smaller. The by far most abundant lake type in the regional model area is the oligotrophic hardwater lake, to which all the larger lakes belong.

The investigated oligotrophic hardwater lakes in the Forsmark area have an average depth of 1 m, whereas the average depth for all lakes in Uppsala County is 2 m. The lakes in the Forsmark area also have small *areas*, compared to other lakes in the county /Brunberg and Blomqvist, 1999/. Due to their small size and shallowness, the lakes also have small water volumes and consequently short renewal times of the water. In some of the lakes, which as yet have not been sufficiently separated from the shoreline, the hydrological conditions also include intrusions of water from the Baltic Sea during low pressure weather conditions which create a high sea level /Brunberg and Blomqvist, 1999/. Some of the lakes in the area have been subject to drainage projects and lowering of the water level. However, both the frequency and the extent of these projects are less than for the other lakes in the county /Brunberg and Blomqvist, 1999/.

Water chemistry in lakes and streams

The specific type of hardwater lakes, which is common in the Forsmark regional model area, are called *Chara* lakes (see further "The littoral zone" in Section 7.1.5). The *Chara* lakes are chemically characterised as hardwater lakes, distinguished from softwater lakes by their high conductivity and by their richness in calcium and magnesium which are dissolved in the water. Hardwater lakes occur all over the world, in areas of alkaline sedimentary rocks or, as in this case, in areas with high content of limestone blocks in the Quaternary till. These rocks/blocks are easily weathered and yield alkaline water rich in calcium and many other elements, e.g. micro-nutrients for the biota. However, due to both chemically and biologically induced interactions in the lake water, the amounts of nutrients (e.g. phosphorus) transported to the lakes may be effectively reduced by precipitation of calcium-rich particulate matter. Nitrogen, on the other hand, tends to be present in relatively high concentrations in the water, due to the combination of high input but low biotic utilisation /Brunberg and Blomqvist, 1999, 2000/. The ionic composition of *Chara* lakes in Uppland, which is used to distinguish two main types ("biocarbonate group", "sulphate group"), is shown in Table 7-1.

Table 7-1. The ionic composition of Chara lakes in Uppland (equiv. %, average values, after /Brunberg and Blomqvist, 1999/).

Lake type	Ca	Mg	Na	K	HCO$_3$	SO$_4$	Cl
Chara lakes of "bicarbonate group"	79.1	10.9	8.3	1.7	71.9	22.7	5.4
Chara lakes of "sulphate group"	73.3	16.0	8.8	1.9	37.2	55.4	7.4
Standard composition*	63.5	17.4	15.7	3.4	73.9	16.0	10.1

* Standard composition of freshwater lakes (according to /Rodhe, 1949/).

7.1.3 Oceanography

The shoreline between Gävle bay and Svartklubben (SMHI station at Singö, approximately 30 km southeast of the Forsmark regional model area) consists, in a relatively large part, of archipelago mixed with open, exposed areas. Water composition and water movements in the area are affected by the freshwater discharge from rivers which flow into the Gävle bay, but also by the wind. The freshwater discharge from Gävle bay moves south along the coast and passes the Öregrundsgrepen, causing a lower salinity in this area compared with the more exposed Grundkallen east of Gräsö. There appears to be no salinity stratification in the area /Larsson-McCann et al, 2002/.

Physical properties

The maximum depth of Öregrundsgrepen is about 60 m, and due to the relatively open water areas, the water exchange is considered good. In a model study, /Engqvist and Andrejev, 1999/ found that the water retention time of Öregrundsgrepen varies between 12.1 days (surface) and 25.8 days (bottom), as an annual average.

During temperature stratification, rapid movements of the thermocline have been observed, indicating substantial exchange of water. During northerly winds, a counter-clockwise circulation is set up. Surface water is then brought into the area, pressing down the thermocline and resulting in deep water leaving the area along the bottom. During southerly winds, the circulation is clockwise and surface water is brought out of the area allowing inflow of deep water along the bottom under the thermocline. Stagnation in the bottom water can occur in the deepest parts of Öregrundsgrepen, west of Gräsö /Larsson-McCann et al, 2002/. The water level show considerable temporal variation, especially during the autumn and winter when monthly mean water level can differ as much as ± 1 m between extreme years (Figure 7-1).

During spring, the increased solar radiation heats the surface water in the Bothnian Sea and usually temperature stratification has developed by the end of June /Larsson-McCann et al, 2002/. The depth of this surface layer is between 20–25 m. In the fall, the surface layer is cooled and the temperature stratification breaks down. By October, the temperature is homogenous throughout the water column. During the winter months, the cooling of the uppermost surface layer can bring the temperature below 0° C, resulting in the formation of sea ice. The variations in water temperature are small from year to year during winter and spring, whereas variations are larger in summer and autumn /Larsson-McCann et al, 2002/.
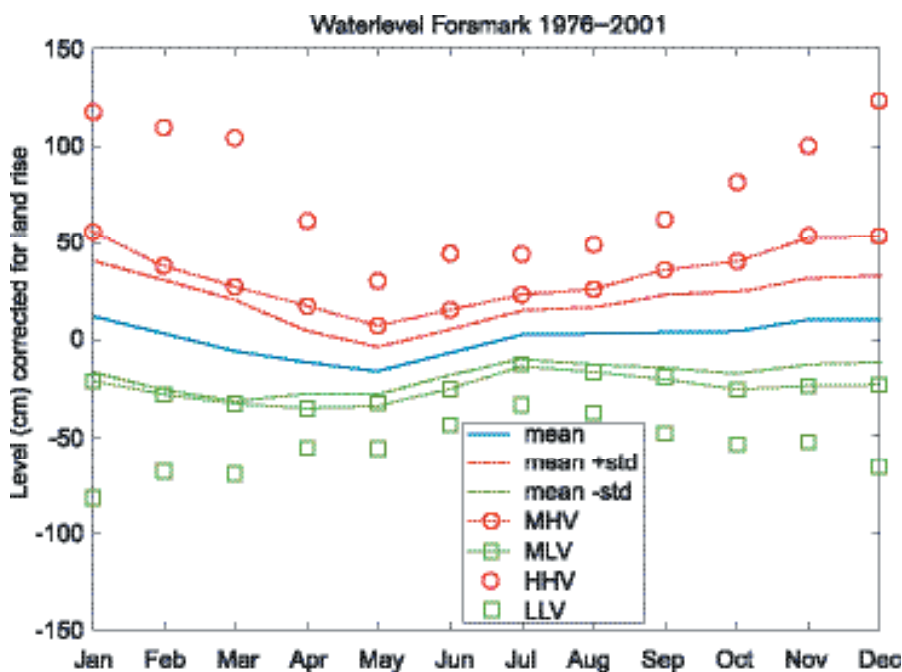
Figure 7-1. *Monthly sea water level (mean ±1 SD) at Forsmark 1976–2001. MHV/MLV signifies mean high/low water level, i.e. mean of all years 1976–2001. HHV/LLV signifies highest/lowest water level ever during 1976–2001. Based on hourly measurements. From /Larsson-McCann et al, 2002/.*

Water chemistry

Due to the rapid water turnover of Öregrundsgrepen, the oxygen saturation is high, on average 95% /Larsson-McCann et al, 2002/. The concentration of nutrients in the water varies throughout the year, with the highest concentration at the time for break-up of the ice. Generally, the open water area is poor in nutrients during summer. The content of total nitrogen in Öregrundsgrepen varies between c 200 and 300 µg/L and total phosphorus between c 10 and 15 µg/L.

The salinity in Öregrundsgrepen in 1977–78 was between 4.5–5.8‰ in surface water and 5.6–6.4‰ at a depth of 40 m /Persson et al, 1993/. A monthly mean from twenty years of salinity measurements in Åland Sea (1971–1991) shows a variation of only 0.5‰. The salinity in Åland Sea is somewhat higher and more stable than that of Öregrundsgrepen. During the winter period, when Öregrundsgrepen can be ice-covered, the salinity can decline to less than 1‰ in the upper decimetre of the water column because freshwater from the ice accumulates /Persson et al, 1993/.

The surface salinity of Öregrundsgrepen was modelled by /Engqvist and Andrejev, 1999/ and the results are partly shown in Figure 7-2. The salinity depletion at the mouth of Kallrigafjärden, where two streams discharge, is clearly visible. Except for this, the salinity surface distribution is homogeneous.
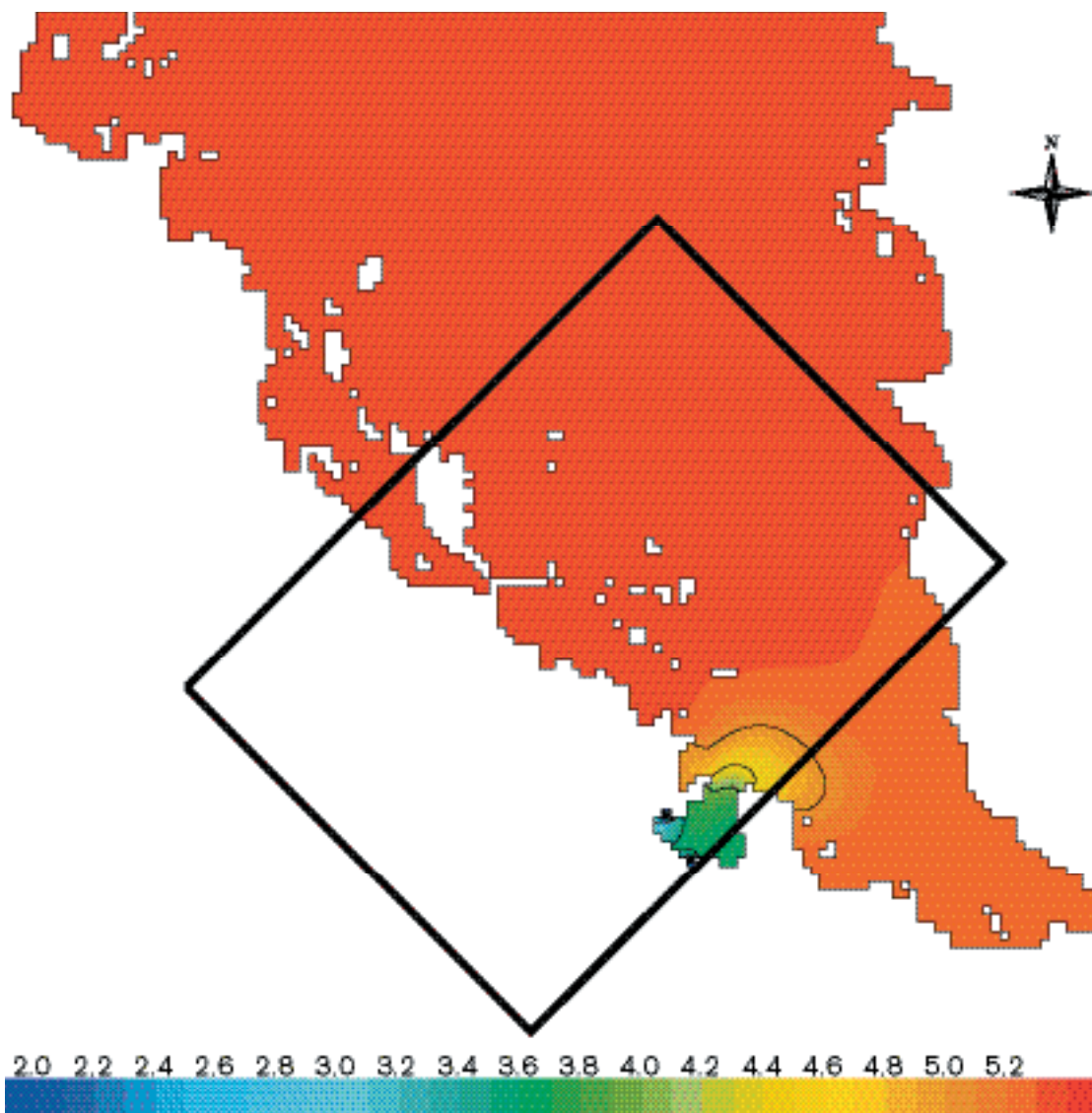
Figure 7-2. *Modelled surface salinity (‰) distribution of Öregrundsgrepen 1992-12-31 /Engqvist and Andrejev, 1999/. The Forsmark regional model area is shown by a black line.*

7.1.4 Quaternary deposits and other regoliths

Surface distribution

Unconsolidated Quaternary deposits cover c 82% of the land area in the regional model area and artificial fill, principally around the Forsmark nuclear power station and an area close to Johannisfors, c 3%. Exposed bedrock or bedrock with only a thin (< 0.5 m) Quaternary cover occupies c 15% of the land area. The frequency of outcrops varies within the mapped area. Areas with low frequency of outcrops are e.g. the eastern part at Storskäret and west of Lake Bolundsfjärden. Areas with high frequency of bedrock outcrops are e.g. the south-western part of the mapped area and the coast north of Lake Bolundsfjärden. Many of the outcrops are Roches mountonnées with a smooth abraded northern side and a rough, steep plucked side towards the south. Ice moving from $350 \pm 10°$ formed a majority of the striae. An older system from north-west is preserved on lee side positions.

Glacial till is the dominating Quaternary deposit, often leaving a flat upper surface. Based on the composition of the surface layer, three areas with different till types were distinguished:

1. The western and northern parts of the mapped area, east and northwest of Lake Eckarfjärden and north of Lake Bolundsfjärden are dominated by sandy till. Gravely till was also identified, mainly close to drillsite 1. Medium bolder frequency dominates.

2. At Storskäret and east of Lake Fiskarfjärden, a clayey till dominates. The boulder frequency is low and the area is used for cultivation.

3. In the easternmost part of the mapped area there is a high frequency of large boulders close to the Börstilåsen esker in the south-eastern part of the investigated area.

Glaciofluvial sediments are deposited in a small esker, the Börstilåsen esker, with a flat crest reaching c 5 m above the present sea level. Wave washing has affected the esker, where a raised shingle shoreline is developed. The Börstilåsen esker has a N-S direction and is the largest glaciofluvial deposit in the Östhammar region and can be followed from Harg situated c 30 km south of the area mapped /Persson, 1985/. The esker is, however, small compared to several of the large eskers found further west around Lake Mälaren.

The till and glacial clay are rich in $CaCO_3$, which originates from Palaeozoic limestone, present at the sea bottom north of the area. A positive correlation appears to exist between the calcite content and areas with clayey till at the surface. At several sites, calcite occurs from the ground surface and downwards. Since the major part of the area has been above sea level for a short period, too little time has passed for weathering processes to dissolve the calcite from the uppermost soil. However, the most elevated areas have been above sea level approximately 1,500 years, which should be sufficient to deplete calcite. A study of soils and soil forming processes will be included in the next model version.

Post-glacial sediment and peat form the youngest group of Quaternary deposits. In general, they overlie till and, locally, glacial clay or crystalline bedrock. Clay gyttja or gyttja clay are the dominating organic deposits in the surface of the wetlands while peat accumulations > 50 cm are rare. Existing peat accumulations are concentrated in the more elevated areas, e.g. south east of Lake Eckarfjärden. The organic sediment is often thinner than 1 m, underlain by sand or gravel and till or glacial clay.

A typical feature of the area is a large number of small (< 50 m) wetlands often submerged by shallow water during the spring and early summer. A typical stratigraphy in these wetlands contains a thin layer of organic cover, sand or gravel and glacial clay on top of bedrock or glacial till. The cover of glacial clay has, most probably, a negative effect on the capacity for water infiltration.

Stratigraphy

The recorded thickness of the Quaternary deposits varies between 0 and 17 m within the investigated area (Figure 7-3). In the north-western part of the investigated area, the depth to bedrock is generally between 4 and 8 m. Close to drillsite 1, the thickness of the Quaternary deposits varies between c 12 m and 4 m in eight corings, located within c 200 m from the drillsite. The altitude of the upper surface of the regolith is flat and varies between c 4 and 2 masl. This indicates an undulating upper surface of the bedrock and a till cover that fills out the depressions.
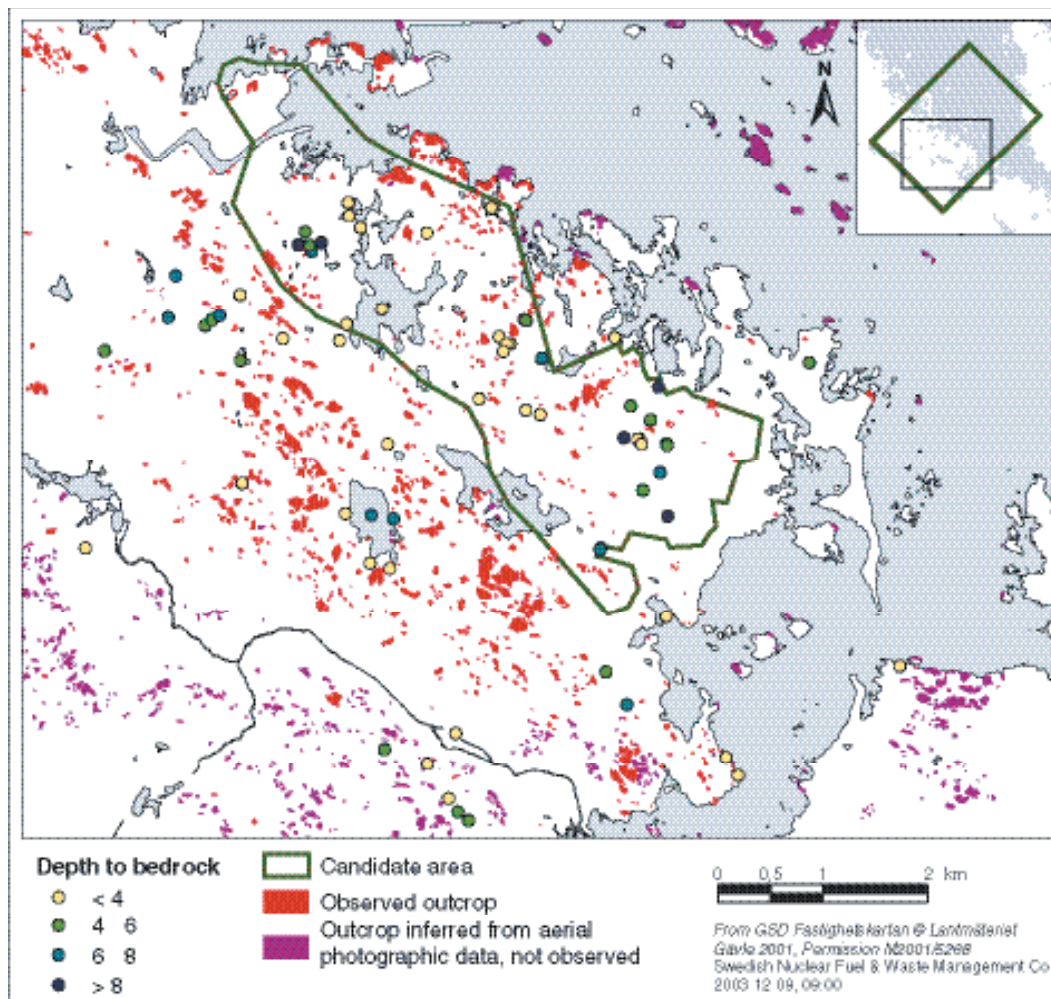
Figure 7-3. *Map showing the distribution of bedrock outcrops together with depth to bedrock. The depth to bedrock is based on percussion corings, auger drillings together with data from SGU archive of wells. In the area with clayey till at the surface the Quaternary deposits are generally thick. However, deep till cover was also identified close to drillsite 1, i.e. in a region with sandy till at the surface.*

In the central part of the candidate area, close to Lake Bolundsfjärden, the thickness of the glacial till is < 4 m, e.g. at SFM0030, c 3.5 m sandy silty till covers the bedrock (Figure 7-4). In the eastern part of the investigated area, at Storskäret, the thickness ranges from < 4 to c 11 m. At PFM002463, c 11 m glacial till covers the bedrock. A consistent feature in the area close to Storskäret is low frequency of bedrock outcrops and relatively thick till cover. At the surface, the till is clayey and a coarser till is situated closer to bedrock (Figure 7-5). At this time, no general till stratigraphy can be defined.

In contrast to the heterogenic composition of the glacial till, the distribution of marine and lacustrine sediments in the Forsmark region is fairly consistent. The total thickness of the sediments in lakes (not including glacial till) is shown in Figure 7-6. In a majority of the corings, the sediments were less than 2 m thick and only three lakes contained sediments thicker than 4 m. The maximum coring depth in the area was 8.8 m (including 0.5 m water), recorded at Lake Fiskarfjärden. A generalised outline of stratigraphical units in the investigated sediments at Forsmark is presented in Table 7-2.
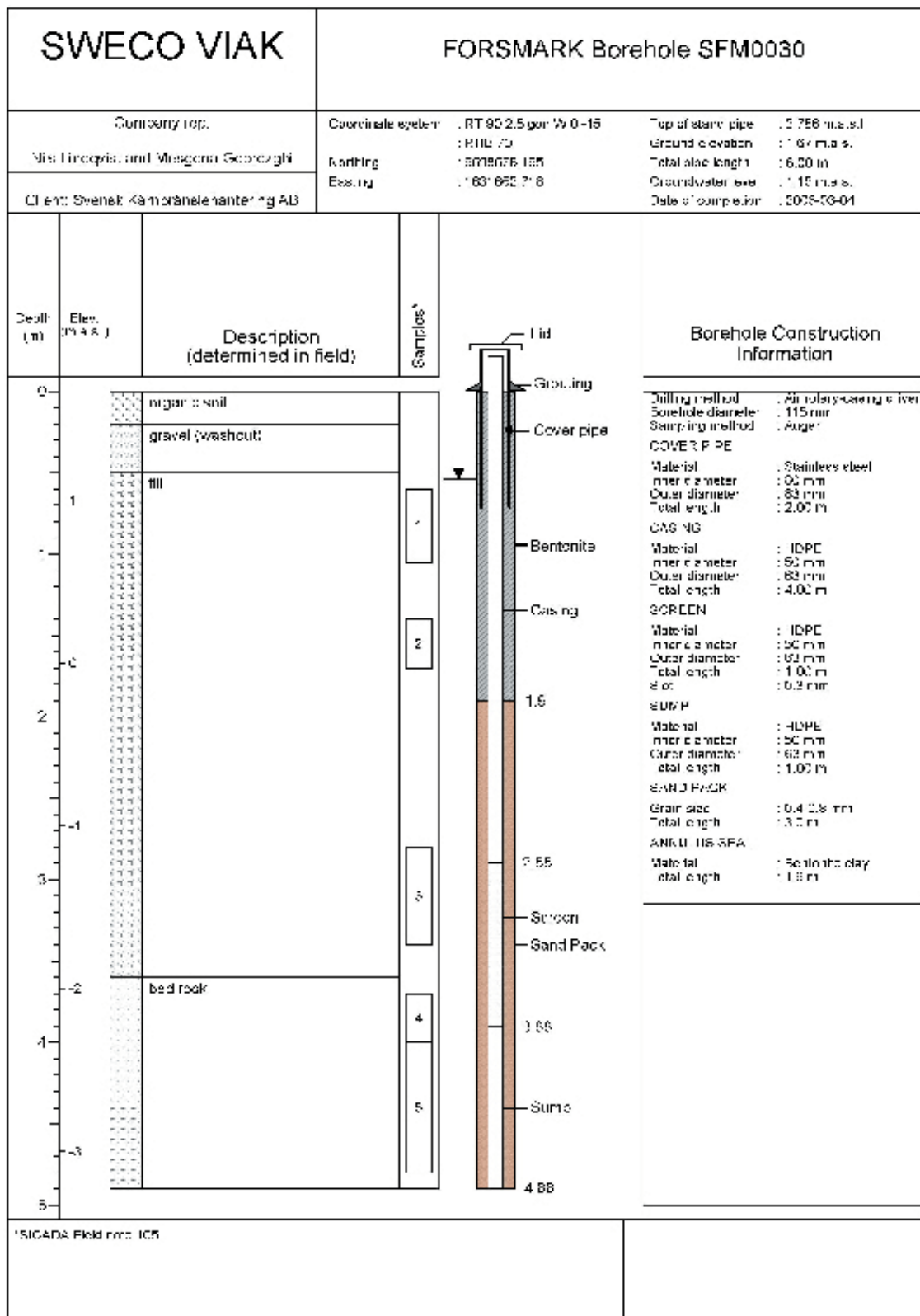
Figure 7-4. *The stratigraphic section at SFM0030, south west of Lake Bolundsfjärden. The bedrock is covered by c 3 m sandy silty till with wave washed sand and gravel at the top.*

Figure 7-5. *The stratigraphical section at PFM002463, situated c 300 m west of drillsite 3. The total depth of the glacial till is 11.2 m. The bedrock is covered by c 4.5 m silty till and c 6 m clayey till at the top.*
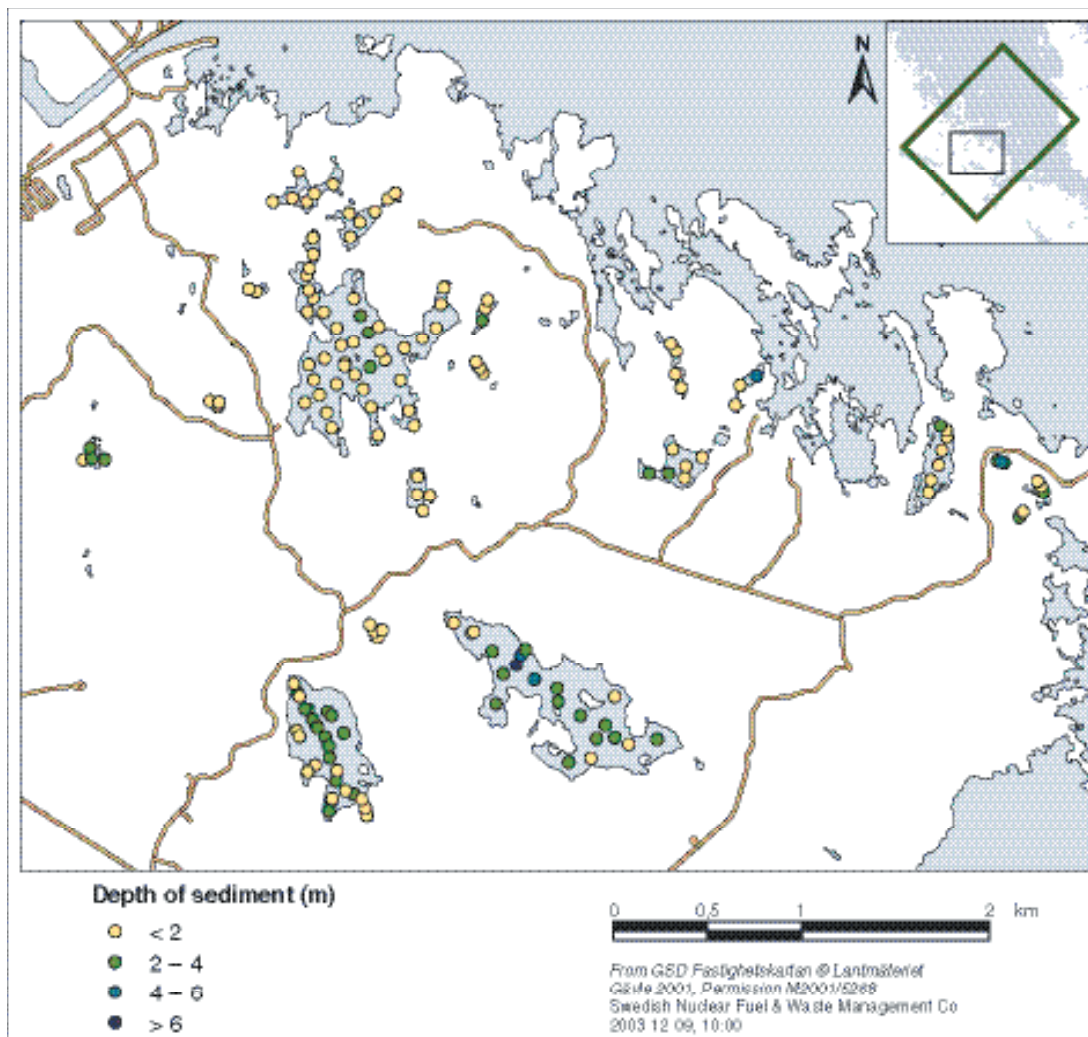
Figure 7-6. *Map showing the location of the coring sites where marine and lacustrine sediment have been investigated from /Bergström, 2001/ and the site investigations. The depth values are the sediment thickness and do not include the water column in the lake or the glacial till.*

Table 7-2. General outline of stratigraphical units from the lakes in Forsmark. The interpretation of the environment at deposition is mainly based on data from Lake Eckarfjärden /Hedenström and Risberg, 2003/.

Environment	Lithology
Freshwater lake	Unclassified detritus
Freshwater lake	Calcareous gyttja
Freshwater lake and coastal lagoons	Algal gyttja
Post glacial Baltic basin	Gyttja clay/clay gyttja
Shallow coast	Sand, gravel
Post glacial Baltic basin	Postglacial clay
Late glacial Baltic basin	Glacial clay

The sedimentary sequence in Lake Eckarfjärden follows a consistent pattern (Figure 7-7). Glacial clay covers the bottom of the basin. The unit was deposited shortly after the deglaciation from c 11,000 years ago onwards. Post-glacial clay only contributes as minor patches. The next stratigraphical unit consists of sand and gravel and forms a permeable layer throughout almost the entire lake basin. The sediment is redeposited, wave washed sand and gravel, formed when the land areas close to the lake started to emerge from the Baltic c 1,500 years ago (Section 3.2) /Hedenström and Risberg, 2003/. Thus, the boundary between the clay and the sand marks a hiatus representing

the major part of the Holocene cf /Brydsten, 1999b/. The ongoing isostatic uplift results in new land areas which transfers the lake basin to a sheltered position favouring deposition of gyttja clay and clay gyttja. The isolation of Lake Eckarfjärden has been dated to c 850 cal years BP, recorded approximately at the transition to the gyttja layer /Hedenström and Risberg, 2003/. After the isolation, algal gyttja and calcareous gyttja has been deposited. Lake Eckarfjärden is a typical oligotrophic hardwater lake, described in several reports /e.g. Blomqvist et al, 2002 and refs therein/.

The sedimentary sequence in Lake Bolundsfjärden is generally less than two m thick (Figure 7-8). The sequence starts with a thin layer of sand covered by gyttja clay and gyttja. The sequence of clay covering the bottom of Lake Eckarfjärden is not present in the stratigraphy of Lake Bolundsfjärden. Probably, erosion has been more effective in this basin with almost no protection from wave activity from the north. Lake Bolundsfjärden is still occasionally in contact with the Baltic.
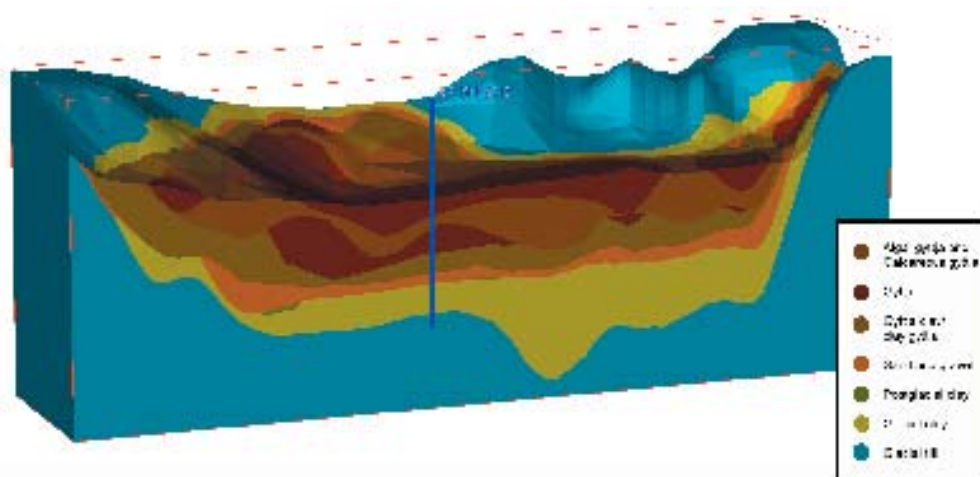
Figure 7-7. *3D distribution of the sediment in Lake Eckarfjärden. From the bottom up, the sediment layers are glacial and postglacial clay, wave-washed sand and gravel, gyttja clay/clay gyttja, algal gyttja, calcareous gyttja and unconsolidated gyttja, i.e. detritus. The blue line shows the location of a groundwater monitoring well, SFM0015. The model is cut along a NNW-SSE profile. A consistent feature is that glacial clay covers the glacial till. Note that the simplified model only schematically indicates the position of the glacial till. The thickness of the till, and thus the depth to bedrock, is not included in this model version.*
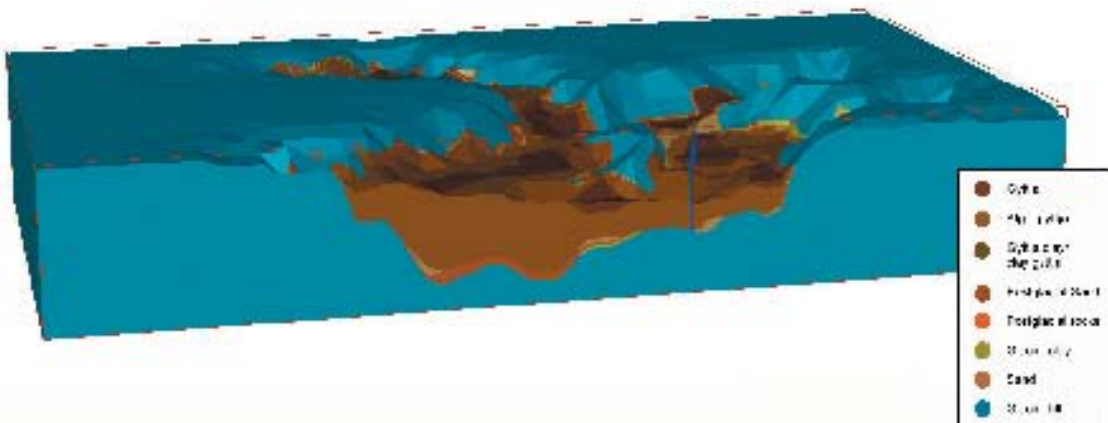
Figure 7-8. *3D distribution of the sediment in Lake Bolundsfjärden. The sediment layers are generally thin; only three corings in the central part of the basin had sediment thicker than 2 m. The blue line shows the location of a groundwater monitoring well, SFM0028. The model is cut along a N-S profile, looking into the sediment from the west. Note that the simplified model only schematically indicates the position of the glacial till. The thickness of the till, and thus the depth to bedrock, is not included in this model version.*

Offshore Quaternary deposits

Offshore Quaternary deposits are dominated by till which rests on the bedrock. Locally, till is covered by clay. Glacial clay is overlain by a thin layer of sand and gravel, i.e. similar to the on shore distribution. The clay in this area occurs most conspicuously in a narrow belt which trends in a NNW direction. /Carlsson et al, 1985/ have speculated that the occurrence of clay may be linked, in some cases, to fracture zones in the bedrock. The thickness of the offshore Quaternary deposits varies considerably from < 2.5 m to > 10 m /Carlsson et al, 1985/. In the area above SFR, till varies in thickness between 4 and 14 m and clay between 0 and 4 m. No new offshore data are available.

Late- or post-glacial faulting

Candidates for young fault movements turned out to be glacially eroded, i.e. not post-glacial in age. Sections in gravel- and sand-pits including silty deposits regarded as susceptible to seismically induced liquefaction were investigated, but no major distortions were noted. Contorted and folded sequences of glacial clay were encountered at several locations, but these were interpreted as a result of sliding. A survey of glacially polished bedrock outcrops in the archipelago was performed but no indications of post-glacial fault movements were found. One c 80 m long trench on the eastern flank of the Börstilåsen esker was excavated. No signs of earthquake vibrations were found. Deformation of the primary sedimentary structures caused by drop-stones and sliding occurred frequently. No distinct indications of late or post-glacial faulting have appeared so far, but the investigations are still in their very initial stage. Furthermore, the most crucial test, the search for seismically generated distortions in strategically located trenches remains to be done.

7.1.5   Biotic entities and their properties

The description of the biotic components of the ecosystem is divided into the entities primary producers and consumers /cf Löfgren and Lindborg, 2003/. The entity consumers includes, beside herbivores and predators, also detrivores, such as invertebrates, fungi and bacteria.

Producers

Terrestrial producers

The vegetation map /Boresjö Bronge and Wester, 2002/ for the Forsmark area is shown in Figure 7-9. The most common *forest type* is the 70-year old pine forest, typical of broken terrain in eastern Svealand. The distribution of forest trees in the region is pine (*Pinus sylvestris*) 40–60%, spruce (*Picea abies*) 20–40%, birch (*Betula pendula*) 10–20%, oak (*Quercus robur*) < 1% and other broad-leaved trees 5–10%. Closer to the coast and the Forsmark region, the amount of pine *(Pinus sylvestris)* increases at the expense of spruce *(Picea abies)*.

The most common undergrowth is the nutrient-rich herb type, which is often found in calcareous areas. Some 25–50% of the undergrowth in the Forsmark region is of this rich herb type, but it decreases further inland to c 15–25% /Jerling et al, 2001/. In general, the coniferous forests in the area often have a major element of deciduous trees and shrubs as undergrowth. In wetter parts, the deciduous trees are dominant together with increasing amounts of herbs and grasses. Pine forest is found on the thin soils of rocky outcrops of bedrock. The shores are often bordered by alder (*Alnus glutinosa*) and sometimes ash (*Fraxinus excelsior*) /Jerling et al, 2001/.

See also Section 5.7.2 for a description of biomass and production of terrestrial producers in the Forsmark regional model area.

Limnic aquatic producers

Since oligotrophic hardwater lakes in general, and those of the county of Uppsala, in particular, are small, shallow, and have relatively clear water, a typical oligotrophic hardwater lake can be characterised as having three distinguishable habitats, the open water (pelagic zone), the emergent macrophyte zone, and the light-exposed soft-bottom zone (littoral zone). The other habitats, the profundal zone and the wind-exposed littoral zone, are missing.
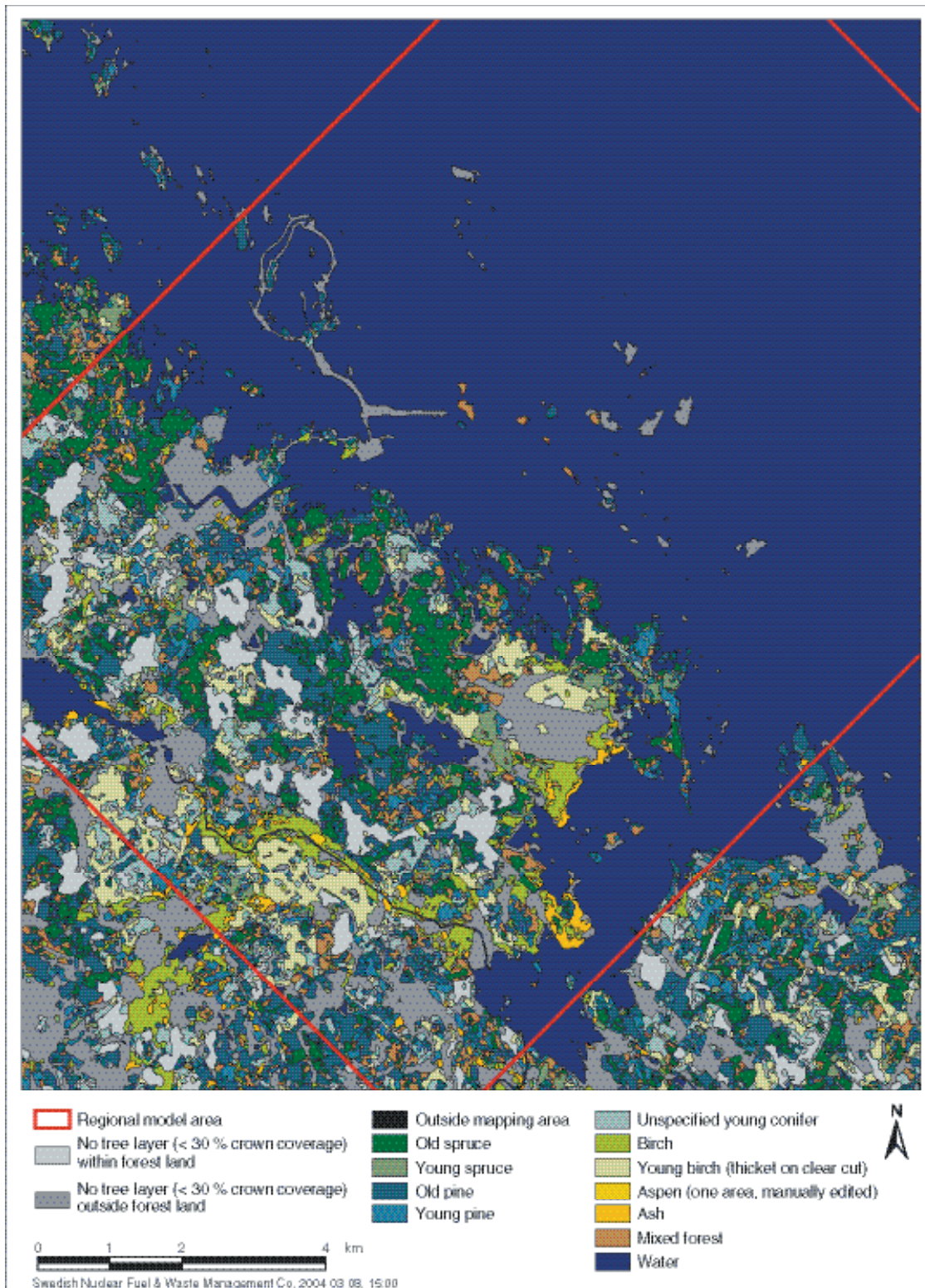
Figure 7-9. *Vegetation map, after /Boresjö Bronge and Wester, 2002/. The Forsmark regional model area is shown by a red line.*

The pelagic zone

There are very few studies of the phytoplankton communities in lakes of the Forsmark area and those that have been performed mainly concern phytoplankton community biomass and composition. /Kleiven, 1991/ studied environmental conditions and phytoplankton in some *Chara* lakes in the county of Uppland and included three lakes in the Forsmark area in that study: Lake Hällefjärd, Lake Käringsjön, and Lake Strönningsvik. The lakes were sampled just once, in September 1984 (two lakes) and in September 1985 (Lake Strönningsvik). Phytoplankton total biomass was low, 113, 815, and 451 µg wet weight/L, respectively, indicating oligotrophic conditions in the systems /Rosén, 1981; Brettum, 1989/. In all three lakes, chrysophytes dominated the community and accounted for approximately 50% (42–62) of the biomass. Green algae was the second most important group in two lakes, and cryptophytes in the third lake. Dinoflagellates and diatoms made up most of the remaining biomass, while cyanobacteria were less important despite the time of the year /Brunberg and Blomqvist, 2000/.

The littoral zone

The macroflora of the littoral zone (i.e. mostly the floating outer edge of the mire) of the lakes in the Forsmark area is characterised by two species: *Sphagnum* in the bottom layer and *Phragmites* in the field layer. Quantitative data on the biomass and production of these organisms in the Forsmark area are lacking /Brunberg and Blomqvist, 2000/.

The stoneworts, *Charales*, is the best studied of all groups of organisms in the oligotrophic hardwater lakes (for references see /Brunberg and Blomqvist, 2000/). These submersed macroalgae strongly dominate parts of the light-exposed soft-bottom sediments, and the characteristic *Chara* meadows have given rise to the name "*Chara* lakes". There are few, if any, quantitative studies of the benthic fauna of the illuminated soft-bottom sediments of the lakes in the Forsmark area /Brunberg and Blomqvist, 2000/. Neither have there been any studies of the biomass, nor of the production of heterotrophic bacteria or fungi, in the light-exposed soft-bottom zone.

The riparian zone

The outermost parts of floating mats constituting the littoral zone of the lakes are mires. These surrounding mire systems have been subject to a large number of inventories, especially concerning their vegetation /Brunberg and Blomqvist, 1998/, but studies of functional aspects are lacking. The mires often have a mixed character with components of pine bog, poor fen, rich fen, extremely rich fen and, at the edge of the lake, *Phragmites*-populated floating *Sphagnum*-mats. The bottom layer of the pine bog is dominated by *Sphagnum*, and in the field layer *Ledum palustre*, *Rubus chamemorus*, and *Eriophorum vaginatum* are important compartments. The poor fen also has *Sphagnum* as a dominant constituent of the bottom layer, and a field layer with *Rhyncospora alba*, *Scheuchzeria palustris*, *Carex rostrata*, and *C lasiocarpa*. Rich fens, interspersed with components of extremely rich fens, often dominate the mires. The bottom layer in these fens is dominated by a variety of brown-coloured mosses. Important constituents of the field layer are *Parnassia palustris*, *Primula farinosa*, *Dactylorhiza incarnata*, *Epipactis palustris*, *Liparis loeserii*, and *Dactylorhiza traunsteineri* /Brunberg and Blomqvist, 2000/.

Marine aquatic producers

The major biological components of the brackish water coastal ecosystem, and the energy flows between these components, are described below.

The pelagic community includes the water mass with phytoplankton, bacterioplankton, zooplankton and fish. During the spring, the phytoplankton community in Öregrundsgrepen is dominated by diatoms (*Bacillariaophyceae*) and dinoflagellates (*Dinophyceae*) whereas the biomass in summer and autumn mainly is composed of bluegreen algae (*Cyanophyceae*) and small flagellates /Lindahl and Wallström, 1980/.

On *shallow soft bottoms* the *vegetation* is dominated by vascular plants. In the bay Forsmarksfjärden, west of the Biotest basin, vascular plants like *Myriophyllum spicatum* and different species of *Potamogeton spp* were common in a survey in 1974. *Chara tomentosa* and/or *Potamogeton pectinatus* can dominate down to a depth of two metres and are often found in the shallow bays called flads and gloes, which have limited water exchange with the sea. On these bottoms, *Chara baltica* and

Najas marina often form small stands. In places where the sediments are more stable, *Chara marina* is usually found, and in sandier sediment the diversity can be great and include many vascular plants like *Potamogeton pectinatus, P perfoliatus, Ranunculus baudotti, Zanichellia palustris, Myriophyllum spicatum* and *Callitriche spp.* Some of the Charophytes found in these areas are Red Listed (i.e. are on the list of species in Sweden which are under threat of extinction) /Kautsky, 2001/.

At 2–4 m depth, the soft bottoms are often covered by *Vaucheria spp.* On these bottoms, sparse stands of *Potamogeton perfoliatus, Myriophyllum spicatum* and *Ranunculus baudotti* can also be found /Kautsky, 2001/.

The occurrence of macrophytes was verified by a diving survey /Kautsky et al, 1999/. On the hard, more stable substrata (boulders, rock), a luxuriant growth of the bladder wrack (*Fucus vesiculosus*) could be seen. Also, the moss *Fontinalis dalecarlica* was common. The filamentous green algae (*Cladophora* spp) and some filamentous brown algae (*Ectocarpus/Pilayella* and *Sphacelaria arctica*) dominate the first two metres. Between 2 to 4 m, the bladder wrack (*Fucus vesiculosus*) dominates the biomass (in total 214 gDW/m^2). Vascular plants (*Potamogeton* spp and *Zostera* sp), as well as perennial red algae (*Furcellaria lumbricalis*), contribute to the total biomass. Perennial red algae dominate the vegetation down to 10 m depth, where the macroscopic vegetation ends.

Compared to what was found in nearby studies, the Forsmark area had somewhat lower maximum biomass in the zone between 2–4 m depth (580 and 214 g DW/m^2, respectively). This is probably due to the lack of suitable substrates in the area. Observations in the area partly indicate a rich growth of *Fucus* especially on hard substrates /Kautsky et al, 1999/.

Consumers

Terrestrial consumers

See Section 5.7.2.

Limnic aquatic consumers

The pelagic zone

Six of the lakes in the Forsmark area have been subject to standardised survey gill-net fishing prior to the site investigations /Brunberg and Blomqvist, 2000/. *Fish* was caught in all lakes. The average catch (catch per unit effort, CPUE) was 3.6 kg in terms of biomass and 36 individuals in terms of abundance. The average number of species found was 3.7. In total for all 6 lakes, 6 species were encountered; roach (*sw mört, Rutilus rutilus*), Crucian carp (*sw ruda, Carassius carassius*), tench (*sw sutare, Tinca tinca*), perch (*sw abborre, Perca fluviatilis*), ruffe (*sw gärs, Gymnocephalus cernua*), and pike (*sw gädda, Esox lucius*). Crucian carp dominated in terms of numbers and/or biomass in four of the lakes. In the two other lakes, roach and perch were dominant. The other three species were less abundant in the lakes in which they occurred, pike and ruffe being found in three lakes and tench in one lake. In one of the lakes in which Crucian carp dominated, it was also the only fish caught.

In comparison with data from the entire fish survey, including 81 lakes in the county of Uppsala, the oligotrophic hardwater lakes have a lower abundance of fish (36 compared to 81 individuals per gill net). The biomass of fish is almost exactly the same (3.6 kg in both cases) whereas the oligo-trophic lakes have a lower diversity in the fish community, 3.7 compared to 5.8 species encountered /Brunberg and Blomqvist, 2000/.

The littoral zone

There are few, if any, quantitative studies of the benthic fauna of the illuminated soft-bottom sediments of the lakes in the Forsmark area /Brunberg and Blomqvist, 2000/. According to /Brunberg and Blomqvist, 2000/, there have not been any studies of biomass, nor of the production of heterotrophic bacteria or fungi in the light-exposed soft-bottom zone.

The riparian zone

There are no known quantitative studies of the fauna, nor of decomposers, in the riparian zone of lakes in the Forsmark area.

Marine aquatic consumers

In the diving survey, the bottom from the surface down to a maximum of 18 m was investigated in an area including the bottoms above SFR. The biomass and diversity of *benthic fauna* peaks between 2–4 m depth with a high contribution of filter feeders (mainly *Cardium* sp), herbivores (*Theodoxus fluviatilis* and *Lymnaea peregra*) and detrivores (mainly *Macoma balthica)* with a mean biomass of 60 gDW/m². At lower depths, the detrivores dominate (mainly *Macoma balthica*), with a high biomass down to 15 m. The blue mussel (*Mytilus edulis*) was to a large extent missing, although suitable substrate was present. In the Bothnian Sea, blue mussels extend up to Norra Kvarken, but usually few individuals are found at each site along the coast and the density is never as high as can be observed further south in the Baltic proper. Data on the soft bottom fauna of Öregrundsgrepen have been collected in studies performed by Swedish Environmental Protection Agency between 1978–1986 /Mo and Smith, 1988/.

/Kumblad, 2001/ compiled data concerning biomass in the coastal ecosystem in the area above SFR from various sources, and used this information to set up an annual carbon budget for the area above SFR. It was based on biomasses and flows of carbon between thirteen functional groups in the ecosystem. The results indicate that the organisms are self-sufficient in carbon, and that the area exports carbon corresponding to approximately 50% of the annual primary production. The largest organic carbon pool is DOC (one and a half time larger than the total biomass) and the major functional organism groups are the macrophytes (37% of the total biomass), benthic macrofauna (36%), and the microphytes (11%). The soft bottom and phytobenthic communities appear to have important roles in the ecosystem since these communities comprise the main part of the living carbon in the studied area. The phytobenthic community contributes to the larger share (61%) of the primary production, whereas the larger part of the consumption takes place in the soft bottom community (53%) /Kumblad, 2001/.

7.1.6   Humans and land use

See Section 5.7.3.

7.1.7   Nature values

During the planning process, a methodology for compiling and assessing areas of environmental and/or cultural concern was developed. This aimed at producing a map showing areas suitable and not suitable for e.g. drilling or other disturbing activities, i.e. an *accessibility map*, but also at documenting site-specific information of environmental and/or cultural interest for a coming Environmental Impact Assessment.

The basis for this map was an aggregation of spatially defined areas, such as legally protected areas, ecologically sensitive areas, buffered watercourses and buildings, cultural amenities etc. In Table 7-3 some examples of defined areas/points, and how these were spatially delimited, are given. For a full description on the procedure, see /Kyläkorpi, 2004/. After the aggregation of all non-suitable areas into one theme, the remaining area can be interpreted as accessible for the various survey activities after a complementary field check.

Table 7-3. Examples of nature, cultural and socio-economical values that have been used to produce the accessibility map for the Forsmark regional model area.

Area of interest	Value	Characteristics	Delimitation
Nature values	Nature reserves	Legally protected	Polygon boundary
	Key biotopes	Ecologically sensitive	Polygon boundary
	Red listed species	Ecologically sensitive / Legally protected	Occurrence buffered 100 m
	Water courses	Ecologically sensitive	Buffered 50 m
	Lakes	Ecologically sensitive	Shoreline buffered 100 m
Cultural values	Ancient monuments	Legally protected	Occurrence buffered 100 m
Socio-economic values	Residental properties	Legally protected / policy reasons	Buildings buffered 100 m
	Wells		Buffered 100 m

7.1.8 Overall ecosystem model

No overall ecosystem model has been produced for the Forsmark Site Descriptive Model version 1.1.

7.2 Bedrock regional scale

7.2.1 Geological description

Rock domain model

A single, three-dimensional regional model, which consists of thirty-four rock domains, is presented here for the Forsmark site. These domains have been distinguished on the basis of their composition and grain size, their degree of inhomogeneity and their degree of ductile deformation.

Felsic, meta-igneous rocks dominate the Forsmark site and all are rich in quartz (mean values of recalculated quartz contents in QAPF plots > 30%). Apart from some younger pegmatites and granites, all rock types show low (mean values < 6 ppm) uranium contents. Most of the rocks formed during the time period 1,910 to 1,840 million years ago, i.e. during phase 1 or phase 2 of the geological evolution in central-eastern Sweden (see Section 3.1).

Detailed information concerning the properties of all the thirty-four rock domains, in accordance with the procedures outlined in Section 5.1.2, are summarised in a group of tables, one for each rock domain (Appendix 4). The properties of two representative examples of these domains, RFM029 that dominates the candidate area and RFM032 that helps to define a major folded structure in the central part of the regional model volume, are illustrated here (Table 7-4 and Table 7-5, respectively). All rock codes are listed in Appendix 3. A key property of each domain is the character of the rock type that forms either the dominant rock or a subordinate rock within the domain. For this reason, the composition, grain size, age and physical properties as well as the uranium contents of the different rock types at the Forsmark site are also presented (Table 7-6, Table 7-7 and Table 7-8).

Table 7-4. Properties of rock domain RFM029.

RFM029 Property	Character	Quantitative estimate	Confidence	Basis for interpretation	Comments
Volume (m³)		Unable to be carried out due to difficulties with RVS.			Borehole data close to reactors 1 and 2 not analysed.
Rock type, dominant	101057	84%	High	See confidence table.	Quantitative estimate based on occurrence in KFM01A. Borehole data close to reactors 1 and 2 not analysed.
Rock type, subordinate	101051	11%	High	See confidence table.	Quantitative estimate based on occurrence in close to KFM01A. Borehole data reactors 1 and 2 not analysed.
	102017	2%			
	101061	1.5%			
	111058	1.3%			
	108019	0.2%			
Degree of homogeneity	High		High	See confidence table.	Borehole data close to reactors 1 and 2 not analysed.
High temperature alteration (dominant rock type)	Amphibolite-facies metamorphism		High	See confidence table.	Borehole data close to reactors 1 and 2 not analysed.
Ductile deformation	Lineated and weakly foliated. More strongly foliated along southwestern and northeastern margins.		High	See confidence table.	Borehole data close to reactors 1 and 2 not analysed.
Class (1–4)*	4				Borehole data close to reactors 1 and 2 not analysed.

Background fracturing	Quantitative estimate	Span	Confidence	Basis for interpretation	Comments
Low temperature alteration around fractures	7% of the fractures. All sets.	5 to 12% in different sets.	Medium	Section 4.4.2	Sealed fracture data from KFM01A. Open fracture data. Oxidation not mapped.
Fracture filling	Open fractures, 60% chlorite.	Open fractures, 38 to 67% in different sets.	Medium	Section 4.4.2	Dominant filling in open and sealed fracture data from KFM01A.
	Sealed fractures, laumontite, hematite, chlorite.	Sealed fractures, highly variable.			

*1 = Inhomogeneous. Banded, foliated and lineated. Inferred higher degree of ductile deformation.
 2 = Inhomogeneous. Lineated and weakly foliated. Inferred lower degree of ductile deformation.
 3 = Homogeneous. Foliated and lineated. Inferred higher degree of ductile deformation.
 4 = Homogeneous. Lineated and weakly foliated. Inferred lower degree of ductile deformation.

Table 7-5. Properties of rock domain RFM032.

RFM032 Property	Character	Quantitative estimate	Confidence	Basis for interpretation	Comments
Volume (m³)		Unable to be carried out due to difficulties with RVS.			Borehole data close to reactors 1 and 2 not analysed.
Rock type, dominant	101058		High	See confidence table	Borehole data close to reactors 1 and 2 not analysed.
Rock type, subordinate	101057 103076 101061 102017 101051 111058		High	See confidence table	Borehole data close to reactors 1 and 2 not analysed.
Degree of homogeneity	Low		Medium	See confidence table	Borehole data close to reactors 1 and 2 not analysed.
High temperature alteration (dominant rock type)	Amphibolite-facies metamorphism		High	See confidence table	Borehole data close to reactors 1 and 2 not analysed.
Ductile deformation	Banded, foliated and lineated		High	See confidence table	Borehole data close to reactors 1 and 2 not analysed.
Class (1–4)*	1				

Background fracturing	Quantitative estimate	Span	Confidence	Basis for interpretation	Comments
Low temperature alteration around fractures	No data				Tunnel 1/2 data and borehole data close to reactors 1 and 2 not analysed.
Fracture filling	No data				Tunnel 1/2 data and borehole data close to reactors 1 and 2 not analysed.

*1 = Inhomogeneous. Banded, foliated and lineated. Inferred higher degree of ductile deformation.
 2 = Inhomogeneous. Lineated and weakly foliated. Inferred lower degree of ductile deformation.
 3 = Homogeneous. Foliated and lineated. Inferred higher degree of ductile deformation.
 4 = Homogeneous. Lineated and weakly foliated. Inferred lower degree of ductile deformation.

Table 7-6. Composition, grain size and age of the different rock types at the Forsmark site.

Code (SKB)	Composition								Grain size	Age
	Name (IUGS/SGU)	Quartz (%) in QAPF plot		Alkali feldspar (%) in QAPF plot		Plagioclase feldspar (%) in QAPF plot		N (No. of obs.)	Class (SGU)	Million years
		Mean	Std	Mean	Std	Mean	Std			
103076	Dacite and andesite, metamorphic	31.8	11.0	4.0	5.8	64.3	13.8	10	Fine-grained	1,906–1,891
106000	Sedimentary rock, metamorphic	No data								1,906–1,891
108019	Calc-silicate rock (skarn)	No data							Finely medium-grained	1,906–1,891
109010	Pyrite-pyrrhotite-chalcopyrite-sphalerite mineralisation	No data							Fine-grained	Not known
109014	Magnetite mineralisation associated with calc-silicate rock	No data							Fine-grained	1,906–1,891
101004	Ultramafic rock (olivine-hornblende pyroxenite)	Not relevant. Quartz (Q), K-feldspar (A) and plagioclase feldspar (P) are absent							Medium-grained	1,891–1,840
101033	Diorite, quartz diorite and gabbro, metamorphic	3.2	5.0	0.0	0.0	96.8	5.0	3	Medium-grained	1,891–1,840
102017	Amphibolite	0.0		0.0		100.0		1	Finely medium-grained	1,891–1,840
101054	Tonalite and granodiorite, metamorphic	31.1	8.7	8.2	4.1	60.7	7.6	12	Medium-grained	1,891–1,840
101056	Granodiorite, metamorphic	35.2	3.5	13.9	2.9	50.9	6.4	3	Medium-grained	1,891–1,840
101057	Granite and granodiorite, metamorphic	37.7	4.4	27.0	7.8	35.3	6.3	20	Medium-grained	1,891–1,840
101058	Granite, metamorphic	35.0	4.3	31.7	23.9	33.4	19.6	2	Fine-grained (aplitic)	1,891–1,840
111051	Granitoid, metamorphic	No data								1,891–1,840
101051	Granodiorite, tonalite and granite, metamorphic	32.2	4.7	12.9	10.5	54.9	11.9	14	Finely medium-grained	1,891–1,750
101061	Pegmatitic granite, pegmatite	37.4	2.7	26.7	6.4	35.9	5.9	3	Coarse-grained (pegmatitic)	1,891–1,750
111058	Granite	32.8	1.4	34.2	7.9	33.0	6.5	2	Fine- to medium-grained	1,850–1,750

Table 7-7. Physical properties of the different rock types at the Forsmark site.

Code (SKB)	Composition (and grain size) Name (IUGS/SGU)	Density (kg/m³) Mean	Std	Porosity (%) Mean	Std	Magnetic susceptibility (SI units) Geometric mean	Std above/below mean	Electrical resistivity in fresh water (ohm m) Geometric mean	Std above/ below mean	N (No. of obs.)
103076	Dacite and andesite, metamorphic	2755	88	0.34	0.08	0.00381	0.06541/0.00360	22696	26316/12186	12
106000	Sedimentary rock, metamorphic	No data								
108019	Calc-silicate rock (skarn)	No data								
109010	Pyrite-pyrrhotite-chalcopyrite-sphalerite mineralisation	No data								
109014	Magnetite mineralisation associated with calc-silicate rock	4177	67	1.36	0.16	0.12310	0.00128/0.00127	233	138/87	2
101004	Ultramafic rock (olivine-hornblende pyroxenite)	3045		1.04		0.04572		52		1
101033	Diorite, quartz diorite and gabbro, metamorphic	2948	108	0.37	0.08	0.00471	0.03135/0.00409	15916	13540/7316	11
102017	Amphibolite	2928		0.30		0.00071		11211		1
101054	Tonalite and granodiorite, metamorphic	2746	42	0.41	0.07	0.00149	0.00881/0.00128	14101	5530/3972	14
101056	Granodiorite, metamorphic	2704		0.50		0.00673		76646		1
101057	Granite and granodiorite, metamorphic, medium-grained	2655	11	0.44	0.06	0.00453	0.01352/0.00339	20362	7713/5594	31
101058	Granite, metamorphic, aplitic	2635	12	0.39	0.04	0.00546	0.00832/0.00330	16190	7662/5201	4
111051	Granitoid, metamorphic	No data								
101051	Granodiorite, tonalite and granite, metamorphic, fine- to medium-grained	2701	30	0.46	0.05	0.00107	0.00583/0.00091	13187	4961/3605	5
101061	Pegmatitic granite, pegmatite	2626	5	0.53	0.08	0.00284	0.00883/0.00215	16868	8881/5818	5/7
111058	Granite, fine- to medium-grained	2632		0.48		0.00204		13017		1

The general character of the rock domains varies in a highly consistent pattern, from southwest to northeast across the regional model volume. This important variation was recognised already in connection with SKB's feasibility study programme /e.g. Bergman et al, 1998/.

The *tectonic lens in approximately the central part of the regional model volume* (Figure 7-10), that includes the candidate area, consists of folded rock domains. One of these domains (RFM032) is inhomogeneous, banded and contains some rocks that show an inferred high degree of ductile deformation. This rock domain is dominated by a fine-grained metagranite that contains few dark minerals, i.e. an aplitic metagranite, and is folded in a synformal structure that plunges moderately to the southeast (Figure 7-10). The strike and dip of domain RFM032 as well as its position in three-dimensional space, in the hinge of this fold, are similar to the important A0–A1 seismic reflector (cf Figure 5-11). However, there remains some uncertainty concerning whether this reflector is related to the inhomogeneous bedrock in rock domain RFM032, a deformation zone (or zones) with an approximately EW strike, or both these features.

Table 7-8. Uranium contents of the different rock types at the Forsmark site, based on in situ, gamma-ray spectrometric measurements (without brackets) and geochemical analyses of bedrock samples (brackets). The natural exposure values are based on the in situ, gamma-ray spectrometric measurements.

Code (SKB)	Composition (and grain size)	Content of uranium					
	Name (IUGS/SGU)	Gamma-ray spectrometric and U geochemical measurements					N (No. of obs.)
		Mean U (ppm). Gamma-ray spec./(geochemical)	Std	Mean natural exposure (microR/h)	Std		
103076	Dacite and andesite, metamorphic	3.9 (3.2)	0.9 (1.9)	8.52	2.0	12 (7)	
106000	Sedimentary rock, metamorphic	No data					
108019	Calc-silicate rock (skarn)	No data					
109010	Pyrite-pyrrhotite-chalcopyrite-sphalerite mineralisation	No data					
109014	Magnetite mineralisation associated with calc-silicate rock	5.7	0.7	6.7	0.1	2	
101004	Ultramafic rock (olivine-hornblende pyroxenite)	0.0 (< 0.1)		0.0		1 (1)	
101033	Diorite, quartz diorite and gabbro, metamorphic	1.0 (0.6)	0.7 (0.2)	2.3	1.6	11 (3)	
102017	Amphibolite	1.1 (1.5)	(0.8)	3.4		1 (13)	
101054	Tonalite and granodiorite, metamorphic	4.0 (3.4)	1.3 (0.6)	8.1	1.6	14 (5)	
101056	Granodiorite, metamorphic	3.3 (4.2)		7.2		1 (1)	
101057	Granite and granodiorite, metamorphic, medium-grained	4.7 (4.2)	1.3 (1.8)	12.1	1.6	31 (11)	
101058	Granite, metamorphic, aplitic	5.5 (3.1)	1.7	12.8	3.9	6 (1)	
111051	Granitoid, metamorphic	No data					
101051	Granodiorite, tonalite and granite, metamorphic, fine- to medium-grained	4.8 (5.1)	2.2 (3.6)	10.7	3.5	6 (4)	
101061	Pegmatitic granite, pegmatite	15.9 (2.8)	13.5 (0.5)	22.5	9.1	22 (2)	
111058	Granite, fine- to medium-grained	10.2 (12.8)	4.3 (2.5)	21.5	1.8	3 (2)	

Both rock domain RFM029, that dominates the candidate area, and rock domain RFM034, that lies northwest of the nuclear power plants, are more homogeneous. These domains are predominantly composed of metamorphosed granite that, in part, merges over to granodiorite. A linear, grain-shape fabric, that is inferred to represent a mineral stretching lineation, dominates the bedrock in these domains. The lineation is parallel to folds that deform a weak, planar grain-shape fabric. Both the folds and the mineral stretching lineation plunge moderately to the southeast. Domain RFM029 shows the same compositional and ductile structural features at c 1,000 m depth as that seen at the surface and has been modelled so that it extends to the base of the regional model volume (Figure 7-10).

Metamorphosed tonalite to granodiorite dominates rock domain RFM017 in the southeastern part of the candidate area. The contacts of this unit and the planar grain-shape fabric dip moderately to the east, and the strong mineral stretching lineation maintains its moderate E to SE plunge. This domain has a lensoid geometry at the surface and is inferred to thin out in a down-dip direction. It has not been extended to the base of the regional model volume (Figure 7-10).

The metamorphosed bedrock in the *marginal rock domains*, both to the southwest and to the northeast, is generally much more inhomogeneous. These domains extend as far as the Forsmark deformation zone to the southwest and into the volume of bedrock that is situated around the Singö deformation zone to the northeast (Figure 7-10).
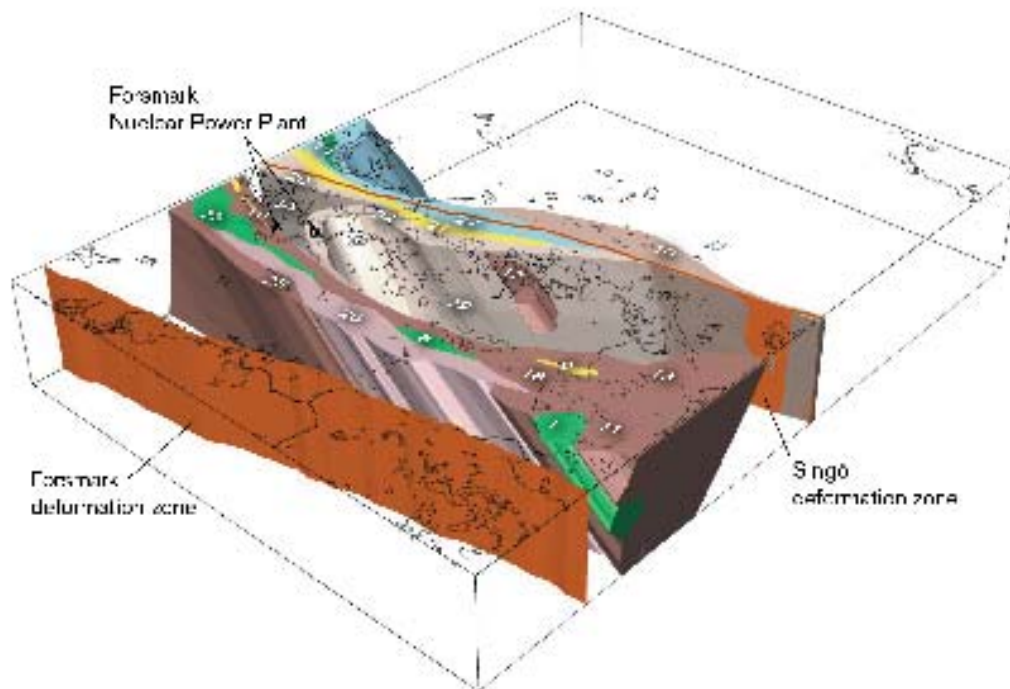
Figure 7-10. *Rock domain model viewed to the north. Domains RFM029 and RFM034 are unshaded in order to show the major folding within the tectonic lens at the Forsmark site. The domains southwest of the rock domain 26 are unshaded in order to show the modelled southeasterly elongation of several domains. The dominant rock type in each domain is illustrated with the help of different colours (see the rock domain map at the surface in Figure 5-6).*

Metamorphosed tonalite and granodiorite as well as metavolcanic rocks with a dacitic to andesitic composition dominate the marginal rock domains. Iron oxide mineralisations are also present in the metavolcanic rocks that are located both to the southwest and to the northwest of the candidate area. In the model, this mineralised domain dips steeply in a southwesterly direction away from the tectonic lens. All these domains strike in a northwesterly direction and dip vertically or steeply to the southwest (Figure 7-10). Several of them show a strong tectonic banding and/or strong planar and linear grain-shape fabrics that are related to a high degree of ductile deformation. Mineral lineations and fold axes plunge once again to the southeast. Folded high-strain zones with a right-lateral component of movement and occasional eye folds are also present.

Intermediate, mafic and ultramafic rocks, in which quartz is generally lacking, are also a conspicuous bedrock component in the marginal domains (e.g. RFM001). The rock domains that are dominated by the rocks within this group show a lensoid form at the surface and have been modelled so that they extend downwards in a southeasterly direction, parallel to the mineral stretching lineation (Figure 7-10).

There are virtually no site investigation data in the *rock domains that are situated both to the southwest of the Forsmark deformation zone and to the northeast of the Singö deformation zone*. The compilation of the bedrock at the surface, that was completed in connection with the SDM version 0 /SKB, 2002a/, has formed the foundation for the three-dimensional rock domain model that is presented in this study.

The variation in the quality of the surface geological data and the paucity of primary data from sub-surface locations are the two important factors that affect the uncertainties in the modelling of the thirty-four rock domains. A higher concentration of quality data from the surface will already be available in version 1.2. However, the high uncertainties for the assessment and modelling of rock domains under Öregrundsgrepen will remain. Sub-surface data will increase during the site investigation programme, in especially rock domain RFM029, but will probably continue to be lacking

346

in virtually all the other domains. Apart from rock domain RFM029, estimates of the quantitative proportions of each rock type in a rock domain are lacking. This gives rise to some uncertainties in the characterisation of especially the more inhomogeneous rock domains. An expert judgement concerning the confidence of the occurrence and geometry of individual rock domains was presented earlier (Section 5.1.2).

As far as the site-specific questions are concerned /SKB, 2002b/, two points are of significance:

- There are already strong indications from the primary data available during SDM version 1.1 that the tectonic lens at Forsmark, within which the candidate area is situated, is a major structural feature that consists of several folded rock domains. This structure extends downwards to at least 1,000 m. Furthermore, the modelling procedure indicates that it extends at least to the base of the regional model volume.

- The complementary study completed by /Lindroos et al, 2004/ shows that the bedrock at the Forsmark site is of little interest for the exploration and exploitation of metal-bearing ore deposits.

Deterministic structural model

A base, three-dimensional model for the deformation zones which have so far been recognised, with variable confidence, at the Forsmark site is presented in this report. Only zones with a length of 1 km or more are addressed in the structural model. Bearing in mind the major uncertainty concerning the continuity of the sub-horizontal and gently dipping fracture zones, an alternative structural model is also briefly described for these zones. Older structural models, a variety of new surface and sub-surface data, and the identification of so-called linked lineaments have all been used in the modelling procedure.

Base structural model

166 deformation zones, four of which consist of both longer and shorter segments, are present in the regional model volume. For this reason, there are 177 zone segments. Thirteen deformation zones, along which there are, to variable extents, confirmatory geological and geophysical data, are judged to show a high level of confidence for their occurrence. However, the majority of deformation zones in the structural models (153) are based solely on the interpretation of linked lineaments. The confidence of occurrence of these zones is judged to vary from medium to very low.

The possible deformation zones with medium confidence (71) are based on well-defined lineaments that have been identified, to a large extent, with the help of the airborne, magnetic data. The remaining possible deformation zones, which are based solely on the interpretation of linked lineaments (82), are presented with a low to very low level of confidence for their occurrence. The lowest level of confidence is assigned to the possible zones that are based on linked lineaments derived solely from electrical conductivity measurements or topographic data. This judgement is steered by the uncertainty concerning whether the lineament represents a geological feature in the crystalline bedrock or in the Quaternary cover.

Detailed information concerning the properties of the deformation zones, in accordance with the procedures outlined in Section 5.1.4, are summarised in a series of tables (Appendix 5). The properties of a representative example of the thirteen high-confidence zones and a representative set of possible deformation zones, which are based solely on the interpretation of linked lineaments, are illustrated here (Table 7-9 and Table 7-10, respectively).

The base structural model for the *thirteen deformation zones, which are based on a variety of geological and geophysical information* and which are not so much affected by the interpretation of linked lineaments, is presented in Figure 7-11. Three important types of deformation zones are present within this group:

- Regionally important deformation zones with northwesterly strike and vertical dip.

- Fracture zones with northeasterly strike and vertical or steep, southeasterly dips.

- Fracture zones that are sub-horizontal or dip gently to the southeast.

Table 7-9. Properties of fracture zone ZFMNE0061.

ZFMNE0061 (656-674 m level in KFM01A)					
Property	**Quantitative estimate**	**Span**	**Confidence level**	**Basis for interpretation**	**Comments**
Position		± 9 m (± 20 m)	High	KFM01A, linked lineaments	Position in borehole (surface)
Orientation (strike/dip)	068/81	± 5/± 10	High	KFM01A, linked lineaments	
Width	5 m	± 1 m		KFM01A	
Length	1730 m	± 200 m	Medium	Linked lineaments	
Ductile deformation	No		High	KFM01A	
Brittle deformation	Yes		High	KFM01A	
Alteration	Yes	± 5 m	High	KFM01A	10 m of oxidized bedrock
Fracture orientation	050/75	± 15/± 10	High	KFM01A	Boremap
Fracture frequency	< 4 m^{-1}, section of crush		High	KFM01A	Concentration of fractures is distinctly higher, mainly sealed fractures. Crush at 652 m.
Fracture filling	Laumontite, chlorite, calcite		High	KFM01A	

Table 7-10. Properties for the NW set of regional deformation zones that have been recognised solely on the interpretation of linked lineaments.

NW set. Regional deformation zones (> 10 km)					
Property	**Quantitative estimate**	**Span**	**Confidence level**	**Basis for interpretation**	**Comments**
Position		± 20 m	High	Linked lineaments, fracture statistical analysis	
Orientation (strike/dip)	306/88	±24/90-62	Low	Statistical analysis of fractures and lineaments (DFN model)	Span 95% confidence level
Width	75 m	±25 m	Low		Assumption
Length	> 10 km		Medium		
Ductile deformation	Yes		Low	Ground geology	
Brittle deformation	Yes		Low	Ground geology	
Alteration					
Fracture orientation					
Fracture frequency					
Fracture filling					

Figure 7-11. Base structural model in the regional model volume for the thirteen deformation zones along which there are confirmatory geological and geophysical data and which are judged to have a high confidence of occurrence. Vertical or steeply dipping zones are shown in red and sub-horizontal and gently dipping zones in orange. This figure should be compared with Figure 4-9 in the model version 0 /SKB, 2002a/.

The Forsmark and Singö deformation zones, which belong to the zones with northwesterly strike and vertical dip, are the two master regional deformation zones at the Forsmark site (Figure 7-11; see also Figure 7-10). The Eckarfjärden deformation zone forms an important splay north of the Forsmark zone. Furthermore, the zones that are referred to as ZFMNW0002 and ZFMNW0805 form splays once again to the north of a master zone, in this case the Singö deformation zone (Figure 7-11). All these splays show strike directions that are more northerly in orientation but their dips are also vertical. Both ductile and brittle deformation are present along these zones. The inferred length of these zones suggests that they all extend to the base of the regional model volume.

The geometric configuration described above was already recognised during the SDM version 0 /SKB, 2002a/. The geometric relationship of the splays to the master zones is consistent with the interpretation that the master deformation zones have a component of dextral strike-slip movement along them. Bearing in mind that the high-temperature (amphibolite-facies), ductile deformation in the Forsmark area, with its strong northwesterly structural grain, also displays this kinematic component, it is possible that these zones were established many hundreds of million years ago, during the Palaeoproterozoic time period, i.e. during phase 2 of the evolutionary history of the site.

One of the high-confidence fracture zones that strikes in a northeasterly direction (ZFMNE0061) dips steeply towards the southeast and cuts across the candidate area. This zone is characterized by a high frequency of sealed fractures with laumontite, chlorite and calcite as fracture fillings. The two other zones within this subgroup (ZFMNE0869 or Zone 3 at SFR and ZFMNE0870 or Zone 9 at SFR) dip vertically and enclose the SFR site. All these zones are locally major in character and only show brittle deformation. They are confined between the regionally more important zones with northwesterly strike (Figure 7-11).

The five remaining zones that are judged with high confidence to be present at the Forsmark site are either sub-horizontal (ZFMEW0865) or strike in a northeasterly direction and dip gently towards the southeast (ZFMNE0871 that is equivalent to Zone H2 at SFR, ZFMNE0866, ZFMNE0867 and ZFMNE0868). All these zones show only brittle deformation. The consistent southeasterly dip of most of the zones is strongly reminiscent of the geometry of many of the seismic reflectors (Figure 5-11). Indeed, fracture zones ZFMNE0867 and ZFMNE0868, which lie close to drillsite 3, correlate with high confidence to the seismic reflectors A5 and A6, respectively. This observation provides support to a correlation between this subgroup of zones and many of the seismic reflectors. However, no unconstrained correlation has been carried out at this stage in the modelling procedure.

The base structural model terminates the sub-horizontal and gently dipping fracture zones at the nearest vertical or steeply-dipping deformation zone. In this model, the regional structural significance of these zones is limited (Figure 7-11). All the five zones modelled in this manner are local major or local minor in character and are restricted to the crustal segment above the critical 400–600 m level in the rock model volume. This feature is consistent with the concentration of sub-horizontal fractures in the upper 400 m of KFM01A (see Section 4.4.3).
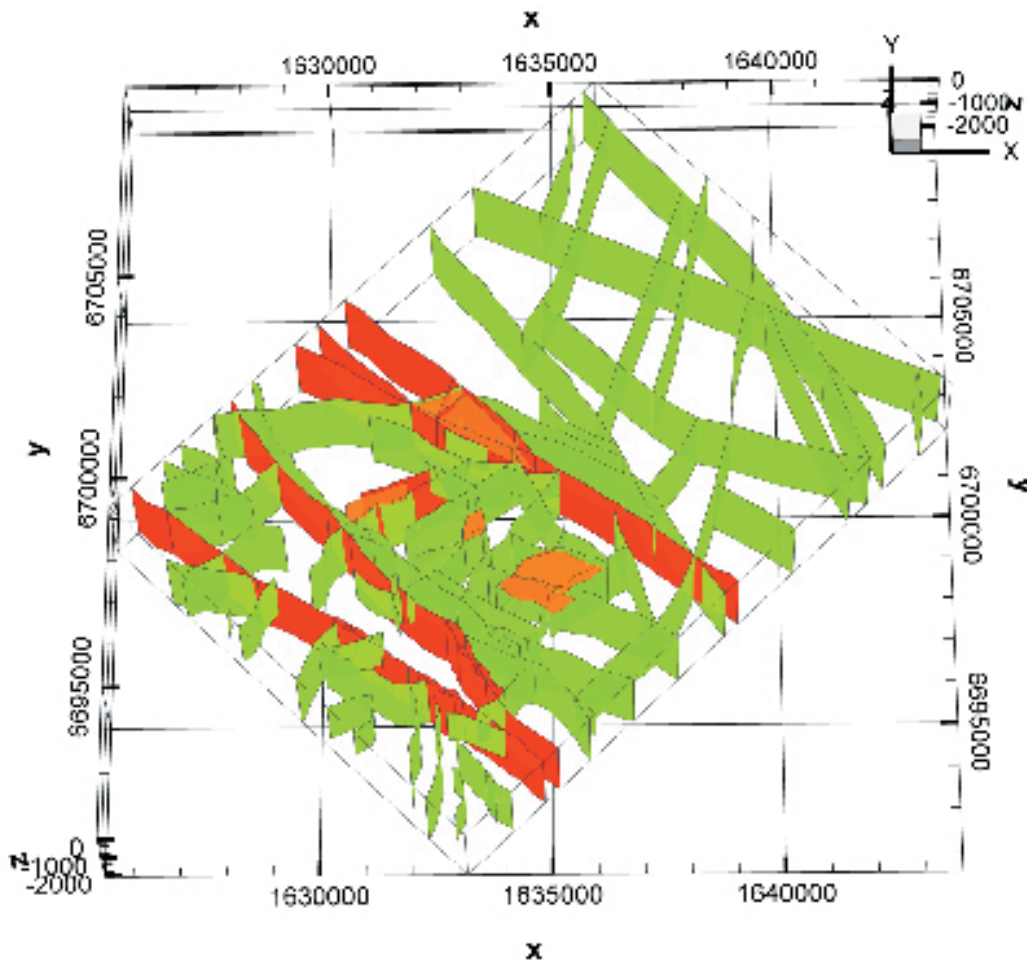
Figure 7-12. *Base structural model in the regional model volume for the deformation zones with both high (red and orange) and medium (green) confidence of occurrence. The red and orange colours distinguish zones with high confidence of occurrence that are vertical or steeply dipping (red) from those that are sub-horizontal or gently dipping (orange).*

The thirteen deformation zones with high confidence are complemented with *153 possible deformation zones that are based solely on the interpretation of linked lineaments*. These possible zones are considered to show a variable, medium to very low confidence of occurrence. The zones with medium confidence are based, at least in part, on distinctive, low-magnetic lineaments. Four of the zones with medium confidence are regional in character and are situated under the sea area. The remaining zones are local major in character. All the zones in the base structural model that show both high and medium confidence of occurrence are shown in Figure 7-12. All the inferred deformation zones in the base structural model, irrespective of the judgement concerning the confidence of occurrence, are shown in Figure 7-13.

The possible deformation zones recognised solely on the basis of linked lineaments have been grouped into four different orientation sets – NW, NE, NS and EW. The zones that strike NW, NE and NS dominate. However, zones with a medium confidence of occurrence are present in all four sets. Four lineation arrays with these trends, which correspond to possible deformation zones, were already recognised during the model version 0 /SKB, 2002a/. The occurrence of distinctive fracture orientation sets that strike NW and NE (see Section 5.1.6) provides some support to the inference that at least the linked lineaments with these trends represent deformation zones.

Besides the question marks concerning the occurrence of these zones, a key uncertainty concerns their dip. All zones except one, which is situated east of drillsite 1, have been modelled with an inferred vertical dip. The zone east of drillsite 1 has been modelled with a steep dip towards the east.
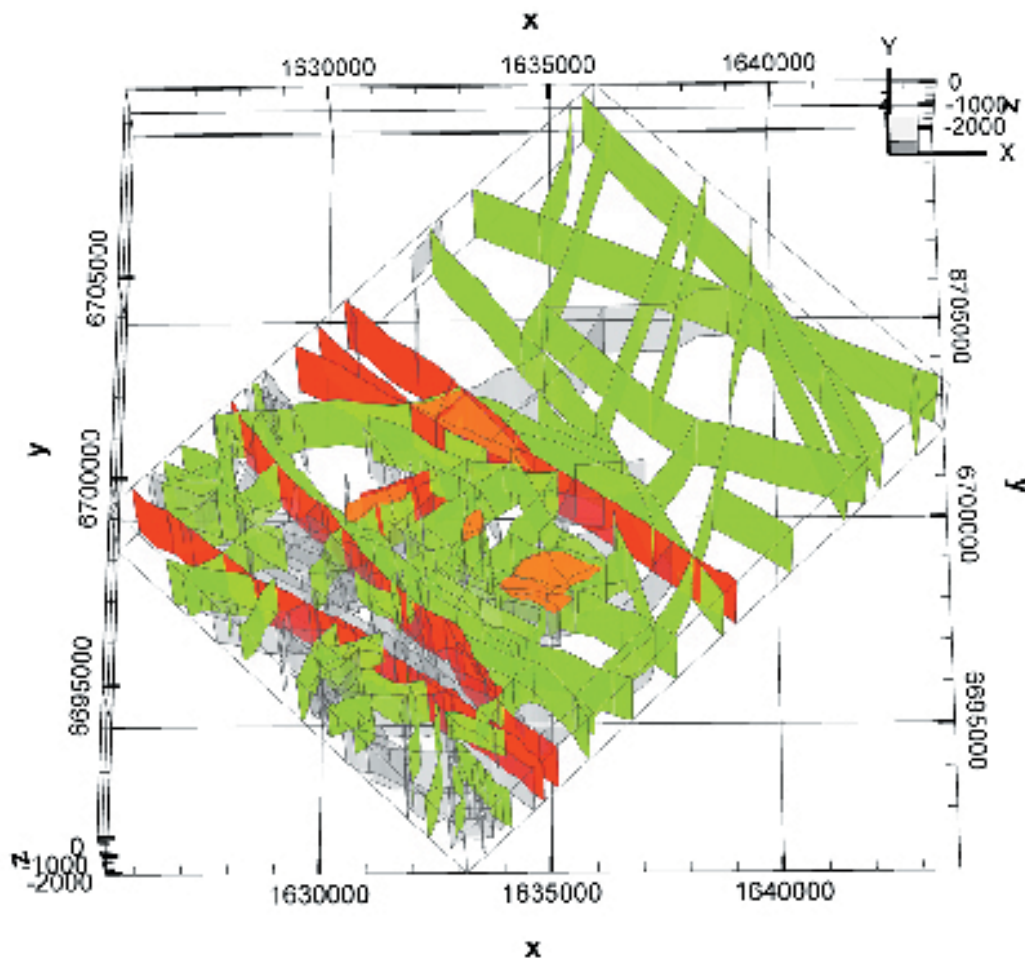
Figure 7-13. Base structural model for all deformation zones in the regional model volume. The red and orange colours mark zones with a high confidence of occurrence; vertical or steeply dipping zones are shown in red and sub-horizontal and gently dipping zones in orange. The green colours show the zones with medium confidence of occurrence and the grey colours indicate zones with low or very low confidence of occurrence. All the zones with medium and lower confidence of occurrence are based solely on the interpretation of linked lineaments and have been modelled with vertical or steep dips.

The along-strike continuity of nearly all the vertical or steeply dipping deformation zones, irrespective of their confidence of occurrence, is steered by the interpretation of the length of the linked lineament that is coupled to the deformation zone. It is considered probable that the number of smaller segments that are present along each individual deformation zone has been underestimated. Such segments may be shorter zones arranged, for example, in an en echelon manner along the main zone. It is difficult to resolve the individual breaks between such segments, bearing in mind the uncertainty inherent in the siting of the lineaments. It is considered likely that many of the deformation zones are far less continuous in their strike direction compared to that shown in the structural model. The recognition of separate segments along the same zone may have important implications for the establishment of respect distances across the deformation zones.

Alternative structural model

The alternative structural model resembles in most aspects the base structural model. It only differs from the base model where it concerns the along-strike and down-dip extension of the five fracture zones that are sub-horizontal or dip gently to the southeast. The alternative model allows these five fracture zones to continue in both strike and dip directions to the margins of the regional model volume. The alternative model has been adopted in order to emphasise the uncertainty in the along-strike continuity and down-dip extension of these zones. It is motivated not least by the historical debate (see summary in /SKB, 2002a/) concerning the continuity of ZFMNE0871 (Zone H2 at SFR).

Assessment of models and site-specific questions

The base and alternative structural models for the sub-horizontal or gently dipping fracture zones provide two extreme concepts as a means to model these structures. In the base model, these zones do not continue for any major distance. In the alternative model, they have a regional structural significance. It is probable that neither of these models is correct. They have been adopted at this stage of the modelling procedure in order to assess, especially, the hydrogeological consequences of the different alternatives.

As far as the site-specific questions are concerned /SKB, 2002b/, the site descriptive model version 1.1 confirms the presence of several sub-horizontal or gently, SE-dipping fracture zones at the Forsmark site. These zones build an important structural feature at the site. Furthermore, at least some of the gently, SE-dipping fracture zones correspond to gently, SE-dipping seismic reflectors. It should be possible to assess whether or not there is a more general link between fracture zones and reflectors during the site descriptive model version 1.2. The key question concerning the extension of the sub-horizontal and gently dipping fracture zones, both along strike and in a down-dip direction, remains.

Finally, it needs to be stated that considerably more work is required to relate more closely the different sets of fracture orientations, the different groups of mineral fracture fillings, kinematic data along the various deformation zones and the geological evolutionary model (see Section 3.1). In this manner, a better understanding of the timing of brittle deformation at the Forsmark site may be achieved.

7.2.2 Rock mechanics description

Regional stress conditions

Based on available stress data bases, it was found that the southern part of the area around the Gulf of Bothnia may have a variable stress field. Along the coast of northern Uppland there are data from Finnsjön and Forsmark supporting a general trend for the major horizontal stress in a NW-SE direction, rather close to alignment with the coast line. Also further to the west in central Sweden (the mining district), as well as towards the south (Stockholm area), the stresses are normally trending somewhat NNW to NW.

Data from the old Dannemora mine, a little more to the west, indicate a more N-S stress orientation. The background to these data is, however, not known. Some 200 km to the ENE, at the Finnish Olkilouto site, the stresses seem to be a little more trending to the NE-SW.

A general trend of NW-SE has been explained for the south-eastern part of Sweden /Hakami et al, 2002/. This explanation fits well to most observations in this part of Sweden. But because some observations show different stress orientations, there may be many reasons to consider perturbation of the stress field at various scales due to influence by rock types of different properties, as well as from fault zones. There will always remain uncertainties in the regional stress field for this reason. But so far it is assumed that the results from Forsmark and Finnsjön show, to a reasonable degree, the trend of the regional stress field. This is also likely, because such a regional stress field is sub-parallel to the regional fault zones in the area.

Regional mechanical properties

Mechanical properties of the rock are described at the local scale only, see Section 7.3.2.

7.2.3 Thermal properties

The temperature in the regional scale at 500 m depth is about 12°C according to Figure 7-14. The regional heat flow is about 45–50 mW/m^2 /Sundberg, 1995/ and the resulting temperature gradient is approximately 13–14°C/km at a thermal conductivity of 3.5 W/(m·K). The temperature at 500 m depth at the nearby Finnsjön is about 11.6°C /Ahlbom et al, 1995/.
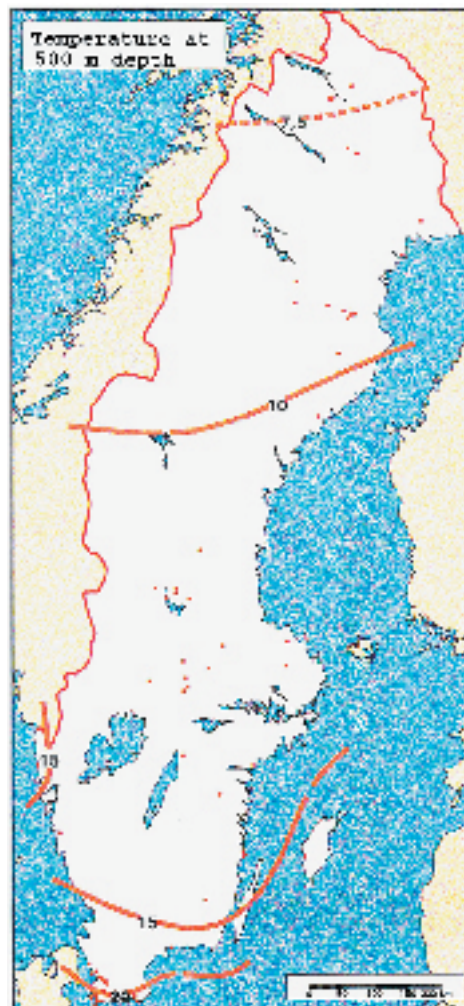
Figure 7-14. *Temperature at 500 m depth /Sundberg, 1995/.*

7.2.4 Hydrogeological description

Hydraulic conductor domains (HCD)

A single, regional scale, three-dimensional model for the deformation zones has so far been recognised in the geological description of the Forsmark site. Out of a total of 166 deformation zones 160 were modelled as vertical. The remaining six were modelled as sub-horizontal or gently dipping. The major uncertainty in the present structural model concerns the spatial continuity of the sub-horizontal or gently dipping deformation zones.

The numerical modelling of groundwater flow and mass (salt) transport presented in this report does not treat the above geological uncertainty concerning the spatial continuity of the sub-horizontal or gently dipping deformation zones, nor does it consider the variable geological confidence of the vertical deformation zones. That is, all of the 166 deformation zones were treated as conductive fracture zones (Hydraulic Conductor Domains) without uncertainty despite their variable geological confidence.

The high-confidence fracture zones that were investigated hydraulically are in minority; 13 out of 166. They have been assigned transmissivity values in accordance with the reported results. Where several data exist intermediate values were adopted. The transmissivity assigned to the non-investigated Forsmark Fault Zone was set to mimic the value of the Singö and the Eckarfjärden deformation zones.

The hydraulic properties of all medium and low confidence HCDs are by definition unknown, both geologically and hydraulically. In order not to exaggerate their hydraulic impact, intermediate hydraulic properties were assigned for model version 1.1, at least compared to the values available from the testing of the high-confidence fracture zones. No sensitivity analyses were carried out at this point as a means of testing their hydraulic property uncertainty.

The database is very limited concerning fracture zone specific storativity. The only value available stems from the short-distance hydraulic interference test conducted at drillsite 1. The specific storativity of the tested fracture zone (ZFMEW0865) was provisionally assigned to all fracture zones. However, for the palaeo-hydrogeological simulations conducted in support of the hydrogeological description the uncertainty associated with this assumption was found to be unimportant.

Likewise, the database for the kinematic porosity is also very limited. The values proposed constitute a reasonable estimation compared to data reported from tests conducted at Äspö.

All parameter settings of the HCDs as used in the numerical simulations are shown in Table 5-38.

7.2.5 Hydrogeochemical description

Groundwater composition

One of the objectives of the Initial Site Investigation (ISI) stage is to produce a preliminary version of the hydrogeochemical descriptive model on a site scale /Smellie et al, 2002/. Visualisation should be based on modelling approaches and also on evaluation where expert judgement is schematically illustrated. Results of applying these preliminary approaches based on presently available Forsmark data are summarised in Figure 7-15. More details are given in /Laaksoharju et al, 2004/.

Figure 7-15 is a conceptual visualisation based on all relevant hydrochemical and isotopic data (although still very limited), and general geological and hydrogeological considerations. The hydrogeochemical trends described and illustrated in Chapter 4, together with information from the post-glacial scenario illustrated in Figure 3-12 and borehole KFM01A structures, have been used to make a first schematic attempt at integrating hydrochemistry with the general hydrostructural character of the Forsmark area. The conceptual model assumes continuity of sub-horizontal zones which is consistent with the alternative geological model. The model will be updated when a more detailed local hydrogeological and geological model becomes available; for example, the sub-horizontal structures are visualised gently dipping to the NW but may be in reality dip towards the SE.
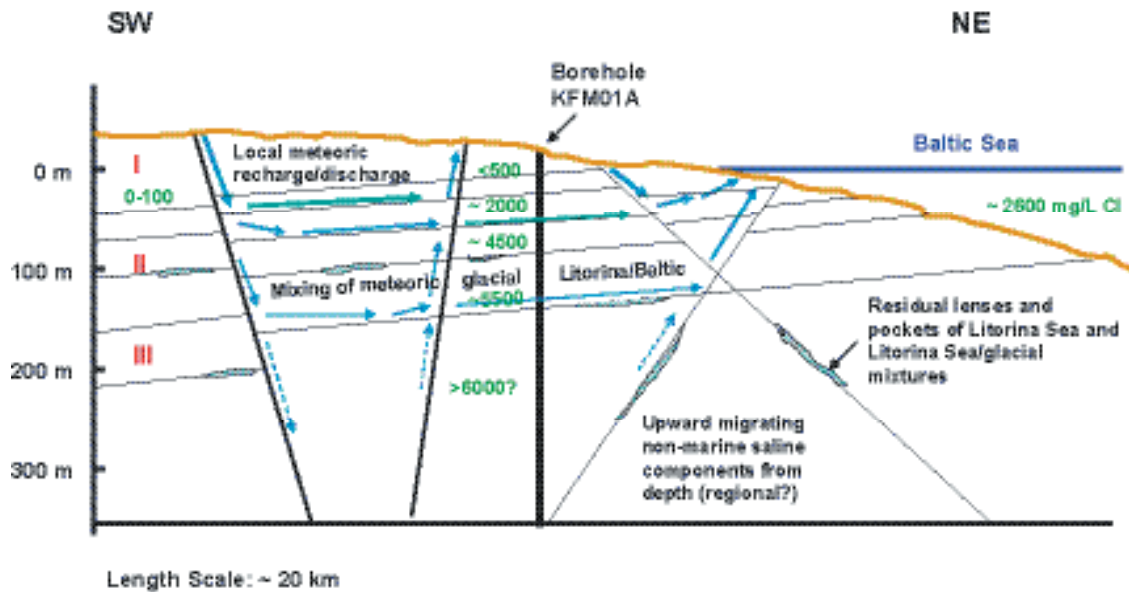
Figure 7-15. Integrated conceptual visualisation of the regional hydrochemistry at the Forsmark site based partly on measured values, on other hydrochemical and isotopic criteria, and general geological and hydrogeological considerations. Note that the geological structures and groundwater flow directions are not based on measurement but are used only for illustration purposes to fit with present conceptual ideas (for example, when more information is available, the sub-horizontal zones may in reality dip towards the SE). Values in green represent mg/L Cl; I, II and III refer to the modelled reaction boxes illustrated in Figure 7-16.

Processes and boundary conditions

These mixing processes, schematically visualised in Figure 7-15, are the result of: a) present-day meteoric recharge/discharge hydraulic gradients of local extent with potentially a more saline regional discharge contribution from depth, b) the forced introduction of glacial melt water to unknown depths during glacial retreat, c) density turnover influences from saline waters introduced during past marine transgressions (e.g. Litorina Sea) since the last glaciation, and d) recent introduction of brackish water when the Baltic Sea covered the Forsmark site area. Because of the generally flat topography close to the coast, the present-day local hydraulic gradients are relatively weak thus preserving the more saline, denser Litorina Sea, Litorina Sea/glacial water and probably brackish Baltic Sea mixtures as pockets and lenses in the bedrock in association with both sub-vertical and sub-horizontal hydraulic structures.

The structural pattern of the area, i.e. a series of vertical and sub-vertical hydraulic fractures which intersect a series of sub-parallel horizontal fracture zones, also hydraulically active, facilitates the groundwater mixing processes. However, this structural system may also partly restrict recharge flow to great depths or, conversely, deep discharge flow to shallow depths by the 'hydraulic cage' effect. This may contribute to the existence of a series of hydraulically (and therefore hydrochemically) separated zones or horizons with only limited vertical flow between them. How realistic or widespread this situation may be is presently not known, but earlier studies at nearby Finnsjön /Ahlbom and Smellie, 1991/ would appear to lend some support to these ideas, together with the suggestion that the preserved Litorina Sea waters may be restricted to around 100–200 m depth.

7.2.6   Transport properties

Only transport properties relevant for the local scale, and more specifically to rock unit 29, are addressed in the present version, see Section 7.3.6.

7.3 Bedrock – local scale

7.3.1 Geological description

Rock domain and deterministic structural models

The rock domain model and deterministic structural model have been developed specifically for the regional model domain and do not change in geometry or properties inside the local model domain.

Stochastic DFN model

A DFN model for the local model domain has been developed for model version 1.1. The main activity has been the evaluation of fracture statistics of linked lineaments, detailed fracture maps of drillsites 2 and 3 and the cored borehole KFM01A. The fracture analysis has aimed at describing the following DFN parameters:

- orientation sets of fractures,

- size distribution in three-dimensions of fractures,

- fracture termination,

- fracture intensity,

- the spatial distribution of fractures.

The orientation analysis shows that lineaments and sub-vertical fractures on outcrops follow essentially the same orientation sets. Four sets are distinguished trending NW, NE, NS and EW. The sub-horizontal fracture population has been analyzed in borehole KFM01A and provides a fifth orientation set.

As a working hypothesis, it is assumed that, for a given orientation, discontinuities observed on outcrops and lineaments are samples from the same population. This assumption may need to be re-evaluated in later model stages, but serves as a first hypothesis of how fracturing has occurred in the Forsmark region. A trace analysis of lineaments and fractures shows a reasonable good fit to a power law distribution for each observed (sub-vertical) set of orientations. The size of sub-horizontal fractures remains an unconstrained parameter in this preliminary model. As a working hypothesis the size distribution for the NS set was used for sub-horizontal fractures.

Fracture termination analysis was performed by calculating the number of terminations of each set against the other. It was assumed that the relative order of fracturing can be deduced by calculating the proportion of terminations against other sets such that the oldest set should have a low proportion of terminations against the other sets. The second oldest should have a dominating proportion of its terminations against the older set, and so forth. Following these assumptions, the order of origin determined was: NW, NS, NE and EW.

The fracture intensity is defined as the amount of fracture area per unit volume of rock, P_{32} (m^2/m^3) /Dershowitz and Herda, 1992/. This parameter cannot be assessed in the field. It can be estimated on the basis of a linear correlation with fracture frequency or from the amount of fracture trace length per unit area. The intensity of sub-vertical fracturing was estimated from the fracture outcrops at drillsites 2 and 3.

However, sub-horizontal fractures are sparse in the outcrops and their density was instead estimated from borehole KFM01A. The borehole shows a relatively high fracture frequency in the topmost 400 m, i.e. 70% of all open fractures (aperture > 0) and slightly less than 60% of all sealed fractures are found in the section 100 m to 400 m. The lower 600 m of the borehole is substantially less fractured. The fracture frequency for sub-horizontal fractures below 400 m borehole depth is c 34% of the fracture frequency above 400 m. The fracture frequency for open sub-horizontal fractures below 400 m borehole depth is c 44% of the fracture frequency above 400 m borehole depth.

Fracture intensities (P_{32}) have been evaluated based on both open and all fractures. The proposed DFN model have high intensity of sub-horizontal fracturing (all and open fractures) above 400 m borehole depth and a lower sub-horizontal fracture intensity (all and open fractures) below 400 m borehole depth. Sub-vertical fracture sets have constant fracture intensities at depth in the proposed DFN model.

The dispersion of fractures is evaluated by counting the amount of fractures or fracture centers in a stepwise increasing reference domain size. The box dimension was calculated for the lineaments data to establish a spatial model for the fracturing in the local model domain. The calculated box dimension of 1.6 suggests that the fracture pattern is somewhat clustered, and the rock mass is divided into blocks of non-uniform size. Despite the low degree of clustering, a Poissonian model was adopted for the spatial representation of stochastic fractures.

A summary of the analyzed fracture statistics for the DFN model are presented in Chapter 5. The values of the DFN parameters are considered to be valid for rock domain 29 and they are summarised in Tables 5-23 and 5-24. An analysis of how these DFN properties can be propagated to other nearby rock domains was performed for model version 1.1.

The entire data sample is derived from within rock domain 29, except for the lineament map, which covers a larger area. Thus, the evaluated fracture statistics are in essence valid only for the fracturing in the central part of the tectonic lens at the Forsmark site. As a working hypothesis it is suggested that orientation and size distributions as well as the spatial model derived for rock domain 29 is valid for all rock domains in the local model.

The sub-vertical fracture intensity of each set is changed between different rock domains by analysing the lineament intensity in rock domain 29 relative to the lineament intensity in other rock domains. Sub-horizontal fracture intensity is kept constant in all rock domains in the local model.

7.3.2   Rock mechanics description

In situ stress conditions

Compared to the information given by the borehole DBT-1, where over-coring was carried out in the late seventies, the following conclusions have been drawn on the information given in this report:

- The borehole KFM01A does not show any significant fractured zones, except the superficial rock, and a minor structure at approximately 660 m depth. It is therefore not clear if the potential "stress jump" discussed as an alternative stress model in model version 0 /SKB, 2002a/ would appear through out the investigation area.

- The re-evaluation of old over-coring data using transient strain analysis /Perman and Sjöberg, 2003/ indicates that the original results to some degree could be over-estimated.

- Compared to the possible problems with over-coring, results of old hydraulic fracturing are regarded as more reliable to determine the minimum horizontal stress (assumed to be approximately equal to σ_3), /SKB, 2002a/.

- Based on the partly fractured, partly very smooth outcrops in the central part of the investigation area (denoted 29a respectively 29b in Section 4.6.4), it is likely that the stresses can vary significantly close to the surface (at least within some tens of metre depth). It is assumed that the maximum principal stress extrapolated to the surface would be, on average, in the range of what old data indicate.

The estimated stress magnitude in the area is given in Table 7-11. No new information is available on stress orientation. As in the previous model version, a rather horizontal σ_1 oriented at 134°, ± 15° is assumed to be realistic.

Table 7-11. Predicted in situ stress magnitudes in Forsmark.

Parameter	σ_1 based on overcoring	σ_2 based on hydraulic fracturing	σ_3
Mean stress magnitude	0.09*z + 4	0.028*z + 1.4	0.027z
Uncertainty, 0–500 m	± 20%	± 20%	± 20
Uncertainty, 500–1000 m	± 50%	± 50	± 20
Spatial variation, rock mass	± 15%	± 15%	± 15%
Spatial variation, fracture zones	± 50%	± 50%	± 50%

Mechanical properties

The estimates of the mechanical properties are obtained based on the surface mapping and core-loggings reported in Sections 4.6 and 5.2.

Uniaxial compressive strength of the rock

The results of all uniaxial testing from the SFR were presented in Table 4-17. It is estimated that the gneissic granite from SFR has properties that are rather similar to the granite in rock domain 29. Therefore the values in Table 7-12 are assumed to be realistic. From a mechanical point of view, the information on rock quality along the core from borehole KFM01A indicates mostly a very good intact rock. It is therefore not unlikely that the SFR data underestimates the strength of the intact rock in rock domain 29.

Table 7-12. Uniaxial compressive strength of gneissic granite (intact rock) from the SFR, assumed here to apply for rock domain 29

	Minimum	Average	Maximum
UCS [MPa]	80	230	330
E [GPa]	60	75	95
ν [–]	0.15	0.24	0.29
Density [g/cm³]	2.6	2.7	2.9

Based on the rock mass characterisation in Section 5.2.4 and Figure 5-6, an evaluation of the equivalent uniaxial compressive strength of the rock mass can be made based on empirical relations with the rock quality for domain 29. In Table 7-13, the ranges of variation of the strength of the rock mass are given for different depths. Also a tentative estimation of the rock mass tensile strength is reported here. Because borehole KFM01A does not intersect any fracture zones, the determination of the mechanical properties of the rock mass for poorer rock was left blank.

Table 7-13. Ranges of variation of the uniaxial compressive and tensile strength of the rock mass in rock domain 29 at different depths.

UCS [MPa]	Competent rock			Fracture zones		
	Minimum	Average	Maximum	Minimum	Average	Maximum
100–200 m	40	100	160			
200–400 m	50	130	200			
400–1000 m	60	170	220			
UTS [MPa]	**Minimum**	**Average**	**Maximum**			
100–1000 m	5	13	20			

Deformation modulus of the rock mass

The deformation modulus of the rock mass was determined in Section 5.2.4 according to the available relations with Q and RMR that assume a continuum medium. For rock domain 29, for which borehole information is available, the rock mass deformation modulus is reported in Table 7-14 for different depth intervals. Here, a tentative estimation of the range of possible variation of the deformation modulus of fracture zones in a similar rock mass as rock domain 29 is also given, based on the analysis of poorer rock section in KFM01A and some engineering judgements.

Table 7-14. Ranges of variation of the deformation modulus of the rock mass in rock domain 29 at different depths.

Em [GPa]	Competent rock			Fracture zones		
	Minimum	Average	Maximum	Minimum	Average	Maximum
100–200 m	25	40	60	3	–	10
200–400 m	30	50	70			
400–1000 m	40	70	85			

Poisson's ratio of the rock mass

For rock domain 29, the ranges of variation of the Poisson's ratio could be empirically determined and the results are reported in Table 7-15 for different depths.

Table 7-15. Ranges of variation of the Poisson's ratio of the rock mass in rock domain 29 at different depths.

| ν [–] | Competent rock | | | Fracture zones | | |
	Minimum	Average	Maximum	Minimum	Average	Maximum
100–200 m	0.10	–	0.18			
200–400 m	0.12	–	0.22			
400–1000 m	0.16	–	0.24			

Cohesion and friction of the rock mass

If the rock mass is assumed as an equivalent continuum, also the Mohr-Coulomb strength parameters can be determined through empirical relations with the rock quality. The rock mass strength linear envelope between normal stresses of 10 and 30 MPa for rock domain 29 is described in Table 7-16 by means of the equivalent cohesion (C') and friction angle (Fi') for different depth intervals. Not enough information was available to allow an estimation of the strength properties of fractured zones in a similar rock volume at the site. The estimated values in Table 7-16 were obtained by averaging the data in Figure 5-7.

Table 7-16. Ranges of variation of the cohesion and friction angle of the rock mass in rock domain 29 at different depths.

| C' [MPa]* | Competent rock | | | Fracture zones | | |
	Minimum	Average	Maximum	Minimum	Average	Maximum
100–200 m	16	20	30			
200–400 m	16	27	35			
400–1000 m	20	35	45			
Fi' [°]*	**Minimum**	**Average**	**Maximum**	**Minimum**	**Average**	**Maximum**
100–1000 m	20	37	45			

* Linear envelope between 10 and 30 MPa.

7.3.3 Thermal properties

In situ temperature

Temperature loggings from KFM01A indicate that the *in situ* temperature increases from about 7°C at a depth of 100 m to about 13°C at 600 m and about 18°C at the depth 1,000 m. The temperature gradient increases with depth, from about 11°C/km at the depth 400 m to about 14°C/km at 900 m. The temperature gradient curve has a relatively constant slope but there is a tendency for the gradient to be lower at larger depths (weak convex shape of the temperature gradient curve).

The behaviour of the temperature gradient could be explained by changes in thermal conductivity with depth, climatic changes in the past, and perturbations by drilling and water flow. This is planned to be further analysed in the next model version.

Thermal transport properties

Thermal conductivity has been calculated from mineral composition of a total of 71 rock samples (SCA-method). Results are categorized in both rock units and rock domains. Rock units and rock domains with only 1–2 rock samples are excluded from the following presentation.

Results for five rock units are available (≥ 3 samples). The rock unit with lowest mean value of thermal conductivity was "Felsic to intermediate volcanic rock, metamorphic" (rock unit 103076), 2.79 W/(m·K), whereas unit "Granite to granodiorite, metamorphic, medium grained" (rock unit

101057, dominates rock domain 29) exhibited the highest mean value, 3.33 W/(m·K). The first mentioned rock unit had the largest statistical variation (standard deviation), 0.42 W/(m·K) and the second rock unit had the lowest, 0.31 W/(m·K).

Results are available for 9 rock domains (≥ 3 samples). Rock domains 29 and 17 dominate the candidate area and the mean values of the thermal conductivity are 3.41 W/(m·K) and 2.73 W/(m·K), respectively. The corresponding standard deviations are 0.206 W/(m·K) and 0.216 W/(m·K), respectively. The other 7 rock domains have mean values in the range of 2.70–3.04 W/(m·K) with standard deviations in the range of 0.286–0.578 W/(m·K).

A Monte Carlo simulation of the thermal properties of borehole KFM01A has been performed with the simplified assumption that 90% of the borehole consists of rock types represented by rock domain 29 och 10% belongs to rock types represented by rock domain 17. The 95% confidence interval for the thermal conductivity data (simulated distribution) is 2.58–3.82 W/(m·K). The mean of the simulated distribution is 3.34 W/(m·K).

Comparisons between measured values of thermal conductivity (TPS-method) and calculated values (SCA-method) for rock units indicate a difference of less than 10% for a specific rock sample. Four rock samples were compared and differences of 1.9–8.8% in both directions were observed for the methods. Earlier comparisons indicate that calculations with the SCA-method produce lower values than measured, in the interval 5–8% /Sundberg, 2003b/.

Measurements of anisotropy of thermal conductivity, parallel and perpendicular to the foliation in the rock, did not give unambiguous results.

Uncertainties

Uncertainties regarding in situ temperature include:

- The increasing temperature gradient with depth is not fully explained and need to be further analysed.

- Temperature loggings are only available from one borehole.

Uncertainties regarding thermal properties:

- Only a few direct measurements of thermal properties have been made. Since the number of samples is low, the statistical basis is weak, and low accuracy is achieved in the comparison with calculated values.

- There are uncertainties in the representativeness of calculated thermal conductivities for different rock units and domains.

- Measurements (TPS) and calculation (SCA) of thermal properties are based on small scale samples. The relation between small scales (cm-dm) and the larger scales is not fully known. Most of the variation in mineral composition is levelled out at the dm scale but other factors may be of importance at larger scales.

- The anisotropy of thermal properties needs a closer investigation and details in the measurement technique must be carefully considered.

- There is a lack of data concerning thermal properties at elevated temperatures.

7.3.4 Hydrogeological description

Brief review of available data

The information extracted from the compilation of historical data and the data freeze 1.1 concerning the hydrogeological conditions in the bedrock 1.1 may be summarised as follows:

- The documentation from the historical investigations shows that the superficial bedrock is extensively fractured and that the thickness varies in space. Available borehole logs indicate an average thickness of several metres, possibly more.

- High transmissivities were recorded in the percussion-drilled boreholes at all drillsites, which indicate that there may be several extensive fractures/fracture zones. The borehole information suggests that all of these fractures/fracture zones are either gently dipping or close to horizontal.

- Fracture infillings classified as fine-grained sediments of Quaternary origin were encountered at different depths within the candidate area. The mechanism behind these infillings is not fully understood. The encountered sediment-filled fracture/fracture zones were generally of low transmissivity according to the flow logging performed at the completion of the percussion drilling. According to the BIPS logs, some of the impervious fractures/fracture zones lacked fracture infillings, which suggests either a heterogeneous fracture aperture and/or a heterogeneously distributed infilling.

- The overlapping difference flow logging in the cored borehole KFM01A suggests that the bedrock in the Forsmark area may be very low-conductive at depth. This hypothesis is supported by the historical information reported from the cored borehole DBT-1, drilled in the reactor area. Compared to the hydrogeological experiences gained in the past from the investigations of the study sites (Kamlunge, Gideå, Svartboberget, Finnsjön, Fjällveden, Klipperås and Sternö), the sparsely fractured and low conductive rock observed in the vicinity of KFM01A is considered exceptional.

Hydraulic rock domains (HRD)

The description of the hydrogeological properties of the rock domains between the fracture zones is highly dependent on the discrete fracture network modelling. It should be noted that the geological classification and the statistical analyses of linked lineaments, outcrop traces and borehole intercepts were based on a many assumptions, some of which need to be revisited as more data are gathered. In particular, the assumptions made for the derivation of a power-law size distribution is of key interest.

The geological classification of potentially conductive fractures is another example of a working hypothesis that needs to be revisited as more data are gathered. For model version 1.1, two different geological classifications of conductive fracture were used leading to two different values of the conductive fracture intensity, P_{32c}.

Above all, it is important to recall that the deep structural and hydraulic data available for model version 1.1 come from a single borehole only and that a minor portion of this borehole was possible to use only because of the absence of flowing fractures below c (–400) masl.

The positive correlation between fracture transmissivity and size presented in Section 5.4.6 constitutes a cornerstone in the hydrogeological description for model version 1.1, yet it must be considered as a working hypothesis. In theory, other relationships between fracture transmissivity and size may exist, including no relationship at all. To our current understanding, however, no relationship whatsoever between fracture transmissivity and size means a much more resistant flow system than a coupled flow system as is used for model version 1.1.

The transmissivity to size correlation used in the numerical simulations is given by Equation (5.14). The remaining parameter settings for the stochastic fracturing of the HRDs as used the numerical simulation are shown in Tables 5-39 and 5-40. It is noted once more that the conductive fracture intensity parameter in Table 5-39, P_{32c}, is of key interest.

By coincidence, the aforementioned change in the geological classification of conductive fractures allows for an assessment of the relative difference between the initial and the changed geological classifications impact on the hydrogeologic description of the HRDs. Regardless of how the two geological classifications of potentially conductive fractures were made, the practical implications for the hydrogeological description of the conditions in Forsmark are more or less the same. That is, either the hydraulic conductivity of the rock domains between the fracture zones is low or very low. Hence, the stochastic fracturing of the HRDs between the HCDs will not contribute significantly to the connectivity of the advective flow system. If the changed geological classification of conductive fractures is considered more correct than the initial classification, the situation becomes quite extreme, suggesting an essentially binary flow system consisting of large volumes of low-conductive rock between a limited number of large features of high transmissivity. If this is the case, a good description of the geometry and transmissivity of the deterministic fracture zones will become very important.

In consequence, the groundwater storage not readily accessible to advective flow constitutes, more or less, an immobile volume of groundwater accessible mainly through diffusion processes. The larger the immobile volume, the longer the "initial" groundwater conditions in the bedrock between the flowing fractures will be preserved. There are no data from data freeze 1.1 to support a quantitative discussion of this situation.

In model version 1.1, the assignment of sub-grid material properties was based on expert judgments rather than precise data. The equivalent hydraulic conductivity of the bedrock intersected by features less than 100 m was assumed to be homogeneous and isotropic, with a magnitude of $1 \cdot 10^{-12}$ m/s. The kinematic porosity was set to $1 \cdot 10^{-5}$ and the rock matrix (immobile) porosity to $1 \cdot 10^{-4}$. Hence, the mobile volume of groundwater in a 100-m cube of background bedrock was set to 10 m^3, whereas the immobile volume was set to 100 m^3. The motivation for using a ratio of ten between the immobile to mobile porosities comes from the experiences of the multi-rate diffusion modelling of non-sorbing tracer experiments (uranine) conducted by the Äspö Task Force.

Preliminary numerical simulations

The main objective of the numerical modelling was to underpin the hydrogeological description of the bedrock conditions. As mentioned above, the present structural model was used "as is" in combination with the results of the initial geological classification of conductive fractures. The justification for this focus is the vital role of the fracture zones (conductors) and the interconnected fractures within the rock domains as potential pathways of groundwater flow.

Numerical simulations of the palaeo-hydrogeological evolution come into play as a means of identifying the most important factors leading to the present-day conditions concerning the groundwater salinity distribution. Conclusive simulations of the palaeo-hydrogeological evolution, in turn, are of interest as a means of gaining credibility for the hydrogeological descriptive model.

Conclusive simulations require high-quality hydrogeological and hydrogeochemical measurements that can be used to constrain the result of the simulations and, hence, discriminate among tentative alternatives. At this point of the site investigations, the uncertainties are still too many and too large for such a discrimination, which implies that the simulation results for version 1.1 are, at the best, indicative.

The simulations of the past palaeo-hydrogeological evolution were conducted between 8,000 BC and 2,000 AD (present). The simulation results appear to be fairly realistic with regards to fluxes and salinities, despite the geological uncertainties in the fracture zone description. However, there are few or no field data to compare the simulation results with, which means that the interpretation is somewhat diffident.

Using a sparse network to represent the conditions seen in the HRDs causes pockets of various water types in the bedrock. The water type simulations also indicate that impact of the Litorina period may be considered as a natural tracer experiment. However, the data available for version 1.1 represent the most conductive parts of the uppermost part of the bedrock flow system down to c (–200) masl. Hence, there are no salinity data from repository depth or below and no data about the salinity in the rock matrix. When salinity data from depth and from the rock matrix become available, it will be fruitful to repeat the palaeo-hydrogeological simulations, hopefully with a more realistic geological description of the sub-horizontal or gently dipping fracture zones.

7.3.5 Hydrogeochemical description

Groundwater composition

The detailed evaluation of the groundwater observations indicates the following features /Laaksoharju et al, 2004/:

Descriptive observations

- Dilute surface waters, mostly represented by the Lake and Stream samples, are usually characterised by very short residence times (days to some years) and high tritium and ^{14}C.

- Dilute near-surface waters, mostly represented by the Soil Pipe waters, but also some discharging groundwater to the surface Lakes and Streams, are probably characterised by longer residence times (months to some years). Despite this, similarly high tritium values are obtained for the surface-derived waters although ^{14}C (based on only a few data) appears to be a little lower due to dissolution of calcite and/or decomposition of organic material.

- Baltic Sea water which in the coastal bays is mixed with varying amounts of: a) meteoric waters (i.e. direct precipitation run-off), b) stream water input, and c) in places discharge of deeper groundwaters.

- Other marine sources with higher salinity are involved, in particular, Litorina Sea water or Litorina Sea/glacial water mixtures with chloride contents of around 4,000–5,500 mg/L and δ^{18}O values between –10 and –12‰ SMOW. For example, taking the SFR data into account, a dilution line between a fresh glacial meltwater with a δ^{18}O of –25‰ SMOW and a Litorina Sea water of 6,500 mg/L Cl and –4.7‰ SMOW can be calculated, corresponding closely to some of the Forsmark data.

- The Litorina Sea water component (twice as saline as the present Baltic Sea water) has intruded into, and mixed with glacial melt waters, some 7,000–5,000 years ago. This glacial-Litorina mixture, where preserved in the bedrock, has in some fractures mixed with present Baltic Sea water and, during the last 1,000 years, probably also with meteoric water. Only in hydraulically favourable 'pockets' or 'lenses/horizons' (e.g. HFM08 between 93–143 m) has a stronger Litorina signature been recorded.

- At present, the indication of Litorina Sea water is based on the δ^{18}O vs. Cl relationship and also the higher Mg and SO_4 contents when compared with saline waters of brine type. With additional data it is hoped to be able to better differentiate between Baltic, Litorina and deep non-marine saline waters.

- Processes in the bedrock fracture systems such as ion exchange (e.g. with clay fractions) have modified the marine water components causing a decrease in Mg and Na and enrichment of Ca. As shown by the Soil Pipe samples, ion exchange with the sediments may have occurred although the mixing with deeper discharge groundwaters richer in Ca cannot be ruled out.

- In one example (HFM05) the decrease in sulphate content and higher δ^{34}S values might indicate activity of sulphate-reducing bacteria.

Modelling outcomes

- Based on the general geochemical characteristics and the apparent age two major water types are present in Forsmark: fresh waters with a bicarbonate imprint and low residence times (tritium values above detection limit), and brackish-marine waters with Cl contents up to 6,000 mg/L and longer residence times (tritium values below detection limit).

- The chemistry of the first water type is mainly controlled by the chemistry of the recharge waters and, most importantly, by water-rock interaction processes in the overburden (surface/ near-surface). Locally, these waters can mix with marine components changing their chemical composition towards more chloride-rich members. Under these conditions, the major water-rock interaction processes are organic matter decomposition, dissolution of the more soluble phases such as calcite and sulphides and the alteration of the upper granitic bedrock. Primary and secondary silicates and aluminosilicates are related by incongruent reactions which seem to control silica and aluminium contents and participate in the loss or gain of elements such as K, Mg and, to some extent, Na (through dissolution-precipitation or ion exchange processes).

- Waters from the brackish-marine type representing deeper bedrock groundwaters have a longer residence time and a higher mixing component with older waters with different origins. Heterogeneous reaction processes, although less important than in the first water type, can be described mostly by the same set of minerals; a major difference is that calcite is precipitating instead of dissolving. Also, in some of these waters microbially mediated reactions and dissolution-precipitation of Fe-mineral phases become important in controlling sulphate and iron contents, as well as the redox state of the system.

Processes and boundary conditions

The major processes affecting the local chemistry at Forsmark are summarised in Figure 7-16.

Figure 7-16 is based on an integration of:

- Measured salinity variations with depth derived from the percussion and cored boreholes; the measured values are from open boreholes in addition to isolated packed-off borehole sections and lengths. Open hole electrical conductivity logging has been utilised also. Estimations of the high saline interface (> 5,000 mg/L), non-saline interface (< 1,000 mg/L Cl) and extent of the brackish groundwaters (1,000–5,000 mg/L Cl) are indicated.

- Modelled calculations integrating the inverse modelling in PREEQEC to explain the evolutionary reaction paths and mixing proportions of the Forsmark groundwaters, with the M3 mixing modelling approach used to select appropriate groundwater end-members. The modelling is preliminary and will be updated when down hole pH and Eh measurements are available for all the samples.

The present state of hydrogeochemical knowledge from modelling of the Forsmark groundwater water system is that the main water-rock interaction processes that affect the chemistry are: (i) decomposition of organic matter, (ii) calcite, plagioclase, biotite and sulphide dissolution, (iii) Na-Ca ion exchange, and (iv) phyllosilicate precipitation. The generic reaction model will be refined when more data concerning the mineralogy of the system and its hydrological functioning become available.

The mixing modelling (Figure 7-16) indicates that two water types dominate, meteoric water and marine water affected by Baltic Sea water and possibly by Litorina Sea water (see also Figure 7-15). The meteoric type of water shows typical seasonal variations. Closer to the coast and with depth the influence of marine water is detected.

As for the brackish-saline waters, the modelling points to a mixing process with multiple end-members as the principal control on their chemistry. The main compositional variations between the brackish (< 5,000 mg/L Cl) and the saline (6,000 mg/L Cl) waters can be explained by an increase in the proportion of the Litorina end-member (see also Figure 7-15). The role of water-rock interaction processes in these waters is assumed to be much less important than in the fresh waters, and secondary to the mixing process. It is important to note that the mixing modelling do not explain the water rock interactions included in the formation of the end-members, e.g. formation of the Brine. This circumstance allows the calculation of the mixing proportions even without a precise knowledge of the detailed mineralogy of the system. However, the influence of the sulphate-reduction processes on the final mixing proportions has not been evaluated rigorously enough and it is therefore likely that further detailed studies would produce a refinement of the generic reaction model used in the present calculations.

The results from the redox modelling suggest that the redox state of the brackish waters from the shallow depth interval (centred at 115.33 m) at borehole KFM01A could be buffered by the presence of iron oxides and hydroxides and by redox reactions among phyllosilicates. The lack of specific mineralogical data precludes a definitive confirmation of this conclusion. On the other hand, the good match between the sulphur redox-pair and measured Eh values points to sulphide minerals as redox buffers. This buffering action, together with the presence of dissolved sulphides, suggests the development of an anoxic-sulphidic state mediated by sulphate reducing bacteria (SRB). Typical precipitation of sulphide minerals associated with this environment is suggested by the equilibrium between the waters and several monosulphide phases, as deduced from speciation-solubility calculations. Note: Pyrite is a relatively common fracture phase but it has not been possible yet to confirm mineralogically these modelled predictions.

The modelling indicates also that the groundwater composition at shallow depth, i.e. far from repository depth, is such that the representative sample from KFM01A:110–121 m can meet the SKB chemical stability criteria (Table 7-17) for Eh, pH, TDS and Ca+Mg /see Anderson et al, 2000/.
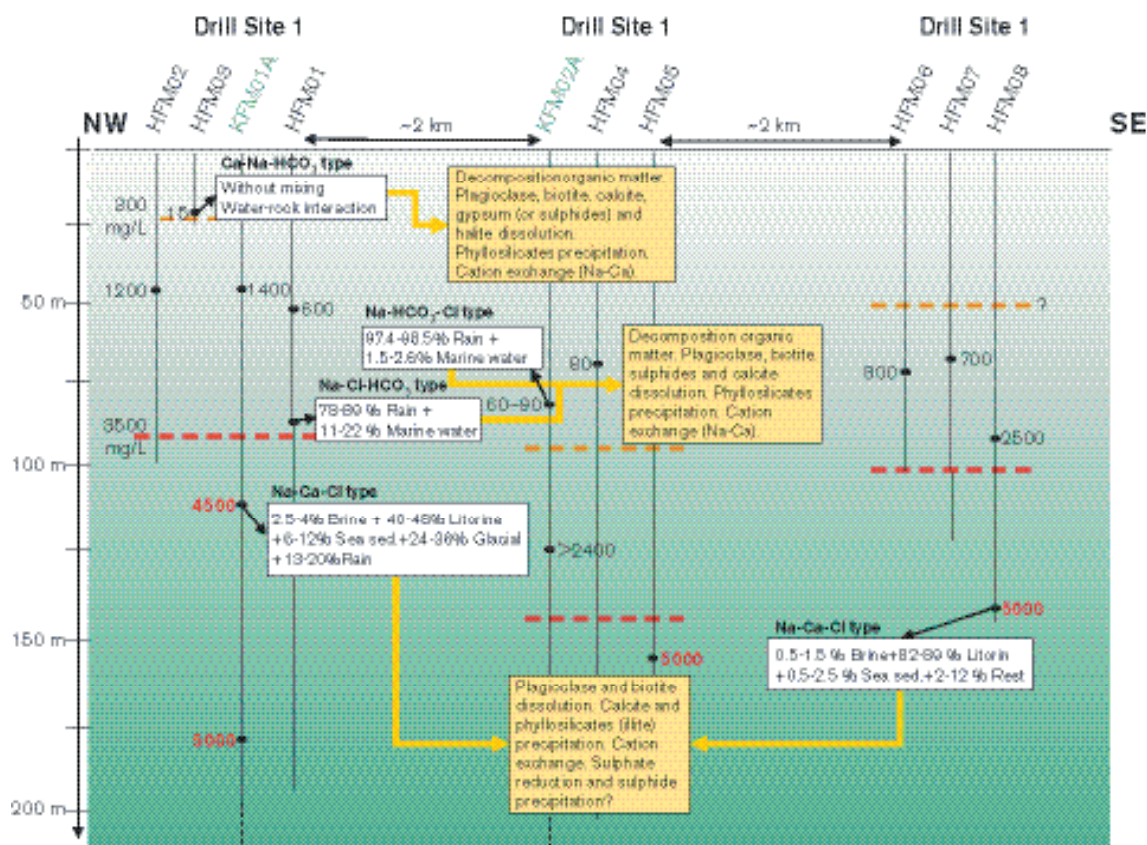
Figure 7-16. Integrated conceptual visualisation of the local hydrochemistry at Forsmark site is based on integration of: 1) Salinity distributions based on measured Cl concentrations (in red) and electrical conductivity values (in black); the saline interface is at > 5,000 mg/L Cl, the non-saline at < 1 000 mg/L the brackish water is between 1,000-5,000 mg/L, Cl, and 2) Modelled evolution paths of the non-saline and brackish-saline groundwater. For each sample the mixing proportions and the main heterogeneous reaction processes are indicated. Mixing calculations are based on inverse modelling in PHREEQC but uses M3 mixing models and expert judgement for selecting appropriate end-members.

Table 7-17. The hydrochemical stability criteria defined by SKB are valid for the analysed values of sample KFM01A (110–121 m).

	Eh mV	pH (units)	TDS (g/L)	DOC (mg/L)	Colloids* (mg/L)	Ca+Mg (mg/L)
Criterion	< 0	6–10	< 100	< 20	< 0.5	> 4
KFM01A: 110–121 m	−180	7.5	7.8	NA	NA	1016

NA = Not analysed

7.3.6 Transport properties

The resulting site-descriptive model for transport properties in model version 1.1 for Forsmark consists of two separate parts. First, a parameterisation of the intact rock (rock matrix) for the processes matrix diffusion and sorption has been made. Secondly, a characterisation of flow paths from depth, primarily with respect to transport resistance, has been performed.

Since no site-specific data on transport properties are available from cores or from boreholes, an attempt has been made to relate existing data from near-by Finnsjön to Forsmark. Specifically, the formation factor has been evaluated for Finnsjön rock materials with mineralogical and geological characteristics similar to that of rock domain 29 in Forsmark. The results indicate that the obtained formation factor is of the same order of magnitude as the one used in previous safety assessments. Thus, based on this limited knowledge, there is no support for assuming other formation factors, and hence, effective diffusivities, for Forsmark than used previously. The uncertainty in the assessment of the effective diffusivity is large, since only few data, originating from a different site, have been used.

The transport resistance has been calculated for three flow paths originating from different locations within the candidate area. The resulting values indicate a good transport resistance, but with a large spread (see Section 5.6.4). Thus, one may expect large variability in transport resistance when the whole domain is considered. Also, the obtained results may be biased by the limited information used when setting up the hydrogeological models.

8   Conclusions

8.1   Overall changes since previous model version

Version 1.1 of the Forsmark Site Descriptive Model is the first model version based on information from the Site Investigation. Before the start of the initial site investigation in Forsmark, version 0 of the site descriptive model was developed /SKB, 2002a/. This model version 0 serves as a platform for the development of new versions during the initial site investigation and during the complete site investigation.

As further explored in Section 6.6 there are two types of principal changes in version 1.1 compared to version 0 /SKB, 2002a/. One concerns additional features/content of the model and the other concerns actual changes in the understanding of the site.

Compared with version 0 there are considerable additional features in the version 1.1, especially in the geological description and in the description of the near surface. This is only natural since there is a considerable increase in data compared to the data available for version 0. In summary, these additions and updates concern:

- The geological model based on on-site borehole information and much higher resolution surface data. A discrete fracture network (DFN) model has also been developed.

- The rock mechanics model is based on strength information from SFR and an empirical, mechanical classification by depth at KFM01A and at outcrops.

- A first model of thermal properties of the rock has been developed, although still rather immature due to few site-specific data in support of the model.

- The hydrogeological description is based on the new geological (structure) model and the fracture transmissivity distribution of the DFN model is based on the data from depth (KFM01A). Hydrogeological simulations of the groundwater evolution since the last glaciation have been performed and compared with the hydrogeochemical conceptual model.

- The conceptual model of the development of post-glacial hydrogeochemistry has been updated. Also, the salinity distribution, mixing processes and the major reactions altering the groundwaters have been described down to a depth of 200 m and a Hydrogeochemical Site Descriptive Model version 1.1 has been produced.

- A first model of the transport properties of the rock has been presented, although still rather immature due to lack of site-specific data in support of the model.

- For the near-surface there is additional information regarding the stratigraphic distribution of glacial till and water-laid sediment, with related updates in the description.

The main changes include:

- The existence of highly fractured sub-horizontal zones has been verified and these are now part of the model of the deformation zones.

- The fracture intensity decreases with depth (below 400 m).

- Very low permeability below 400 m (modelled as decrease in conductive fracture intensity).

- Strong variability in depth (thickness) of the Quaternary deposits.

It was expected that the site should be quite low-permeable, but the very low fracture intensity and very tight rock below 400 m in borehole KFM01A was more extreme than expected. This may also have rock mechanics implications. Also the variability in depth (thickness) of Quaternary deposits and that it was fairly uncorrelated to the bedrock surface variability was not fully expected. These findings suggest that the overall understanding of the Forsmark site may be more an issue than in general in the Fennoscandian crystalline basement.

8.2 Overall understanding of the site

The overall understanding of the site is addressed in Chapter 6 – confidence assessment. The following section draws on the conclusion made there.

8.2.1 General

As further discussed in Section 6.3 there is much uncertainty in version 1.1 of the site descriptive model, but the main uncertainties have been identified, some are also quantified and others are left as input to alternative hypotheses. However, since a main reason for uncertainty in version 1.1 is lack of data and poor data density and as much more data are expected in coming data freezes, it has not been judged meaningful to carry the uncertainty quantification or the alternative model generation too far. These efforts would soon be outdated, whereas the types of uncertainties and alternative hypotheses identified are judged to be very useful input to the uncertainty and alternative model assessment in coming model versions.

Numerous interdisciplinary interactions are considered and good cross-discipline understanding of the interactions has been established. There is direct consistency in geometry between the geological, rock mechanics, thermal and bedrock hydrogeological models. However, no attempts were made, mainly due to lack of data from depth in the bedrock, to quantitatively explore implications from e.g. rock mechanics, hydrogeological or hydrogeochemical measurements on the geological description. Such evaluations are expected in coming model versions.

The model as presented is in general agreement with current understanding of the past evolution, but the overall hydrogeochemical understanding of the site is restricted to the processes taking place at the surface and down to a depth of 200 m. The confidence in this description is high since independent model approaches were utilised in the work. The origin and the post glacial evolution of the water is fairly well understood. The confidence concerning the spatial variation is low due to few observations at depth. The ongoing sampling programme will provide better spatial information and will increase this confidence.

Compared to version 0 there are considerable additional features in the version 1.1, especially in the geological description and in the description of the near surface. In terms of actual changes of the understanding of the site there are no really big surprises.

The overriding issue affecting confidence in models based on the version 1.1 data freeze is the bias and uncertainty resulting from varying spatial coverage of data and very few and unidirectional deep borehole data. These biases will evidently be rectified in coming model versions.

8.2.2 Advance on important site-specific questions

In planning the execution programme for the Forsmark area /SKB, 2002b/ some important site specific questions were formulated. They concerned the *three-dimensional shape of the tectonic lens, potential for ore occurrence at depth, occurrence of gently dipping fracture zones and the occurrence of high rock stresses*. Based on model version 1.1 the following advances have been made on these questions:

- The understanding of the three dimensional shape of the rock domains in the local model area is now fair, even if there still remain uncertainty on the extension of rock domain boundaries at depth, especially outside the candidate area (see further discussion in Section 5.1.2 and Section 6.3).

- A special study /Lindroos et al, 2004/ has evaluated the ore potential of the site. It concludes that the Forsmark candidate area is virtually sterile with respect to ore, although some additional assessments and measurements might be advisable to completely rule out the possibility.

- Model version 1.1 contains some near-horizontal, permeable fracture zones, but it is also noted (see Section 6.3) that the extension in both the strike and dip directions as well as the hydraulic properties of these zones are still uncertain. Furthermore, other sub-horizontal zones may possibly exist in addition to the ones in the version 1.1 model.

- Due to lack of on-site rock stress measurement in version 1.1 the understanding of the rock stress distribution has not advanced very much in model version 1.1.The very low fracture intensity and very tight rock below 400 m in borehole KFM01A was more extreme than expected. This may also have rock mechanics implications.

In conclusion, it seems that the remaining issues after model version 1.1 are the sub-horizontal deformation zones and the rock stress distribution. In addition, uncertainties still exist on several other issues as already noted in the previous section.

8.3 Implications for further modelling

The model version presented in this report will soon be updated with data available at the next data freeze. In preparation for this updating work it is necessary to assemble experience, both regarding technical/scientific issues and modelling procedures, which could be considered for the coming modelling work. Experience on both these aspects has been assembled during the course of the modelling work, and has also been discussed at some of the modelling project meetings.

8.3.1 Technical aspects and scope of the version 1.2 modelling

The requirements on resolution and accuracy within the model volume in local and regional scale primarily depend on the needs within Safety Assessment and Repository Engineering. If very high resolution and very low uncertainty are needed in the local model, its current volume will need to be reduced. However, model version 1.1 does not really have a spatial coverage to allow for assessments on where such focusing would be worthwhile. For model version 1.2, where also the expected data will cover a large volume, the selected size of the local model may possibly be retained, but the modelling must be able to serve as a background for this focusing.

Data freeze 1.2 will include several deep boreholes with associated loggings, geophysics, rock mechanics, hydrogeological and chemical tests. This will potentially improve the description of the bedrock, but also implies several modelling challenges. The need for integration between disciplines will increase. This e.g. implies that:

- the geological modelling will need to consider input, mainly from rock mechanics and hydro-geology, in evaluating possible geometrical alternatives,

- modelling the rock stress development using the geological model may be a means to enhance the understanding of the rock stress distribution,

- hydraulic interference tests and interference observations between boreholes would require more exploratory hydrogeologic modelling in order to make use of the new information and to explore how the site works,

- a 3D hydrochemical description of the site should be produced, which together with enhanced capacity for modelling the surface waters and existence of water samples from depth would allow for more conclusive integration between hydrogeological and hydrogeochemical modelling.

There will be a need to pay more attention to alternatives, as this would be required by the users of the models and as the added data would allow for more meaningful alternatives to be developed. In particular:

- Given the importance of the lineaments for the continued deformation zone modelling it may be worthwhile to carry out an alternative, independent lineament interpretation, within the local model area, using another team, in order to explore its sensitivity to "modelling style".

- Various assumptions regarding the fracture transmissivity distribution and its correlation to size and fracture orientation should be explored.

The use of independent modelling approaches within the hydrogeochemical modelling gave a possibility to compare the outcome of the different models and to use discrepancies between models to guide further modelling efforts. The noted similarities in the modelling results gave confidence in the obtained results.

8.3.2 Modelling procedures and organisation of work

Experience has also been gained on the modelling procedures and organisation of work. Generally, it must be concluded that interdisciplinary modelling is a continuous learning processes and that this learning process must go on also in coming modelling steps. During the course of the version 1.1 modelling, the following observations were made on issues that would benefit from improvements in coming steps.

Capturing and evaluating the primary field data, as presented in Chapters 2 and 4 of this report, is a very demanding effort. Possibly, the procedures and experiences developed during the version 1.1 modelling work will make this step less cumbersome in the future modelling.

Some method development, geological single-hole evaluation in particular, was not completed at the onset of the modelling. However, these methods have now been established, which should allow for an easier analysis in the future.

The information exchange with the on-site investigation activities has been extensive, but can still be improved. For example, the data freeze makes the modelling work potentially out-dated if new data are obtained during the investigation programme and the necessary interaction with the people on the site may be confused. The concept of a data freeze is necessary to allow traceability and consistency in the staged modelling. It must be clear what the information base for the modelling is and this information base must be shared among disciplines. Still, means of improving the dynamics between the investigation work and the modelling work would be very helpful, although possibly this potential information mismatch may decrease as the new findings in the site investigation data level off.

As already stated, the coming model versions will require further integration efforts. Careful activity planning with assessment of when and what results different disciplines need to deliver to other disciplines will be required. Furthermore, an increased strictness in meeting these requirements in deliveries, as set out in this planning, is needed.

Finally, the reporting needs further development, both as regards structure and style. One obvious conclusion for coming steps is to define and establish additional supporting documents, which would allow less detail in the modelling report itself. Dividing the report into different volumes is another possibility.

8.4 Implications for the ongoing site investigation programme

One of the objectives of the site modelling project version 1.1 is to give recommendations on continued field investigations during the initial site investigation, based on results and experience gained during the work with the development of the site descriptive model version 1.1. The recommendations arising from the work with model version 1.1 are compiled in this section divided into recommendations or feed-back that have been given to the site investigation organisation during the course of the modelling work and recommendations arising from the uncertainties in the model version 1.1.

8.4.1 Recommendations/feed-back given during the modelling work

During the work with model version 1.1, the project group has had continuous information exchange with the site investigation team, among other things concerning questions related to the field investigation programme. These questions have ranged from more extensive ones, like where drilling should be carried out, to details e.g. concerning sampling methods. Recommendations given on the siting of new drill holes have been documented in so called decision papers. Recommendations and feedback from the hydrogeochemical modelling work have also been provided in various documents. However, much of the feedback to the site investigation team has been given in a more "informal" form via mail, via telephone, in meetings and so forth, not necessarily associated with a documentation of the contents of the feedback. A log has been used in order to try to keep track of some of this "informal" information exchange.

Recommendations concerning drilling of new holes

On account of the rapid progress made with the drilling activities in the Forsmark candidate area and the necessity to maintain continuity in the drilling programme, a need to select the site for borehole KFM04 developed somewhat earlier than included in the original planning. On request from the site investigation team at Forsmark the modelling project completed the task and provided recommendations concerning the siting of the cored borehole KFM04A and two percussion boreholes along the Eckarfjärden fracture zone. These recommendations were documented in a decision paper (Appendix 6).

The rapid progress made with the drilling activities in Forsmark was also the cause of a second request from the site investigation team on selection of a site for the cored borehole KFM05. Again the modelling project completed the task and recommended a location for borehole KFM05 east of Lake Bolundsfjärden. The recommendation was documented in a decision paper (Appendix 7), which also contained suggestions on the location of a future additional drilling site north of Bolundsfjärden, just east of Lake Puttan.

A question that has been discussed between the geologists in the model project and the site investigation team is how well lineaments of various character (low magnetic, high electrically conductive and topographic) reflect fracture zones. The uncertainty mainly concerns short, topographic lineaments in areas where the Quaternary cover is substantial. These lineaments might rather reflect the Quaternary history than being an indication of a fracture zone in the bedrock. As a result of these discussions, and written recommendations from the geologists in the project group (Appendix 8) a percussion drilling programme was set up and drilling started in autumn 2003. The aim of this programme was to assess the presence and character of a limited number of possible regional or local major fracture zones in the candidate area that are based on the interpretation of lineaments.

In connection with the motivation for the selection of the site for and the orientation of the cored borehole KFM05A, it was recognised that a second cored borehole may be necessary to the east, in order to ensure that the lineaments with NS trend through Bolundsfjärden are sufficiently well-understood. A site was proposed (Appendix 7) and this suggestion was adopted by the site investigation team who established drillsite 6 at the proposed location. On request, an additional document with recommendations and motivations to the orientation of the cored borehole KFM06 was prepared and delivered to the site investigation team (Appendix 9)

Feed-back to the hydrogeochemical site investigation programme

The hydrogeochemical analyses and modelling work has been carried out by a group of experts, the Hydrogeochemical Analysis Group (HAG). During their work, they have continuously provided feed-back to the hydrogeochemical site investigation programme via the activity leader for hydro-geochemistry at Forsmark. The feed-back as well as the response from the site has been documented by the representative for hydro-geochemistry in the modelling project and this documentation is reproduced in Table 8-1.

Log for "informal feedback"

An attempt has been made to keep track of "informal" information exchange between the modelling project and the site investigation team. In order to exemplify the type of information contained in the log, extracts related to feedback from the modelling project to the site investigation team are shown in Table 8-2. It should be emphasised that this log-file in no way claims to contain all information exchange of informal character that have been taken place during the work with model version 1.1, since the content is restricted to information exchange that the project leader has been aware of.

Table 8-1. Hydrogeochmical feed-back from the modelling project (HAG) to site investigation and the response from the site investigation.

Feed-back	Response
All samples should have x, y, z coordinates in order to be useful in the visualisation work.	The z-coordinates are missing for surface samples such as lakes since the SICADA database can not handle coordinates that varies with time for a sampling point. A reference level will be used for future sampling so the z-coordinate can be calculated.
The tube samplings in boreholes with low hydrogeological conductivity are of limited use for reflecting water compositions in fractures. But the information may be useful for reflecting the disturbances in the open borehole.	The electrical conductivity measurements will be used to guide when tube sampling can add more information.
Much more background information is required to evaluate sample representativeness. For example: a) At which stage during the Chemac monitoring of pH, Eh, O_2 and Temp. is it decided to take samples and why? b) When there are time constraints and it is not possible to wait for chemical stability - sampling should be planned to cover the complete sampling period, rather than choosing just one time interval. This will give a spread of sampling which should also show up time variations which can be important. c) SICADA only indicates the 'Start' and 'Completion' dates of the sampling. It is necessary to know the actual day of sampling for proper evaluation. d) Information concerning drilling/sampling protocols (e.g. pump stops; other pauses etc.) and the sequences of events carried out in the boreholes are needed. Some of this information (sampling protocol) was forthcoming from Simpevarp but not Forsmark.	Chemac measurements were not included in the "data freeze" and much of the above information will be available for the next model version.
Analytical questions have been taken up with the site and moves are being made for improvement (e.g. Br data quality; U-series data). Also proper presentation of some data to the required precision (e.g. Sr isotope ratios; B[11] etc.) have been improved in the SICADA data base.	
The flushing/drilling waters should be allocated Class 5 status which is useful to track contamination especially trace elements and isotopic signatures which may be quite sensitive.	The used Class 3 status should be sufficient for tracing contamination since most of the isotopes included in class 5 is optional in the Class 3 program.
Some data such as REEs are always below detection limits with the result that all granitic waters will show the same range of REE contents. Can other analytical techniques be used so this information can be used in models?	The technique used is ICP-MS and INAA will not provide an improved resolution.
DIS (Drilling Impact Study) should be made during drilling in order to identify the degree of contamination and guide the sampling strategy. The drilling data should be available earlier concerning: a) the drilling water volume pumped in and out from the borehole, b) the uranine concentration in the drilling water pumped in and out from the borehole, and c) the water pressure along the borehole. The drilling water volume and the uranine records in the water pumped in and out from the borehole should be done simultaneously in time to make a comparision possible.	This is generally a logistic problem and much of the needed information for DIS evaluation is available only after accomplishing the drilling work and processing the data or after performing DIFF measurements.
The fracture minerals in the drill cores from the Forsmark site (only the first three KFM01A, KFM02A and KFM03A have been sampled so far) are not as well-preserved as expected from triple tube drilling. Instead, many fractures/and fractures zones show loss of loose material, disturbances of surfaces and grinding of fracture coatings. This significantly reduces the possibility of getting good samples for palaeohydrogeological interpretations. For example, low temperature minerals like clays and calcite are the minerals that are most easily destroyed and/or flushed away. It is therefore important to improve further drilling methodology in order to get intact drill cores suitable for hydrogeochemical investigations.	The site will make a test by changing the drilling team and equipment.

Table 8-2. Example of items related to feed-back to site investigation extracted from log for "informal" information exchange between the modelling project and site investigations (original log-file is in Swedish).

ID	Specification	When?	Follow up?
03	Need to compile and interpret data on depths of Quaternary deposits and location of upper surface of the bedrock.	February 2003	Yes (see ID11)
04	Important that the problem with "black gauge" in the drillholes is solved.	February 2003	Yes (see ID12
05	Asked for more transparent print-outs from the planning tool in order to get a better overview of the on-going and planned field activities.	February 2003	Yes (see ID16)
06	Reply to the question from SI regarding the need for more detailed analyses of gas that has been observed during the work with lake mapping. Reply: Of primary interest to find out if it is marsh gas or deep gas. Should, however, also be checked with Safety Assessment.	February 2003	Yes (see ID09)
07	Input regarding siting and orientation of KFM01B in order to give as much information as possible, not only rock mechanical data. (minutes project meeting #4). Also suggestions on measurements (minutes project meeting #5).	February, March 2003	
08	Modelling group asked for prioritisation of geologic single-hole interpretation of percussion-drilled holes so that results will be available in time for data freeze 1.1.	March 2003	Yes (see ID14)
09	Response to Site Investigation that SA (Ulrik K) primarily is interested in knowing if the gas is deep or surficial gas. In a later stage it will be interesting to measure the flow of gas.	March 2003	Yes
11	Sven Follin takes the responsibility for an Activity Plan for compilation of depths of QD.	March 2003	
12	Model group gives suggestions on how to keep drilling tubes in between drilling in order to avoid corrosion and rust that can contaminate the boreholes during drilling (minutes project meeting #5).	March 2003	Yes (see ID19)
13	Model group suggested that porewater analyses of clays should be carried out to get information on the salinity in the porewater.	March 2003	
14	Respons from SI that there will be no geologic single-hole interpretation of percussion-drilled holes in time for data freeze 1.1, but that all data necessary for such an interpretation will be available.	March 2003	
19	Written document to SI from the HAG-group highlighting the importance a cored borehole for complete chemical characterisation that is free from black gauge.	April 2003	
20	Model group recommends that VSP is carried out in KFM03A as soon as possible so that results will be available in time for data freeze 1.2.	April 2003	Yes (see ID36)
34	Discussions with SI concerning how to carry out a percussion-drlling program for investigation of critical lineamnets in the candidate area.	November 2003	
35	HAG-group (E-L T) express concerns about the quality of drillcores. Fracture filling materials are flushed away during drilling.	November 2003	
36	Model group asks about plans for geologic single-hole interpretation and VSP. Reply: geologic single-hole interpretation will start in the beginning of 2004. No defined plans yet as to VSP measurements.	November 2003	Yes

8.4.2 Recommendations based on uncertainties in the integrated site descriptive model version 1.1

The site-specific critical issues that were raised in FUD-K /SKB, 2001b/ and later in the planning of the site investigations in Forsmark /SKB, 2002b/ are in essence still valid, see Section 8.2.2. Model version 1.1 provides a certain increase in understanding of the geological features of the site, but large uncertainties in the site description still remain. These uncertainties are shown and discussed in Section 6.3 where it also is concluded that the main reason for these uncertainties is the lack of data from depth in the bedrock and poor data density. Using these uncertainties as a starting point, the project group has made an effort to assess whether the identified uncertainties will be reduced by additional site data and if so, how those data should be obtained.

The assessment was carried out by filling in a table with the following information:

- A specification of the uncertainty in model version 1.1 and the cause of this uncertainty, i.e. the information already documented in the protocols described in Section 6.3.

- An assessment of how much this uncertainty can be reduced by additional data that will become available for model version 1.2 and how this can be achieved.

- An assessment of how much the uncertainties remaining in model version 1.2 can be reduced by site data provided during the complete site investigation phase and how this can be achieved.

The results of the assessments are shown in Table 8-3 and summarised below. No specific recommendations are given in Table 8-3 on site investigations to reduce uncertainties in transport properties of the rock. The reason is that no site-specific data at all were available for version 1.1, but some data will be available for model version 1.2, according to the strategy document for laboratory measurements of transport properties in the rock /Widestrand et al, 2003/. Therefore, it is premature at this stage to suggest additional measurements prior to the initialisation of the planned strategy.

Location of boreholes

Obviously, continued drilling and new borehole information from investigations during and after completion of drilling will contribute to an improved description of the bedrock. As already indicated in Section 8.3.1, the need of a reduction in the local model volume has developed during the work with model version 1.1. This will also imply a focusing of future drilling activities and accompanying investigations to a smaller area. However, model version 1.1 cannot give input to the selection of this target area, but it is envisaged that the interpretation and modelling of the extensively larger data set that will be available for model version 1.2 will provide the basis for this. This requires though that critical data, like results from stress measurements from the drillsites 1, 2 and 3, are reported in time for data freeze 1.2.

Even with a future focusing of new holes to a smaller area, some new holes upstream and downstream of the candidate area might be needed for verification of hydrogeological and hydrogeochemical conditions.

Occurrence, geometry and properties of deformation zones

The occurrence and geometry of deformation zones are associated with large uncertainties. This is also the case for near-surface, sub-horizontal zones. Suggested field activities in order to reduce these uncertainties in model version 1.2 and in later versions are:

- Field investigations of selected lineaments in order to confirm the occurrence of zones are carried out by stripping away the Quaternary cover.

- Vertical Seismic Profile, VSP, measurements in selected boreholes and seismic reflection profile measurements at the surface, which can give valuable information on the occurrence of zones and their geometry.

- Hydrogeological interference tests between boreholes, which can give information on the occurrence and continuity of deformation zones.

Fracture statistics – fracture mapping

The present version of the DFN-model is based on several assumptions, which need verification. For example, this concerns whether surface mapped fracture sizes could represent the fracture size distribution at depth and whether the fracture traces on the surface should be statistically related to the size distribution of lineaments (which in fact are made up by small fractures).

In order to check the representativity of fractures mapped on the surface there is a need for fracture mapping on drill cores at shallow depth (i.e. including the first 100 m) and in various directions. Due to the orientation bias, KFM01A and the mapped surfaces essentially displays different fracture sets – and tests on the consistency between these mappings cannot be made meaningfully. Some multiple directional borehole data will be available in data freeze 1.2, but additional holes may be required. Interaction with the hydraulic DFN-modelling and its interpretation of interference tests is also essential for this.

Another assumption concerns the couplings between fracture intensity and lineaments. Detailed fracture mapping in rock domains outside rock domain 29 may give more input to the uncertainties associated with these assumptions. This can possibly be combined with specified field investigations giving input to estimates of the proportions of different rock types in rock domains.

Rock stress distribution – rock mechanics properties

The uncertainty in rock stress magnitudes and distribution with depth will probably be reduced significantly by the measurements planned for data freeze 1.2. Given the importance of the issues, additional rock stress measurement and mechanical tests may still be needed, especially in the tentative construction area (to be selected).

Transmissivity distribution – hydraulic tests

The uncertainty in geometry of water-bearing structures and transmissivity distribution in zones and fractures will be reduced by enhanced understanding of the geological structural model and by interpreting information from additional boreholes and hydro tests. Such data will be available already in data freeze 1.2. However, in order to address key issues – like the transmissivity/size relation there is a need to change the current program of investigation and focus more on hydraulic interference testing.

Groundwater composition – rock matrix pore water

The conceptual understanding of the hydrogeology and hydrogeochemistry are associated with uncertainties concerning the past evolution. There is generally a need to obtain chemical data from depth – and such data are expected in data freeze 1.2. Also regionally placed boreholes would be a valuable support for the conceptual model.

In addition, information on the composition of the rock matrix water and on the rock matrix porosity will give valuable input to this understanding as well as to the present hydrogeological and hydrogeo-chemical conditions at the site. Measurements of these entities are therefore strongly recommended.

Surface System

Table 8-3 shows that much of the current uncertainty in the surface system properties and proc-esses is expected to be significantly reduced by the data that will be available at data freeze 1.2. Continuation of the monitoring programmes of e.g. meteorology, hydrology (water levels, runoff) hydrochemistry and eco-systems, which will result in longer time series, is expected and will further reduce uncertainties.

More directed efforts may be required on further characterizing the Quaternary deposits in order to give information on their hydraulic properties, varying thickness and the spatial variability of bedrock surface. Additional data may e.g. be obtained from investigations of stratigraphy in trenches and additional boreholes, from additional slug-tests in existing and new boreholes in the Quaternary deposits, from marine geology data and from mapping of Quaternary deposits in shallow coastal areas. This should produce a continuous Quaternary deposit map from present land areas to the sea bottom.

Table 8-3. Uncertainties in the site descriptive model version 1.1 and field data/activities that can reduce these uncertainties.

Discipline	Model version 1.1		Will 1.2 data reduce this uncertainty?		Can remaining uncertainty in SDM v 1.2 be reduced by more field data?	
	Uncertainty	Cause	Much/To some extent/ Little	How	Much/To some extent/Little	How
Geology – rock domain model	Extension of rock domains at depth.	Limited sub-surface data.	To some extent, predominantly in the candidate area.	Observations in additional cored boreholes. Assessment of borehole and tunnel data around NPP and SFR (predominantly shallow depths).	To some extent.	Observations in additional cored boreholes. Modelling of geophysical data.
	Composition, degree of inhomogeneity and degree of ductile deformation of rock domains in areas south of road 76 and northeast of the candidate area.	Little or no data.	To some extent.	Surface data south of road 76 and from small islands will be available.	High uncertainty will remain in the sea area.	
	Numerical estimates of the proportions of different rock types in especially the inhomogeneous rock domains.	No data.	Little.		Much.	Specified field investigation at a limited number of outcrops in key rock domains.
Geology – structural model	Presence of undetected deformation zones.	Large area where airborne geophysical data are lacking or are disturbed in the vicinity of the NPP, major power lines and sub-surface cables. Original topography in the NPP area is disturbed by building activities. Poor data coverage for the interpretation of lineaments in the sea area.	Much.	Interpretation of older seismic refraction and topographic data close to the NPP. Use of new bathymetric data and processed EM data beneath the sea area. New borehole information.	To some extent.	New borehole information.
	Occurrence of inferred vertical or steeply dipping deformation zones based solely on the interpretation of linked lineaments.	Uncertain how well especially topographic and EM lineaments reflect geological features in the bedrock. Very few field observations that confirm lineament = deformation zone.	To some extent in the candidate area.	Drilling activity. Field investigation of selected lineaments by stripping away the Quaternary cover. Ground geophysics. Hydrogeological interference tests between boreholes.	To some extent in the candidate area.	Same methods as for 1.2. Include VSP measurements in selected boreholes.

| Discipline | Model version 1.1 | | Will 1.2 data reduce this uncertainty? | | Can remaining uncertainty in SDM v 1.2 be reduced by more field data? | |
	Uncertainty	Cause	Much/To some extent/ Little	How	Much/To some extent/Little	How
	Continuity (along-strike and down-dip) and dip of deformation zones based on the inter-pretation of linked lineaments. Length and dip are critical.	Very few surface and sub-surface observations.	To some extent in the candidate area.	Drilling activity. Field investigation of selected lineaments by stripping away the Quaternary cover. Ground geophysics. Interference tests between boreholes.	To some extent in the candidate area.	Same methods as for 1.2. Include VSP measurements in selected boreholes.
	Near-surface, sub-horizontal and gently dipping zones – continuity in both along-strike and down-dip directions.	Very few sub-surface observations.	To some extent in the candidate area.	Additional boreholes. Interference tests between boreholes.	To some extent in the candidate area.	Same methods as for 1.2. Complementary seismic reflection profiles at the surface.
	Geological feature(s) that gives (give) rise to seismic reflectors.	Several alternative geological features can give rise to reflectors.	Much.	Careful correlation of the BOREMAP data from KFM02A and KFM03A with the seismic reflection data.		
Geology – DFN model	Spatial distribution of fracture intensity, size.	Few observations of sub-horizontal fracture size.	To some extent.	More information regarding sub-horizontal fracture orientations and intensity in new boreholes.		
	Representativity of surface fractures for DFN-model.	Few boreholes and sub-surface data.	To some extent.	Availability of more fracture data from tunnels around SFR.		
	Assumption about statistical distribution of size.	No observations of fractures in the range 20 to 500 m.	To some extent.	The lack of observations in this scale range will persist. Other approaches such as lognormal distributions may need to be analysed.	To some extent.	Detailed fracture mapping in other domains outside rock domain 29 may give indications to the variability of fracture intensity, size and orientation.
	Assumption of fracture intensity coupled to ductile deformation and lineaments.	Detailed fracture data available only in rock domain 29.	To some extent.	Detailed fracture mapping in other domains outside rock domain 29.	To some extent.	Detailed fracture mapping in other domains outside rock domain 29.
Geology – late- or post-glacial faulting	Occurrence of late- or post-glacial faults that are related to major palaeoseismic activity.	Criteria to recognise such geological features. Little data.	To some extent in northern Uppland.	Rigid documentation of criteria. Field investigations including excavation work.	Some uncertainty will remain.	

Discipline	Model version 1.1		Will 1.2 data reduce this uncertainty?		Can remaining uncertainty in SDM v 1.2 be reduced by more field data?	
	Uncertainty	Cause	Much/To some extent/ Little	How	Much/To some extent/Little	How
Geology – evolutionary aspects	Poor control on the tectonic history in the brittle régime after c. 1,750 million years.	Little data. Difficulties to date movement along brittle deformation zones.	To some extent.	Assembly of new high- and low-temperature geochronological data. More data concerning the mineralogy of fracture fillings.	To some extent.	Relate fracture-filling mineralogy to the different fracture orientation sets. Assembly of low-temperature geochronological data along different fracture sets. Assemble data that documents the kinematics of the different sets of deformation zones. Compare with the established geological evolutionary model for central-eastern Sweden.
Bedrock mechanical properties	Rock stress magnitudes and distribution with depth.	No direct measurements available.	Much.	Stress measure-ments KFM01B. Hydraulic fracturing in intact rock and pre-excisiting fractures in KFM01A, 1B, 2A and 3A.		Further stress measurement. Focus on tentative construction area.
	High stresses in connections with subhorizontal zones.	No measure-ments, no observations of subhorizontal zones.	If observed.	Geological investigations and modelling with focus on subhorizontal zones.		Further geological investigations.
	Mechanical properties – spatial variability.	No direct measurements. Model based on rock domain model. Possibly also insuffcient information on the variation of lithology in 3D (limited data from deep boreholes).	Much/To some extent.	KFM01B + labdata+ modelling.		
	Mechanical properties – fractured zones.	No direct observations	If observed.	Furher investigations, study of old data from construction site.		Further geological and geophysical investigations.
Bedrock thermal properties	Thermal conductivity – rock type.	Too few measurements, variability within rock type.	Much/To some extent.	Additional lab data + modelling.		
	Thermal properties – spatial variability	No direct measurements. Model based on rock domain model. Possibly also insuffcient information on the variation of lithology in 3D (limited data from deep boreholes).	Much/To some extent			
	Thermal expansion.	No direct measurements.	Much/To some extent.	Additional lab data+ modelling		

Discipline	Model version 1.1		Will 1.2 data reduce this uncertainty?		Can remaining uncertainty in SDM v 1.2 be reduced by more field data?	
	Uncertainty	Cause	Much/To some extent/ Little	How	Much/To some extent/Little	How
Bedrock hydro-geology	Geometry of water-bearing structures.	Uncertainties in geological structural model.	Little.	Response tests during drilling.	Much.	Focus on hydraulic interference testing.
	Transmissivity in zones.	Few site data, impact of drilling on hydraulic properties of horizontal zones.	Little.	Response tests during drilling.	Much.	Additional boreholes and hydrotests (difference flow logging).
	Transmissivity distribution in fractures.	Few site data.	Much.	Additional boreholes and hydrotests (difference flow logging).	Much.	Additional boreholes and hydrotests (difference flow logging).
	Depth dependence of transmissivity distribution.	Few site data.	Little.	Additional boreholes and hydrotests (difference flow logging).	Much.	Additional boreholes and hydrotests (difference flow logging).
	Bedrock topography.	Few site data.	To some extent.	Geostatistical analysis.	Much.	Changing the current program of investigation and focus on borings in the Quaternary deposits.
	Matrix porosity and salinity in matrix porosity.	Few site data.	To some extent.	Data from measurements of matrix porosity and matrix water composition .	Much.	More data from measurements of matrix porosity and matrix water composition .
Paleohydro-geology	Initial conditions (in particular, the salinity profile).	Few site data.	To some extent.	Additional boreholes and hydrotests (difference flow logging).	Much.	Additional boreholes and hydrotests (difference flow logging).
	Boundary conditions.	Current size of the model domain does not coincide with natural physical boundaries.	To some extent.	Exploration numerical simulation.	Little.	
	Processes; shoreline displacement, evapo-transpiration, upconing, surface runoff.	Few site data.	To some extent.	Additional monitoring wells, dams' and hydrotests.	Much.	Additional monitoring wells, dams' and hydrotests.
Hydrogeo-chemistry	Spatial variability at depth.	Few site data.	Much, but remaining uncertainty.	Additional borehole data at depth (KFM02, 03, 04, 05) and samples from the rock matrix.	To some extent. Confirmation aspects. Details of resolution aspects will not be resolved	Boreholes in regional model volume, upstream + already planned borehole in Singö zone. Long-term hydro monitoring. Detailed analyses of fracture minerals. Microbes.
	Description of processes.	Few site data.	Much, but remaining uncertainty.	Additional borehole data at depth (KFM02, 03, 04, 05) and samples from the rock matrix.	To some extent. Confirmation and verification.	Boreholes in regional model volume, upstream + already planned borehole in Singö zone. Long-term hydro monitoring. Detailed analyses of fracture minerals. Microbes.

| Discipline | Model version 1.1 | | Will 1.2 data reduce this uncertainty? | | Can remaining uncertainty in SDM v 1.2 be reduced by more field data? | |
	Uncertainty	Cause	Much/To some extent/ Little	How	Much/To some extent/Little	How
Paleohydro-geochemistry	Origin and development of water composition.	Few site data		Additional borehole data and samples from the rock matrix, paleomodelling + hydromodelling.	To some extent. Confirmation and verification.	Boreholes in regional model volume, upstream + already planned borehole in Singö zone. Long-term hydro monitoring. Detailed analyses of fracture minerals. Microbes.
Surface system – Quaternary geology	Terrestrial – composition, spatial distribution and depth.	Inhomogeneity: Large variations in depth over short distances. QD-mapping only in minor parts of local model area.	Much.	QD-mapping of central part of regional model area. Stratigraphic data from trenches and additional boreholes.	To some extent.	Continued investigations.
	Stratigraphic distribution and character of organic deposits.	Lack of data.	To some extent.	Investigation of peat in two mires.	To some extent.	Continued investigation of organic deposits in wetlands.
	Deglaciation history.	Lack of data.	Little.	Additional stratigraphic data from trenches and investigations of varved clay.	To some extent.	Clay varve chronology, deglaciation history, better dating and understanding of the retreat of the inland ice.
	Off-shore Quaternary deposits, sediments – character, thickness and spatial distribution.	Data not available.	Much.	Marine geology data will become available.	To some extent.	QD mapping of shallow coastal areas. Results in a continous QD map from present land areas to sea bottom. Stratigraphic analyses of one sediment core.
	Neo-tectonic movements.	Data incomplete.	To some extent.	Further investigations of evidence of neo tectonic movements in Quaternary deposits.	To some extent.	Further investigations.
Surface system – Surface hydrology, near-surface hydrogeology	Meteorology – spatial variability in precipitation.	Representativity of SMHI data – all stations outside regional model area.	Little.	Short time series from two meteorological stations in the area.	Much.	Longer time series from the two existing meteorological stations in the area. Campaign with additional precipitation gauge.
	Spatial variability in runoff.	Runoff measured outside regional model area. Variation in vegetation, topography, geology etc. not considered.	Little.	Short time series from one runoff station within the area.	Much.	Time series from the existing and 4 planned runoff stations in the area. Investigation of the possibility to establish a runoff station at the outlet of Lake Bolundsfjärden.

| Discipline | Model version 1.1 | | Will 1.2 data reduce this uncertainty? | | Can remaining uncertainty in SDM v 1.2 be reduced by more field data? | |
	Uncertainty	Cause	Much/To some extent/ Little	How	Much/To some extent/Little	How
	Spatial variability of transmissivity in QD and transmissivity of fractures in QD.	Data from the contact between bedrock and QD. No representation of variation in depth. Inhomogeneity of QD.	To some extent.	Additional slug-tests in existing and new bore-holes in soil.	To some extent.	Test of the hydraulic contact between the till aquifers and major wetlands. Additional hydraulic tests based on the result from the version 1.2 modelling.
	GW level – spatial and temporal variability.	Measurements concentrated to topographic depressions and no temporal variation.	Much.	One year´s time series from more than 30 observation wells.	Much.	Longer time series from existing and additional observation wells.
Surface system – Chemistry	Temporal and spatial variation in water composition in surface water.	No evaluation carried out.	Much.		To some extent.	Continued measurements combined with flow logging.
	Chemistry of regolith and regolith water.	No lab. analyses carried out.	Much.		Much.	Continued investigations.
Ecosystems – biotic	Chemistry in biota.	No lab. analyses carried out.	To some extent.	Lab analyses will become available.	To some extent.	Continued investigations.
	Terrestrial: Biotic processes in regolith. Biomass and production.	No data available.	Much.	Data will become available.	Not possible to judge at present.	
	Limnic: Biomass, production and decomposition. Flow of matter.	Lack of data.	Much.	More data will become available.	Not possible to judge at present.	
	Marine: Biomass, production and decomposition. Flow of matter.	Lack of data.	Much.	More data will become available.	Not possible to judge at present.	
	Humans and land use					
Ecosystems – historical development	Shoreline displacement, paleoecology, historical land use.	Lack of data.	Much.	More data will become available, e.g. pollen analyses.	Not possible to judge at present.	

9   References

Aaro S, 2003. Regional gravity survey in the Forsmark area, 2002 and 2003. SKB P-03-42, Svensk Kärnbränslehantering AB.

Adl-Zarrabi B, 2003. Outcrop samples from Forsmark. Determination of thermal properties by the TPS-Method. SKB P-03-08, Svensk Kärnbränslehantering AB.

Agrell, H 1981. Gillberga Gryt – En sentida sprickgrotta i Uppland. Sveriges Speleolog-Förbund, Grottan Nr 4 (in Swedish).

Ahlbom K, Smellie J A T, 1991. Overview of the fracture zone project at Finnsjön, Sweden. J. Hydrol., 126, 1–15.

Ahlbom K, Andersson J-E, Andersson P, 1992. Finnsjön study site. Scope of activities and main results. SKB TR 92-03, Svensk Kärnbränslehantering AB.

Ahlbom K, Olsson O, Sehlstedt S, 1995. Temperaure conditions at the SKB study sites. SKB TR 95-16, Svensk Kärnbränslehantering AB.

Allen R L, Lundström I, Ripa M, Simeonov A, Christofferson H, 1996. Facies Analysis of a 1.9 Ga, Continental Margin, Back –Arc, Felsic Caldera Province with Diverse Zn-Pb-Ag-(Cu-Au) Sulfide and Fe Oxide Deposits, Bergslagen Region, Sweden. Economic Geology 91.

Amadei B, Stephansson O, 1997. Rock stress and its measurement. Chapman and Hall, London, p 490.

Ambros M, 1988. Beskrivning till berggrundskartorna Avesta NV och SV. SGU series Af 152 and 153, Sveriges Geologiska Undersökning (in Swedish).

Andersson J, Ström A, Svemar C, Almén K-E, Ericsson L O, 2000. What requirements does the KBS-3 repository make on the host rock? Geoscientific suitability indicators and criteria for siting and site evaluation. SKB TR-00-12, Svensk Kärnbränslehantering AB.

Andersson J, Christiansson R, Munier R, 2001. Djupförvarsteknik: Hantering av osäkerheter vid platsbeskrivande modeller. Tech. Doc. (TD-01-40), SKB, Stockholm, Sweden.

Andersson J, Berglund J, Follin S, Hakami E, Halvarson J, Hermanson J, Laaksoharju M, Rhén I, Wahlgren C-H, 2002a. Testing the methodology for site descriptive modelling. Application for the Laxemar area. SKB TR-02-19, Svensk Kärnbränslehantering AB.

Andersson J, Christiansson R, Hudson J, 2002b. Site Investigations. Strategy for Rock Mechanics Site Descriptive Model. SKB TR-02-01, Svensk Kärnbränslehantering AB.

Andersson J, 2003. Site descriptive modelling – strategy for integrated evaluation. SKB R-03-05, Svensk Kärnbränslehantering AB.

Andersson J (ed), 2004. T-H-M in Safety Assessments. Findings of DECOVALEX III, SKI Report (in progress).

Anonymous, 1997. Länsstyrelsen för Uppsala län. Kulturmiljöer I Uppsala län. Områden av riksintresse. Beskrivningar. Länsstyrelsens meddelandeserie 1997:13 (in Swedish).

Antal I, Bergman S, Gierup J, Johansson R, Persson C, Stephens M, Thunholm B, 1998a. Översiktsstudie av Uppsala län: Geologiska förutsättningar. SKB R-98-32, Svensk Kärnbränslehantering AB (in Swedish).

Antal I, Bergman T, Gierup J, Johansson R, Lindén A, Stephens M, Thunholm B, 1998b. Översiktsstudie av Östergötlands län: Geologiska förutsättningar. SKB R-98-26, Svensk Kärnbränslehantering AB (in Swedish).

Antal I, Bergman T, Johansson R, Persson C, Stephens M, Thunholm B, Åsman M, 1998c. Översiktsstudie av Södermanlands län: Geologiska förutsättningar. SKB R-98-28, Svensk Kärnbränslehantering AB (in Swedish).

Antal I, Bergman T, Johansson R, Persson C, Stephens M, Thunholm B, Åsman M, 1998d. Översiktsstudie av Stockholms län: Geologiska förutsättningar. SKB R-98-30, Svensk Kärnbränslehantering AB (in Swedish).

Axelsson C-L, Hansen L M, 1997. Update of structural models at SFR nuclear waste repository, Forsmark, Sweden. SKB R-98-05, Svensk Kärnbränslehantering AB.

Axelsson C-A, Ekstav A, Lindblad Påsse A, 2002. SFR – Utvärdering av hydrogeologi. SKB R-02-14, Svensk Kärnbränslehantering AB.

Banwart S A, 1999. Reduction of iron (III) minerals by natural organic matter in groundwater. Geochim. Cosmochim. Acta, 63, 2919–2928.

Barton N, Lien R, Lunde J, 1974. Engineering classification of rock masses for the design of tunnel support. Rock Mech., Vol 6, pp 189–236.

Barton N, Choubey V, 1977. The shear strength of rock joints in theory and practice. Roch. Mech., vol 10, pp 1–54.

Barton N, 2002. Some new Q-value correlations to assist in site characterisation and tunnel design. Int. J. Rock Mech. & Min. Sci., Vol 39, p 185–216.

Barton N, 2003. KFM01A. Q-logging. SKB P-03-29, Svensk Kärnbränslehantering AB.

Barton N, 2004. Q-logging of surface exposure in Forsmark. SKB P-report in press, Svensk Kärnbränslehantering AB.

Bein A, Arad A, 1992. Formation of saline groundwaters in the Baltic region through freezing of seawater during glacial periods. Journal of Hydrology, 140, pp 75–87.

Berggren J, Kyläkorpi L, 2002. Ekosystemen I Forsmarksområdet. Sammanställning av befintlig information, SKB R-02-08, Svensk Kärnbränslehantering AB (in Swedish).

Berglund B E, 1971. Littorina transgressions in Blekinge, South Sweden. A preliminary survey. Geologiska Föreningens I Stockholm Förhandlingar 93, 625–652.

Berglund J, 1997. Compressional and extensional ductile shearing along a terrane boundary in south-western Sweden. In J. Berglund, Mid-Proterozoic evolution in south-western Sweden. Thesis, Earth Sciences Centre, Göteborg University, A15 1997.

Berglund S, Selroos J-O, 2004. Transport Properties Site Descriptive Model. Guidelines for evaluation and modelling. SKB R-03-09, Svensk Kärnbränslehantering AB.

Bergman S, Sjöström H, 1994. The Storsjön-Edsbyn Deformation Zone, central Sweden. Unpublished research report, Sveriges Geologiska Undersökning.

Bergman S, Isaksson H, Johansson R, Lindén A, Persson Ch, Stephens M, 1996. Förstudie Östhammar. Jordarter, bergarter och deformationszoner. SKB PR-D-96-016, Svensk Kärnbränslehantering AB (in Swedish).

Bergman S, Bergman T, Johansson R, Stephens M, Isaksson H, 1998. Förstudie Östhammar. Delprojekt jordarter, bergarter och deformationszoner. Kompletterande arbeten 1998. Del 1: Fältkontroll av berggrunden inom Forsmarks- och Hargshamnsområdena. SKB R-98-57, Svensk Kärnbränslehantering AB (in Swedish).

Bergman T, Isaksson H, Johansson R, Lindèn A H, Lindroos H, Rudmark L, Stephens M, 1999. Förstudie Tierp. Jordarter, bergarter och deformationszoner. SKB R-99-53, Svensk Kärnbränslehantering AB (in Swedish).

Bergman T, Fredén C, Gierup J, Johansson R, Kübler L, Stephens M, Stølen L K, Thunholm B, 1999a. Översiktsstudie av Örebro län: Geologiska förutsättningar. SKB R-99-23, Svensk Kärnbränslehantering AB (in Swedish).

Bergman T, Gierup J, Johansson R, Kübler L, Lindén A, Stephens M, Stølen L K, Thunholm B, 1999b. Översiktsstudie av Västmanlands län: Geologiska förutsättningar. SKB R-99-31, Svensk Kärnbränslehantering AB (in Swedish).

Bergström E, 2001. Late Holocene distribution of lake sediment and peat in NE Uppland, Sweden. SKB R-01-12, Svensk Kärnbränslehantering AB.

Berman R G, Brown H, 1985. Heat capacity of minerals in the system Na_2O-K_2O-CaO-MgO-FeO-Fe_2O_3-Al_2O_3-SiO_2-TiO_2-H_2O-CO_2: representation, estimation, and high temperature extrapolation. Contrib. Mineral Petrol., 89, p 163–183.

Beunk F F, Page L M, 2001. Structural evolution of the accretional continental margin of the Paleoproterozoic Svecofennian orogen in southern Sweden. Tectonophysics 339.

Bieniawski ZT, 1979. The Geomechanics Classification in rock engineering applications, Proc. 4th Congr. Int. Soc. For Rock Mech., Montreux: Switzerland.

Bieniawski ZT, 1989. Engineering rock mass classifications. John Wiley & Sons.

Björck S, 1995. A review of the history of the Baltic Sea 13-8 ka. Quaternary International 27, 19–40.

Björnbom S, 1979. Clayey basal till in central and northern Sweden. A deposit from an old phase of the Würm glaciation. SGU Series C 753, Sveriges Geologiska Undersökning.

Blomqvist P, Nilsson E, Brunberg A-K, 2002. Habitat distribution, water chemistry, and biomass and production of pelagic and benthic microbiota in Lake Eckarfjärden, Forsmark. SKB R-02-41, Svensk Kärnbränslehantering AB.

Boresjö Bronge L, Wester K, 2002. Vegetation mapping with satellite data of the Forsmark and Tierp region. SKB R-02-07, Svensk Kärnbränslehantering AB

Bratt P (ed), 1998. Forntid I ny dager – Arkeologi I Stockholmstrakten, Raster Förlag, Stockholm. (in Swedish)

Brettum P, 1989. Alger som indikator på vannkvalitet I norske innsjøer. Planteplankton.NIVA, Oslo, 111 p. ISBN 82 557 1627 8 (in Norwegian).

Brunberg A-K, Blomqvist P, 1998. Vatten I Uppsala län 1997. Beskrivning, utvärdering, åtgärdsförslag. Rapport nr 8/1998. Upplandsstiftelsen. 944 pp (in Swedish).

Brunberg A-K, Blomqvist P, 1999. Characteristics and ontogeny of oligotrophic hardwater lakes in the Forsmark area, central Sweden. SKB R-99-68, Svensk Kärnbränslehantering AB.

Brunberg A-K, Blomqvist P, 2000. Post-glacial, land rise-induced formation and development of lakes in the Forsmark area, central Sweden. SKB TR-00-02, Svensk Kärnbränslehantering AB.

Brunberg A-K, Nilsson E, Blomqvist P, 2002. Characteristics of oligotrophic hardwater lakes in a postglacial landrise area in mid-Sweden. Freshwater Biology (2002) 47, p 1451–1462.

Brunberg A-K, Blomqvist P, 2003. Ontogeny of lake ecosystems in the Forsmark area – chemical analyses of deep sediment cores. SKB R-03-28, Svensk Kärnbränslehantering AB.

Bruno J, Cera E, Grivé M, Rollin C, Ahonen L, Kaija J, Blomqvist R, El Aamrani F.Z, Casas I, de Pablo J, 1999. Redox Processes in the Palmottu uranium deposit. Redox measurements and redox controls in the Palmottu system. Draft. Informe 64023. ENRESA, 76 p.

Bruno J, 2004. Personal communication, Enviros, Spain

Brydsten L, 1999a. Shore line displacement in Öregrundsgrepen. SKB TR-99-16, Svensk Kärnbränslehantering AB.

Brydsten L, 1999b. Change in coastal sedimentation conditions due to positive shore displacement in Öresundsgrepen. SKB TR-99-37, Svensk Kärnbränslehantering AB.

Butler J J Jr, 1998. The design, performance and analysis of slug tests. Lewis Publisher.

Byegård J, Johansson H, Skålberg M, Tullborg E-L, 1998. The interaction of sorbing and non-sorbing tracers with different Äspö rock types – Sorption and diffusion experiments in the laboratory scale, SKB TR-98-18, Svensk Kärnbränslehantering AB.

Carlsson A, 1979. Characteristic features of a superficial rock mass in southern central Sweden – Horizontal and subhorizontal fractures and filling material. Striae, vol 11, pp 79.

Carlsson A, Olsson T, 1982. Characterisation of deep-seated rock masses by means of borehole investigations. Vattenfall Research and Development, Final Report, April 1982, Report 5:1.

Carlsson L, Carlsten S, Sigurdsson T, Winberg A, 1985. Hydraulic modelling of the final repository for reactor waste (SFR). Compilation and conceptualization of available geological and hydrogeological data. Edition 1. SKB Progress Report SFR 85-06, Svensk Kärnbränslehantering AB.

Carlsson A, Christiansson R, 1987. Geology and tectonics at Forsmark, Sweden. SKB SFR-87-04, Svensk Kärnbränslehantering AB.

Cederlund G, Hammarström A, Wallin K, 2003. Survey of mammal populations in the areas adjacent to Forsmark and Tierp. SKB P-03-18, Svensk Kärnbränslehantering AB.

Chapin III F S, Matson P A, Mooney H A, 2002. Principles of Terrestrial Ecosystem Ecology. Springer Verlag New York, Inc. ISBN 0-387-95439-2.

Christiansson R, Martin C D, 2001. In-situ stress profiles with depth from site characterization programs for nuclear waste repositories. Proc. of EUROCK 2001 (Särkää P and Eloranta P eds), Espoo, Finland, AA Balkema, Rotterdam, p 732–42

Christiansson R, Hudson J A, 2003. ISRM suggested methods for rock stress estimation – Part 4: Quality control of rock stress estimation. I.J.R.M. & Min. Sci., vol 40, p 1021–25

Chryssanthakis P, 2003. Borehole KFM01A – Results of Tilt Testing, SKB P-03-128, Svensk Kärnbränslehantering AB.

Cobbold P R, Quinquis H, 1980. Development of sheath folds in shear zones. Journal of Structural Geology 2.

Cooper H H Jr, Bredhoeft J D, Papadopoulos I S, 1967. Response of a finite diameter well to an instantaneous charge of water. Water Resour. Res. 3(1), 263–269.

Cosma C, Balu L, Enescu N, 2003. Estimation of 3D positions and orientations of reflectors identified in the reflection seismic survey at the Forsmark area. SKB R-03-22, Svensk Kärnbränslehantering AB.

Cousins S A O, 2001. Plant species diversity patterns in a Swedish rural landscape. Effects of the past and consequences for the future. Doctoral thesis, No 17. Department of Physical Geography and Quaternary Geology, Stockholm University.

Cramer J, Smellie J, 1994 (eds). Final report of the AECL /SKB Cigar Lake Analog Study. SKB TR 94-04. Svensk Kärnbränslehantering AB

Delin P, 1983. Uttagna kärnbitar för tryckförsök och point-load tester på KTH. KTH/Hagkonsult (personal communication).

Delin H, 1993. The radiometric age of the Ljusdal granodiorite of central Sweden. In T. Lundqvist (ed), Radiometric dating results. SGU series C 823, Sveriges Geologiska Undersökning.

Delin H, 1996. U-Pb zircon ages of granitoids in the Kårböle region, central Sweden. In T. Lundqvist (ed), Radiometric dating results 2. SGU series C 828, Sveriges Geologiska Undersökning.

Delin H, Persson P-O, 1999. U-Pb zircon ages of three Palaeoproterozoic igneous rocks in the Loos-Hamra area, central Sweden. In S Bergman (ed), Radiometric dating results 4. SGU series C 831, Sveriges Geologiska Undersökning.

Dershowitz W, Herda H, 1992. Interpretation of fracture spacing and intensity. Proceedings, 32nd US rock symposium, Santa Fe, New Mexico.

Dershowitz W, Winberg A, Hermanson J, Byegård J, Tullborg E-L, Andersson P, Mazurek M, 2003. Äspö Task Force on modelling of groundwater flow and transport of solutes. Task 6c. A semi-synthetic model of block scale conductive structures at the Äspö HRL. Äspö Hard Rock Laboratory, International Progress Report IPR-03-13, Svensk Kärnbränslehantering AB.

Deutsch W J, Jenne E A, Krupka K M, 1982. Solubility equilibria in basalt aquifers: The Columbia Plateau, Eastern Washington, U.S.A. Chemical Geology, 36, 15–34.

Ekman M, 1996. A consistent map of the postglacial uplift of Fennoscandia. Terra-Nova 8/2, 158–165.

Engqvist A, Andrejev O, 1999. Water exchange of Öregrundsgrepen. A baroclinic 3D-model study. SKB TR-99-11, Svensk Kärnbränslehantering AB.

Ericsson B, Lidén E, 1988. Description to the Quaternary map Söderfors NO. SGU Ae 87, Sveriges Geologiska Undersökning (in Swedish with English summary).

Erlström M, Sivhed U, 2001. Intra-cratonic dextral transtension and inversion of the southern Kattegat on the southwest margin of Baltica – Seismostratigraphy and structural development. SGU series C 832, Sveriges Geologiska Undersökning.

Espeby B, 1989. Water flow in a forested till slope – field studies and physically based modelling. Dept. of Land and Water Resources, Rep. Trita-Kut No 1052, Royal Inst.of Technology, Stockholm.

Fairbanks R, 1989. A 17 000-year glacio-eustatic sea level record: influence of glacial melting rates on the Younger Dryas event and deep-ocean circulation. Nature 342, 637–642.

Follin S, Hermanson J, 1996. A discrete fracture network model of the Äspö TBM tunnel rock mass. Äspö Hard Rock Laboratory, International Progress Report IPR-01-71, Svensk Kärnbränslehantering AB.

Follin S, Svensson U, 2003. On the role of mesh discretisation and salinity for the occurrence of local flow cells. Results from a regional scale groundwater flow model of Östra Götaland. SKB R-03-23, Svensk Kärnbränslehantering AB.

Frape S, 2003. Personal communication. University of Waterloo, Canada

Fredén C (ed), 1994. Geology. National Atlas of Sweden.

Fredén C (ed), 2002. Berg och jord. Sveriges nationalatlas. Tredje upplagan.

Fridriksson G, Öhr J, 2003. Forsmark site investigation. Assessment of plant biomass of the ground, field and shrub layers of the Forsmark area. SKB P-03-90, Svensk Kärnbränslehantering AB.

Frietsch R, 1975. Brief outline of the metallic mineral resources of Sweden. SGU series C 718, Sveriges Geologiska Undersökning.

Fromm E, 1976. Beskrivning till jordartskartan Linköping NO. SGU Ae 19, Sveriges Geologiska Undersökning (in Swedish with English summary).

Garrels R M, 1984. Montmorillonite/illite stability diagrams. Clays and Clay Minerals, 32, 161–166.

Geocon, 2002. Stomnätsmätning I plan och höjd vid PLU Forsmark. Geocon S1020, September 2002 (in Swedish).

Gidlund J, Moreno L, Neretnieks I, 1990. Porosity and diffusivity measurements of samples from Finnsjön, SKB AR 90-34, Svensk Kärnbränslehantering AB.

Gierup J, Kübler L, Lindén A, Ripa M, Stephens M, Stølen L K, Thunholm B, 1999. Översiktsstudie av Dalarnas län (urbergsdelen): Geologiska förutsättningar. SKB R-99-29, Svensk Kärnbränslehantering AB (in Swedish).

Gilbert R O, 1987. Statistical Methods for Environmental Pollution Monitoring. Van Nostrand Reinhold, New York, 320 p.

Glynn P D, Voss C I, 1999. Geochemical characterization of Simpevarp ground waters near Äspö Hard Rock Laboratory. SITE-94 SKI Report 96:29, Statens Kärnkraftinspektion, Stockholm, Sweden.

Green M, 2003. Fågelundersökningar inom SKB:s platsundersökningar 2002 – Forsmark. SKB P-03-10, Svensk Kärnbränslehantering AB (in Swedish).

Grenthe I, Stumm W, Laaksoharju M, Nilsson A C, Wikberg P, 1992. Redox potentials and redox reactions in deep groundwater systems. Chem. Geol., 98, 131–150.

Grimaud D, Beaucaire C, Michard G, 1990. Modeling of the evolution of ground waters in a granite system at low temperature: the Stripa ground waters, Sweden. Applied Geochemistry, 5, 515–525.

Grånäs K, 1985. Description to the Quaternary map Söderfors NV. SGUAe 74, Sveriges Geologiska Undersökning (in Swedish with English summary).

Grönlund T, 1991a. The diatom stratigraphy of the Eemian Baltic Sea on the basis of sediment discoveries in Ostrobothnia, Finland. Geological Survey of Finland, Report of investigation 102, 26 pp.

Grönlund T, 1991b. New cores from Eemian interglacial deposits in Ostrobothnia, Finland. Geological Survey of Finland, Bulletin 352, 23 pp.

Gurban I, Laaksoharju M, 2002. Drilling Impact Study (DIS); Evaluation of the influences of drilling, in special on the changes on groundwater parameters. SKB report in progress, Svensk Kärnbränslehantering AB.

Gustafsson S, 1991. Transient plane source techniques for thermal conductivity and thermal diffusivity measurements of solid materials. Rev. Sci. Instrum. 62, p 797–804. American Institute of Physics, USA.

Gustafsson L, Ahlén I, 1996. (Editors) Geography of plants and animals. National Atlas of Sweden.

Gustafsson C, Nilsson P, 2003. Forsmark site investigation. Geophysical, radar and BIPS logging in boreholes HFM01, HFM02, HFM03 and the percussion drilled part of KFM01A. SKB P-03-39, Svensk Kärnbränslehantering AB.

Hagkonsult AB, 1982a. Geologiska undersökningar och utvärderingar för lokalisering av SFR till Forsmark, Del 1. SKB SFR 81-13, Svensk Kärnbränslehantering AB (in Swedish).

Hagkonsult AB, 1982b. Geologiska undersökningar och utvärderingar för lokalisering av SFR till Forsmark, Del 2. SKB SFR 81-13, Svensk Kärnbränslehantering AB (in Swedish).

Hakala M, Hudson J A, Christiansson R, 2003. Quality control of overcoring stress measurement data. Int. J Rock. Mech. Min. Sci., 40, No 7–8, pp 1141–1159.

Hakami E, Hakami H, Cosgrove J, 2002. Strategy for a Rock mechanics Site Descriptive Model. Development and testing of an approach to modelling the state of stress. SKB R-02-03, Svensk Kärnbränslehantering AB.

Hansen L, 1989. Bedrock of the Forsmark area. Technical Report, Swedish State Power Board, Stockholm.

Haveman S A, Pedersen K, Ruotsalainen P, 1998. Geomicrobial investigations of groundwaters from Olkilouto, Hästholmen, Kivetty and Romuvaara, Finland. POSIVA Report 98-09, Helsinki, Finland, 40 p.

Hedenström A, Risberg J, 1999. Early Holocene shore-displacement in southern central Sweden as recorded in elevated isolated basins. Boreas 28, 490–504.

Hedenström A, 2001. Shore displacement in south eastern Uppland during the early Litorina Sea stage. Quaternaria Ser A. No 10, paper IV. 48 pp.

Hedenström A, 2003. Forsmark site investigation: Investigation of marine and lacustrine sediment in lakes. Field data 2003. SKB P-03-24, Svensk Kärnbränslehantering AB**.**

Hedenström A, Risberg J, 2003. Shore displacement in northern Uppland during the last 6500 calendar years. SKB TR-03-17, Svensk Kärnbränslehantering AB.

Heinsalu A, 2001. Diatom stratigraphy and the palaeoenvironment of the Yoldia Sea in the Gulf of Finland, Baltic Sea. Doctoral Thesis. Annales Universitatis Turkuensis Ser. A II, 144, 41pp.

Helgeson H C, 1969. Thermodynamics of hydrothermal systems at elevated temperatures. Am. J. Sci., 267, 729–804.

Helgeson H C, Delany J M, Nesbitt H W, Bird D K, 1978. Summary and critique of thermodynamic properties of rock forming minerals. Am. J. Sci., 278-A.

Helsel D R, Hirsch R M, 1991. Statistical Methods in Water Resources. Chapter A3 in: Techniques of Water-Resources Investigations of the United States Geological Survey, Book 4, Hydrologic Analysis and Interpretation. USGS

Henkel H, Pesonen L J, 1992. Impact craters and craterform structures in Fennoscandia. Tectonophysics 216.

Hermanson J, Stigsson M, 1998. A discrete fracture network model of the Äspö Zedex tunnel section. SKB PR-HRL-98-29, Svensk Kärnbränslehantering AB**.**

Hermanson J, Hansen L, Olofsson J, Sävås J, Vestgård J, 2003. Detailed fracture mapping at the KFM02 and KFM03 drill sites. SKB P-03-12, Svensk Kärnbränslehantering AB.

Hoek E, Brown ET, 1980. Underground excavations in rock, The institution of Mining and Metallurgy: London, pp 527.

Hoek E, Brown ET, 1997. Practical estimates of rock mass strength. International Journal of Rock Mechanics and Mining Sciences, Vol 34, No 8, pp 1165–1186.

Holmén J G, Stigsson M, 2001. Modelling of future hydrogeological conditions at SFR. SKB R-01-02, Svensk Kärnbränslehantering AB.

Holmén J G, Stigsson M, Marsic N, Gylling B, 2003. Modelling of froundwater flow and flow paths for a large regional domain in northeast Uppland. A three-dimensional, mathematical modelling of groundwater flows and flow paths on a super-regional scale, for different complexity levels of the flow domain. SKB R-03-24, Svensk Kärnbränslehantering AB.

Holtedahl O, 1953. On the oblique uplift of some northern lands. Norsk Geologisk Tidsskrift 14.

Horai K, Simmons G, 1969. Thermal conductivity of rock-forming minerals. Earth Planet. Sci. Lett., 6, p 359–368.

Horai K, 1971. Thermal conductivity of rock-forming minerals. J. Geophys. Res. 76, p 1278–1308.

Hättestrand C, Stroeven A. 2002. A preglacial landscape in the centre of Fennoscandian glaciation: geomorphological evidence of minimal Quaternary glacial erosion. Geomorphology, 44, 127–143.

Högdahl K, 2000. Late-orogenic, ductile shear zones and protolith ages in the Svecofennian Domain, central Sweden. Meddelande från Stockholms Universitets Institution för Geologi och Geokemi 309.

Ingmar T, 1963. Från havsvik till mosse – något om Florornas utveckling. Sveriges Natur, Årsbok 1963, 120–132, (in Swedish).

Isaksson H, 2003. Forsmark site investigation. Interpretation of topographic lineaments 2002. SKB P-03-40, Svensk Kärnbränslehantering AB.

Isaksson H, Mattsson H, Thunehed H, Keisu M, 2004a. Interpretation of petrophysical surface data. Stage 1 (2002). SKB P-03-102, Svensk Kärnbränslehantering AB.

Isaksson H, Thunehed H, Mattsson H, Keisu M, 2004b. Interpretation of airborne geophysics and integration with topography. Stage 1 (2002). SKB P-04-29, Svensk Kärnbränslehantering AB.

Jacobsson O, 1978. Skog för framtid. SOU 1978:7, bilaga 1 pp 200–205 (in Swedish).

Jerling L, Isæus M, Lanneck J, Lindborg T, Schüldt R, 2001. The terrestrial biosphere in the SFR region. SKB R-01-09, Svensk Kärnbränslehantering AB.

Johansson P-O, 1986. Diurnal groundwater level fluctuations in sandy till – a model analysis. J. of Hydrology, 87, 125–134.

Johansson P-O, 1987a. Estimation of groundwater recharge in sandy till with two different methods using groundwater level fluctuations. J. of Hydrology, 90, 183–198.

Johansson P-O, 1987b. Spring discharge and aquifer characteristics in a sandy till area in southeastern Sweden. Nordic Hydrol., 18, 203–220.

Johansson P-O, 2003. Forsmark site investigation. Drilling and sampling in soil. Installation of groundwater monitoring wells and surface water level gauges. SKB P-03-64, Svensk Kärnbränslehantering AB.

Juhlin C, Bergman B, Palm H, 2002. Reflection seismic studies in the Forsmark area – stage 1. SKB R-02-43, Svensk Kärnbränslehantering AB.

Kautsky H, Plantman P, Borgiel M, 1999. Quantitative distribution of aquatic plant and animal communities in the Forsmark-area. SKB R-99-69, Svensk Kärnbränslehantering AB.

Kautsky U (ed), 2001. The biosphere today and tomorrow in the SFR area. A summary of knowledge for the SAFE project. 2001. SKB R-01-27, Svensk Kärnbränslehantering AB.

Kleiven S, 1991. An analysis of allelopathic effects of Chara on phytoplankton development. PhD-thesis. Acta Universitatis Upsaliensis 313, 20 p.

Koistinen T, Stephens M B, Bogatchev V, Nordgulen O, Wennerström M, Korhonen J, 2001. Geological map of the Fennoscandian Shield, scale 1:2 000 000. Geological Surveys of Finland, Norway and Sweden and the North-West Department of Natural Resources of Russia.

Kumblad L, 1999. A carbon budget for the aquatic ecosystem above SFR in Öregrundsgrepen. SKB R-99-40, Svensk Kärnbränslehantering AB.

Kumblad L, 2001. A transport and fate model of C-14 in a bay of the Baltic Sea at SFR. Today and in future. SKB TR-01-15, Svensk Kärnbränslehantering AB.

Kyläkorpi L, 2004. Nature values and site accessibility maps of Forsmark and Simpevarp. SKB R-04-12, Svensk Kärnbränslehantering AB (in prep).

Källgården J, Ludvigson J-E, Jönsson S, 2003. Forsmark site investigation. Pumping tests and flow logging. Boreholes KFM03A (0–100 m), HFM06, HFM07 and HFM08. SKB P-03-36, Svensk Kärnbränslehantering AB.

Laaksoharju M, Smellie J, Nilsson A-C, Skårman C, 1995. Groundwater sampling and chemical characterisation of the Laxemar deep borehole KLX02. SKB TR 95-05, Svensk Kärnbränslehantering AB.

Laaksoharju M, Wallin B (eds), 1997. Evolution of the groundwater chemistry at the Äspö Hard Rock Laboratory. Proceedings of the second Äspö International Geochemistry Workshop, June 6–7, 1995. SKB International Co-operation Report ISRN SKB-ICR-91/04-SE. ISSN 1104-3210. Svensk Kärnbränslehantering AB.

Laaksoharju M, 1999. Groundwater Characterisation and Modelling: Problems, Facts and Possibilities. Dissertation TRITA-AMI-PHD 1031; ISSN 1400-1284; ISRN KTH/AMI/PHD 1031-SE; ISBN 91-7170-. Royal Institute of Technology, Stockholm, Sweden. Also as SKB TR-99-42, Svensk Kärnbränslehantering AB.

Laaksoharju M, Skårman C, Skårman E, 1999a. Multivariate Mixing and Mass-balance (M3) calculations, a new tool for decoding ydrogeochemical information. Applied Geochemistry Vol 14, #7, 1999, Elsevier Science Ltd, pp 861–871.

Laaksoharju M, Tullborg E-L, Wikberg P, Wallin B, Smellie J, 1999b. Hydrogeochemical conditions and evolution at Äspö HRL, Sweden. Applied Geochemistry Vol 14, #7, 1999, Elsevier Science Ltd., pp 835–859.

Laaksoharju M (ed), Gimeno M, Smellie J, Tullborg E-L, Gurban I, Auqué L, Gómez J, 2004. Hydrogeochemical evaluation of the Forsmark site, model version 1.1. SKB R-04-05, Svensk Kärnbränslehantering AB.

Lagerbäck R, 1988a. The Veiki moraines in northern Sweden – widespread evidence of an Early Weichselian deglaciation. Boreas, vol 17, 469–486.

Lagerbäck R, 1988b. Periglacial phenomena in the wooded areas of Northern Sweden – relicts from the Tärendö Interstadial. Boreas, vol 17, 487–499.

Lagerbäck R, Robertsson A-M, 1988. Kettle holes – stratigraphical archives for Weichselian geology and palaeoenvironment in northernmost Sweden. Boreas, vol 17, 439–468.

Lagerbäck R, Sundh M, 2003. Forsmark site investigation. Searching for evidence of late- or post-glacial faulting in the Forsmark region. Results from 2002. SKB P-03-76, Svensk Kärnbränslehantering AB.

Lanaro F, 2004. Rock mechanics characterisation of borehole KFM01A. SKB P-04-XX, Svensk Kärnbränslehantering AB (in prep).

LaPointe P R, Wallmann P C, Follin S, 1995. Estimation of effective block conductivities based on discrete network analyses using data from the Äspö site. SKB TR 97-07, Svensk Kärnbränslehantering AB.

LaPointe P R, Burago A, Lee K, Dershowitz W, 2000. geoFractal: Geostatistical and Fractal Analysis for Spatial Data. User manual, version 1.0. Golder Associates Inc.

LaPointe P R, 2002. Derivation of parent fracture population statistics from trace length measurements of fractal fracture populations. Int. J. of Rock Mech. and Min. Sci., Vol 39, p 381–388.

Larsson W, 1973. Forsmark kraftstation, aggregat 1 och 2, avloppstunneln: Berggeologiska förhållanden efter tunnellinjen. Technical Report, Swedish State Power Board, Stockholm (in Swedish).

Larson S Å, Tullborg E-L, 1993. Tectonic regimes in the Baltic Shield during the last 1200 Ma – A review. SKB TR 94-05, Svensk Kärnbränslehantering AB.

Larson S Å, Tullborg E-L, Cederbom C, Stiberg J-A, 1999. Sveconorwegian and Caledonian foreland basins in the Baltic Shield revealed by fission-track thermochronology. Terra Nova 11.

Larsson-McCann S, Karlsson A, Nord M, Sjögren J, Johansson L, Ivarsson M, Kindell S, 2002. Meteorological, hydrological and oceanographical information and data for the site investigation program in the communities of Östhammar and Tierp in the northern part of Uppland. SKB TR-02-02, Svensk Kärnbränslehantering AB.

Lidmar-Bergström K, 1994. Morphology of the bedrock surface. In C Fredén (ed), Geology, National Atlas of Sweden.

Lidmar-Bergström K, 1996. Long term morphotectonic evolution in Sweden. Geomorphology 16.

Lidmar-Bergström K, Olsson S, Olvmo M, 1997. Paleosurfaces and associated saprolites in southern Sweden. Geological Society 120, 95–124.

Lindahl G, Wallström K, 1980. Växtplankton I Öregrundsgrepen, SV Bottenhavet. Meddelande från Växtbiologiska Institutionen, Uppsala Universitet, 1980:8 (in Swedish).

Lindborg T, Schüldt R, 1998. The biosphere at Aberg, Beberg and Ceberg – a description based on literature concerning climate, physical geography, ecology, land use and environment. SKB TR-98-20, Svensk Kärnbränslehantering AB.

Lindborg T, Kautsky U, 2000. Variabler i olika ekosystem, tänkbara att beskriva vid platsundersökning för ett djupförvar. SKB R-00-19, Svensk Kärnbränslehantering AB (in Swedish).

Lindell S, Ambjörn C, Juhlin B, Larsson-McCann S, Lindqvist K, 2000. Available climatological and oceanographical data for site investigation program. SKB R-99-70, Svensk Kärnbränslehantering AB.

Lindroos H, Isaksson H, Thunehed H, 2004. The potential for ore and industrial minerals in the Forsmark area. SKB R-04-18, Svensk Kärnbränslehantering AB.

Lindström G, Rodhe A, 1986. Modelling water exchange and transit times in till basins using oxygen-18. Nordic Hydrol., 17, 325–334.

Ludvigson J-E, 2002. Brunnsinventering I Forsmark. SKB R-02-17, Svensk Kärnbränslehantering AB (in Swedish).

Ludvigson J-E, Jönsson S, 2003. Forsmark site investigation. Hydraulic interference tests. Boreholes HFM01, HFM02 and HFM03. SKB P-03-35, Svensk Kärnbränslehantering AB

Ludvigson J-E, Jönsson S, Levén J, 2003a. Pumping tests and flow logging. Boreholes KFM01A (0–100 m), HFM01, HFM02 and HFM03. SKB P-03-33, Svensk Kärnbränslehantering AB.

Ludvigson J-E, Jönsson S, Svensson T, 2003b. Pumping tests and flow logging. Boreholes KFM02A (0–100 m), HFM04 and HFM05. SKB P-03-34, Svensk Kärnbränslehantering AB.

Lundin L, 1982. Soil and groundwater in moraine and the influence of the soil type on the runoff. Dept. of Phys. Geogr., Rep. No 56, Univ. of Uppsala.

Lundmark, J-E, 1986. Skogsmarkers ekologi – Ståndortsanpassat skogsbruk. Del 1 – Grunder. Skogsstyrelsen Förlag, Jönköping. ISBN 91-85748-50-1 (in Swedish).

Lundqvist G, 1963. Beskrivning till jordartskarta ode Gävleborgs län. SGU series Ca 42, Sveriges Geologiska Undersökning (in Swedish with English summary).

Lundqvist T, 1968. Precambrian geology of the Los-Hamra Region, Central Sweden. SGU series Ba 23, Sveriges Geologiska Undersökning.

Lundqvist J, 1985. Deep-weathering in Sweden. Fennia 163, 287–292.

Lundström I, 1988. Regional inter-relationships in the Proterozoic geology of Bergslagen and Southeastern Central Sweden. Geologie en Mijnbouw 67.

Lång G, Cederlund G, Wallin K, 2004. Mammal population in three areas of site survey for deep-level repositories of radioactive waste: existing data and suggested additions. SKB R-04-XX, Svensk Kärnbränslehantering AB (in prep).

Löfgren A, Lindborg T, 2003. A descriptive ecosystem model – a strategy for model development during site investigations. SKB R-03-06, Svensk Kärnbränslehantering AB.

Martin C D, Christiansson R, 1991. Overcoring in highly stressed granite – the influence of microcracking. Int. J. Rock. Mech. Min. Sci. & Geomech. Abstr., Vol 28, No 1, 53–70.

Mattsson H, Isaksson H, Thunehed H, 2003. Forsmark site investigation. Petrophysical rock sampling, measurements of petrophysical rock parameters and in situ gamma-ray spectrometry measurements on outcrops carried out 2002. SKB P-03-26, Svensk Kärnbränslehantering AB.

McDonough W F, Sun S S, Ringwood A E, Jagoutz E, Hofmann A W, 1992. Potassium, rubidium, and cesium in the Earth and Moon and the evolution of the mantle of the Earth. Geochimica et Cosmochimica Acta 56.

Miliander S, Punakivi M, Kyläkorpi L, Rydgren B, 2004. Forsmark site description: Human population and human activities. SKB R-04-10, Svensk Kärnbränslehantering AB (in press).

Miller U, Robertsson A-M, 1979. Biostratigraphical investigations in the Annundsjö region, Ångermanland, northern Sweden. Early Norrland 12. Kungliga Vitterhets Historie och Antikvitets Akademien, 1–76.

Mo K, Smith S, 1988. Mjukbottenfaunan I Öregrundsgrepen 1978–1986. Naturvårdsverket Rapport 3467. 43 p (in Swedish).

Muir Wood R, 1995. Reconstructing the tectonic history of Fennoscandia from its margins: The past 100 million years. SKB TR-95-36, Svensk Kärnbränslehantering AB.

Munier R, Stenberg L, Stanfors R, Milnes A G, Hermanson J, Triumf C-A, 2003. Geological Site Descriptive Model. A strategy for the model development during site investigations. SKB R-03-07, Svensk Kärnbränslehantering AB.

Månsson A G M, 1996. Brittle reactivation of ductile basement structures; a tectonic model for the Lake Vättern basin, southern Sweden. GFF 118 (extended abstract).

Mörner N A, 2003. Paleoseismicity of Sweden a novel paradigm. Paleogeophysics & Geodynamics, Stockholm.

Nilsson P, Aaltonen J, 2003. Forsmark site investigation. Geophysical, radar and BIPS logging in boreholes HFM06, HFM07 and HFM08. SKB P-03-54, Svensk Kärnbränslehantering AB.

Nilsson P, Gustafsson C, 2003. Forsmark site investigation. Geophysical, radar and BIPS logging in boreholes HFM04, HFM05 and the percussion drilled part of KFM02A. SKB P-03-53, Svensk Kärnbränslehantering AB.

Nilsson A-C, Karlsson S, Borgiel M, 2003. Forsmark site investigations. Sampling and analyses of surface waters. Results from sampling in the Forsmark area, March 2002 to March 2003. SKB P-03-27, Svensk Kärnbränslehantering AB.

Nilsson A-C, 2003a. Forsmark site investigation. Sampling and analyses of groundwater in percussion drilled boreholes at drill site DS3. Results from the percussion boreholes HFM06 and HFM08. SKB P-03-49, Svensk Kärnbränslehantering AB.

Nilsson A-C, 2003b. Forsmark site investigation. Sampling and analyses of groundwater in percussion drilled boreholes and shallow monitoring wells at drill site DS2. Results from the percussion boreholes HFM04, HFM05, KFM02A (borehole section 0–100 m) and the monitoring wells SFM0004 and SFM0005. SKB P-03-48, Svensk Kärnbränslehantering AB.

Nilsson A-C, 2003c. Forsmark site investigation. Sampling and analyses of groundwater in percussion drilled boreholes and shallow monitoring wells at drillsite DS1. Results from the percussion boreholes HFM01, HFM02, HFM03, KFM01A (borehole section 0–100 m) and the monitoring wells SFM0001, SFM0002 and SFM0003. SKB P-03-47, Svensk Kärnbränslehantering AB.

NMR, 1984. Naturgeografisk regionindelning av Norden. Nordiska ministerrådet (in Swedish).

Nordstrom D K, Andrews J N, Carlsson L, Fontes J-Ch, Fritz P, Moser H, Olsson T, 1985. Hydrogeological and hydrogeochemical investigations in boreholes – final report of the Phase I geochemical investigations of the Stripa groundwaters. SKB TR 85-06, Svensk Kärnbränslehantering AB.

Nordstrom D K, Puigdomenech I, 1989. Redox chemistry of deep ground water in Sweden. SKB TR 86-03, Svensk Kärnbränslehantering AB

Nordstrom D K, Ball J W, Donahoe R J, Whittemore D, 1989. Groundwater chemistry and water-rock interactions at Stripa. Geochim. Cosmochim. Acta, 53, 1727–1740.

Ohlsson Y, Neretnieks I, 1997. Diffusion data in granite – recommended values. SKB TR 97-20, Svensk Kärnbränslehantering AB.

Parkhurst D L, Appelo C A J, 1999. User's Guide to PHREEQC (Version 2), a computer program for speciation, batch-reaction, one-dimensional transport, and inverse geochemical calculations. U.S. Geological Survey Water-Resources Investigations Report 99-4259, 312 p.

Passchier C W, Trouw R A J, 1998. Microtectonics. Springer-Verlag, Berlin, Heidelberg.

Perman F, Sjöberg J, 2003. Transient strain analysis of overcoring measurements in boreholes DBT-01 and DBT-03. Forsmark site investigation. SKB P-03-119, Svensk Kärnbränslehantering AB.

Persson C, 1985. Jordartskarta 12I Östhammar NO med beskrivning. SGU Ae 73, Sveriges Geologiska Undersökning (in Swedish with English summary).

Persson C, 1986. Jordartskarta 13I Österlövsta SO/13J Grundkallen SV med beskrivning. SGU Ae 76, Sveriges Geologiska Undersökning (in Swedish with English summary).

Persson C, 1990. Description to the Quaternary map Grisslehamn SV. SGU Ae 105, Sveriges Geologiska Undersökning (in Swedish with English summary).

Persson C, 1992. The latest ice recession and till deposits in northern Uppland, eastern central Sweden. SGU Series Ca 81, Sveriges Geologiska Undersökning.

Persson J, Wallin M, Wallström K, 1993. Kustvatten i Uppsala län 1993. Upplandsstiftelsen, Report nr 2 (in Swedish).

Petersson J, Wägnerud A, 2003. Forsmark site investigation. Boremap mapping of telescopic drilled borehole KFM01A. SKB P-03-23, Svensk Kärnbränslehantering AB, Stockholm, Sweden.

Pitkänen P, Luukkonen A, Ruotsalainen P, Leino-Forsman H, Vuorinen U, 1998. Geochemical modelling of groundwater evolution and residence time at the Kivetty site. POSIVA Report 98-07, Helsinki, Finland, 139 p.

Pitkänen P, Luukkonen A, Ruotsalainen P, Leino-Forsman H, Vuorinen U, 1999. Geochemical odelling of groundwater evolution and residence time at the Olkilouto site. POSIVA Report 98-10, Helsinki, Finland.

Pusch R, Börgesson L, Knutsson S, 1990. Origin of silty fracture fillings in crystalline bedrock. Geologiska Föreningens I Stockholm Förhandlingar, vol 112, 209–213.

Påsse T, 1996. A mathematical model of the shore level displacement in Fennoscandia. SKB TR 96-24, Svensk Kärnbränslehantering AB.

Påsse T, 1997. A mathematical model of past, present and future shore level displacement in Fennoscandia. SKB TR 97-28, Svensk Kärnbränslehantering AB.

Påsse T, 2001. An empirical model of glacio-isostatic movements and shore-level displacement in Fennoscandia. SKB R-01-41, Svensk Kärnbränslehantering AB.

Ranheden H, 1989. Barknåre and Lingnåre, human impact and vegetational development in an area of subrecent landuplift. Striae 33.

Renberg I, Segerström U, 1981. Applications of varved lake sediments in palaeoenvironmental studies. Wahlenbergia 7, 125–133.

Rhén I, Bäckblom G, Gustafson G, Stanfors R, Wikberg P, 1997a. Äspö HRL – Geoscientific evaluation 1997/2. Results from pre-investigations and detailed site characterisation. Summary report. SKB TR 97-03, Svensk Kärnbränslehantering AB.

Rhén I, Gustafson G, Stanfors R, Wikberg P, 1997b. Äspö HRL – Geoscientific evaluation 1997/4. Results from pre-investigations and detailed site characterisation. Comparison of predictions and observations. Geohydrology, groundwater chemistry and transport of solutes. SKB TR 97-05, Svensk Kärnbränslehantering AB.

Rhén I, Gustafson G, Stanfors R, Wikberg P, 1997c. Äspö HRL – Geoscientific evaluation 1997/ 5. Models based on site characterization 1986–1995. SKB TR 97-06, Svensk Kärnbränslehantering AB.

Rhén I, Smellie J, 2003 (eds). Comparison and summary of TASK#5. SKB-IC report in preparation.

Rhén I, Follin S, Hermanson J, 2003. Hydrogeological Site Descriptive Model. A strategy for the model development during site investigations. SKB R-03-08, Svensk Kärnbränslehantering AB.

Risberg J, 1991. Palaeoenvironment and sea level changes during the early Holocen on the Södertörn peninsula, Södermanland, eastern Sweden. Stockholm University, Department of Quaternary Rechearch. Report 20.

Robertsson A-M, Persson C, 1989. Biostratigraphical studies of three mires in Northern Uppland, Sweden. SGU Series C. No 821, Sveriges Geologiska Undersökning.

Robertsson A-M, Svedlund J-O, Andrén T, Sundh M, 1997. Pleistocene stratigraphy in the Dellen region, central Sweden. Boreas, Vol 26, pp 237–260.

Rodhe W, 1949. The ionic composition of lake waters. Verh. Int. Verein. Theor. Angew. Limnol. 10:377–386.

Rodhe A, 1987. The origin of streamwater traced by oxygen-18. Dept. of Phys. Geogr., Rep. Series A No 41, Univ. of Uppsala.

Rosén G, 1981. Tusen sjöar. Växtplanktons miljökrav. Liber förlag, Stockholm (in Swedish).

Rouhiainen P, Pöllänen J, 2003. Forsmark site investigation. Difference flow logging of borehole KFM01A. SKB P-03-28, Svensk Kärnbränslehantering AB.

Rønning H J S, Kihle O, Mogaard J O, Walker P, Shomali H, Hagthorpe P, Byström S, Lindberg H, Thunehed H, 2003. Forsmark site investigation. Helicopter borne geophysics, Östhammar, Sweden. SKB P-03-41, Svensk Kärnbränslehantering AB.

Röshoff R, Lanaro F, Jing L, 2002. Strategy for a Rock Mechanics Site Descriptive Model. Development and testing of the empirical approach. SKB R-02-01, Svensk Kärnbränslehantering AB.

Samuelsson M, 1996. Interannual salinity variations in the Baltic Sea during the period 1954–1990. Continental Shelf Research. Vol 16, No 11, pp 1463–1477.

Sandegren R, Asklund B, Westergård A H, 1939. Beskrivning till kartbladet Gävle. SGU Aa 178, Sveriges Geologiska Undersökning (in Swedish).

Sandegren R, Asklund B, 1948. Beskrivning till kartbladet Söderfors. SGU Aa 190, Sveriges Geologiska Undersökning (in Swedish).

Schoning K, 2001. Marine conditions in middle Sweden during the Late Weichselian and Early Holocene as inferred from foraminifera, Ostracoda and stable isotopes. Doctoral thesis. Department of Physical Geography and Quaternary Geology. Quaternaria Ser A. No 8.

Serafim JL, Pereira JP, 1983. Consideration of the geomechanics classification of Bieniawski, Proc. Int. Symp. Eng. Geol. & Underground Constr., p 1133–1144.

SGU, 1983. Description and appendices to the hydrogeological map of Uppsala County. Swedish Geological Survey, Uppsala.

Shackelton N J, Berger A, Peltier W R, 1990. An alternative astronomical calibration of the lower Pleistocene timescale based on ODP Site 677. Transactions of the Royal Society of Edinburgh: Earth Sciences, 81, 251–261.

Shackelton N J, 1997. The deep-sea sediment record and the Pliocene-Pleistocene boundary. Quaternary International, vol 40, 33–35.

Ŝibrava V, 1992. Should the Pliocene-Pleistocene boundary be lowered? SGU Series Ca 81, 327–332, Sveriges Geologiska Undersökning.

Sigurdsson T, 1987. Bottenundersökning av ett område ovanför SFR, Forsmark. SFR 87-07, Svensk Kärnbränslehantering AB (in Swedish).

Sjöberg R, 1994. Bedrock caves and fractured rock surface in Sweden. Paleogeophysics & Geodynamics, Stockholm University, Stockholm.

SKB, 2000a. Förstudie Östhammar. Slutrapport. Svensk Kärnbränslehantering AB. IBSN 91-972810-4-2 (in Swedish).

SKB, 2000b. Geoscientific programme for investigation and evaluation of sites for the deep repository. SKB TR-00-20, Svensk Kärnbränslehantering AB.

SKB, 2001a. Site investigations. Investigation methods and general execution programme. SKB TR-01-29, Svensk Kärnbränslehantering AB

SKB, 2001b. Integrated account of method, site selection and programme prior to the site investigation phase. SKB TR-01-03, Svensk Kärnbränslehantering AB.

SKB, 2002a. Forsmark – site descriptive model version 0. SKB R-02-32, Svensk Kärnbränslehantering AB.

SKB, 2002b. Execution programme for the initial site investigations at Forsmark. SKB P-02-03, Svensk Kärnbränslehantering AB.

SKB, 2002c. Preliminary safety evaluation, based on initial site investigation data. Planning document. SKB TR-02-28, Svensk Kärnbränslehantering AB.

SKB, 2003. Planning report for the safety assessment SR-Can. SKB TR-03-08, Svensk Kärnbränslehantering AB.

SKB GIS, 2003. Forsmark Fieldnote 115. Umeu_FM-vtn_1345_1371.

SKB SICADA, 2003. Forsmark Fieldnote 169.

Slunga R, Nordgren L, 1990. Earthquake measurements in southern Sweden. Apr 1 1987–Nov 30 1988. SKB AR 90-19, Svensk Kärnbränslehantering AB.

Smellie J A T, Wikberg P, 1991. Hydrochemical investigations at Finnsjön, Sweden. J. Hydrol., 126, 129–158.

Smellie J, Laaksoharju M, 1992. The Äspö hard rock laboratory: final evaluation of the rojectureical pre-investigations in relation to existing geologic and hydraulic conditions. SKB TR 92-31, Svensk Kärnbränslehantering AB

Smellie J, Laaksoharju M, Tullborg E-L, 2002. Hydrogeochemical Site Descriptive Model. A strategy for the model development during site investigations. SKB R-02-49, Svensk Kärnbränslehantering AB.

Snellman M, Pitkänen P, Luukkonen A, Ruotsalainen P, Leino-Forsman H, Vuorinen U, 1998. Summary of recent observations from Hästholmen groundwater studies. POSIVA Working Report 98-44, Helsinki, Finland, 71 p.

Sohlenius G, Rudmark L, 2003. Forsmark site investigation. Mapping of unconsolidated Quaternary deposits. Stratigraphical and analytical data. SKB P-03-14, Svensk Kärnbränslehantering AB.

Sohlenius G, Rudmark L, Hedenström A, 2003. Forsmark. Mapping of unconsolidated Quaternary deposits. Field data 2002. SKB P-03-11, Svensk Kärnbränslehantering AB.

Stanfors R, Erlström M, Markström I, 1997. Äspö HRL – Geoscientific evaluation 1997/1. Overview of site characterization 1986–1995. SKB TR-97-02, Svensk Kärnbränslehantering AB.

Stephansson O, Eriksson B, 1975. Pre-Holocene joint fillings at Forsmark, Uppland, Sweden. Geologiska Föreningens I Stockholm Förhandlingar, vol 97, 91–95.

Stephansson O, Ångman P, 1984. Hydraulic fracturing stress measurements at Forsmark and Stidsvig, Sweden. Research Report TULEA 1984:30.

Stephens M B, Wahlgren C-H, Weihed P, 1994. Geological Map of Sweden, scale 1:3 000 000. SGU series Ba 52, Sveriges Geologiska Undersökning.

Stephens M B, Wahlgren C-H, 1996. Post-1.85 Ga tectonic evolution of the Svecokarelian orogen with special reference to central and SE Sweden. GFF 118 (extended abstract).

Stephens M B, Wahlgren C-H, Weijermars R, Cruden A R, 1996. Left-lateral transpressive deformation and its tectonic implications, Sveconorwegian orogen, Baltic Shield, southwestern Sweden. Precambrian Research 79.

Stephens M B, Wahlgren C-H, Weihed P, 1997. Sweden. In E. M. Moores & R. W. Fairbridge (edits), Encyclopedia of European and Asian Regional Geology. Chapman & Hall, London.

Stephens M B, Ahl M, Bergman T, Lundström I, Persson L, Ripa M, Wahlgren C-H, 2000. Syntes av berggrundsgeologisk och geofysisk information, Bergslagen och omgivande områden. I H. Delin (red.): Regional berggrundsgeologisk undersökning – sammanfattning av pågående undersökningar 1999. SGU Rapporter och meddelanden 102, Sveriges Geologiska Undersökning (in Swedish).

Stephens M B, Bergman T, Andersson J, Hermansson T, Wahlgren C-H, Albrecht L, Mikko H, 2003a. Forsmark bedrock mapping. Stage 1 (2002) – Outcrop data including fracture data. SKB P-03-09, Svensk Kärnbränslehantering AB.

Stephens M B, Lundqvist S, Ekström M, Bergman T, Andersson J, 2003b. Rock types, their petrographic and geochemical characteristics, and a structural analysis of the bedrock based on stage 1 (2002) surface data. SKB P-03-75, Svensk Kärnbränslehantering AB.

Stigsson M, Follin S, Andersson J, 1998. On the simulation of variable density flow at SFR, Sweden. SKB R-98-08, Svensk Kärnbränslehantering AB.

Stigsson M, Outters J, Hermanson J, 2001. Äspö Hard Rock Laboratory, prototype repository. Hydraulic DFN model no: 2. International Progress Report IPR-01-39, Svensk Kärnbränslehantering AB.

Stille H, Groth T, Fredriksson A, 1982. FEM-analysis of rock mechanical problems with JOBFEM. Stiftelsen Bergteknisk Forskning – BeFo, Stockholm, 307:1/82.

Stille H, Fredriksson A, Widing E, Åhrling G, 1985. Bergmekaniska beräkningar – FEM-analys av Silo med anslutande tunnlar. SKB SFR 85-05, Svensk Kärnbränslehantering AB (in Swedish).

Stille H, 1986. Experiences of design of large caverns in Sweden, Proc. Conf. Large Rock Caverns, 1986, Stockholm, Sweden.

Streckeisen A, 1976. To each plutonic rock its proper name. Earth Science Reviews 12.

Streckeisen A, 1978. IUGS Subcommission on the Systematics of Igneous Rocks. Classification and nomenclature of volcanic rock, lamprophyres, carbonatites and melilitic rocks. Recommendations and suggestions. Neues Jahrbuch für Mineralogie 134.

Strömberg B, 1989. Late Weichselian deglaciation and clay varve chronology in east-central Sweden. SGU Series Ca 73, Sveriges Geologiska Undersökning.

Stålhös G, 1991. Beskrivning till berggrundskartorna Östhammar NV, NO, SV, SO. SGU serie Af 161, 166, 169 och 172. Sveriges Geologiska Undersökning (in Swedish).

Sundberg J, 1988. Thermal properties of soils and rocks, Publ. A 57 Dissertation, doctoral thesis, Geologiska institutionen, Chalmers Univerity of Technology and University of Göteborg.

Sundberg J, 1995. Termiska egenskaper för kristallint berg i Sverige. Kartor över värmekonduktivitet, värmeflöde och temperatur på 500 m djup. SKB Projektrapport D-95-018, Svensk Kärnbränslehantering AB (in Swedish).

Sundberg J, 2003a. Thermal Site Descriptive Model, A Strategy for the Model Development during Site Investigations. SKB R-03-10, Svensk Kärnbränslehantering AB.

Sundberg J, 2003b. Thermal Properties at Äspö HRL, Analysis of Distribution and Scale Factors. SKB R-03-17, Svensk Kärnbränslehantering AB.

Svenonius F, 1887. Beskrifning till kartbladen Forsmark och Björn. SGU serie Aa 98 och 99, Sveriges Geologiska Undersökning (in Swedish).

Svensson S A, 1988. Skattning av årlig tillväxt i stamvolym. Rapport 46, Sveriges lantbruksuniversitet, inst. F skogstaxering, pp 65–74, 77–78, 82–83 (in Swedish).

Svensson N-O, 1989. Late Weichselian and early Holocene shore displacement in the central Baltic, based on stratigraphical and morphological records from eastern Småland and Gotland, Sweden. LUNDQUA, vol 25, 181 pp.

Svensson U, 1996. SKB Palaeohydrogeological programme. Regional groundwater flow due to advancing and retreating glacier-scoping calculations. In: SKB Project Report U 96-35, Svensk Kärnbränslehantering AB.

Svensson U, Laaksoharju M, Gurban I, 2002. Impact of the tunnel construction on the groundwater chemistry at Äspö. SKB report in progress. Svensk Kärnbränslehantering AB.

Svensson U, Follin S, 2003. Äspö Hard Rock Laboratory. Äspö Task Force on modelling groundwater flow and transport of solutes. Task 6a, 6b and 6b2. Simulation of tracer transport, considering both experimental and natural, long time scales. International Progress Report IPR-03-XX, Svensk Kärnbränslehantering AB (in print).

Svensson U, Kuylenstierna H-O, Ferry M, 2004. Darcy Tools V 2.1. Concepts, methods, equations and demo simulations. SKB R-04-19, Svensk Kärnbränslehantering AB.

Thunehed H, Pitkänen T, 2002. Markgeofysiska mätningar inför placering av de tre första kärnborrhålen i Forsmarksområdet. SKB P-02-01, Svensk Kärnbränslehantering AB (in Swedish).

Tullborg E-L, Larson S Å, 1984. $\delta^{18}O$ and $\delta^{13}C$ for limestones, calcite fissure infillings and calcite precipitates from Sweden. Geologiska föreningens i Stockholm förhandlingar 106(2).

Tullborg E-L, Larson S Å, Björklund L, Samuelsson L, Stigh J, 1995. Thermal evidence of Caledonide foreland, molasse sedimentation in Fennoscandia. SKB TR-95-18, Svensk Kärnbränslehantering AB.

Tullborg E-L, Larson S Å, Stiberg J-A, 1996. Subsidence and uplift of the present land surface in the southeastern part of the Fennoscandian Shield. GFF 118.

Tunbridge L, Chryssanthakis P, 2003. Forsmark site investigation. Borehole: KFM01A. Determination of P-wave velocity, transverse borehole core. SKB P-03-38, Svensk Kärnbränslehantering AB.

Wahlgren C-H, Cruden A R, Stephens M B, 1994. Kinematics of a fan-like structure in the eastern part of the Sveconorwegian orogen, Baltic Shield, south-central Sweden. Precambrian Research 70.

Wastegård S, Andrén T, Sohlenius G, Sandgren P, 1995. Different phases of the Yoldia Sea in the north western Baltic Proper. Quaternary International 27, 121–129.

Welin E, 1964. Uranium disseminations and vein fillings in iron ores of northern Uppland, Central Sweden. Geologiska Föreningens i Stockholm Förhandlingar 86.

Welinder S, Pedersen E A, Widgren M, 1998. Det svenska jordbrukets historia: Jordbrukets första femtusen år. Natur och Kultur/LTs förlag, Borås (in Swedish).

Werner K, Johansson P-O, 2003. Forsmark site investigation. Slug tests in groundwater monitoring wells in soil. SKB P-03-65, Svensk Kärnbränslehantering AB.

Westman P, Wastegård S, Schoning K, Gustafsson B, Omstedt A, 1999. Salinity change in the Baltic sea during the last 8500 years: evidence, causes and models. SKB TR-99-38, Svensk Kärnbränslehantering AB.

Wetzel R G, 2001. Limnology: Lake and River Ecosystems. 3rd Edition, Academic Press, San Diego. 1006 pp.

Wickman F E, Åberg G, Levi B, 1983. Rb-Sr dating of alteration events in granitoids. Contributions to Mineralogy and Petrology 83.

Wickman F E, 1988. Possible impact structures in Sweden. In A Boden and K-G Eriksson, (eds), Deep Drilling in Crystalline Bedrock. Volume 1: The Deep Gas Drilling in the Siljan Impact Structure, Sweden and Astroblemes. Springer-Verlag, Berlin.

Widestrand H, Byegård J, Ohlsson Y, Tullborgh E-L, 2003. Strategy for the use of laboratory methods in the site investigations programme fort the transport properties of the rock. SKB R-03-20, Svensk Kärnbränslehantering AB.

Widgren M, 1983. Settlement and farming systems in early Iron Age. A study of fossil agrarian landscapes in Östergötland, Sweden. Stockholm studies in Human Geography 3, Dissertation in Human geography. Almquist & Wiksell International, Stockholm. 132 pp.

Wikberg P, 1998. Äspö Task Force on modelling of groundwater flow and transport of solutes. SKB progress report HRL-98-07, Svensk Kärnbränslehantering AB.

Wiklund S, 2002. Digitala ortofoton och höjdmodeller. Redovisning av metodik för platsundersökningsområdena Oskarshamn och Forsmark samt förstudieområdet Tierp Norra. SKB P-02-02, Svensk Kärnbränslehantering AB (in Swedish).

Wikström A, 1996. U-Pb zircon dating of a coarse porphyritic quartz monzonite and an even-grained, grey tonalitic gneiss from the Tiveden area, south central Sweden. In T Lundkvist (ed), Radiometric dating results 2. SGU series C 828, Sveriges Geologiska Undersökning.

Wikström A, Karis L, 1998. Beskrivning till berggrundskartorna Askersund NO och SO. SGU serie Af 186, 195, Sveriges Geologiska Undersökning (in Swedish).

Åkerman C, 1994. Ores and mineral deposits. In C Fredèn (ed), Geology. National Atlas of Sweden.

Humans and land use

Input data sources and calculated figures for the variables used to describe humans and land use in the Forsmark regional model area. Absolute numbers and calculated numbers per km^2 are for the Forsmark parish, since much of the data were available on the parish level.

Humans

Table 1. Variable group - Demography

Variable	Time series	Data source	Method	Results No.	No. per km^2
Total population	1993 - 2002	Statistics Sweden	The latest statistical figure concerning the total population in Forsmark parish is from 2002	168 (82 men and 86 women)	1.8
			A mean value for 1993-2002 was calculated	169.5 (83 men and 86 women)	1.8
Age structure	1993 - 2002	Statistics Sweden	The distribution over the five age classes was calculated for the year 2002	0-15 y 17.9 % 16-24 y 6.0 % 25-44 y 23.8 % 45– 64 y 31.5 % ≥ 65 y 20.8 %	
Excess of births over deaths	1993 - 2002	Statistics Sweden	The latest birth figure is from 2002	0	
			A mean value for 1993-2002 was calculated	2.4	
			The latest death figure is from 2002	4	
			A mean value for 1993-2002 was calculated	1.7	
			The excess of births over deaths was calculated for 2002	-4	
			A mean excess value was calculated for 1993-2002	0.7	
Net-migration	1993 - 2002	Statistics Sweden	The latest figure concerning in-migration is from 2002	9	
			A mean value for 1993-2002 was calculated	14.1	
			The latest out-migration figure is from 2002	7	
			A mean value for 1993-2002 was calculated	13.7	
			A net-migration value was calculated for 2002	2	
			A mean net-migration value was calculated for 1993-2002	1	
Ill-health number	1998-2002	Statistics Sweden	The latest figure over the ill-health number is from 2002	70.8	
			A mean value for 1998-2002 was calculated	41.6	
			The latest figure over the men ill-health number is from 2002	51.8	
			A mean value for 1998-2002 was calculated	21.9	
			The latest figure over the women ill-health number is from 2002.	90.2	
			A mean value for 1998-2002 was calculated	61.4	

Table 2. Variable group – Properties and buildings

Variable	Time series	Data source	Method	Results		No. per km²
				No.		
Type of properties	1996 and 2002	Statistics Sweden	The actual number of properties was obtained from Statistics Sweden for 2002 and 1996. The number was calculated as a procentage			
			Number of farms in 2002 (1996).	49 (53)	28.2 %	0.52
			Number of one- or two dwelling buildings in 2002 (1996).	52 (52)	29.9 %	0.55
			Number of holiday-houses in 2002 (1996).	65 (65)	37.4 %	0.69
			Number of multi-dwelling buildings in 2002 (1996).	0 (0)	0 %	0.00
			Number of "other" buildings in 2002 (1996).	8 (9)	4.6 %	0.08
Building permits	1996 - 2002	Statistics Sweden	The latest figure over the number of building permits for dwellings is from 2002	0		
			A mean value for 1996-2002 was calculated	0.9		
			The latest figure over the number of building permits for business premises is from 2002	3		
			A mean value for 1996-2002 was calculated	0.4		
Completed dwellings	1993 - 2002	Statistics Sweden	The latest figure over completed dwellings in one- two or multi dwelling buildings is from 2002	0		0
			A mean value for 1993-2002 was calculated	0		0

Table 3. Variable group – Employment

The following course classification of lines of business, according to SE-SIC Swedish Standard Industrial Classification, is used in the table:

1   Agriculture, forestry, hunting, fishing
2   Mining and manufacturing
3   Electricity-, gas- and water supply. Sewage and refuse disposal
4   Construction
5   Trade and communication
6   Financial intermediation, business activities

7   Education and research
8   Health and social work
9   Personal and cultural activities
10 Public administration etc.
11 Unknown activity

Variable	Time series	Data source	Method	Results		No.	No. per km^2
The total employed night-population (20-64 y)	1997-2002	Statistics Sweden	The latest figure over the total number of employed night population is from 2001			71	0.75
			A mean value for 1997-2001 was calculated			70	0.74
The employed night-population by lines of business* (20-64 y)	1997-2002	Statistics Sweden	The distribution over the eleven lines of business was calculated for the year 2001.		1	5.6 %	
					2	9.9 %	
					3	19.7 %	
					4	4.2 %	
					5	7.0 %	
					6	28.2 %	
					7	7.0 %	
					8	9.9 %	
					9	5.6 %	
					10	0.0 %	
					11	0.0 %	
The total employed day-population (20-64 y)	1997-2002	Statistics Sweden	The latest figure over the total number of employed day population is from 2001			929	9.9
			A mean value for 1997-2001 was calculated			958	10.2
The employed day-population by lines of business (20-64 y)	1997-2002	Statistics Sweden	The distribution over the eleven lines of business was calculated for the year 2001. *		1	0.0 %	
					2	0.0 %	
					3	79.0 %	
					4	1.0 %	
					5	0.3 %	
					6	18.4 %	
					7	0.0 %	
					8	0.0 %	
					9	1.2 %	
					10	0.0 %	
					11	0.0 %	

Variable	Time series	Data source	Method	Results		
					No.	No. per km^2
The total number of working sites	1997-2002	Statistics Sweden	The latest figure over the total number of working sites is from 2002		17	0.18
			A mean value for 1997-2002 was calculated		11	0.12
Working sites by lines of business	2001	Statistics Sweden	The distribution over the eleven lines of business was calculated for the year 2001. *	1	0.0 %	
				2	0.0 %	
				3	0.0 %	
				4	17.6 %	
				5	0.0 %	
				6	52.9 %	
				7	0.0 %	
				8	0.0 %	
				9	17.6 %	
				10	0.0 %	
				11	0.0 %	
Commuting (20-64 y)	2001	Statistics Sweden	A figure from 2001 over the number of outgoing-commuters has been obtained.		32	
			A figure from 2001 over the number of ingoing-commuters has been obtained.		902	
			The net commuting was calculated for 2001.		870	
The total non-employed population (20-64 y)	1997-2001	Statistics Sweden	The latest figure over the total number of non employed population is from 2001		26	0.28
			A mean value for 1997-2001 was calculated		25	0.27
			The percentage non employed of the total population was calculated		15.3 %	
The non employed population by category	1997-2001	Statistics Sweden	The latest figures over the different categories within the non employed population are from 2001. The number per category was calculated as a percentage of the non employed			
			Number of students in 2001.	3	11.5 %	
			Number of unemployed in 2001.	3	11.5 %	
			Number of inhabitants in the military service in 2001.	0	0.0 %	
			Number of inhabitants with early retirement in 2001.	9	34.6 %	
			Number of inhabitants non employed of other reasons in 2001.	12	46.2 %	

Human activities

Table 4. Variable group – Forestry

Variable	Time series	Data source	Method	Results	
				No.	No. per km^2
Wood extraction	1999	Forestry Manage-ment Plan, Sveaskog 1999	The amount of wood extracted from the model area during the past 10 years was calculated. Here, the average amount of wood extracted per year is given.	10119 m^{3}sk	176 m^{3}sk

Table 5. Variable group – Agriculture

Variable	Time series	Data source	Method	Results	
				Total production kg/year	Production kg/km^2/year
Production of Rye	1990, 1995, 1999	Statistics Sweden	Production is calculated with the crop distribution (hectare rye) multiplied with the standard yield in the appropriate area	56 251 (1990) 4 327 (1995) 0 average 20 193	547 (1990) 45 (1995) 0 (1999) average 214
Production of Barley	1990, 1995, 1999	Statistics Sweden	Production is calculated with the crop distribution (hectare barley) multiplied with the standard yield in the appropriate area	113 069 (1990) 137 96 (1995) 61 175 (1990) average 104 068	1 200 (1990) 1 464 (1995) 649 (1999) average 1 104
Production of Oats	1990, 1995, 1999	Statistics Sweden	Production is calculated with hte crop distribution (hectare oats) multiplied with the standard yield in the appropriate area	0 (1990) 3 808 (1995) 0 (1999) average 1 269	0 (1990) 40 (1995) 0 (1999) average 13
Production of Potatoes	1990, 1995, 1999	Statistics Sweden	Production is calculated with the crop distribution (hectare potatoes) multiplied with the standard yield in the appropriate area	15 532 (1990) 7 766 (1995) 5 177 (1990) average 9 492	165 (1990) 82 (1995) 55 (1999) average 101
Production of Hay, Silage, Green Fodder	1990, 1995, 1999	Statistics Sweden	Production is calculated with the crop distribution (hectare hay, silage, fodder) multiplied with the standard yield in the appropriate area	529 928 (1990) 558 030 (1995) 600 216 (1999) average 562 658	5 623 (1990) 5 924 (1995) 6 371 (1999) average 5 973
Veal	1990, 1995, 1999	Statistics Sweden	Production kg/km^2 is calculated with the help of the number of animals, average slaughter weight and national average percentage of slaughtered animals in a flock	12 137 (1990) 15 130 (1995) 15 211 (1999) average 14 159	129 (1990) 161 (1995) 161 (1999) average 150

Mutton	1990, 1995, 1999	Statistics Sweden	Production kg/km^2 is calculated with the help of the number of animals, average slaughter weight and national average percentage of slaughtered animals in a flock	307 (1990) 239 (1995) 247 (1999) average 264	3.26 (1990) 2.54 (1995) 2.62 (1999) average 2,81
Pork	1990, 1995, 1999	Statistics Sweden	Production kg/km^2 is calculated with the help of the number of animals, average slaughter weight and national average percentage of slaughtered pigs in a flock	860 (1990) 0 (1995) 0 (1999) average 287	9.1 (1990) 0 (1995) 0 (1999) average 3
Eggs	1990, 1995, 1999	Statistics Sweden	Production is calculated with the help of the number of laying hen and national average egg production by hen	2 173 (1990) 1 630 (1995) 1 304 (1999) average	23 (1990) 17 (1995) 13 (1999) average 18
Milk	1990, 1995, 1999	Statistics Sweden	Production is calculated with the help of the number of dairy cows and national average milk production by cow	8450 (1990) 5850 (1995) 8320 (1999) average 7540	90 (1990) 62 (1995) 88 (1999) average 80

Table 6. Variable group – Horticulture

Variable	Time series	Data source	Method	Results	
				No.	No. per km^2
Number of horticultural holdings	2003	See right	There are no holdings in the parish according to www.gulasidorna.se and www.onab.net (Östhammars Näringslivsutveckling AB)	0	0
Production of fruit and vegetables	2003	As above	As above	0	0

Table 7. Variable group – Aquaculture

Variable	Time series	Data source	Method	Results	
				No.	No. per km^2
Number of enterprises/ production for consumption	2002	The report *Aquaculture 2002*, Statistics Sweden and Östhammar key plan (ÖP) 2002.	The number of enterprises in Uppsala County was obtained from Statistics Sweden. The number and location of the enterprises in the municipality was obtained from the key plan for the municipality. There is no aquaculture within the parish of Forsmark.	0	0

Table 8. Variable group – Mineral extraction

Variable	Time series	Data source	Method	Results No.	No. per km^2
Number of mineral extraction leases	2003	Data from the County Administrative Board	Coordinates for the leases acquired from the County Administrative Board was plotted on a GIS-map and compared to the spatial delimitation of the Forsmark parish.	0	0

Table 9. Variable group – Water supply

Variable	Time series	Data source	Method	Results No.	No. per km^2
Water use, by category; house-holds, agriculture, industry and other	1990, 1995 and 2000	Statistics Sweden	The water use by households is calculated with the average use per person according to Statistics Sweden (189 litres/ day) multiplied with the number of inhabitants in the parish.	11590 m^3/year	
			The water use within agriculture has been estimated with the average use per farm in the municipality in 1995 (571000 m^3 /513 farms) multiplied with the number of farms in the parish (four in 1999).	4450 m^3/year	
			The extensive water use within Forsmark power plant can represent the water use within the industry.	257 000 m^3/year	
Water withdrawal subdivided in private and public supply	1990, 1995 and 2000	Statistics Sweden	If we assume that the allocation between public and private is the same as in the municipality in 1995 (water used in Formark power plant is excluded) we can estimate a rough figure over the water withdrawal from public water supplies.	Approx. 5800 m^3/year	
			If we assume that the allocation between public and private is the same as in the municipality in 1995 (water used in Formark power plant is included) we can estimate a rough figure over the water withdrawal from private water supplies. Forsmark power plant use a private water supply (Forsmarksån)	Approx. 267 000 m^3/year	
Water withdrawal subdivided in ground water and surface water	1990, 1995 and 2000	Statistics Sweden	As the allocation between ground water and surface water is almost the same as between public and private supply in Östhammar municipality in 1995, we can assume that the amount of ground water is comparable with the amount of public water.	Approx. 5800 m^3/year	
			As the allocation between ground water and surface water is almost the same as between public and private supply in Östhammar municipality in 1995, we can assume that the amount of surface water is comparable with the amount of private water.	Approx. 267 000 m^3/year	

Table 10. Variable group – Commercial fishing

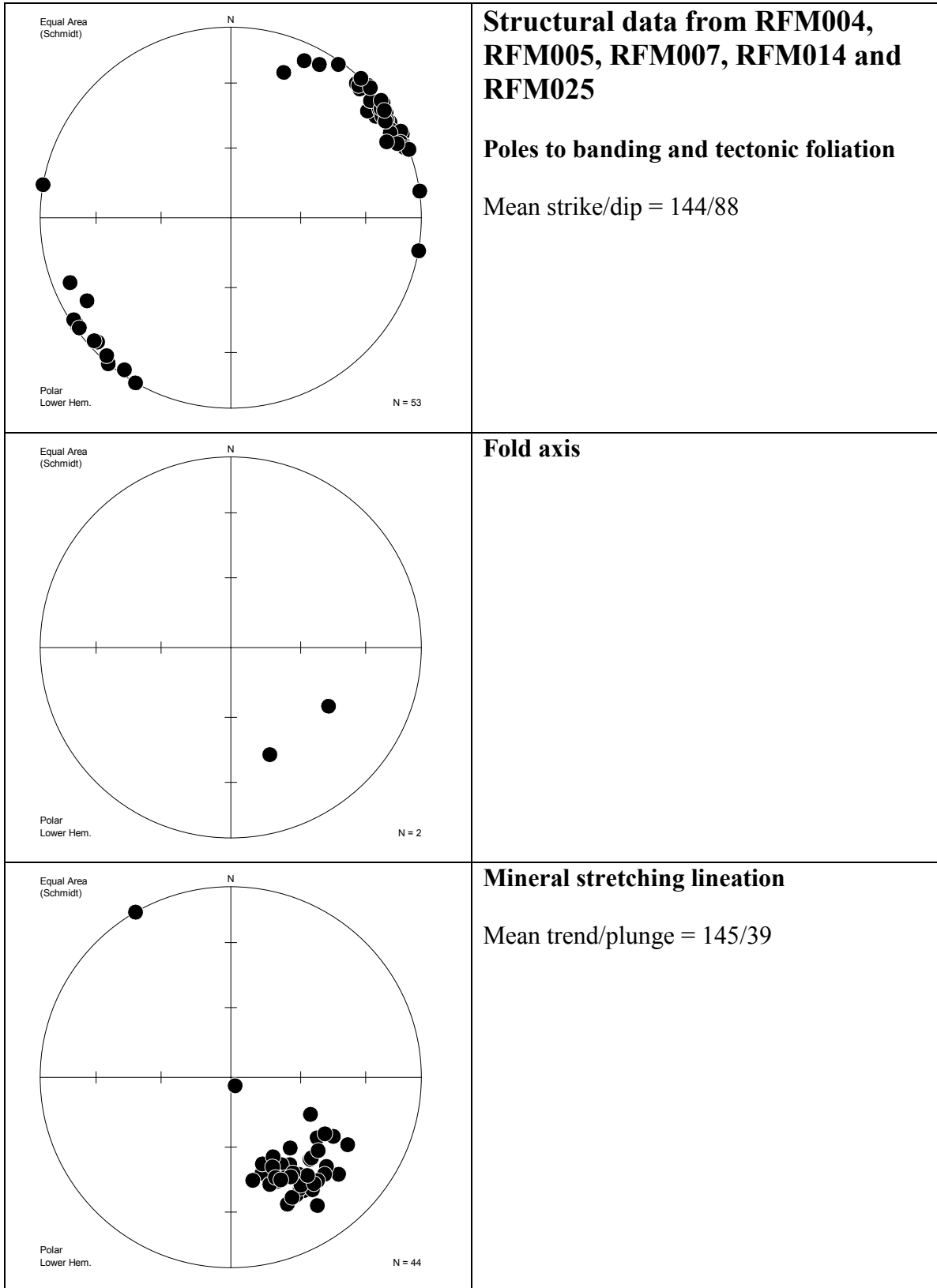| Variable	Time series	Data source	Method	Results	
				No.	No. per km^2
Number of fishermen	1995-2002	National Board of Fisheries	Through the postcode catalogue it could be established that no fisherman lives within the parish of Forsmark.	0	0
Total catch	1995-2002	National Board of Fisheries	As there is no active fisherman in the parish, there is no catch registered in the parish.	0	0

Table 11. Variable group – Outdoor life

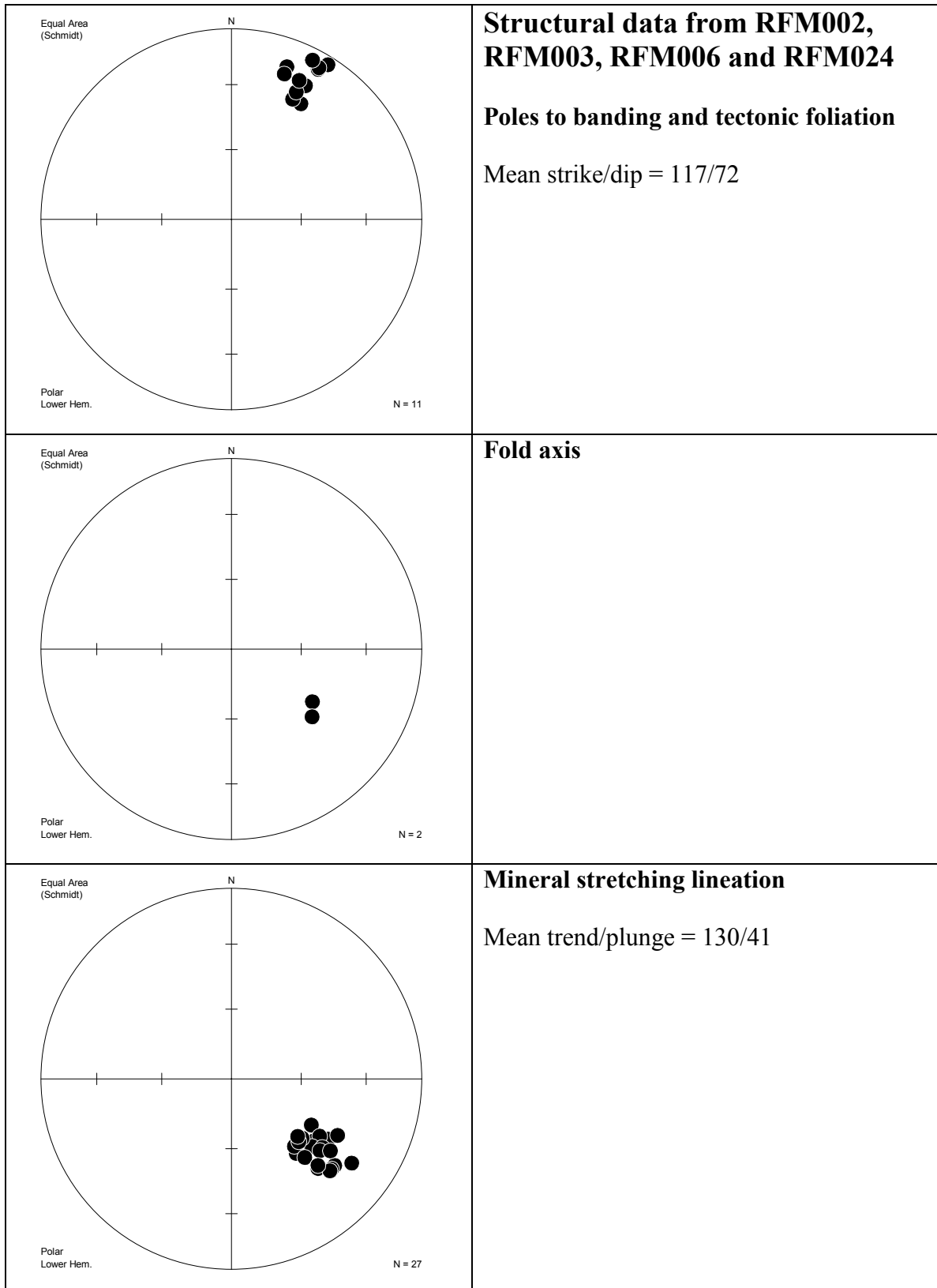| Variable	Time series	Data source	Method	Results			
				No.			No. per km^2
Harvested moose in number	1999-2003	County Administra-tive Board of Uppsala	The number of harvested moose from the different hunting zones has been summarised for the last hunting season (ended in 2003).	22 (bulls)	21 (cows)	26 (calves)	0.53
			A mean value for 1999-2003 was calculated	20.6 (bulls)	20.0 (cows)	27.6 (calves)	0.53
Harvested moose in weight	1999-2003	County Administra-tive Board of Uppsala	According to Swedish Association for Hunting and Wildlife Management the carcass weight is 180-230 kg for a bull, 170-200 kg for a cow and 70 kg for a calf (55% of the living weight). When calculating we have chosen to use a carcass weight of 205 kg for a bull, 185 kg for a cow and 70 kg for calves.	10215 kg/year			78 kg/km^2/year
			A mean value for 1999-2003 was calculated	9855 kg/year			76 kg/km^2/year
Harvested roe deers in number	1997-2001	Swedish Association for Hunting and Wildlife Management	The latest coarse estimate of the harvested roe deers per km^2 is from 2001. The actual number of harvested roe deers within the parish was calculated from the number per unit area.	94.2			1.0
			A mean value for 1997-2001 was calculated	179.5			1.9
Harvested roe deers in weight	1997-2001	Swedish Association for Hunting and Wildlife Management	According to Swedish Association for Hunting and Wildlife Management the roe deer weight is 20-30 kg. If we assume that the carcass weight is 55 % of the living weight as for the moose, we get a carcass weight of approx. 14 kg for an adult.	1319 kg/year			14.0 kg/km^2/year
			A mean value for 1997-2001 was calculated	2514 kg/year			26.7 kg/km^2/year
Picking of wild berries	1997	Statistics Sweden	According to surveys conducted by Statistics Sweden, an approximate average amount of 200-500g/ha of wild berries is picked in Sweden. This figure was multiplied with the land area of the Forsmark parish.	1880 – 4700 kg/year			20 – 50 kg/ km^2/year

Variable	Time series	Data source	Method	Results	
				No.	No. per km^2
Picking of fungi	1997	Statistics Sweden	According to surveys conducted by Statistics Sweden, an approximate average amount of 30-100g/ha of fungi is picked in Sweden. This figure was multiplied with the land area of the Forsmark parish.	280 – 940 kg/year	3 – 10 kg/km^2/year
Number of attractive fishing-waters	2003	www.cinclusc.com/spfguide/ Cinclus C Sportfiskeguide	Södra Åsjön is a fishing water that requires a fishing licence, according to Fiskeguide, Uppsala län 2000-2001. Furthermore, the waters around the Forsmark power plant are considered attractive for fishing.	2	
Number of sport-fishing clubs	2003	www.sportfiskarna.se Swedish Sport Fishing Association	According to www.sportfiskarna.se (Sveriges sportfiske- och fiskevårdsförbund) there is no sport fishing club registered in Östhammar municipality.	0	
Catch by sport fishermen	2002	Report Fiske 2000 – En undersökning om svenskarnas sport- och husbehovsfiske, Fiskeri-verket (ISSN 1404-8590)	A theoretically value has been calculated based on the facts in the report Fiske 2000. 55 % of the inhabitants between 16-64 years catch 18 kg fish per person and year.	1026 kg/year	10.9 kg /km^2/year
Number of golf courses	2003	www.upplandsgolf.org.se Upplands golfförbund	There are no golf-courses within the parish of Forsmark according to www.upplandsgolf.org.se (Upplands Golfförbund)	0	
Number of jogging tracks	2003	www.osthammar.se Östhammar municip-ality	There are no jogging tracks within the parish of Forsmark according to www.osthammar.se	0	
Number of areas for country walks	2003	The County Administrative Board of Uppsala	There are three nature reserves in the parish according to www.c.lst.se. These are often attractive areas for out-door life.	3	
Number of attractive spots for bird watching	2003	www.uof.nu Upplands ornithological association	According to Upplands ornithological association, www.uof.nu, there are two attractive spots within the parish. Biotestsjön is one of them.	2	
Number of canoe-routes	2003	www.kanotguiden.com	According to www.kanotguiden.com there are no canoe-routes within Östhammar municipality.	0	
Number of canoe-renters	2003	www.kanotguiden.com	According to www.kanotguiden.com there are no canoe-renters within the parish.	0	

Variable	Time series	Data source	Method	Results	
				No.	No. per km^2
Number of open-air baths	2003	www.onab.net Östhammars Näringslivsutveckling AB www.osthammar.se	There are no public open-air baths within the parish according to www.osthammar.se. According to www.onab.net there is a bathing bridge and diving tower at Berkinge.	1	
Number of campsites and holiday villages	2003	www.onab.net www.upplandsstiftelsen.c.se Upplandsstiftelsen	There is one nature campsite at Kallerö according to www.onab.net (Östhammars Näringslivsutveckling). There is a small tentsite att Stora Rångsen in the nature reserve Skaten-Rångsen according to www.upplandsstiftelsen.c.se	1	
Number of marinas	2003	www.osthammar.se	There is no marinas within the parish according to www.osthammar.se	0	
Number of guest harbours	2003	www.osthammar.se	There is no guest harbours within the parish according to www.osthammar.se	0	
Number of boat renters	2003	www.onab.net www.upplandsstiftelsen.c.se	There is a boat rental at Berking, according to www.onab.net and at Södra Åsjön according to Fiskeguide Uppsala län 2000-2001. There is also a boat rental at Stora Rångsen in the nature reserve Skaten-Rångsen according to www.upplandsstiftelsen.c.se	3	

410

Lower hemisphere, Schmidt sterographic plots of ductile structural data arranged according to rock domains

The rock domains have been arranged into 10 structurally and lithologically homogeneous groups (subareas). Few data are available for rock domains RFM002, RFM003, RFM004, RFM006, RFM021 and RFM024. No data are available for rock domains RFM001, RFM009, RFM010, RFM015, RFM016, RFM019, RFM020, RFM022, RFM027 and RFM033. All these domains are situated southwest and northeast of the candidate area at the Forsmark site, predominantly in the peripheral parts of the regional model volume.

Structural data from RFM004, RFM005, RFM007, RFM014 and RFM025

Poles to banding and tectonic foliation

Mean strike/dip = 144/88

Fold axis

Mineral stretching lineation

Mean trend/plunge = 145/39

Equal Area
(Schmidt)

N

Polar
Lower Hem.

N = 11

Structural data from RFM002, RFM003, RFM006 and RFM024

Poles to banding and tectonic foliation

Mean strike/dip = 117/72

Equal Area
(Schmidt)

N

Polar
Lower Hem.

N = 2

Fold axis

Equal Area
(Schmidt)

N

Polar
Lower Hem.

N = 27

Mineral stretching lineation

Mean trend/plunge = 130/41

413

Structural data from RFM008, RFM018, RFM026 and RFM028

Poles to banding and tectonic foliation

Mean strike/dip = 139/86

Fold axis

Mineral stretching lineation

Mean trend/plunge = 140/39

Equal Area
(Schmidt)

N

Polar
Lower Hem.

N = 15

Structural data from RFM013

Poles to banding and tectonic foliation

Mean strike/dip = 108/55

Equal Area
(Schmidt)

N

Polar
Lower Hem.

N = 19

Mineral stretching lineation

Mean trend/plunge = 150/38

There are no measurements of fold axes.

Structural data from RFM011 and RFM023

Poles to banding and tectonic foliation

The pole to the π-circle that can possibly be constructed through all the points is 153/38. Compare with measured fold axes and mineral stretching lineations below.

Fold axis

Mineral stretching lineation

Mean trend/plunge = 143/36

Structural data from RFM012 and RFM032

Poles to banding and tectonic foliation

Mean strike/dip = 117/83

Fold axis

Mineral stretching lineation

Mean trend/plunge = 122/36

Structural data from RFM017

Poles to banding and tectonic foliation

The pole to the π-circle that can possibly be constructed through all the points is 120/21. Compare with measured mineral stretching lineations below.

Mineral stretching lineation

Mean trend/plunge = 138/30

There are no measurements of fold axes.

Structural data from RFM021

Poles to banding and tectonic foliation

Mean strike/dip = 135/90

Equal Area (Schmidt)
N
Polar Lower Hem.
N = 12

Fold axis

Equal Area (Schmidt)
N
Polar Lower Hem.
N = 4

Mineral stretching lineation

Mean trend/plunge = 128/48

Equal Area (Schmidt)
N
Polar Lower Hem.
N = 6

419

Structural data from RFM029 and RFM034

Poles to tectonic foliation and banding

The pole to the π-circle that can be constructed through all the points is 150/55. Compare with measured fold axes and mineral stretching lineations below.

Fold axis

Mineral stretching lineation

Mean trend/plunge = 148/38

Structural data from RFM030 and RFM031

Poles to banding and tectonic foliation

Mean strike/dip = 125/81

Fold axis

Mean trend/plunge = 145/40

Mineral stretching lineation

Mean trend/plunge = 137/39

Dominant and subordinate rock types in rock domains

Few (<5 observation points) or no data are available for rock domains RFM002, RFM003, RFM004, RFM006, RFM009, RFM015, RFM016, RFM019, RFM020, RFM022, RFM027 and RFM033. All these domains are situated southwest and northeast of the candidate area at the Forsmark site, predominantly in the peripheral parts of the regional model volume.
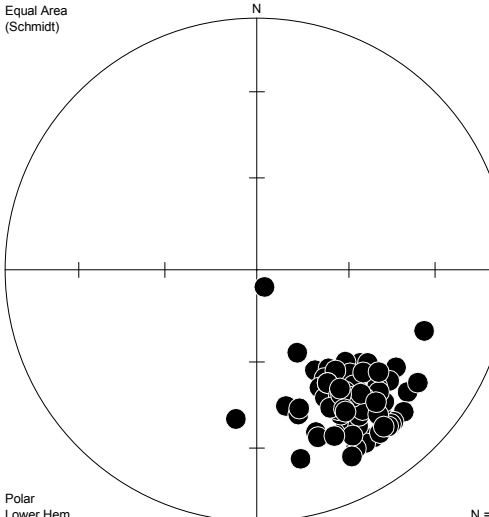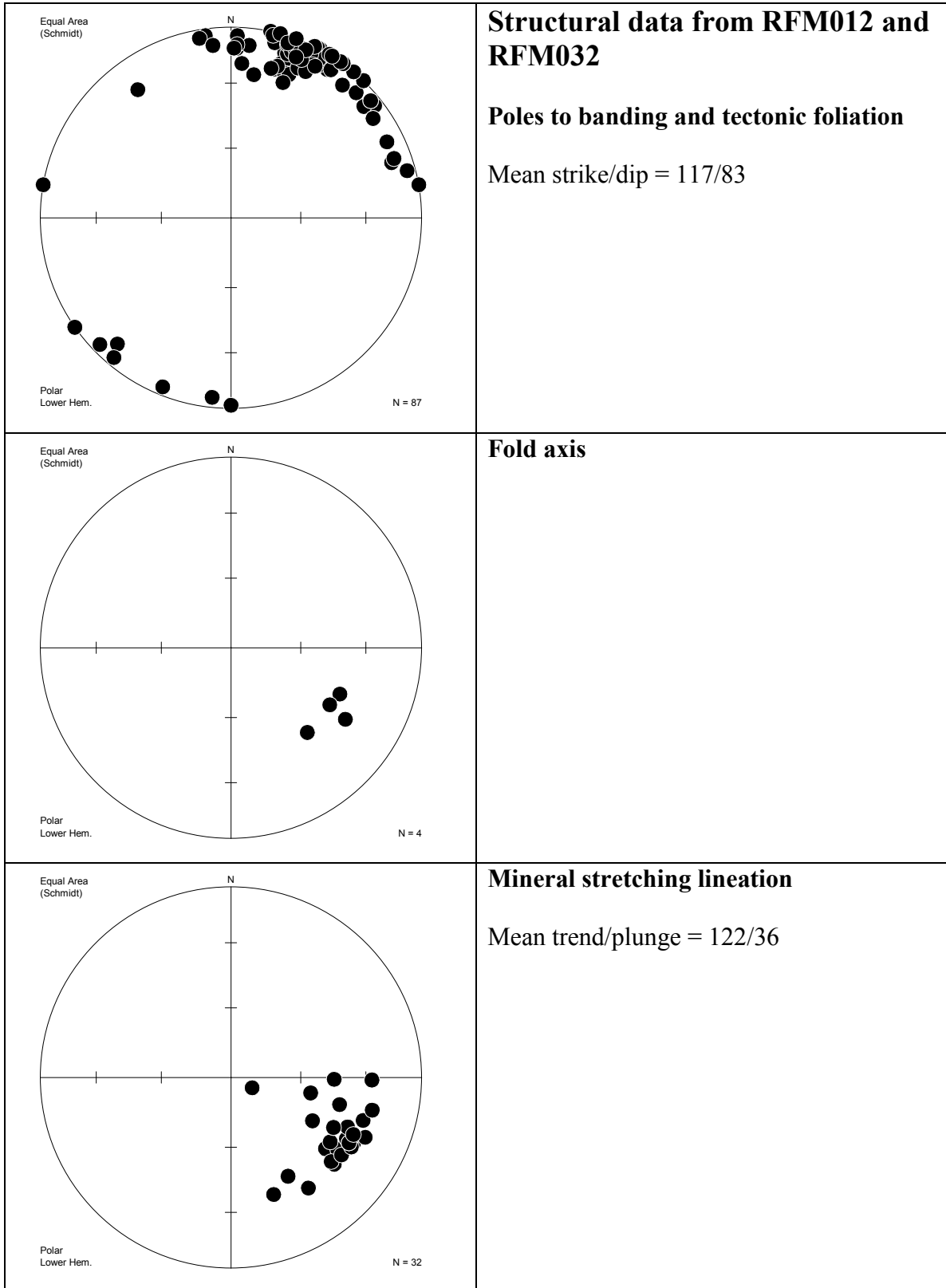
The table below translates the various rock codes in the following rock domain diagrams to rock names. The different groups (A to D), that are essentially a stratigraphic classification of the rocks, are described in Section 4.2.2. The oldest rocks of supracrustal character are included in Group A. The rocks in Groups B and C belong to different generations of younger, calc-alkaline intrusive rocks. The youngest intrusive rocks are included in Group D.

Rock code	Rock composition	Complementary characteristics		
Rock codes and rock names adopted by SKB				
111058	Granite		Fine- to medium-grained	Group D
101061	Pegmatite, pegmatitic granite			Group D
101051	Granite, granodiorite and tonalite	Metamorphic	Fine- to medium-grained	Group C
111051	Granitoid	Metamorphic		Group B
101058	Granite	Metamorphic	Aplitic	Group B
101057	Granite to granodiorite	Metamorphic	Medium-grained	Group B
101056	Granodiorite	Metamorphic		Group B
101054	Tonalite to granodiorite	Metamorphic		Group B
101033	Diorite, quartz diorite, gabbro	Metamorphic		Group B
101004	Ultramafic rock	Metamorphic		Group B
102017	Amphibolite			Group B
108019	Calc-silicate rock (skarn)			Group A
109014	Magnetite mineralisation associated with calc-silicate rock (skarn)			Group A
109010	Sulphide mineralisation			Group A
103076	Felsic to intermediate volcanic rock	Metamorphic		Group A
106000	Sedimentary rock	Metamorphic		Group A
Additional rock codes and rock names of strongly subordinate character				
1051	Granitoid	Metamorphic	Uncertain classification 101051, 111051	Group B or Group C
1053	Tonalite	Metamorphic	Uncertain classification 101051 or 101054	Group B or Group C
1054	Tonalite to granodiorite	Metamorphic	Uncertain classification 101051 or 101054	Group B or Group C
1056	Granodiorite	Metamorphic	Uncertain classification 101051 or 101056	Group B or Group C
1057	Granite to granodiorite	Metamorphic	Uncertain classification 101051 or 101057	Group B or Group C
1058_120	Granite	Metamorphic	Uncertain classification 101057 or 101058	Group B
1058	Granite		Uncertain classification 101051, 101057, 101058 or 111058	Group B, Group C or Group D
1059	Leucocratic granite		Uncertain classification 101058 or 111058	Group B or Group D
1062	Aplite		Uncertain classification 101058 or 111058	Group B or Group D
111058_101051	Granite		Uncertain classification 101051 or 111058	Group C or Group D
5103	Felsic rock	Metamorphic	Uncertain classification 103076 or 101058	Group A or Group B
6053	Quartz-hematite rock			
8003	Cataclastic rock			
8004	Mylonite			
8011	Gneiss			
8020	Hydrothermal vein or segregation			
8021	Quartz-rich hydrothermal vein or segregation			
8023	Hydrothermally altered rock			

Rock domain 1

Number of outcrops where each rock type is dominating.
Y-axis indicates total number of outcrops in the rock domain.
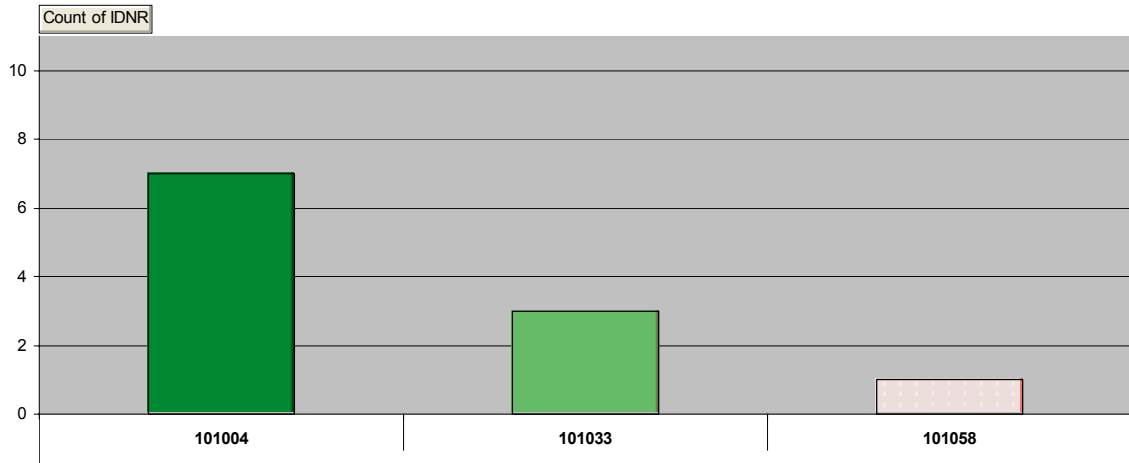
Rock domain 1

Number of outcrops composed solely of one rock type.
Y-axis indicates total number of outcrops in the rock domain.

Rock domain 1

Number of occurrences of each rock type.

Rock domain 5

Number of outcrops where each rock type is dominating.
Y-axis indicates total number of outcrops in the rock domain.

Rock domain 5

Number of outcrops composed solely of one rock type.
Y-axis indicates total number of outcrops in the rock domain.

Rock domain 5

Number of occurrences of each rock type.

Rock domain 7

Number of outcrops where each rock type is dominating.
Y-axis indicates total number of outcrops in the rock domain.

Rock domain 7

Number of outcrops composed solely of one rock type.
Y-axis indicates total number of outcrops in the rock domain.

Rock domain 7

Number of outcrops where each rock type is found.
Y-axis indicates total number of outcrops in the rock domain.

426

Rock domain 8

Number of outcrops where each rock type is dominating.
Y-axis indicates total number of outcrops in the rock domain.

Rock domain 8

Number of outcrops composed solely of one rock type.
Y-axis indicates total number of outcrops in the rock domain.

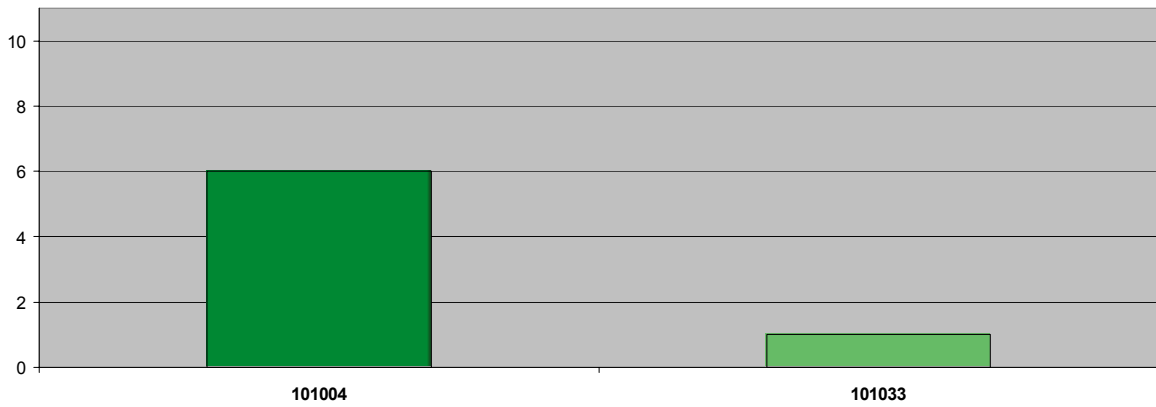## Rock domain 8

Number of occurrences of each rock type.

Rock domain 10

Number of outcrops where each rock type is dominating.
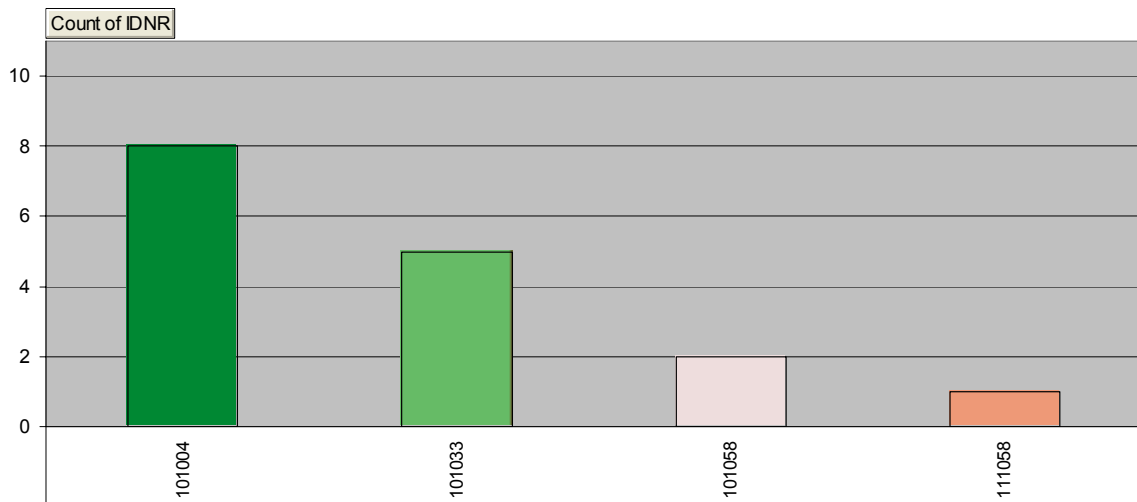Y-axis indicates total number of outcrops in the rock domain.

Rock domain 10

Number of outcrops composed solely of one rock type.
Y-axis indicates total number of outcrops in the rock domain.

Rock domain 10

Number of occurrences of each rock type.

428

Rock domain 11

Number of outcrops where each rock type is dominating.
Y-axis indicates total number of outcrops in the rock domain.

Rock domain 11

Number of outcrops composed solely of one rock type.
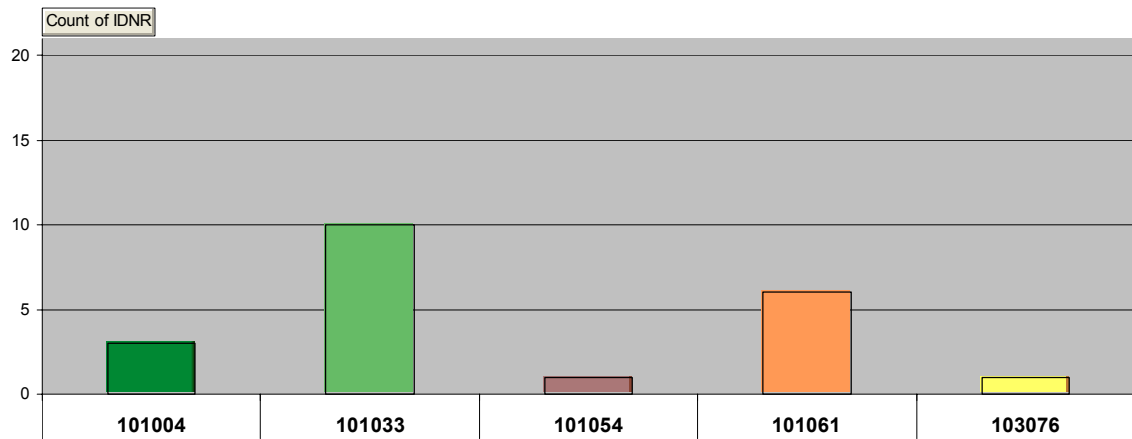Y-axis indicates total number of outcrops in the rock domain.

Rock domain 11

Number of occurrences of each rock type.

429

Rock domain 12

Number of outcrops where each rock type is dominating.
Y-axis indicates total number of outcrops in the rock domain.

Rock domain 12

Number of outcrops composed solely of one rock type.
Y-axis indicates total number of outcrops in the rock domain.

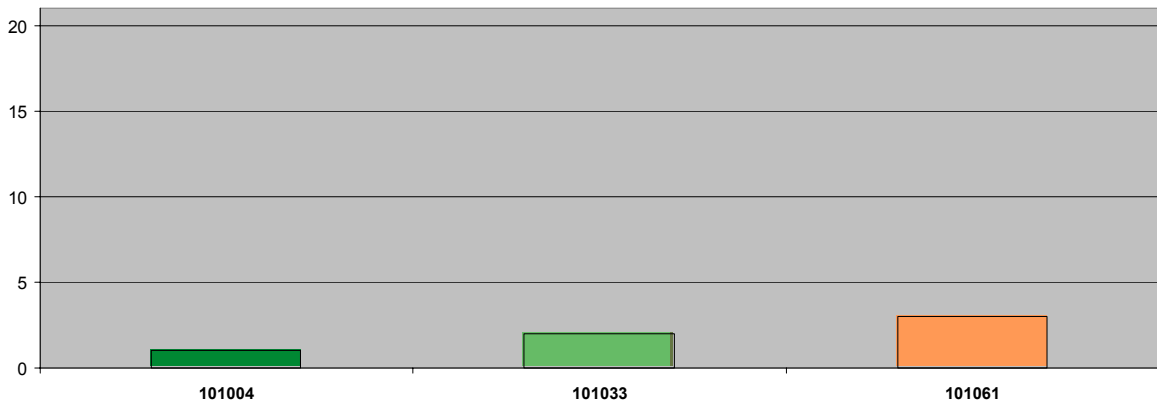
Rock domain 12

Number of occurrences of each rock type.

Rock domain 13

Number of outcrops where each rock type is dominating.
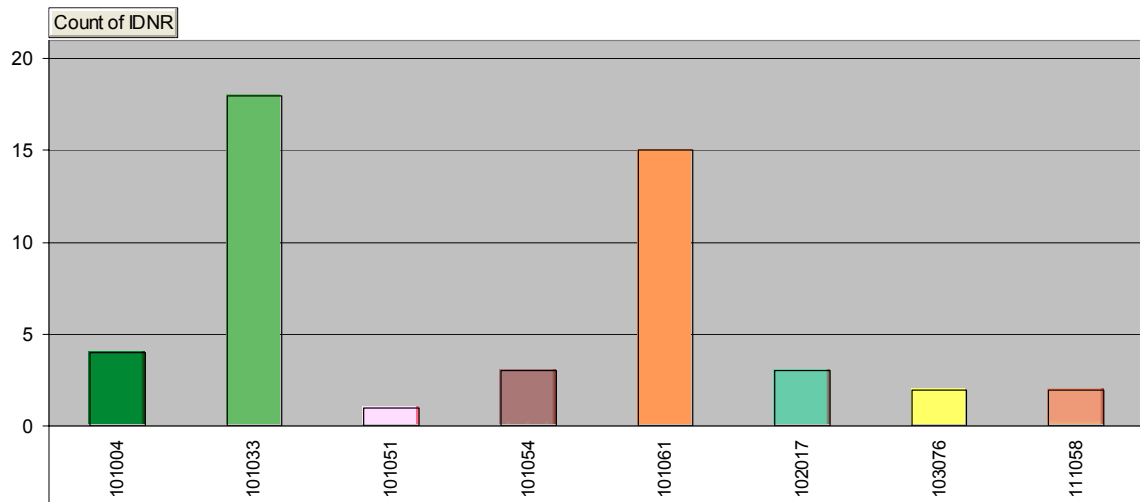Y-axis indicates total number of outcrops in the rock domain.

Rock domain 13

Number of outcrops composed solely of one rock type.
Y-axis indicates total number of outcrops in the rock domain.

Rock domain 13

Number of occurrences of each rock type.

431

Rock domain 14
Number of outcrops where each rock type is dominating.
Y-axis indicates total number of outcrops in the rock domain.

Rock domain 14
Number of outcrops composed solely of one rock type.
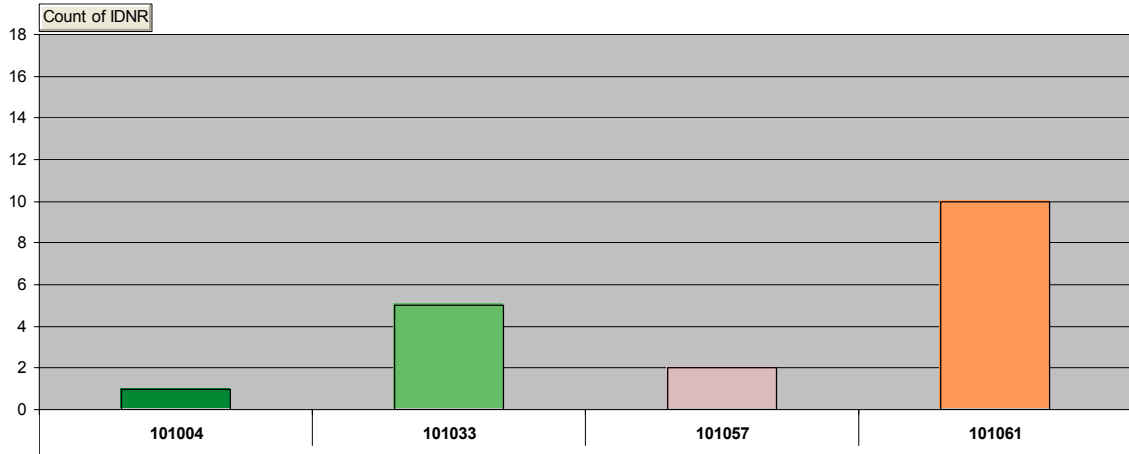Y-axis indicates total number of outcrops in the rock domain.

Rock domain 14
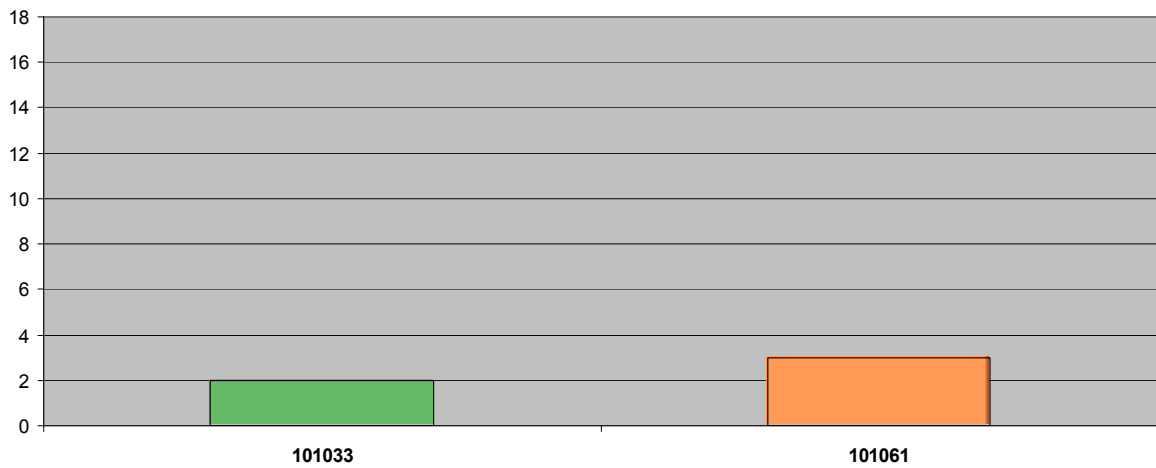Number of occurrences of each rock type.

432

Rock domain 17

Number of outcrops where each rock type is dominating.
Y-axis indicates total number of outcrops in the rock domain.

Rock domain 17

Number of outcrops composed solely of one rock type.
Y-axis indicates total number of outcrops in the rock domain.
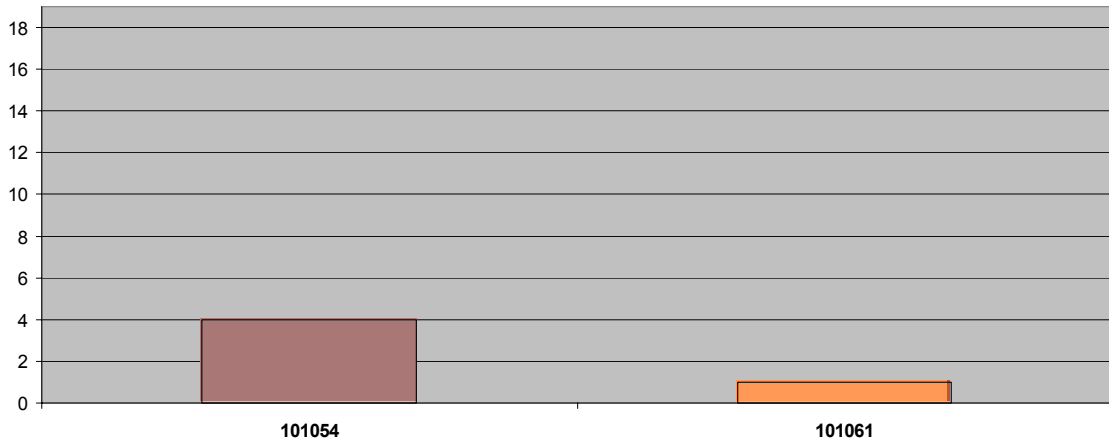
Rock domain 17

Number of occurrences of each rock type.
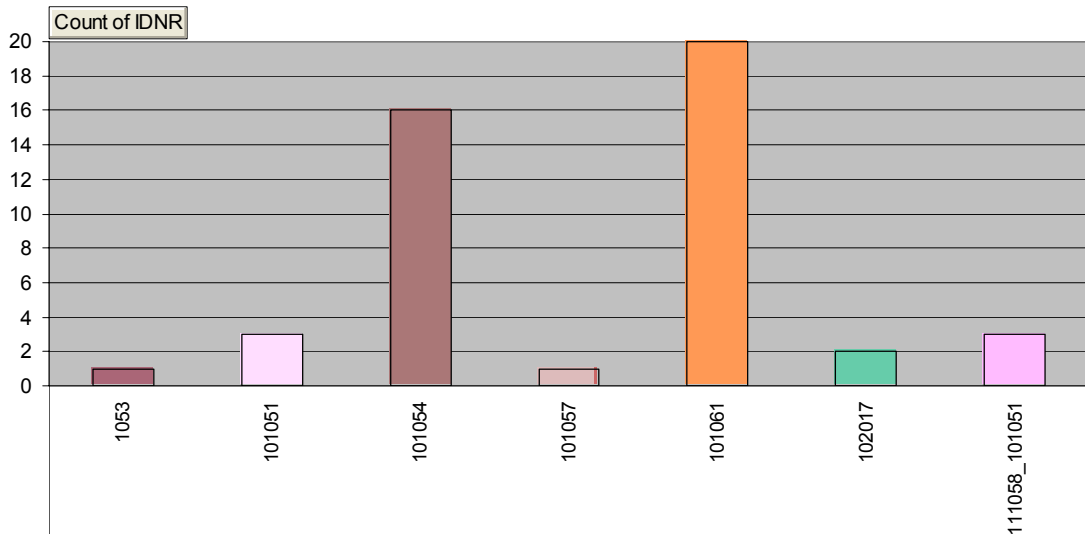
433

Rock domain 18

Number of outcrops where each rock type is dominating.
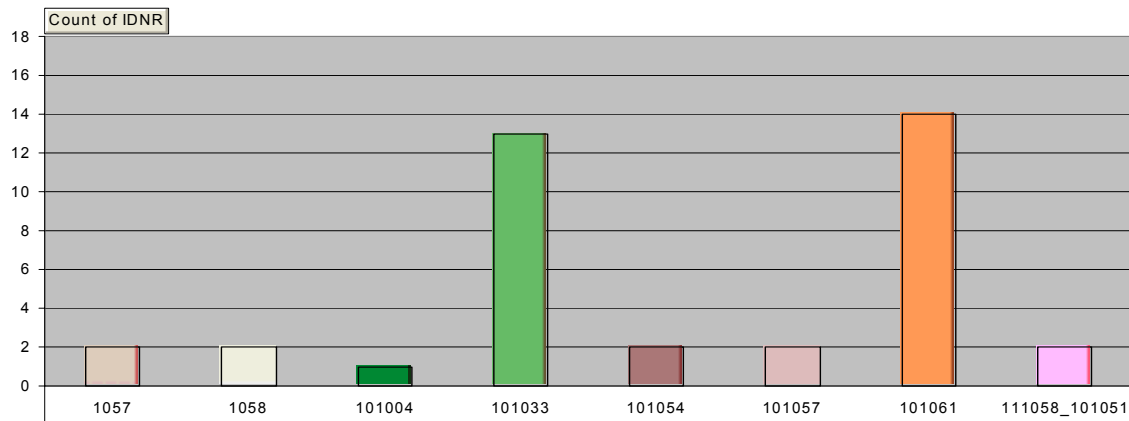Y-axis indicates total number of outcrops in the rock domain.
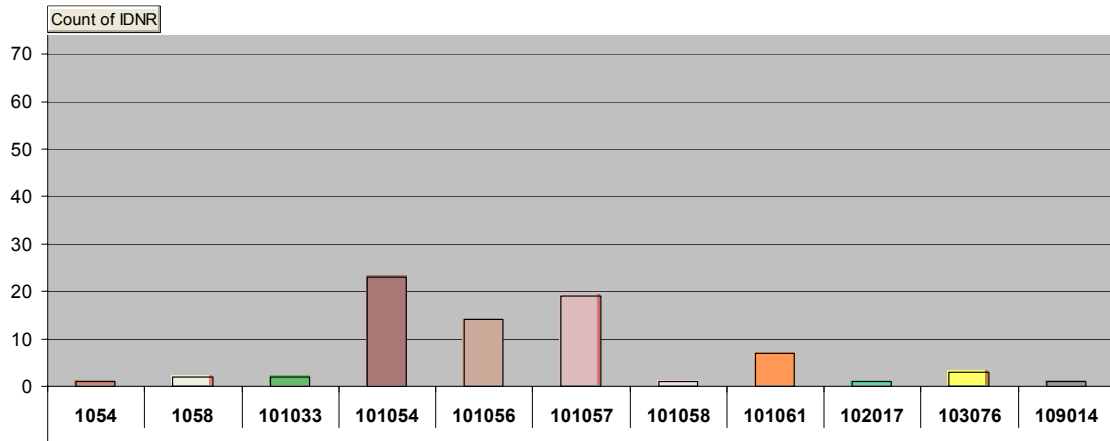
Rock domain 18

Number of outcrops composed solely of one rock type.
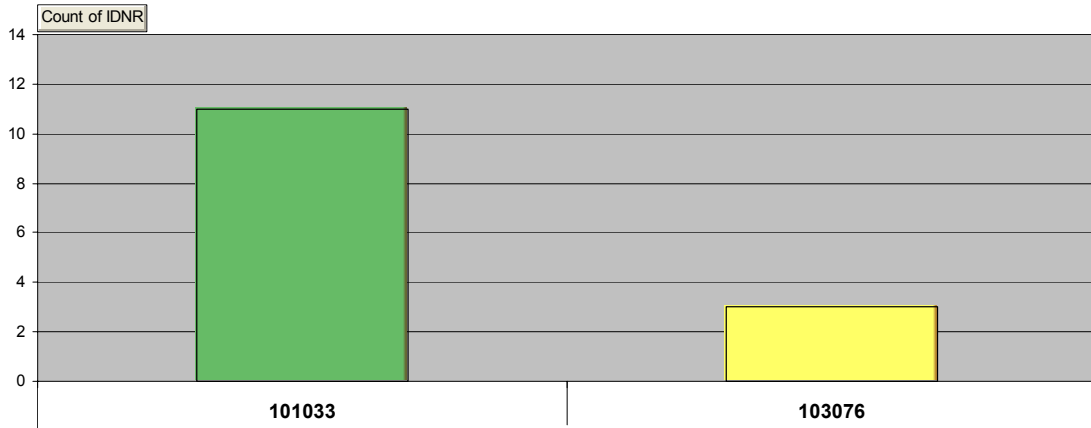Y-axis indicates total number of outcrops in the rock domain.
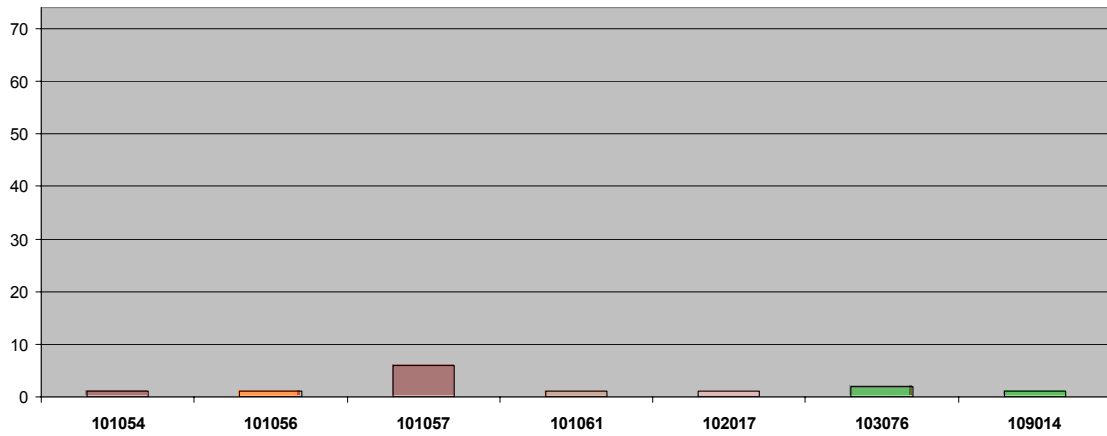
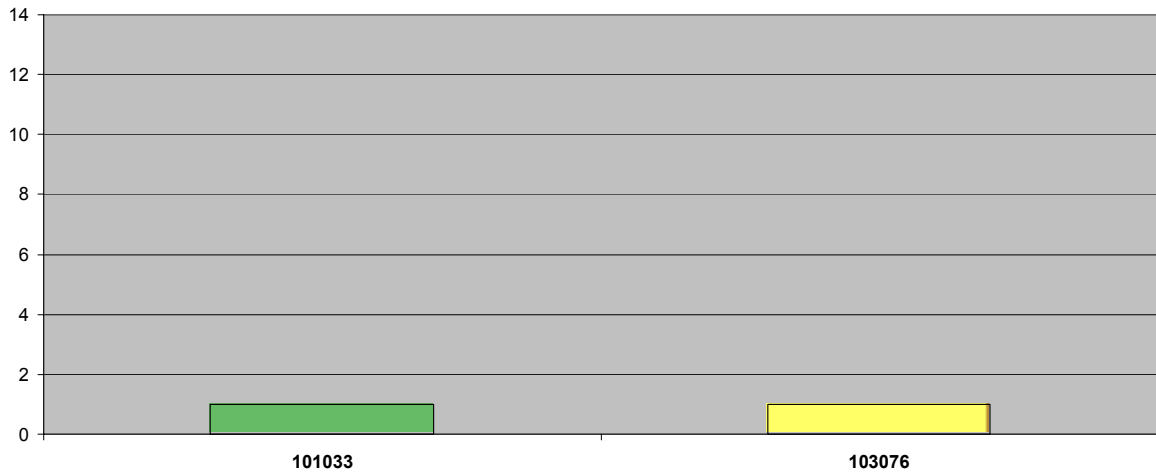# Rock domain 18

Number of occurrences of each rock type.
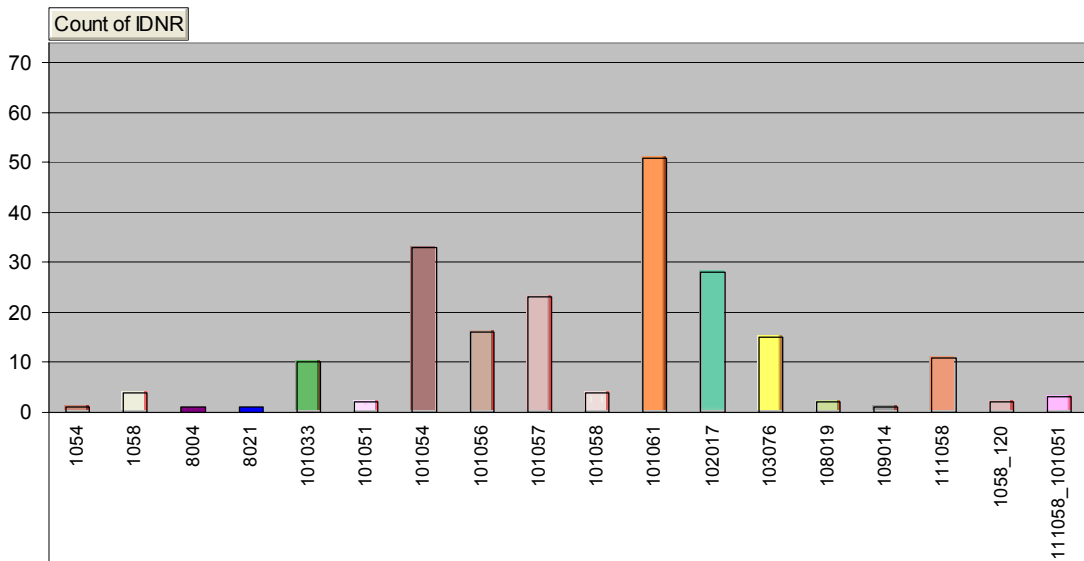
Rock domain 21

Number of outcrops where each rock type is dominating.
Y-axis indicates total number of outcrops in the rock domain.
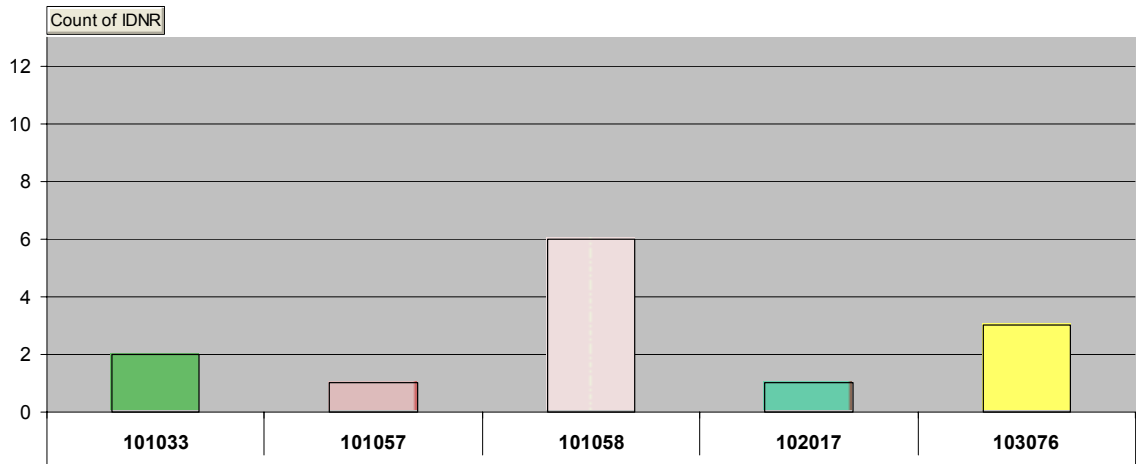
Rock domain 21

Number of outcrops composed solely of one rock type.
Y-axis indicates total number of outcrops in the rock domain.
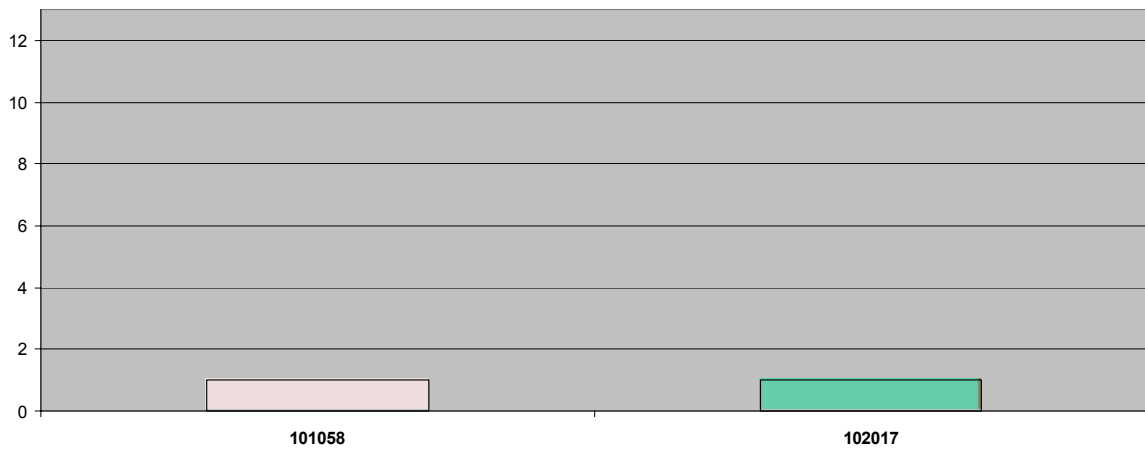
Rock domain 21

Number of occurrences of each rock type.
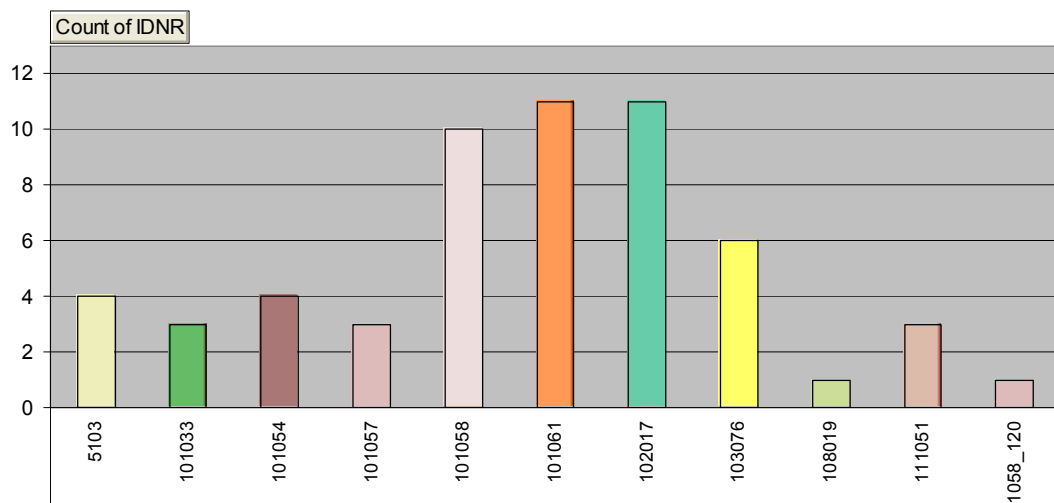
435

Rock domain 23

Number of outcrops where each rock type is dominating.
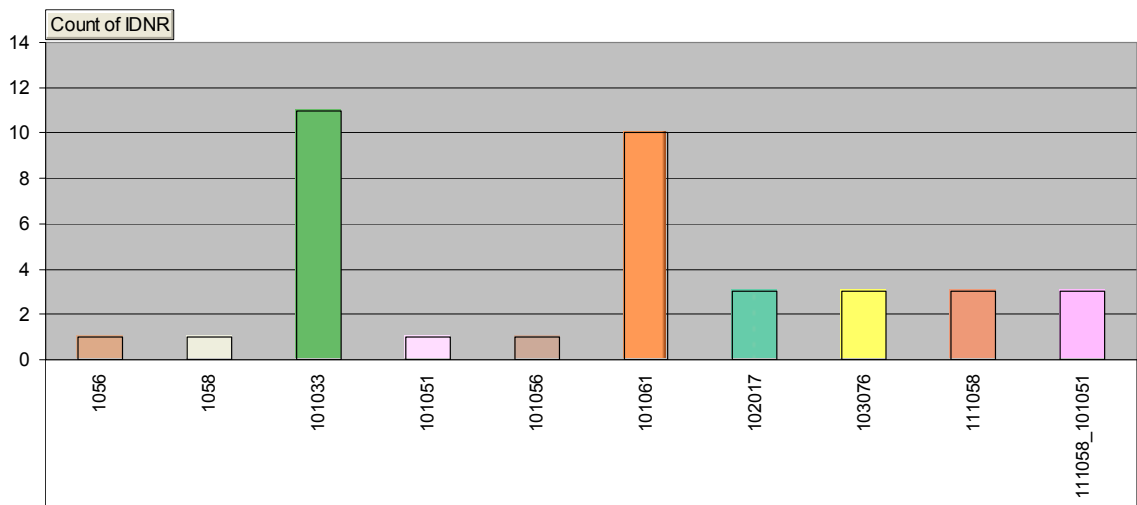Y-axis indicates total number of outcrops in the rock domain.
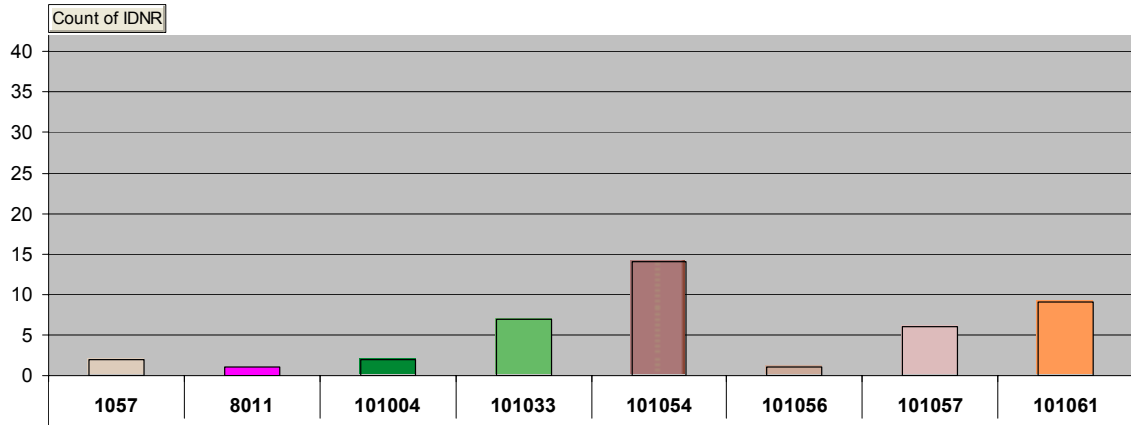
Rock domain 23

Number of outcrops composed solely of one rock type.
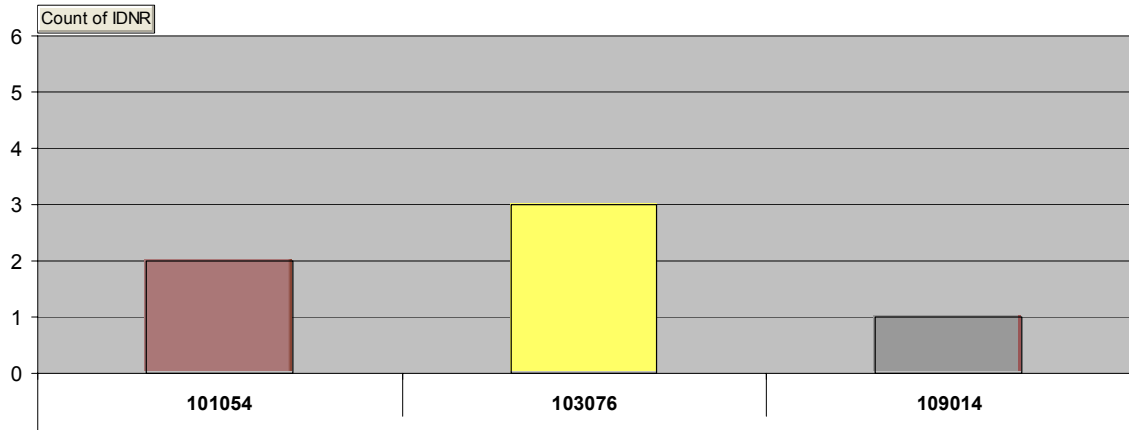Y-axis indicates total number of outcrops in the rock domain.
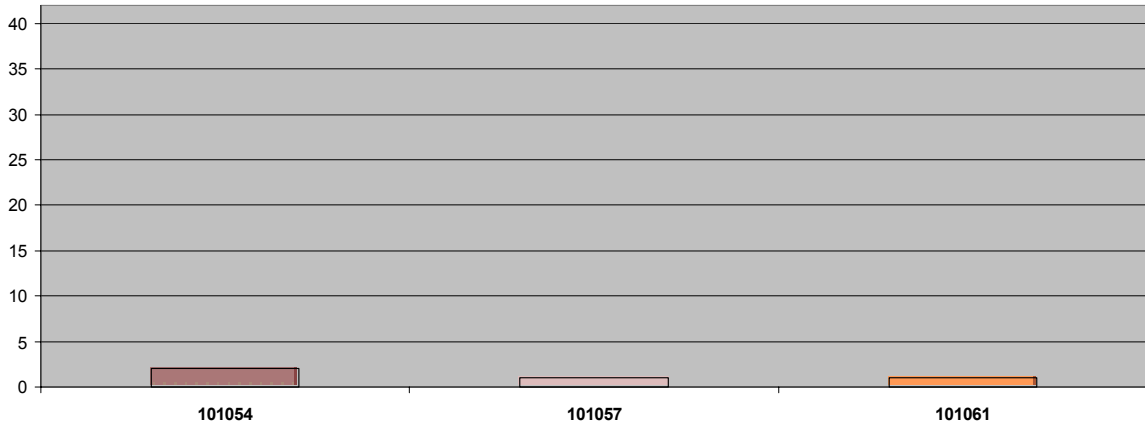
Rock domain 23

Number of occurrences of each rock type.
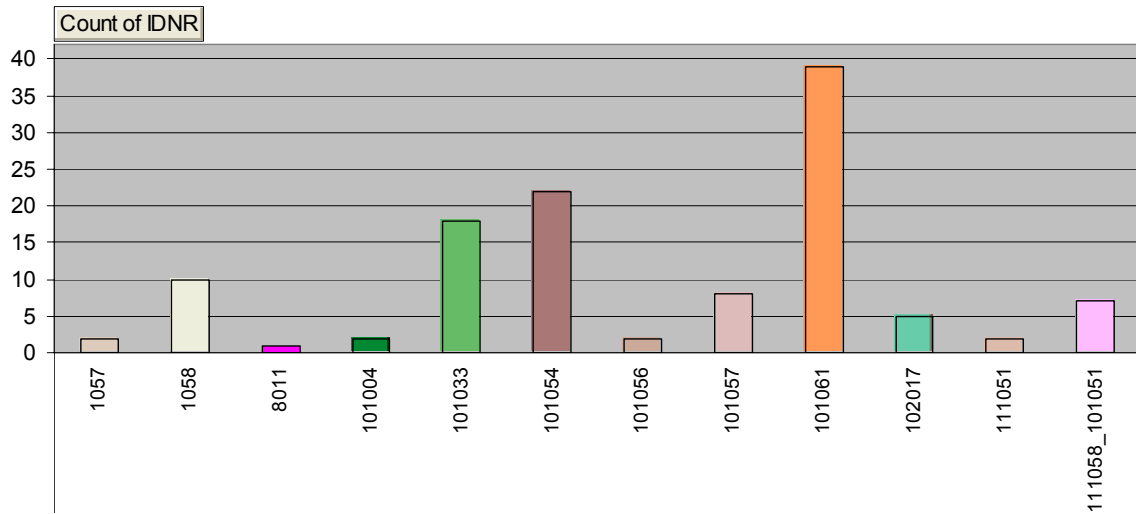
Rock domain 24

Number of outcrops where each rock type is dominating.
Y-axis indicates total number of outcrops in the rock domain.
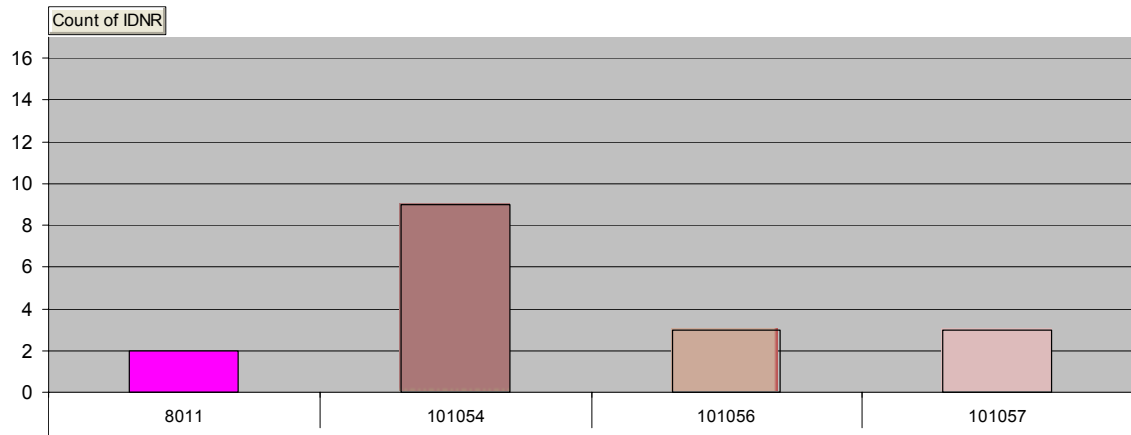
Rock domain 24

Number of occurrences of each rock type.
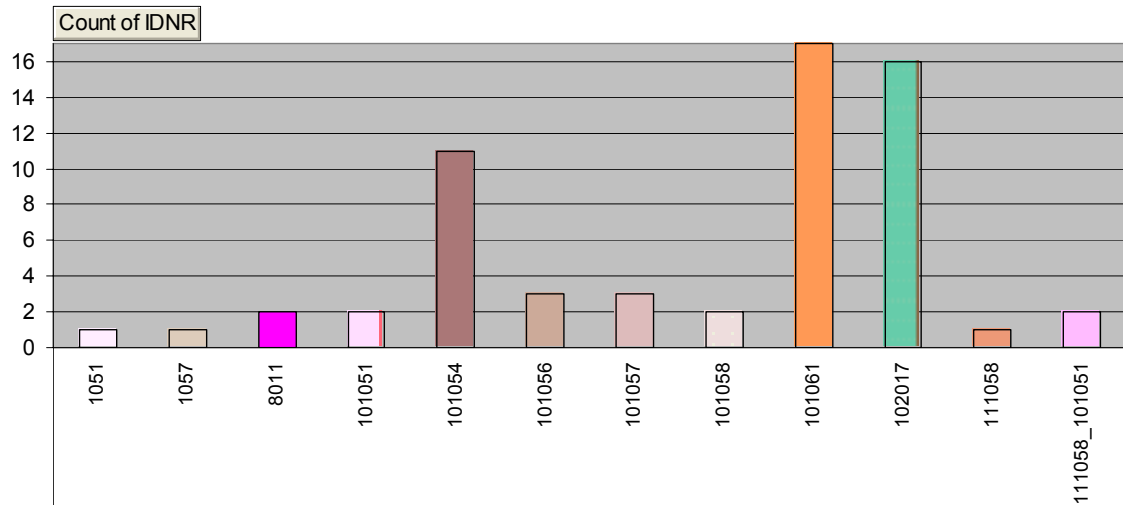
No outcrop in this rock domain are composed solely of one rock type.

Rock domain 25

Number of outcrops where each rock type is dominating.
Y-axis indicates total number of outcrops in the rock domain.
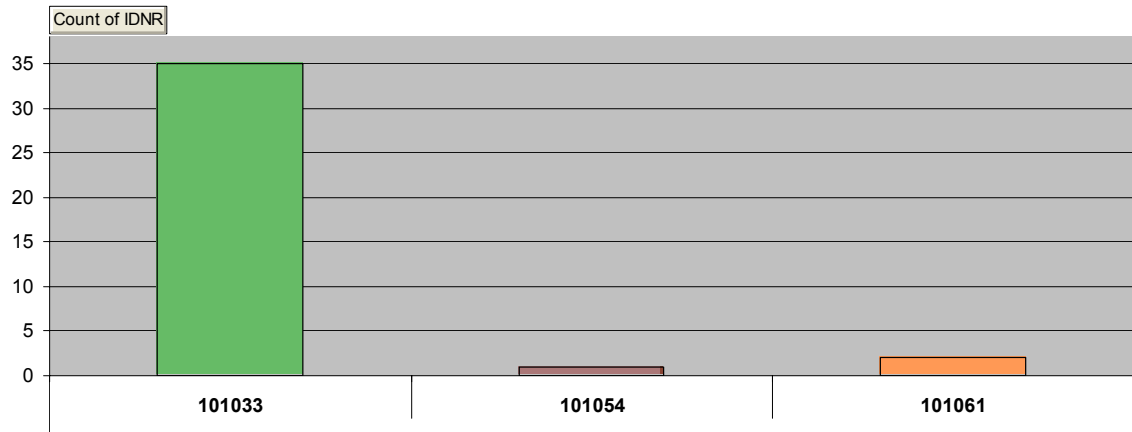
Rock domain 25

Number of outcrops composed solely of one rock type.
Y-axis indicates total number of outcrops in the rock domain.
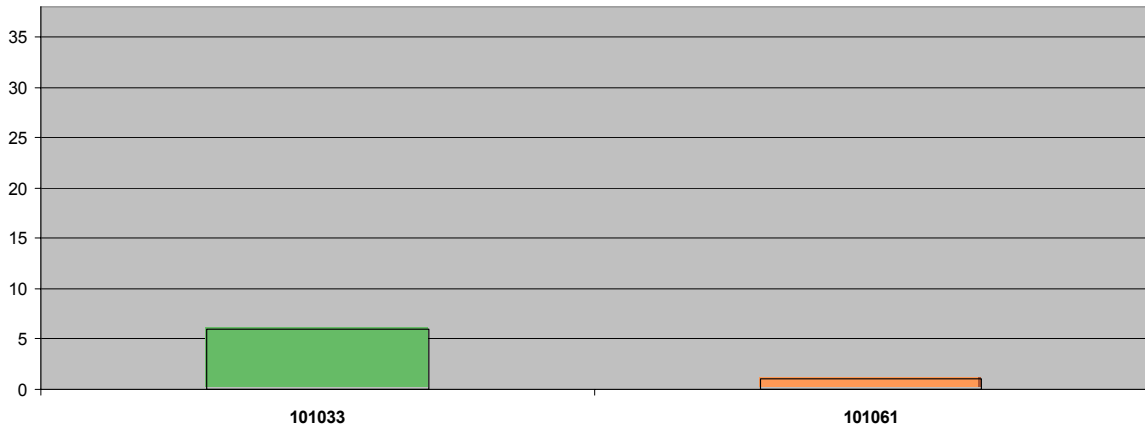
Rock domain 25
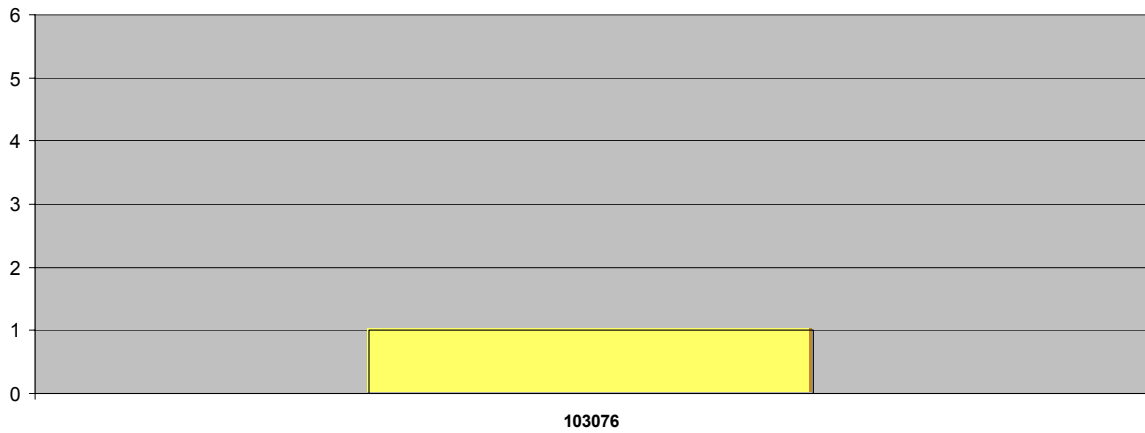
Number of occurrences of each rock type.
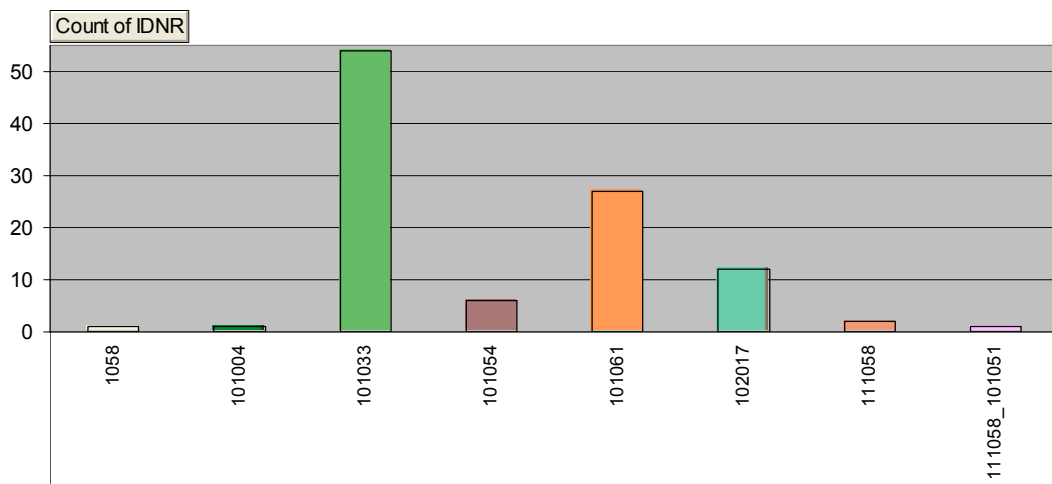
438

Rock domain 26
Number of outcrops where each rock type is dominating.
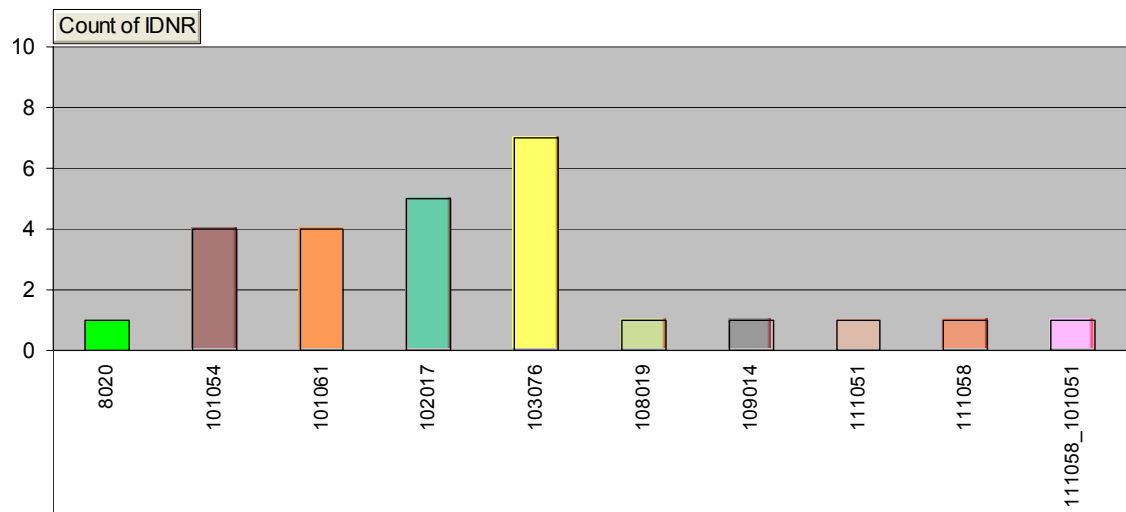Y-axis indicates total number of outcrops in the rock domain.
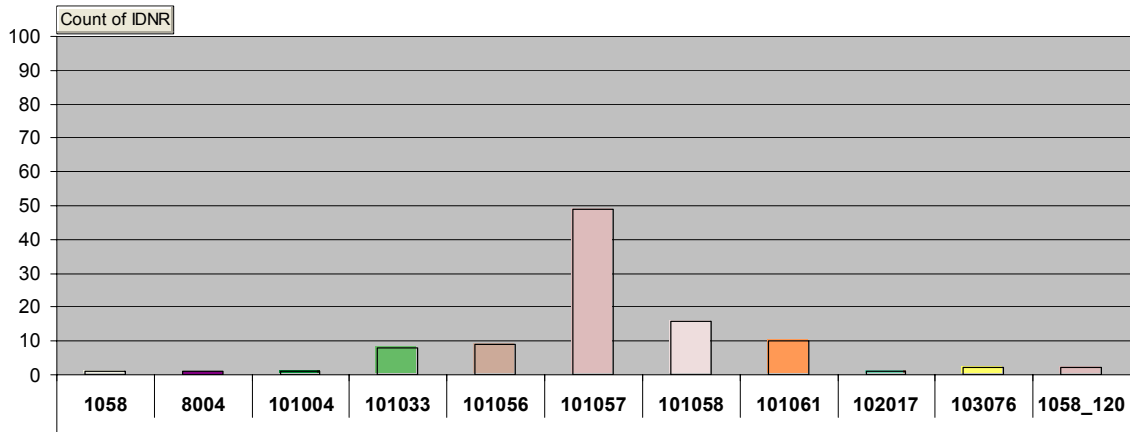
Rock domain 26
Number of outcrops composed solely of one rock type.
Y-axis indicates total number of outcrops in the rock domain.
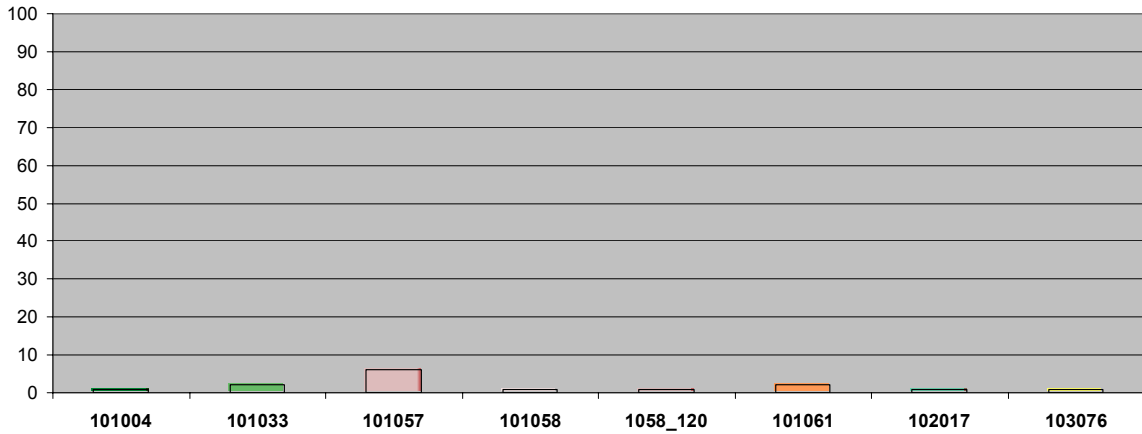
Rock domain 26
Number of occurrences of each rock type.
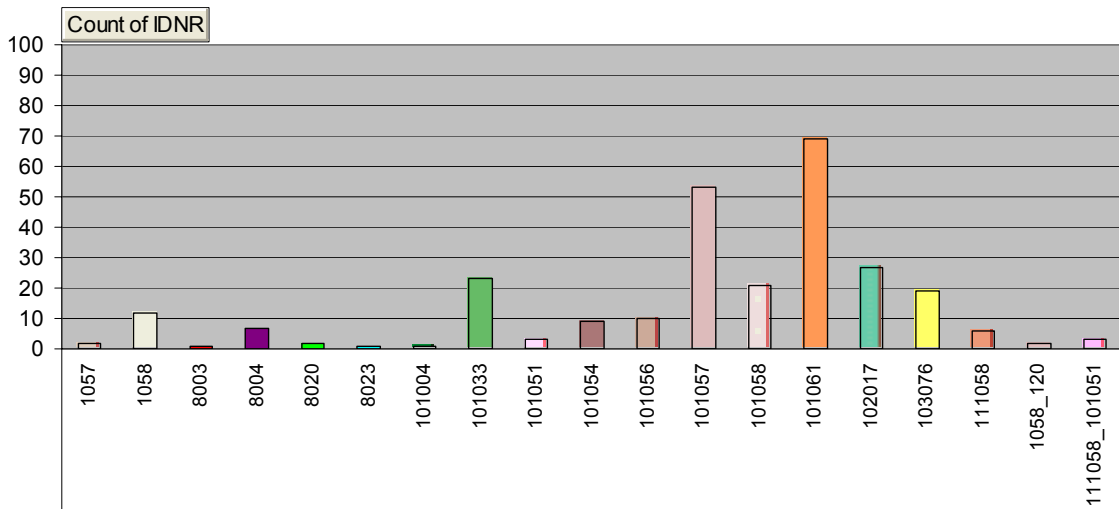
439

Rock domain 28

Number of outcrops where each rock type is dominating.
Y-axis indicates total number of outcrops in the rock domain.
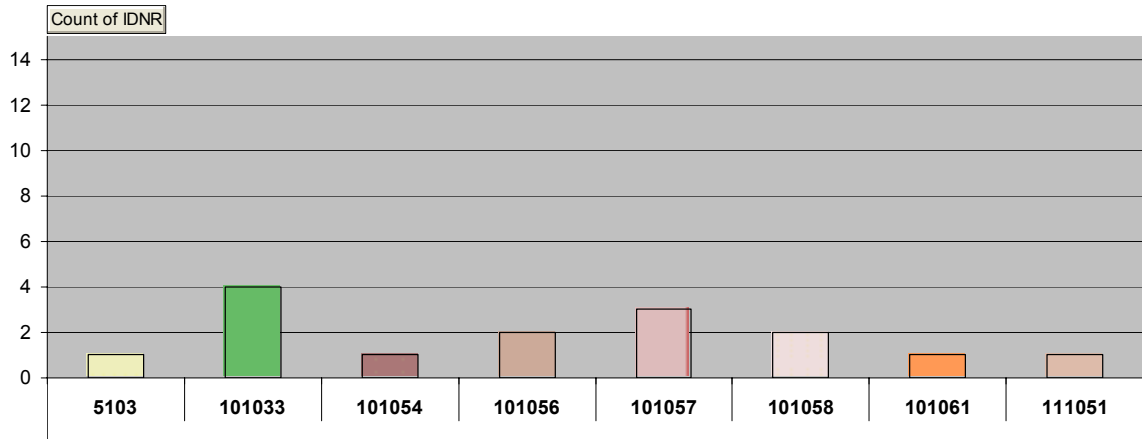
Rock domain 28

Number of outcrops composed solely of one rock type.
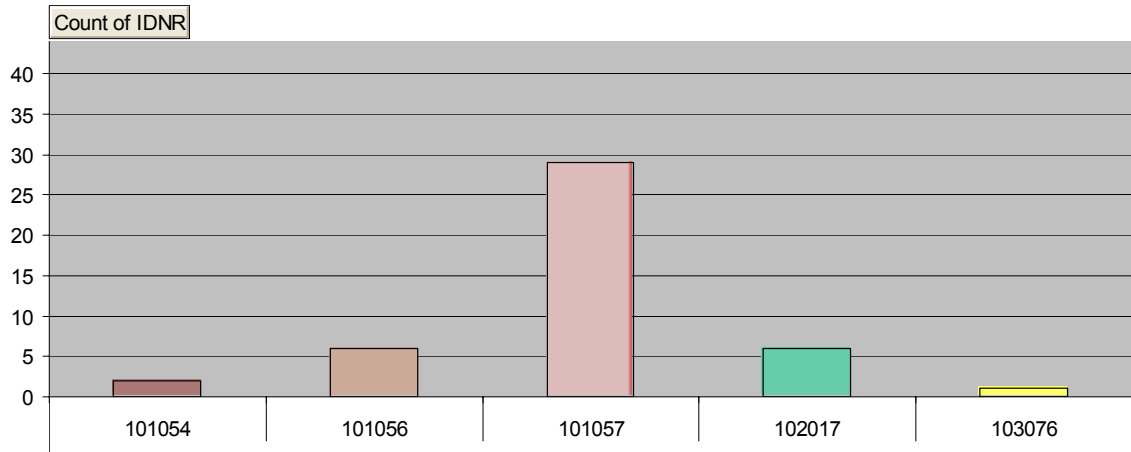Y-axis indicates total number of outcrops in the rock domain.
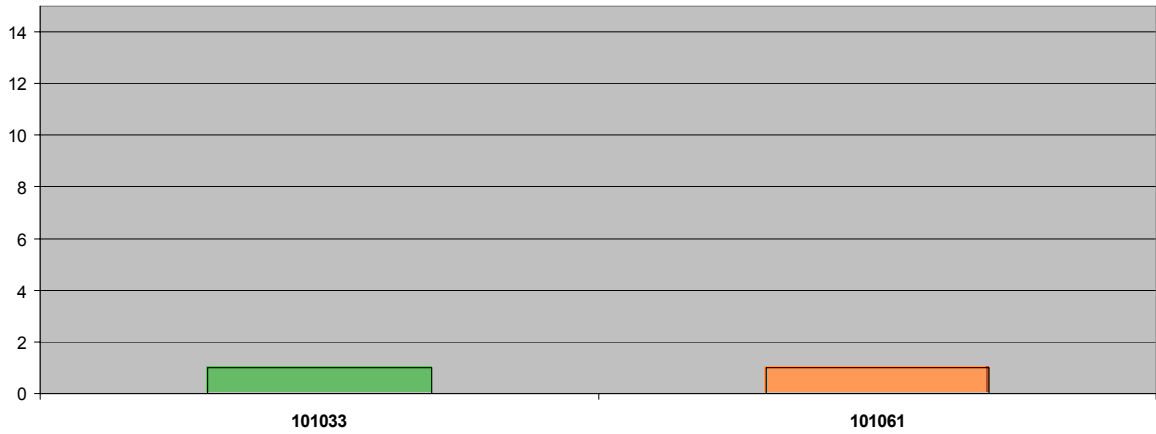
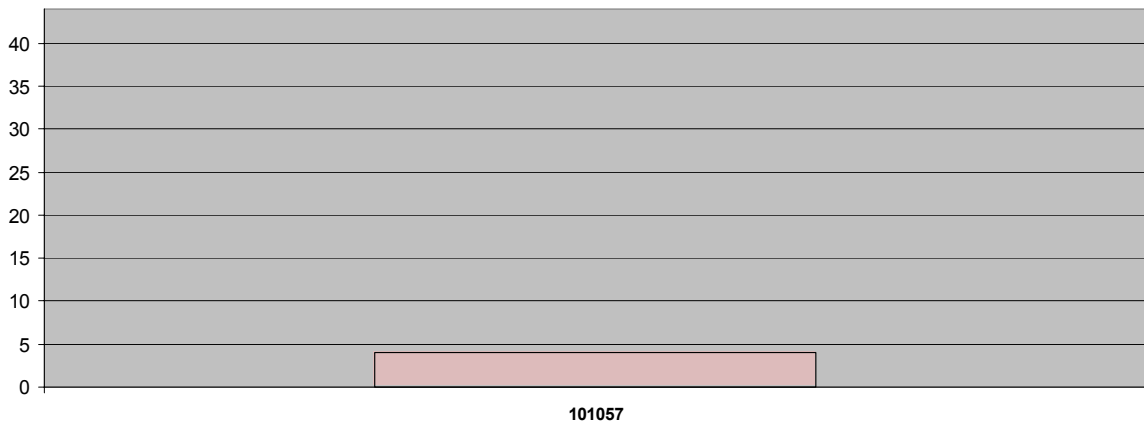
Rock domain 28

Number of occurrences of each rock type.
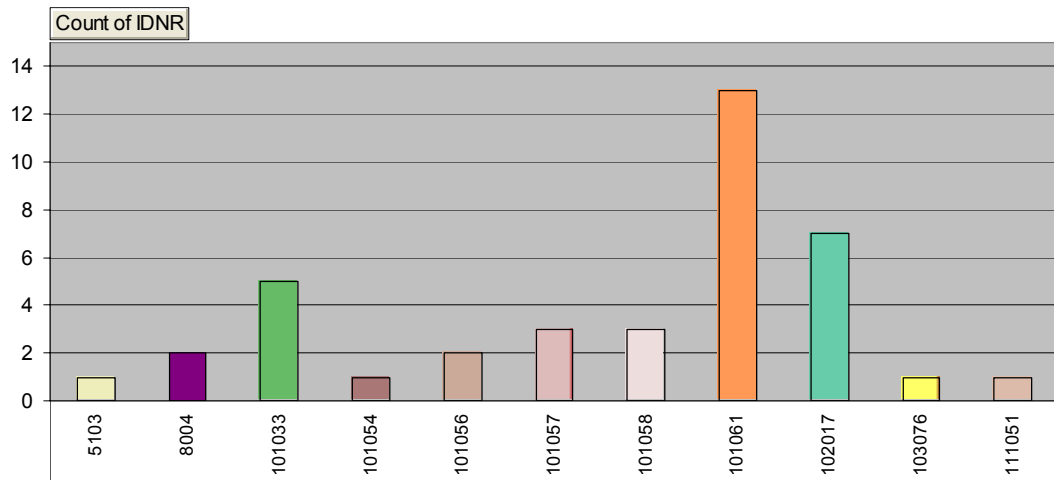
440

Rock domain 29

Number of outcrops where each rock type is dominating.
Y-axis indicates total number of outcrops in the rock domain.
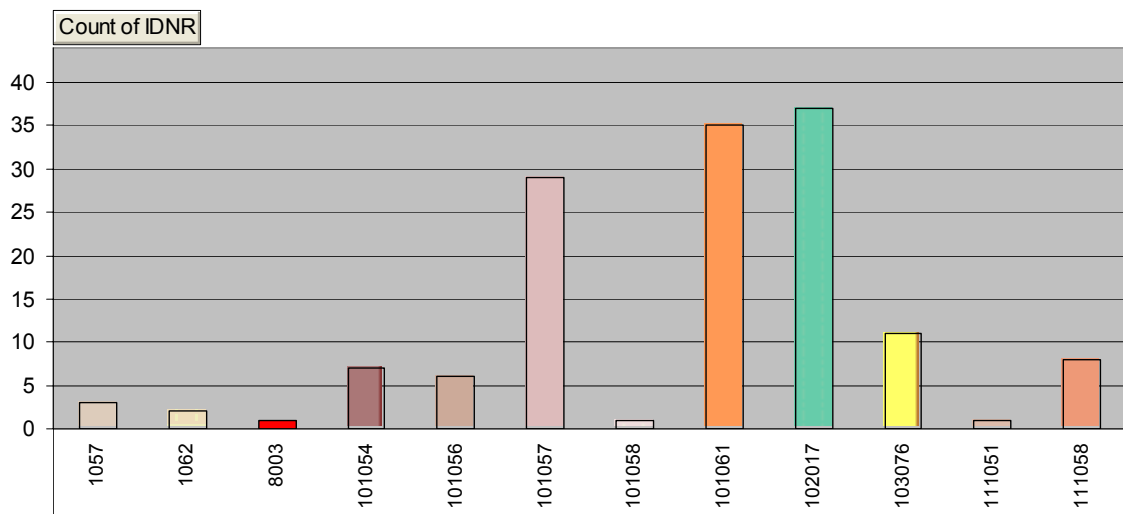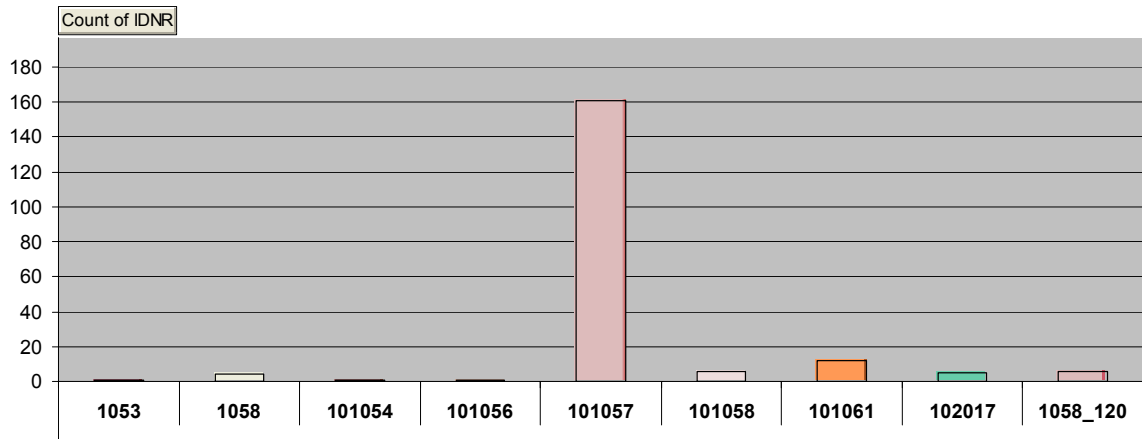

Rock domain 29

Number of outcrops composed solely of one rock type.
Y-axis indicates total number of outcrops in the rock domain.
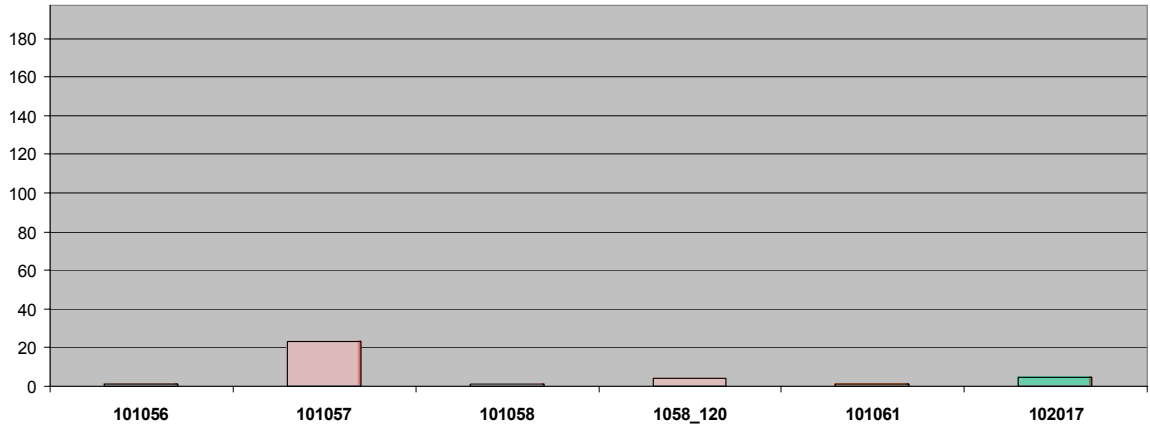
Rock domain 29

Number of occurrences of each rock type.
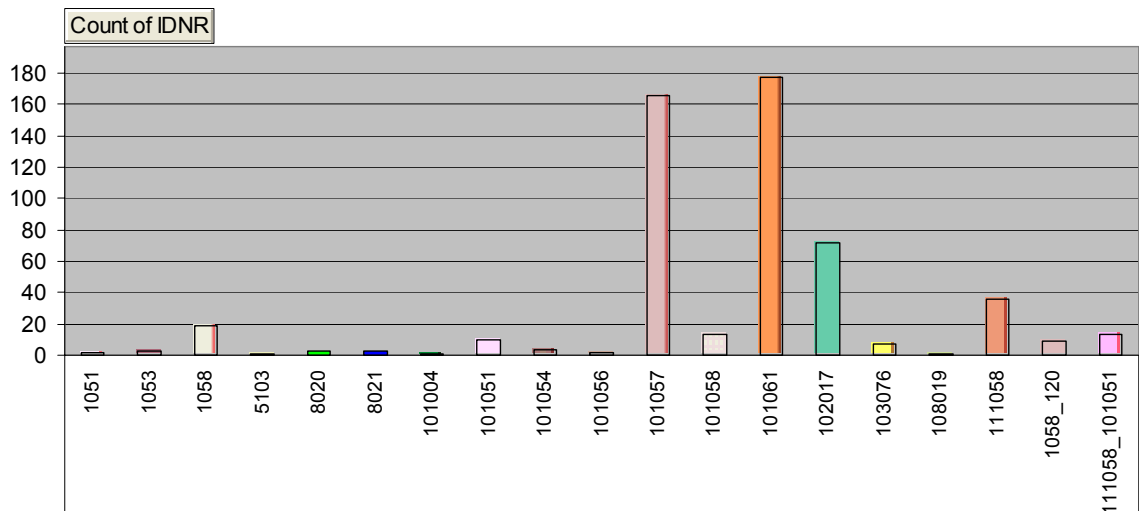
441

Rock domain 30

Number of outcrops where each rock type is dominating.
Y-axis indicates total number of outcrops in the rock domain.
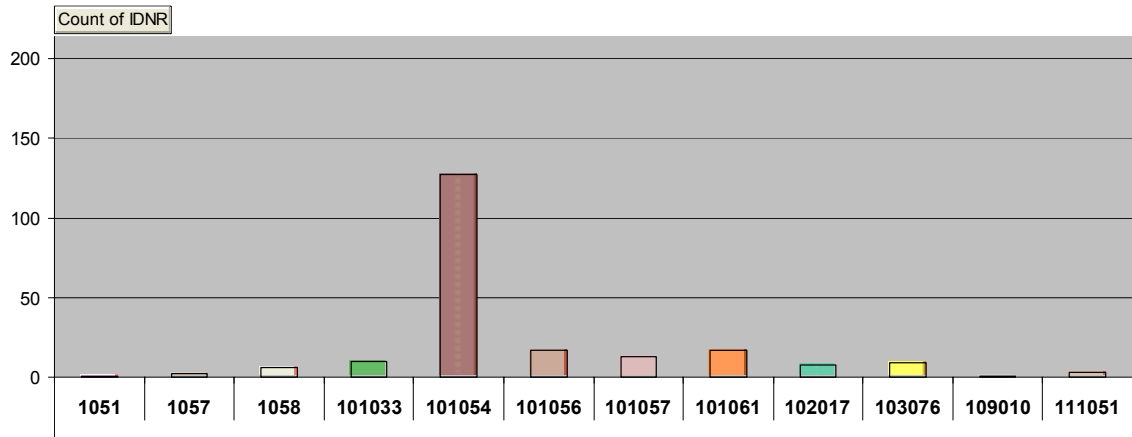
Rock domain 30

Number of outcrops composed solely of one rock type.
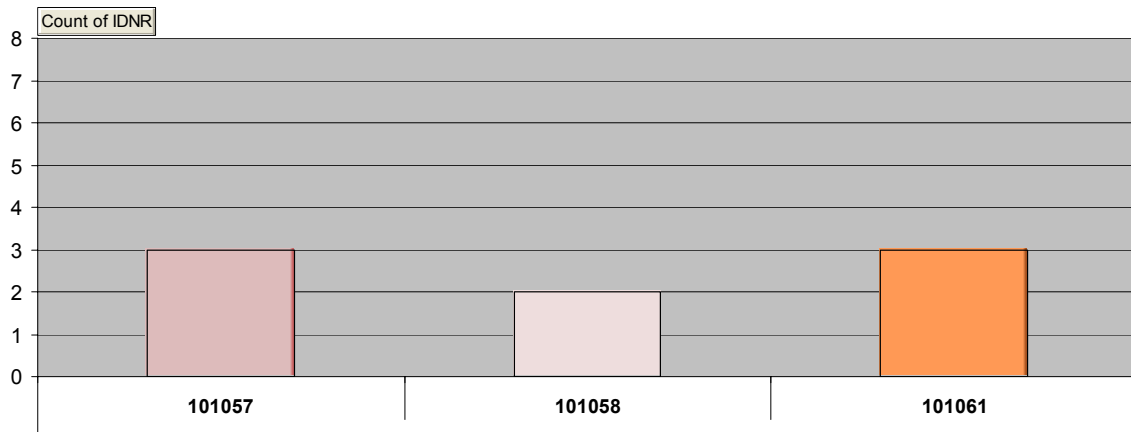Y-axis indicates total number of outcrops in the rock domain.
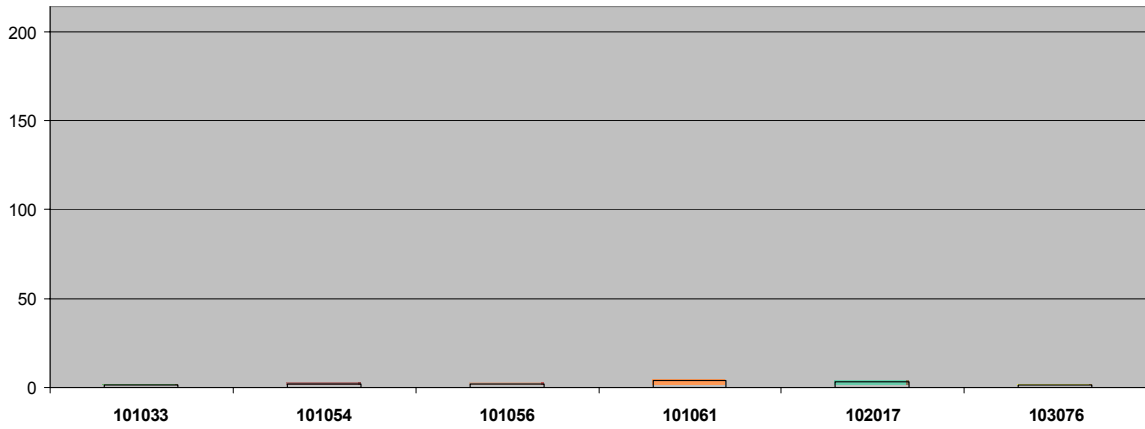
Rock domain 30
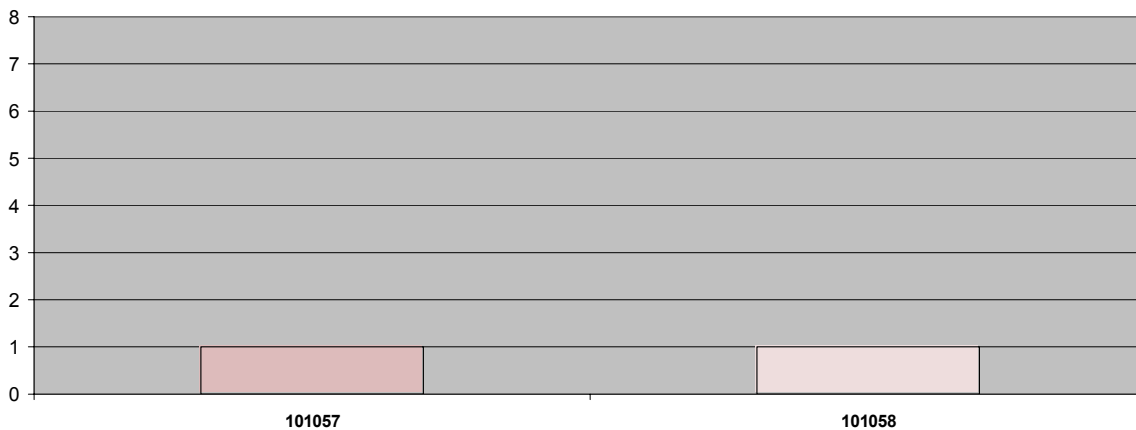
Number of occurrences of each rock type.
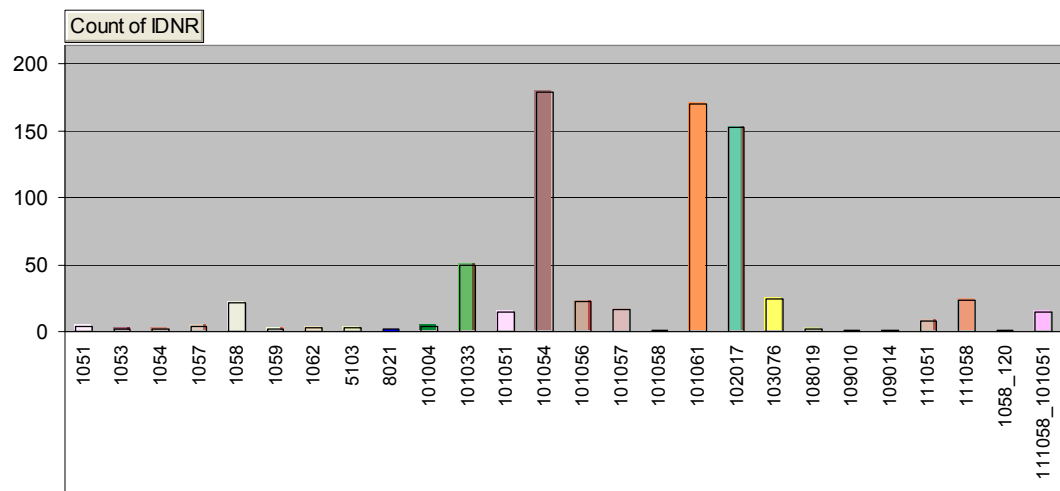
442

Rock domain 31

Number of outcrops where each rock type is dominating.

Y-axis indicates total number of outcrops in the rock domain.
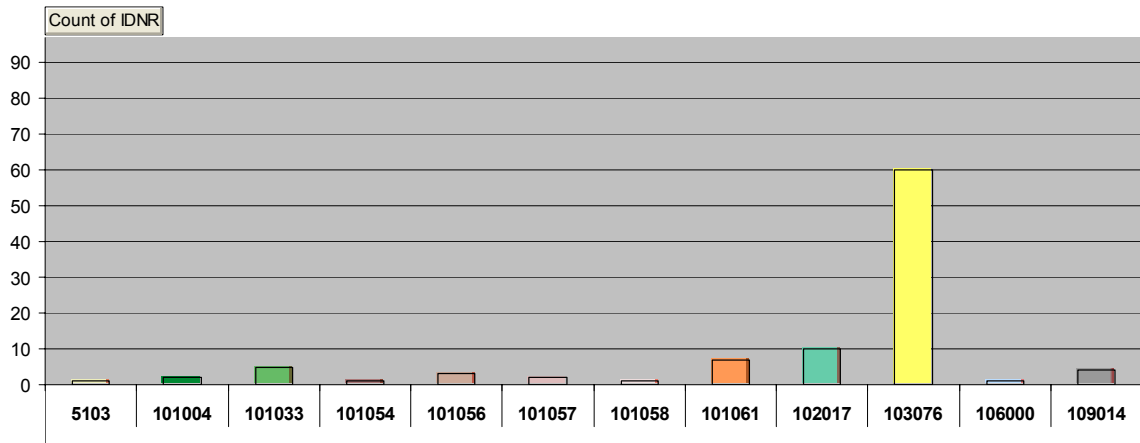
Rock domain 31

Number of outcrops composed solely of one rock type.

Y-axis indicates total number of outcrops in the rock domain.
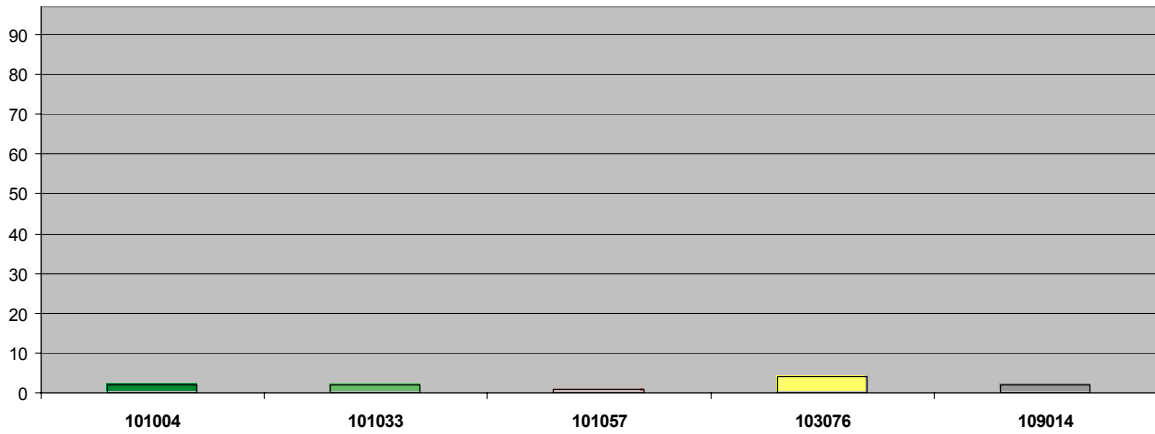
Rock domain 31

Number of occurrences of each rock type.
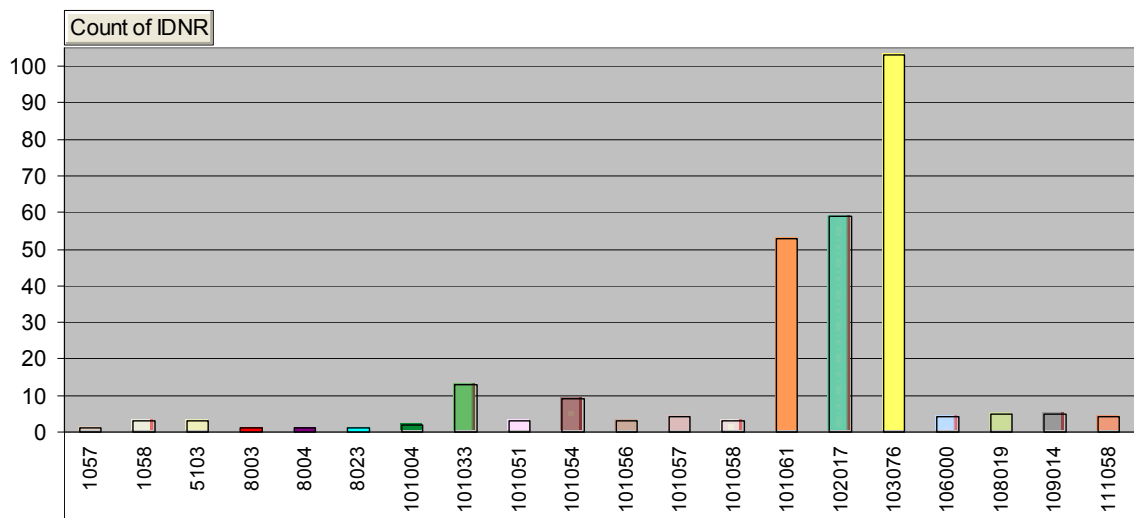
Rock domain 32

Number of outcrops where each rock type is dominating.
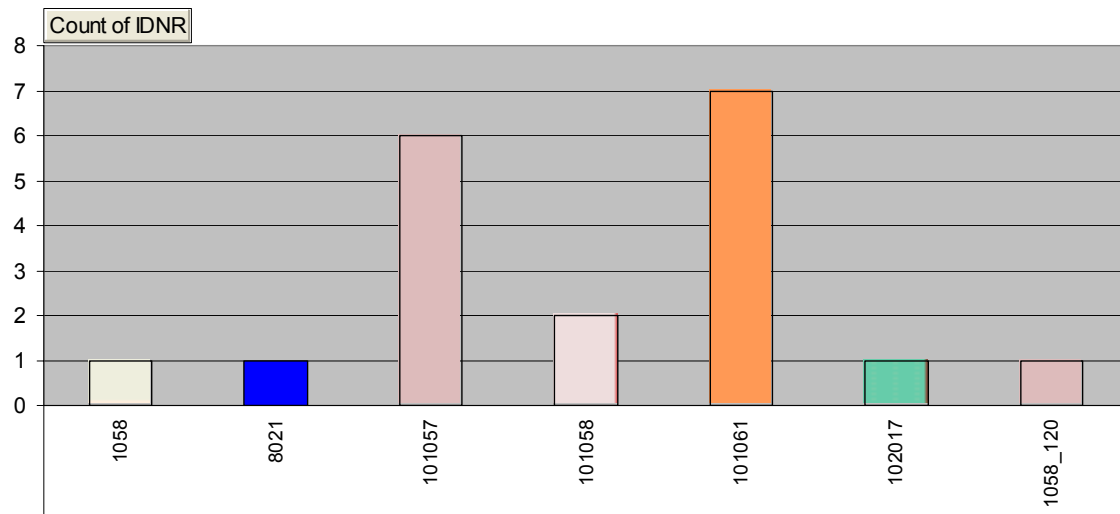Y-axis indicates total number of outcrops in the rock domain.
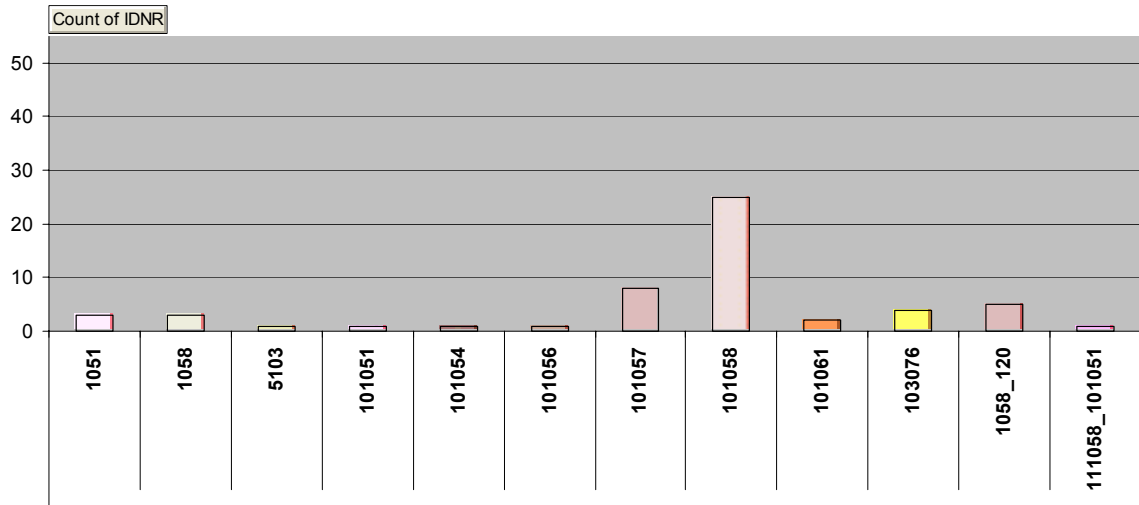
Rock domain 32

Number of outcrops composed solely of one rock type.
Y-axis indicates total number of outcrops in the rock domain.
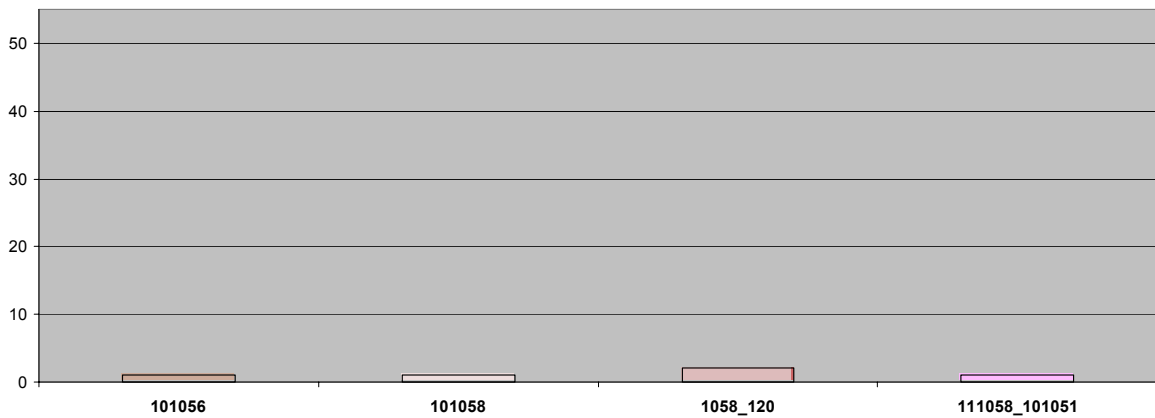
Rock domain 32

Number of occurrences of each rock type.
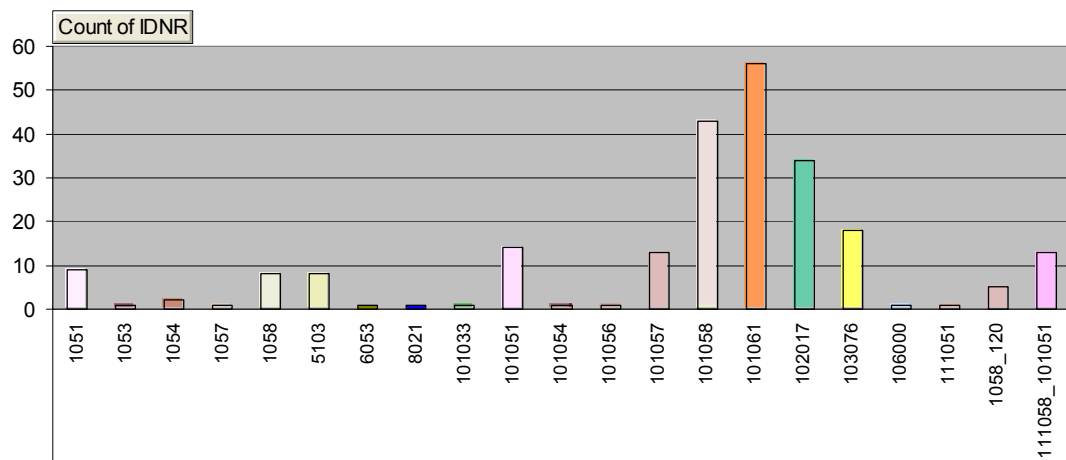
444

Rock domain 34

Number of outcrops where each rock type is dominating.
Y-axis indicates total number of outcrops in the rock domain.
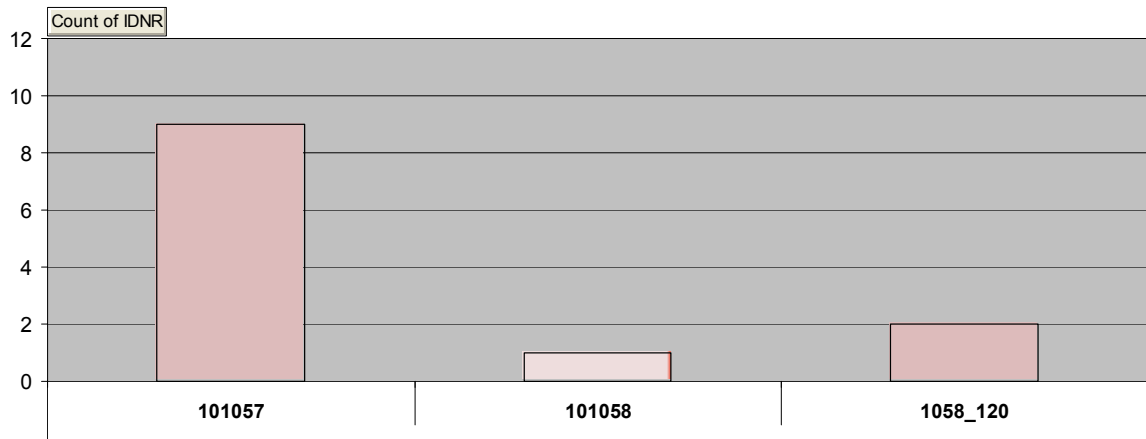
Rock domain 34

Number of outcrops composed solely of one rock type.
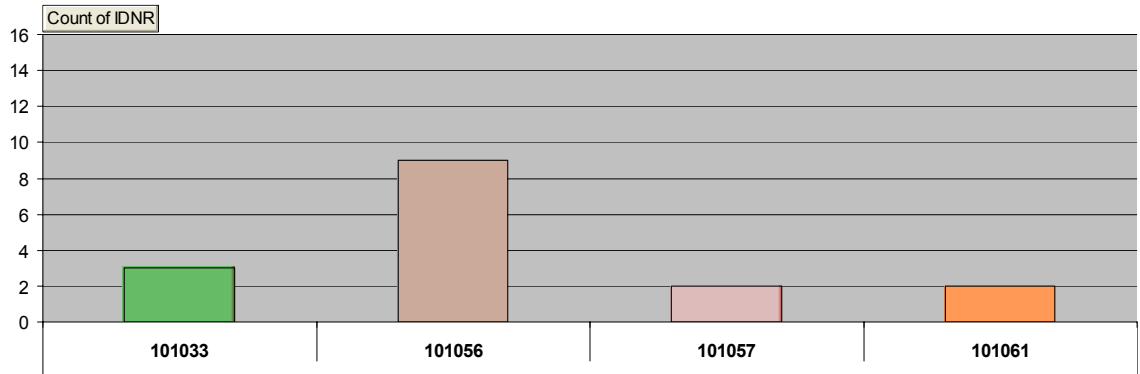Y-axis indicates total number of outcrops in the rock domain.

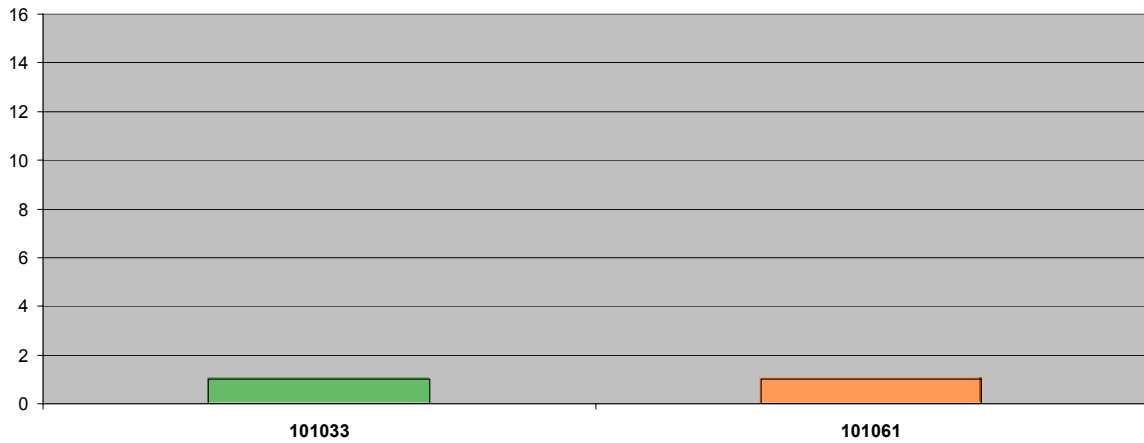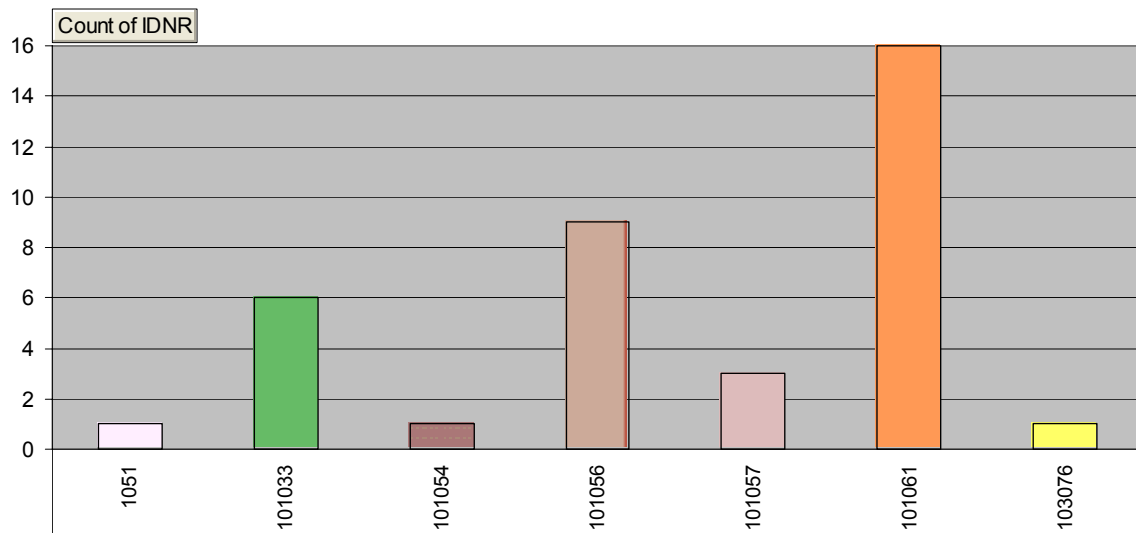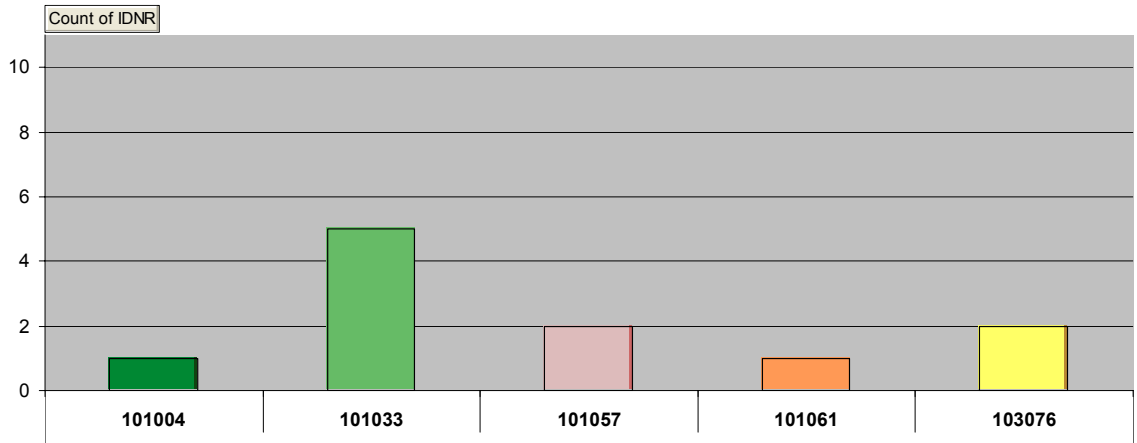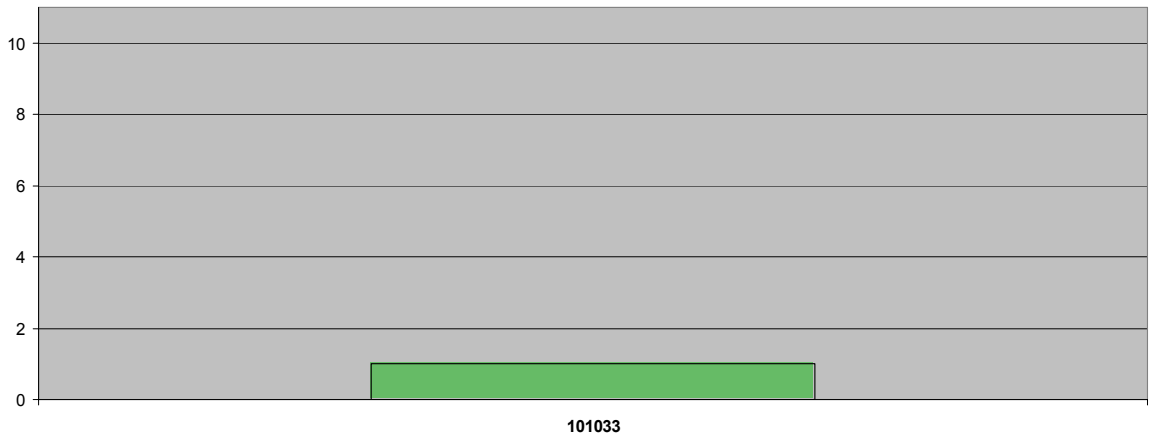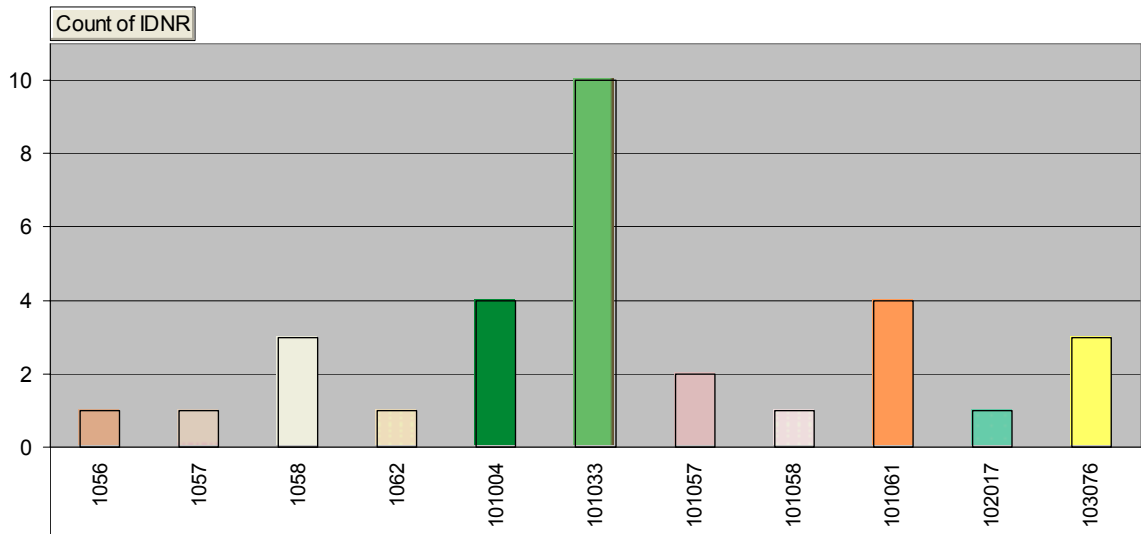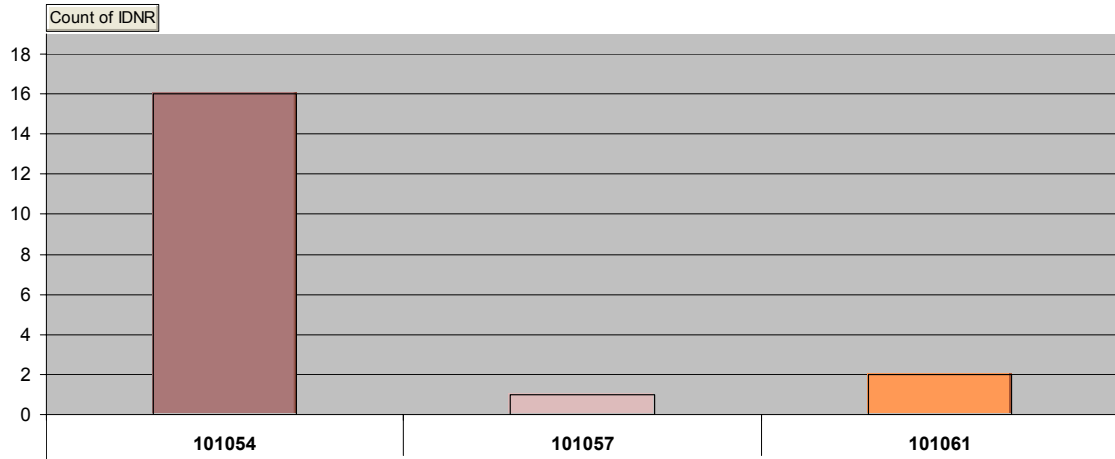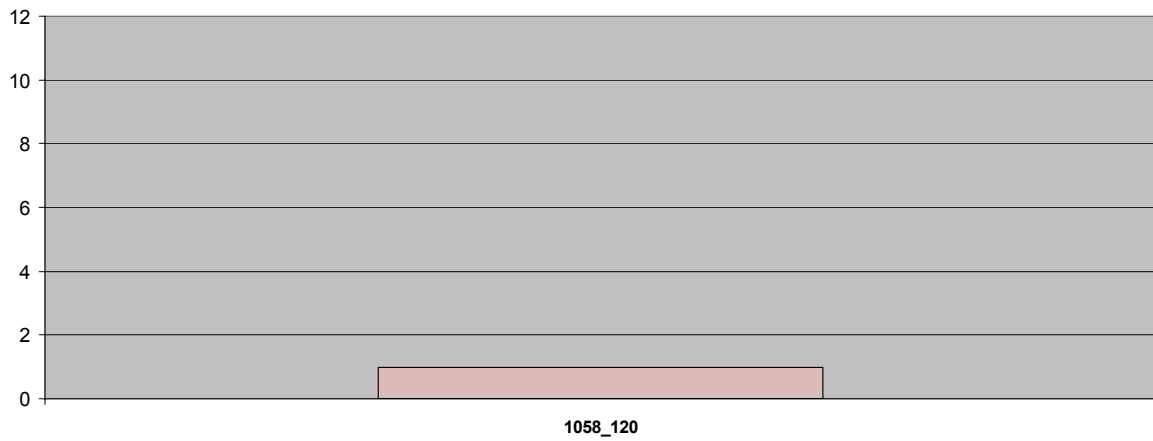## Rock domain 34

Number of occurrences of each rock type.

445
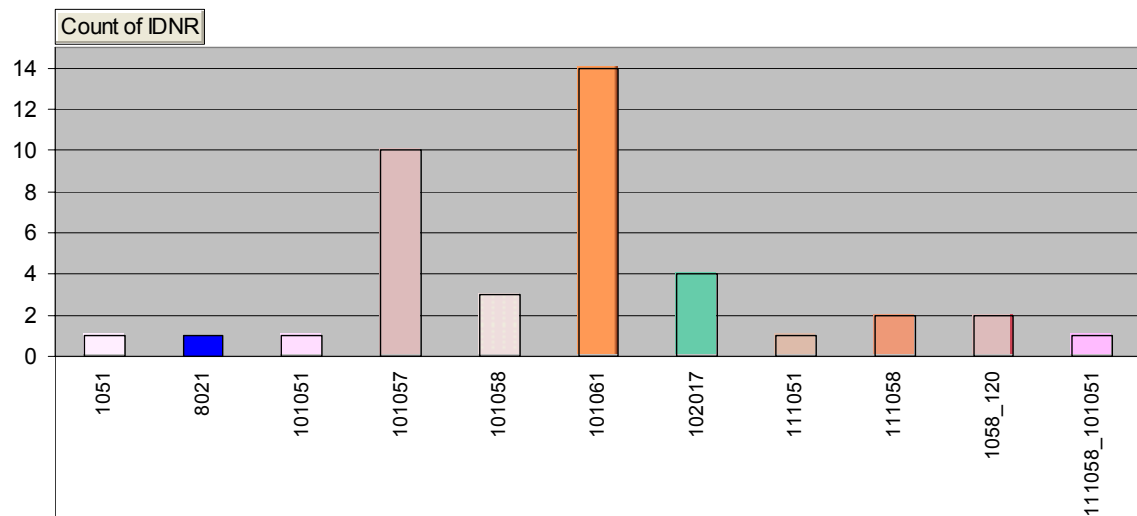
Properties of rock domains (RFM001 to RFM034) in the regional model volume

The construction of these tables is described in Section 5.1.2. The translation of rock codes to rock names is provided in Appendix 3.

RFM001					
Property	**Character**	**Quantitative estimate**	**Confidence**	**Basis for interpretation**	**Comments**
Volume (m^3)		5.31E+08	Medium		
Rock type, dominant	101004		High	See confidence table	
Rock type, subordinate	101033 101058		High	See confidence table	
Degree of homogeneity	High		Medium	See confidence table	
High temperature alteration (dominant rock type)	Amphibolite-facies metamorphism		High	See confidence table	
Ductile deformation	Isotropic or lineated and weakly foliated		High	See confidence table	
Class (1-4)*	4				
Background fracturing	**Quantitative estimate**	**Span**	**Confidence**	**Basis for interpretation**	**Comments**
Low temperature alteration around fractures	No data				
Fracture filling	No data				

*1=Inhomogeneous. Banded, foliated and lineated. Inferred higher degree of ductile deformation.
2=Inhomogeneous. Lineated and weakly foliated. Inferred lower degree of ductile deformation.
3=Homogeneous. Foliated and lineated. Inferred higher degree of ductile deformation. 4=Homogeneous. Lineated and weakly foliated. Inferred lower degree of ductile deformation.

RFM002					
Property	**Character**	**Quantitative estimate**	**Confidence**	**Basis for interpretation**	**Comments**
Volume (m^3)		1.57E+09	Low		
Rock type, dominant	101033		Medium	See confidence table	
Rock type, subordinate	101004		Medium	See confidence table	
Degree of homogeneity	High		Medium	See confidence table	
High temperature alteration (dominant rock type)	Amphibolite-facies metamorphism		High	See confidence table	
Ductile deformation	Lineated and weakly foliated		Low	See confidence table	
Class (1-4)*	4				
Background fracturing	**Quantitative estimate**	**Span**	**Confidence**	**Basis for interpretation**	**Comments**
Low temperature alteration around fractures	No data				
Fracture filling	No data				

*1=Inhomogeneous. Banded, foliated and lineated. Inferred higher degree of ductile deformation.
2=Inhomogeneous. Lineated and weakly foliated. Inferred lower degree of ductile deformation.
3=Homogeneous. Foliated and lineated. Inferred higher degree of ductile deformation. 4=Homogeneous.
Lineated and weakly foliated. Inferred lower degree of ductile deformation.

RFM003					
Property	**Character**	**Quantitative estimate**	**Confidence**	**Basis for interpretation**	**Comments**
Volume (m^3)		3.66E+07	Low		
Rock type, dominant	103076		Medium	See confidence table	
Rock type, subordinate	102017 101061		Medium	See confidence table	
Degree of homogeneity	Low		Low	See confidence table	
High temperature alteration (dominant rock type)	Amphibolite-facies metamorphism		High	See confidence table	
Ductile deformation	Banded, foliated and lineated		Low	See confidence table	
Class (1-4)*	4				
Background fracturing	**Quantitative estimate**	**Span**	**Confidence**	**Basis for interpretation**	**Comments**
Low temperature alteration around fractures	No data				
Fracture filling	No data				

*1=Inhomogeneous. Banded, foliated and lineated. Inferred higher degree of ductile deformation.
2=Inhomogeneous. Lineated and weakly foliated. Inferred lower degree of ductile deformation.
3=Homogeneous. Foliated and lineated. Inferred higher degree of ductile deformation. 4=Homogeneous.
Lineated and weakly foliated. Inferred lower degree of ductile deformation.

RFM004					
Property	**Character**	**Quantitative estimate**	**Confidence**	**Basis for interpretation**	**Comments**
Volume (m^3)		5.13E+07	Low		
Rock type, dominant	101033		Medium	See confidence table	
Rock type, subordinate	101061		Medium	See confidence table	
Degree of homogeneity	High		Medium	See confidence table	
High temperature alteration (dominant rock type)	Amphibolite-facies metamorphism		High	See confidence table	
Ductile deformation	Lineated and weakly foliated		Low	See confidence table	
Class (1-4)*	4				
Background fracturing	**Quantitative estimate**	**Span**	**Confidence**	**Basis for interpretation**	**Comments**
Low temperature alteration around fractures	No data				
Fracture filling	No data				

*1=Inhomogeneous. Banded, foliated and lineated. Inferred higher degree of ductile deformation.
2=Inhomogeneous. Lineated and weakly foliated. Inferred lower degree of ductile deformation.
3=Homogeneous. Foliated and lineated. Inferred higher degree of ductile deformation. 4=Homogeneous.
Lineated and weakly foliated. Inferred lower degree of ductile deformation.

RFM005					
Property	**Character**	**Quantitative estimate**	**Confidence**	**Basis for interpretation**	**Comments**
Volume (m^3)		1.48E+09	Medium		
Rock type, dominant	101033		High	See confidence table	
Rock type, subordinate	101061 101004 101054 103076 102017		High	See confidence table	
Degree of homogeneity	High		Medium	See confidence table	
High temperature alteration (dominant rock type)	Amphibolite-facies metamorphism		High	See confidence table	
Ductile deformation	Lineated and weakly foliated		High	See confidence table	
Class (1-4)*	4				
Background fracturing	**Quantitative estimate**	**Span**	**Confidence**	**Basis for interpretation**	**Comments**
Low temperature alteration around fractures	No data				
Fracture filling	No data				

*1=Inhomogeneous. Banded, foliated and lineated. Inferred higher degree of ductile deformation.
2=Inhomogeneous. Lineated and weakly foliated. Inferred lower degree of ductile deformation.
3=Homogeneous. Foliated and lineated. Inferred higher degree of ductile deformation. 4=Homogeneous.
Lineated and weakly foliated. Inferred lower degree of ductile deformation.

RFM006					
Property	**Character**	**Quantitative estimate**	**Confidence**	**Basis for interpretation**	**Comments**
Volume (m^3)		1.24E+09	Low		
Rock type, dominant	101054		Medium	See confidence table	
Rock type, subordinate	102017		Medium	See confidence table	
Degree of homogeneity	High		Low	See confidence table	
High temperature alteration (dominant rock type)	Amphibolite-facies metamorphism		High	See confidence table	
Ductile deformation	Lineated and weakly foliated		Low	See confidence table	
Class (1-4)*	4				
Background fracturing	**Quantitative estimate**	**Span**	**Confidence**	**Basis for interpretation**	**Comments**
Low temperature alteration around fractures	No data				
Fracture filling	No data				

*1=Inhomogeneous. Banded, foliated and lineated. Inferred higher degree of ductile deformation.
2=Inhomogeneous. Lineated and weakly foliated. Inferred lower degree of ductile deformation.
3=Homogeneous. Foliated and lineated. Inferred higher degree of ductile deformation. 4=Homogeneous.
Lineated and weakly foliated. Inferred lower degree of ductile deformation.

RFM007					
Property	**Character**	**Quantitative estimate**	**Confidence**	**Basis for interpretation**	**Comments**
Volume (m^3)		1.90E+09	Medium		
Rock type, dominant	101033		Medium	See confidence table	
Rock type, subordinate	101061 101057 101004 101054		Medium	See confidence table	
Degree of homogeneity	High		Medium	See confidence table	
High temperature alteration (dominant rock type)	Amphibolite-facies metamorphism		High	See confidence table	
Ductile deformation	Lineated and weakly foliated		High	See confidence table	
Class (1-4)*	4				
Background fracturing	**Quantitative estimate**	**Span**	**Confidence**	**Basis for interpretation**	**Comments**
Low temperature alteration around fractures	No data				
Fracture filling	No data				

*1=Inhomogeneous. Banded, foliated and lineated. Inferred higher degree of ductile deformation.
2=Inhomogeneous. Lineated and weakly foliated. Inferred lower degree of ductile deformation.
3=Homogeneous. Foliated and lineated. Inferred higher degree of ductile deformation. 4=Homogeneous. Lineated and weakly foliated. Inferred lower degree of ductile deformation.

RFM008					
Property	**Character**	**Quantitative estimate**	**Confidence**	**Basis for interpretation**	**Comments**
Volume (m³)		7.02E+08	Medium		
Rock type, dominant	101033		High	See confidence table	
Rock type, subordinate	103076 101061 102017 111058		High	See confidence table	
Degree of homogeneity	High		Medium	See confidence table	
High temperature alteration (dominant rock type)	Amphibolite-facies metamorphism		High	See confidence table	
Ductile deformation	Foliated and lineated		High	See confidence table	
Class (1-4)*	3				
Background fracturing	**Quantitative estimate**	**Span**	**Confidence**	**Basis for interpretation**	**Comments**
Low temperature alteration around fractures	No data				
Fracture filling	No data				

*1=Inhomogeneous. Banded, foliated and lineated. Inferred higher degree of ductile deformation.
2=Inhomogeneous. Lineated and weakly foliated. Inferred lower degree of ductile deformation.
3=Homogeneous. Foliated and lineated. Inferred higher degree of ductile deformation. 4=Homogeneous.
Lineated and weakly foliated. Inferred lower degree of ductile deformation.

RFM009					
Property	**Character**	**Quantitative estimate**	**Confidence**	**Basis for interpretation**	**Comments**
Volume (m³)		3.62E+07	Medium		
Rock type, dominant	101061		Medium	See confidence table	
Rock type, subordinate	103076		Medium	See confidence table	
Degree of homogeneity	High		Medium	See confidence table	
High temperature alteration (dominant rock type)	Greenschist facies metamorphism		High	See confidence table	
Ductile deformation	Isotropic or weakly foliated and lineated (in 101061)		High	See confidence table	
Class (1-4)*	4				
Background fracturing	**Quantitative estimate**	**Span**	**Confidence**	**Basis for interpretation**	**Comments**
Low temperature alteration around fractures	No data				
Fracture filling	No data				

*1=Inhomogeneous. Banded, foliated and lineated. Inferred higher degree of ductile deformation.
2=Inhomogeneous. Lineated and weakly foliated. Inferred lower degree of ductile deformation.
3=Homogeneous. Foliated and lineated. Inferred higher degree of ductile deformation. 4=Homogeneous.
Lineated and weakly foliated. Inferred lower degree of ductile deformation.

RFM010					
Property	**Character**	**Quantitative estimate**	**Confidence**	**Basis for interpretation**	**Comments**
Volume (m^3)		4.19E+08	Medium		
Rock type, dominant	103076		High	See confidence table	
Rock type, subordinate	101054 102017 101054 101061 111058 109014 108019		High	See confidence table	
Degree of homogeneity	Low		Medium	See confidence table	
High temperature alteration (dominant rock type)	Amphibolite-facies metamorphism		High	See confidence table	
Ductile deformation	Banded, foliated and lineated		High	See confidence table	
Class (1-4)[*]	1				
Background fracturing	**Quantitative estimate**	**Span**	**Confidence**	**Basis for interpretation**	**Comments**
Low temperature alteration around fractures	No data				
Fracture filling	No data				

[*]1=Inhomogeneous. Banded, foliated and lineated. Inferred higher degree of ductile deformation.
2=Inhomogeneous. Lineated and weakly foliated. Inferred lower degree of ductile deformation.
3=Homogeneous. Foliated and lineated. Inferred higher degree of ductile deformation. 4=Homogeneous.
Lineated and weakly foliated. Inferred lower degree of ductile deformation.

RFM011					
Property	**Character**	**Quantitative estimate**	**Confidence**	**Basis for interpretation**	**Comments**
Volume (m^3)		Unable to be carried out due to difficulties with RVS			
Rock type, dominant	101057		Medium	See confidence table	
Rock type, subordinate	102017 101056 101054 103076 101061 111058		Medium	See confidence table	
Degree of homogeneity	High		Medium	See confidence table	
High temperature alteration (dominant rock type)	Amphibolite-facies metamorphism		High	See confidence table	
Ductile deformation	Lineated and weakly foliated		Medium	See confidence table	
Class (1-4)*	4				
Background fracturing	**Quantitative estimate**	**Span**	**Confidence**	**Basis for interpretation**	**Comments**
Low temperature alteration around fractures	No data				
Fracture filling	No data				

*1=Inhomogeneous. Banded, foliated and lineated. Inferred higher degree of ductile deformation.
2=Inhomogeneous. Lineated and weakly foliated. Inferred lower degree of ductile deformation.
3=Homogeneous. Foliated and lineated. Inferred higher degree of ductile deformation. 4=Homogeneous.
Lineated and weakly foliated. Inferred lower degree of ductile deformation.

RFM012					
Property	**Character**	**Quantitative estimate**	**Confidence**	**Basis for interpretation**	**Comments**
Volume (m³)		4.63E+08	Medium		
Rock type, dominant	101057		High	See confidence table	
Rock type, subordinate	101061 101058 102017		High	See confidence table	
Degree of homogeneity	High		Medium	See confidence table	
High temperature alteration (dominant rock type)	Amphibolite-facies metamorphism		High	See confidence table	
Ductile deformation	Foliated and lineated		High	See confidence table	
Class (1-4)*	3				
Background fracturing	**Quantitative estimate**	**Span**	**Confidence**	**Basis for interpretation**	**Comments**
Low temperature alteration around fractures	No data				
Fracture filling	No data				

*1=Inhomogeneous. Banded, foliated and lineated. Inferred higher degree of ductile deformation.
2=Inhomogeneous. Lineated and weakly foliated. Inferred lower degree of ductile deformation.
3=Homogeneous. Foliated and lineated. Inferred higher degree of ductile deformation. 4=Homogeneous.
Lineated and weakly foliated. Inferred lower degree of ductile deformation.

RFM013					
Property	**Character**	**Quantitative estimate**	**Confidence**	**Basis for interpretation**	**Comments**
Volume (m^3)		2.45E+09	Medium		
Rock type, dominant	101056		High	See confidence table	
Rock type, subordinate	101033 101061 101057		High	See confidence table	
Degree of homogeneity	High		Medium	See confidence table	
High temperature alteration (dominant rock type)	Amphibolite-facies metamorphism		High	See confidence table	
Ductile deformation	Lineated and weakly foliated.		High	See confidence table	
Class (1-4)*	4				
Background fracturing	**Quantitative estimate**	**Span**	**Confidence**	**Basis for interpretation**	**Comments**
Low temperature alteration around fractures	No data				
Fracture filling	No data				

*1=Inhomogeneous. Banded, foliated and lineated. Inferred higher degree of ductile deformation.
2=Inhomogeneous. Lineated and weakly foliated. Inferred lower degree of ductile deformation.
3=Homogeneous. Foliated and lineated. Inferred higher degree of ductile deformation. 4=Homogeneous.
Lineated and weakly foliated. Inferred lower degree of ductile deformation.

RFM014					
Property	**Character**	**Quantitative estimate**	**Confidence**	**Basis for interpretation**	**Comments**
Volume (m^3)		Unable to be carried out due to difficulties with RVS			
Rock type, dominant	101033		High	See confidence table	
Rock type, subordinate	103076 101057 101004 101061		High	See confidence table	
Degree of homogeneity	High		Medium	See confidence table	
High temperature alteration (dominant rock type)	Amphibolite-facies metamorphism		High	See confidence table	
Ductile deformation	Lineated and weakly foliated		High	See confidence table	
Class (1-4)*	4				
Background fracturing	**Quantitative estimate**	**Span**	**Confidence**	**Basis for interpretation**	**Comments**
Low temperature alteration around fractures	No data				
Fracture filling	No data				

*1=Inhomogeneous. Banded, foliated and lineated. Inferred higher degree of ductile deformation.
2=Inhomogeneous. Lineated and weakly foliated. Inferred lower degree of ductile deformation.
3=Homogeneous. Foliated and lineated. Inferred higher degree of ductile deformation. 4=Homogeneous.
Lineated and weakly foliated. Inferred lower degree of ductile deformation.

RFM015					
Property	**Character**	**Quantitative estimate**	**Confidence**	**Basis for interpretation**	**Comments**
Volume (m^3)		9.61E+08	Low		
Rock type, dominant	101033		Medium	See confidence table	
Rock type, subordinate	101061 102017 106000		Medium	See confidence table	
Degree of homogeneity	High		Medium	See confidence table	
High temperature alteration (dominant rock type)	Amphibolite-facies metamorphism		High	See confidence table	
Ductile deformation	Foliated and lineated		Low	See confidence table	
Class (1-4)*	3				
Background fracturing	**Quantitative estimate**	**Span**	**Confidence**	**Basis for interpretation**	**Comments**
Low temperature alteration around fractures	No data				Tunnel 3 data not analysed
Fracture filling	No data				Tunnel 3 data not analysed

*1=Inhomogeneous. Banded, foliated and lineated. Inferred higher degree of ductile deformation.
2=Inhomogeneous. Lineated and weakly foliated. Inferred lower degree of ductile deformation.
3=Homogeneous. Foliated and lineated. Inferred higher degree of ductile deformation. 4=Homogeneous.
Lineated and weakly foliated. Inferred lower degree of ductile deformation.

RFM016					
Property	**Character**	**Quantitative estimate**	**Confidence**	**Basis for interpretation**	**Comments**
Volume (m^3)		5.05E+09	Low		
Rock type, dominant	101033		Medium	See confidence table	
Rock type, subordinate	106000		Low	See confidence table	
Degree of homogeneity	High		Medium	See confidence table	
High temperature alteration (dominant rock type)	Amphibolite-facies metamorphism		High	See confidence table	
Ductile deformation	Lineated and weakly foliated, in part isotropic		Medium	See confidence table	
Class (1-4)[*]	4				
Background fracturing	**Quantitative estimate**	**Span**	**Confidence**	**Basis for interpretation**	**Comments**
Low temperature alteration around fractures	No data				
Fracture filling	No data				

[*]1=Inhomogeneous. Banded, foliated and lineated. Inferred higher degree of ductile deformation.
2=Inhomogeneous. Lineated and weakly foliated. Inferred lower degree of ductile deformation.
3=Homogeneous. Foliated and lineated. Inferred higher degree of ductile deformation. 4=Homogeneous.
Lineated and weakly foliated. Inferred lower degree of ductile deformation.

RFM017					
Property	**Character**	**Quantitative estimate**	**Confidence**	**Basis for interpretation**	**Comments**
Volume (m^3)		2.82E+08	Medium		
Rock type, dominant	101054		High	See confidence table	
Rock type, subordinate	101061 101051 101057 102017		High	See confidence table	
Degree of homogeneity	High		Medium	See confidence table	
High temperature alteration (dominant rock type)	Amphibolite-facies metamorphism		High	See confidence table	
Ductile deformation	Lineated and weakly foliated.		High	See confidence table	
Class (1-4)*	4				
Background fracturing	**Quantitative estimate**	**Span**	**Confidence**	**Basis for interpretation**	**Comments**
Low temperature alteration around fractures	No data				
Fracture filling	No data				

*1=Inhomogeneous. Banded, foliated and lineated. Inferred higher degree of ductile deformation.
2=Inhomogeneous. Lineated and weakly foliated. Inferred lower degree of ductile deformation.
3=Homogeneous. Foliated and lineated. Inferred higher degree of ductile deformation. 4=Homogeneous.
Lineated and weakly foliated. Inferred lower degree of ductile deformation.

RFM018					
Property	**Character**	**Quantitative estimate**	**Confidence**	**Basis for interpretation**	**Comments**
Volume (m^3)		Unable to be carried out due to difficulties with RVS			Borehole data close to reactor 3 not analysed
Rock type, dominant	101054		High	See confidence table	Borehole data close to reactor 3 not analysed
Rock type, subordinate	101057 101056 101061 103076 101033 102017 111058		High	See confidence table	Borehole data close to reactor 3 not analysed
Degree of homogeneity	Low		Medium	See confidence table	Borehole data close to reactor 3 not analysed
High temperature alteration (dominant rock type)	Amphibolite-facies metamorphism		High	See confidence table	Borehole data close to reactor 3 not analysed
Ductile deformation	Banded, foliated and lineated		High	See confidence table	Borehole data close to reactor 3 not analysed
Class (1-4)[*]	1				
Background fracturing	**Quantitative estimate**	**Span**	**Confidence**	**Basis for interpretation**	**Comments**
Low temperature alteration around fractures	No data				Borehole data close to reactor 3 not analysed
Fracture filling	No data				Borehole data close to reactor 3 not analysed

[*]1=Inhomogeneous. Banded, foliated and lineated. Inferred higher degree of ductile deformation.
2=Inhomogeneous. Lineated and weakly foliated. Inferred lower degree of ductile deformation.
3=Homogeneous. Foliated and lineated. Inferred higher degree of ductile deformation. 4=Homogeneous.
Lineated and weakly foliated. Inferred lower degree of ductile deformation.

RFM019					
Property	**Character**	**Quantitative estimate**	**Confidence**	**Basis for interpretation**	**Comments**
Volume (m^3)		7.22E+09	Very low		
Rock type, dominant	111051		Low	See confidence table	SFR data not analysed
Rock type, subordinate	101061		Low	See confidence table	SFR data not analysed
Degree of homogeneity	Low		Low	See confidence table	SFR data not analysed
High temperature alteration (dominant rock type)	Amphibolite-facies metamorphism		Low	See confidence table	SFR data not analysed
Ductile deformation	Banded, foliated and lineated		Low	See confidence table	SFR data not analysed
Class (1-4)[*]	1				
Background fracturing	**Quantitative estimate**	**Span**	**Confidence**	**Basis for interpretation**	**Comments**
Low temperature alteration around fractures	No data				SFR data not analysed
Fracture filling	No data				SFR data not analysed

[*]1=Inhomogeneous. Banded, foliated and lineated. Inferred higher degree of ductile deformation.
2=Inhomogeneous. Lineated and weakly foliated. Inferred lower degree of ductile deformation.
3=Homogeneous. Foliated and lineated. Inferred higher degree of ductile deformation. 4=Homogeneous.
Lineated and weakly foliated. Inferred lower degree of ductile deformation.

RFM020					
Property	**Character**	**Quantitative estimate**	**Confidence**	**Basis for interpretation**	**Comments**
Volume (m³)		2.79E+09	Low		
Rock type, dominant	101058		Medium	See confidence table	
Rock type, subordinate	101057 101061 102017		Medium	See confidence table	
Degree of homogeneity	High		Low	See confidence table	
High temperature alteration (dominant rock type)	Amphibolite-facies metamorphism		High	See confidence table	
Ductile deformation	Banded, foliated and lineated		Low	See confidence table	
Class (1-4)*	1				
Background fracturing	**Quantitative estimate**	**Span**	**Confidence**	**Basis for interpretation**	**Comments**
Low temperature alteration around fractures	No data				Tunnel data (1/2 and 3) not analysed
Fracture filling	No data				Tunnel data (1/2 and 3) not analysed

*1=Inhomogeneous. Banded, foliated and lineated. Inferred higher degree of ductile deformation.
2=Inhomogeneous. Lineated and weakly foliated. Inferred lower degree of ductile deformation.
3=Homogeneous. Foliated and lineated. Inferred higher degree of ductile deformation. 4=Homogeneous. Lineated and weakly foliated. Inferred lower degree of ductile deformation.

RFM021					
Property	**Character**	**Quantitative estimate**	**Confidence**	**Basis for interpretation**	**Comments**
Volume (m^3)		4.57E+09	Medium		
Rock type, dominant	103076		High	See confidence table	
Rock type, subordinate	101058 101033 102017 101057 101061 101054 108019		High	See confidence table	
Degree of homogeneity	Low		Medium	See confidence table	
High temperature alteration (dominant rock type)	Amphibolite-facies metamorphism		High	See confidence table	
Ductile deformation	Banded, foliated and lineated		High	See confidence table	
Class (1-4)[*]	1				
Background fracturing	**Quantitative estimate**	**Span**	**Confidence**	**Basis for interpretation**	**Comments**
Low temperature alteration around fractures	No data				Tunnel data (1/2 and 3) not analysed
Fracture filling	No data				Tunnel data (1/2 and 3) not analysed

[*]1=Inhomogeneous. Banded, foliated and lineated. Inferred higher degree of ductile deformation.
2=Inhomogeneous. Lineated and weakly foliated. Inferred lower degree of ductile deformation.
3=Homogeneous. Foliated and lineated. Inferred higher degree of ductile deformation. 4=Homogeneous.
Lineated and weakly foliated. Inferred lower degree of ductile deformation.

RFM022					
Property	**Character**	**Quantitative estimate**	**Confidence**	**Basis for interpretation**	**Comments**
Volume (m^3)		1.87E+08	Very low		
Rock type, dominant	111058		Low	See confidence table	
Rock type, subordinate	101061		Low	See confidence table	
Degree of homogeneity	High		Low	See confidence table	
High temperature alteration (dominant rock type)	Greenschist facies metamorphism		Low	See confidence table	
Ductile deformation	Isotropic or weakly foliated and lineated		Low	See confidence table	
Class (1-4)*	4				
Background fracturing	**Quantitative estimate**	**Span**	**Confidence**	**Basis for interpretation**	**Comments**
Low temperature alteration around fractures	No data				
Fracture filling	No data				

*1=Inhomogeneous. Banded, foliated and lineated. Inferred higher degree of ductile deformation.
2=Inhomogeneous. Lineated and weakly foliated. Inferred lower degree of ductile deformation.
3=Homogeneous. Foliated and lineated. Inferred higher degree of ductile deformation. 4=Homogeneous.
Lineated and weakly foliated. Inferred lower degree of ductile deformation.

RFM023					
Property	**Character**	**Quantitative estimate**	**Confidence**	**Basis for interpretation**	**Comments**
Volume (m^3)		Unable to be carried out due to difficulties with RVS			
Rock type, dominant	101054		High	See confidence table	
Rock type, subordinate	101061 101033 101057 101004 101056 101051 102017		High	See confidence table	
Degree of homogeneity	High		Medium	See confidence table	
High temperature alteration (dominant rock type)	Amphibolite-facies metamorphism		High	See confidence table	
Ductile deformation	Lineated and weakly foliated		High	See confidence table	
Class (1-4)*	4				
Background fracturing	**Quantitative estimate**	**Span**	**Confidence**	**Basis for interpretation**	**Comments**
Low temperature alteration around fractures	No data				
Fracture filling	No data				

*1=Inhomogeneous. Banded, foliated and lineated. Inferred higher degree of ductile deformation.
2=Inhomogeneous. Lineated and weakly foliated. Inferred lower degree of ductile deformation.
3=Homogeneous. Foliated and lineated. Inferred higher degree of ductile deformation. 4=Homogeneous.
Lineated and weakly foliated. Inferred lower degree of ductile deformation.

RFM024					
Property	**Character**	**Quantitative estimate**	**Confidence**	**Basis for interpretation**	**Comments**
Volume (m^3)		1.95E+10	Low		
Rock type, dominant	101054		Medium	See confidence table	
Rock type, subordinate	102017 101061		Medium	See confidence table	
Degree of homogeneity	High		Low	See confidence table	
High temperature alteration (dominant rock type)	Amphibolite-facies metamorphism		High	See confidence table	
Ductile deformation	Lineated and weakly foliated		Low	See confidence table	
Class (1-4)[*]	4				
Background fracturing	**Quantitative estimate**	**Span**	**Confidence**	**Basis for interpretation**	**Comments**
Low temperature alteration around fractures	No data				
Fracture filling	No data				

[*]1=Inhomogeneous. Banded, foliated and lineated. Inferred higher degree of ductile deformation.
2=Inhomogeneous. Lineated and weakly foliated. Inferred lower degree of ductile deformation.
3=Homogeneous. Foliated and lineated. Inferred higher degree of ductile deformation. 4=Homogeneous.
Lineated and weakly foliated. Inferred lower degree of ductile deformation.

RFM025					
Property	**Character**	**Quantitative estimate**	**Confidence**	**Basis for interpretation**	**Comments**
Volume (m^3)		Unable to be carried out due to difficulties with RVS			
Rock type, dominant	101033		High	See confidence table	
Rock type, subordinate	101061 101054 102017		High	See confidence table	
Degree of homogeneity	High		Medium	See confidence table	
High temperature alteration (dominant rock type)	Amphibolite-facies metamorphism		High	See confidence table	
Ductile deformation	Lineated and weakly foliated		High	See confidence table	
Class (1-4)*	4				
Background fracturing	**Quantitative estimate**	**Span**	**Confidence**	**Basis for interpretation**	**Comments**
Low temperature alteration around fractures	No data				
Fracture filling	No data				

*1=Inhomogeneous. Banded, foliated and lineated. Inferred higher degree of ductile deformation.
2=Inhomogeneous. Lineated and weakly foliated. Inferred lower degree of ductile deformation.
3=Homogeneous. Foliated and lineated. Inferred higher degree of ductile deformation. 4=Homogeneous.
Lineated and weakly foliated. Inferred lower degree of ductile deformation.

RFM026					
Property	**Character**	**Quantitative estimate**	**Confidence**	**Basis for interpretation**	**Comments**
Volume (m^3)		Unable to be carried out due to difficulties with RVS			
Rock type, dominant	101057		High	See confidence table	
Rock type, subordinate	101058 101061 101056 101033 103076 102017 101054 101051 111058		High	See confidence table	
Degree of homogeneity	High		Medium	See confidence table	
High temperature alteration (dominant rock type)	Amphibolite-facies metamorphism		High	See confidence table	
Ductile deformation	Foliated and lineated		High	See confidence table	
Class (1-4)*	1				
Background fracturing	**Quantitative estimate**	**Span**	**Confidence**	**Basis for interpretation**	**Comments**
Low temperature alteration around fractures	No data				
Fracture filling	No data				

*1=Inhomogeneous. Banded, foliated and lineated. Inferred higher degree of ductile deformation.
2=Inhomogeneous. Lineated and weakly foliated. Inferred lower degree of ductile deformation.
3=Homogeneous. Foliated and lineated. Inferred higher degree of ductile deformation. 4=Homogeneous.
Lineated and weakly foliated. Inferred lower degree of ductile deformation.

RFM027					
Property	**Character**	**Quantitative estimate**	**Confidence**	**Basis for interpretation**	**Comments**
Volume (m³)		Unable to be carried out due to difficulties with RVS			
Rock type, dominant	106000		Low	See confidence table	SFR data not analysed
Rock type, subordinate	101061		Low	See confidence table	SFR data not analysed
Degree of homogeneity	Low		Low	See confidence table	SFR data not analysed
High temperature alteration (dominant rock type)	Amphibolite-facies metamorphism		Low	See confidence table	SFR data not analysed
Ductile deformation	Banded, foliated and lineated		Low	See confidence table	SFR data not analysed
Class (1-4)*	1				
Background fracturing	**Quantitative estimate**	**Span**	**Confidence**	**Basis for interpretation**	**Comments**
Low temperature alteration around fractures	No data				SFR data and data from tunnels (1/2 and 3) not analysed
Fracture filling	No data				SFR data and data from tunnels (1/2 and 3) not analysed

*1=Inhomogeneous. Banded, foliated and lineated. Inferred higher degree of ductile deformation.
2=Inhomogeneous. Lineated and weakly foliated. Inferred lower degree of ductile deformation.
3=Homogeneous. Foliated and lineated. Inferred higher degree of ductile deformation. 4=Homogeneous.
Lineated and weakly foliated. Inferred lower degree of ductile deformation.

RFM028					
Property	**Character**	**Quantitative estimate**	**Confidence**	**Basis for interpretation**	**Comments**
Volume (m^3)		Unable to be carried out due to difficulties with RVS			
Rock type, dominant	101057		Medium	See confidence table	
Rock type, subordinate	101033 101056 101058 101054 101061 102017		Medium	See confidence table	
Degree of homogeneity	Low		Medium	See confidence table	
High temperature alteration (dominant rock type)	Amphibolite-facies metamorphism		High	See confidence table	
Ductile deformation	Banded, foliated and lineated		High	See confidence table	
Class (1-4)*	1				
Background fracturing	**Quantitative estimate**	**Span**	**Confidence**	**Basis for interpretation**	**Comments**
Low temperature alteration around fractures	No data				
Fracture filling	No data				

*1=Inhomogeneous. Banded, foliated and lineated. Inferred higher degree of ductile deformation.
2=Inhomogeneous. Lineated and weakly foliated. Inferred lower degree of ductile deformation.
3=Homogeneous. Foliated and lineated. Inferred higher degree of ductile deformation. 4=Homogeneous.
Lineated and weakly foliated. Inferred lower degree of ductile deformation.

RFM029					
Property	**Character**	**Quantitative estimate**	**Confidence**	**Basis for interpretation**	**Comments**
Volume (m^3)		Unable to be carried out due to difficulties with RVS			Borehole data close to reactors 1 and 2 not analysed.
Rock type, dominant	101057	84%	High	See confidence table	Quantitative estimate based on occurrence in KFM01A. Borehole data close to reactors 1 and 2 not analysed.
Rock type, subordinate	101051 102017 101061 111058 108019	11% 2% 1.5% 1.3% 0.2%	High	See confidence table	Quantitative estimate based on occurrence in close to KFM01A. Borehole data reactors 1 and 2 not analysed.
Degree of homogeneity	High		High	See confidence table	Borehole data close to reactors 1 and 2 not analysed.
High temperature alteration (dominant rock type)	Amphibolite-facies metamorphism		High	See confidence table	Borehole data close to reactors 1 and 2 not analysed.
Ductile deformation	Lineated and weakly foliated. More strongly foliated along southwestern and northeastern margins		High	See confidence table	Borehole data close to reactors 1 and 2 not analysed.
Class (1-4)*	4				Borehole data close to reactors 1 and 2 not analysed.
Background fracturing	**Quantitative estimate**	**Span**	**Confidence**	**Basis for interpretation**	**Comments**
Low temperature alteration around fractures	7% of the fractures. All sets	5 to 12 % in different sets	Medium	section 4.4.2	Sealed fracture data from KFM01A. Open fracture data. Oxidation not mapped.
Fracture filling	Open fractures, 60% chlorite. Sealed fractures, laumontite, hematite, chlorite	Open fractures, 38 to 67% in different sets. Sealed fractures, highly variable	Medium	section 4.4.2	Dominant filling in open and sealed fracture data from KFM01A.

*1=Inhomogeneous. Banded, foliated and lineated. Inferred higher degree of ductile deformation.
2=Inhomogeneous. Lineated and weakly foliated. Inferred lower degree of ductile deformation.
3=Homogeneous. Foliated and lineated. Inferred higher degree of ductile deformation. 4=Homogeneous.
Lineated and weakly foliated. Inferred lower degree of ductile deformation.

RFM030					
Property	**Character**	**Quantitative estimate**	**Confidence**	**Basis for interpretation**	**Comments**
Volume (m^3)		2.92E+10	Medium		
Rock type, dominant	101054		High	See confidence table	
Rock type, subordinate	101056 101061 101057 101033 103076 102017 101051 111058 109010		High	See confidence table	
Degree of homogeneity	Low		Medium	See confidence table	
High temperature alteration (dominant rock type)	Amphibolite-facies metamorphism		High	See confidence table	
Ductile deformation	Banded, foliated and lineated		High	See confidence table	
Class (1-4)*	1				
Background fracturing	**Quantitative estimate**	**Span**	**Confidence**	**Basis for interpretation**	**Comments**
Low temperature alteration around fractures	No data				
Fracture filling	No data				

*1=Inhomogeneous. Banded, foliated and lineated. Inferred higher degree of ductile deformation.
2=Inhomogeneous. Lineated and weakly foliated. Inferred lower degree of ductile deformation.
3=Homogeneous. Foliated and lineated. Inferred higher degree of ductile deformation. 4=Homogeneous.
Lineated and weakly foliated. Inferred lower degree of ductile deformation.

RFM031					
Property	**Character**	**Quantitative estimate**	**Confidence**	**Basis for interpretation**	**Comments**
Volume (m^3)		Unable to be carried out due to difficulties with RVS			
Rock type, dominant	103076		High	See confidence table	
Rock type, subordinate	102017 101061 101033 101056 101054 109014 108019		High	See confidence table	
Degree of homogeneity	Low		Medium	See confidence table	
High temperature alteration (dominant rock type)	Amphibolite-facies metamorphism		High	See confidence table	
Ductile deformation	Banded, foliated and lineated		High	See confidence table	
Class (1-4)*	1				
Background fracturing	**Quantitative estimate**	**Span**	**Confidence**	**Basis for interpretation**	**Comments**
Low temperature alteration around fractures	No data				
Fracture filling	No data				

*1=Inhomogeneous. Banded, foliated and lineated. Inferred higher degree of ductile deformation.
2=Inhomogeneous. Lineated and weakly foliated. Inferred lower degree of ductile deformation.
3=Homogeneous. Foliated and lineated. Inferred higher degree of ductile deformation. 4=Homogeneous.
Lineated and weakly foliated. Inferred lower degree of ductile deformation.

RFM032					
Property	**Character**	**Quantitative estimate**	**Confidence**	**Basis for interpretation**	**Comments**
Volume (m^3)		Unable to be carried out due to difficulties with RVS			Borehole data close to reactors 1 and 2 not analysed.
Rock type, dominant	101058		High	See confidence table	Borehole data close to reactors 1 and 2 not analysed.
Rock type, subordinate	101057 103076 101061 102017 101051 111058		High	See confidence table	Borehole data close to reactors 1 and 2 not analysed.
Degree of homogeneity	Low		Medium	See confidence table	Borehole data close to reactors 1 and 2 not analysed.
High temperature alteration (dominant rock type)	Amphibolite-facies metamorphism		High	See confidence table	Borehole data close to reactors 1 and 2 not analysed.
Ductile deformation	Banded, foliated and lineated		High	See confidence table	Borehole data close to reactors 1 and 2 not analysed.
Class (1-4)*	1				
Background fracturing	**Quantitative estimate**	**Span**	**Confidence**	**Basis for interpretation**	**Comments**
Low temperature alteration around fractures	No data				Tunnel 1/2 data and borehole data close to reactors 1 and 2 not analysed
Fracture filling	No data				Tunnel 1/2 data and borehole data close to reactors 1 and 2 not analysed

*1=Inhomogeneous. Banded, foliated and lineated. Inferred higher degree of ductile deformation.
2=Inhomogeneous. Lineated and weakly foliated. Inferred lower degree of ductile deformation.
3=Homogeneous. Foliated and lineated. Inferred higher degree of ductile deformation. 4=Homogeneous.
Lineated and weakly foliated. Inferred lower degree of ductile deformation.

RFM033					
Property	**Character**	**Quantitative estimate**	**Confidence**	**Basis for interpretation**	**Comments**
Volume (m³)		1.61E+11	Very low		
Rock type, dominant	111051		Low	See confidence table	
Rock type, subordinate	101061		Low	See confidence table	
Degree of homogeneity	Low		Low	See confidence table	
High temperature alteration (dominant rock type)	Amphibolite-facies metamorphism		Low	See confidence table	
Ductile deformation	Lineated and weakly foliated		Low	See confidence table	
Class (1-4)*	2				
Background fracturing	**Quantitative estimate**	**Span**	**Confidence**	**Basis for interpretation**	**Comments**
Low temperature alteration around fractures	No data				SFR data not analysed
Fracture filling	No data				SFR data not analysed

*1=Inhomogeneous. Banded, foliated and lineated. Inferred higher degree of ductile deformation.
2=Inhomogeneous. Lineated and weakly foliated. Inferred lower degree of ductile deformation.
3=Homogeneous. Foliated and lineated. Inferred higher degree of ductile deformation. 4=Homogeneous.
Lineated and weakly foliated. Inferred lower degree of ductile deformation.

RFM034					
Property	**Character**	**Quantitative estimate**	**Confidence**	**Basis for interpretation**	**Comments**
Volume (m^3)		Unable to be carried out due to difficulties with RVS			Borehole data close to reactor 3 not analysed
Rock type, dominant	101057		High	See confidence table	Borehole data close to reactor 3 not analysed
Rock type, subordinate	101058 101061 102017 111058 101051		High	See confidence table	Borehole data close to reactor 3 not analysed
Degree of homogeneity	High		Medium	See confidence table	Borehole data close to reactor 3 not analysed
High temperature alteration (dominant rock type)	Amphibolite-facies metamorphism		High	See confidence table	Borehole data close to reactor 3 not analysed
Ductile deformation	Lineated and weakly foliated. More strongly foliated along southwestern margin		High	See confidence table	Borehole data close to reactor 3 not analysed
Class (1-4)[*]	4				
Background fracturing	**Quantitative estimate**	**Span**	**Confidence**	**Basis for interpretation**	**Comments**
Low temperature alteration around fractures	No data				Tunnel data (1/2 and 3) and borehole data close to reactor 3 not analysed.
Fracture filling	No data				Tunnel data (1/2 and 3) and borehole data close to reactor 3 not analysed.

[*]1=Inhomogeneous. Banded, foliated and lineated. Inferred higher degree of ductile deformation.
2=Inhomogeneous. Lineated and weakly foliated. Inferred lower degree of ductile deformation.
3=Homogeneous. Foliated and lineated. Inferred higher degree of ductile deformation. 4=Homogeneous.
Lineated and weakly foliated. Inferred lower degree of ductile deformation.

Properties of deformation zones in the regional model volume

The construction of these tables is described in Section 5.1.4.

ZFMNW0001 (Singö deformation zone)					
Property	**Quantitative estimate**	**Span**	**Confidence level**	**Basis for interpretation**	**Comments**
Position		± 20 m	High	Linked lineaments, seismic refraction data, tunnel, borehole	Position on surface
Orientation (strike/dip)	300/90	± 10/± 10	High for strike, medium for dip	Linked lineaments, seismic refraction data, tunnel, borehole	Dip from model version 0
Width	200 m	± 50 m	Low	Tunnel, borehole	
Length[1]	30 km	+ 25 km	High	Linked lineaments, model version 0	Extension outside regional model domain based on model version 0
Ductile deformation	Yes		High	Tunnel, borehole	
Brittle deformation	Yes		High	Tunnel, borehole	
Alteration					
Fracture orientation	210/75, 55/75, 170/40, subhorizontal	± 5/± 5	High	Tunnel, borehole	Carlsson and Christiansson 1987
Fracture frequency	10 m^{-1}	± 4/ m	High	Tunnel, borehole	
Fracture filling	Chlorite, calcite, quartz, clay, sandy material		High	Tunnel, borehole	

[1]Concerns total length. Extends outside regional model volume

ZFMNW0002 (splay from Singö deformation zone through tunnel 3)					
Property	**Quantitative estimate**	**Span**	**Confidence level**	**Basis for interpretation**	**Comments**
Position		± 20 m	High	Linked lineaments, tunnel	Position on surface
Orientation (strike/dip)	315/90	± 10/± 10	High for strike, medium for dip	Linked lineaments, tunnel	Dip from model version 0
Width	75 m	± 10 m	Low	Tunnel	
Length[1]	13 km	± 1 km	High	Linked lineaments, model version 0	Extension outside regional model domain based on model version 0
Ductile deformation	Yes		High	Tunnel	Zones of foliated rocks and chlorite schist documented during mapping of tunnel from block 3
Brittle deformation	Yes		Medium	Tunnel	
Alteration	Yes. Chloritization		High	Tunnel	
Fracture orientation	NW/70S, NE/90, NNW/90		High	Tunnel	
Fracture frequency	1 m^{-1}	0.5/ m	High	Tunnel	Low fracture frequency
Fracture filling	Chlorite, calcite		High	Tunnel	

[1]Concerns total length. Extends outside regional model volume

ZFMNW003A, B, C, D, E (Eckarfjärden deformation zone)					
Property	**Quantitative estimate**	**Span**	**Confidence level**	**Basis for interpretation**	**Comments**
Position		± 20 m	High	Linked lineaments	Position on surface
Orientation (strike/dip)	320/90	± 15/± 10	High for strike, low for dip	Linked lineaments	
Width	100 m	± 50 m	Low	Comparison with ZFMNW0001	
Length[1]	35 km	± 1 km	High	Linked lineaments, model version 0	Extension outside regional model domain based on model version 0
Ductile deformation	Yes		High	Ground geology	
Brittle deformation	Yes		High	Ground geology	
Alteration	Yes		High	Ground geology	
Fracture orientation					
Fracture frequency					
Fracture filling	Quartz, epidote		High	Ground geology	

[1]Concerns total length. Extends outside regional model volume

ZFMNW004A, B, C, D, E (Forsmark deformation zone)					
Property	**Quantitative estimate**	**Span**	**Confidence level**	**Basis for interpretation**	**Comments**
Position		± 20 m	High	Linked lineaments	Position on surface
Orientation (strike/dip)	310/90	± 10/± 10	High for strike, low for dip	Linked lineaments	
Width	100 m	± 50 m	Low	Comparison with ZFMNW0001	
Length[1]	70 km	± 5 km	High	Linked lineaments, model version 0	Extension outside model domain based on model version 0
Ductile deformation	Yes		High	Ground geology	
Brittle deformation	Yes		High	Ground geology outside regional model domain, summarized in model version 0	
Alteration	Yes		High	Ground geology outside regional model doamian, summarized in model version 0	
Fracture orientation					
Fracture frequency					
Fracture filling					

[1]Concerns total length. Extends outside regional model volume

ZFMNE0869 (Zone 3, SFR)					
Property	**Quantitative estimate**	**Span**	**Confidence level**	**Basis for interpretation**	**Comments**
Position		± 1 m	High	Seismic refraction data, tunnel, borehole	Position in tunnel, borehole
Orientation (strike/dip)	012/90	±10/±10	Medium	Tunnel	SSW/steep W in Axelsson and Hansen (1997)
Width	10 m	± 1 m	High	Tunnel	
Length	1 km	± 200 m	High	Ground geophysics, borehole, tunnel	
Ductile deformation					
Brittle deformation	Yes		High	Seismic refraction data, tunnel, borehole	
Alteration					
Fracture orientation					
Fracture frequency	15 m^{-1}	± 5/ m	High	Borehole	
Fracture filling					

ZFMNW0805 (Zone 8, SFR)					
Property	**Quantitative estimate**	**Span**	**Confidence level**	**Basis for interpretation**	**Comments**
Position		±1 m	High	Linked lineaments, seismic refraction data, borehole	Position on surface
Orientation (strike/dip)	133/90	±10/±10	High	Linked lineaments, borehole	NW/steep NE in Axelsson and Hansen (1997)
Width	10 m	± 5 m	Low	Borehole	Uncertainty concerning the width and significance of this zone (c.f. Carlsson et al 1986, Axelsson and Hansen 1997)
Length[1]	6 km	±1 km	High	Linked lineaments, borehole	Extends outside regional model volume
Ductile deformation	Yes		Low	Borehole	Degree of foliation development is uncertain. See Axelsson and Hansen (1997)
Brittle deformation	Yes		High	Borehole	
Alteration					
Fracture orientation					
Fracture frequency	15 m^{-1}	± 5/ m	Low	Borehole	Uncertain to which zone highly fractured bedrock is related (Axelsson and Hansen 1997)
Fracture filling					

[1]Concerns minimum length. Total length not estimated

ZFMNE0870 (Zone 9, SFR)					
Property	Quantitative estimate	Span	Confidence level	Basis for interpretation	Comments
Position		±1 m	High	Tunnel, borehole	Position in tunnel, borehole
Orientation (strike/dip)	50/90	±10/±10	Medium	Tunnel	ENE/steep in Axelsson and Hansen (1997)
Width	2 m	± 1 m	High	Tunnel, borehole	
Length	1 km	±200 m	High	Tunnel, borehole	
Ductile deformation	Mylonite present		Low	Tunnel	
Brittle deformation	Yes		High	Tunnel, borehole	Water-bearing, clayey gouge
Alteration					
Fracture orientation					
Fracture frequency	15 m^{-1}	± 5/ m	High	Borehole	
Fracture filling	Clay, chlorite, calcite, Fe-bearing mineral		High	Tunnel	

ZFMNE0871 (H2, SFR)					
Property	**Quantitative estimate**	**Span**	**Confidence level**	**Basis for interpretation**	**Comments**
Position		±1 m	High	Tunnel, borehole	Position in tunnel and boreholes. Projection to surface differs in Axelsson and Hansen (1997) and Holmén and Stigsson (2001)
Orientation (strike/dip)	048/16	±15 dip	Medium	Tunnel	ENE/20 in Axelsson and Hansen (1997). NE/15-20 in Holmén and Stigsson (2001)
Width	10 m	± 5 m	High	Tunnel, borehole	
Length[1]	3 km	± 500 m	Low	Tunnel, borehole	Model assumption. Truncated in base structural model against nearest steep deformation zone
Ductile deformation					
Brittle deformation	Yes		High	Tunnel, borehole	
Alteration	Yes		High	Borehole	
Fracture orientation					
Fracture frequency	15 m^{-1}	± 5/ m	High	Borehole	
Fracture filling	Clay		High	Borehole	

[1]Concerns length in base structural model

ZFMEW0865 (40 m level in KFM01A)					
Property	**Quantitative estimate**	**Span**	**Confidence level**	**Basis for interpretation**	**Comments**
Position		±1 m	High	KFM01A, HFM01, HFM02	Position in borehole
Orientation (strike/dip)	266/01	± 15 dip	High	KFM01A, HFM01, HFM02	
Width	3 m	± 1 m	High	KFM01A, HFM01, HFM02	
Length[1]	1500 m	±500 m	Low		Model assumption. Truncated in base structural model against nearest steep deformation zone
Ductile deformation	No		High	KFM01A, HFM01, HFM02	
Brittle deformation	Yes		High	KFM01A, HFM01, HFM02	
Alteration	Oxidized walls		High	KFM01A	
Fracture orientation	Subhorizontal	± 10 dip		KFM01A, HFM01, HFM02	Open fractures in KFM01A
Fracture frequency	>9 m^{-1}, sections of crush			KFM01A, HFM01, HFM02	Open fractures in KFM01A, crush in HFM01 and HFM02 at 43 m
Fracture filling	Chlorite, calcite, clay			KFM01A, HFM01, HFM02	

[1]Concerns length in base structural model

ZFMNE0061 (640-680 m level in KFM01A)					
Property	**Quantitative estimate**	**Span**	**Confidence level**	**Basis for interpretation**	**Comments**
Position		± 9 m (± 20 m)	High	KFM01A, linked lineaments	Position in borehole (surface)
Orientation (strike/dip)	068/81	± 5/± 10	High	KFM01A, linked lineaments	
Width	5 m	± 1 m		KFM01A	
Length	1730 m	± 200 m	Medium	Linked lineaments	
Ductile deformation	No		High	KFM01A	
Brittle deformation	Yes		High	KFM01A	
Alteration	Yes	± 5 m	High	KFM01A	10 m of oxidized bedrock
Fracture orientation	050/75	± 15/± 10	High	KFM01A	Boremap
Fracture frequency	<4 m^{-1}, section of crush		High	KFM01A	Concentration of fractures is distinctly higher, mainly sealed fractures. Crush at 652 m
Fracture filling	Laumontite, chlorite, calcite		High	KFM01A	

ZFMNE0866 (62 m level in HFM04)					
Property	**Quantitative estimate**	**Span**	**Confidence level**	**Basis for interpretation**	**Comments**
Position		± 1 m	High	HFM04, HFM05, KFM02A (0-100 m), seismic reflection data	Position in boreholes. Possible correlation with reflector A3 in Juhlin et al. (2002)
Orientation (strike/dip)	058/36	± 10/± 10	High	HFM04, HFM05, KFM02A (0-100 m)	
Width	2 m	± 1 m	High	HFM04, HFM05	
Length[1]	500 m	± 200 m	Low		Model assumption. Truncated in base structural model against nearest steep deformation zone
Ductile deformation	No		High	HFM04, HFM05	
Brittle deformation	Yes		High	HFM04, HFM05	
Alteration	Yes		High	HFM04	Oxidation, chloritization
Fracture orientation	086/51	± 30/ ± 30	High	HFM04, HFM05	High variability in orientation of open fractures
Fracture frequency	5 m^{-1}		High	HFM04, HFM05	Low frequency of open fractures, crush in HFM05
Fracture fillings	Chlorite, calcite		High	HFM04, HFM05	

[1]Concerns length in base structural model

ZFMNE0867 (70 m level in HFM06)					
Property	**Quantitative estimate**	**Span**	**Confidence level**	**Basis for interpretation**	**Comments**
Position		± 1 m	High	HFM06, HFM08, KFM03A (0-100 m), seismic reflection data	Position in borehole. Correlation with reflector A3 in Juhlin et al. (2002)
Orientation (strike/dip)	055/20	± 10/± 15	High	HFM06, HFM08, KFM03A (0-100 m)	
Width	2 m	± 1 m	High	HFM06, HFM08	
Length[1]	1300 m	± 200 m	Low		Model assumption. Truncated in base structural model against nearest steep deformation zone
Ductile deformation	No		High	HFM06, HFM08	
Brittle deformation	Yes		High	HFM06, HFM08	
Alteration	Yes		High	HFM06	Oxidized walls
Fracture orientation	Dominating subhorizontal fractures	± 20 dip	High	HFM06, HFM08	Open fractures, Crush at 61 and 70 m in HFM06
Fracture frequency	>9 m^{-1}, sections of crush		High	HFM06, HFM08	Open fractures, Crush at 61 and 70 m in HFM06
Fracture filling	Chlorite, calcite		High	HFM06, HFM08	

[1]Concerns length in base structural model

ZFMNE0868 (55-67 m level in HFM07)					
Property	**Quantitative estimate**	**Span**	**Confidence level**	**Basis for interpretation**	**Comments**
Position		± 5 m	High	HFM07, seismic reflection data	Position in borehole. Correlation with reflector A6 in Juhlin et al. (2002)
Orientation (strike/dip)	077/30	± 10/± 15	Medium	Seismic reflection data	
Width	10 m	± 2 m	High	HFM07	
Length[1]	2 km	± 500 m	Low		Model assumption. Truncated in base structural model against nearest steep deformation zone
Ductile deformation	No		High	HFM07	
Brittle deformation	Yes		High	HFM07	
Alteration	Yes		High	HFM07	Oxidation, chloritization
Fracture orientation	030/60	± 6/± 6	High	HFM07	Open fractures (at 58 m)
Fracture frequency	>10 m^{-1}		High	HFM07	Open fractures (at 58 m)
Fracture filling	Calcite, chlorite		High	HFM07	

[1]Concerns length in base structural model

NE set. Regional deformation zones (>10 km)					
Property	**Quantitative estimate**	**Span**	**Confidence level**	**Basis for interpretation**	**Comments**
Position		± 20 m	High	Linked lineaments, fracture statistical analysis	
Orientation (strike/dip)	43/90	±26/90-60	Low	Statistical analysis of fractures and lineaments (DFN model)	span 95% confidence interval
Width	75 m	±25 m	Low		Assumption
Length	>10 km		Medium		
Ductile deformation	No		Low	Ground geology	
Brittle deformation	Yes		Low	Ground geology	
Alteration					
Fracture orientation					
Fracture frequency					
Fracture filling					

NE set. Local major deformation zones (1-10 km)					
Property	**Quantitative estimate**	**Span**	**Confidence level**	**Basis for interpretation**	**Comments**
Position		± 20 m	High	Linked lineaments, fracture statistical analysis	
Orientation (strike/dip)	43/90	±26/90-60	Low	Statistical analysis of fractures and lineaments (DFN model)	span 95% confidence interval
Width	15 m	± 10 m	Low		Assumption
Length	1-10 km		Medium		
Ductile deformation	No		Low	Ground geology	
Brittle deformation	Yes		Low	Ground geology	
Alteration					
Fracture orientation					
Fracture frequency					
Fracture filling					

NW set. Regional deformation zones (>10 km)					
Property	**Quantitative estimate**	**Span**	**Confidence level**	**Basis for interpretation**	**Comments**
Position		± 20 m	High	Linked lineaments, fracture statistical analysis	
Orientation (strike/dip)	306/88	±24/90-62	Low	Statistical analysis of fractures and lineaments (DFN model)	span 95% confidence interval
Width	75 m	±25 m	Low		Assumption
Length	>10 km		Medium		
Ductile deformation	Yes		Low	Ground geology	
Brittle deformation	Yes		Low	Ground geology	
Alteration					
Fracture orientation					
Fracture frequency					
Fracture filling					

	NW set. Local major deformation zones (1-10 km)				
Property	**Quantitative estimate**	**Span**	**Confidence level**	**Basis for interpretation**	**Comments**
Position		± 20 m	High	Linked lineaments, fracture statistical analysis	
Orientation (strike/dip)	306/88	±24/90-62	Low	Statistical analysis of fractures and lineaments (DFN model)	span 95% confidence interval
Width	15 m	± 10 m	Low		Assumption
Length	1-10 km		Medium		
Ductile deformation	Yes		Low	Ground geology	
Brittle deformation	Yes		Low	Ground geology	
Alteration					
Fracture orientation					
Fracture frequency					
Fracture filling					

NS set. Regional deformation zones (>10 km)					
Property	**Quantitative estimate**	**Span**	**Confidence level**	**Basis for interpretation**	**Comments**
Position		± 20 m	High	Linked lineaments, fracture statistical analysis	
Orientation (strike/dip)	356/88	±25/90-61	Low	Statistical analysis of fractures and lineaments (DFN model)	Span 95% confidence interval
Width	75 m	±25 m	Low		Assumption
Length	>10 km		Medium		
Ductile deformation	No		Low	Ground geology	
Brittle deformation	Yes		Low	Ground geology	
Alteration					
Fracture orientation					
Fracture frequency					
Fracture filling					

NS set. Local major deformation zones (1-10 km)					
Property	**Quantitative estimate**	**Span**	**Confidence level**	**Basis for interpretation**	**Comments**
Position		± 20 m	High	Linked lineaments, fracture statistical analysis	
Orientation (strike/dip)	356/88	±25/90-61	Low	Statistical analysis of fractures and lineaments (DFN model)	Span 95% confidence interval
Width	15 m	± 10 m	Low		Assumption
Length	1-10 km		Medium		
Ductile deformation	No		Low	Ground geology	
Brittle deformation	Yes		Low	Ground geology	
Alteration					
Fracture orientation					
Fracture frequency					
Fracture filling					

EW set. Regional deformation zones (>10 km)					
Property	**Quantitative estimate**	**Span**	**Confidence level**	**Basis for interpretation**	**Comments**
Position		± 20 m	High	Linked lineaments, fracture statistical analysis	
Orientation (strike/dip)	278/87	±18/89-67	Low	Statistical analysis of fractures and lineaments (DFN model)	Span 95% confidence interval
Width	75 m	±25 m	Low		Assumption
Length	>10 km		Medium		
Ductile deformation	No		Low	Ground geology	
Brittle deformation	Yes		Low	Ground geology	
Alteration					
Fracture orientation					
Fracture frequency					
Fracture filling					

EW set. Local major deformation zones (1-10 km)					
Property	**Quantitative estimate**	**Span**	**Confidence level**	**Basis for interpretation**	**Comments**
Position		± 20 m	High	Linked lineaments, fracture statistical analysis	
Orientation (strike/dip)	278/87	±18/89-67	Low	Statistical analysis of fractures and lineaments (DFN model)	Span 95% confidence interval
Width	15 m	± 10 m	Low		Assumption
Length	1-10 km		Medium		
Ductile deformation	No		Low	Ground geology	
Brittle deformation	Yes		Low	Ground geology	
Alteration					
Fracture orientation					
Fracture frequency					
Fracture filling					

Selection of sites for cored borehole KFM04 and a batch of percussion boreholes across the Eckarfjärden fracture zone

Introduction

On account of the rapid progress made with the drilling activities in the Forsmark candidate area and the necessity to maintain a continuity in the drilling programme, there has developed a need to select the site for borehole KFM04 somewhat earlier than that originally included in the planning activities. The site investigation team at Forsmark has directed the question of site selection to the SKB analytical unit (Forsmark) under the leadership of Kristina Skagius. Michael Stephens (Geological Survey of Sweden) and Jan Hermanson (Golder Associates) from the Forsmark analytical panel have received the specific instruction to complete the task.

The question concerning the siting of KFM04 has been discussed within an informal group of geologists (GeoNet) who are working with site investigation and analytical studies at both Forsmark and Simpevarp, under the leadership of Raymond Munier (SKB). Stephens and Hermanson are also members of this network. The site selection work has also been carried out in close collaboration with Hans Isaksson (GeoVista AB), who is responsible for the interpretation of new airborne geophysical data in the candidate area and its surroundings, as well as Jenny Andersson, Rune Johansson and Sara Karlsson who are responsible for the activitites geology, geophysics and ecology, respectively, at the Forsmark site.

Motivation for drilling activities

One of the objectives of the initial site investigations in the Forsmark area is to study the boundary zones of the candidate area, both to the northeast and to the southwest /P-02-03, p.15/. Since there is already some information from both boreholes and tunnels through the Singö fault zone to the northeast, it is feasible that the first borehole which aims to address the boundary conditions should be placed in the vicinity of the southwestern boundary.

Which geological factors have steered the definition of the southwestern boundary of the candidate area?

The candidate area at Forsmark /SKB 2000/ was defined on the basis of the results of the geological and environmental investigations carried out during the feasibility study in the Östhammar municipality. The definition of the southwestern boundary was steered essentially by the assessment of available geological data.

In this area (Fiskarfjärden-Vamborsfjärden-southern part of Bolundsfjärden), there are distinctive changes in two geological features from northeast to southwest across the proposed boundary (Figure 1):
- An increase in the degree of bedrock inhomogeneity.
- An increase in the degree of ductile deformation.

Two other, important geological features can also be noted:
- Felsic metavolcanic rocks that are known to contain Fe-rich mineralizations associated with calc-silicate rocks (skarn) appear in the more inhomogeneous bedrock in the area to the southwest of the lakes (Figure 1).
- Low-temperature mylonites and cataclastic rocks have been observed in outcrop, immediately adjacent to a pronounced magnetic and topographic lineament which trends in a northwesterly direction through the lake Eckarfjärden. This lineament was upgraded to a regional fracture zone (ZFM0003A0) within the site descriptive model, version 0 /R-02-32/.

Mapping work during 2002 indicates that the high-temperature tectonic foliation in the rocks along and immediately to the southwest of the candidate area strikes 130-140° and dips 70-90° to the southwest. The dip of the Eckarfjärden fracture zone is poorly understood. The low-temperature mylonites in the outcrops closest to the lineament strike 325° and dip 85-90° to the northeast. The reflection seismic data /reflector D1 with rank 3 in R-02-43/ provide some support to the conclusion that the zone dips steeply to the northeast.

Using a conservative approach, the boundary to the area where the ductile deformation was judged to increase in intensity was adopted as the southwestern border of the area recommended for further investigations in the feasibility study. This boundary is clearly difficult to locate and is, almost certainly, transitional in character and, thereby, poorly defined. There are also some questions concerning the significance of the variation in the intensity of ductile deformation in the context of the suitability of bedrock for nuclear waste disposal. The distance along the surface from the southwestern boundary of the candidate area to the lineament along the Eckarfjärden zone is c. 800 m in the northwest (southwest of KFM01) and c. 1200 m in the southeast (close to the lake Eckarfjärden).

What are the key questions to be solved with the drilling?

The geological considerations discussed above awaken the following key questions and, thereby, motivate a drilling campaign:

- What are the detailed lithological, structural, rock mechanical, hydrogeological and hydrogeochemical characteristics of the transitional change in geological features described above?
- Can the volume of potentially suitable bedrock be extended to the southwest of the candidate area? If so, how far?
- What are the structural, hydrogeological and hydrogeochemical characteristics of the Eckarfjärden fracture zone with its distinctive lineament association?

A general strategy for borehole orientation and choice of site

When boundary conditions along the southwestern side of the candidate area are concerned, it is apparent that all the questions listed above need to be addressed. However, it is clear that a single cored borehole with a length of 1000 m and a dip greater than or equal to 60° will not solve all the relevant questions. It is highly probable that a satisfactory understanding of the relationships along the southwestern border will only be gained with the help of more than one cored borehole. Bearing in mind these considerations and the orientation of the various structures summarized above, the following general strategy is recommended at this stage in the investigations:

- A cored borehole (KFM04) is sited southwest of, i.e. outside, the candidate area, in bedrock judged to be affected by the various negative aspects listed above. This borehole should be drilled at an angle of 60° in the direction 045°, i. e. towards the candidate area. The borehole direction is at a high angle to both the strike of the tectonic foliation and to the inferred bedrock contacts in the area (Figure 1). The borehole should also descend into the bedrock in the opposite direction to the dip of these structural features. Such a borehole orientation may have some problems picking up the fracture set in the area that strikes in a northeasterly direction. However, this borehole will be an excellent complement to KFM01A which appears to have underestimated somewhat the fracture set that strikes in a northwesterly direction.
- The Eckarfjärden fracture zone is investigated at this stage with a set of percussion boreholes. These boreholes should be drilled, if possible, at an angle of 45-50° in order to gain the maximum horizontal coverage. Since the dip of the brittle deformational component of the Eckarfjärden zone is poorly understood, it is recommended that a careful analysis with the help of BIPS, radar and geophysical logging is carried out after completion of the first two percussion boreholes and prior to the final selection of the exact site for the remaining boreholes. If the percussion drilling does not satisfactorily answer the key questions concerning the structural, hydrogeological and hydrogeochemical characteristics of this zone, then a cored borehole should be considered at a later stage in the site investigation.

Geographic, geological and geophysical data available along the southwestern boundary of the candidate area

The following geographic, geological and geophysical information exists along the southwestern boundary area. The data have been generated by SKB in the context of the initial site investigation programme and have been made use of in the site selection work:

- Detailed geographic information (available 2002).
- Reflection seismic data and interpretation (R-02-43).
- Bedrock outcrop data (data available January 2003).
- A preliminary, detailed bedrock geological map (interpretation available April 2003).
- Detailed digital elevation model (available 2002).
- Airborne geophysical data measured from a helicopter (data available January 2003)
- A preliminary interpretation of lineaments based on the integrated interpretation of the topographic and airborne geophysical data (interpretation available April 2003).

Recommendation concerning the siting of KFM04

The following general considerations have been taken account of in the site selection procedure:

- Since the various geoinformation available from older boreholes in the area close to and immediately southeast of the Forsmark nuclear power station has not as yet been reassessed, it was decided to leave this part of the southwestern border area for later investigations.

- A strategic decision was made to avoid cored drilling in an area that is distal to the northwestern central part of the candidate area around Bolundsfjärden. This essentially restricts the potentially interesting part to the area between the northwestern end of Fiskarjärden and the accommodation buildings southeast of the nuclear power station.
- Since it is desirable that a detailed fracture analysis is carried out on the surface at the selected site, as at KFM02 and KFM03, it was decided to place the drilling site on a bedrock outcrop.
- The borehole with a recommended strike and dip of 045° and 60°, respectively, should avoid siting along an inferred lineament.

On this basis, two alternative sites have been selected (Figures 1 and 2).

The first alternative to the northwest lies in a fairly open forest area with new tree growth, directly southwest of a minor road. A 1000 m long borehole with strike and dip 045° and 60°, respectively, in this area should intersect initially a complexly banded bedrock with important components of metamorphosed tonalite and lenses of felsic metavolcanic rocks, metamorphosed and deformed granodiorite with possible lenses of felsic metavolcanic rocks, and a metamorphosed and strongly foliated granite to granodiorite (Figure 1). The bedrock mapping at the surface indicates that the latter corresponds to the metamorphosed granite to granodiorite in the southwestern part of the candidate area (rock unit which dominates KFM01A). The borehole should end at a point which is c. 870 m below the surface and c. 500 m from the borehole site. The projection of this point to the surface lies within the candidate area, c. 175 m northeast of its southwestern boundary. The borehole site is situated c. 450 m northeast of the lineament inferred to correspond to the Eckarfjärden fracture zone.

The second alternative to the southeast is situated within a forest area, immediately adjacent to an open area to the southeast. The site lies directly southwest of a minor road. This road was recently strengthened in connection with the site investigation programme. A 1000 m long borehole with strike and dip 045° and 60°, respectively, in this area should intersect initially an inhomogeneous bedrock with possible lenses of felsic metavolcanic rocks, a distinctive lineament with a northwesterly trend, metamorphosed and deformed granodiorite with possible lenses of felsic metavolcanic rocks, and a metamorphosed and strongly foliated granite to granodiorite (Figure 1). The bedrock mapping at the surface indicates that the latter corresponds to the metamorphosed granite to granodiorite in the southwestern part of the candidate area. The borehole should end at a point which is c. 870 m below the surface and c. 500 m from the borehole site. The projection of this point to the surface lies outside the candidate area, c. 250 m southwest of the boundary. The borehole site is situated c. 475 m northeast of the lineament inferred to correspond to the Eckarfjärden fracture zone.

Following selection of both these sites, ground electromagnetic (EM) and magnetic measurements have been carried out along several short profiles in both areas /AP PF 400-03-31; see also Figures 1 and 2/. Preliminary results indicate that a borehole at both alternatives will not be drilled along a lineament with a northeasterly trend. A brief field visit has also been carried out and a more exact borehole position has been selected for both sites (Table 1).

Table 1. Length, direction, dip and coordinates of the alternative sites for the cored borehole KFM04.

Cored borehole KFM04	Northing in RT 90, 2.5 gon V (metres)	Easting in RT 90, 2.5 gon V (metres)	Length (m)	Direction	Dip
Alt.1. Northwest	6698922	1630969	1000	045°	60°
Alt. 2. Southeast	6698029	1631632	1000	045°	60°

Both sites have clear advantages and disadvantages:

1. ***Knowledge build-up:*** Choice of the site to the southeast has the advantage that the build-up of knowledge at an early stage in the site investigations will be spread out over a broader area. However, bearing in mind the distance between the boreholes, it will probably be difficult to link many of the results from the investigations at the KFM04 site with those derived from the investigations at the sites KFM01-KFM03. By contrast, there is an interesting opportunity to compare and possibly investigate the interplay between the results from KFM01 with the results from KFM04, if the northwestern site is chosen. In this case, our knowledge will be more restricted in space but potentially will provide us with a better understanding of the characteristics of the southwestern boundary area.
2. ***Surface control:*** The frequency of outcrops is higher and, thereby, the surface control of the geology is better in the area around the northwestern site.
3. ***Relationship to candidate area:*** Selection of the site to the northwest has the advantage that a borehole from this site will end with its projection point at the surface *within* the candidate area.
4. ***Future cored borehole to the southwest:*** By placing a second cored borehole at a later stage at either the northwestern or the southeastern site, but directed to the southwest instead of to the northeast, there opens the possibility that the whole deformation zone which passes through Eckarfjärden, with its ductile and brittle components, can be investigated by cored drilling. The northwestern site has a minor advantage in this respect since it lies marginally closer to the Eckarfjärden zone. There is the added bonus that such a borehole from the northwestern site will intersect the lineament which is the northwesterly continuation of the lineament through the southwestern part of Fiskarfjärden (Figure 1).

- In summary, the advantages of the northwestern site are judged to outweigh the advantages of the southeastern site. For this reason, the northwestern site is recommended. It is predicted that the results from KFM01, KFM04 (northwestern site, direction 045°/60°) and a possible later borehole directed to the southwest, at the same site as KFM04, will together provide data which will permit a close and well-intergrated understanding of the southwestern border zone of the candidate area.

Recommendation concerning the siting of percussion boreholes along the Eckarfjärden fracture zone

The following general considerations have been taken account of in the site selection procedure:

- The sites have been spread out along various segments of the lineament which is coupled to the Eckarfjärden fracture zone.
- In order to minimize the environmental disturbance, sites with close proximity to a minor road have been selected.

Three sites have been selected (Figures 1 and 2). The northwestern site lies close to the minor road which passes north of Gällsboträsket. The central site is situated northwest of Eckarfjärden and directly northwest of the minor road which passes through Habbalsbo. The southeastern site lies close to the minor road which links road 76 with Storkäret.

In connection with the ground geophysical surveys over the areas containing the possible sites for KFM04, EM and magnetic measurements were carried out along three profiles which trend NE-SW across the Eckarfjärden lineament in the vicinity of the central site /AP PF 400-03-31; see also Figures 1 and 2/. Preliminary results show that the Eckarfjärden lineament appears on all three profiles as a distinct, although weak EM anomaly. The location coincides very well with the lineament as inferred from other data sets and the drilling target is thought to be well defined. A brief field visit to the three percussion borehole sites has also been completed.

The following recommendations are provided concerning the percussion boreholes:

- Two percussion boreholes each with a length of 200-250 m and a dip of 45-50° are drilled in the central site, one on each side of the lineament. Bearing in mind the possible dip of the Eckarfjärden fracture zone to the northeast, it is recommended that the borehole on the northeastern side of the lineament is drilled first in a direction 240°, slightly oblique to the trend of the lineament in this area (310°). The second percussion borehole on the southwestern side of the lineament should be drilled in a direction 060°. With a borehole length of 200 m and a dip of 45°, each borehole should end at a point which is c. 140 m below the surface and c. 140 m from the borehole site. The coordinates of the two boreholes are shown in Table 2. This drilling should take place during the same campaign as the normal percussion drilling which will be necessary in the vicinity of the KFM04 site.

- BIPS, radar and geophysical logging should be completed and the results analysed after completion of the two percussion boreholes at the central site and prior to a planned, later round of percussion drilling at the other two sites.

- Decisions concerning whether one or two percussion boreholes should be drilled at the northwestern and southeastern sites and exactly where these boreholes should be placed should be made after analysis of the borehole data from the central site.

Table 2. Coordinates, length, direction and dip of the percussion boreholes at the central site
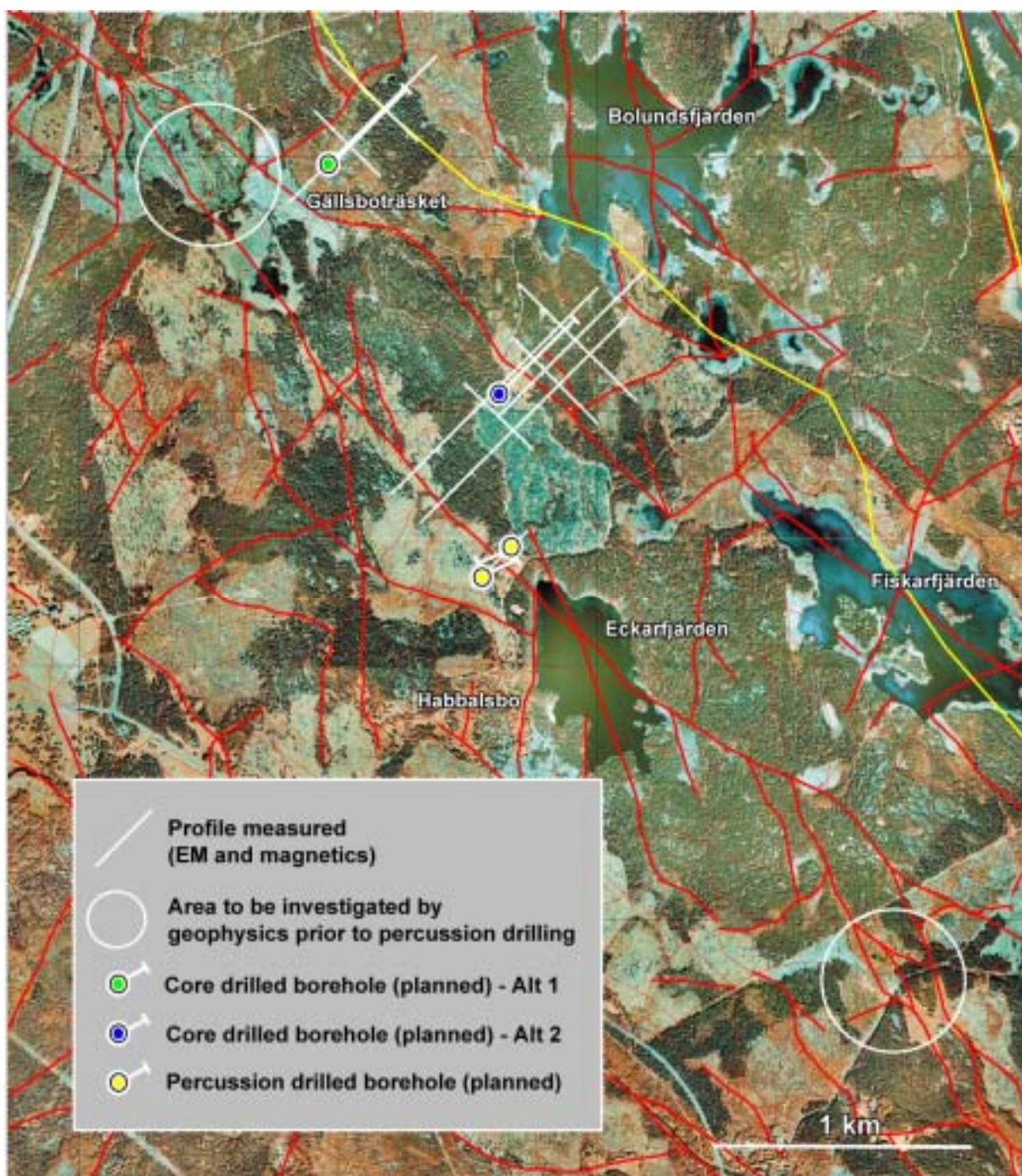
Percussion borehole, central site	Northing in RT 90, 2.5 gon V (metres)	Easting in RT 90, 2.5 gon V (metres)	Length (m)	Direction	Dip
NE of lineament	6697439	1631699	200-250	240°	45-50°
SW of lineament	6697336	1631572	200-250	060°	45-50°

Michael B. Stephens (Geological Survey of Sweden)
Jan Hermanson (Golder Associates)

2002-04-23
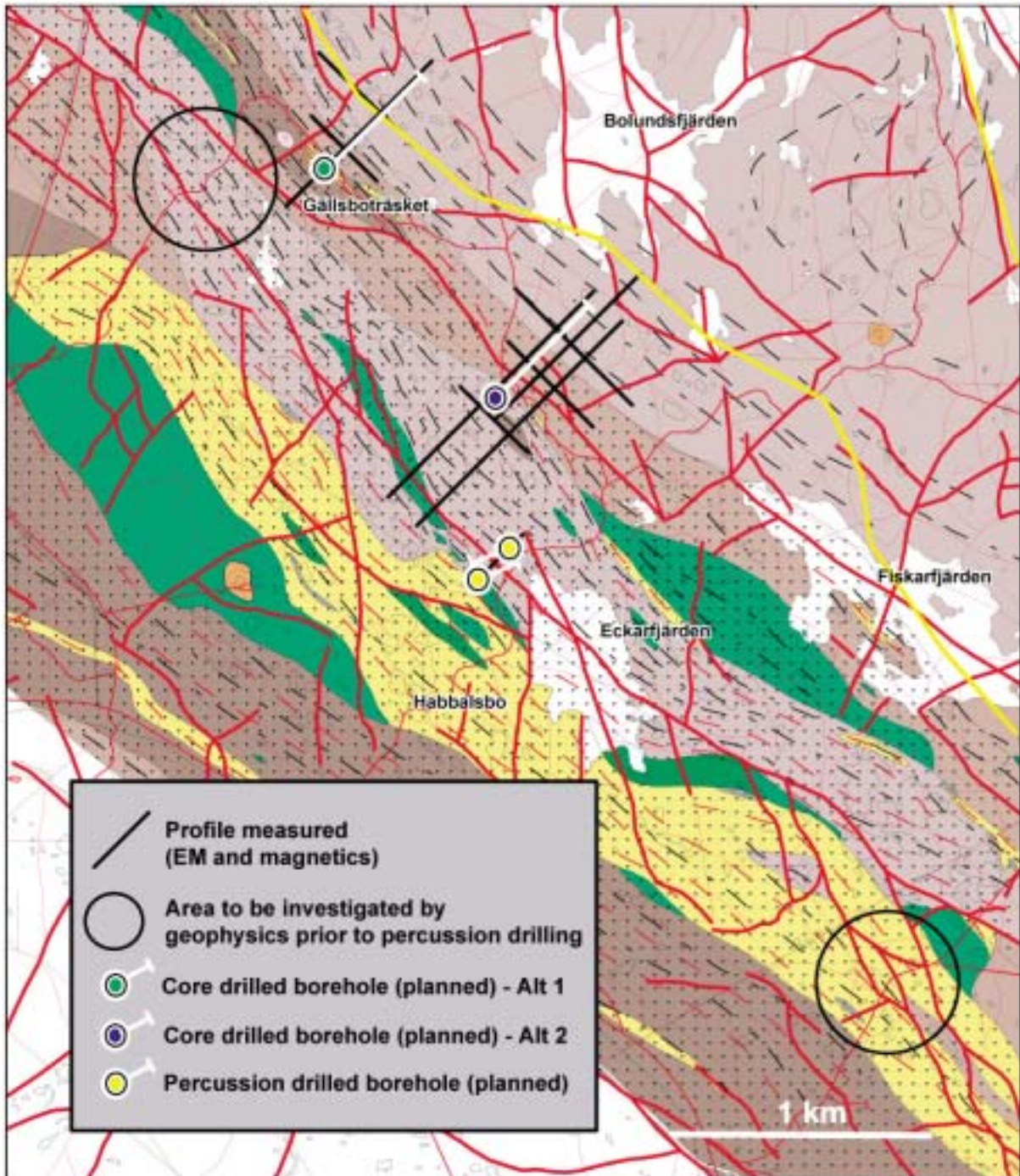
Figure 1. Preliminary geological map of the area from Fiskarfjärden to Gällsboträsket. Outcrops are shown as small areas ringed by a black line. The various colours indicate the dominant rock types. Yellow represents felsic metavolcanic rocks (locally with Fe-mineralization in grey colour), brown represents various metagranitoids (dark=tonalitic to granodioritic composition, medium=granodioritic and pale=granitic to granodioritic), green represents metagabbro and metadiorite, and orange represents pegmatitic granite. Form lines for foliation and banding are shown with thin dashed lines (black and red, respectively). The dotted ornament indicates the area judged to be affected, in general, by more intense ductile deformation. Lineaments inferred from various data sets are shown as continuous red lines. The yellow line marks the boundary to the Forsmark candidate area.

Figure 2. Map showing the location of the profiles along which ground geophysical measurements have been carried out, and the proposed sites for the cored borehole KFM04 (alternatives 1 and 2) and the percussion boreholes across the lineament inferred to be coupled to the Eckarfjärden fracture zone. Lineaments inferred from various data sets are shown as continuous red lines. The yellow line marks the boundary to the Forsmark candidate area.

Selection of the site for cored borehole KFM05 and a future cored borehole east of the small lake Puttan

Introduction

On account of the rapid progress made with the drilling activities in the Forsmark candidate area and the necessity to maintain a continuity in the drilling programme, there has developed a need to select the site for borehole KFM05 somewhat earlier than that originally included in the planning activities. The site investigation team at Forsmark has directed the question of site selection to the SKB analytical unit (Forsmark) under the leadership of Kristina Skagius. Michael Stephens (Geological Survey of Sweden) and Jan Hermanson (Golder Associates) from the Forsmark analytical panel have received the specific instruction to complete the task.

The work with the selection of the drillsite for KFM05 has been carried out in collaboration with Hans Isaksson (GeoVista AB), who is responsible for the interpretation of topographic and new airborne geophysical data in the candidate area and its surroundings, as well as Lena Albrecht, Rune Johansson and Sara Karlsson who are responsible for the activitites geology, geophysics and ecology, respectively, at Forsmark.

Motivation for drilling activities

Five deep (1000 m in length) cored boreholes were planned in the initial site investigation programme in the Forsmark area /P-02-03, p. 15/. The aim of these boreholes, together with a number of shallower percussion boreholes (0-200 m in length), was to provide data on the following four site specific questions:

- The vertical extension of the tectonic lens at Forsmark.
- The potential for metallic ore deposits at depth.
- The occurrence of subhorizontal fracture zones.
- The occurrence of high rock stresses.

In order to provide some answers to these questions, three vertical boreholes were proposed in the initial site investigation programme. The programme also includes two additional deep, but inclined, boreholes. The aim of the additional boreholes was to study the boundary conditions of the candidate area, both to the northeast and to the southwest /P-02-03, p. 15/. The programme envisaged that the exact locations of these additional boreholes were to be decided after detailed geological and geophysical surveys had been completed.

In a PM dated 2003-04-24 (Document ID 1013788), the selection of a site for borehole KFM04 and a batch of percussion boreholes across the Eckarfjärden fracture zone was presented. In accordance with the original objectives, borehole KFM04 is located so as to address the properties of the bedrock along the southwestern boundary of the tectonic lens. The present document provides a proposal for the location of the site for cored borehole KFM05.

The location of borehole KFM05 proposed here diverges somewhat from the site specific programme, where it was planned that this borehole should provide new data along the northeastern boundary of the tectonic lens. Instead, it is proposed to locate the site for KFM05 within the candidate area, close to the lake Bolundsfjärden. It is important to keep in mind that drilling across the northeastern boundary is not removed from the programme. If site investigations continue at Forsmark, drilling across the northeastern boundary will be carried out during the complete site investigation phase. It should be noted that the main fracture zone at this boundary, the so-called Singö fault zone, has been penetrated earlier by four tunnels, with associated borehole and other investigations. Although data regarding properties at greater depth regarding this fault are lacking, there are considerable data at shallower depth that can be utilized as a first approximation in the site descriptive model.

The key points that motivate the minor adjustment of the planned drilling programme and, thereby, define the objectives for KFM05 are as follows:

- Bolundsfjärden is situated in the central part of the area which is of high interest for a repository site at c. 500 m depth. The recently completed and detailed lineament interpretation of the candidate area and its surroundings confirms earlier interpretations that the area around Bolundsfjärden is transected by several north-south trending lineaments that potentially are local major fracture zones. It is argued that in order to judge the feasibility of the site for further investigations in the context of the complete site investigation programme, it is vital that the lithological, structural, rock mechanical, hydrogeological and hydrogeochemical characteristics of these potential fracture zones are investigated with the help of an inclined, deep cored borehole.

- One of the important features that drilling in the Forsmark area has demonstrated is the local occurrence of vuggy metagranite in borehole KFM02A. The occurrence of this type of bedrock was not foreseen in the previous investigations and, for this reason, no measures were undertaken to include any studies in the execution programme for the initial site investigations /P-02-03/. As emphasized in the report recently submitted to SKB that concerns the mineralogical and microstructural characteristics of this hydrothermally altered and mechanically weak metagranite, there is little control on the geometry, extent and properties of vuggy metagranite in the candidate area. Bearing in mind its potentially unfavourable character, it is judged to be of high priority that the site descriptive model version 1.2 is able to address the possible relative occurrence of vuggy metagranite in the Forsmark area.

Bearing in mind these circumstances, an inclined deep cored borehole within the candidate area is judged to be of higher priority at this stage in the site investigation programme than a borehole across the northeastern boundary. It is highly unlikely that the lineaments with a north-south trend through Bolundsfjärden will be transected by an inclined borehole sited along or immediately adjacent to the present road system in the area. It is also apparent that, in order to meet the two objectives noted above, borehole KFM05 can be located close to either the eastern or the western shores of the lake.

Consideration of nature conservation aspects

The main constraints regarding the location of the drilling site concerns aspects of nature conservation. The whole candidate area at Forsmark is located within an area of national interest for nature conservation and parts of the candidate site have been classified with high nature conservation values. In general, special consideration should be taken when considering drilling sites close to lakes. For these reasons, all drilling sites must be approved by the county board (Länsstyrelsen) before any work can commence. This also applies if a road has to be constructed to connect the drilling site with existing roads.

There is no road leading to the shores of the lake Bolundsfjärden. A drilling site will, therefore, require a new road. Consultation with the site ecologist reveals that it is possible, from a nature conservation standpoint, to locate a drilling site close to both shores. However, the main impact on the environment will probably be caused by establishment of the new road.

The site ecologist recommends that a site close to the western shore is selected for the drilling activities. Choice of such a site will minimize the environmental impact since:

- This area lies closer to the already established road system.
- The nature conservation values are probably lower on the western relative to the eastern sides of the lake Bolundsfjärden.

However, a detailed inventory of flora and fauna will need to be carried out before a proposal for the location of the drillsite and the new road can be established and submitted to the county board for approval.

Geographic, geological and geophysical data available in the area around Bolundsfjärden

The following geographic, geological and geophysical information exists in the area around Bolundsfjärden. The data have been generated by SKB in the context of the initial site investigation programme and have been utilized in the site selection work:

- Detailed geographic information (available 2002).
- Reflection seismic data and interpretation (R-02-43).
- Bedrock outcrop data (data available January 2003).
- A detailed bedrock geological map, version 1.1 (available May 2003).
- Detailed digital elevation model (available 2002).
- Airborne geophysical data measured from a helicopter (data available January 2003)
- An interpretation of lineaments based on the integrated interpretation of the topographic and airborne geophysical data (available May 2003).

Recommendation concerning the siting of borehole KFM05

The following general considerations have been adopted in the site selection procedure:

- Bearing in mind the environmental considerations summarized earlier, the drillsite should be located west of Bolundsfjärden.
- The drillsite should be located within a block that is enclosed by the lineament network.
- It is recommended that the drillsite includes a bedrock outcrop. Siting of the borehole on an outcrop will allow a detailed fracture analysis to be carried out at the ground surface and the fracture data obtained from such an investigation can then be compared with that derived from the borehole. This procedure has been implemented at the drillsites for KFM02, KFM03 and KFM04.
- In order to minimize the environmental impact, it is desirable that the site chosen is potentially suitable for further drilling activities in a different orientation at a later date.
- Since it is feasible at this stage to consider that both the potential local major fracture zones that pass through Bolundsfjärden and the vuggy metagranite in borehole KFM02A are steeply-dipping structures, it is recommended that borehole KFM05 is inclined. Bearing in mind the various technical limitations with the BIPS and geophysical logging surveys, an inclination of 60° is recommended. The borehole should be drilled in an approximately easterly direction, at a high-angle to the north-south lineaments that trend through Bolundsfjärden. Since both borehole KFM04 across the southwestern boundary of the candidate area and borehole KFM05 at Bolundsfjärden will be drilled inclined, 60° from the horizontal, they will each have a 500 m horizontal component. Furthermore, by drilling these two boreholes at significantly different directions (approximately 45°), it is possible that an estimate of the relative occurrence of vuggy metagranite in two separate directions can be made. The drilling configuration also facilitates better statistical representation of fractures and other features in the bedrock.

A recommendation for the location of borehole KFM05 is shown as a small area with an elliptical form in the geological (Figure 1) and orthorectified aerial photographic (Figure 2) maps that accompany this document. The area is situated in a forest area at a minimum distance of c. 240-370 m from the nearest road. The area enclosed within the ellipse is the only one which fulfils the five criteria listed above. In order to avoid potentially complex areas where lineaments with different trends intersect each other, **it is recommended that a 1000 m cored borehole at this site is inclined at 60° in a direction 080°.**

The inferred outcrop in the eastern part of the ellipse at coordinates 6699328/1631730 was discovered in connection with the Quaternary geology mapping work during the later part of the field season 2002. It is situated c. 85 m west of the shoreline of the lake Bolundsfjärden. Inspection of this locality (Hermanson and Stephens on 2003-05-14; Albrecht, Johansson and Stephens on 2003-06-05) showed that foliated and lineated metagranite, similar to that in a larger part of the candidate area, is exposed at this locality. However, some discussion was raised concerning whether the exposure is an outcrop or the upper part of a large boulder. It was therefore decided to carry out a limited number of ground penetration radar (GPR) profiles over the small area around this probable outcrop. The GPR survey, which was conducted on 2003-06-10, strongly supports the initial judgement that the metagranite is exposed in a bedrock outcrop.

Based on the background information presented above, the field inspections and the radar survey, it is recommended that the area selected for borehole KFM05 should include the outcrop in question. Full documentation of the bedrock components at this locality will be carried out during June 2003.

If the county board do not approve the establishment of the borehole site at a distance of less than 100 m from the shoreline to Bolundsfjärden, then the site for KFM05 should be moved within the elliptical area to the southwest so as to lie at least 100 m from the shoreline. The location will be determined in more detail following the inventory of flora and fauna on the western side of Bolundsfjärden.

A 1000 m long borehole with a direction and inclination of 080° and 60°, respectively, in this area should intersect metagranite with subordinate amphibolite, pegmatite and finer-grained metagranitoid. The borehole should end at a point which is c. 870 m below the surface and c. 500 m from the borehole site. The projection of this point to the surface lies close to a small outcrop on the eastern shore of Bolundsfjärden (Figure 1). In accordance with the procedures adopted at KFM01, KFM02, KFM03 and KFM04, it is recommended that ground electromagnetic (EM) and magnetic measurements are carried out prior to the final establishment of the coordinates for the location of the borehole.

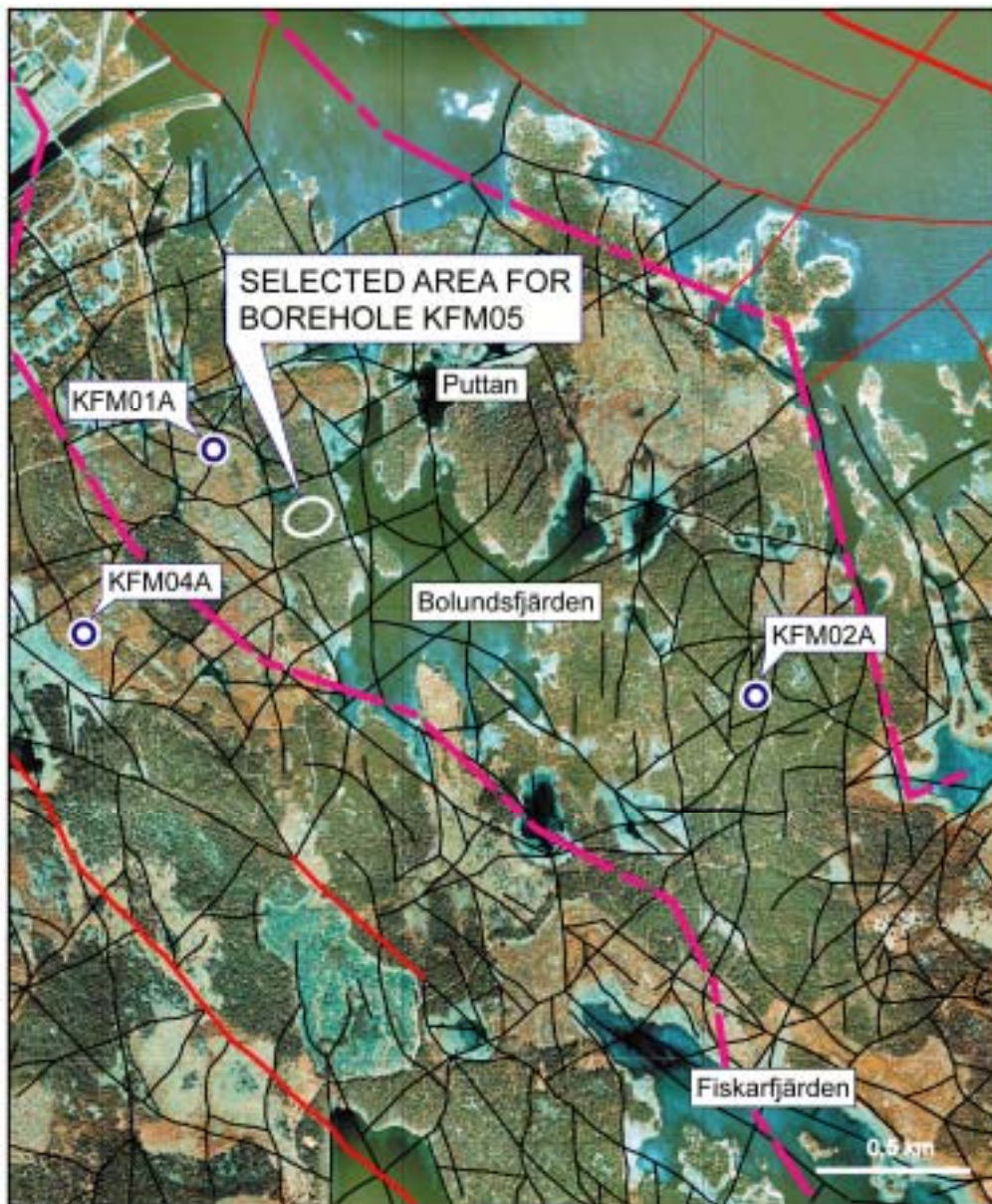**Considerations of future cored boreholes in the area around Bolundsfjärden**

The proposed location of borehole KFM05 opens interesting possibilities for future drilling from the same site towards the southeast, in order to investigate the orientation and properties of possible fracture zones in the Bolundsfjärden area with a northeasterly strike. Furthermore, if the north-south lineaments through Bolundsfjärden represent fracture zones that dip c. 80-45° towards the east, it is probable that both the proposed KFM05 borehole (and the near-vertical borehole KFM02) will fail (have failed) to penetrate most (or all) of these structures. In order to take account of this possibility, it is suggested that a future drilling site is established at a later stage in the site investigations at the end of the existing road, east of the small lake Puttan. An inclined borehole should be drilled approximately westwards at this site so that the orientation and properties of the structures around Bolundsfjärden can be investigated with an even greater degree of confidence.

Michael B. Stephens (Geological Survey of Sweden)
Jan Hermanson (Golder Associates)

2003-06-16 (title modified 2004-01-19)
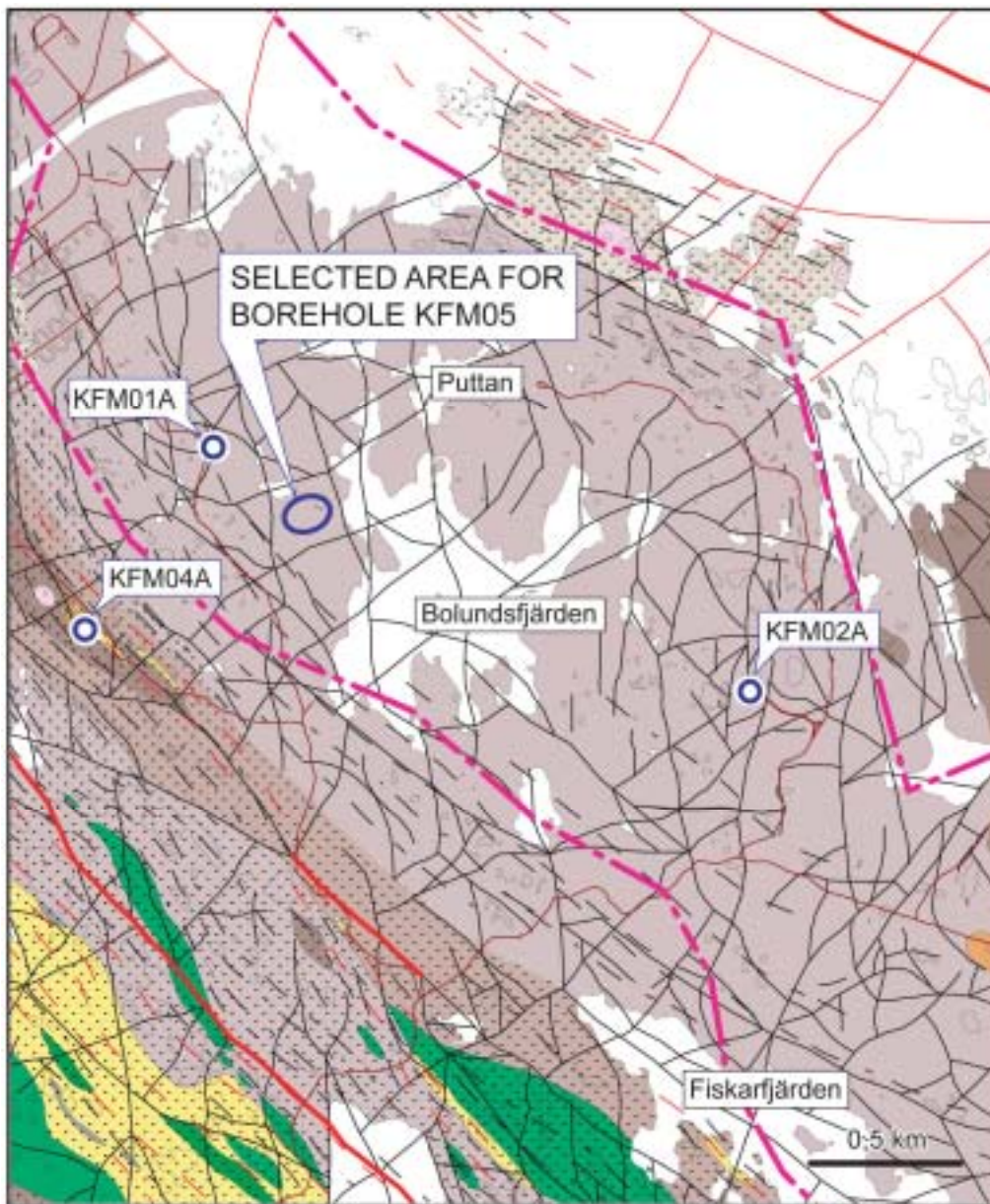
Figure 1. Geological map (version 1.1) of the area around Bolundsfjärden showing the selected area for borehole KFM05 and the sites for boreholes KFM01A, KFM02A and KFM04A. Outcrops are shown as small areas ringed by a black line. The various colours indicate the dominant rock types. Yellow represents felsic metavolcanic rocks (locally with Fe-mineralization in grey colour), brown represents various metagranitoids (dark=tonalitic to granodioritic composition, medium=granodioritic and pale=granitic to granodioritic), green represents metagabbro and metadiorite, and orange represents pegmatitic granite. Form lines for foliation and banding are shown with thin dashed lines (black and red, respectively). The dotted ornament indicates the area judged to be affected, in general, by more intense ductile deformation. Lineaments are shown as continuous black (integrated topographic and airborne geophysical data) or thin red (only magnetic data) lines. Thick red lines indicate fracture zones. The thick, dashed line in lilac marks the boundary to the Forsmark candidate area.

Figure 2. Orthorectified aerial photographic map showing the location of the selected area for borehole KFM05 and the sites for boreholes KFM01A, KFM02A and KFM04A. Lineaments are shown as continuous black (integrated topographic and airborne geophysical data) or thin red (only magnetic data) lines. Thick red lines indicate fracture zones. The thick, dashed line in lilac marks the boundary to the Forsmark candidate area.

Lineaments and fracture zones – a comment to some comments

Afterthought

The lithological and deterministic structural components in the geological model version 1.1 were presented for the first time at the ALF meeting in Forsmark on the 28th August, 2003. These parts of the model and the complementary statistical analysis of fractures (DFN analysis) were also presented at the 9th Forsmark analysis group meeting in Stockholm on the 3rd September. The presentation at the ALF meeting provoked a lively and, I would hasten to add, healthy reaction from the site investigation team at Forsmark. Further constructive discussions between Kaj Ahlbom, Rune Johansson, Hans Isaksson (Geovista AB) and myself took place at Forsmark on the 8th September.

The principal matter that has been discussed at all these meetings and in the e-mail correspondence is how well lineaments of various character (low magnetic, high electrically conductive and topographic) reflect fracture zones. Both Jan Hermanson and I are in full agreement with both Kaj and Lennart Ekman that this is a major question and that there is considerable uncertainty regarding the direct matching of lineaments with fracture zones. Indeed, lineaments without any other geological or geophysical information which indicate that the bedrock is disturbed by brittle deformation were not included in the version 0 model. The following points need to be kept in mind:

1. Hans Isaksson (Geovista AB) delivered to PLU Forsmark in late April the interpretation of the individual geophysical and topographic data sets and an integrated lineament interpretation. With the help of the table that accompanies each lineament segment, it is possible to trace the uncertainty of an individual integrated lineament and upon what data set (magnetic, EM, VLF and topographic data) the lineament is based. These various interpretations were placed in SKB´s GIS database.
2. If a lineament does represent a fracture zone, it is necessary to record the correct length of this structural feature. For this reason Jan H. and I made the decision in May to combine into one lineament the individual segments that lie along, what can be judged with confidence is, the same lineament. The production of these combined (linked) lineaments was carried out by Hans Isaksson (Geovista AB) for the analysis group as part of the necessary ongoing work within the analysis group. The combined (linked) lineaments were delivered to Jan H. and myself during mid June and to PLU Forsmark in late August. It is still possible to trace the judgement concerning the uncertainty of the lineament and upon what data set the lineament is based.
3. The deterministic structural model only translates to possible fracture zones the combined (linked) lineaments that are equal to or longer than 1 km. Nearly 180 lineaments of this type are present in the regional model volume. Only six of these longer lineaments are based solely on topographic data and only one is based solely on electrical conductivity data (EM and VLF). It is clear that the magnetic data **not** topography has played the most important role in the interpretation of the longer lineaments. As pointed out by Kaj, lineaments based in part or entirely on magnetic data can with confidence be related to processes in the bedrock, not in the Quaternary cover.

4. The interpretations of the seismic reflection data carried out originally by Chris Juhlin and coworkers (Uppsala University) and later by Calin Cosma and coworkers (Vibrometric Oy), in connection with the analysis group work, have been of prime help in the interpretation of some of the more confidently interpreted fracture zones in the local model area. However, since there are some difficulties concerning the interpretation of exactly what these reflectors represent, we have not directly translated all reflectors to fracture zones. The seismic reflection data has had a support function in the modelling procedure.

Where do go from here?

The analysis of lineaments has shown that there are four sets of lineaments with NW, NE, N-S and E-W trends. Bearing in mind the general plan that is starting to emerge for the whole site investigation programme at Forsmark, with its necessary cost-effectivity considerations, I recommend the following:

1. At this stage in the investigation programme, a percussion drilling programme is carried out to assess the presence and character of a limited number of possible regional or local major fracture zones that are based on the interpretation of lineaments. Representative examples from each of the lineament sets should be selected for study.
2. After presentation of the version 1.2 geological model and hopefully after a focussing of the site investigation programme to a more restricted area, a more aggressive drilling programme could be initiated to assess the presence and character of the possible regional or local major fracture zones that are based on the interpretation of lineaments and that bound the blocks in the critical, more restricted area.

The Eckarfjärden fault zone with NW strike has just been investigated by percussion drilling (see small red rings on enclosed map). More drilling along this major zone should be carried out during the spring, after the BIPS images from HFM11 and HFM12 have been obtained and interpreted. Percussion drilling of the possible NW zone through Fiskarfjärden could also be carried out at this time.

Cored drilling at BP5 aims, in the first hand, to address the N-S lineaments that trend through Bolundsfjärden. This activity will be completed during the late winter.

Bearing in mind that there are several possible local major fracture zones with NE strike that transect the candidate area, it is recommended that a percussion drilling programme to assess the presence and character of these zones is completed during the autumn, 2003. Following discussions at the ALF meeting and at the meeting on the 8th September, it is suggested that the percussion drilling campaign during the autumn at BP5, BP6 and at two other sites (see the four, large blue rings on the map enclosed) addresses the possible fracture zones linked to lineaments with NE (and possibly even N-S) trend. The exact location of the drilling site should await the assessment of the ground geophysical measurements which were carried out at all these sites during week 37.

I fully agree with Kaj that we need to produce a family of quality maps that show:

1. The interpretation of lineaments based on each data set (magnetic, EM, VLF and topography).

2. The interpretation of all integrated lineaments (delivery to SKB in April, 2003), on a topographic background.
3. The selection of the c. 180 combined lineaments included in the geological model, on a topographic background.
4. The selection of the c. 180 combined lineaments included in the geological model on the geological map background.

Finally, if a study of shorter lineaments is to be carrried out, BP1 (as suggested by Kaj) or BP2 can be considered as possible study areas. However, it is highly unlikely that the results of such a study can be included in version 1.1.

Michael B. Stephens
Geological Survey of Sweden

Uppsala, 2003-09-22
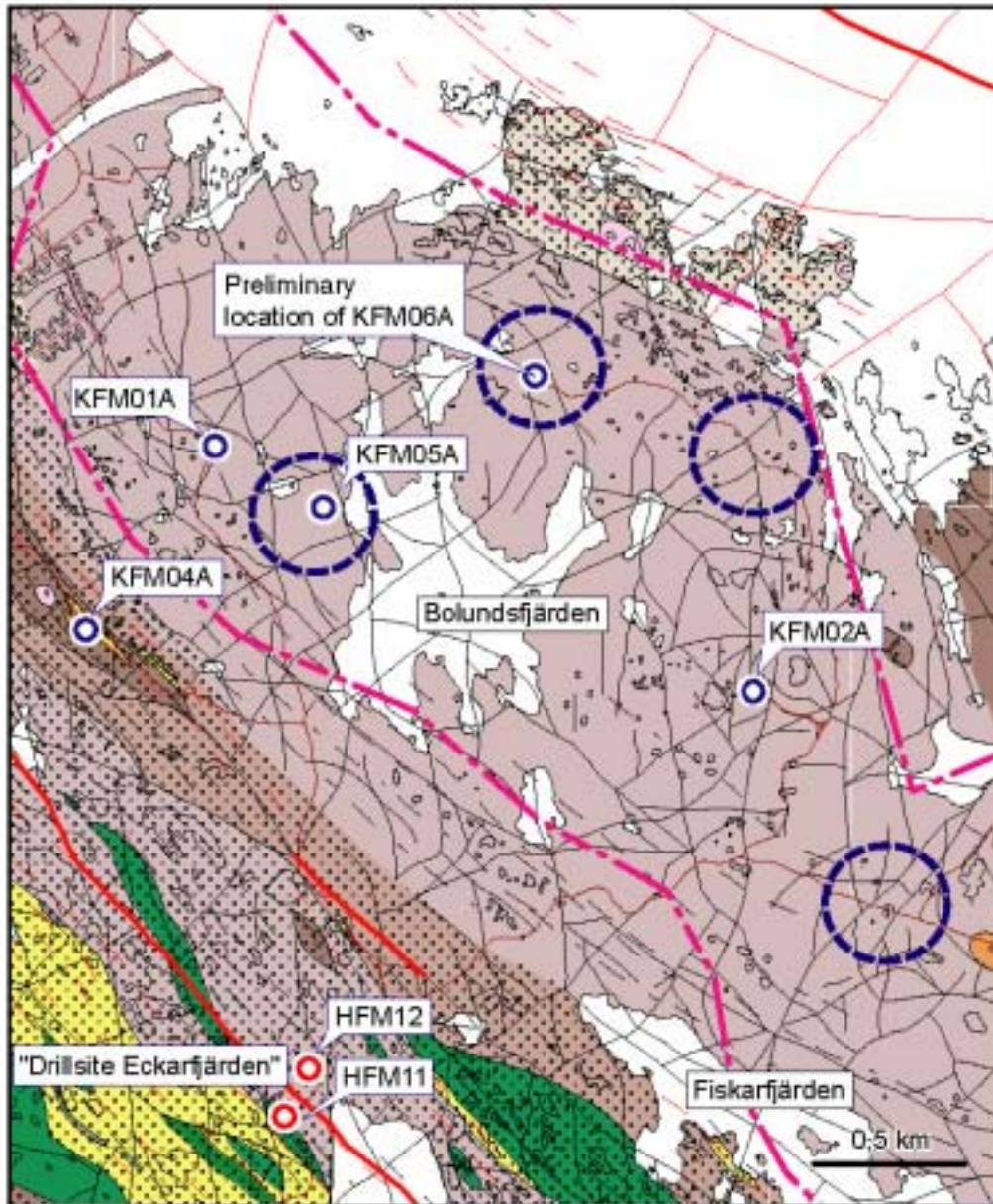
Orientation of the cored borehole KFM06A

Background

In connection with the motivation for the selection of the site for and the orientation of the cored borehole KFM05A (document by Stephens and Hermanson, date 2003-06-16), it was recognised that a second cored borehole may be necessary to the east, in order to ensure that the lineaments with NS trend through Bolundsfjärden are sufficiently well-understood. A fundamental problem is the uncertainty concerning the dip of these potentially critical fracture zones. A site for the second borehole in the Bolundsfjärden area was also proposed in the document presented by Stephens and Hermanson. The site is situated at the end of the small road that transects the candidate area and ends just east of the small lake referred to as Puttan (Figure 1).

The international panel of experts, that operate under commission for SKI (INSITE), have pointed out the key importance for our understanding of the structural geological and hydrogeological significance of the NS lineaments through Bolundsfjärden. The Bolundsfjärden area is also of central importance for an assessment concerning whether or not the Forsmark site is a feasible alternative for waste disposal. Bearing in mind these considerations and the original motivation in the document presented by Stephens and Hermanson, the site investigation team at Forsmark decided to build drillsite 6 at the end of the small road close to the small lake Puttan. This document provides a short motivation for the orientation of cored borehole KFM06A.

Motivation

The area in the vicinity of the small lake Puttan is transected by three lineaments with a length longer than 1 km. One of these lineaments trends c. NS and the other two c. NE-SW (Figure 1). There are also other minor lineaments in the area that show lengths less than 1 km. These trend approximately NW and NS, and have been recognised primarily on the basis of their topographic signature. They show no low magnetic anomaly and are not considered further here. The three lineaments longer than 1 km have all been included in the version 1.1, deterministic structural model for the Forsmark area as possible deformation zones.

The NS zone, referred to as ZFMNS0098 in the site descriptive model (Figure 1), has been recognised predominantly on the basis of topographic and electrical conductivity data. However, a subordinate component with a low magnetic signature is also present along this possible zone. Both the NE zones, ZFMNE0060 that strikes through the lake Puttan and ZFMNE0061 that is situated to the northwest of Puttan (Figure 1), have been recognised primarily on the basis of their low magnetic signature. They are also topographically distinctive and show, at least in part, a linear anomaly in the electrical conductivity data. The drilling campaign during the autumn has indicated the importance of strongly water-conductive zones in the uppermost part of the crystalline bedrock with NE strike that are gently dipping to the southeast, a pattern that is reminiscent of the seismic reflectors inside the

candidate area. An important, yet unresolved question concerns whether or not these strongly water-conductive zones can be related to the lineaments that are recognised at the surface.

With this background information in mind, it is recommended that KFM06A is oriented so that there is a possibility to transect and characterise the attributes of all the three zones described above. As far as ZFMNS0098 is concerned, borehole KFM06A will complement borehole KFM05A. If the NS zones through Bolundsfjärden dip westwards they will be intersected in KFM05A. If they dip eastwards, KFM06A should be oriented in such a manner that at least ZFMNS0098 intersects this borehole. Assuming that ZFMNE0060 and ZFMNE0061 dip to the southeast, KFM06A should be oriented so that this borehole also transects these zones.

It is recommended that KFM06A is inclined at 60° in a direction 300° (Figure 1). This orientation is oblique to both the NS zone and the NE zones and should hopefully meet the aims established above. This orientation will also provide some spread in the orientation of the inclined boreholes in the area (Figure 1).

Michael B. Stephens (Geological Survey of Sweden)
2003-12-02
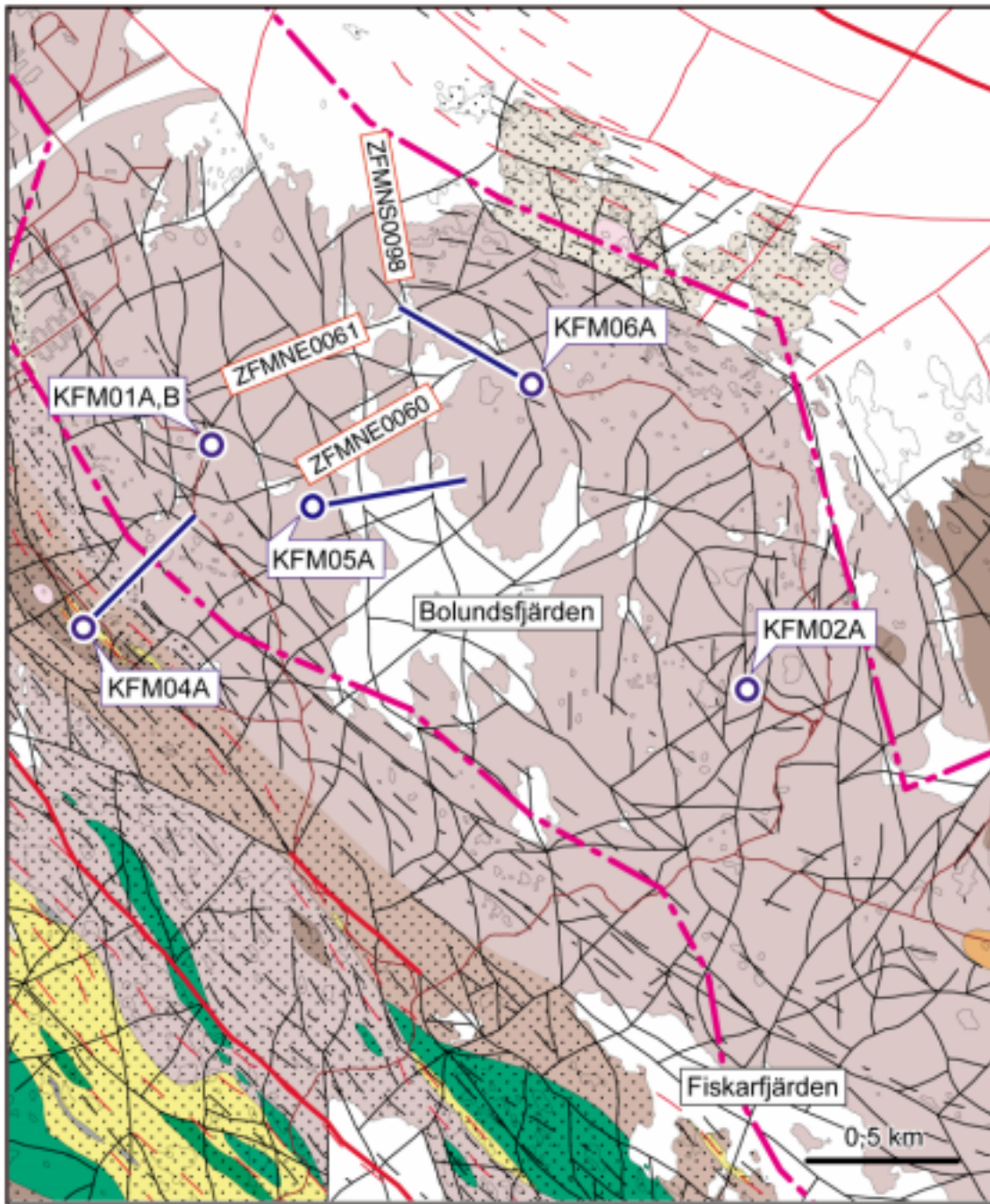
Figure 1. Geological map (version 1.1) of the area around Bolundsfjärden showing the sites for boreholes KFM01A, KFM01B, KFM02A, KFM04A, KFM05A and KFM06A. Outcrops are shown as small areas ringed by a black line. The various colours indicate the dominant rock types. Yellow represents felsic metavolcanic rocks (locally with Fe-mineralization in grey colour), brown represents various metagranitoids (dark=tonalitic to granodioritic composition, medium=granodioritic and pale=granitic to granodioritic), green represents metagabbro and metadiorite, and orange represents pegmatitic granite. Form lines for foliation and banding are shown with thin dashed lines (black and red, respectively). The dotted ornament indicates the area judged to be affected, in general, by more intense ductile deformation. Lineaments are shown as continuous black (integrated topographic and airborne geophysical data) or thin red (only magnetic data) lines. Thick red lines indicate fracture zones. The thick, dashed line in lilac marks the boundary to the Forsmark candidate area.